UNIVERSITY OF
BIRMINGHAM

NOVEL BIONANOCATALYSTS FOR GREEN CHEMISTRY APPLICATIONS

by

JACOB B. OMAJALI

A thesis submitted to the University of Birmingham for the degree of DOCTOR OF PHILOSOPHY

School of Biosciences

College of Life and Environmental Sciences

The University of Birmingham

August 2015

Abstract

Desulfovibrio desulfuricans have been known to synthesize good catalysts in a number of industrially and environmentally relevant reactions but the underlying reasons and /or mechanisms for such catalysis have largely remained elusive. This study has shown that in addition to nanoparticle (NP) size, the catalytic properties of *D. desulfuricans* is hinged on several factors such as the textural surface of the bacterial support, binding mechanism to surface functional groups and the crystal structure of the resulting catalyst NPs. In this study, various characterization techniques: AFM, EDX, SEM, HAADF-STEM, HRTEM, XRD and XPS and catalytic hydrogenation of soybean oil, reductive dehalogenation of chlorinated benzene, biomass conversion and heavy oil upgrading were used to evaluate the activity of bio-supported catalysts. Here, *D. desulfricans* NCIMB 8307 with rougher cell surface was found to be more active (~65% difference in conversion to *cis*-fatty acid methyl esters during soy bean oil partial hydrogenation) than *D. desulfuricans* NCIMB 8326 with smoother surface. The former was found *via* XPS to bind more strongly to amide nitrogen groups while the latter binds more strongly to phosphoryl groups (largely due to the presence of extracellular polymeric substances observed on the surface). The binding mechanisms were proposed to be via calcium ion and proton exchange in both organisms as a result of the absence of calcium following Pd sorption. However, endogenous reduction of palladium (II) was observed in both strains of bacteria which were suggested to be *via* a biochemical rather than abiotic process due to its absence in heat-killed cells determined *via* XPS study.

The concept of intracellular trafficking of palladium into the cells of both Gram-negative (*Desulfovibrio desulfuricans*) and Gram-positive (*Bacillus benzeovorans*) bacteria was pioneered. While *D. desulfuricans* produced multiply twinned crystalline icosahedral NPs, *B. benzeovorans* produced single nanocrystalline and amorphous palladium NPs under formate and hydrogen as electron acceptor respectively. However, the biologically different *D. desulfuricans* NCIMB 8307 and *B. benzeovorans* NCIMB 12555 produced highly monodispersed intracellular NPs than *D. desulfuricans* NCIMB 8326 which was more polydispersed. The membrane integrity and membrane potentials

of “palladized” cells (‘bio-Pd’) were found to be retained through flow cytometry analysis.

Due to the current increasing global demand for fossil energy and continuous depletion of world reserve, heavy oils are potential alternative sources but their viscous nature and inherent heavy ends makes exploitation and transportation challenging if not upgraded. Catalytic upgrading using commercial catalyst is expensive. Hence, bio-supported bimetallic (bio-Pd/Pt) catalyst from *D. desulfuricans* and *B. benzeovorans* were developed which has demonstrated comparable catalytic properties to a commercial catalyst (Ni-Mo/Al_2O_3) as a potential ‘green’ alternative. Generally, the extent of viscosity reduction was: 98.7% (thermal), 99.2% (bio-NPs) and 99.6% (Ni-Mo/Al_2O_3) below 1031 mPa.s of the feed heavy oil. Also the bimetallic bio-NPs produced an increament of ~2^o in API (American petroleum institute) gravity (~9.1^o) than monometallic (~7.6^o) on average while the API gravity using thermal was lower (6.3^o) while that of a commercial catalyst was 11.1^o. The bio-NPs also produced more liquids and less coking of catalyst surface than the commercial catalyst. In addition, the precious metals can be sourced cheaply from waste sources for catalytic synthesis.

Towards tandem (one-pot) catalytic remediation of chlorinated aromatic contaminants *B. benzeovorans* was selected due to ease of scalability. With combined flow cytometry and enzyme analysis of palladized cells of *B. benzeovorans*, it was found that the palladized cells retained viability and membrane potential and also the activity of catechol 1, 2-dioxygenase enzyme. 1wt% bio-Pd on cells retained the highest enzyme activity (~130U/ml) than 5wt% and 20wt% bio-Pd. This concept was pioneered as a potential platform for the remediation of chlorinated benzenes e.g chlorobenzene where the viable cells will act under aerobic condition to de-aromatize chlorobenzene and the Pd (0) to perform reductive dehalogenation in a one-pot tandem process.

This study has demonstrated the potential of using novel ‘green’ synthesis of bionanocatalyst in key industrially and environmentally important reactions. However, further future improvements are needed for bionanocatalyst to be more competitive with commercial counterparts.

Author's Declaration

I certify that this thesis is entirely the product of my original intellectual effort and materials which are not mine have been identified and duely acknowledged. To the best of my knowledge, no material contained in this thesis has been accepted or is in consideration for the award of any other degree or diploma in any University.

Jacob B. Omajali

To

My loving wife, Angela and precious daughter, Olivia

My beloved mother, Veronica Omajali

And

The loving memory of my dear father, Alexander Omajali

Acknowledgements

I would like to first and foremost give thanks to God Almighty for the gift of strength, good health and courage to be able to successfully complete my PhD studies. I would like to specially thank my supervisor, Prof. Lynne E. Macaskie for her guidance, moral support and training and for always pushing me to achieve the best while believing in myself, especially during challenging projects all through the entire duration of my studies. My profound gratitude also goes to my second supervisor, Prof. Joseph Wood for his support and guidance.

In a special way, I would like to thank my wife, Angela and daughter, Olivia for their unwavering support, love, understanding and patience in dealing with my absence most of the times when I was away. To my mother (Veronica Omajali), in-laws (Dr Isaac Achoba and Mrs Mary Achoba and children: Albert, Aaron, Alfred, Andrew), uncles (HRH John O. Egwemi and Mr Paul Omajali), brothers, cousin (Dr Victor O. Egwemi and family) and sisters (Felicia and Gloria), I express my utmost appreciation for all their prayers all through the years.

To our collaborators, Dr Marc Walker, Warwick University, Prof. Mohamed L. Merroun, University of Granada, Spain, Dr Hart Abarasi and Mr Bayonle Kayode, both of the University of Birmingham. I am grateful for useful discussions during writing, training, analysis and experiments. Special thanks also go to the great technical support staff of the University of Birmingham: Dr Jackie Deans, Theresa Morris, Paul Stanley, and Dr James Bowen for their technical assistance.

To the immense support of every member of the Unit of Functional Bionanomaterials: Dr Iryan Mikheenko, Dr Angela Murray, Dr Raf Orozco, Dr Jimmy Roussel, Dr Rajkumar Gangappa, Ms. Anna Williams, Ms. Sarah Singh and Mrs Rachel Priestley for the various help and useful discussion rendered during the course of this studies. You guys are the best one can ever wish for in any research group. Thanks a lot!

Finally, I would like to thank the Commonwealth Scholarships Commission of the United Kingdom for funding my PhD.

Thesis layout and organization

This thesis is divided into five main chapters. Chapter one, the introduction, gives a background to the study while chapter two described the main methodologies and materials employed in the study. Chapter three deals with the results and findings and each section has been written in the form of a scientific paper, each with a summary to the study, introduction, materials and methods, results, discussion and conclusion with acknowledgements and independent reference lists. Chapter four captures and discusses the entire findings and pinpoints the challenges and fundamental questions emanating from this study for future projects. The appendices make up chapter five and also contain additional methodologies and collaborative projects relating to this study but not yet ready for publication. Also contained in the appendices are published papers in journals and conference papers, proceedings, abstracts, posters, seminars and symbosia.

Table of contents

List of Figures

1. Introduction

2. Materials and methods

3. Results

3.1.1 Catalytic Hydrogenation of Soybean Oil Using Bio-Pd and X-ray Photoelectron Spectroscopy Studies on the Mechanisms of Palladium (II) Coordination in *Desulfovibrio desulfuricans*

3.1.2 Uptake of Pd (II) by *Desulfovibrio desulfuricans*: coordination to cell surface functional groups and endogenous reduction at the cell surface shown by X-ray photoelectron spectroscopy

3.3.2 Probing the Viability of Palladium-Challenged Bacterial Cells Using Flow Cytometry

3.4.1 Synthesis of Biogenic Palladium Catalyst by *Bacillus benzeovorans* pregrown by two methods

List of Tables

1. Introduction

2. Materials and methods

3. Results

3.1.1. Catalytic hydrogenation of Soybean Oil Using Bio-Pd and X-ray Photoelectron Spectroscopy Studies on the Mechanisms of Palladium (II) Coordination in *Desulfovibrio desulfuricans*

3.1.2 Uptake of Pd (II) by *Desulfovibrio desulfuricans*: coordination to cell surface functional groups and endogenous reduction at the cell surface shown by X-ray photoelectron spectroscopy

3.2.1 Bio-manufacture of heterogeneous Palladium catalysts: Effects of Biomass type in the reductive Dechlorination of Chlorobenzene

3.2.2 *In-Situ* Catalytic Upgrading of Heavy Oil Using Dispersed Bionanoparticles Supported on Gram-positive and Gram-negative Bacteria

3.3.2 Probing the Viability of Palladium-Challenged Bacterial Cells Using Flow Cytometry

3.4.1 Synthesis of Biogenic Palladium Catalyst by *Bacillus benzeovorans* pregrown by two methods

3.4.2 Potential of Palladized Cells of *Bacillus Benzeovorans* in Tandem Catalytic Remediation of Chlorobenzene

4. Discussion, conclusion and future work

5. Appendices

Abbreviations

ADI	Arginine Deiminase pathway
AMD	Acid Mine Drainage
ADP	Adenosine-5'-diphosphate
AFM	Atomic Force Microscopy
AR	Aqua Regia
ATR	Acid Tolerance Response
AMP	Adenosine-5'-monophosphate
ATP	Adenosine-5'-triphosphate
Bb	*Bacillus benzeovorans*
CALB	*Candida Antarctica* lipase B
CAPRI	Catalytic Upgrading Process *In-situ*
CDTA	Calcium-Dependent Transacylase
Dd	*Desulfovibrio desulfuricans*
dSir	Dissimilatory Sulfite Reductase
EDX	Energy Dispersive X-ray Spectrometry
EPR	Electron Paramagnetic Resonance
EPS	Extracellular Polymeric Substance
FAAH	Fatty Acid Amide Hydrolase
FAD	Flavin Adenine Dinucleotide
$FADH_2$	Flavin Adenine Dinucleotide (reduced form)
FAMEs	Fatty Acid Methyl Esters
FC	Fuel Cell
FCV	Fuel Cell Vehicle
FDA	Fluorescein Diacetate
FDH	Formate Dehydrogenase

FHL	Formate Hydrogen Lyase
FITC	Fluorescein Isocyanate
FMN	Flavin Mononucleotide
GC/MS	Gas Chromatography-Mass Spectrometry
HAADF	High Angle Annula Dark Field
HRTEM	High Resolution Transmission Electron Microscopy
ICEVs	Internal-Combustion Engine Vehicles
MALDI	MS- Matrix-Assited Laser Desorption/Ionization-Mass Spectrometry
MOPS	3-(-N-morpholino) propanesulfonic acid
NADH	Nicotinamide Adenicleotide (reduced form)
NADPH	Nicotinamide Adenicleotide Phosphate (reduced form)
NAG-	*N*-acetylglucosamine
NAM-	*N*-acetyl muramic acid
NAE	*N*-acyl ethanolamine
NAPEs	*N*- acyl phosphatidylethanolamine
NPs	Nanoparticles
PGMs	Platinum Group Metals
PI	Propidium Iodide
PCD	Programmed Cell Death
PMF	Proton Motive Force
SEM-	Scanning Electron Microscopy
SRB	Sulfate-Reducing Bacteria
STEM-	Scanning Transmission Electron Microscopy
TEM	Transmission Electron Microscopy
VAMAS-	Versailles Project on Advanced Materials and Standards
XPS	X-ray Photelectron Spectroscopy

CHAPTER 1 Introduction

1.1 Sulfate-reducing bacteria and *Bacillus* spp. as Gram-negative and Gram-positive paradigms with potential for metal bio-refining

Sulfate – reducing bacteria (SRB) are a diverse group of organisms in terms of their ecology and physiology. They are highly versatile and ubiquitous in anoxic habitats, in marine sediments, soils, surface and subsurface waters, pipelines, sewage and petroleum reservoirs (Muyzer and Stams, 2008) where they play important roles in both sulfur and carbon cycles. They derive their energy from anaerobic respiration through dissimilatory sulfate reduction, coupled to proton-driven and substrate-level ADP phosphorylation. In this case, sulfate is used as a terminal electron acceptor. Although named after the electron acceptor sulfate, some SRB are also capable of utilizing other forms of electron acceptors such as nitrate (Bursakov et al., 1995), thereby performing dissimilatory nitrate reduction to ammonia. Some can use oxygen (Dilling and Cypionka, 1990; Mogensen et al., 2005; Ramel et al., 2015) or oxidized forms of heavy metals such as Cr(VI), uranium(VI), Iron(III), and manganese (IV) (Tebo and Obraztsova, 1998).

According to taxonomic classification of the group (Postgate, 1979), two genera were named; *Desulfovibrio* (non- sporulating) and *Desulfotomaculum* (spore-forming). Seven species of *Desulfovibrio* were identified, with the ability to grow on lactate and malate, but not acetate and glucose. On the other hand, four of the five species of *Desulfotomaculum* can also grow on lactate while the related, *Desulfuromonas acetoxidans* grows on acetate but not lactate. With increasing research, more species and genera of the SRB have been identified. Widdel and Pfennig (1981) suggested that SRB can be classified into two groups based on their nutritional requirements: those that can only partially oxidize lactate and related compounds to produce acetate as the end product of metabolism (incomplete oxidizers) and the other group, which has a wide range of catabolic activity, ranging from the ability to grow on fatty acids, aromatics (benzoate) and authotrophically (CO_2). Subsequent studies by Feio et al., (1998) have led to the isolation of a novel SRB called Ind 1 (with a proposed name of *Desulfovibrio*

indonensis) from biofilm of a severely corroded carbon steel structure. It shares close similarity with *D. gabonensis* and possesses periplasmic proteins, hydrogenase and cytochrome c_3, and two cytoplasmic proteins: ferrodoxin and sulfite reductase which have been purified and are similar to that of *D. gigas*.

Sulfate reduction by the SRB in industry produces many challenges. In the agro - industries for instance, wastes, which also contain sulfuric acid, are released into waste water and reduced under anaerobic digestion conditions. Sulfate reduction leads to lower methane yield in addition to the additional odour, toxicity and corrosion caused by the production of H_2S (Tang et al., 2009). In the petrochemical industries, sulfate reduction leads to the formation of toxic hydrogen sulfide which is implicated in corrosion of oil platforms which can weaken structures. The threshold odour concentration of the gas is about 0.0005 ppm (Leonardos et al., 1969), but concentrations greater than 10 ppm could lead to adverse physiological effects while concentrations greater than 300 ppm could be life-threatening (Mori et al., 1992). However, the presence of metal ions can trap H_2S, thereby reducing its environmental exposure.

Sulfate-reducing bacteria also play very important roles in nature. Their relevance in bioremediation has been well documented especially in the reduction of heavy metals to insoluble forms in ground water and waste water. This also occurs via precipitating metals as insoluble metal sulfides (Gramp et al., 2010) which are easily recovered and reused. Such metal sulfates that are reduced under anoxic conditions include; cadmium, copper, cobalt, nickel, iron and zinc (Lee and Pandey, 2012). The mining industries use this application to immobilize metals from surface water and process water – a process which, in conjunction of bio-oxidation of metals from ores, called biomining.

The genus *Bacillus* comprises a group of over 70 species of Gram-positive bacteria. They are generally classified as aerobes or, less commonly, as facultative anaerobes except for the species *B. infernus* (Boone et al., 1995) which is the only obligate anaerobe described in the group. *Bacillus subtilis* has also been found to be able to adapt to an anaerobic environment by altering its metabolic activities, anaerobically, performing mixed acid fermentation with lactate, acetate and acetoin as the major product (Nakano et al., 1997). It has also been reported that some species of *Bacillus*

were able to produce lactic acid under aerobic and anaerobic conditions (Ohara and Yahata, 1996), but more lactic acid was produced when the bacteria were grown anaerobically. This metabolic switch has been linked to the presence of the *fnr* regulon, which is a transcriptional activator of anaerobically induced genes (Nakano and Zuber, 1998; Geng et al., 2007).

Morphologically, *Bacillus* spp are spore-forming and rod-shaped with the ability of the spore to resist extreme environmental conditions (Maughan and Van der Auwera, 2011). They are widely found in different environments and also as laboratory contaminants. While most of them are non-pathogenic, *B. anthracis* and *B. cereus* are human pathogens (Maughan and Van der Auwera, 2011). *Bacillus* spp, apart from being very important as one of the model organisms of industrial importance and research, are currently becoming potential key players in environmental bioremediation. They have been linked to selective accumulation of heavy metals (Selenska-Pobell et al., 1999), biosorption of heavy metals (Tuzen et al., 2007) and recently in the removal of trivalent chromium from tannery effluent (Fathima et al., 2012). Their ability to reduce metals has equally been reported (Boone et al., 1995) as well as the synthesis of nanosized metallic deposits on their S-layer proteins (Pollman et al., 2005; Fahmy et al., 2006). The S-layers (surface layers) are made up of protein monomers with the ability to assemble in two-dimensions with different structures. The protein array has identical sizes of regularly arranged pores which allow the exchange of ions and small molecules between living cells and their environment via the cell membrane beneath.

The ability of SRB (e.g. *Desulfovibrio desulfuricans*) and some *Bacillus* spp. to reduce metals has raised substantial interest in recent research, especially in the areas of metal recovery and catalysis. The increasing demand in the use of precious metals (e.g. the PGMs (Platinum Group Metals); platinum (Pt), rhodium (Rd), ruthenium (Ru) and palladium (Pd)), their increasing price on the world market and scarcity of supply calls for an alternative source of precious metal production. These metals are generally very important in medicine, optical devices, electronics and catalysis (Das, 2010). The PGMs are widely used in automotive catalytic converters to reduce a harmful gaseous emission, which produces the greatest drain on global supply (see section 1.4.6). Among the PGMs, palladium is more widely used in catalysis but falls in its supply lead

due to an increase in price. Therefore, there is a need to move from conventional methods of hydro and pyrometallurgical processes from primary sources which require capital, labour, time and a large amount of chemicals (Jacobsen, 2005) to a simple method of recovery of palladium (and other PGMs) from wastes.

In parrallel, it has become necessary to move from laborious and expensive use of toxic and synthetic chemicals in the production of catalysts to "green chemistry" approaches. Often, the finished commercial catalyst lacks the desired selectivity, resulting in wasteful production of unwanted side products. The concepts of green chemistry also include a focus on catalysts with high selectivity and hence less waste.

The use of bacteria to reduce soluble palladium (Pd (II)) as nanoparticles (Pd (0)) on bacterial biomass has attracted a lot of attention as an alternative, not only in sustainable nanomaterials production but also as a way of recovering palladium and other precious metals from wastes. Several examples of 'new bionanocatalysts from wastes' have been reported (Deplanche, 2008; 2011; Murray et al., 2015) with, in some cases, better catalytic activity than biogenic catalysts made from pure metal solutions. The underlying reason that makes some organisms (especially *Desulfovibrio desulfuricans*) a platform for the synthesis of better catalysts when compared with other members of the same genus has remained elusive and will form a major objective of this study. It is worthy of note that the production of catalysts using bacteria is also not without its challenges.

1.2 Metal bio-sorption and reduction by bacteria

The activities of bacteria in metal reduction has captured interest, not only in bioremediation or detoxification of heavy metals and radionuclides in polluted environments, but also in the emerging areas of metal recovery and catalyst biogenesis *via* mechanisms whereby metals are reduced and precipitated on bacterial surfaces for the production of nanoparticles of great catalytic importance.

The co-existence of metals and microorganisms has long been known as a result of their importance in biogeochemical processes in the biosphere and the interactions of metals with enzymes (Liermann et al., 2007), where they play catalytic roles. Such metals are

needed in minute amounts sufficient for normal metabolic processes of the cell and not in excess (Valls and de Lorenzo, 2002). Generally, these metals are divided into three main groups: (a) the essential and non-toxic metals e.g. Ca and Mg; (b) essential but harmful metals at high concentrations e.g. Fe, Mn, Cu, Co, Zn, Ni and Mo and (c) toxic metals for which no metabolic role is known e.g. Cd and Hg. In nature the noble metals (Pd, Pt, Au) generally occur as metallic components of ores and are considered biologically unavailable although platinum compounds have found therapeutic use as potent anticancer agents (see section 1.4.6). With the exception of Au, almost nothing was reported on microbial interaction with Pd and Pt and current research focuses almost exclusively on metallic nanoparticle biogenesis.

The heavy metals in (b) and (c) above are widely found naturally as toxic elements and compounds and their pollution in soil and aquatic environments has negative impacts on the ecosystem. As a result, a wide range of strategies has been adopted for their removal. The use of chemical processes for remediation is considered to be expensive and also lacks the specificity needed in the treatment of target metals in the presence of other competing ions (Lloyd and Lovley, 2001). Such chemical processes include precipitation, lime coagulation, ion exchange, reverse osmosis and solvent extraction (Aravindhan et al., 2004). Disadvantages include incomplete metal removal, high reagent and energy requirements and the generation of toxic sludge and other toxic wastes which could pose challenges of disposal. The use of microbial approaches has been considered to be more sustainable considering their potential in selective removal of toxic metals and the flexibility in either in-situ or ex-situ bioreactor applications (Lloyd and Lovley, 2001).

The complete removal of heavy metals from metal solutions by microorganisms is brought about by biosorption, bioaccumulation or biominerization. Bioaccumulation deals with the transport of the metal from the outer membrane (in Gram-negative cells) through the cellular membrane where the metal is finally sequestered (Wong and So, 1993) or further metabolized. The mechanisms of biosorption have been well documented (e.g. Volesky, 1994; Kratochvil and Volesky, 1998; Blanco et al., 1999; Yin et al., 1999; Sofu et al., 2015) and involve the formation of chemical links between functional groups on the biosorbent and metal ions. These biosorbents in bacteria are

usually macromolecules such as polysaccharides, proteins, lipids, and uronic acids – generally (where produced outside the cell) called extracellular polymeric substances (EPS) (Veglió et al., 1997). The EPS contain a range of charged functional groups such as carboxyl, phosphoric, amide and hydroxyl groups which can bind metal ions (Omoike and Chorover, 2006). The interaction of these electronegative sites with metal ions results in nucleation and formation of fine-grained particles. The adsorption of metal ions on the external surfaces of bacteria is also reported to be a biomass defence mechanism against toxic heavy metals by preventing their penetration into the cell wall. This is achieved by the production of external polymeric layers by the microorganism (Scott and Palmer, 1990).

Prior to the reduction of metals on bacterial biomass towards the bio-fabrication of bionanocatalysts (see section 1.5.1), biosorption is known to be a key stage required for the adsorption of in-coming metal ions onto bacterial surfaces. Bacteria (and see **Figure 1.1**) have a large surface area to volume ratio and this provides them with the interfaces for the sorption of metal cations. This equally makes them efficient scavengers of dilute metals while concentrating them from the aqueous environment (Schultze-Lam et al., 1996).

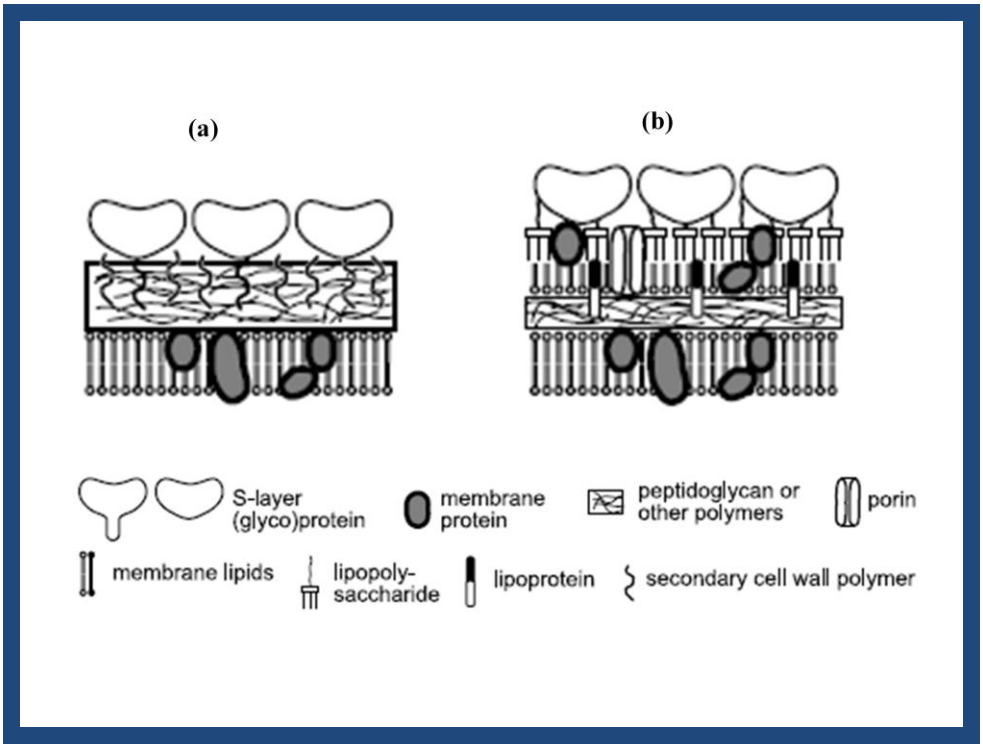

Figure 1. 1 Structure of the bacterial cell surface ((a) and (b)). Cell envelop of (a) is primarily composed of peptidoglycan whereas (b) is composed of a thin layer of peptidoglycan and an outermembrane. Adapted from Sleytr et al (2001).

1.2.1 Use of XPS (X-ray Photoelectron Spectroscopy) to study the bio-sorption of metal ions on bacterial surfaces

The determination of the interaction between metals and bacterial functionalized surfaces can be made possible by surface techniques e.g. XPS, which has the ability to determine elemental and functional group interaction on surfaces of materials. The possibility of determining functional groups associated with metal interactions with the bacterial surface could open up an entirely new area towards the synthesis or 'fine-tuning' of surface-localized nanocatalysts manufactured from biomass e.g. by manipulation of the cell surface groups *via* molecular techniques.

XPS is a technique used to investigate the chemistry at the surface of a sample and involves bombarding the sample with photons, electrons or ions in order to excite the emission of photons, electrons or ions (Kai, 2000). It is an easy method for the

determination of chemical composition, presence of impurities and the nature of chemical bonds (Estrade-Szwarckopf, 2004). It is also a quantitative technique due to the fact that the number of electrons recorded for a given transition is proportional to the number of atoms at the surface (Fairley, 2013), making it a very powerful technique with a very good precision. XPS probes only the outermost surface, ~5-10 nm of a sample (see **Figure 1.2**).

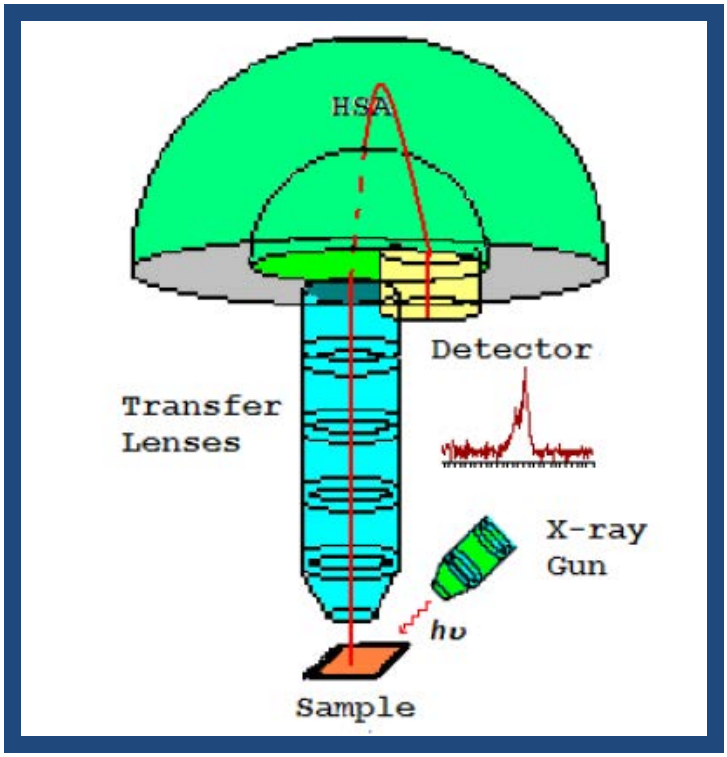

Figure 1. 2 A schematic diagram of an XPS instrument adapted from Fairley (2013)

The above technique has been widely used in the studies of conjugated polymers (Hasik et al., 2002), particularly to investigate changes in the polymer chain occurring upon doping, e.g. in the structure determination of chitosan-stabilized Pd and Pt bimetallics (Wu et al., 2012) and in the location of Pd atoms in a silica lattice (Zienkiewicz-Strzalka and Pikus, 2012).

However, the use of XPS in the study of the interaction between metal ions and bacterial surfaces is very sparse. The interaction of metal ion like Pd (II) and nitrogen

species has been well exemplified (Charbonnier et al., 2006) and amines have been well established previously to coordinate to palladium (II) and other metal ions in bacteria during biosorption (Du et al., 2012). These interactions have been analysed and confirmed with XPS (de Vargas et al., 2005) and infrared spectroscopy (Rotaru et al., 2012), while Niu and Volesky (1999), through Fourier transformed infrared (FTIR) analyses, showed that an N-containing group in the biomass might be involved in gold sorption.

However, XPS studies by Bunge et al., (2010) did not elucidate the interaction of Pd (II) to functional groups on bacterial cells, but only analysed for the presence of Pd (II) and Pd (0) reduced under formate added to the samples. The involvement of amine groups has prompted the use of amine-functionalized abiotic surfaces as supports for the synthesis of Pd nanoparticles (De Corte et al., 2013). Other functional groups on Gram-positive (Ahimou et al., 2007) and Gram-negative (Dufrêne and Rouxhet, 1996) bacterial surfaces have been analysed with XPS but available data on their interaction with metals (e.g. Pd or Pt) is very limited. Therefore, this means that a complete study on the involvement of groups like phosphoryl and sulfuryl is very important, as phosphate groups are believed to be involved in coordinating to divalent metals and the presence of sulfuryl group interaction with metals might mean an involvement of sulfur-containing proteins on bacterial surface (Azcarate et al., 2014). This could become relevant to the bio-fabrication or ‘fine-tuning ‘of the final nanocatalyst produced using bacterial biomass for improved catalysis. In this respect, sulfide is a potent catalyst poison but in some cases some partial poisoning can enhance catalytic specificity (Dunleavy, 2006).

1.2.2 Assimilatory and dissimilatory metal reduction

Assimilatory metal reduction involves the intracellular incorporation of metals into proteins such as metalloenzymes (Liermann et al., 2007), cofactors or magnetosomes (Lovely, 1991) unlike dissimilatory metal reduction whereby significant amounts of the metal tend to accumulate outside the cell during normal physiological conditions. The best understood and well studied mechanism of assimilatory metal reduction is that of iron (Fe) reduction. This is as a result of the relevance of iron in most microorganisms,

as it plays an exclusive role in the synthesis of haem and non-haem Fe-containing proteins.

Table 1. 1 Examples of metals commonly found in cellular enzymes

Metals	Enzymes containing metals
Mn	Phosphatases, dioxygenase, catalase
Fe	Phosphatases, nitrogenases, reductases, peroxidases, hydrogenases, oxidases
Co	Mutases, ribonucleotide reductase (as B_{12} cofactor)
Ni, W	Urease, hydrogenases
Cu	Laccase, oxidases, hydroxylases
Zn	Phosphatases, peptidases, polymerases carbonic anhydrase
Mo	Nitrogenases, oxidases, reductases

Adapted from Liermann et al., (2007) with slight modifications.

The assimilatory pathway of Fe reduction involves key enzymes called the assimilatory ferric reductases which are found in all living organisms with the exception of a small group of homofermentative lactic acid bacteria (Schröder et al., 2003). Most Fe reductases use NADH or NADPH as electron donor for ferric iron reduction. However, bacterial ferric reductases lack bound flavin and therefore require flavin as a diffusible cofactor in the form of FMN, FAD or riboflavin. Many organisms have evolved different mechanisms for chelating Fe^{3+} before reduction by a ferric reductase prior to or after transport into the cell. These microbes produce chelates or low molecular weight molecules called siderophores to chelate the Fe^{3+} making reduction and cellular uptake possible (Schröder et al., 2003). Following reduction of Fe^{3+} to Fe^{2+}, the Fe^{2+} becomes available for the synthesis of haem and other non-haem containing proteins while excess iron is stored by iron storage proteins (Arosio and Levi, 2002).

The discovery of dissimilatory metal reduction, on the other hand, brought about a paradigm shift in the study of subsurface environments and microorganisms as well as the many potential technological applications. Dissimilatory metal reduction involves the generation of energy to fuel cell growth and development (Laguna et al., 2011). This has been observed in a diverse group of specialist bacteria and archeae where

dissimilatory metal reduction is used to conserve energy for growth under anaerobic conditions (Lovely and Philip 1988; Ahmann et al., 1994). Geological evidence identifies nitrate, Mn (IV), Fe (III), and sulphate as primary terminal electron acceptors in the decomposition of organic matter in anaerobic environments (Reeburgh, 1983). These terminal electron acceptors are of immense importance in subsurface environments.

The above led to the identification of many organisms capable of dissimilatory metal reduction based on preferred terminal electron acceptors. These organisms include the dissimilatory Fe (III) reducers, dissimilatory Mn (IV) reducers, dissimilatory sulphate reducers, dissimilatory nitrate reducers and methanogens. However, of these, the dissimilatory Fe (III) reducers and the dissimilatory sulphate reducers have received most attention in the study of dissimilatory metal reduction and its potential applications. Therefore, more focus will be given to these two groups in this review.

1.2.3 Dissimilatory Fe (III) reduction

A diverse group of bacteria and archeae uses iron respiration as a means of generating energy to support growth. This form of respiration is regarded as dissimilatory iron reduction, as Fe (III) is the terminal electron acceptor. Both Fe (III) reduction and Mn (IV) reduction have been well documented as they play very important roles in the cycling of organic matter in the biosphere (Hines et al., 1991) with Fe (III) as one of the dominant terminal electron acceptors in subsurface environments. It has been suggested that the dissimilatory reduction of Fe (III) might have been the earliest form of respiration on earth and also very important as the resulting mineral 'fingerprint' may provide information on life in other planets (Vargas et al., 1998). However, most of the respiratory pathways were not well understood until recently (Schröder et al., 2003). The mechanism of 'export' of electrons onto extracellular bulk minerals is becoming clear but is still controversial.

A phylogenetically diverse group of bacteria has been identified with the ability to grow by oxidizing hydrogen, sulfur, fermentable organic substances, aromatic compounds, fatty acids while simultaneously reducing Fe (III) (Laguna et al., 2011). The first group

of organisms discovered with the ability to utilize Fe (III) under anaerobic conditions includes *Shewanella oneidensis* (formerly *Alteromonas putrefaciens*) and *Geobacter metallireducens* (formerly called strain GS-15) (Lloyd, 2003). Since then many dissimilatory Fe (III) reducers have been characterised including hyperthermophilic bacteria and archea.

The mechanism of Fe (III) respiration is still not well understood but three different strategies have been proposed as utilized by different organisms (Schröder et al., 2003). It has been reported that humic substances which contain quinone-like groups can act as electron shuttles for Fe^{3+} oxide. They can act as terminal electron acceptors in their oxidized states for a respiratory chain. The reduced humic substances can then be chemically reoxidized using solid forms of Fe^{3+} as electron sink. This form of respiratory chain was thought to be a primitive form of electron transport chain and that the respiratory chain that utilizes specific iron-reducing enzymes may have evolved through this primitive process. It has been found also that bacteria can reduce Fe^{3+} by secreting small diffusible redox compounds and therefore this does not require bacteria to have contact with the Fe^{3+} before reduction can occur. This has been demonstrated by embedding Fe^{3+} oxide in alginate beads without any contact with the bacteria and yet the Fe^{3+} oxide was reduced confirming that small diffusible compounds were involved (Newman and Kolter, 1997; Nevin and Lovely, 2002). Since then, flavins have been used as diffusible electron shuttles for the reduction of iron by *Shewanella oneidensis* strain MR-1 and *Geobacter fermentans*, and also the use of melanin (a humic acid precursor) by *Shewanella alga* strain BrY (Laguna et al., 2011). *G. fermentans* and *S.alga* strain BrY also secreted Fe^{3+} chelating compounds with the ability to significantly solubilise Fe^{3+} oxides. However, the ability of such siderophores produced by bacteria to act as electron shuttles and therefore serve as terminal electron acceptors for dissimilatory iron reduction is still a matter of debate, but in contrast their involvement in assimilatory iron reduction is widely known.

The anaerobic iron-reducing bacterium *Geobacter metallireducens* has demonstrated the ability of dissimilatory iron reduction by direct contact (Tremblay et al., 2012). This differs from the mechanism observed in *Shewanella* species which can undergo dissimilatory iron reduction without any contact with the Fe^{3+} oxide particles but by

releasing soluble quinones that can take electron from the cell surface to Fe^{3+} oxide (Coursolle and Gralnick, 2010). However, this is controversial. For the reduction of Fe^{3+} oxide, the bacterium using its pili (bacterial nanowire) or flagella must come in contact with Fe^{3+} oxide *via* chemotaxis (except where Fe^{3+} - citrate, which is a soluble electron acceptor, is provided) (Childers et al., 2002).

In *Shewanella* species proteins are involved in respiration of insoluble ferric ion. In *S. oneidensis* MR-1 it has been demonstrated that *c*-type cytochromes are key components in iron respiration by either serving in electron transfer or by acting as the possible terminal reductase (Myers and Myers, 1997). These cytochromes are found in the periplasm or are membrane-bound and expressed under anaerobic conditions irrespective of the final electron acceptor. Over 50% of the ferric iron reductases found in *S. oneidensis* MR-1 were located in the outer membrane (Myers and Myers, 1993), which is regarded as an unusual site for such an important respiratory enzyme more typical of the cytoplasmic membrane or periplasm of an organism. Even with the difficulty of isolating the ferric reductase from the outer membrane of *S.oneidensis* MR-1 (Schröder et al., 2003), biochemical analysis suggested (Myers and Myers, 1997) the presence of four *c*-type cytochrome-containing proteins that could be reduced with formate and reoxidized with Fe^{3+} , suggesting that one or more of these proteins could be acting as the ferric reductase. Also, the involvement of outer membrane *c*-type cytochromes has been reported in *Geobacter* species supporting their relevance in dissimilatory metal reduction (Leang et al., 2003).

1.2.4 Dissimilatory sulfate-reducing bacteria (SRB)

The physiology, diversity and classification of this group of bacteria have been earlier highlighted. The activities of the SRB were reported by the German scientist, F. Hoppe-Seyler in 1886, where he observed that when gypsum ($CaSO_4.2H_2O$) was added to anaerobic mud containing organic matter, cellulose was completely oxidized and "rotten egg" gas (H_2S) was produced (see Shen and Buick, 2004). At that time the process of sulfate reduction was not known but this process was later attributed to obligately anaerobic sulfate reducing bacteria, although some can survive temporary exposure to oxygen (Krekeler and Cypionka, 1995; van Niel et al., 1996; Mogensen et

al., 2005; Lobo et al., 2007), again becoming active under anaerobic conditions. Microbial sulfate reduction is a very important process in the sulphur biogeochemical cycle.

According to Postgate (1984), microbial sulphate reduction is an energy generating mechanism which involves the reduction of sulphate to sulphide coupled with the oxidation of organic matter or hydrogen (H_2). (As shown in equation 1: dissimilatory sulfate reduction) (Hao, 2003). This differs from the assimilatory reduction of sulfate which is carried out by a variety of organisms except animals, providing the cell with sulphur in the oxidation state of -2, which is necessary for the biosynthesis of amino acids and cofactors (Wirtz and Droux, 2005).

$$SO_4^{2-} + 2C + 2H_2O \xrightarrow{SRB} H_2S + 2HCO_3^- \qquad (1)$$

Equation 1 above explains that alkalinity is produced and there is a stoichiometric relationship between the milligrams (mg) of carbon required per mg of sulfate reduced. The reaction stoichiometry also depends on the electron donor.

Sulfate is the preferred terminal electron acceptor for the SRB. The importance of SRB in metal reduction has become of great technological importance. It has been reported that sulphate-reducing bacteria such as *Desulfovibrio desulfuricans* can equally couple the oxidation of molecular H_2 or simple organic acids to metal reduction in the absence of sulphate, although metal reduction is not coupled to energy generation (Lloyd, 2003). Examples of metals reduced under this condition includes Au(III), Cr(VI), Fe(III), Mo(VI), Pd(II), Pt(IV), Tc(VII) and U(VI). There were reports however, that some species of SRB (e.g. *Desulfotomaculum*) could grow with As(V), Cr(VI), Mn(IV) and U(VI) using other sulphur containing compounds as additional electron acceptors (Newman et al. 1997; Tebo and Obraztsova, 1998).

The mechanism of sulfate reduction and energy generation has been widely demonstrated in *Desulfovibrio* spp. This process, in which hydrogen cycling (see **Figure 1.4**) plays a key role, was thought to be *via* a mixture of oxidation of organic

electron donors, such as lactate to acetate *via* pyruvate and anaerobic respiration (the reduction of sulphate to sulphide via lactate oxidation) (Postgate, 1979).

A key enzyme of this anaerobic process is the dissimilatory sulfite reductase (dSir), which catalyzes the six-electron reduction of sulphite (see **Figure 1.3**) to hydrogen sulfide in the presence of a special magnetically coupled siroheme-[4Fe-4s] centre (Schiffer et al., 2008). The pathway proceeds by activating sulphate ($E^{0'}$ = -516 mV) to adenosine-5'-phosphosulfate ($E^{0'}$ = -60 mV) by ATP sulfurylase at the expense of ATP (**Figure 1.3**). This results in the hydrolysis of adenosine-5'-phosphosulfate and reduction to sulfite and AMP by adenosine-5'-phosphosulfate reductase (Thauer et al., 1977). The resulting sulfite is finally reduced to hydrogen sulfide by sulfite reductase (Sir) in a six-electron transfer process (Thauer et al., 1977). The involvement of the enzyme hydrogenase (**Figure 1.3**) in metal reduction is discussed later.

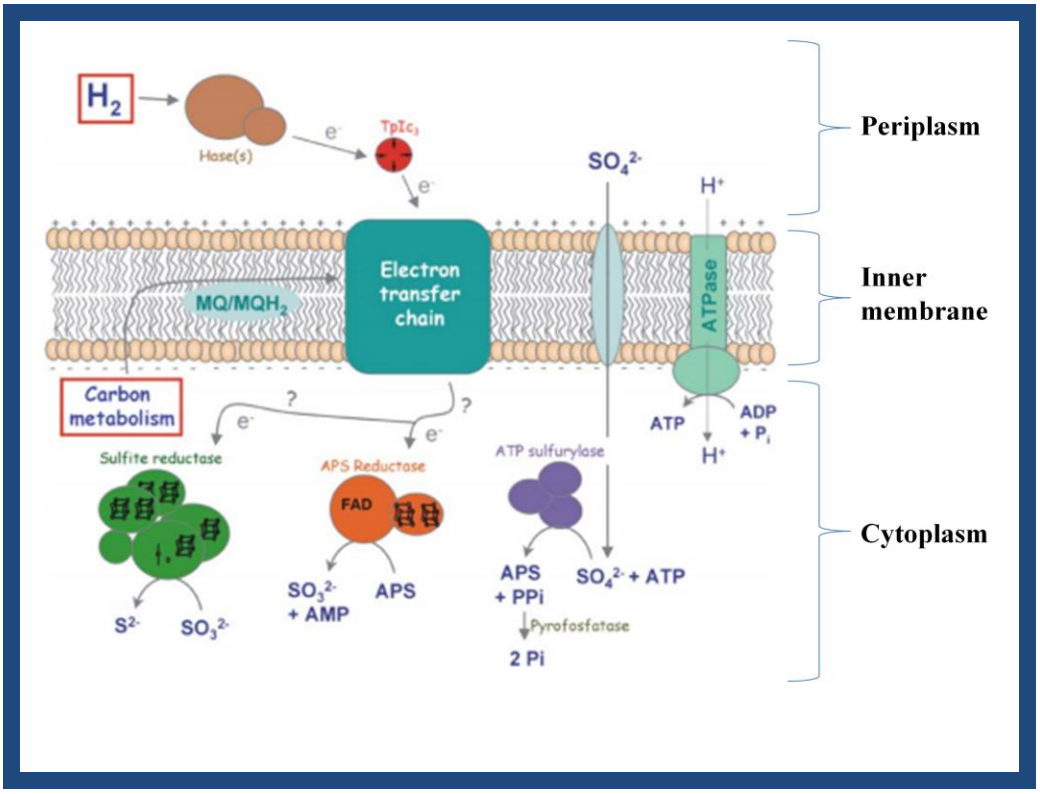

Figure 1. 3 Sulfate respiration in *Desulfovibrio* spp. adapted from Matias et al., (2005) with hydrogen or an organic compound as electron donor and sulphate as the terminal electron acceptor. TpI-c_3 (tetraheam Type I tetrahaem cytochrome), MQ/MQH_2 (Menaquinone/menahydroquinone), Hase(s) (Hydrogenase(s)).

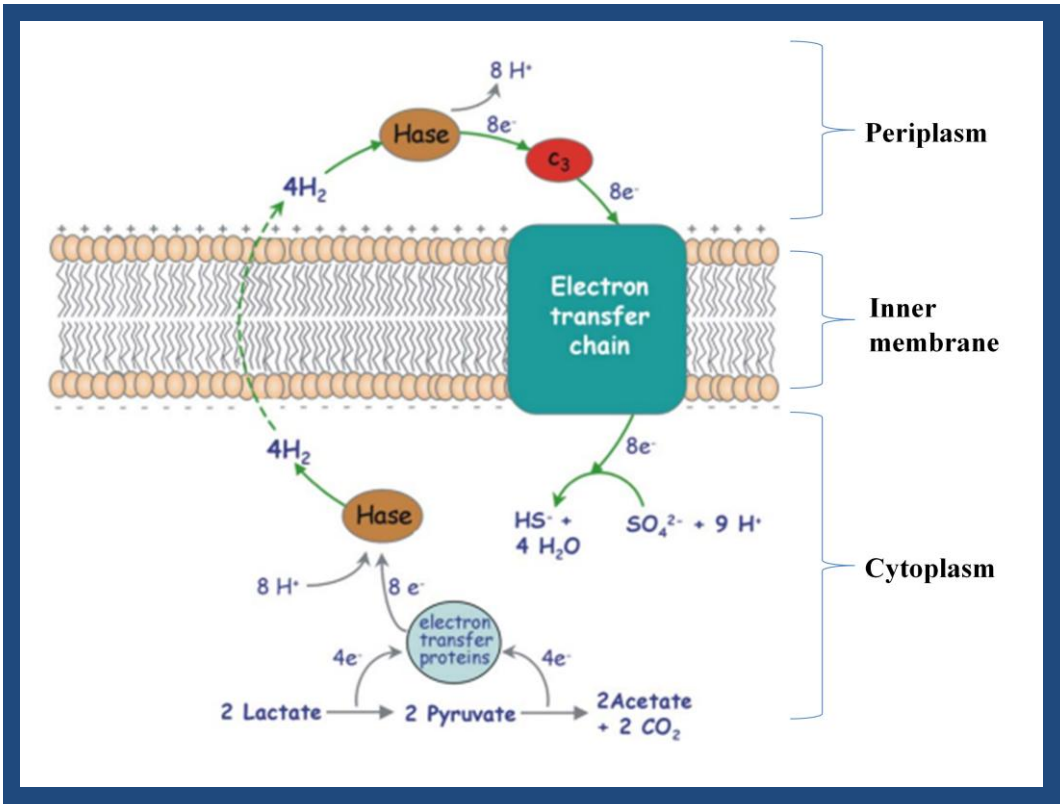

Figure 1. 4 Mechanism of hydrogen cycling as proposed by Odom and Peck (1981).

1.2.5 The involvement of hydrogenase(s) and cytochrome(s) in metal reduction

A hydrogenase, also called ferrodoxin: H^+ oxidoreductase, EC 1.18.3.1 (Pulvin and Bourdillon, 1986) is an enzyme responsible for the metabolism of molecular hydrogen by reversible oxidation of molecular hydrogen (Ogata et al., 2015). Hydrogen plays a key role in energy metabolism of the sulfate-reducing bacteria especially the *Desulfovibrio* spp. As a result of the importance of hydrogen to this group of organisms, two major metabolic mechanisms for hydrogen metabolism were proposed. The first model (hydrogen cycling) was described by Odom and Peck (1981). They proposed that the oxidation of lactate (a key intermediate in energy metabolism) leads to the production of molecular hydrogen by cytoplasmic hydrogenase, the H_2 then diffuses outwards across the cell membrane. Reoxidation of the hydrogen by periplasmic hydrogenase results in the generation of electrons that are shuttled across the membrane for the cytoplasmic reduction of sulfate (**Figure 1.4**). This leaves protons at the

periplasm to be translocated by ATP synthase (Matias et al., 2005). However, this model was criticised for lack of evidence of cytoplasmic hydrogenases in many *Desulfovibrio* species and that the mechanism might be too simple to explain the complex mechanisms involved in the energy metabolism of the genus *Desulfovibrio*. The involvement of several other possible pathways and cycling of intermediates such as carbon monoxide, hydrogen, ethanol and formate were also suggested (Voordouw, 2002). Genome sequencing of *Desulfovibrio vulgaris* Hildenborough reveals a fourth periplasmic hydrogenase (HyBA-2 isozyme) for hydrogen oxidation which was previously unknown. Also three additional c_3-type cytochromes responsible for accepting electron from periplasmic hydrogenases have been found. One of the cytochromes encodes formate dehydrogenase by accepting electrons from formate oxidation (Heidelberg et al., 2004). This has further provided new insights into hydrogen metabolism (cycling) in *Desulfovibrios*.

In the second model, hydrogen metabolism is said to control the redox levels of electron carriers such as ferredoxin or/and cytochromes which can then regulate the shuttling of electrons and transfer of protons that generate membrane bound proton motive force (Lupton et al., 1984). These two models have however given insights into the involvement of key enzymes (hydrogenases) and proteins (cytochromes) in the metabolism of hydrogen and energy generation by the sulfate-reducing bacteria, especially the genus *Desulfovibrio*.

Hydrogenases are localized in the cytoplasm, periplasm and some are membrane-bound, where they carry out different physiological functions. These hydrogenases are generally common in bacteria and it is normal to find more than one type of hydrogenase in a single species of bacteria. They are generally divided into two major groups with respect to the metals present in the active sites: The [Fe] only hydrogenases and the [Ni-Fe] hydrogenases which also includes the sub-group [NiSeFe] hydrogenases, where a cysteinyl ligand is replaced by a selenocysteine (Carepo et al., 2002). The [Ni-Fe] and [Fe] hydrogenases are the major forms of hydrogenases found and both contain a binuclear metal active site. [Ni-Fe] hydrogenases, along with ureases are one of the few examples of enzymes that require Ni (II) as a functional component, with redox cycling of Ni between the +1, +2 and +3 states during activity as shown by

electron paramagnetic resonance (EPR) (Lill and Siegbahn, 2009). To achieve the formation of the active enzyme requires recognition, uptake and trafficking of Ni (II) (Higgins et al., 2012) and for actual assembly of the enzyme it is thought that Ni (II) is removed from a periplasmic binding protein like NikA and HypA-type nickel metallochaperone (Higgins et al., 2012) for incorporation into the enzyme, but the specific mechanism for the final transfer of Ni atoms into the enzyme from a cytoplasmic carrier are not known.

The synergy between hydrogenases and cytochromes in the absence of sulfate to reduce metals in bacteria, especially *Desulfovibrio,* is crucial. The periplasmic hydrogenases are very important in this process as they are responsible for the oxidation of molecular hydrogen at the periplasm. The tetrahaem type I tetrahaem cytochrome c_3 (TpI-c_3), is a small 13.5-15 kDa soluble protein; this being the most abundant periplasmic protein in *Desulfovibrio* spp. (Legall et al., 1994) and the best characterised electron transport protein, has been reported to be the physiological electron acceptor for the periplasmic-facing hydrogenase (Legall et al., 1994). This interaction results in the transfer of electrons to other multihaem cytochromes associated with membrane-bound redox complexes, such as the respiratory membrane complex, quinone-reductase complex (Qrc) found in SRB (Venceslau et al., 2010).

Reduction of metals occurs under anaerobic conditions, the perfect condition for hydrogenase activity, as oxygen species have been reported to inactivate the enzyme (Marques et al., 2010), leading to irreversible damage in the [Fe-Fe] hydrogenases; inactivation is reversible in the [Ni-Fe] hydrogenases.

Hydrogenase and cytochrome c_3 have become important in understanding the process of metal reduction in this group of bacteria. The sensitivity of the *Desulfovibrio* "Pd (II) reductase" to Cu^{2+} (Lloyd et al., 1998) suggested a possible role of hydrogenase in metal reduction. Mikheenko et al. (2008) later confirmed the involvement of periplasmic hydrogenases by using hydrogenase deficient mutants of *D. fructosovorans* in the reduction of palladium (II) in which Pd (0) relocated to the site of the remaining hydrogenase. Other evidences *via* mutant analyses had previously suggested the role of cytochrome c_3 as part of the *in vivo* electron transfer pathway to uranium (VI) from hydrogen through hydrogenase (Payne et al., 2002) and recently a deletion mutant

devoid of an outer membrane cytochrome was able to reduce metal and humic acid when a suppressor mutation was used as a rescue (Bucking et al., 2012). Hydrogenase was also reported to be involved in the reduction of palladium (II) in mutants of *Escherichia coli* (Deplanche et al., 2010) which had no periplasmically located hydrogenase, although the membrane-bound [Ni-Fe] hydrogenases (Hyd-1 and Hyd-2) are periplasmic-facing.

1.3 Effects of acid stress in bacteria

Some bacteria can survive in low pH (<3) and diverse environments (Johnson, 1998). Acidification of environments can be brought about by the microbial dissimilatory oxidation of elemental sulfur and ferrous iron (Johnson, 1998). Oxidation of sulfur by autotrophic and heterotrophic microorganisms produces sulfuric acid. This process results in acid mine drainage (AMD) with pH generally from 2-4 (Bechard et al., 1994). The activities of SRB have been shown to raise the pH of AMD resulting in remediation with the ability to remain viable at pH 3.25-4.5 after 21 days (Elliott et al., 1998). Changes in environmental pH can be caused by oxygen supply, initial pH, buffering, ionic strength and temperature and microbial activities like fermentation of available sugar (forming organic acid) and ammonia production (*via* dissimilatory nitrate reduction), decarboxylation reactions (Yang et al., 2015) and other pH regulatory mechanisms in bacteria (Stincone et al., 2011).

The ability of bacteria to survive in acidic environments such as in acid mine drainage (pH 2-4) and during transit through the highly acidic gastric juice (pH ~1.5) of the stomach has prompted a renewed interest as to how these bacteria especially pathogenic, probiotic and lactic acid bacteria, regulate acid stress (Hecker , 2007, Senouci-Rezkallah et al., 2015). For example, diarrhogenic *E. coli* can pass through the stomach with pH as low as 1 to cause disease in humans (Stincone et al., 2011) while acido-tolerant *Bacillus* e.g. *Bacillus cereus* (Senouci-Rezkallah et al., 2015) and *Bacillus licheniformis* (Yang et al., 2015) are important food-poisoning organisms. This ability to survive at pH shock is a key factor for most entero pathogenic bacteria. However, growth of *Staphylococcus aureus* in excess of glucose (35mM) was suppressed due to carbon overflow (Thomas et al., 2014) which results in excess

accumulation of the product (acetate) in the medium (intracellular acidification and respiratory inhibition) resulting in programmed cell death (PCD). Intracellular acidification results in lost of purines and pyrimidines from DNA at a greater rate than at neutral or alkaline pH due to protonation of base followed by cleavage of glycosyl bonds (Lindahl and Nyberg, 1972).

As a result of acid stress, bacteria have developed various regulatory or resistance mechanisms for acid adaptation and prevention of intracellular acidification. This includes: the use of proton pumps (F_1F_0-ATPase), glutamate decaboxylase, electrogenic transport, two-component signal transduction systems (Johnson et al., 2014), production of alkali and urease (urease and arginine deiminase pathway, ADI), protection or repair of macromecules, cell membrane changes (e.g. fatty acid profile), and the use of regulators (sigma factors) (Cotter and Hill, 2003). Considering the use of proton pumps (F_1F_0-ATPase), ATP is produced in respiring cells which is coupled to transmembrane proton motive force (PMF) while PMF is generated by ATP produced during fermentative substrate level phosphorylation. Therefore, under acid stress in bacteria, the PMF performs an efflux function by extruding protons from the cell cytoplasm in order to maintain intracellular pH (due to a drop in intracellular pH). The F_1F_0-ATPase also helps to induce the acid tolerance response (ATR); such tolerance to lethal pH increases as a result of a prior exposure to a sub-lethal pH (Cotter et al., 2000). Details of the involvement of other mechanisms can be found in an extensive review by Cotter and Hill, (2003) and work by Johnson et al., (2014).

These mechanisms can provide insight into understanding the effects of low pH (2-3) used in the treatment of bacterial cells during biosorption and reduction of precious metal solutions for the synthesis of catalytically active material at acidic pH which is the main goal of this study.

1.4 Platinum-Group Metals (PGMs)

The platinum-group metals (PGMs); ruthenium (Ru), rhodium (Rh), palladium (Pd), osmium (Os), iridium (Ir), platinum (Pt), together with gold (Au) and silver (Ag) are generally referred to as "precious" metals as a result of their rarity, increasing value, and demand to meet today's technological needs. Platinum was the first PGM to be discovered in the 16th century in the Choco District of Columbia (see Xiao and Laplante, 2004). Palladium, osmium, iridium, and rhodium were all discovered in 1803, while ruthenium was the last to be discovered. Apart from osmium which has a bluish tinge, all other PGMs are silvery white lustrous metals and are ductile and malleable, and hence can easily be drawn into wires, rolled into sheets or formed by spinning and stamping. The PGMs are classified into two groups, based on their comparison with the specific gravity of gold: ruthenium, rhodium and palladium are classified as elements lighter than gold (their specific gravity is around 12.0-12.4). The others; osmium, iridium and platinum are heavier than gold, with a specific gravity in the range of 21-22.5 (Xiao and Laplante, 2004), and with a higher atomic number of 76, 77 and 78 respectively.

1.4.1. Major deposits and global producers

PGMs are obtained from major mines across the world; e.g. the Busveld igneous complex (South Africa); There are about 20 active mines in the region that mine about 250 tonnes of PGMs per year (Jollie, 2010), making South Africa the largest global producer (see **Figure 1.5, 1.6, 1.7**). Although several of the mines are open pits, there are mostly underground mines, producing significant amounts of nickel, copper, cobalt, silver and gold as by-products. The Ni-Cu-PGM sulphide deposit of Noril'sk in the Russian Arctic and placer deposits in the Ural Mountains (Russia) is the second largest producer of palladium (~ 45%) and platinum (~15%) of the world's total production (Crundwell et al., 2011). There are six underground and one open pit mines (Kendall, 2004), producing about 120 tonnes of PGMs per year along with several quantities of nickel, copper, cobalt, silver and gold.

Other deposits include; Sudbury (Ontario, Canada), the Hartley mine (Zimbabwe), the Still-water complex (Montana, USA), Northern Territory (Australia) and the Zechstein copper deposit in Poland. South Africa is the leading producer with 85% of the world production of PGM and 82% of the world's economic resources. As a result of uncertainties in the major supplying zones and monopoly by these countries, alternative efforts are being channelled towards search for new deposits. Also, there is an intensified effort in the recycling and recovery of PGMs from scrap metals to help offset the increase in demand (Jimenez de Aberasturi et al., 2011). Fig 1.5-1.7 identify that most "insecure" metal in socioeconomic term is Pd, due to artificially-controlled availability and hence price (Fig 1.6).

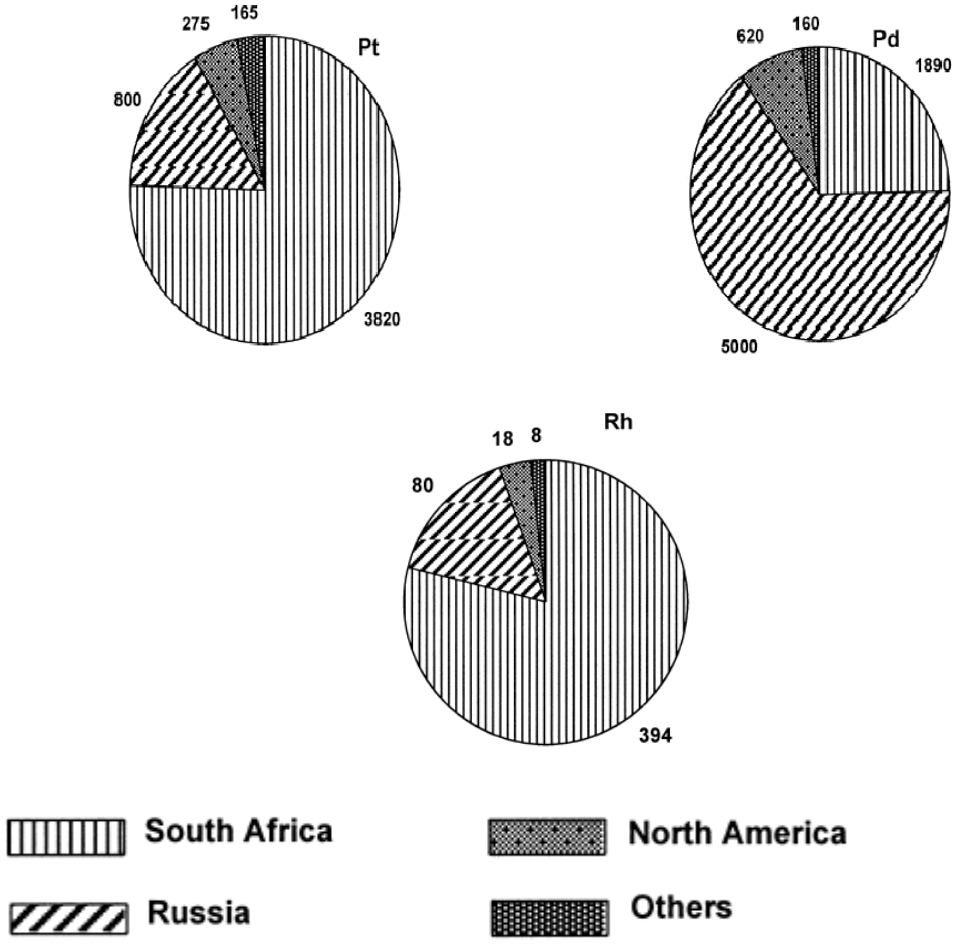

Figure 1. 5 Major producers of Pt, Pd and Rh (in 10^3 oz) adapted from Rao and Reddi (2000)

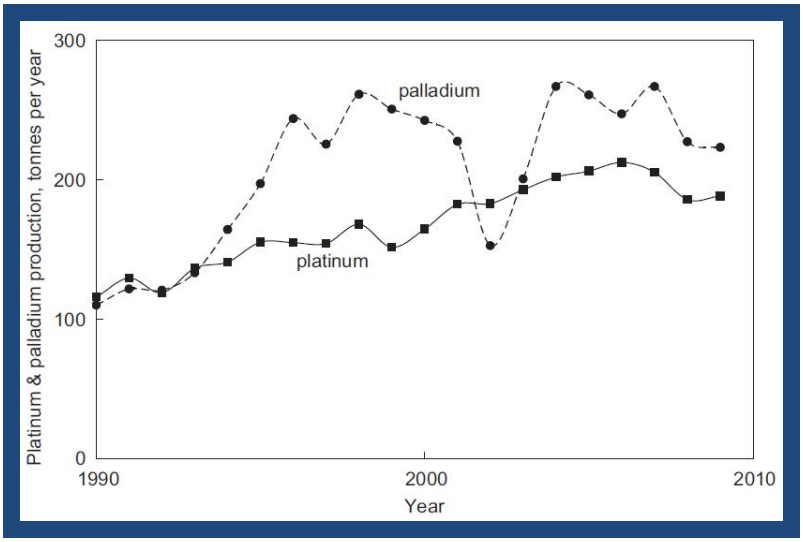

Figure 1. 6 Annual primary production of palladium and platinum (Jollie, 2010). Growth has been steady except for transient swings in palladium production from about 1995 onward. This attributed to rapid growth in demand for palladium catalyst and subsequent releases of palladium from the Russian stockpile; since Russia is the primary producer (Figure 1.5) the market price of Pd is to a large extent artificially controlled.

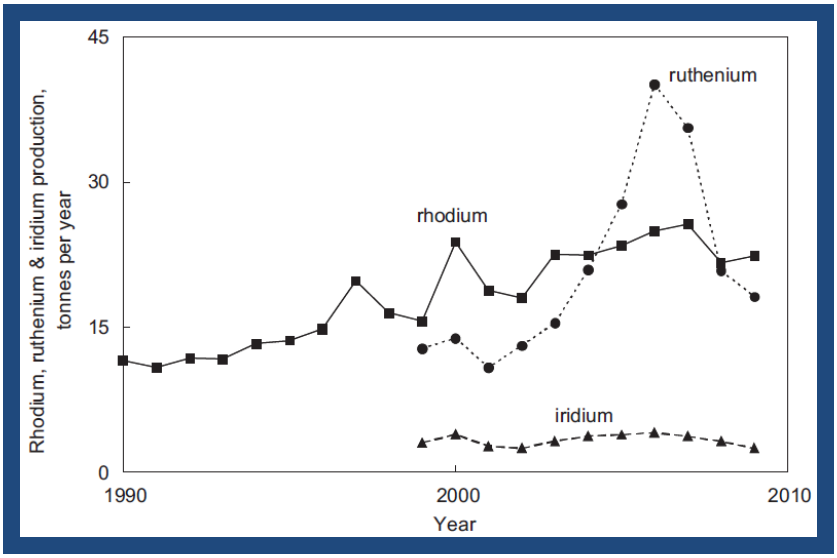

Figure 1. 7 Annual primary production of rhodium, ruthenium and iridium (Jollie, 2010). Ruthenium and iridium production comfortably meets demand (Jollie, 2009).

1.4.2 Properties

PGMs possess unique chemical and physical properties underlie their various uses. Pd and Pt dissolve in aqua regia (AR), whereas Ru, Rh, Ir and Os are relatively inert. They can all be dissolved in strong, alkaline oxidizing agents. PGMs dissolve in molten bases e.g. sodium, phosphorus, silicon, antimony and lead (Rao and Reddi, 2000). PGMs generally have the following properties:

(a) Ability to catalyse chemical reactions
(b) Ability to resist corrosion and oxidation
(c) Visual appeal
(d) The ease with which they can be worked (ductility and malleability)
(e) High electrical conductivities, densities and melting points (Crundwell et al 2011; Xiao and Laplante, 2004).

1.4.3 Crustal abundance levels and distribution

The abundance and distribution of PGMs in the earth's crust is very low: 1-10 (Pt), 0.1-3 (Pd), < 0.5 (Rh), < 1 (Ru), 0.3-5 (Ir), and < 0.1 (Os) ng g^{-1}. The concentrations of platinum are 21.9 ng g^{-1} in ocean sediments; 0.03-0.3ng dm^{-3} in seawater; 0.08-0.32 ng g^{-1} in marine algae; 56 ng g^{-1} in limber pines; 100-830 ng g^{-1}in plants in ultrabasic soils; <0.8-6.9 ng l^{-1} (Kanický et al., 1999) in blood and 0.5-14.3 ng l^{-1} in urine (Barefoot, 1999) with the exception of patients receiving cisplatin. Platinum is found in the range of < 50 fg m^{-3} in ambient air near road. With the introduction of the implementation of the use of catalysts in automobiles, there has been an increase in the level of platinum along the highway to 1-13 pg m^{-3} and up to 33 pg m^{-3} in routes with very dense traffics (Schierl and Fruhmann, 1996). There has also been a parallel increase of Pd of 0.3 μg g^{-1} in dust particles accumulated on plants on busy motorways (Barefoot, 1999). In water, the Pd concentration was estimated at 0.4-0.6 ng l^{-1} (Kanický et al., 1999). The key features is that due to the low concentration and high dispersion of PGMs, once discharged into the environment the metals are lost to mankind forever and hence their use from finite resources is not sustainable.

1.4.4 Occurrence

PGMs are usually sulfur–loving and as a result are called chalcophiles, often found in sulphide minerals e.g. Ru, Pd and Pt have some important sulphide minerals. PGMs are also called siderophiles (iron-loving). Ru and Rh are generally found in chromites. However, most PGMs are associated with tellurides, selenides, arsenides and antimonides.

PGMs in the earth's crust usually occur in native form and in association with one or more of the other PGMs along with gold, iron, copper and chromium (Rao and Reddi, 2000). Their natural alloys have variable degree of composition and often form more or less continuous series in which no sharp boundaries exist between the various minerals. A very good example is the alloy of osmium and iridium known as osmiridium (syserkskite) or iridosmium (neyanskite).

PGMs occur in basic or ultrabasic igneous rocks such as peridotites, pyroxenites and dunites. They are also found in sedimentary rocks in association with quartz, copper, nickel, silver etc. but found associated with chromites, magnetites, ilmenite, etc in alluvial deposits. Among these PGMs, Pd and Pt are present at higher concentrations in the platinum-group ores than the other platinum group elements (Crundwell et al., 2011).

1.4.5 Extraction and refining

PGMs generally occur either as sulfides or in association with sulfides of copper and nickel and the mined ore contains between 3g/tonne and 10g/tonne (0.0003-0.001%) of PGMs (Norilsk Nickel, 2008). Froth flotation of the sulfide component results in a concentrate containing between 35g/tonne and 150g/tonne PGMs, a 20 times upgrade from the ore. The general extraction and refining process of PGMs involves the following steps:

(a) Mining of ore rich in PGMs while leaving behind rocks with less or without PGMs.

(b) Isolation of the PGMs in the ore into a flotation concentrate consisting of nickel-copper-iron sulphide that is rich in PGMs.

(c) Smelting and conversion of the flotation concentrate to a nickel-copper sulphide matte that is richer than the concentrate in PGMs.

(d) Separation of the PGMs in the converter matte from the base metals, either by magnetic concentration or leaching, to produce a PGM-rich concentrate with about 60% by mass of platinum-group elements.

(e) Refining of the PGM-rich concentrate to individual PGMs with purities in excess of 99.9%.

However, the two major producing countries (South Africa and Russia) use different approach in the extraction of PGMs from their crude states.

The South African Anglo American Platinum's refinery in Rustenburg is the only major producer that uses the slow-cooling process prior to magnetic separation (**Figure 1.8**). This process allows converter matte to cool over several days leading to the development of large crystals of metal alloys, heazlewoodite, Ni_3S_2, and chalcocite, Cu_2S to develop. The converter matte is deficient in sulphur of which 10% is in the form of alloys which are magnetic. The PGMs concentrate in the alloy phase during the slow-cooling process, resulting in their separation from the base metal sulphides by magnetic separation. The slow-cooling process has an advantage of the PGM production to be less dependent on the production of the base metals. This means that the base metals which form the major components of the non-magnetic fraction could be stockpiled or refined elsewhere, which could save time and boost the extraction and refining of PGMs (Crundwell et al., 2011).

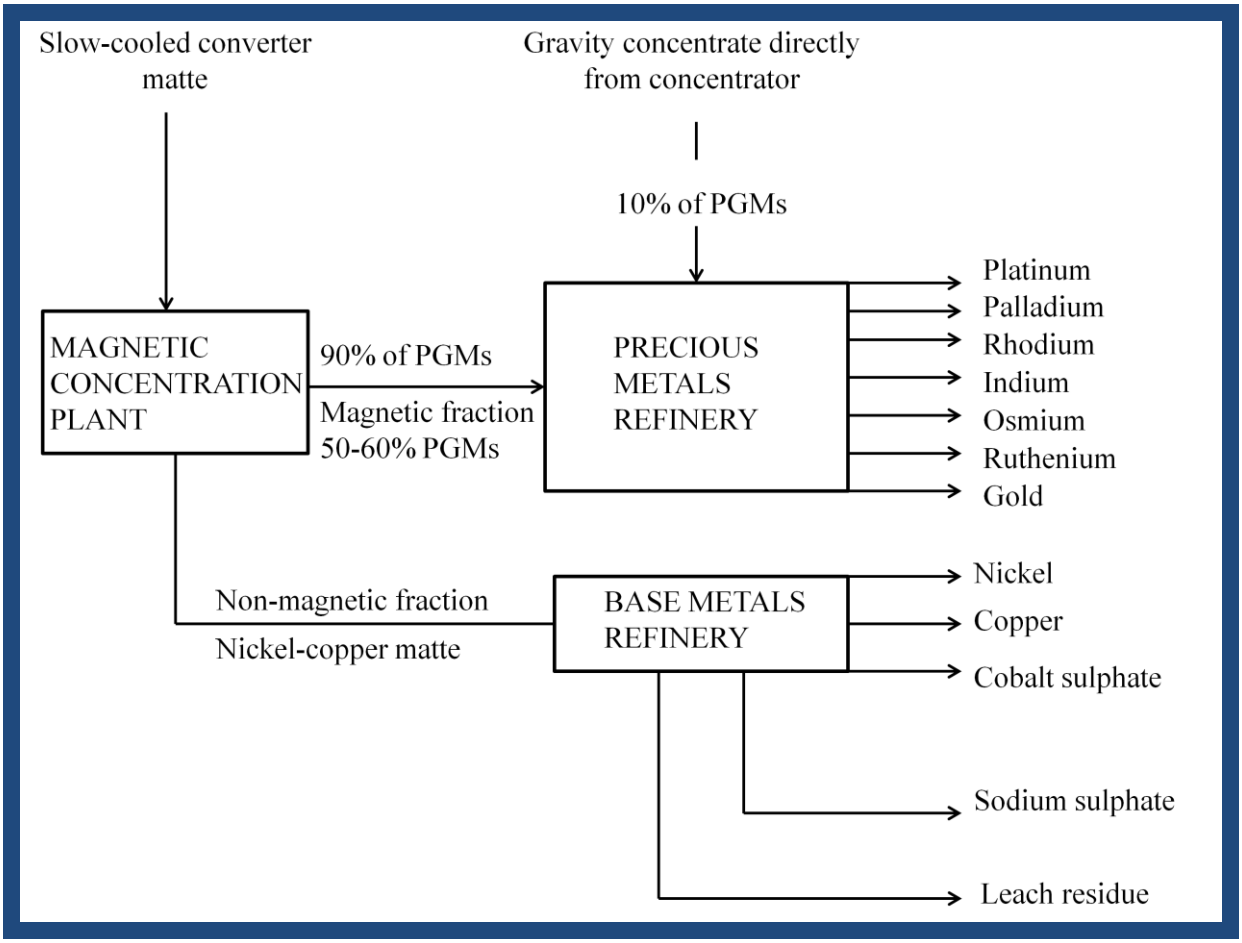

Figure 1. 8 The magnetic concentration process used by the South African Anglo American Platinum refinery for the separation of PGMs from base metals showing the slow-cooling process. About 10% PGM feed to the precious metal refinery comes directly from the concentrator. Adapted from Crundwell et al.(2011).

In the Russian production, the ore is first passed through a centrifugal density separator before proceeding to froth flotation, which improves the recovery of PGMs into the concentrate and also bypasses the nickel and copper production steps directly to refining. The ultimate objective of this process is to reduce the amounts of the PGMs held up in the process and to improve the overall economics of the process.

Refining is done in the region or in distant refineries whereas concentration and smelting/conversion are carried out in or near the mining regions. Differences exist in the percentage composition of base metals and concentration of PGMs between the ores

of the two major producing countries. The Russian ores from Norilsk-Talnakh region contains up to 50 times more nickel, copper and cobalt than the South African ores. The former also contains about 7% of each of these base metals, while the South African ores contain only 0.15% of these metals. The Russian ores (10g/tonne) are also more concentrated in PGMs than the South African ores (6g/tonne) *in situ*. Palladium is more concentrated in the Russian ores, while platinum, which usually has a higher price, is more concentrated in the South African ores (c.f. Fig 1.5).

The operating cost for the extraction and refining of PGMs is very high. For instance, the annual operating cost to the South African platinum mining companies for the production of PGMs is around US$ 20 million/tonnes of refined platinum metals (Impala Platinum, 2009), which is divided between plant areas. Other methods such as direct hydrometallurgical processing of flotation concentrates have been impossible (Liu, 2001) due to the complicated solution components and low recoveries. Cyanidation, such as the use of sodium cyanide to extract sulphide flotation concentrates from PGMs has been economically unsuccessful. This is because it was previously reported that at room temperature and atmospheric pressure, sodium cyanide cannot react slowly with PGMs like its reaction of gold (Feather, 1978; Dawson, 1984).

On the other hand, the smelting stages during extraction have been reported (Chen and Huang, 2006) to have serious environmental impacts and the lengthy overall flowsheet leads to unavoidable losses of PGMs. When the mattes are leached with acid to separate the base metals, the content of the PGMs in the residue never goes beyond 50%, making it difficult for PGM refining. To overcome some of these challenges, a new all hydrometallurgical two-stage process (pressure cyanidation) for the extraction of PGMs from sulphide flotation concentrates was proposed by Chen et al (2005). This method was used by Chen and Huang (2006) to achieve up to 90-94% and 99% extraction of Pt and Pd respectively. Here, a flotation concentrate containing about 80g/t Pt and Pd was pre-treated using pressure acid leaching, which was followed by two stages of high-temperature pressure cyanide leaching at 160^0C. Zinc cementation was then used to obtain a final precipitate containing 70-90% of the precious metals from the cyanide leach solution.

Further to the very capital intensive processes of extraction, and the increasing demand for precious metals especially in the automobile industries as emission-control catalysts, alternative approaches are needed for the extraction, refining and recovery of PGM (Nejad and Kazemeini, 2012; Yin et al., 2013). As a result, there is now a renewed interest in the development of new sensitive and reliable techniques for the detection of PGMs which would subsequently lead to their extraction and refining. In addition, the PGMs provide important information on metal geochemistry. For instance, the determination of iridium at a very low amount provides an account of some anomalies in iridium distribution in sedimentary rock samples, due to catastrophic events (Rao and Reddi, 2000).

1.4.6 Uses of PGMs

As a result of the unique chemical and physical properties of PGMs, they have become increasingly very important in environmentally-related technologies, chemical industries such as petroleum refining, fertilizers and plastics, automobile industries, hydrogen fuel cell technology, medical uses, jewellery or investment and they also form parts of electronic components (Mudd, 2012). In order to meet current technological and environmental challenges, there is a need to expand the uses of PGMs. However, the demand for PGMs is expected to remain sustained in the future (i.e. supply from reserves would be increased) as a result of their importance. However, despite the early claim by economic geologists that there are abundant PGM resources for many decades (Cawthorn, 1999), there is still fear in the long-term ability to meet future demands for PGMs (Gordon et al., 2006; Yang 2009). The consumption of palladium and platinum has been relatively similar to each other over the years, whereas, the use of rhodium, ruthenium and iridium has been very low. Osmium, on the other hand, is rarely used (Shott, 2013). It used to be very important in the production of incandescent light bulbs, but that has long been replaced by tungsten but osmium is currently used primarily in pen nibs and armor-piercing weapon shells.

One of the major uses of PGMs is in catalysis; substitution by other metals has been very difficult in some major industrial reactions. The automobile industry is the largest consumer of PGMs, where they are used in the catalytic converters of cars and trucks

for the controlled emission of exhaust gases. Motor vehicles release their fumes in addition to CO_2 and H_2O, as a result of the consumption of hydrocarbons as fuel. This leads to the release of other compounds such as carbon monoxide, nitrogen oxides and unburnt hydrocarbons, which combine to form photochemical smog in ultra-violet light (Twigg, 2011).

As a result of the environmental concerns regarding these harmful and toxic wastes and the increasing use of diesel engines, the USA proposed a legislation to control their emission (Twigg, 2011). Engine modification could not solve these problems and this led to the introduction of catalytic converters using PGMs (palladium, platinum and rhodium) to control the emission of these particulate pollutants (Acre , 1987). The exhaust gases are passed over the catalytic converter (**Figure 1.9**) with a catalyst which contains Pt, Pd and Rh in an example ratio 67:26:7 (Xiao and Laplante, 2004), which makes up about 30% Pt, 50% Pd and 85% Rh of metals available (Crundwell, 2011), converting CO and hydrocarbons to CO_2 and water by oxidation and reduces nitrogen oxides to nitrogen. The actual proportions of PGMs may vary according to market price at the time of manufacture.

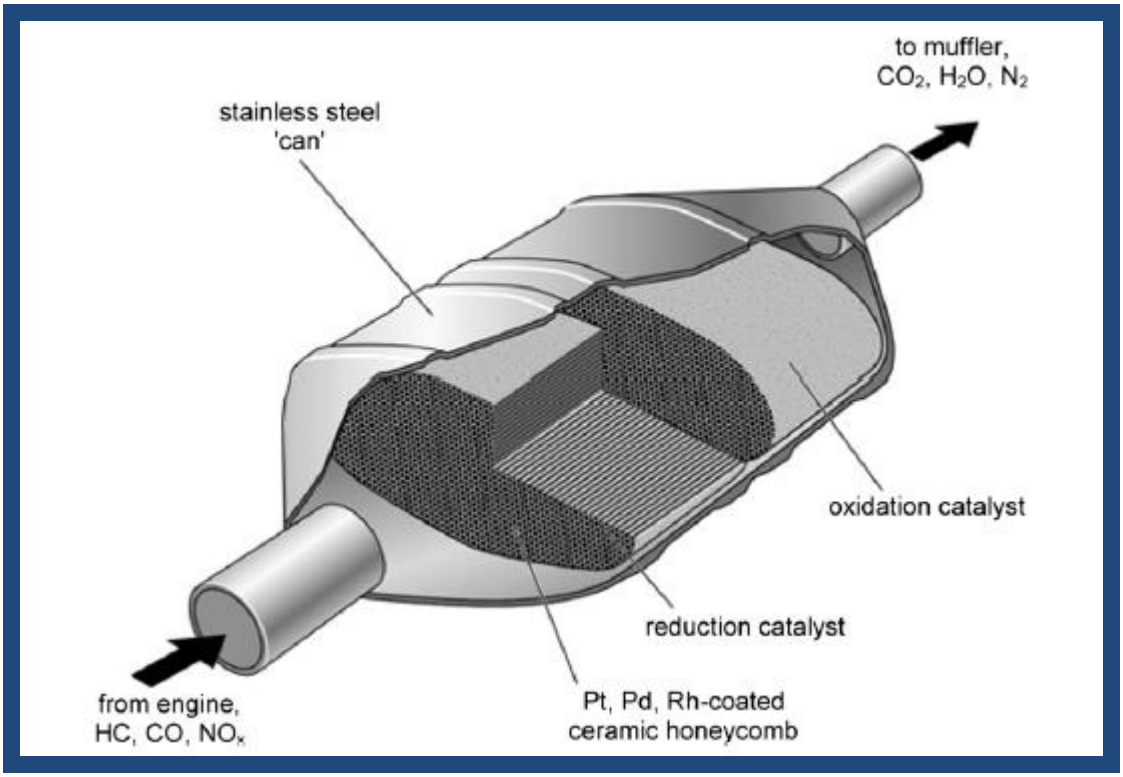

Figure 1. 9 A catalytic converter adapted from Crundwell, (2011). It catalyzes the oxidation of carbon (II) oxide and hydrocarbons to carbon (IV) oxide and water and the reduction of nitrogen oxides to nitrogen. It operates at ~200^{o}C during start ups and 800^{o}C during cruising. Typically oval in shape, ~0.35 m long and ~0.25 m across the oval (sometimes round). The total content of PGMs in a typical car catalyst is always lower than 0.1% (Jimenez de Aberasturi et al., 2011).

As a 'clean' alternative to hydrocarbon-based fuels the advent of hydrogen fuel cell technology has potential as a clean and efficient alternative power source for light-duty vehicle applications. Currently, a 50-kW fuel cell vehicle (FCV) contains about 46g/loading of platinum and this costs about $2200 (Sun et al., 2011). The deployment of more FCVs has been proposed (Sun et al., 2011) to lead to a decline in platinum loading and a subsequent reduction in price. This however, has been viewed differently (Mock and Schmid, 2009) as the wide substitution of FCVs for internal-combustion engine vehicles (ICEVs) might increase platinum demand and prices. However, in many countries the use of catalytic converters is mandatory for the controlled-emission of exhaust gases, and hence a large proportion of the catalytic converters is shed onto the

road and lost to the environment, out of man's use. Hence, the use of traditional vehicles is clearly impacting upon tomorrow's fuel cell technologies and the switch needs to happen as soon as possible. However, the short lifetime of fuel cell catalyst due to poisoning continues to be a major limitation. Such catalyst poison arises from the use of petrochemically-derived hydrogen that must be filtered prior to use; hence the supply of pure hydrogen in sufficient quality impacts upon FC usage. Hydrogen availability in turn, is limited by the lack of suitable methods to store and transport hydrogen from its point of generation (e.g. by solar-powered electrolysis of water) to the point of usage.

The rapid rise in the price of platinum has become another major challenge to the commercialization of FCVs, and it has been shown historically that platinum prices have been sensitive to changes in demand. Sun et al., (2011) proposed that if platinum loading per FCV does not meet its goal of 6g/FCV, and remains at 15g/FCV beyond 2025, this could lead to an increase in demand of virgin platinum to nearly 600 metric tonnes by 2050, which is three times its current supply. On the other hand, if platinum loading meets its goal but the recycling rate of platinum remains at 50%, then the demand for virgin platinum will again continue to rise beyond 2050. Even when some of these technical goals are met, it has been proposed that the future mid-size requirement of platinum in FCVs will be around 4-8 g, which is twice the 2-4 g of what is currently in use by catalytic converters by internal combustion engine vehicles (Sun et al., 2011). There is a strong focus towards part-substitution of the Pt by the cheaper Pd in FCs (Antolini, 2009) but the longer term durability of such alloys also requires elaboration.

Platinum has alternative major applications. In 1965, the synthesis of cisplatin became a breakthrough in cancer chemotherapy and many cisplatin analogues have been biologically evaluated (see Cutillas et al., 2013).Today, three platinum-based anticancer drugs (cisplatin, carboplatin and oxaliplatin) have been approved and currently in use worldwide, in more than 50% of the treatment regimes for cancer patients (**Figure 1.10**). Notwithstanding the huge global market for platinum-based drugs (billions of Euros) factors such as nephrotoxicity and sensitivity to resistance mechanism (Fuertes et al., 2003) have remained major challenges to effective use of the drugs. Agaist this

backdrop, other research groups (Rjiba-Touati et al., 2013) and many pharmaceutical companies have initiated research into alternative transition-metal drug candidates.

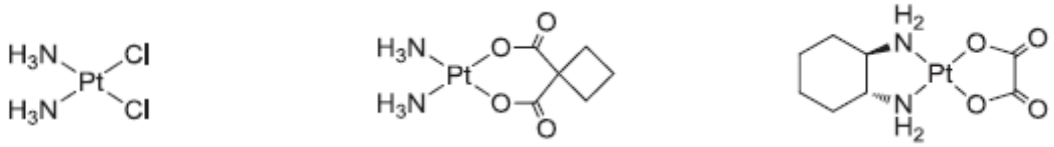

Cisplatin Carboplatin Oxaliplatin

Figure 1. 10 Anti-cancer drugs currently used globally (adapted from Cutillas et al., 2013)

Organometallic compounds with intermediate properties between the classical inorganic and organic drugs are emerging on the global stage as potential alternatives for several reasons. These hybrid compounds combine features of the metallic centre and the organic entities, coupled with their versatile stereochemistry, relative lipophilic nature, and variety of functionalized ligands with very specific reactivities.

The redox property of the metal ion and the ability to bind to its biological target is very crucial to drug design. Cutillas et al. (2013) has extensively reviewed the importance of cyclometalated complexes of PGMs (platinum (II), palladium (II), rhuthenium (II), rhodium (III), iridium (III)) and also gold (III) with potential anticancer properties. The properties of the anionic cyclometalated or the ancillary ligands can easily be modified and "tuned" to enhance their cytotoxicity and pharmacokinetics. This modification improves the stability of the complexes against biological reduction and ligand exchange reactions, as they also contain a strong C-M δ bond. Karaküçük-İyidoğan et al., (2011) have also successfully synthesized platinum (II) and palladium (II) complexes with both antiviral and cytotoxic properties. Recently, palladium (II) complexes (Pd (II)-Schiff base complexes) were synthesized by Prasad et al., (2013) with the ability to interact with DNA, and have also demonstrated promising antimicrobial activities against selected microorganisms which is of interest given the emergence of bacteria with resistance to almost all known antibiotics (Davies and Davies, 2010).

1.4.7 Recovery of PGMs

In recent years, the prices of internationally traded metals especially the PGMs have reached record highs. This is due to the high demand by mostly the automobile industries (Butler, 2012) as seen above. This increase in demand is partially due to emerging economies like China and India (Chen, 2010). In addition, there is considerable uncertainty concerning the future of PGMs. In 2013, Johnson-Matthey (Cowley, 2013) reported a decline in the average prices of Pt, Pd, Rh and Ru in 2012 except for Ir whose price was increased from US$ 1,036/oz the previous year (2011) to US$ 1070/oz. This follows a general increase in the average prices of Pt, Pd, Rh and Ru until 2011 (**Table 1.2**).

Table 1.2 Average prices of PGMs (US$ per oz)

	Year					
PGMs	**2007**	**2008**	**2009**	**2010**	**2011**	**2012**
Pt	1,304	1,576	1,205	1,611	1,721	1,552
Pd	355	352	264	526	733	643
Rh	6,191	6,564	1,592	2,458	2,022	1,276
Ru	580	323	95	197	166	112
Ir	447	450	425	642	1,036	1070

Summarized from Cowley (2013), Johnson Matthey Ltd (JM), 2013-2015 review not available as at the time of writing this review. An ounce (oz) is equivalent to 28.35g or one-sixteenth of a pound while one international troy ounce (oz t) is equivalent to 31.1034768 g.

As a result of the limited availability and high market values along with the various industrial applications of PGMs, there is a great need for their recovery. Scrap catalysts from catalytic converters of automotive vehicles form the major source for the recovery of PGMs. The global consumption of PGMs made by recycling end-of-use consumer products was reported at 25% (Jollie, 2010; Shed , 2010). This recovery process has

become an economically attractive business for companies with an efficient process and many such companies have started in recent years.

Conventional industrial techniques like hydrometallurgical and pryrometallurgical processes have been widely used in the recovery of precious metals from scraps and wastewater (Jacobsen, 2005). The hydrometallurgical method involves solubilisation of metals followed by adsorption by ion exchange resins, solvent extraction, and the reduction of precious metal precipitate by reagents. This method has been used more often than the pyrometallurgical approach. Both of these methods are very expensive and require extensive labour, time and the addition of toxic chemicals for the precipitation and reduction processes. As a result, large quantities of secondary wastes are generated.

Economically and environmentally sustainable techniques have become necessary for the recovery of PGM wastes from solutions. Biosorption, as discussed earlier has the potential of becoming an alternative technology for the recovery of PGMs from metal solutions. This is due the properties of certain microbial biomass materials whether live, inactive or dead to bind and concentrate metal ions from industrial effluents and aqueous solutions. There are many comprehensive reviews on biosorption (see Volesky, 1994; Dobson and Burgess, 2007; Wang and Chen, 2009; Das , 2010; Mudhoo et al., 2012). Critically, live-cell biotechnologies cannot be used under the aggressive conditions of most hydrometallurgical PGM waste waters. However, by pre-seeding biomass under ‘permissive’ conditions of the initially-produced metallic deposit can autocatalyse the reduction of further metal from acidic waste water.

1.4.8 Environmental behaviour and evaluation of health risks

The use of catalytic converters has improved air quality since their introduction in 1975 in the US and 1986 in Europe (Wiseman and Zereini, 2009), but these have also become the primary source of PGMs in the environment. Due to the inert and immobile nature of PGMs, they were considered harmless and proper investigation into their environmental behaviour and health risk was given scant attention.

PGMs are now known to be present at elevated levels in the environments (initially in airborne particulate matter, roadside dust, soil, sludge, and water etc) taken up by plants, with the possibility of entering the food chain (Rao and Reddi, 2000). PGMs are emitted into the environment in small quantities together with particles (e.g. alumina) from the washcoat of the catalyst due to chemical and physical stresses like sintering and thermal shock (Artelt et al., 1999; Palacios et al., 2000). The amount and rate of PGM emission might be dependent on the speed of driving, type and age of the catalyst and engine type (Artelt et al., 1999). Chronic exposure to soluble platinum compounds can result in toxic effects known as 'platinosis' and certain Pt species are known to exhibit allergenic potentials (Ravindra et al., 2004). Hence, it is necessary to understand the bio-availability, bio-accumulation and bio-magnification of PGMs in living organisms and to have the ability to evaluate their toxic effects.

Earlier reviews (Merget and Rosner 2002; Ravindra et al., 2004) which were based on data collected from the 1970s through to the 1990s on the emission, environmental concentration and related toxicity of PGMs, resulted in two similar conclusions; that data on PGM toxicity, speciation and behaviour are limited, making it quite difficult to adequately assess the risks related to environmental exposure. Based on the lack of adequate information, the current levels of PGMs in the environment were assumed to be too low to cause any serious threat to human health.

However, studies by Colombo et al. (2008) have now shown that PGM uptake in the human body could increase significantly through respiratory exposure versus ingestion. It was reported that ambient particulate matter (PM) aerodynamic diameter of less than 10μm (PM_{10}), particularly the $PM_{2.5}$ fraction, has been associated with morbidity and mortality (Burnett et al., 2000). Other studies (Artelt et al., 1999; Gómez et al., 2002; Zereini et al., 2004; 2012) have shown that about 30% to 57% of the total PGM measured in airborne samples fall within this fraction, posing a potential health risk from traffic emissions. Further studies have reported measured PGM level of $PM_{2.5}$ (see Wiseman and Zereini, 2009) and PGM concentrations in airborne samples from different countries. The airborne concentration was dependent on the traffic density. However, there were some inconsistencies in the order of which PGM has the highest

concentration in airborne samples, presumably since the actual metal concentration in the catalyst material differs according to the correct metal values at the time of catalyst manufacture.

Toxicity studies have also shown the potential toxic nature of PGMs. Most of the earlier reports were mostly on Pt and Pt-containing substances that were used in chemotherapy; there were less available data on PGM particles emitted from catalytic converters into roadside dusts. The toxic effects of most metals were dependent on their speciation ability and adsorption route, with soluble compounds (ingested) being most toxic. For instance, hexachloroplatinate solution is more toxic, exhibiting more nephrotoxicity in rats (Ward et al., 1976) than metallic Pt. A study has also shown that soluble Pt and Rh compounds were more genotoxic than Pd (Migliore et al., 2002), thought to be mediated by an ability of the former two to induce oxidative stress (e.g. $10^{-2} – 10^{-8}$ mol/l of Pt-salts have been diagnosed for their potential in causing occupational diseases). It has now been confirmed in *in vitro* studies that PGMs could impact on mammalian cell viability and cellular processes and functions (Frazzoli et al., 2007). This conclusion was supported by Schmid et al., (2007), who used human bronchial epithelial cells (BEAS-2B) to monitor the effect of PGM exposure on cellular viability and their capacity to induce oxidative stress. It was found that Pt (II) and Pt (IV) led to an increase in the production of reactive oxygen species, while Pd (II) and Rh (III) had no effect. Additional information on further toxic effects of PGMs on health can be found in an extensive review by Ravindra et al. (2004).

Even when the entire population might not be exposed to a higher concentration of PGMs in the short term as would workers working in the precious metal refineries and catalyst production (although the effect of long term exposure to urban atmospheric dust has still to be evaluated), it has become very important to carry out more research so that additional data can be documented on their toxicity, biotransformation, speciation, and bioavailability in order to help in the prevention of potential sub-clinical health issues or, indeed, in apparently unrelated problems e.g. the long term effect of organo-lead compounds on the human brain was not confirmed until a number of years after routine addition of organo-leads as anti-knock additives in petrol (Patocka, 2008). By

this analogy (as well as due to diminishing supplies of oil reserves and CO_2 impacts on fossil fuels) the move towards hydrogen and fuel cell technologies, and hence development of alternative routes of PGM catalyst manufacture is warranted. Yong et al. (2007) showed that biogenic fuel cell catalysts could make as much electricity in 'PEM' fuel cell as commercial counterparts, and further showed (Yong et al., 2010) that PGM biorecovered from waste were superior for this purpose.

1.5 Biocatalysis

Catalysts are substances with the ability to accelerate a chemical reaction without being altered at the end of the reaction (see Gates, 1992) for review. For example, ammonia formation did not occur when nitrogen and hydrogen were passed through a tube at high temperature and pressure, even when the chemical equilibrium was favourable. However, when particles of iron were placed in the tube, the gases came in contact with each other on the Fe and were converted to ammonia. This catalytic mechanism has become a key industrial process for the synthesis of raw materials like fertilizers for agricultural purposes. Catalysts are also applied in other forms of industrial processes such as petroleum refining, gas synthesis and in fuel processing as well as in control of vehicle exhaust emissions but a major application is in synthetic chemistry. A good catalyst should have the following essential properties; activity, selectivity and long life as well as ease of recovery. In practice the cost is a major consideration; especially in low-value applications like detoxification of hazardous materials. The cost of a catalyst and the possibility to recover it (i.e. minimal treatment of the product stream) are very major industrial consideration (Crundwell, 2011).

The activity of a catalyst refers to the rate to convert feedstock to (various) products (e.g. number of molecules reacting s^{-1}/active site) and rapid dissociation of the 'leaving' group from the catalyst. The selectivity is the ability of a catalyst to give the desired product, out of all possible products, e.g. products as percentage of reactant converted (yield); the selectivity of a catalyst may even be more important than its activity for large-scale application (Gates, 1992). On the other hand, every catalyst should have a long life time and be robust against potential poisons. The life of a catalyst is the time

for which the catalyst keeps a sufficient level of activity and/or selectivity (Twigg, 1996). A deactivated catalyst can often be treated to restore its activity.

Biocatalysis, which involves the use of organisms or enzymatic systems of organisms, is well established in biotechnology. Pre-extracted immobilized enzymes can be processed and purified from living systems (Lester and Sherrington, 1995) and used for catalytic reactions at industrial scale. Catalysts fall into different categories; heterogeneous and homogenous catalysts, and supported and unsupported catalysts.

Homogeneous catalysts are in the same phase (e.g. liquid) as the reactants and products and are usually considered as 'one through' since their recovery is difficult and their removal adds significantly to process costs (Cole-Hamilton, 2003) unlike heterogeneous catalysts which are present in a different phase (usually solids) as considered in this study. Considering supported catalyst (e.g. supported metals), these have more advantages over the unsupported metals (bulk metals) by maximizing the active surface area for increased catalytic efficiency. For instance, when supported platinum group metal catalysts are used, they exhibit good metal dispersion and also no loss of metal within the support phase is observed (Twigg, 1996). In chemical industries, a porous refractory oxide, usually fired at high temperature to give stability is used as the support (e.g. TiO_2). Also, high-area carbons are used as support especially for the platinum group metals. Since small nanoparticles sinter (growth of larger particles by aggregating with neighbouring particles) easily, the use of a support reduces particle sintering during reaction although this does happen eventually (e.g. in fuel cell catalyst) (Gasteiger et al., 2008).

The use of chemical substances as the support is considered expensive and some of the chemicals are toxic (Jacobsen, 2005), hence, the use of microorganisms or other biomass as the support (**Table 1.3**) as a sustainable way of producing supported catalyst is becoming promising. Catalyst can now be made by recovery of the very expensive precious metals from wastes sources (Creamer et al., 2006; Mabbet et al., 2006; Murray et al., 2015) which is more sustainable, less expensive and more environmentally friendly than the conventional use of hydro and pyrometallurgical processes (Jacobsen, 2005; Macaskie et al., 2010). In addition, previous studies have shown that

microorganisms synthesized nanoparticles of sizes of about 1-6 nm by reduction of Pd (II) which exhibited comparable catalytic activity with chemically produced palladium on carbon support (Creamer et al., 2007). This study following initial studies by (e.g. Baxter-Plant et al 2003; Mabbet et al., 2004) opened the way to a large contemporary literature in this area. The study by Creamer et al. (2006) showed the potential for 'bio-Pd' on both (*D. desulfuricans*) and (*B. sphaericus*) cells to perform an effective hydrogenation reaction (of itaconic acid) that is an accepted "reference" reaction in industrial synthesis. However, with a burgeoning literature on the activity of bio-supported PGM-nanoparticle catalysts on bacterial cells, information about the underlying pathway of NP synthesis and 'steering' of NP morphology (and with this the chemical selectivity of the catalyst) is almost totally lacking.

1.5.1 Biomass-supported catalysts

Biomass-supported catalyst production has been well exemplified by the sulphate-reducing bacterium *Desulfovibrio desulfuricans* (e.g. Baxter-Plant et al 2003; Mabbet et al., 2006; Deplanche et al., 2014), and metal-respiring bacterium *Shewanella oneidensis* (De Windt et al., 2005). This has further been produced by facultatively grown cells e.g. *E.coli* (Deplanche et al., 2010; Foulkes et al., 2011) and by the obligately anaerobic *Clostridium pasteurianum* (Chidambaram et al., 2010). Catalyst has also been produced using the aerobic bacterium *Bacillus sphaericus* (Creamer et al., 2007). Besides the use of whole bacterial biomass, more recently, Iron and palladium binding by extracellular polymeric substances (EPS) was obtained and material was purified from cultures of *Klebsiella oxytoca* BAS-10 with the ability to grow under an anaerobic condition (Baldi et al., 2011). Chitin is a key component of fungal cell walls and its derivative, chitosan, has been the subject of an extensive development of chitosan-supported metallic catalysts (Guibal et al., 2005; Kadib et al., 2015). Chitin is a polymer made up of *N-acetylglucosamine* (NAG) units. Petitoglyglycan (or murein) on the other hand is a polymer of NAG and *N*-acetyl muramic acid (NAM) (van Heijenoort, 2001) which is found more in Gram-positive bacteria like *Bacillus* spp. than Gram-negative bacteria. Both chitin and petidoglycans contain NAG which is lined with functional group like amine which can bind to metal ions in acidic solution. The

presence of these bio-polymers (**Figure 1.11**) is an important platform in the synthesis of metallic catalyst.

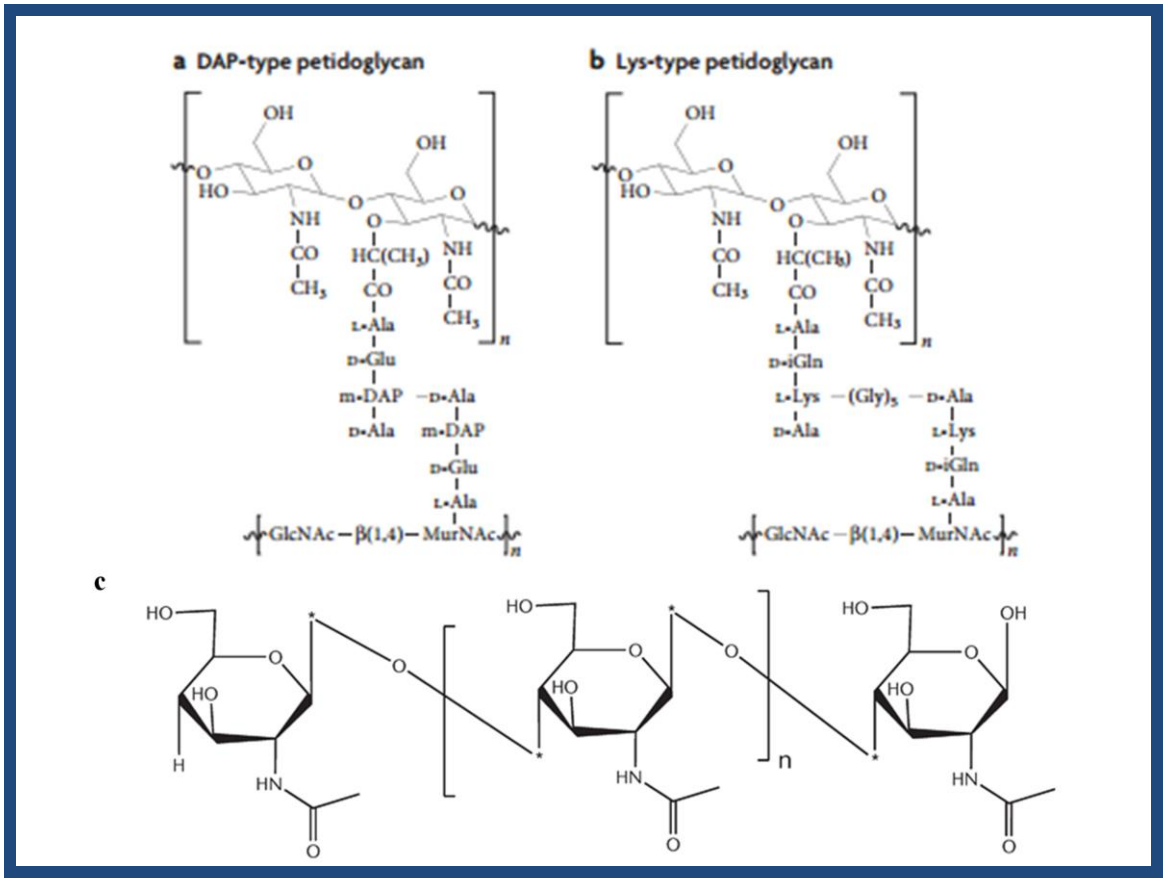

Figure 1. 11 Structure of peptidoglycan polymer of β(1-4)-*N*-acetylglucosamine (NAG) and *N*-acetylmuramic acid (NAM). Adapted from Royet and Dziarsk (2007) and Martinez (2001).

The ability of palladium to catalyse reactions in either form of Pd (0) or Pd (II) makes it the most sought-after PGM metal in the manufacture of biomass-supported catalysts; biomass-supported PGM biocatalysts especially 'bio-Pd (0)' have been widely used either as a single metal or as a bimetallic doped with other precious metals, especially gold. The synthesis of the biomass-supported palladium or bimetallic catalysts is brought about by the reduction of metal solutions on the cell surface (outer membrane), periplasm or the S-layer of bacteria acting as support, using electron donors like hydrogen, formate, and, in some cases, lactate, pyruvate or ethanol (De Windth et al., 2005). In *E.coli* and the sulfate-reducing bacteria, this bioreduction is brought about

with involvement of hydrogenase (Mikheenkho et al., 2008; Deplanche et al., 2010) and C_3-type cytochromes (Elias et al., 2004), leading to the formation of fine nanoparticles on the bacterial surface, with great potential in green chemistry. It is noteworthy that it is the inner membrane that comprises the cellular permeability barrier. However, substances like ions can be transported *via* high conductance porins in the outer membrane of Gram-negative bacteria but Gram-positive bacteria also have the cell (plasma) membrane (Alcayaga et al., 1992) that allows the selective passage of these substances from the external environment into the cell, hence the possibility of NP synthesis inside the cell of both bacteria.

1.5.2 Applications of Biomass-supported PGM catalysts

1.5.2.1 *In-situ* environmental applications

Biomass-supported palladium catalyst on *Desulfovibrio desulfuricans* has shown potential in *ex-situ* environmental applications; e.g. in the reduction of toxic Cr (VI) to Cr (III) (Mabbet et al. 2004; 2006) in the reductive dehalogenation of highly toxic polychlorinated biphenyls (PCBs) (Baxter-Plant et al., 2003; De Windt et al., 2005), and reductive debromination of polybrominated diphenyl ether (PBDE) (Harrad et al., 2007; Deplanche et al., 2009) and in the dehalogenation of chlorobenzene by the use of bio-generated metal binding exopolysaccharides (Baldi et al., 2011). Deplanche et al., (2008) also carried out the dehalogenation of halogenated compounds in contaminated ground water by observing the reaction with ^{31}P NMR.

The ability of bimetallics (Pd/Au) was shown (Nutt et al., 2006) previously to catalyse the dehalogenation of recalcitrant halogenated compounds in contaminated ground water. This approach was adopted by De Corte et al., (2012) to synthesise a bio-Pd/Au on *Shewanella oneidensis* with the ability to dehalogenate about 78% of diclofenac after 24h and was better than the monometallic bio-Pd catalyst. Converesly, there were other reactions where the monometallic bio-Pd catalyst performed better. Recently, Pretzer et al., (2013) produced a bimetallic Au nanoparticle that was partially coated with Pd ("Pd-on-Au NPs) capable of degrading trichloroethene, a common carcinogen and ground water contaminant in industrialized nations. With competition from commercial

bimetallic catalysts, improvements could be made especially in the ability of bio-generated catalysts to dehalogenate environmentally recalcitrant contaminants. To clean up wastes, the catalyst has to be cheap (i.e. dirty catalyst for dirty application), hence the scope also includes the potential use of bio-PGM mixed catalyst from waste sources (e.g. road dust) in dehalogenation and other important reactions.

1.5.2.2 Synthesis of platform chemicals

The use of biogenic catalysts made from PGMs or in combination (bimetallic) with other precious metals (e.g. gold) is currently receiving increasing attention in the synthesis of platform chemicals. Biomass-supported palladium catalysts for instance has been reported in some important industrial reactions, comparing very well with chemically synthesised palladium catalyst on either carbon or alumina support (Bennett et al., 2013).

Biomass-supported palladium catalyst on *Desulfovibrio desulfuricans* was used for an active and selective hydrogenation of 2-pentyne (Bennett et al., 2010). In their work, Bennett et al. (2010) observed that at 92% alkyne conversion, the bio-Pd produced a *cis/trans* ratio of 2.5 and pentene/pentane ratio of 3.3 as compared with the 2.2 and 2.0 respectively observed when 5% Pd/Al_2O_3 was used. Wood et al.(2010) also demonstrated the hydrogenation of 2-butyne-1,4, diol using biopalladium catalyst. The hydrogenation of itaconic acid (methylene succinate) was carried out by biopalladium nanocatalysts supported on *Desulfovibrio desulfuricans* and *Bacillus sphaericus* (Creamer et al., 2007). The nanocatalyst of both compared favourably with a commercial 5% Pd-graphite catalyst.

Bennett et al., (2013) have since demonstrated the potential of reusing a bio-Pd (0) in the Heck coupling reaction of styrene and iodobenzene. In addition, they showed that the biogenic catalyst was more effective than colloidal Pd catalyst under the same experimental conditions. Moreover, the bio-derived catalyst was re-usable in several sequential reactions whereas the commercial catalyst lost activity. More recently, Deplanche et al., (2014) have shown the potential of bio-Pd in pharmaceutical applications such as Heck and Suzuki reactions, using bromoacetophenone and 4-

bromanisole (Heck) and 4-chloroanisole with more than 90% conversion (Suzuki) using 4-bromobenzotriflouride.

However, in recent times, scientific interest is driven towards new ways of synthesizing bimetallics (e.g. bio-Au/Pd), using easy and scalable approaches on bacterial surfaces (Deplanche et al., 2012) and with selectivity. Such an approach has been used successfully in the selective oxidation of benzyl alcohol in air at low temperature (Deplanche et al., 2011; 2012; Zhu, 2014), making it suitable towards green chemistry approaches; there is currently no commercial way to achieve this reaction selectively.

More recently, studies have equally demonstrated the potential applications of biogenic bimetallic Pd/Au in organic synthesis, such as in carbon-carbon coupling reactions. Heugebaert et al., (2012) synthesized bio-Pd/Au on *Shewanella oneidensis* with the ability to catalyse a Suzuki coupling reaction, with more reproducible results and broader reaction scope than the monometallic bio-Pd. These approaches will open new ways in the future for making improvements to the biogenic catalysts with enhanced reactivity and selectivity in an environmentally viable way.

1.5.2.3 Tandem catalysis

Previous transformations and chemical syntheses have not considered environmentally benign reactions where there is little or no waste of time, energy and other resources. However, current studies and methodologies are becoming available and two or more synthetic steps can now be combined into a single step operation, enabling a multistep synthesis of complex molecules within a short time (Kolarovic et al., 2011). This concept is called “Tandem catalysis” - a one-pot procedure that embraces multiple catalytic transformations in a single process.

The term ‘tandem catalysis’ is often used interchangeably with “Domino catalysis”, “Cascade catalysis”, “Multifunctional catalysis”, “Multicomponent catalysis” and “ One-Pot reactions” (Fogg and dos Santos, 2004), and these terms often describe a reaction wherein a single catalytic process results in a stoichiometric reaction. Foggs and dos Santos (2004) further stated that “tandem catalysis is a term used to describe coupled catalyses whereby sequential transformation of the substrate occurs via two (or

more) mechanistically distinct processes, with all catalytic species – whether masked or apparent - present from the outset." These reactions can be subdivided as follows:

Orthogonal tandem catalysis involves two or more functionally distinct catalysts and (in principle) non-interfering catalysts or pre-catalyst. The catalytic mechanisms are meant to operate concurrently, with a sequential transformation of the substrate. Loones et al., (2006) have shown the possibility of using orthogonal tandem catalysts (Pd and Cu) or auto tandem catalyst (Pd) in the synthesis of dipyrido[1,2-a:2',3'-d]imidazole via regioselective inter and intramolecular C-N bond formation.

In auto-tandem catalysis, two or more mechanistically distinct reactions are promoted by a single catalyst. Here, both catalytic cycles take place spontaneously with a cooperative interaction of species present from the outset of reactions. There is no change in conditions required to trigger the change in catalytic reactions. Transition metal complexes of Rh, Ru, Pd and Au have been associated with various auto-tandem catalysis and those of Pd, Pt, Au and In were found to be capable of simultaneously acting as a σ Lewis acid to activate C=X (X= heteroatom) bond and acting as a π Lewis acid to activate C-C multiple bond in tandem catalysis (Wang et al., 2011).

Wang et al., (2011) further demonstrated the use of Ag-catalysed auto-tandem catalysis of acetylinic aldehydes with indoles to form highly substituted tetrahydrocarbazoles – a common compound found in natural products and bioactive molecules. This was made possible because silver (I) salts are good catalysts for the development of auto-tandem catalysis involving the dual activation of C=X and unsaturated C-C bonds. Recently, Kanbayashi et al., (2013) have demonstrated for the first time an asymmetric auto tandem catalysis using a planar-chiral Ru complex (as a single catalyst) for the sequential regio-, enantio-, and diastereoselective reactions of allylic chlorides with amide derivatives, involving completely different reaction mechanisms.

In assisted tandem catalysis, a change in reaction conditions (with the exclusion of catalyst addition) results in a shift from one catalytic mechanism to a different mechanism, and the transformations are not concurrent.

There is currently a lot of work on the use of metal-containing compounds or complexes in tandem catalysis (Burns et al., 1992; Pollino and Weck, 2000; Foggs and santos, 2004; van As et al., 2007; Yamada et al., 2011; Nakatani et al., 2012; Tang et al., 2013; Yao et al., 2013) but literature on the use of whole microbial cell or metallobiological catalysts as tandem catalysts is very sparse and just emerging.

According to Yan et al., (2012), biodiesel was produced from grease in a one pot esterification and transesterification with tandem lipases engineered in an *E.coli*. The immobilized lipases were obtained from *Candida antarctica* lipase B (CALB) (Novozyme 435) which favours an esterification reaction, and *Thermomyces lanuginosus* lipase (TLL) (Lipozyme TLIM) which prefers transesterifaction. The use of wet or dry cells (4% wt) of the recombinant *E.coli* (Calb/Tll) co-expressing CALB and TLL was a better tandem lipases system, resulting in 87% or 95% yield of FAME (fatty acid methyl ester), better than when the *E.coli* was engineered with either CALB or TLL alone. The catalyst (cells of *E.coli* (Calb/Tll)) retained about 75% productivity after five cycles of reactions.

On the other hand, Foulkes et al., (2011) engineered for the first time, a biometallic whole cell catalyst of aerobic *E. coli* for deracemization of racemic amines, which was achieved through a discrete sequential oxidation/reduction steps using a separate enantiomer-specific catalyst and a metal catalyst on the cell respectively. The *E. coli* culture carrying the cloned monoamine oxidase gene and nanoscale bioreduced Pd (0) particles was used for the conversion of racemic 1-methyltetrahydroisoquinoline (MTQ) to (R)–MTQ, via the intermediate 1-methyl-3,4-dihydroisoquinoline, with an enantiomeric excess of up 96%. There was no loss of activity after five cycles of oxidation/reduction and also there was minimal loss of palladium into the supernatant.

The use of the rapidly advancing tools of molecular and synthetic biology and the very high possible combination could open a new direction for the synthesis of whole cell or biometallic whole cell tandem catalysts with multifunctional activities of industrial importance. However, the fate of genetically modified organisms is still debatable. Therefore, identifying natural organisms with specific catalytic abilities and enhancing or 'tuning' them as tandem whole cell catalysts by the introduction of metals (while still keeping them alive) could be a novel and promising research area in the fabrication of

biometallic and tandem catalysts. This could be particularly of interest for example in the remediation of contaminated chlorinated aromatic compounds, where an organism identified to decompose a particular aromatic compound may be limited by the presence of halide substituents; this could also be 'fine-tuned' as a nanoscale biometallic catalyst, for example, for the dehalogenation and degradation process, resulting in a multistep catalytic reaction whereby chemical catalysis effects reductive dehalogenation followed by metabolism of the generated aromatic compound.

1.5.2.4 Heavy oil upgrading

The world's energy demand continues to rise with increasing pressure on fossil fuel or light oil. The consequence of such high demand is the depletion in global oil reserves which can lead to energy crises, unless new alternative sources are developed to sustain global need. Heavy oil and bitumen are potential alternatives owing to their large deposits found in the Alberta Basin of Canada and the Orionoco Belt of Venezuela, together making up about 80% of global oil reserves (de Sena et al., 2013). Of these vast deposits, only about 2-3% (2 Million barrels/day, Mb/d) is currently being supplied globally (Total, 2015). This is due to the inherent properties of the oil *i.e.* high viscosity, low hydrogen content, presence of high molecular weight compounds (resins and asphaltenes) and richness in hetero-elements (nitrogen, sulfur and oxygen), as well as high metal contents, especially nickel and vanadium which requires new upgrading technologies to improve their economics and transportability. In addition, extraction and transportation of the highly viscous materials are more environmentally damaging than for lighter oils and hence there is strong pressure to upgrade the heavy oil, reducing its viscosity *in-situ*.

The use of commercial catalyst (*e.g.* Ni-Mo/Al_2O_3) in the upgrading of heavy oil *via* THAI-CAPRI (Toe-to-Heel Air Injection coupled with Catalytic Upgrading Process *In-situ*) technology combines thermally enhanced oil recovery with down-hole *in-situ* catalytic upgrading of heavy oil into light fractions and THAI is establised in use (Hart et al., 2014) with CAPRI toeing a more recent developmental addition. However, the high cost of the commercial catalyst and the fact that they are easily deactivated due to coking, calls for the use of an alternative 'green' approach involving catalyst

synthesized by bacterial cells using precious metals (Pd and Pt) which can be biorefined cheaply from wastes (Mabbet et al., 2006; Murray et al., 2015). This holds great potential since the bacteria are potentially amenable to modification and tuning (see above).

1.5.2.5 Other applications of biomass-supported nanomaterials

Apart from the use of biomass –supported catalysts in catalysis and bioremediation, recent advances have also included the use of fungal cultures to synthesize silver nanoparticles (AgNps) as antimicrobials. For instance, *Trichoderma viride* was used for the extracellular synthesis of AgNps from silver nitrate solution. The AgNps were active against both Gram-positive and Gram-negative bacteria and were able to increase the potency of conventional antibiotics particularly ampicillin when used in combination (Fayaz et al., 2010). The same authors reported earlier that there was also the possibility of controlling the size and monodispersity of the *Trichoderma* AgNps by e.g. temperature manipulation during biosynthesis (Fayaz et al., 2009).

Furthermore, AgNps have been produced from bacterial sources such as *Geobacter sulfurreducens* (Law et al., 2008) and *Shewanella oneidensis* (Suresh Ak Fau - Pelletier et al., 2010) with enhanced antimicrobial activities. However, as a result of the potential toxicity of AgNps, metabolomic studies (Wang et al., 2010) showed that *S.oneidensis* could only tolerate up to 50μM of Ag (I) added to the cultures, while at higher concentrations, the doubling time and biomass yield was affected. This was as a result of a drop in phospholipid fatty acids, membrane damage, and the penetration of the cell by the Ag (I), causing intracellular toxicity. For further details on the use of other bacteria in the synthesis of antimicrobial AgNps, the reader is referred to a comprehensive review by Lloyd et al., (2011).

Magnetic iron-based nanoparticles (nanomagnets) especially magnetite (Fe_3O_4) synthesized by bacteria (e.g. *Geobacter spp. and Shewanella spp*.) are becoming relevant for potential application in cancer therapies. For instance, tumours that are beyond reach using conventional approaches (such as pancreas and brain) can now be targeted and thermally destroyed by the heat generated by magnetic nanoparticles in the presence of an alternating magnetic field (see Lloyd et al., 2011).

Further application of biomass supported nanoparticles also includes the synthesis of semi-conductors called quantum dots (QDs) with unique electronic and optical properties to quantum confinement effects. Instead of the usual chemical synthetic pathways, microbial metabolism through the reduction of oxyanions of the group 16 metalloids selenium, tellurium, or sulphur can now synthesize QDs in the presence of cationic metals, metal selenides, tellurides and sulphides (Bai et al, 2009; Zhou et al., 2009; Shen et al., 2010).

Microbial nanowires (pilus-like filaments) (Malvankar et al., 2015) are also receiving attention; especially focusing on dissimilatory metal reducing bacteria such as *Geobacter spp. and Shewanella spp*. Strycharz-Glaven et al., (2011) demonstrated an *in situ* electrical conductivity of an anode-grown *G. sulfurreducens* DL1 biofilm, thereby suggesting the role of bacterial nanowires of *S.oneidensis and G. sulfurreducens* in biofilm conductivity with potential in fuel cell technology. Earlier work by Yong et al., (2007) had demonstrated the use of bio-Pt (0) and bio-Pd (0)-supported bacterial nanoparticles as fuel cell electro-catalysts achieving 100% and 81% maximum power generation respectively but in this case the metallised biomass was sintered (carbonized) to achieve conductivity.

1.6 Challenges of using *Desulfovibrio desulfuricans* as bacterial support in catalyst bio-fabrication

A paradigm bacterial support for catalytic NP fabrication is *Desulfovibrio desulfuricans* (**Table 1.3**). However, some challenges abound when using *D. desulfuricans* as the biomass support; the slow growth which usually takes days for biomass to be ready for harvest, and the production of hydrogen sulfide (a catalyst poison), which can be fatal when inhaled in high concentrations by humans. Some sulfate-reducers are also human opportunistic pathogens. The use of an alternative organism which would not only grow fast, producing sufficient biomass in a limited period of time, but equally produce very active metallic biocatalyst should be considered. *Bacillus* spp. which are fast growing and have been demonstrated to produce effective catalyst (Creamer et al., 2007) could offer an alternative opportunity since *Bacillus* spp. are produced at large scale as wastes from commercial production of enzymes (e.g. by Novozymes). Since the enzymes are extracellular the bio-waste comprises intact, metabolising cells that could find 'second-

life' as bioinorganic catalysts, hence, potentially removing the cost of biomass growth specially while reducing the cost of waste biomass disposal.

While *E.coli* the laboratory "workhorse" for molecular strain development and which produces catalyst with activity compared to *D. desulfuricans* (Deplanche et al., 2014) has been used in some manufacturing processes (e.g. recombinant human insulin production) its availability as a waste (i.e. catalyst precursor) is limited. The problem is that primary use of *E. coli* breaks the cell for product harvest. Current work (I. Henderson, University of Birmingham unpublished) is developing protein exporting strains of *E.coli* for primary production; the spent whole cells could then be used as 'second life' bio-Pd catalysts.

Table 1.3 summarizes the microorganisms currently evaluated as palladium nanocatalyst supports, of these, clostridia are well established in fermentation but, like *D. desulfuricans* have the limitation of obligately anaerobic growth and sporulate readily. Other candidate groups like actinomycetes are used industrially (e.g. Streptomycetes) but appear not to have been evaluated as catalyst support. Of the archaea, tests using methanogens gave catalytically poor bio-Pd (0) while *Pyrococcus furiosus* was found to give poor growth, insufficient for catalyst manufacture (K. Deplanche, unpublished).

Table 1.3 Examples of biomass-supported nanocatalyst produced using bacteria as support

Metal	Microorganism support and Gram stain	Catalytic test	References
Pd	*Arthrobacter oxydans* (+)	Cr (VI) reduction Mizoro-Heck coupling Hydrogenation of 2-butyne 1, 4-diol	Deplanche (2008) Wood et al., (2010)
	Bacillus sphaericus (+)	Hydrogenation of itaconic acid and 3-nitrostyrene	Creamer et al., (2007)
	Bacillus benzeovorans (+)	Reductive dechlorination of chlorobenzene Heavy oil upgrading	This study
	Clostridium pasteuranium (+)	Cr (VI) reduction	Chidambaram et al., 2010
	Cupriavidus necator (-)	H_2 evolution from hypophosphite Suzuki-Miyaura couplings Hydrogenation of (E)-3-(4-methoxyphenyl)-N-methylacrylamide Reductive dechlorination of 4-	Sobjerg et al., (2009) Bung et al., (2010) Sobjerg et al., (2011)

		chloro-nitrobenzene	
	Cupriavidus metallidurans (-)	Cr (VI) reduction Mizoroki-Heck coupling Fuel cell electrocatalyst	Deplanche (2008) Deplanche et al., (2014) Yong et al., 2010
	Desulfovibrio desulfuricans (-)	H_2 evolution from hydrophosphite Cr (VI) reduction Reductive dechlorination of chlorophenol, chlorobenzene, PCBs Reductive debromination flame retardants Mizoroki-Heck coupling Fuel cell electrocatalyst Heavy oil upgrading Hydrogenation of soybean oil	Yong et al., (2002, 2007), Mabbet et al., (2004, 2006), Baxter-Plant et al., (2003), Macaskie et al., (2005), This study, Redwood et al., (2008) Humphries et al., (2006), Deplanche et al., (2009, 2014), Harrad et al., (2007), Bennett et al., (2013), Yong et al., (2007) This study
	Desulfovibrio vulgaris (-)	Reductive dechlorination of	Baxter-Plant et al., (2003)

		chlorophenol, PCBs Cr (VI) reduction	Humphries et al., (2006)
	Desulfovibrio sp. Oz-7 (-)	Reductive dechlorination of chlorophenol, PCBs	Baxter-Plant et al., (2003)
	Escherichia coli (-)	Reductive dechlorination of chlorinated ground water. Cr (VI) reduction Mizoroki-Heck coupling, Fuel cell electrocatalyst Enantioselective deracemization reaction (tandem catalysis)	Deplanche et al., (2008, 2014), Yong et al., (2010), Foulkes et al., 2011
	Paracoccus denitrificans (+)	H_2 evolution from hypophosphite Suzuki-Miyaura and Mizoroki-Heck couplings	Sobjerg et al., (2009), Bunge et al., (2010)
	Pseudomonas putida (-)	H_2 evolution from hypophosphite Suzuki-Miyaura and Heck couplings	Sobjerg et al., (2009), Bunge et al., (2010)

	Rhodobacter capsulatus (-)	Hydrogenation of 2-butyne 1, 4-diol	Wood et al., (2010)
	Rhodobacter sphaeroides (-)	Reductive dechlorination of chlorophenol, PCBs Fuel cell electrocatalyst	Redwood et al., (2008), Yong et al., (2010)
	Serratia sp. (-)	Cr (VI) reduction Mizoroki-Heck couplings	Deplanche (2008)
	Schewanella oneidensis (-)	Cr (VI) reduction Mizoroki-Heck couplings Reductive dechlorination dichlofenac, waste water and ground water	De Windt et al., (2005, 2006), Deplanche (2008), Hennebel et al., (2011), De Corte et al., (2013)
	Staphylococcus sciuri (-)	Suzuki-Miyaura and Mizoroki-Heck couplings Hydrohenation(E)-3-(4-methoxyphenyl)-N-methylacrylamide Reductive dechlorination of 4-	Sobjerg et al., (2011)

		chloro-nitrobenzene	
Pd/Au	*Escherichia coli* (-)	Selective oxidation of benzyl alcohol	Deplanche et al., (2012) Zhu, (2014)
	Desulfovibrio desulfuricans (-)	Selection oxidation of benzyl alcohol	Deplanche et al., (2012), Zhu, (2014)
Pt	*Desulfovibrio desulfuricans* (-)	Fuel cell electrocatalyst	Yong et al (2007)
Pd/Pt	*Bacillus benzeovorans* (-)	Heavy oil upgrading	This study
	Desulfovibrio desulfuricans (-)	Heavy oil upgrading	This study

Adapted from Deplanche et al., (2011) with modifications

There was so many reports of bio-Pd and the new frontier are to understand the mechanism of metal deposition so as to target catalysts for particular applications. An early study (de Vargas et al., 2005) identified, using XPS, that incoming Pd (II) coordinates to oxygen and amide groups in *D. desulfuricans* and recent work (A.R. Williams, unpublished; Priestley et al., 2015) has reinforced this conclusion using *E. coli*. Hence, potential amide-based candidates for molecular improvements were sought from literature reports as reviewed in the next section.

1.7 The enzyme aspartyl/glutamyl t-RNA amidotransferase and the possible role of amine membrane precursor in catalyst production by *Desulfovibrio desulfuricans*

Fatty acid amides are regarded as a new class of endogenous signalling molecules and are classified into; fatty acid ethanolamides (with anandamides as the model) and the fatty acid primary amides (oleoamide is the most explored member) (Ezzili et al., 2010) (**Figure 1.12**). Fatty acid amides are incorporated into some lipid molecules like ceramides, glycol-sphingolipids, *N*-acylated lipids and bacterial lipoproteins. Their

presence in plants (Faulds and Williamson, 1999), grasses (Kawasaki et al., 1998) and algae (Dembitsky et al., 2000) has been reported. Anandamide, also called *N*-arachidonoyl ethanolamide (AEA), is a member of a large group of signalling lipids called *N*-acylethanolamines (NAEs) and was the first endogenous ligand identified for cannabinoid receptors. It was identified and isolated from porcine brain extracts (Devane et al., 1992) and other mammalian peripheral tissues, and found as a very competitive ligand with the ability to inhibit specific binding of a radiolabelled cannabinoid probe [^{3}H]HU-243 to synaptosomal membranes (Ezzili et al., 2010). The functions of fatty acid amides have been extensively reviewed (Farrell and Merkler, 2008; Ezzili et al., 2010). Generally, the anandamides are involved in the regulation of body temperature, locomotion, feeding and perception of pain, anxiety and fear (Walker et al., 1999; Marscicano et al., 2002). Their biosynthesis has not been fully understood. It is generally accepted that *N*-acyl phosphatidylethanolamines (NAPEs) are the precursors, but the detailed enzymatic pathway leading to the synthesis of NAEs from NAPEs is still unclear. A two-step pathway has been proposed as the possible route for NAEs synthesis. The first involves a calcium-dependent transacylase (CDTA) that transfers the *sn*-1 acyl chain of phospholipids onto the primary amine of phosphatidylethanolamine (PE) to generate *N*-acyl phosphatidylethanolamines (NAPEs), and the second step involves a D-type phospholipase that hydrolyzes NAPEs to produce NAEs (Ezzili et al., 2010). However, other alternative pathways have also been suggested (Liu et al., 2008).

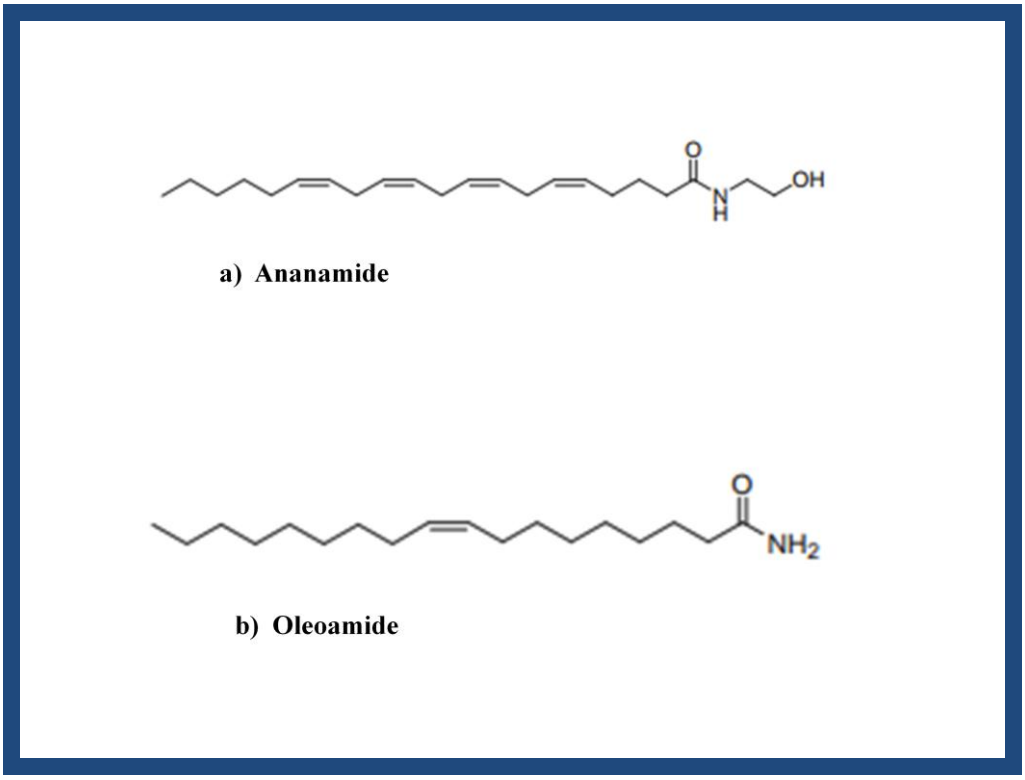

Figure 1. 12 Structures of Ananamide and Oleoamide. Adapted from Ezzili et al (2010).

Although, the functions of the fatty acid amides are relatively well known in mammals, their role in bacteria, especially Gram-negative bacteria, may be connected with pathogenicity (Cox and Wilkinson, 1989) with *Pseudomonas cepacia* (*Burkhoderia cepacia*) as an example. The presence of amide-bound fatty acid found in lipid A, an endotoxin component in non-pathogenic *Desulfovibrio desulfuricans* (Wolny et al., 2011) underlies its ability to trigger an inflammatory response in a host's immune system. In a moderately halophilic bacterium, the fatty acid amides were found as phosphatidylethanolamines (Ohno et al., 1976) just as in *Burkholderia* and *Ralstonia* species (Galbraith et al., 1999) in both cases serving as precursors of fatty acid ethanolamide.

It is important to note that these fatty acid amides (anandamide) in mice are not stored in the cell. They are produced only when needed and then rapidly inactivated and hydrolyzed by a membrane-bound enzyme with an amidase activity, fatty acid amide hydrolase (FAAH) found in mammals (Cravatt et al., 2001) and *Arabidopsis thaliana* (Shrestha et al., 2003) but not yet sought in bacteria. This was supported by the fact that

mice lacking the enzyme FAAH were severely impaired in their ability to degrade anandamide (Cravatt et al., 2001), although detailed information is not yet available. In bacteria, the A subunit of aspartyl/glutamyl t-RNA amidotransferase has an amidase signature (Curnow et al., 1997). The enzyme aspartyl/glutamyl t-RNA amidotransferase is involved in a pathway that generates the relevant aminoacyl-tRNAs, glutaminyl-tRNA (Gln-tRNA^{Gln}) and asparagynyl-tRNA (Asn-tRNA^{Asn}) by converting glutamyl-tRNA (Glu-tRNA^{Gln}) and aspartyl-tRNA (Asp-tRNA^{Asn}) in the presence of ATP and an amide donor such as glutamine or asparagine (Wu et al., 2009). The heterotrimeric form of the enzyme with subunits A, B and C is common to most bacteria and archaea while the heterodimeric form with subunits D and E is only found in archaea. Curnow et al (1997) demonstrated that genetic knockout of the 5' portion of the gene is lethal, suggesting its vital role in cell survival. Wu et al. (2009) further described the structures and roles of the various subunits.

A PhD thesis (Goldsworthy, 2011) reported the presence of the enzyme aspartyl/glutamyl t-RNA amidotransferase in two strains of *Desulfovibrio desulfuricans,* strains NCIMB 8307 (i.e. the strain used extensively in the biomanufacture of nano Pd (0)) and NCIMB 8326. The enzyme was over-expressed in the strain NCIMB 8326 but under-expressed in the strain NCIMB 8307. Accordingly, it was found that membrane extracts of the strain NCIMB 8307 contain fatty acid ethanolamide which was absent in strain NCIMB 8326 (possible to its more efficient enzymatic removal). A previous report showed that strain NCIMB 8307 produced a better biosorption of palladium and platinum than other strains of *Desulfovibrio* (de Vargas et al., 2004). While bio-Pd (0) of *D. desulfuricans* was more catalytically effective than the corresponding bio-Pd on *D. vulgaris* (Baxter-Plant et al., 2003) it is possible, and a working hypothesis of this study, that the over-expression of the enzyme aspartyl/glutamyl t-RNA amidotransferase in the strain NCIMB 8326 prevents the accumulation of the fatty acid ethanolamide as found in strain NCIMB 8307 where the enzyme was under-expressed. This is supported by the fact that fatty acid amides are perfect substrates for the enzyme FAAH, which might have shared a similar phylogenetic origin with the subunit A of aspartyl/glutamyl t-RNA amidotransferase. If the conceptual flow is that t-RNA is made cytoplasmically, whereas Pd (II) biosorption occurs to cell surface ligands, it can be proposed that the hydrolysis of fatty acid amides could be a novel function of the

subunit A of aspartyl/glutamyl t-RNA amidotransferase in *Desulfovibrio desulfuricans*. This bifunctionality was proposed and discussed at length by Goldsworthy (2011) and may suggest evolution of a dual role for the enzyme.

Based on the foregoing, the involvement of the amine groups and preferentially amide groups (G. Attard, personal communication) in the strain NCIMB 8307 as part of a very reactive ligand to palladium cannot be overlooked because the binding of metal ions to functional groups such as amine groups present in the extracellular polymeric substances (EPS) of bacteria has been reported (Omoike and Chorover, 2006; Baldi et al., 2011). The ligands coordinating this reaction might be produced by the fatty acid ethanolamide in *Desulfovibrio desulfuricans* strain NCIMB 8307. It was also reported that palladium coordinates to nitrogen ligands of amine groups (de Vargas et al., 2005) and that N-coordination ensures better catalytic properties (Van Asselt and Elsevier, 1994; Groen et al., 1999; Abu-Surrah et al., 1999; Canovese and Visentin, 2010). These reports have been demonstrated in chemical catalysis, but there is no literature to support nitrogen-ligand fatty acid amide donor to metal coordination in biometallic catalysis. Fatty acid amides could possibly play a role in steering catalytic activity in *Desulfovibrio desulfuricans* by serving as nitrogen ligand donor for coordination to palladium in biocatalyst production. Such steering could be accountable as a 'manipulation' of the final nanoparticle shape via crystal growth of the long chain of fatty acid component. The influence of nanoparticle shape on its catalytic activity is at the cutting edge of our understanding of catalysis (Johnson Matthey: personal communication; via J.V. Hanna, University of Warwick, 2012). This study will report for the first time attempt to 'steer' metallic nanoparticle functionality by virtue of the selection and manipulation of cell surface coordinating ligands.

1.8 Objectives of this study

In this project, two different strains of *Desulfovibrio desulfuricans* and *Bacillus* are identified for use in the production of biogenic catalyst (bio-palladium catalyst). The project aim is to start to develop 'designer' catalysts for particular applications by virtue of understanding the process responsible for catalyst biofabrication and resulting effect on catalyst structure:

1. The first objective is to confirm a role for fatty acid amide as key groups for 'steerage' of bio-Pd synthesis and to establish their role in the production of bio-Pd with enhanced catalytic activity and specificity. Attention will be paid to understanding what actually steers the catalytic activity of the bio-palladium produced by *Desulfovibrio desulfuricans* (strain NCIMB 8307) and makes it a better catalyst than other strains of the same genus based on published data. de Vargas et al., (2005) used X-ray photoelectron spectroscopy (XPS) to confirm the role of cellular amine groups in the biosorption of Pd (II) and Pt (IV).

   Therefore, the following fundamental questions will be addressed using XPS: (a) Does Pd (II) "prefer" to coordinate to cellular amides versus amines? (b) Then does Pd (0) catalyse the hydrogenation across the amide to make an amine? If so, is this a key step in making "good" bio-Pd? And if not, are there other functional groups on the bacterial surface or characteristics that could be of relevance to catalytic activities or any form of ion-exchange mechanism at the bacterial surface? Does any endogenous reduction of Pd (II) occur in the absence of added electron donor?
2. The second objective is to develop the concept of bio-Pd as a new type of catalyst for reactions involving oils using two examples: selective hydrogenation of soybean oil and as a 'cracking catalyst' for heavy oils to facilitate their 'green' extraction from the environment. Since it has been demonstrated that *Bacillus* spp. has the ability to reduce palladium (II) (Creamer et al., 2007) and other metals (Selenska-Pobell et al., 1999). The aim is to probe into the possibility of producing an active biocatalyst using some strains of *Bacillus* spp. and to test the catalytic activities of their bio-Pd (0) in comparison with that of *D. desulfuricans*. It is proposed that the production of an active biogenic palladium catalyst from *Bacillus* spp. would provide a more facile route to produce bio-Pd as compared with *Desulfovibrio desulfuricans*. For industrial process, the use of *Desulfovibrio desulfuricans* may not be desirable due to its production at scale and the production of H_2S, a powerful catalyst poison. *Bacillus* spp. are industrial 'workhorses' for production of many key products (e.g. enzymes) and tonnages of wastes are produced. Key to this concept is that *Bacillus* spp. are used commercially in aerobic growth but the possibility of

harnessing their anaerobic metabolism (little-reported and never explored for commercial potential) could provide a novel route to the scalable synthesis of bio-Pd (0) which is an anaerobic process.

3. Towards environmental decontamination, the third objective is to develop a novel concept of tandem catalysis whereby palladized cells perform a chemical pre-treatment and then the metabolic degradation of a target halogenated aromatic compound that is resistant to microbial attack per se.

Within the limited duration of a PhD project it is clear that all objectives will not be achieved in full and hence the overall aim is to provide key information towards an overall program goal of a rationally designed bionanocatalyst manufacture from wastes. The 'global' issues that follow naturally from this are resource efficiency and low carbon and 'green technologies' for avoiding petrochemical products or by making their manufacture and use as environmentally friendly as possible. It is grossly uneconomic to 'sacrifice' precious metals into the environment and this project will develop the concept of a 'dirty' catalyst (otherwise lost) to a 'dirty' application before its final sacrifice.

1.9 References

Acres, G.J.K. 1987. Platinum group metal catalysis at the end of this century. *Materials and Design*. 8:258-262.

Ahimou, F., C.J.P. Boonaert, Y. Adriaensen, P. Jacques, P. Thonart, M. Paquot, and P.G. Rouxhet. 2007. XPS analysis of chemical functions at the surface of *Bacillus subtilis*. *Journal of Colloid and Interface Science*. 309:49-55.

Alcayaga, C., R. Venegas, A. Carrasco, and D. Wolff. 1992. Ion channels from the *Bacillus-subtilis* plasma-membrane incoorporated into planar lipid bilayers. *FEBS Letters*. 311:246-250.

Antolini, E. 2009. Palladium in fuel cell catalysis. *Energy and Environmental Science*. 2:915-931.

Aravindhan, R., B. Madahan, J.R. Rao, B.U. Nair, and R. T. 2004. Bioacumulation of chromium from tannery waste waters: an approach for chrome recovery and reuse. *Environ Sci Technol*. 38:300-306.

Arosio, P., and S. Levi. 2002. Ferritin, iron homeostasis, and oxidative damage. *Free Radical Biology and Medicine*. 33:457-463.

Artelt, S., H. Kock, H.P. König, K. Levsen, and G. Rosner. 1999. Engine dynamometer experiments: platinum emissions from differently aged three-way catalytic converters. *Atmospheric Environment*. 33:3559-3567.

Azcarate, J.C., M.A. Floridia Addato, A. Rubert, G. Corthey, G.S. Kuerten Moreno, G. Benitez, E. Zelaya, R.C. Salvarezza, and M.H. Fonticelli. 2014. Surface Chemistry of Thiomalic Acid Adsorption on Planar Gold and Gold Nanoparticles. *Langmuir*. 30:1820-1826.

Bai, H.J., Z.M. Zhang, Y. Guo, and G.E. Yang. 2009. Biosynthesis of cadmium sulfide nanoparticles by photosynthetic bacteria *Rhodopseudomonas palustris*. *Colloids and Surfaces B: Biointerfaces*. 70:142-146.

Baldi, F., D. Marchetto, S. Paganelli, and O. Piccolo. 2011. Bio-generated metal binding polysaccharides as catalysts for synthetic applications and organic pollutant transformations. *New Biotechnology*. 29:74-78.

Barefoot, R.R. 1999. Distribution and speciation of platinum group elements in environmental matrices. *TrAC Trends in Analytical Chemistry*. 18:702-707.

Baxter-Plant, V.S., I.P. Mikheenko, and L.E. Macaskie. 2003. Sulphate reducing bacteria, palladium and the reductive dehalogenation of chlorinated compounds. *Biodegradation*. 14:83-90.

Bechard, G., H. Yamazaki, W.D. Gould, and P. Bedard. 1994. Use of cellulosic substrates for the microbial treatment of acid-mine drainage. *Journal of Environmental Quality*. 23:111-116.

Bennett, J.A., N.J. Creamer, K. Deplanche, L.E. Macaskie, I.J. Shannon, and J. Wood. 2010. Palladium supported on bacterial biomass as a novel heterogeneous catalyst: A comparison of Pd/Al_2O_3 and bio-Pd in the hydrogenation of 2-pentyne. *Chemical Engineering Science*. 65:282-290.

Bennett, J.A., I.P. Mikheenko, K. Deplanche, I.J. Shannon, J. Wood, and L.E. Macaskie. 2013. Nanoparticles of palladium supported on bacterial biomass: New re-usable heterogeneous catalyst with comparable activity to homogeneous colloidal Pd in the Heck reaction. *Applied Catalysis B: Environmental*. 140–141:700-707.

Blanco, A., B. Sanz, M.a.J. Llama, and J.L. Serra. 1999. Biosorption of heavy metals to immobilised *Phormidium laminosum* biomass. *Journal of Biotechnology*. 69:227-240.

Boone, D.R., Y.T. Liu, Z.J. Zhao, D.L. Balkwill, G.R. Drake, T.O. Stevens, and H.C. Aldrich. 1995. *Bacillus-infernus* sp-nov, an Fe(III)-reducing and Mn(IV)-reducing anaerobe from the deep terrestrial subsurface. *International Journal of Systematic Bacteriology*. 45:441-448.

Bucking, C., A. Piepenbrock, A. Kappler, and J. Gescher. 2012. Outer-membrane cytochrome-independent reduction of extracellular electron acceptors in *Shewanella oneidensis*. *Microbiology-Sgm*. 158:2144-2157.

Bunge, M., L.S. Sobjerg, A.E. Rotaru, D. Gauthier, A.T. Lindhardt, G. Hause, K. Finster, P. Kingshott, T. Skrydstrup, and R.L. Meyer. 2010. Formation of palladium(0) nanoparticles at microbial surfaces. *Biotechnology and Bioengineering*. 107:206-215.

Burnett, R.T., J. Brook, T. Dann, C. Delocla, O. Philips, S. Cakmak, R. Vincent, M.S. Goldberg, and D. Krewski. 2000. Association between particulate- and gas-phase components of urban air pollution and daily mortality in eight Canadian cities. *Inhalation Toxicology*. 12:15-39.

Burns, B., R. Grigg, V. Santhakumar, V. Sridharan, P. Stevenson, and T. Worakun. 1992. Palladium catalysed tandem cyclisation-anion capture processes. Part 1.

Background and hydride ion capture by alkyl- and π-allyl-palladium species. *Tetrahedron*. 48:7297-7320.

Bursakov, S., M.-Y. Liu, W.J. Payne, J. LeGall, I. Moura, and J.J.G. Moura. 1995. Isolation and preliminary characterization of a soluble nitrate reductase from the sulfate reducing organism *Desulfovibrio desulfuricans* ATCC 27774. *Anaerobe*. 1:55-60.

Carepo, M., J.F. Baptista, A. Pamplona, G. Fauque, J.J.G. Moura, and M.A.M. Reis. 2002. Hydrogen metabolism in *Desulfovibrio desulfuricans* strain New Jersey (NCIMB 8313) - comparative study with *D. vulgaris and D. gigas* species. *Anaerobe*. 8:325-332.

Cawthorn, R.G. 1999. The platinum and palladium resources of the Bushveld Complex. *South African Journal of Science*. 95:481-489.

Charbonnier, M., M. Romand, Y. Goepfert, D. Léonard, F. Bessueille, and M. Bouadi. 2006. Palladium (+2) reduction: A key step for the electroless Ni metallization of insulating substrates by a tin-free process. *Thin Solid Films*. 515:1623-1633.

Chen, J., and K. Huang. 2006. A new technique for extraction of platinum group metals by pressure cyanidation. *Hydrometallurgy*. 82:164-171.

Chen, J.H., K. Chen, Y.R. 2005. Hydrometallurgical leaching method for extracting platinum, palladium, copper and nickel from the sulfide flotation concentrates containing platinum metals. South Africa.

Chen, M.-H. 2010. Understanding world metals prices—Returns, volatility and diversification. *Resources Policy*. 35:127-140.

Chidambaram, D., T. Hennebel, S. Taghavi, J. Mast, N. Boon, W. Verstraete, D. Van der leslie, and J.P. Fitts. 2010. Concomittant microbial generation of palladium nanoparticles and hydrogen to immobilize chromate. *Environmental Science and Technology*. 44:7635-7640.

Childers, S.E., S. Ciufo, and D.R. Lovley. 2002. *Geobacter metallireducens* accesses insoluble Fe(III) oxide by chemotaxis. *Nature*. 416:767-769.

Cole-Hamilton, D.J. 2003. Homogeneous Catalysis: New Approaches to Catalyst Separation, Recovery, and Recycling. *Science*. 299:1702-1706.

Colombo, C., A.J. Monhemius, and J.A. Plant. 2008. The estimation of the bioavailabilities of platinum, palladium and rhodium in vehicle exhaust catalysts and road dusts using a physiologically based extraction test. *Science of The Total Environment*. 389:46-51.

Cotter, P.D., C.G.M. Gahan, and C. Hill. 2000. Analysis of the role of the Listeria monocytogenes F0F1-ATPase operon in the acid tolerance response. *International Journal of Food Microbiology*. 60:137-146.

Cotter, P.D., and C. Hill. 2003. Surviving the acid test: Responses of bacteria to low pH. *Microbiology and Molecular Biology Reviews*. 67:429-453.

Coursolle, D., and J.A. Gralnick. 2010. Modularity of the Mtr respiratory pathway of Shewanella oneidensis strain MR-1. *Molecular Microbiology*. 77:995-1008.

Cowley, A. 2013. Platinum 2013 Interim Review. Johnson Matthey PLC, Hertfordshire, England. 2-35.

Cox, A.D., and S.G. Wilkinson. 1989. Polar lipids and fatty acids of *Pseudomonas cepacia*. *Biochimica et Biophysica Acta - Lipids and Lipid Metabolism*. 1001:60-67.

Cravatt, B.F., K. Demarest, M.P. Patricelli, M.H. Bracey, D.K. Giang, B.R. Martin, and A.H. Lichtman. 2001. Supersensitivity to anandamide and enhanced endogenous cannabinoid signaling in mice lacking fatty acid amide hydrolase. *Proceedings of the National Academy of Sciences of the United States of America*. 98:9371-9376.

Creamer, N.J., V.S. Baxter-Plant, J. Henderson, M. Potter, and L.E. Macaskie. 2006. Palladium and gold removal and recovery from precious metal solutions and electronic scrap leachates by *Desulfovibrio desulfuricans*. *Biotechnology Letters*. 28:1475-1484.

Creamer, N.J., I.P. Mikheenko, P. Yong, K. Deplanche, D. Sanyahumbi, J. Wood, K. Pollmann, M. Merroun, S. Selenska-Pobell, and L.E. Macaskie. 2007. Novel supported Pd hydrogenation bionanocatalyst for hybrid homogeneous/heterogeneous catalysis. *Catalysis Today*. 128:80-87.

Crundwell, F.K., M.S. Moats, V. Ramachandran, T.G. Robinson, and W.G. Davenport. 2011. Chapter 31 - Platinum-Group Metals, Production, Use and Extraction Costs. *In* Extractive Metallurgy of Nickel, Cobalt and Platinum Group Metals. Elsevier, Oxford. 395-409.

Curnow, A.W., K.-W. Hong, R. Yuan, S.-I. Kim, O. Martins, W. Winkler, T.M. Henkin, and D. Soll. 1997. Glu-tRNA^{Gln} amidotransferase: A novel heterotrimeric enzyme required for correct decoding of glutamine codons during translation. *Proc. Natl. Acad. Sci. USA*. 94:11819-11826.

Cutillas, N., G.S. Yellol, C. de Haro, C. Vicente, V. Rodríguez, and J. Ruiz. 2013. Anticancer cyclometalated complexes of platinum group metals and gold. *Coordination Chemistry Reviews*. In Press.

Das, N. 2010. Recovery of precious metals through biosorption - A review. *Hydrometallurgy*. 103:180-189.

Davies, J., and D. Davies. 2010. Origins and evolution of antibiotic resistance. *Microbiology and Molecular Biology Reviews*. 74:417-433.

Dawson, M.F. 1984. Testwork on samples of oxidized ore from the Potgietersrus Prospect. *MINTEK Rep. M59D, Council for Mineral Technology, Randburg, S. Africa.*

De Corte, S., S. Bechstein, A.R. Lokanathan, J. Kjems, N. Boon, and R.L. Meyer. 2013. Comparison of bacterial cells and amine-functionalized abiotic surfaces as support for Pd nanoparticle synthesis. *Colloids and Surfaces B: Biointerfaces*. 102:898-904.

De Corte, S., T. Sabbe, T. Hennebel, L. Vanhaecke, B. De Gusseme, W. Verstraete, and N. Boon. 2012. Doping of biogenic Pd catalysts with Au enables dechlorination of diclofenac at environmental conditions. *Water Research*. 46:2718-2726.

de Sena, M.F.M., L.P. Rosa, and A. Szklo. 2013. Will Venezuelan extra-heavy oil be a significant source of petroleum in the next decades? *Energy Policy*. 61:51-59.

de Vargas, I., L.E. Macaskie, and E. Guibal. 2004. Biosorption of palladium and platinum by sulfate-reducing bacteria. *Journal of Chemical Technology and Biotechnology*. 79:49-56.

de Vargas, I., D. Sanyahumbi, M.A. Ashworth, C.M. Hardy, and L.E. Macaskie. 2005. Use of X-ray photoelectron spectroscopy to elucidate the mechanism of palladium and platinum biosorption by *Desulfovibrio desulfuricans* biomass. *In* 25th - 29th September; 16th int. Biohydrometallurgy Symp. S.T.L. Harrison, Rawlings, D.E., Petersen, J., editor, Cape Town. 605-616.

De Windt, W., P. Aelterman, and W. Verstraete. 2005. Bioreductive deposition of palladium (0) nanoparticles on *Shewanella oneidensis* with catalytic activity towards reductive dechlorination of polychlorinated biphenyls. *Environmental Microbiology*. 7:314-325.

Dembitsky, V.M., I. Shkrob, and O.A. Rozentsvet. 2000. Fatty acid amides from freshwater green alga Rhizoclonium hieroglyphicum. *Phytochemistry*. 54:965-967.

Deplanche, K. 2008. New nanocatalysts made by bacteria from metal solutions and recycling of metal wastes. Vol. PhD Thesis. PhD Thesis, University of Birmingham, UK.

Deplanche, K., J.A. Bennett, I.P. Mikheenko, J. Omajali, A.S. Wells, R.E. Meadows, J. Wood, and L.E. Macaskie. 2014. Catalytic activity of biomass-supported Pd nanoparticles: Influence of the biological component in catalytic efficacy and potential application in 'green' synthesis of fine chemicals and pharmaceuticals. *Applied Catalysis B: Environmental*. 147:651-665.

Deplanche, K., I. Caldelari, I.P. Mikheenko, F. Sargent, and L.E. Macaskie. 2010. Involvement of hydrogenases in the formation of highly catalytic Pd(0) nanoparticles by bioreduction of Pd(II) using *Escherichia coli* mutant strains. *Microbiology-SGM*. 156:2630-2640.

Deplanche, K., M.L. Merroun, M. Casadesus, D.T. Tran, I.P. Mikheenko, J.A. Bennett, J. Zhu, I.P. Jones, G.A. Attard, J. Wood, S. Selenska-Pobell, and L.E. Macaskie. 2012. Microbial synthesis of core/shell gold/palladium nanoparticles for applications in green chemistry. *Journal of the Royal Society Interface*. 9:1705-1712.

Deplanche, K., I.P. Mikheenko, J.A. Bennett, M. Merroun, H. Mounzer, J. Wood, and L.E. Macaskie. 2011a. Selective Oxidation of Benzyl-Alcohol over Biomass-Supported Au/Pd Bioinorganic Catalysts. *Top Catal*. 54:1110-1114.

Deplanche, K., A. Murray, S. Taylor, and L.E. Macaskie. 2011b. Biorecycling of precious metals and rare earth elements. *In* Nanomaterials. M.M. Rahman, editor. In Tech publishing principles.

Deplanche, K., T.J. Snape, S. Hazrati, and L.E. Macaskie. 2009. Versatility of a new bioinorganic catalyst: palladized cells of *Desulfovibrio desulfuricans* and application to dehalogenation of flame retardant materials. *Environ. Technol*. 30:681-692.

Devane, W.A., L. Hanus, A. Breuer, R.G. Pertwee, L.A. Stevenson, G. Griffin, D. Gibson, A. Mandelbaum, A. Etinger, and R. Mechoulam. 1992. Isolation and structure of a brain constituent that binds to the cannabinoid receptor. *Science*. 258:1946-1949.

Dobson, R.S., and J.E. Burgess. 2007. Biological treatment of precious metal refinery wastewater: A review. *Minerals Engineering*. 20:519-532.

Du, L.-N., B. Wang, G. Li, S. Wang, D.E. Crowley, and Y.-H. Zhao. 2012. Biosorption of the metal-complex dye Acid Black 172 by live and heat-treated biomass of Pseudomonas sp. strain DY1: Kinetics and sorption mechanisms. *Journal of Hazardous Materials*. 205–206:47-54.

Dufrêne, Y.F., and P.G. Rouxhet. 1996. X-ray photoelectron spectroscopy analysis of the surface composition of Azospirillum brasilense in relation to growth conditions. *Colloids and Surfaces B: Biointerfaces*. 7:271-279.

Dunleavy, J.K. 2006. Sulfur as a catalyst poison. *Platinum Metals Review*. 50:110.

El Kadib, A. 2015. Chitosan as a Sustainable Organocatalyst: A Concise Overview. *Chemsuschem*. 8:217-244.

Elias, D.A., J.M. Suflita, M.J. McInerney, and L.R. Krumholz. 2004. Periplasmic cytochrome c(3) of Desulfovibrio vulgaris is directly involved in H-2-mediated metal but not sulfate reduction. *Applied and Environmental Microbiology*. 70:413-420.

Elliott, P., S. Ragusa, and D. Catcheside. 1998. Growth of sulfate-reducing bacteria under acidic conditions in an upflow anaerobic bioreactor as a treatment system for acid mine drainage. *Water Research*. 32:3724-3730.

Estrade-Szwarckopf, H. 2004. XPS photoemission in carbonaceous materials: A "defect" peak beside the graphitic asymmetric peak. *Carbon*. 42:1713-1721.

Ezzili, C., K. Otrubova, and D.L. Boger. 2010. Fatty acid amide signaling molecules. *Bioorganic & Medicinal Chemistry Letters*. 20:5959-5968.

Fahmy, K., M. Merroun, K. Pollmann, J. Raff, O. Savchuk, C. Hennig, and S. Selenska-Pobell. 2006. Secondary structure and Pd-(II) coordination in S-layer proteins from *Bacillus sphaericus* studied by infrared and x-ray absorption spectroscopy. *Biophysical Journal*. 91:996-1007.

Fairley, N. 2013. CasaXPS. Casa Software Ltd. www.casaxps.com.

Farrell, E.K., and D.J. Merkler. 2008. Biosynthesis, degradation and pharmacological importance of the fatty acid amides. *Drug Discovery Today*. 13:558-568.

Fathima, A., J.R. Rao, and B.U. Nair. 2012. Trivalent chromium removal from tannery effluent using kaolin-supported bacterial biofilm of *Bacillus* sp. isolated from chromium polluted soil. *J. Chem Technol Biotechnol*. 87:271-279.

Faulds, C.B., and G. Williamson. 1999. The role of hydroxycinnamates in the plant cell wall. *Journal of the Science of Food and Agriculture*. 79:393-395.

Fayaz, A.M., K. Balaji, M. Girilal, R. Yadav, P.T. Kalaichelvan, and R. Venketesan. 2010. Biogenic synthesis of silver nanoparticles and their synergistic effect with antibiotics: a study against and bacteria. *Nanomedicine: Nanotechnology, Biology and Medicine*. 6:103-109.

Feather, C.A. 1978. Mineralogical considerations in the recovery of platinum group minerals from Witwatersrand Mines gravity concentrates. *Transactions of the Geological Society of South Africa*. 81:229-231.

Feio, M.J., I.B. Beech, M. Carepo, J.M. Lopes, C.W.S. Cheung, R. Franco, J. Guezennec, J.R. Smith, J.I. Mitchell, J.J.G. Moura, and A.R. Lino. 1998. Isolation and characterisation of a novel sulphate-reducing bacterium of the Desulfovibrio genus. *Anaerobe*. 4:117-130.

Fogg, D.E., and E.N. dos Santos. 2004. Tandem catalysis: a taxonomy and illustrative review. *Coordination Chemistry Reviews*. 248:2365-2379.

Foulkes, J.M., K.J. Malone, V.S. Coker, N.J. Turner, and J.R. Lloyd. 2011. Engineering a biometallic whole cell catalyst for enantioselective deracemization reactions. *ACS Catalysis*. 1:1589-1594.

Frazzoli, C., R. Dragone, A. Mantovani, C. Massimi, and L. Campanella. 2007. Functional toxicity and tolerance patterns of bioavailable Pd(II), Pt(II), and Rh(III) on suspended *Saccharomyces cerevisiae* cells assayed in tandem by a respirometric biosensor. *Analytical and Bioanalytical Chemistry*. 389:2185-2194.

Fuertes, M.A., J. Castilla, C. Alonso, and J.M. Perez. 2003. Cisplatin biochemical mechanism of action: From cytotoxicity to induction of cell death through

interconnections between apoptotic and necrotic pathways. *Current Medicinal Chemistry*. 10:257-266.

Galbraith, L., M.H. Jonsson, L.C. Rudhe, and S.G. Wilkinson. 1999. Lipids and fatty acids of *Burkholderia* and *Ralstonia* species. *FEMS Microbiology Letters*. 173:359-364.

Gasteiger, H.A., W. Gu, B. Litteer, R. Makharia, B. Brady, M. Budinski, E. Thompson, F.T. Wagner, S.G. Yan, and P.T. Yu. 2008. Catalyst Degradation Mechanisms in PEM and Direct Methanol Fuel Cells. *In* Mini-Micro Fuel Cells. S. Kakaç, A. Pramuanjaroenkij, and L. Vasiliev, editors. Springer Netherlands. 225-233.

Gates, B.C. 1992. Catalytic chemistry. John Wiley & Sons, New York, U.S.A.

Geng, H., Y. Zhu, K. Mullen, C.S. Zuber, and M.M. Nakano. 2007. Characterization of ResDE-dependent *fnr* transcription in *Bacillus subtilis*. *Journal of Bacteriology*. 189:1745-1755.

Goldsworthy, M.J.H. 2011. Hydrocarbon biosynthesis in *Mycobacterium* sp. NCIMB 10403 and *Desulfovibrio desulphuricans*. PhD Thesis. Unversity of Exeter, Exeter.

Gómez, B., M.A. Palacios, M. Gómez, J.L. Sanchez, G. Morrison, S. Rauch, C. McLeod, R. Ma, S. Caroli, A. Alimonti, F. Petrucci, B. Bocca, P. Schramel, M. Zischka, C. Petterson, and U. Wass. 2002. Levels and risk assessment for humans and ecosystems of platinum-group elements in the airborne particles and road dust of some European cities. *Science of The Total Environment*. 299:1-19.

Gordon, R.B., M. Bertram, and T.E. Graedel. 2006. Metal stocks and sustainability. *Proceedings of the National Academy of Sciences of the United States of America*. 103:1209-1214.

Gramp, J.P., J.M. Bigham, F.S. Jones, and O.H. Tuovinen. 2010. Formation of Fe-sulfides in cultures of sulfate-reducing bacteria. *Journal of Hazardous Materials*. 175:1062-1067.

Guibal, E. 2005. Heterogeneous catalysis on chitosan-based materials: a review. *Progress in Polymer Science*. 30:71-109.

Hao, J.O. 2003. The sulphate-reducing bacteria. *In* The Hand book of water and waste water microbiology. D. Mara and N. Horan, editors. Academic press, London, UK.

Harrad, S., M. Robson, S. Hazrati, V.S. Baxter-Plant, K. Deplanche, M.D. Redwood, and L.E. Macaskie. 2007. Dehalogenation of polyclorinated biphenyls and polybrominated dipheny ethers using a hybrid bioinorganic catalyst. *J.Environ Monito*. 9:314-318.

Hart, A., G. Leeke, M. Greaves, and J. Wood. 2014. Downhole Heavy Crude Oil Upgrading Using CAPRI: Effect of Steam upon Upgrading and Coke Formation. *Energy & Fuels*. 28:1811-1819.

Hasik, M., A. Bernasik, A. Drelinkiewicz, K. Kowalski, E. Wenda, and J. Camra. 2002. XPS studies of nitrogen-containing conjugated polymers–palladium systems. *Surface Science*. 507–510:916-921.

Hecker, M., J. Pane-Farre, and U. Volker. 2007. SigB-dependent general stress response in Bacillus subtilis and related bacteria. *In* Annual Review of Microbiology. Vol. 61. 215-236.

Heidelberg, J. F. Seshadri, R. Haveman, S. A. Hemme, C. L. Paulsen, I. T. Kolonay, J. F. Eisen, J. A. Ward, N. Methe, B. Brinkac, L. M. Daugherty, S. C. Deboy, R. T. Dodson, R. J. Durkin, A. S. Madupu, R. Nelson, W. C. Sullivan, S. A. Fouts, D.

Haft, D. H. Selengut, J. Peterson, J. D. Davidsen, T. M.; Zafar, N. Zhou, L. Radune, D. Dimitrov, G. Hance, M. Tran, K.; Khouri, H. Gill, J. Utterback, T. R.; Feldblyum, T. V. Wall, J. D. Voordouw, G. Fraser, C. M., The genome sequence of the anaerobic, sulfate-reducing bacterium *Desulfovibrio vulgaris* Hildenborough. *Nat Biotech.* 22: 554-559.

Hennebel, T., J. Benner, P. Clauaert, L. Vanhaecke, P. Aelterman, N. Boon, and W. Verstraete. 2011. Dehalogenation of environmental pollutants in microbial electrolysis cells with biogenic palladium nanoparticles. *Biotechnol Lett*. 33:89-95.

Hennebel, T., B. De Gusseme, N. Boon, and W. Verstraete. 2009. Biogenic metals in advanced water treatment. *Trends in Biotechnology*. 27:90-98.

Heugebaert, T.S.A., S. De Corte, T. Sabbe, T. Hennebel, W. Verstraete, N. Boon, and C.V. Stevens. 2012. Biodeposited Pd/Au bimetallic nanoparticles as novel Suzuki catalysts. *Tetrahedron Letters*. 53:1410-1412.

Higgins, K.A., C.E. Carr, and M.J. Maroney. 2012. Specific Metal Recognition in Nickel Trafficking. *Biochemistry*. 51:7816-7832.

Hines, M.E., D.A. Bazylinski, J.B. Tugel, and W. Berry Lyons. 1991. Anaerobic microbial biogeochemistry in sediments from two basins in the Gulf of Maine: Evidence for iron and manganese reduction. *Estuarine, Coastal and Shelf Science*. 32:313-324.

Humphries, A.C., I.P. Mikheenko, and L.E. Macaskie. 2006. Chromate reduction by immobilized palladized sulfate-reducing bacteria. *Biotechnology and Bioengineering*. 94:81-90.

Jacobsen, R.T. 2005. Catalyst recovery - Part 3: Removing contaminants from spent catalysts. *Chemical Engineering Progress*. 101:41-43.

Jimenez de Aberasturi, D., R. Pinedo, I. Ruiz de Larramendi, J.I. Ruiz de Larramendi, and T. Rojo. 2011. Recovery by hydrometallurgical extraction of the platinum-group metals from car catalytic converters. *Minerals Engineering*. 24:505-513.

Johnson, D.B. 1998. Biodiversity and ecology of acidophilic microorganisms. *FEMS Microbiology Ecology*. 27:307-317.

Johnson, M.D., J. Bell, K. Clarke, R. Chandler, P. Pathak, Y. Xia, R.L. Marshall, G.M. Weinstock, N.J. Loman, P.J. Winn, and P.A. Lund. 2014. Characterization of mutations in the PAS domain of the EvgS sensor kinase selected by laboratory evolution for acid resistance in *Escherichia col*i. *Molecular Microbiology*. 93:911-927.

Jollie, D. 2009. Palladium use in diesel oxidation catalyst. In *Platinum* 2009. *Johnson Matthey*.

Jollie, D. 2010. Platinum 2010. *Johnson Matthey*.

Kai, S. 2000. XPS Theory. John Wiley & Sons, Ltd.

Kanbayashi, N., K. Takenaka, T.-a. Okamura, and K. Onitsuka. 2013. Asymmetric auto-tandem catalysis with a planar-chiral ruthenium complex: sequential allylic amidation and atom-transfer radical cyclization. *Angewandte Chemie-International Edition*. 52:4897-4901.

Kanický, V., V. Otruba, and J.M. Mermet. 1999. Comparison of some analytical performance characteristics in inductively coupled plasma spectrometry of platinum group metals and gold. *Talanta*. 48:859-866.

Karaküçük-İyidoğan, A., D. Taşdemir, E.E. Oruç-Emre, and J. Balzarini. 2011. Novel platinum(II) and palladium(II) complexes of thiosemicarbazones derived from 5-

substitutedthiophene-2-carboxaldehydes and their antiviral and cytotoxic activities. *European Journal of Medicinal Chemistry*. 46:5616-5624.

Kawasaki, W., K. Matsui, Y. Akakabe, N. Itai, and T. Kajiwara. 1998. Volatiles from *Zostera marina*. *Phytochemistry*. 47:27-29.

Kendall, T. 2004. 30 years in the development of autocatalysts and PGM mining in Russia. In

Platinum 2004. *Johnson Matthey*.

Kolarovic, A., M. Schnurch, and M.D. Mihovilovic. 2011. Tandem catalysis: from alkynoic acids and aryl iodides to 1,2,3-triazoles in one pot. *Journal of Organic Chemistry*. 76:2613-2618.

Krekeler, D., and H. Cypionka. 1995. The preferred electron acceptor of *Desulfovibrio desulfuricans* CSN. *FEMS Microbiology Ecology*. 17:271-277.

Laguna, C., F. González, C. García-Balboa, A. Ballester, M.L. Blázquez, and J.A. Muñoz. 2011. Bioreduction of iron compounds as a possible clean environmental alternative for metal recovery. *Minerals Engineering*. 24:10-18.

Law, N., S. Ansari, F.R. Livens, J.C. Renshaw, and J.R. Lloyd. 2008. Formation of Nanoscale Elemental Silver Particles via Enzymatic Reduction by Geobacter sulfurreducens. *Applied and Environmental Microbiology*. 74:7090-7093.

Leang, C., Coppi, M. V. Lovley, D. R. 2003. OmcB, a c-type polyheme cytochrome, involved in Fe (III) reduction in *Geobacter sulfurreducens*. *J Bacteriol* 185: 2096-103.

Lee, J.-c., and B.D. Pandey. 2012. Bio-processing of solid wastes and secondary resources for metal extraction – A review. *Waste Management*. 32:3-18.

Legall, J., W.J. Payne, L. Chen, M.Y. Liu, and A.V. Xavier. 1994. Localization and specificity of cytochromes and other electron-transfer proteins from sulphate-reducing bacteria. *Biochimie*. 76:655-665.

Leonardos, G., D. Kendall, and N. Bardard. 1969. Odour threshold determinations of 53 odourant chemicals. *J. Air Pollut. Control Assoc*. 29:91-95.

Lester, T., and D.C. Sherrington. 1995. Chemistry for waste minimisation. Blackie Academic, London. U.K.

Liermann, L.J., E.M. Hausrath, A.D. Anbar, and S.L. Brantley. 2007. Assimilatory and dissimilatory processes of microorganisms affecting metals in the environment. *Journal of Analytical Atomic Spectrometry*. 22:867-877.

Lill, S.O., and P.E. Siegbahn. 2009. An autocatalytic mechanism for NiFe-hydrogenase: reduction to Ni(I) followed by oxidative addition. *Biochemistry*. 48:1056-1066.

Lindahl, T., and B. Nyberg. 1972. Rate of depurination of native deoxyribonuleic acid. *Biochemistry*. 11:3610.

Liu, J., L. Wang, J. Harvey-White, B.X. Huang, H.-Y. Kim, S. Luquet, R.D. Palmiter, G. Krystal, R. Rai, A. Mahadevan, R.K. Razdan, and G. Kunos. 2008. Multiple pathways involved in the biosynthesis of anandamide. *Neuropharmacology*. 54:1-7.

Liu, S.J. 2001. Metallurgy of Platinum Group Metals. Metallurgical Industry Press, Beijin. 140, 181.

Lloyd, J.R. 2003. Microbial reduction of metals and radionuclides. *FEMS Microbiology Reviews*. 27:411-425.

Lloyd, J.R., J.M. Byrne, and V.S. Coker. 2011. Biotechnological synthesis of functional nanomaterials. *Current Opinion in Biotechnology*. 22:509-515.

Lloyd, J.R., and D.R. Lovley. 2001. Microbial detoxification of metals and radionuclides. *Current Opinion in Biotechnology*. 12:248-253.

Lloyd, J.R., P. Yong, and L.E. Macaskie. 1998. Enzymatic recovery of elemental palladium by using sulfate-reducing bacteria. *Applied and Environmental Microbiology*. 64:4607-4609.

Loones, K.T.J., B.U.W. Maes, C. Meyers, and J. Deruytter. 2006. Orthogonal and auto-tandem catalysis: Synthesis of dipyrido 1,2-a : 2 ',3 '-d imidazole and its benzo and aza analogues via inter- and intramolecular C-N bond formation. *Journal of Organic Chemistry*. 71:260-264.

Lovely, D.R. 1991. Dissimilatory Fe(III) and Mn(IV) reduction. *Microbiol Rev*. 55:259-287.

Lovely, D.R., and E.R. Philips. 1988. Novel mode of microbial energy metabolism: organic carbon oxidation coupled to dissimilatory reduction of iron or manganese. *Appl. Environ. Microbiol*. 54:1472-1480.

Lupton, F.S., R. Conrad, and J.G. Zeikus. 1984. Physiological-function of hydrogen metabolism during growth of sulfidogenic bacteria on organic substrates. *Journal of Bacteriology*. 159:843-849.

Mabbett, A.N., D. Sanyahumbi, P. Yong, and L.E. Macaskie. 2006. Biorecovered precious metals from industrial wastes. Single step conversion of a mixed metal liquid waste to a bioinorganic catalyst with environmental applications. *Environmental Science and Technology*. 40:1015-1021.

Mabbett, A.N., P. Yong, J.P.G. Farr, and L.E. Macaskie. 2004. Reduction of Cr(VI) by "Palladized" - Biomass of *Desulfovibrio desulfuricans* ATCC 29577. *Biotechnology and Bioengineering*. 87:104-109.

Macaskie, L.E., V.S. Baxter-Plant, N.J. Creamer, A.C. Humphries, I.P. Mikheenko, P.M. Mikheenko, D.W. Penfold, and P. Yong. 2005. Applications of bacterial hydrogenases in waste decontamination, manufacture of novel bionanocatalysts and in sustainable energy. *Biochemical Society Transactions*. 33:76-79.

Macaskie, L.E., I.P. Mikheenko, P. Yong, K. Deplanche, A.J. Murray, M. Paterson-Beedle, V.S. Coker, C.I. Pearce, R. Cutting, R.A.D. Pattrick, D. Vaughan, G. van der Laan, and J.R. Lloyd. 2010. Today's wastes, tomorrow's materials for environmental protection. *Hydrometallurgy*. 104:483-487.

Malvankar, N.S., M. Vargas, K. Nevin, P.L. Tremblay, K. Evans-Lutterodt, D. Nykypanchuk, E. Martz, M.T. Tuominen, and D.R. Lovley. 2015. Structural Basis for Metallic-Like Conductivity in Microbial Nanowires. *Mbio*. 6.

Marques, M.C., R. Coelho, A.L. De Lacey, I.A.C. Pereira, and P.M. Matias. 2010. The Three-Dimensional Structure of NiFeSe hydrogenase from *Desulfovibrio vulgaris* Hildenborough: A Hydrogenase without a bridging ligand in the active site in its oxidised, "as-Isolated" state. *Journal of Molecular Biology*. 396:893-907.

Martínez, J.P., M.P. Falomir, and D. Gozalbo. 2001. Chitin: A Structural Biopolysaccharide with Multiple Applications. *In* eLS. John Wiley & Sons, Ltd.

Matias, P.M., I.A.C. Pereira, C.M. Soares, and M.A. Carrondo. 2005. Sulphate respiration from hydrogen in *Desulfovibrio* bacteria: a structural biology overview. *Progress in Biophysics and Molecular Biology*. 89:292-329.

Maughan, H., and G. Van der Auwera. 2011. Bacillus taxonomy in the genomic era finds phenotypes to be essential though often misleading. *Infection, Genetics and Evolution*. 11:789-797.

Merget, R., and G. Rosner. 2001. Evaluation of the health risk of platinum group metals emitted from automotive catalytic converters. *Science of The Total Environment*. 270:165-173.

Migliore, L., G. Frenzilli, C. Nesti, S. Fortaner, and E. Sabbioni. 2002. Cytogenetic and oxidative damage induced in human lymphocytes by platinum, rhodium and palladium compounds. *Mutagenesis*. 17:411-417.

Mikheenko, I.P., M. Rousset, S. Dementin, and L.E. Macaskie. 2008. Bioaccumulation of palladium by *Desulfovibrio fructosovorans* wild-type and hydrogenase-deficient strains. *Applied and Environmental Microbiology*. 74:6144-6146.

Mock, P., and S.A. Schmid. 2009. Fuel cells for automotive powertrains—A techno-economic assessment. *Journal of Power Sources*. 190:133-140.

Mohammed Fayaz, A., K. Balaji, P.T. Kalaichelvan, and R. Venkatesan. 2009. Fungal based synthesis of silver nanoparticles—An effect of temperature on the size of particles. *Colloids and Surfaces B: Biointerfaces*. 74:123-126.

Mori, T., T. Nonaka, and K. Tazaki. 1992. Interaction of nutrients, moisture and pH on microbial corrosion of concrete sewer pipes. *Water Research*. 26:29-37.

Mudd, G.M. 2012. Key trends in the resource sustainability of platinum group elements. *Ore Geology Reviews*. 46:106-117.

Mudhoo, A., V.K. Garg, and S.B. Wang. 2012. Removal of heavy metals by biosorption. *Environmental Chemistry Letters*. 10:109-117.

Muyzer, G., and A.J.M. Stams. 2008. The ecology and biotechnology of sulphate-reducing bacteria. *Nature reviews. Microbiology*. 6:441-454.

Myers, C.R., and J.M. Myers. 1993. Ferric reductase is associated with the membranes of anaerobically grown *Shewanella-putrifuciens* MR-1. *FEMS Microbiology Letters*. 108:15-22.

Myers, C.R., and J.M. Myers. 1997. Outer membrane cytochromes of *Shewanella putrefaciens* MR-1: spectral analysis, and purification of the 83-kDa c-type cytochrome. *Biochim Biophys Acta*. 12:307-318.

Nakano, M.M., Y.P. Dailly, P. Zuber, and D.P. Clark. 1997. Characterization of anaerobic fermentative growth of *Bacillus subtilis*: Identification of fermentation end products and genes required for growth. *Journal of Bacteriology*. 179:6749-6755.

Nakano, M.M., and P. Zuber. 1998. Anaerobic growth of a "strict aerobe" (*Bacillus subtilis*). *Annual Review of Microbiology*. 52:165-190.

Nakatani, K., Y. Ogura, Y. Koda, T. Terashima, and M. Sawamoto. 2012. Sequence-Regulated Copolymers via Tandem Catalysis of Living Radical Polymerization and In Situ Transesterification. *Journal of the American Chemical Society*. 134:4373-4383.

Nejad, H.H., and M. Kazemeini. 2012. Optimization of Platinum Extraction by Trioctylphosphine Oxide in the Presence of Alkaline-Metal Salts. *Procedia Engineering*. 42:1302-1312.

Newman, D.K., E.K. Kennedy, J.D. Coats, D. Ahmann, and D.J. Ellis. 1997. Dissimilatory arsenate and sulfate reduction in *Desulfotomaculum auripigmentum* sp. nov. *Archives of Microbiology*. 168:380-388.

Niu, H., and B. Volesky. 1999. Characteristics of gold biosorption from cyanide solution. *Journal of Chemical Technology and Biotechnology*. 74:778-784.

Norilsk Nickel. 2008. Mineral reserves and resources statement.

Nutt, M.O., K.N. Heck, P. Alvarez, and M.S. Wong. 2006. Improved Pd-on-Au bimetallic nanoparticle catalysts for aqueous-phase trichloroethene hydrodechlorination. *Applied Catalysis B: Environmental*. 69:115-125.

Odom, J.M., and H.D. Peck Jr. 1981. Hydrogen cycling as a general mechanism for energy coupling in the sulphate-redcuing bacteria, *Desulfovibrio* sp. *FEMS Microbiol. Lett*. 12:47-50.

Ogata, H., K. Nishikawa, and W. Lubitz. 2015. Hydrogens detected by subatomic resolution protein crystallography in a NiFe hydrogenase. *Nature*. 520:571.

Ohara, H., and M. Yahata. 1996. L-Lactic acid production by *Bacillus* sp in anaerobic and aerobic culture. *Journal of Fermentation and Bioengineering*. 81:272-274.

Ohno, Y., I. Yano, T. Hiramatsu, and M. Masui. 1976. Lipids and fatty acids of a moderately halophilic bacterium, no. 101. *Biochimica et Biophysica Acta (BBA) - Lipids and Lipid Metabolism*. 424:337-350.

Omoike, A., and J. Chorover. 2006. Adsorption to goethite of extracellular polymeric substances from *Bacillus subtilis*. *Geochimica et Cosmochimica Acta*. 70:827-838.

Palacios, M.A., M.M. Gómez, M. Moldovan, G. Morrison, S. Rauch, C. McLeod, R. Ma, J. Laserna, P. Lucena, S. Caroli, A. Alimonti, F. Petrucci, B. Bocca, P. Schramel, S. Lustig, M. Zischka, U. Wass, B. Stenbom, M. Luna, J.C. Saenz, . Santamar a, and J.M. Torrens. 2000. Platinum-group elements: quantification in collected exhaust fumes and studies of catalyst surfaces. *Science of The Total Environment*. 257:1-15.

Patocka, J. 2008. Organic lead toxicity. *Acta medica*. 51:209-213.

Payne, R.B., D.A. Gentry, B.J. Rapp-Giles, L. Casalot, and J.D. Wall. 2002. Uranium reduction by Desulfovibrio desulfuricans strain G20 and a cytochrome c3 mutant. *Applied and Environmental Microbiology*. 68:3129-3132.

platinum, I. 2009. Impala platinum fact sheet.

Pollino, J.M., and M. Weck. 2002. Tandem catalysis and self-assembly: A one-pot approach to functionalized polymers. *Organic Letters*. 4:753-756.

Pollmann, K., J. Raff, M. Schnorpfeil, G. Radeva, and S. Selenska-Pobell. 2005. Novel surface layer protein genes in *Bacillus sphaericus* associated with unusual insertion elements. *Microbiology-SGM*. 151:2961-2973.

Postgate, J.R. 1979. The sulphate-reducing bacteria. Cambridge University Press, Cambridge, U.K. 1st edition.

Prasad, K.S., L.S. Kumar, S. Chandan, R.M.N. Kumar, and H.D. Revanasiddappa. 2013. Palladium(II) complexes as biologically potent metallo-drugs: Synthesis, spectral characterization, DNA interaction studies and antibacterial activity. *Spectrochimica Acta Part a-Molecular and Biomolecular Spectroscopy*. 107:108-116.

Pretzer, L.A., H.J. Song, Y.-L. Fang, Z. Zhao, N. Guo, T. Wu, I. Arslan, J.T. Miller, and M.S. Wong. 2013. Hydrodechlorination catalysis of Pd-on-Au nanoparticles varies with particle size. *Journal of Catalysis*. 298:206-217.

Pulvin, S., and C. Bourdillon. 1986. Kinetic-studies of hydrogen production by an hydrogenase reactor. *Enzyme and Microbial Technology*. 8:137-140.

Ramel, F., G. Brasseur, L. Pieulle, O. Valette, A. Hirschler-Rea, M.L. Fardeau, and A. Dolla. 2015. Growth of the Obligate Anaerobe *Desulfovibrio vulgaris* Hildenborough under Continuous Low Oxygen Concentration Sparging: Impact of the Membrane- Bound Oxygen Reductases. *Plos One*. 10.

Rao, C.R.M., and G.S. Reddi. 2000. Platinum group metals (PGM); occurrence, use and recent trends in their determination. *TrAC Trends in Analytical Chemistry*. 19:565-586.

Ravindra, K., L. Bencs, and R. Van Grieken. 2004. Platinum group elements in the environment and their health risk. *Science of The Total Environment*. 318:1-43.

Redwood, M.D., K. Deplanche, V.S. Baxter-Plant, and L.E. Macaskie. 2008. Biomass-supported palladium catalysts on *Desulfovibrio desulfuricans* and *Rhodobacter sphaeroides*. *Biotechnology and Bioengineering*. 99:1045-1054.

Reeburgh, W.S. 1983. Rates of biogeochemical processes in anoxic sediments. *Annu. Rev. Earth Planet. Sci*. 11:269-298.

Rjiba-Touati, K., I. Ayed-Boussema, A. Belarbia, A. Azzebi, A. Achour, and H. Bacha. 2013. Protective effect of recombinant human erythropoeitin against cisplatin cytotoxicity and genotoxicity in cultured Vero cells. *Experimental and Toxicologic Pathology*. 65:181-187.

Rotaru, A.E., W. Jiang, K. Finster, T. Skrydstrup, and R.L. Meyer. 2012. Non-enzymatic palladium recovery on microbial and synthetic surfaces. *Biotechnology and Bioengineering*. 109:1889-1897.

Royet, J., and R. Dziarski. 2007. Peptidoglycan recognition proteins: pleiotropic sensors and effectors of antimicrobial defences. *Nature Reviews Microbiology*. 5:264-277.

Schierl, R., and G. Fruhmann. 1996. Airborne platinum concentrations in Munich city buses. *Science of The Total Environment*. 182:21-23.

Schiffer, A., K. Parey, E. Warkentin, K. Diederichs, H. Huber, K.O. Stetter, P.M.H. Kroneck, and U. Ermler. 2008. Structure of the Dissimilatory Sulfite Reductase from the Hyperthermophilic Archaeon *Archaeoglobus fulgidus*. *Journal of Molecular Biology*. 379:1063-1074.

Schmid, M., S. Zimmermann, H.F. Krug, and B. Sures. 2007. Influence of platinum, palladium and rhodium as compared with cadmium, nickel and chromium on cell viability and oxidative stress in human bronchial epithelial cells. *Environment International*. 33:385-390.

Schröder, I., E. Johnson, and S. de Vries. 2003. Microbial ferric iron reductases. *FEMS Microbiology Reviews*. 27:427-447.

Schultze-Lam, S., D. Fortin, B.S. Davis, and T.J. Beveridge. 1996. Mineralization of bacterial surfaces. *Chemical Geology*. 132:171-181.

Scott, J.A., and S.J. Palmer. 1990. Sites of cadmium uptake in bacteria used for biosorption. *Applied Microbiology and Biotechnology*. 33:221-225.

Selenska-Pobell, S., P. Panak, V. Miteva, I. Boudakov, G. Bernhard, and H. Nitsche. 1999. Selective accumulation of heavy metals by three indigenous *Bacillus* strains, *B-cereus*, *B-megaterium* and *B-sphaericus*, from drain waters of a uranium waste pile. *FEMS Microbiology Ecology*. 29:59-67.

Senouci-Rezkallah, K., M.P. Jobin, and P. Schmitt. 2015. Adaptive responses of Bacillus cereus ATCC14579 cells upon exposure to acid conditions involve ATPase activity to maintain their internal pH. *Microbiologyopen*. 4:313-322.

Shed, K.G. 2010. *Cobalt*. *Washington, DC: United States Geological Survey*.

Shen, L.M., N.Z. Bao, P.E. Prevelige, and A. Gupta. 2010. Escherichia coli Bacteria-Templated Synthesis of Nanoporous Cadmium Sulfide Hollow Microrods for Efficient Photocatalytic Hydrogen Production. *Journal of Physical Chemistry C*. 114:2551-2559.

Shott, I. 2013. Osmium, chemical and engineering news. Available from. http://pubs.acs.org/cen/80th/osmium.html.

Shrestha, R., R.A. Dixon, and K.D. Chapman. 2003. Molecular identification of a functional homologue of the mammalian fatty acid amide hydrolase in *Arabidopsis thaliana*. *Journal of Biological Chemistry*. 278:34990-34997.

Sleytr, U.B., M. Sára, D. Pum, and B. Schuster. 2001. Characterization and use of crystalline bacterial cell surface layers. *Progress in Surface Science*. 68:231-278.

Sobjerg, L.S., D. Gauthier, A.T. Lindhardt, M. Bunge, K. Finster, R.L. Meyer, and T. Skrydstrup. 2009. Bio-supported palladium nanoparticles as a catalyst for Suzuki-Miyaura and Mizoroki-Heck reactions. *Green Chemstry*. 11:2041-2046.

Sobjerg, L.S., A.T. Lindhardt, T. Skrydstrup, K. Finster, and R.L. Meyer. 2011. Size control and catalytic activity of bio-supported palladium nanoparticles. *Colloids and Surfaces B: Biointerfaces*. 85:373-378.

Sofu, A., E. Sayilgan, and G. Guney. 2015. Experimental Design for Removal of Fe(II) and Zn(II) Ions by Different Lactic Acid Bacteria Biomasses. *International Journal of Environmental Research*. 9:93-100.

Stincone, A., N. Daudi, A.S. Rahman, P. Antczak, I. Henderson, J. Cole, M.D. Johnson, P. Lund, and F. Falciani. 2011. A systems biology approach sheds new light on *Escherichia coli* acid resistance. *Nucleic Acids Research*. 39:7512-7528.

Strycharz-Glaven, S.M., R.M. Snider, A. Guiseppi-Elie, and L.M. Tender. 2011. On the electrical conductivity of microbial nanowires and biofilms. *Energy & Environmental Science*. 4:4366-4379.

Sun, Y., M. Delucchi, and J. Ogden. 2011. The impact of widespread deployment of fuel cell vehicles on platinum demand and price. *International Journal of Hydrogen Energy*. 36:11116-11127.

Suresh Ak Fau - Pelletier, D.A., W. Pelletier Da Fau - Wang, J.-W. Wang W Fau - Moon, B. Moon Jw Fau - Gu, N.P. Gu B Fau - Mortensen, D.P. Mortensen Np Fau - Allison, D.C. Allison Dp Fau - Joy, T.J. Joy Dc Fau - Phelps, M.J. Phelps Tj Fau - Doktycz, and D. MJ. 2010. - Silver nanocrystallites: biofabrication using *Shewanella oneidensis*, and an evaluation of their comparative toxicity on and bacteria. *Environ Sci Technol*. 44:5210-5215.

Tang, K., V. Baskaran, and M. Nemati. 2009. Bacteria of the sulphur cycle: An overview of microbiology, biokinetics and their role in petroleum and mining industries. *Biochemical Engineering Journal*. 44:73-94.

Tang, Q.Z., D.X. Xia, X.Q. Jin, Q. Zhang, X.Q. Sun, and C.Y. Wang. 2013. Re/Mg bimetallic tandem catalysis for annulation of benzamides and Alkynes via C-H/N-H Functionalization. *Journal of the American Chemical Society*. 135:4628-4631.

Tebo, B.M., and A.Y. Obraztsova. 1998. Sulfate-reducing bacterium grows with Cr(VI), U(IV), Mn(IV), and Fe(III) as electron acceptors. *FEMS Microbiology Letters*. 162:193-198.

Thauer, R.K., K. Jungermann, and K. Decker. 1977. Energy conservation in chemotrophic anaerobic bacteria. *Bacteriol. Rev.* 41:100-180.

Thomas, V.C., M.R. Sadykov, S.S. Chaudhari, J. Jones, J.L. Endres, T.J. Widhelm, J.S. Ahn, R.S. Jawa, M.C. Zimmerman, and K.W. Bayles. 2014. A Central Role for Carbon-Overflow Pathways in the Modulation of Bacterial Cell Death. *Plos Pathogens*. 10.

Total. Reserves for the future. Vol. 2015. Total oil and Gas.
Tremblay, P.L., M. Aklujkar, C. Leang, K.P. Nevin, and D. Lovley. 2012. A genetic system for Geobacter metallireducens: role of the flagellin and pilin in the reduction of Fe(III) oxide. *Environmental Microbiology Reports*. 4:82-88.
Tuzen, M., O.D. Uluozlu, C. Usta, and M. Soylak. 2007. Biosorption of copper(II), lead(II), iron(III) and cobalt(II) on *Bacillus sphaericus*-loaded Diaion SP-850 resin. *Analytica Chimica Acta*. 581:241-246.
Twigg, M.V. 1996. Catalyst handbook. Manson Publishing Ltd, London, England.
Twigg, M.V. 2011. Catalytic control of emissions from cars. *Catalysis Today*. 163:33-41.
Valls, M., and V.c. de Lorenzo. 2002. Exploiting the genetic and biochemical capacities of bacteria for the remediation of heavy metal pollution. *FEMS Microbiology Reviews*. 26:327-338.
van As, B.A.C., J. van Buijtenen, T. Mes, A.R.A. Palmans, and E.W. Meijer. 2007. Iterative tandem catalysis of secondary diols and diesters to chiral polyesters. *Chemistry-a European Journal*. 13:8325-8332.
van Heijenoort, J. 2001. Formation of the glycan chains in the synthesis of bacterial peptidoglycan. *Glycobiology*. 11:25R-36R.
Vargas, M., K. Kashefi, E.L. Blunt-Harris, and D.R. Lovley. 1998. Microbiological evidence for Fe(III) reduction on early Earth. *Nature*. 395:65-67.
Veglió, F., F. Beolchini, and A. Gasbarro. 1997. Biosorption of toxic metals: an equilibrium study using free cells of Arthrobacter sp. *Process Biochemistry*. 32:99-105.
Venceslau, S.S., R.R. Lino, and I.A.C. Pereira. 2010. The Qrc Membrane Complex, Related to the Alternative Complex III, Is a Menaquinone Reductase Involved in Sulfate Respiration. *Journal of Biological Chemistry*. 285:22772-22781.
Volesky, B. 1994. Advances in biosorption of metals: Selection of biomass types. *FEMS Microbiology Reviews*. 14:291-302.
Voordouw, G. 2002. Carbon monoxide cycling by *Desulfovibrio vulgaris* Hildenborough. *J. Bacteriol.* 184:5903-5911.
Wang, H., N. Law, G. Pearson, B.E. van Dongen, R.M. Jarvis, R. Goodacre, and J.R. Lloyd. 2010. Impact of Silver(I) on the Metabolism of Shewanella oneidensis. *Journal of Bacteriology*. 192:1143-1150.
Wang, J., and C. Chen. 2009. Biosorbents for heavy metals removal and their future. *Biotechnology Advances*. 27:195-226.
Wang, M.Z., C.Y. Zhou, and C.M. Che. 2011. A silver-promoted auto-tandem catalysis for the synthesis of multiply substituted tetrahydrocarbazoles. *Chemical Communications*. 47:1312-1314.
Ward, J.M., D.M. Young, K.A. Fauvie, M.K. Wolpert, R. Davis, and A.M. Guarino. 1976. Comparative nephrotoxicity of platinum cancer chemotherapeutic-agents. *Cancer Treatment Reports*. 60:1675-1678.
Widdel, F., and N. Pfennig. 1981. Studies on dissimilatory sulphate-reducing bacteria that decompose fatty-acids. 1. Isolation of new sulphate-reducing bacteria enriched with acetate from saline environments - description of *Desulfobacter Postgatei* gen-nov, sp-nov. *Archives of Microbiology*. 129:395-400.
Wirtz, M., and M. Droux. 2005. Synthesis of the sulfur amino acids: cysteine and methionine. *Photosynth. Res.* 86:345-362.

Wiseman, C.L.S., and F. Zereini. 2009. Airborne particulate matter, platinum group elements and human health: A review of recent evidence. *Science of The Total Environment*. 407:2493-2500.

Wolny, D., J. Lodowska, M. Jaworska-Kik, S. Kurkiewicz, L. Weglarz, and Z. Dzierzewicz. 2011. Chemical composition of *Desulfovibrio desulfuricans* lipid A. *Archives of Microbiology*. 193:15-21.

Wong, P.K., and C.M. So. 1993. Copper accumulation by a strain of *Pseudomonas putida*. *Microbios*. 73:113-121.

Wood, J., L. Bodenes, J. Bennett, K. Deplanche, and L.E. Macaskie. 2010. Hydrogenation of 2-butyne-1,4-diol using novel bio-palladium catalysts. *Industrial & Engineering Chemistry Research*. 49:980-988.

Wu, J., W. Bu, K. Sheppard, M. Kitabatake, S.-T. Kwon, D. Söll, and J.L. Smith. 2009. Insights into tRNA-Dependent Amidotransferase Evolution and Catalysis from the Structure of the *Aquifex aeolicus* Enzyme. *Journal of Molecular Biology*. 391:703-716.

Wu, L., S. Shafii, M.R. Nordin, K.Y. Liew, and J. Li. 2012. Structure determination of chitosan-stabilized Pt and Pd based bimetallic nanoparticles by X-ray photoelectron spectroscopy and transmission electron microscopy. *Materials Chemistry and Physics*. 137:493-498.

Xiao, Z., and A.R. Laplante. 2004. Characterizing and recovering the platinum group minerals—a review. *Minerals Engineering*. 17:961-979.

Yamada, Y., C.K. Tsung, W. Huang, Z.Y. Huo, S.E. Habas, T. Soejima, C.E. Aliaga, G.A. Somorjai, and P.D. Yang. 2011. Nanocrystal bilayer for tandem catalysis. *Nature Chemistry*. 3:372-376.

Yan, J., A. Li, Y. Xu, T.P.N. Ngo, S. Phua, and Z. Li. 2012. Efficient production of biodiesel from waste grease: One-pot esterification and transesterification with tandem lipases. *Bioresource Technology*. 123:332-337.

Yang, C.J. 2009. An impending platinum crisis and its implications for the future of the automobile. *Energy Policy*. 37:1805-1808.

Yang, Z.Q., X. Meng, F. Breidt, L.L. Dean, and F.M. Arritt. 2015. Effects of Acetic Acid and Arginine on pH Elevation and Growth of Bacillus licheniformis in an Acidified Cucumber Juice Medium. *Journal of Food Protection*. 78:728-737.

Yao, F., W. Hao, and M.-Z. Cai. 2013. Copper(I)-catalyzed tandem reaction of 2-iodophenols with isothiocyanates in room temperature ionic liquids. *Journal of Organometallic Chemistry*. 723:137-142.

Yin, C.-Y., A.N. Nikoloski, and M. Wang. 2013. Microfluidic solvent extraction of platinum and palladium from a chloride leach solution using Alamine 336. *Minerals Engineering*. 45:18-21.

Yin, P., Q. Yu, B. Jin, and Z. Ling. 1999. Biosorption removal of cadmium from aqueous solution by using pretreated fungal biomass cultured from starch wastewater. *Water Research*. 33:1960-1963.

Yong, P., I.P. Mikheenko, K. Deplanche, M.D. Redwood, and L.E. Macaskie. 2010. Biorefining of precious metals from wastes: an answer to manufacturing of cheap nanocatalysts for fuel cells and power generation via an integrated biorefinery? *Biotechnology Letters*. 32:1821-1828.

Yong, P., M. Paterson-Beedle, I.P. Mikheenko, and L.E. Macaskie. 2007. From bio-mineralisation to fuel cells: biomanufacture of Pt and Pd nanocrystals for fuel cell electrode catalyst. *Biotechnology Letters*. 29:539-544.

Yong, P., N.A. Rowson, J.P.G. Farr, I.R. Harris, and L.E. Macaskie. 2002. Bioaccumulation of palladium by *Desulfovibrio desulfuricans*. *Journal of Chemical Technology and Biotechnology*. 77:593-601.

Zereini, F., H. Alsenz, C.L.S. Wiseman, W. Puettmann, E. Reimer, R. Schleyer, E. Bieber, and M. Wallasch. 2012. Platinum group elements (Pt, Pd, Rh) in airborne particulate matter in rural vs. urban areas of Germany: Concentrations and spatial patterns of distribution. *Science of The Total Environment*. 416:261-268.

Zereini, F., F. Alt, J. Messerschmidt, A. Von Bohlen, K. Liebl, and W. Puttmann. 2004. Concentration and distribution of platinum group elements (Pt, Pd, Rh) in airborne particulate matter in Frankfurt am Main, Germany. *Environmental Science & Technology*. 38:1686-1692.

Zhou, H., T.X. Fan, T. Han, X.F. Li, J. Ding, D. Zhang, Q.X. Guo, and H. Ogawa. 2009. Bacteria-based controlled assembly of metal chalcogenide hollow nanostructures with enhanced light-harvesting and photocatalytic properties. *Nanotechnology*. 20.

Zhu, J. 2014. Synthesis of Precious Metal Nanoparticles Supported on Bacterial Biomass for Catalytic Applications in Chemical Transformations. Vol. PhD. University of Birmingham.

Zienkiewicz-Strzalka, M., and S. Pikus. 2012. The study of palladium ions incorporation into the mesoporous ordered silicates. *Applied Surface Science*. 261:616-622.

CHAPTER 2 Materials and Methods

This chapter outlines the key methodologies used in this study. Details not included here can be found in the appendix. Each result chapter contains a self-contained materials and methods section for the purpose of clarity; general methods are described in this chapter.

2.1 Reagents and chemicals.

All reagents and chemicals used in this study were of analytical grade and were supplied by globally recognised chemical companies (Sigma-aldrich, UK and Fisher Scientific, UK). All solutions were prepared using ultra pure double-distilled water.

2.2 Bacterial strains used in this study

The bacterial strains used in this study were *Bacillus benzeovorans* NCIMB 12555 and *Desulfovibrio desulfuricans* (NCIMB 8326 and NCIMB 8307). All bacteria were obtained as lyophilised cultures from the National Collection for Industrial and Marine Bacteria (NCIMB), Aberdeen, United Kingdom, except for the *Desulfovibrio desulfuricans* strain NCIMB 8307 which was obtained from laboratory stock.

2.3 Media preparation and bacterial growth

Media for bacterial growth were prepared as specified in individual sections. *Bacillus benzeovorans* NCIMB 12555 (subsequently abbreviated as Bb) was grown aerobically using a rotary shaker (180 rpm, 30^{o}C) in a nutrient medium with the following composition in grams per litre: Lab-Lemco beef extract (1g), yeast extract (2g), peptone (5g), and NaCl (5g). The pH of the medium was adjusted to 7.3 before autoclaving at 121^{o}C for 15 min prior to use. Growth of *Desulfovibrio desulfuricans* (NCIMB 8307 and NCIMB 8326, abbreviated subsequently as Dd8307 and Dd8326) was done anaerobically at 30^{o}C without shaking. The *D. desulfuricans* were initially grown in a Postgate's B medium with the following composition in grams per litre: K_2HPO_4 (0.5g), NH_4Cl (1g), $CaSO_4$ (1g), $MgSO_4.7H_2O$ (2g), Sodium lactate (60%, 4ml), yeast extract (1g), thioglycollic acid (0.1g), ascorbic acid (0.1g), and $FeSO_4.7H_2O$ (0.5g). Note that the last three components (filter-sterilized) were added after autoclaving. The pH was adjusted to 7.4 ± 0.2 using 2M NaOH, dispensed in anaerobic bottles and sealed with

butyl rubber septa, degassed for 30 minutes under oxygen-free nitrogen and then autoclaved at 115^{o}C for 10 minutes. In this project, the inocula (10% v/v) of *Desulfovibrio desulfuricans* from Postgate's B medium were then transferred into Postgate's C production medium with the following composition in grams per litre: KH_2PO_4 (0.5g), NH_4Cl (1g), $NaSO_4$ (4.5g), $CaCl_2$. $6H_2O$ (0.06g), $MgSO_4.7H_2O$ (0.06g), yeast extract (1g), sodium lactate (1%v/v), $FeSO_4$. $7H_2O$ (0.004g) and trisodium citrate dehydrate ($C_6H_5O_7.2H_2O.3Na$) (0.3g) prepared by adjusting the pH to 7.5 ± 0.2 using 2M NaOH followed by autoclaving for 15 min at 121^{o}C.

2.4 Preparation of cells for metallisation

Prior to metallisation experiments, cells of *B. benzeovorans* and *D. desulfuricans* were harvested (Beckman Coulter Avati J-25 Centrifuge, U.S.A) by centrifugation (9,000 x g, 4^{o}C, 15 minutes) during exponential growth (OD_{600} 0.7 -1.0) and (OD_{600} 0.5-0.7) respectively and then washed three times in MOPS (4-morpholinepropanesulfonic acid)-NaOH buffer (20 mM, pH 7.0). The harvested cells were finally resuspended in the same buffer to give a concentration usually of 20-30mg/ml as determined by reference to a pre-determined OD_{600} to dry weight conversion (see Deplanche et al., 2008 and appendix for details). The cells were then stored at 4^{o}C until use, usually within 24 h.

2.4.1 Preparation of biocatalyst (mono- and bimetallic) by metallisation

Monometallic palladium biocatalyst is herein and subsequently called 'bio-Pd' while bimetallic palladium and platinum mixture as 'bio-Pd/Pt'. During monometallic biocatalyst preparation, a known volume of a concentrated resting cell suspension as described above was transferred into a volume of degassed (30 minutes) 2 mM Pd (II) solution (Na_2PdCl_4, pH 2 with 0.01 M HNO_3, 634µl) as appropriate (volume of Pd (II) solution will vary according to volume of cells used) to make 5wt% or 20wt% Pd (mass of Pd/mass of cells i.e. 1mg Pd/ 19mg cell or 4mg Pd/16mg cells respectively) on cells of *B. benzeovorans* and *Desulfovibrio desulfuricans*. The cells and palladium mixture were then allowed to stand in the solution (30 min, at 30^{o}C) for biosorption of the Pd (II) onto the cell surfaces. This was followed by reduction of the sorbed Pd (II) to Pd (0) under H_2 or with formate (to 20 mM) as exogenous electron donors (sees **Figure 2.1**). During Pd (II) reduction with hydrogen, Pd sorbed content was sparged with hydrogen

via rubber septum of anaerobic bottle while reduction with formate was achieved by injecting formate *via* rubber septum of anaerobic bottle. The reduction of the Pd (II) (removal from solution) was confirmed by a tin (II) chloride assay method described below. The metallised cells were harvested by centrifugation (9,000 x g, 4^{o}C, 15 minutes) and washed three times in distilled water and once in acetone. The washed bioPd (0) (palladized cells) was further resuspended in a small volume of acetone, dried in air to constant weight, and finely ground in an agate mortar with pestle and sieved (100 mesh size, i.e. 149-150µm) to give a dry black powder (biocatalyst, bio-Pd) while some samples (aqueous suspension), not ground, were prepared for characterization.

To prepare bimetallic palladium and platinum biocatalyst, a 2mM palladium (II) (Na_2PdCl_4) solution as above and 1mM platinum (IV) (K_2PtCl_6) solution set at pH 2 with 0.01M HNO_3 were prepared and degassed separately. First an appropriate cell suspension as above was transferred into a degassed solution of 2mM Pd (II) to make a 2.5wt% or 10wt% loading on cells followed by biosorption at the same condition as above. The Pd (II) solution was then purged with hydrogen for 15 min and then saturated for an additional 15 min and transferred to a rotary shaker (180 rpm, 30^{o}C) for complete reduction overnight due to a possible slow rate of reduction in samples with lower metal loading (2.5% Pd). Subsequently, the reduced Pd was washed twice with distilled water and resuspended in water (Deplanche et al., 2012) and was then used to reduce Pt (IV) solution under hydrogen to give a final metal loading of 5wt% (2.5%Pd/2.5%Pt) or 20wt% (10%Pd/10%Pt) on bacterial cells. The mixture was then saturated with hydrogen for 15 min in an anaerobic bottle and then placed in a rotary shake (180 rpm, 30^{o}C) for 1 hour to ensure complete reaction between the two metals while measuring the removal of Pd (II) and Pt (IV) by tin (II) chloride assay. The bimetallic catalyst was then washed and processed as the monometallic counterpart. In an alternative experiment, a 5wt% bio-Pd/Pt was prepared by initial seeding with 2wt% Pd (II) solution (2mM solution) followed by reduction of 1.5wt%Pd (from a 0.42mM) and 1.5wt%Pt (from a 0.34mM) mixed solutions by the 2wt% Pd (0) seed to give a final metal loading of 5wt% (2%Pd[/1.5%Pd/1.5%Pt] i.e 3.5%Pd/1.5%Pt) or as stated.

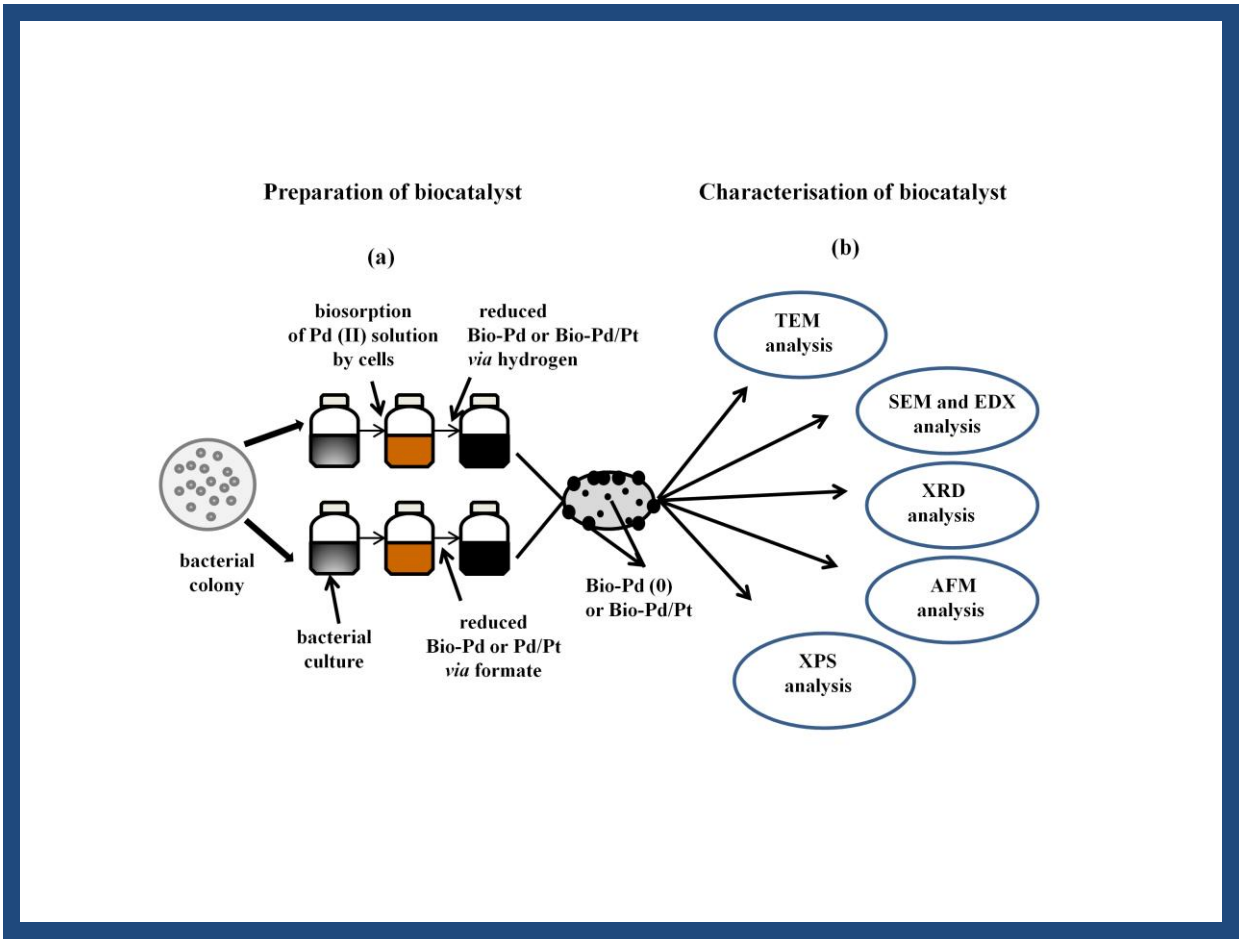

Figure 2. 1 An overview of catalyst preparation (a) from bacterial cells. Details of the characterisation techniques (b) are given in the section below. TEM, SEM, EDX, AFM, and XPS: see table of abbreviations and below.

2.5 Assay of metallic residual ions [Pd (II) and Pt (IV)]

Prior to harvesting the metalized cells, the complete reduction of Pd (II) or Pt (IV) was confirmed by a tin (II) chloride assay method previously described (Deplanche et al., 2010) spectrophotometrically (Ultraspec III, Pharmacia Biotech, Little Chalfront, Buckinghamshire, UK) by taking the absorbance reading of the sample at 463 nm after adding (800µl) tin (II) chloride to the sample supernatant (200µl). The tin (II) chloride solution was freshly prepared by dissolving 29.9 g $SnCl_2$ powder into 500 ml HCl.

2.6 Characterization of biocatalyst

2.6.1 Electron microscopy

Electron microscopy is a technique for obtaining high resolution images of biological and non-biological samples using electron beams with short wavelengths as a source of illuminating radiation (Massover, 2011). The two main types include transmission electron microscopy (TEM) which produces images of thin specimens (e.g. tissue or cell sections) (Mielanzyk et al., 2014) and scanning electron microscopy (SEM) which uses secondary electron emission from the surface of samples to view detailed images of specimen and whole organism (Peckys et al, 2009) that is not possible using TEM. The interaction of the primary electron beam with the surface of the sample generates low energy electrons, high energy backscattered electrons, X-rays and photons. The X-ray emission and backscattered electrons are used to identify elemental composition on samples *via* energy dispersive X-ray spectrometry (EDX) usually coupled to SEM or the thick section of TEM. Here Pd or Pd/Pt-loaded cells of *B. benzeovorans* NCIMB 12555 and *D. desulfuricans* (NCIMB 8307 and NCIMB 8326) were washed twice with distilled water and fixed with 2.5% (w/v) glutaraldehyde fixative in 0.1M phosphate buffer (pH 7.0, 4^{o}C) and stained with 1% osmium tetraoxide. For SEM (Scanning Electron Microscopy), the Pd-loaded cells were mounted on microscope stubs and examined by SEM (Philips XL-30, LaB6) fitted with an INCA energy dispersive X-ray Spectroscopy (EDX) system with peaks sought corresponding to X-ray emission energies of Pd (Yong et al., 2002) using a backscattering detector. For TEM (Transmission Electron Microscopy), the metal-loaded fixed cells were dehydrated using an ethanol series and washed twice in propylene oxide (Deplanche et al., 2010). The cells were embedded in epoxy resin and cut into thin sections (100-150nm thick), mounted on carbon-coated copper grids and viewed with a JEOL 1200EX transmission electron microscope, accelerating voltage 80Kv (initial studies) or using a FEI image Cs-corrector configuration Titan^{TM} G2 60-300 STEM microscope at the University of Granada, Spain, equipped with a HAADF (high angle annular dark field) detector, accelerating voltage of 300kV. This instrument enables detailed visualization of samples which was not possible with the JOEL 1200EX.

2.6.2 X-ray powder diffraction (XRD)

XRD is a non-destructive bulk technique that is used to characterize the crystalline component of materials. It also provides information on phases and crystal orientation and defects and provides information to structural properties like lattice parameter (e.g. strain and average grain size) and measure thickness of materials and also determining their atomic arrangement (Banaciu et al., 2015). For XRD analysis, bioPd (0) or bio-Pd/Pt was washed three times in distilled water and once in acetone, then resuspended in a small volume of acetone. This was then air dried and ground into a fine black powder in an agate mortar with pestle and then sieved as above. 50 mg of biocatalyst powder was mounted onto Scotch tape on a transmission ring and samples were rotated during data collection. The X-ray powder diffraction patterns were acquired using a Bruker AXS D8 Autosampler (Transmission) Diffractometer using a monochromatic high-intensity $CuK_{\alpha 1}$ radiation (λ = 1.5406 Å) equipped with a solid-state LynxEye position sensitive detector (PSD) with a 3^{o} electronic window. The XRD powder patterns were then compared to a reference standard in the Joint Committee for Powder Diffraction Standards (JCPDS) database (now International Committee for Diffraction Data (ICDD) database). The particle size of the biocatalyst was determined using Scherrer equation (Eq 2) using all peaks or major peaks (Jaboyedoff et al., 1999) as appropriate. The average crystallite size was calculated from the Scherrer equation:

$$D = 0.9\lambda/\beta\cos\theta\,, \qquad (2)$$

Where D is the crystallite size in angstrom (Å, finally converted to nanometer, nm), λ is the X-ray wavelength, $CuK_{\alpha 1}$ radiation (λ = 1.5406 Å), θ is the Bragg angle, and β is the full width at half maximum (fwhm, in radians) of the peaks considered.

2.6.3 Atomic force microscopy (AFM)

Atomic force microscopy is used to measure the topography of samples by using a sharp tip supported on a micro cantilever which deflects as it comes close to the sample (Wang et al., 2015). This deflection can then be detected by a sensitive detector, subsequently producing an image of the sample (Wang et al., 2015). In this study, an aliquot of metallised and metal-unsupplemented live cells were washed (16,000 x g, 4min) and distributed uniformly in sterile distilled water (for metallised cells) and 20 mM MOPS-NaOH buffer, pH 7.0 (live cells). The samples were then diluted

appropriately, mounted on a silicon wafer and dried in air at room temperature for 30 min. Topographies were acquired using a NanoWizard II atomic force microscope (JPK Instruments, UK) operating in intermittent contact mode at a tip velocity of 20 μm/s, employing pyramidal tipped Si cantilevers (PPP-NCL, Windsor Scientific, UK) while the data was processed using "JPK data processing software."

2.6.4 X-ray photoelectron spectroscopy (XPS)

XPS is a very important quantitative surface technique for the analysis of surface and chemical composition of organic, inorganic and hybrid materials by providing key information about their chemistry *via* binding energies between atoms in a sample (Zienkiewickz-Strzalka and Pikus, 2012). As many elements vary in their binding energies due to chemical changes, the interaction of an atom for instance with other neighbouring atoms results in chemical shifts in binding energies. These changes in energy can then be used as a measure to identify an atom and its oxidation state or type of chemical interaction with other neighbouring atoms (see section 1.2.1 for details). In this study, prior to XPS measurement, aliquots of metallised samples (biocatalyst) on cells were dropped and dried on a boron-doped silicon wafer (7x7mm in diameter) until enough deposits were acquired (usually ~5-10mg). The X-ray photoelectron spectroscopy (XPS) data were collected at the Science City Photoemission Facility, University of Warwick, UK. The samples were mounted on Omicron sample plates using electrically conductive carbon tape and loaded in to the fast-entry chamber. Once a pressure of less than 1 x 10^{-7} mbar was achieved (approx. 1 hour), the samples were transferred under vacuum to a 12-stage storage carousel, located between the preparation and main analysis chambers, for storage at pressures of less than 2 x 10^{-10}mbar. XPS measurements were made in the main analysis chamber (base pressure 2 x 10^{-11} mbar), with the sample being illuminated using an XM1000 monochromatic Al k_{α} x-ray source (Omicron Nanotechnology). The measurements were made at room temperature and at a take-off angle of 90°, allowing a maximum probe depth of approximately 5-10nm. The photoelectrons were detected using a Sphera electron analyser (Omicron Nanotechnology), with the core levels recorded using a pass energy of 10 eV (resolution approx. 0.47eV). Due to the insulating nature of the samples, a CN10 charge neutralizer (Omicron Nanotechnology) was used in order to prevent surface charging, whereby a low energy (typically 1.5 eV) beam of electrons was

directed on to the sample during XPS data acquisition. The data were converted into VAMAS format and analysed using the CasaXPS package, using Shirley backgrounds, mixed Gaussian-Lorentzian (Voigt) lineshapes and asymmetry parameters where appropriate. All binding energies were calibrated to the C 1s peaks originating from adventitious carbon at 284.6 eV. Control samples include metal-unsupplemented biomass, heat-killed cells and metal solution.

2.7 Catalytic test

2.7.1 Soybean oil hydrogenation

Soy bean oil was purchased from Sigma-Aldrich, UK and the derived fatty acid composition was determined using gas chromatography. The commercial soy bean oil contains mainly linolenic acid (*cis*-C18:3), linoleic acid (*cis*-C18:2), oleic acid (*cis*-C18:1), stearic acid (C18:0) and palmitic acid (C16:0) [1, 2 and 3 is the number of double bonds present]. The catalytic test was carried out by partial hydrogenation of soybean oil. This was performed in a 0.5 litre capacity batch reactor (Baskerville reactors and autoclaves Ltd Manchester, England) at 100^{o}C and 5 bar hydrogen pressure (agitation speed of 800 rpm, 5 h) by using a 150 mg of 5wt% bio-Pd (0) catalyst produced on cells. 150 ml of soybean oil was introduced into the reactor followed by catalyst addition and the reactor and its contents were purged with nitrogen. The first sample was withdrawn as the reaction temperature reached 100^{o}C prior to hydrogenation. Nitrogen was then released before hydrogen was introduced immediately for hydrogenation to proceed. Samples were then withdrawn at various suitable time intervals up to 5 hours and stored in the dark until analysis. Prior to sample analysis, the fatty acid content of the soybean oil was converted to fatty acid methyl esters (FAMEs) by derivatisation according to the method of Christy et al. (2009) with slight modification. In the derivatisation of hydrogenated soybean oil, 2ml of 0.5M NaOH/methanol was added to 0.2ml of hydrogenated soybean oil sample followed by heating in a water bath at 60^{o}C (15 min). After cooling, boron triflouride in methanol (BF3/methanol, vol/vol) mixture was added (2 ml) and heated for an additional 10 min. Then, 2ml of a saturated solution of NaCl and 1ml of hexane were added and shaken for a few minutes. The content was allowed to settle for a few minutes and the top hexane (organic) layer was extracted into a clean vial and stored in the dark prior to GC

analysis. Untreated soybean oil was used as control. GC analysis of samples (0.5µl) was done in a gas chromatograph (Varian CP-3380) equipped with a flame ionization detector (FID) with a 75 m SP^{TM}-2560 capillary column (Sigma-Aldrich, UK) and helium as carrier gas (flow rate, 30 ml/min), injector temperature (250^{o}C), detector temperature (265^{o}C), oven temperature (200-240^{o}C) at a ramp rate of 4^{o}C/min for a total analysis time of 30 min. Conversion of final product and selectivity to *trans* and *cis* fatty acid methyl esters was determined according to the following equations:

$$\textit{cis}\text{-C18:i Conversion (\%)} = \frac{[\textit{cis}\text{-C18:i}]_0 - [\textit{cis}\text{-C18:i}]_t}{[\textit{cis}\text{-C18:i}]_0} \times 100\% \qquad (2.4)$$

Note that i is the number of double bonds (1, 2, 3) present in soy bean oil sample analysed at time = 0 (untreated or unhydrogenated sample) and at various intervals of reaction, time = t (treated or hydrogenated samples).

$$\text{Selectivity (\%)} = \frac{\text{Amount of desired product formed}}{\text{Amounts of all products formed}} \times 100\% \qquad (2.5$$

2.7.2 Reductive dechlorination of chlorinated compounds

Reductive dechlorination is described in a later section (3.2.1). In this study, the catalytic activity of biocatalyst was determined by the release of chloride from chlorinated compounds (method based on those of Baxter-Plant et al., (2003) and Redwood et al., (2008). Bio-Pd (0) or bio-Pd/Pt (2mg) was suspended in 9ml of sterile and degassed MOPS-NaOH buffer (20mM, pH 7.0) in a 12ml serum bottle. The metal loading was 20wt% (0.4 mg Pd) and 0.4mg Pd of 5wt% palladium on carbon catalyst (Pd/C) (Sigma-Aldrich, UK). This was followed by the addition of chlorinated compound (concentration as specified in individual experiments) in hexane (1:1 v/v). The hexane partitioned the substrate (hexane) from the catalyst and chloride product (aq) (Redwood et al., 2008). After shaking (5 min) and separation, sample (1 ml aq) was taken to determine the chloride concentration (time = 0) and the catalyst was separated by centrifugation (16,000 x g, 4min). Reductive dehalogenation was initiated by the addition of sodium formate (1M, pH 7.0) to a final concentration of 10 mM. Samples were then taken from the aqueous phase at suitable time intervals, centrifuged (16,000 x g, 4min), and the supernatant was transferred into cuvettes. Reductive dehalogenation

was monitored by the release of Cl^- by measuring absorbance of sample supernatant at 460 nm. Controls included catalyst free mixture and unmetallised cells (metal-unsupplemented control). All experiments were in triplicate.

2.7.3 *In-situ* upgrading of heavy oil

The heavy oil feedstock used in this study was recovered from oil sands at Kerrobert, Saskatchewan by THAI (Toe-to-Heel Air Injection) and provided by Touchstone Exploration Inc, Canada. Since the feedstock was produced by the THAI process, it was partially upgraded by pyrolysis and its properties are shown in **Table 2**. Commercial catalyst (Ni-Mo/Al_2O_3) was supplied by Akzo Nobel (Amsterdam, Netherlands). The catalytic test was done by Dr Hart Abarasi, Chemical Engineering, University of Birmingham.

The catalytic activity of the biocatalyst and Ni-Mo/Al_2O_3 commercial catalyst (a reference) was tested in a stirred batch reactor (100 mL capacity, Baskerville, United Kingdom) using 15 g of heavy oil as feedstock. The reaction was done at an optimum reaction temperature of 425 ^oC, 30 min, stirring speed of 500 rpm and nanoparticles-to-oil ratio of 1 mg/g as reported by Hart et al. (2013). The reaction time includes heat-up-time (~2h 15 min) since it was reported that activation of commercial catalyst occurred as a result of the sulfidation of the metals by the sulphur in the feed oil during the heating up state (Ortiz-Moreno et al., 2012). The gas atmosphere was nitrogen with initial pressure of 20 bar which increases with the ramp temperature rise and the added gas due to cracking reactions to 74-80 bar. Upon cooling to room temperature after the reaction the pressure decreases (24-26 bars). During the heating up stage (about 2 h 15 min to reach 425 ^oC) some reactions occurred. Therefore, 30 minutes of reaction time was allowed at 425 ^oC with the obtained results being the product of the combined high and lower temperature reactions. A detailed experimental procedure can be found in Hart et al. (2013). The experimental conditions for dispersed nanoparticles are summarised in **Figure 2.2**. In order to evaluate the effect of the biocatalyst, other experiments were conducted without biocatalyst (thermal cracking only) and also with bacterial biomass (without added metals) as controls.

The mass balances of the three products i.e., liquid, gas, and coke were calculated as percentage of the mass of feed oil into the reactor using equations 2.1 and 2.2:

$$\text{Yield (wt. \%)} = W_i/W_{Feed} \times 100 \quad (2.1)$$

$$\text{Yield of gas (wt \%)} = (W_{Feed} - W_{\text{autoclave content after reaction}}) / W_{Feed} \times 100 \quad (2.2)$$

Where W_i is the weight of component i and W_{Feed} is the weight of the heavy oil fed into the reactor.

Table 2 Properties and composition of heavy oil used in this study

Parameter	**Value**
API gravity (^{o})	13.8
Viscosity at 20 ^{o}C (mPa.s)	1031
Sulfur (wt. %)	3.52
Nickel (ppm)	41
Vanadium (ppm)	108
Ni + V (ppm)	149
Asphaltene (wt. %)	10.3
Elemental analysis	
C	88.82 wt.%
H	10.17 wt.%
N	0.57 wt.%
H/C	0.114

Heavy oil was supplied by Touchstone Exploration Inc, Canada

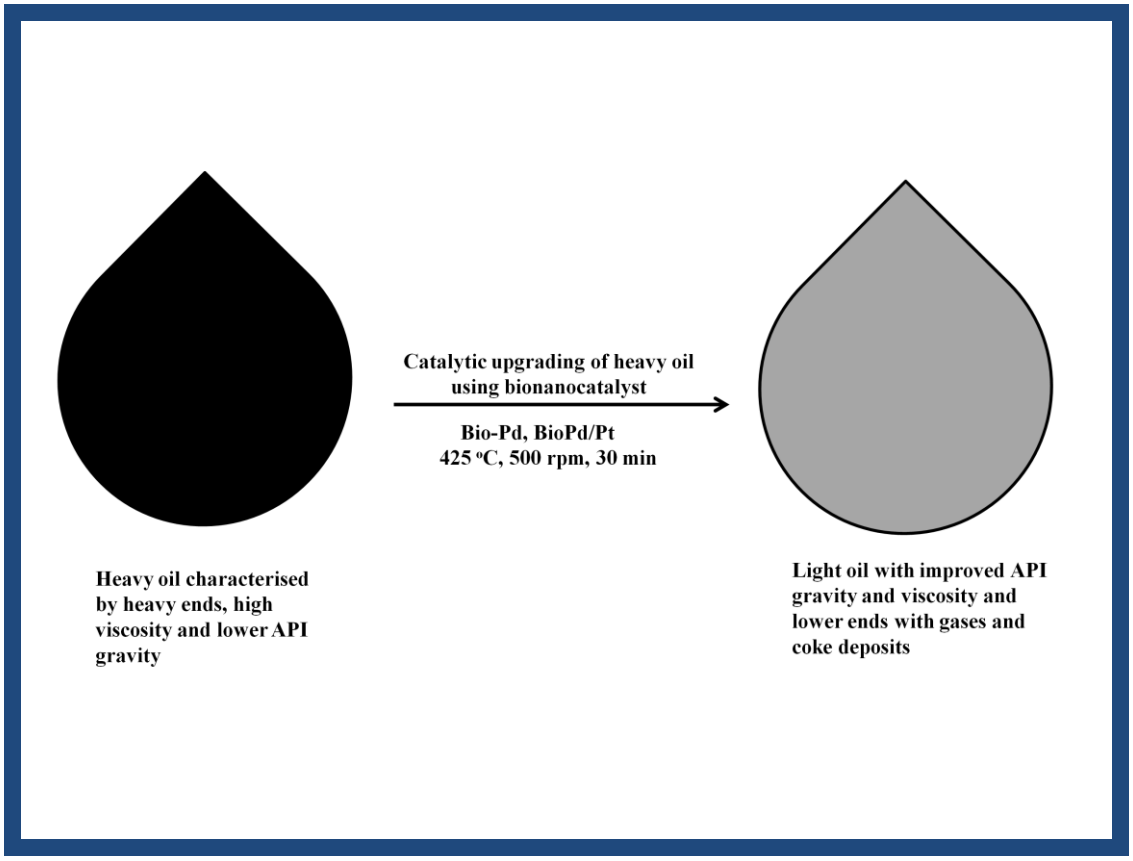

Figure 2. 2 Upgrading of heavy oil using bionanocatalyst made by bacteria

2.8 Biochemical activities of metallised cells

2.8.1 Flow cytometry measurement of membrane integrity and membrane potential of metallised cells

Flow cytometry provides qualitative and quantitative analytical measurement of individual cells using fluorescence emission of labelled cells when they pass individually through a light source (*e.g.* laser) (Davey and Kell, 1996; Davies, 2007). See section 3.3.2 for details of the applications. Harvested cell suspensions were determined based on predetermined OD_{600} and dry weight conversion for *D. desulfuricans* (Deplanche, 2008) and *B. benzeovorans* (see appendix A, section 5.2) and cells were challenged by adding 1 mM Pd (II) solution of Na_2PdCl_4 (pH 2) to make various metal loadings on cells as detailed above. Samples were divided into two; Pd-cell suspension supplemented with 1 M sodium formate (final concentration of 20 mM)

for 1 h with shaking. Samples were then stored (4^{o}C) overnight (16-20 h) prior to flow cytometry measurement.

Cell samples (5 ml) were divided into four: Pd (II)-challenged cells (without formate), Pd-challenged cells with Pd (II) (reduced with formate), Pd-free live cells and heat-killed (70^{o}C for 1h) cells as controls. After incubation as above and prior to flow cytometry measurement, the cells were washed by centrifugation (12,000 x g, 15 min, 4^{o}C) to remove unbound metal ion and MOPS buffer and then suspended in ice cold (10 ml) phosphate buffered saline, PBS (10 mM, containing NaCl (8g), KCl (0.2g), Na_2HPO_4 (1.44g), KH_2PO_4 (0.2g) per L), pH 7.4, washed twice (12,000 x g, 15 min, 4^{o}C) and 0.1 ml of each type of cell was resuspended to approx 10^6 cells/ml in PBS (1.9 ml) to a final volume of 2 ml (Lopez-Fernandez et al., 2014). For measurement of membrane integrity, solutions of flourochromes, flourescein diacetate (FDA) (40µl, 0.1 mg/ml aq) and of propidium iodide (IP) (4µl, 1 mg/ml aq) were added simultaneously to the 2 ml cell mixture. Meanwhile, for the measurement of membrane potential, 3, 3'-Dihexyloxacarbocyanine iodide [$DiOC_6$ (3)] (20µl, 1 µM) was added to a separate sample. Mixtures were stored in the dark for 15 minutes. Then flow cytometry measurements were taken immediately in triplicates (viable cells stain green while non-viable or dead cells stain red) using a FACS Cantoll flow cytometer, Becton Dickson (San Jose Palo Alto, California) equipped with three lasers: 488 nm blue, 620 nm red and 405 nm UV. Samples were measured in a green fluorescence detector or filter, FL1 (for fluorescein isothiocyanate, FITC) and a red fluorescence detector or filter, FL2 (for phycoerythrin-propidium iodide, PE-IP) mode in logarithmic scale channels at medium speed. The band pass filters used were 530 nm and 580 nm and results were analysed using BD Diva 6.1 software.

2.8.2 Determination of the activity of catechol-1, 2-dioxygenase and catechol-2, 3-dioxygenase in Bacillus benzeovorans towards tandem catalysis

Catechol-1, 2 and 2, 3- dioxygenases are ring cleavage enzymes for the aerobic degradation of various aromatic compounds *via* catchecol as the central intermediate of aerobic degradation of aromatic compounds (Schmidt et al., 2013). In this study, cells of *Bacillus benzeovorans* were harvested by centrifugation (9,000 x g, 10 min at 4^{o}C) and washed twice in ice cold 100 mM potassium phosphate buffer (50 mM KH_2PO_4: 50 mM

K_2HPO_4 mixture) at pH 7.2. The cells were suspended in ice cold potassium phosphate buffer (10 ml) in triplicates and disrupted with a homogenizer (Aminco, Md; 140 Pa, 0^oC) for 2-cycles of 2 min with cooling on ice for 30 sec in-between each cycle. The cell pellets were seperated by centrifugation (74, 235 x g, 1 h at 4^oC) and the clear supernatant solution was used as the cell extract (Reinke and Knackmuss, 1984; Zaki, 2006). For enzyme assay, catechol-1, 2-dioxygenase and catechol-2, 3-dioxygenase were measured individually using different assays based on two combined methods (Reinke and Knackmuss, 1984; Hupert-Kocurek et al., 2012) but using the same reaction condition and a total reaction volume of 1 ml (40^oC incubation time, 10 min). Samples were kept on ice throughout the duration of assay. First, the activity of catechol-1, 2- dioxygenase was determined spectrophotometrically at 260 nm by measuring the formation of the product, *cis, cis*-muconic acid (CCMA) with a molar extinction coefficient (ε_{CCMA} = 16800 M^{-1} cm^{-1}) (Hupert-Kocurek et al., 2012) followed by incubation: Crude cell extract (20 µl) was incubated with 30% H_2O_2 (30 µl) for 5 min to in order to inactivate catechol 2, 3-dioxygenase activity followed by addition of 67 µl (20 mM) of Na_2EDTA, 863 µl (50 mM) of buffer and finally 20 µl (50 mM) of catechol was added. For the determination of catechol-2, 3- dioxygenase, mixture contains 20 µl of crude cell extract, 960 µl (50 mM) of buffer and 20 µl (50 mM) of catechol which was then incubated at the same condition as above and the enzyme measured based on the formation of the product 2-hydroxymuconic semialdehyde (2-HMS) at 375 nm ($\varepsilon_{2\text{-}HMS}$ = 36, 000 M^{-1} cm^{-1}). One unit (U) of enzyme activity was defined as the enzyme amount generating 1µmol of product per min at 40^oC.

2. 9 References

Baxter-Plant, V. S.; Mikheenko, I. P.; Macaskie, L. E., Sulphate reducing bacteria, palladium and the reductive dehalogenation of chlorinated compounds. *Biodegradation* **2003,** *14*, 83-90.

Bunaciu, A. A.; Udristioiu, E. G.; Aboul-Enein, H. Y., X-Ray Diffraction: Instrumentation and Applications. *Critical Reviews in Analytical Chemistry* **2015,** *45*, 289-299.

Christy, A. A.; Xu, Z.; Harrington, P. d. B., Thermal degradation and isomerisation kinetics of triolein studied by infrared spectrometry and GC-MS combined with chemometrics. *Chemistry and Physics of Lipids* **2009,** *158*, 22-31.

Davey, H. M.; Kell, D. B., Flow cytometry and cell sorting of heterogeneous microbial populations: the importance of single-cell analyses. *Microbiol Rev* **1996,** *60*, 641-96.

Davies, D., Cell sorting by flow cytometry. In *flow cytometry: Principles and applications.* Macey, M. G., Ed. Humana Press Inc: Totowa, New Jersey, 2007; pp. 257-276.

Deplanche, K. New nanocatalysts made by bacteria from metal solutions and recycling of metal wastes. PhD Thesis, University of Birmingham, UK, 2008.

Deplanche, K.; Caldelari, I.; Mikheenko, I. P.; Sargent, F.; Macaskie, L. E., Involvement of hydrogenases in the formation of highly catalytic Pd(0) nanoparticles by bioreduction of Pd(II) using *Escherichia coli* mutant strains. *Microbiology-SGM* **2010,** *156*, 2630-2640.

Hart, A.; Shah, A.; Leeke, G.; Greaves, M.; Wood, J., Optimization of the CAPRI Process for Heavy Oil Upgrading: Effect of Hydrogen and Guard Bed. *Industrial & Engineering Chemistry Research* **2013,** *52*, 15394-15406.

Hupert-Kocurek, K.; Guzik, U.; Wojcieszynska, D., Characterization of catechol 2,3-dioxygenase from Planococcus sp strain S5 induced by high phenol concentration. *Acta Biochimica Polonica* **2012,** *59*, 345-351.

Jaboyedoff, M.; Kubler, B.; Thelin, P. H., An empirical Scherrer equation for weakly swelling mixed-layer minerals, especially illite-smectite. *Clay Minerals* **1999,** *34*, 601-617.

Massover, W. H., New and unconventional approaches for advancing resolution in biological transmission electron microscopy by improving macromolecular specimen preparation and preservation. *Micron* **2011,** *42*, 141-151.

Mielanczyk, L.; Matysiak, N.; Michalski, M.; Buldak, R.; Wojnicz, R., Closer to the native state. Critical evaluation of cryo-techniques for Transmission Electron Microscopy: preparation of biological samples. *Folia Histochemica Et Cytobiologica* **2014,** *52*, 1-17.

Peckys, D. B.; Veith, G. M.; Joy, D. C.; de Jonge, N., Nanoscale Imaging of Whole Cells Using a Liquid Enclosure and a Scanning Transmission Electron Microscope. *Plos One* **2009,** *4* (12).

Redwood, M. D.; Deplanche, K.; Baxter-Plant, V. S.; Macaskie, L. E., Biomass-supported palladium catalysts on *Desulfovibrio desulfuricans* and *Rhodobacter sphaeroides*. *Biotechnology and Bioengineering* **2008,** *99*, 1045-1054.

Reineke, W.; Knackmuss, H. J., Microbial-metabolism of haloaromatics-isolation and properties of a chlorobenzene-degrading bacterium. *Applied and Environmental Microbiology* **1984,** *47*, 395-402.

Schmidt, E.; Mandt, C.; Janssen, D. B.; Pieper, D. H.; Reineke, W., Degradation of chloroaromatics: structure and catalytic activities of wild-type chlorocatechol 2,3-dioxygenases and modified ones. *Environmental Microbiology* **2013,** *15*, 183-190.

Wang, Y.; Wan, J.; Hu, X.; Xu, L.; Wu, S.; Hu, X., A rate adaptive control method for Improving the imaging speed of atomic force microscopy. *Ultramicroscopy* **2015,** *155*, 49-54

Yong, P.; Rowson, N. A.; Farr, J. P. G.; Harris, I. R.; Macaskie, L. E., Bioaccumulation of palladium by *Desulfovibrio desulfuricans*. *Journal of Chemical Technology and Biotechnology* **2002,** *77*, 593-601.

Zaki, S., Detection of *meta*- and *orthor*-cleavage dioxygenase in bacterial phenol-degraders. *Journal of Applied Science and Environmental Management* **2006,** *10*, 75-81

Zienkiewicz-Strzalka, M.; Pikus, S., The study of palladium ions incorporation into the mesoporous ordered silicates. *Applied Surface Science* **2012,** *261*, 616-622.

CHAPTER 3 Results

This section is divided into four main study areas with each section focused on two key studies and have been written as papers for publication. Some are in submission, while one section has been published.

3.1 Interaction of Pd (II) with Two Strains of *Desulfovibrio desulfuricans*

3.2 Catalytic Activities of Bionanocatalysts Made by *Bacillus benzeovorans* and *Desulfovibrio desulfuricans*

3.3 Interaction of Palladium with Bacterial Cells

3.4 Towards Tandem Catalysis

3.1 Interaction of Pd (II) with Two Strains of *Desulfovibrio desulfuricans*

This section contains the following studies:

3.1.1 Catalytic Hydrogenation of Soybean Oil Using Bio-Pd and X-ray Photoelectron Spectroscopy Studies on the Mechanism of Palladium (II) Coordination in *Desulfovibrio desulfuricans*

Journal: Journal of the Royal Society Interface, in submission

3.1.2 Uptake of Pd (II) by *Desulfovibrio desulfuricans*: Coordination to Cell Surface Functional Groups and Endogenous Reduction at the Cell Surface Shown by X-ray Photoelectron Spectroscopy.

Journal: Biotechnology and Bioengineering, in submission.

3.1.1. Catalytic Hydrogenation of Soybean Oil Using Bio-Pd and X-ray Photoelectron Spectroscopy Studies on the Mechanisms of Palladium (II) Coordination in *Desulfovibrio desulfuricans*

Jacob B. Omajali [1], Marc Walker [2], Joseph Wood [3] and Lynne E. Macaskie [1]*

[1] Unit of Functional Bionanomaterials, Institute of Microbiology and Infection, School of Biosciences, University of Birmingham, Edgbaston, Birmingham, B15 2TT, United Kingdom

[2]Department of Physics, Warwick University, Coventry, CV4 7AL, United Kingdom

[3]School of Chemical Engineering, University of Birmingham, Edgbaston, Birmingham, B15 2TT, United Kingdom

*Corresponding author. Tel.: +441214145889; fax: +441214145925

Email address: L.E.Macaskie@bham.ac.uk

Journal: Journal of the Royal Society Interface, in submission

This paper was written by J.B Omajali. All experiments and analysis were performed by the author. Technical assistance on X-ray photoelectron spectroscopy was rendered by Dr Marc Walker, Warwick University.

Abstract

A Pd-nanoparticle catalyst (bio-Pd) made by two strains of *D. desulfuricans* was compared in the partial hydrogenation of soybean oil. *D. desulfuricans* NCIMB 8307 produced a better Pd-catalyst than *D. desulfuricans* NCIMB 8326 with ~65% difference in conversion; both catalysts displayed selectivity (45-60%) to *cis*-fatty acid with 10-16% selectivity to the less important *trans* fatty acid. The surface topology of the two strains as a host surface for Pd (0) nanoparticles was compared using atomic force microscopy (AFM). The binding mechanism of in-coming Pd (II) to the cell surface of each bacterium prior to Pd synthesis was determined using X-ray photoelectron spectroscopy (XPS). The two strains behaved differently, with *D. desulfuricans* NCIMB 8307 binding more strongly to amine nitrogen of peptide and not fatty acid amide as reflected by higher positive chemical shifts in binding energy and increased amount of sulfur and oxygen groups. *D. desulfuricans* NCIMB 8326 contained more phosphate and calcium and bound Pd (II) strongly due to the presence of these materials on its surface. The Pd binding mechanism was suggested to be *via* ion-exchange with calcium ion which supports coordination to phosphate as well as hydrogen-substitution at amide nitrogen site during Pd (II) uptake in both strains. This study concludes that the better catalytic properties of *D. desulfuricans* NCIMB 8307 could be attributed to cell surface topography, increased number of oxygen-containing sites and stronger Pd binding interaction due to positive shifts in binding energies. As this strain has a reduced P and Ca interaction sites this mechanism of Pd (II) deposition may not be implicated in the formation of Pd-nanoparticles with high catalytic activity.

Key words: *D. desulfuricans; Palladium; Soy bean oil; Hydrogenation; surface functional groups; XPS*

Introduction

Palladium is a very important platinum group metal (PGM) due to its chemical and physical properties which are relevant in catalysis and other industrial applications (Das, 2010). The high cost and demand (especially from the automotive industry) has led to unconventional methods of catalyst manufacture that also overcomes the problem of agglomeration (Maillard et al., 2005) that beset traditional nanocatalyst synthesis. Often, the finished catalyst using conventional methods lacks selectivity, resulting in production of unwanted side products. Hence, the concepts of "green chemistry" include a focus on catalysts with high selectivity, less waste and easy separation from product streams. Bio-Pd which refers to biologically synthesized catalyst outperformed its chemical counterpart in several reactions (Deplanche, 2008; Bennett et al., 2013). The metal catalysts are stabilized on the bacterial cell surface, preventing particle growth and agglomeration and can be separated for re-use (Bennett et al., 2013) while the use of immobilized bacterial biofilms forms a natural method of catalyst immobilization (Beauregard et al., 2010; Yong et al., 2015).

The use of bacteria to precipitate soluble palladium (Pd (II)) as nanoparticles (Pd (0)) onto bacterial cells has attracted increasing focus (Schroefel et al., 2014) not only in sustainable nanocatalyst production but also in recovering palladium and other precious metals from aqueous and waste solutions (Macaskie et al 2007; Won et al., 2014; Murray et al., 2015). The sulfate-reducing bacterium, *D. desulfuricans* in which this property was first reported (Lloyd et al., 1998) produces supported palladium catalyst, a heterogeneous catalyst with potential in *ex-situ* environmental applications (Baxter-Plant et al., 2003; De Windt et al., 2005; Harrad et al., 2007; Schlüter et al., 2014), selective hydrogenation (Creamer et al., 2007; Wood et al., 2010) and oxidation reactions (Deplanche et al., 2012; Zhu, 2014) and, recently, in (for example) Heck-coupling reactions (Bennett et al., 2013; Deplanche et al., 2014). However, despite many reports on comparative bionanocatalyst activities, less attention has been paid to the orthogonal process of catalyst biomanufacture which is an essential prerequisite to application of the tools of synthetic biology to engineer catalysts for specific purposes. A comparative study of the 'bio-Pd' of some representative Gram-negative and Gram-positive bacteria showed a higher catalytic activity of the former in Cr (VI) reduction

(Deplanche et al., 2014), selective hydrogenation of 2-pentyne and selective oxidation of benzyl alcohol (Zhu, 2014). In contrast, the bio-Pd of *Bacillus sphearicus* (Gram-positive) showed comparable catalytic activity to that of *D. desulfuricans* (Gram-negative) in hydrogenation of itaconic acid (Creamer et al., 2007).

The bacterial cell surface, which varies between Gram-positive and Gram-negative bacteria, is an important platform towards catalytic synthesis. It is well known (Beveridge and Murray, 1980) that anionic functional groups such as teichoic acid, teichuronic acid and peptidoglycans, comprising 90% of the cellular surface material are found in Gram-positive bacteria whereas phospholipids and lipopolysaccharides are found in the Gram-negative bacterial outer membrane and are responsible for the negative charge and some metal-binding properties of the bacterial cell wall with a peptidoglycan layer beneath the outer membrane also being contributory. Studies (e.g. Volesky, 2001; Vijayaraghavan and Yun, 2008) have reported that bacteria use these natural compounds to accumulate metals through a range of mechanisms *e.g.* biosorption (ion-exchange between metal ions and charged functional groups *e.g.* amine, carboxyl, hydroxyl and phosphate, on bacterial cell surfaces), sequestration and/or various enzymatically-driven mechanisms like oxidation/reduction of metals and precipitation *via* enzymatic ligand production (Gadd, 2010). The bacteria-metal interactions lead to initial metal nucleation and the formation of nanoparticle deposits on bacterial surfaces (e.g. see Deplanche et al., 2011; 2014; Murray et al., 2015).

Early work to compare different species of *Desulfovibrio* (de Vargas et al., 2004) showed that *D. desulfuricans* NCIMB 8307 showed the best Pd (II) binding ability and previously produced the best catalyst in reductive dehalogenation of chlorinated aromatic compounds (Baxter-Plant et al., 2003). The underlying reason(s) for this relationship remains unknown. However, *D. desulfuricans* NCIMB 8307 has never been compared with another member of the same species and *D. desulfuricans* NCIMB 8326 was selected for that purpose as a first step towards pinpointing key interactions in deposition of catalytic Pd-nanoparticles.

In order to understand the differences between the *D. desulfuricans* in terms of the mechanistic interaction of incoming palladium ions on the cell surfaces, X-ray photoelectron spectroscopy (XPS) was employed. XPS analysis has been used in

several studies (Rouhex et al., 1994; Dufrene et al., 1996; van der Mei et al., 2000) due to its ability to provide chemical information on a layer 3-5nm thick at the surfaces of Gram-positive (*e.g. Bacillus subtilis*: Ahimou et al., 2007) and Gram-negative (*e.g. Azospirillum brasilense*: Dufrene and Rouxhet, 1996) bacteria without the need to disrupt and isolate cell wall components and therefore, providing key information on the mechanism of initial steps of metal binding and hence patterning on bacterial cell surfaces.

The first objective of this study was to compare the catalytic properties of the bio-Pd (0) produced by *D. desulfuricans* NCIMB 8307 and *D. desulfuricans* NCIMB 8326 in the hydrogenation of soybean oil. Soy bean oil hydrogenation was chosen as a suitable catalytic test because hydrogenation is a very important process towards the modification of fat and oil in order to increase the melting point and improve the oxidation property of the oil. There are three major simultaneous reactions in the process of hydrogenation including; saturation of double bonds, and geometric (*cis-trans*) and positional isomerism. The order of hydrogenation of the soy bean oil is from C18:3 (linolenates) to C18:2 (linoleates) to C18:1 (oleates) to C18:0 (stearate) (Bouriazos et al., 2010). The property of the hydrogenated oil is dependent both the number of double bonds and the *cis-trans* isomers of fatty acid (Fernández et al., 2009).

The key features of *D. desulfuricans* NCIMB 8307 that determine the catalytic properties of its bio-Pd are not known but since coordination of Pd (II) to cellular nitrogen-containing groups was reported (de Vargas et al., 2005), a possible involvement of fatty acid amides is hypothesized. This could be attributed to such amides forming the primary binding site and 'steering' the bio-Pd into a catalytically-active nano-entity or, alternatively, by 'diverting' in-coming Pd (II) away from other sites that provide a critical steer. Fatty acid ethanolamide was shown to be present in cell extracts of *D. desulfuricans* NCIMB 8307 but absent in *D. desulfuricans* NCIMB 8326 from a previous study (Goldsworthy, 2011) and a comparison Pd (II) uptake and catalytic activity of the two strains underpins the second objective; to relate the differences in cell surface binding and Pd (0) formation with respect to ability to selectively hydrogenate soy bean oil. The aim is to gain insight into the mechanism(s) involved in the interaction of Pd (II) with functional groups on the cell surfaces of the

two strains of *D. desulfuricans* during Pd (II) sorption and to inform bio-Pd (0) catalyst manufacture in order to provide insights into strain-dependent catalytic nanomaterials to produce 'designer green catalyst' prior to manipulation of cell surface structures.

Materials and Methods

Microorganisms, growth conditions and harvest

Desulfovibrio desulfuricans NCIMB 8307 and NCIMB 8326 were grown anaerobically under oxygen-free nitrogen in Postgate's medium C at 30^{o}C (inoculated from a 24 hour pre-culture, 10%v/v) in sealed anaerobic bottles. Cells were harvested (Beckman Coulter Avati J-25 Centrifuge, U.S.A) by centrifugation (9,000 x g, 15minutes at 4^{o}C) at mid exponential phase (OD_{600} 0.5-0.7), washed three times in air with 20mM MOPS (morpholinepropanesulfonic acid)-NaOH buffer, pH 7.0 and then concentrated in a small amount of the same buffer to usually (20-30mg/ml) as determined by reference to a pre-determined OD_{600} to dry weight conversion (Deplanche et al., 2010). The cells were degassed and then stored under oxygen-free nitrogen (OFN) at 4^{o}C until use, usually within 24h.

Preparation of Bio-Pd (0) biocatalyst

For bio-reduction of Pd (II) sorbed cells, a known volume of a concentrated resting cell suspension as described above was transferred into an appropriate volume of degassed (30 minutes) 2mM Pd (II) salt solution (Na_2PdCl_4, pH 2 ± 0.1 adjusted with 0.01 M HNO_3) to make a 5% metal loading (1:19) on cells of both strains of *Desulfovibrio desulfuricans.* The cells and palladium mixture were then allowed to stand in water (30 min, at 30^{o}C) for biosorption of the Pd (II) onto the cell surfaces with occasional shaking. This was followed by reduction of the Pd (II) bound to the surface of the cells to Pd (0) with H_2 as the exogenous electron donor. The reduction of the Pd (II) (removal from solution) was confirmed by the tin (II) chloride assay method described below. The metallized biomass was harvested by centrifugation (9,000 x g, 4^{o}C, 15 minutes) and washed thrice in distilled water and once in acetone (3079 x g, 4^{o}C, 15 minutes). The washed bio-Pd (0) (palladized biomass) was further resuspended in a small volume of acetone, dried in air to constant weight, finely ground in an agate mortar with pestle and sieved (100 mesh size) to give a dry black powder.

Assay of Pd (II)

Prior to harvesting the palladized cells, the complete reduction of Pd (II) was confirmed by the tin (II) chloride assay method previously described (Deplanche et al., 2010) spectrophotometrically (Ultraspec III, Pharmacia Biotech, Little Chalfront, Buckinghamshire, UK) by taking the absorbance of the sample supernatants at 463 nm. The Sn (II) chloride was freshly prepared by dissolving 29.9 g $SnCl_2$ powder into 500 ml HCl.

Electron Microscopy

Pd-loaded cells of *D. desulfuricans* NCIMB 8307 and NCIMB 8326 were washed twice with distilled water and fixed with 2.5% (w/v) glutaraldehyde fixative in 0.1M cacodylate buffer (pH 7.0) at 4^oC and stained with 1% osmium tetraoxide. For SEM (Scanning Electron Microscopy), the Pd-loaded cells were mounted on carbon-coated copper grid and electron opaque deposits were examined by energy dispersive X-ray Spectroscopy (EDX) with peaks sought corresponding to X-ray emission energies of Pd (Yong et al., 2002). For TEM (Transmission Electron Microscopy), the Pd-loaded cells were dehydrated using an ethanol series and washed twice in propylene oxide (Deplanche et al., 2010). The cells were embedded in epoxy resin and cut into sections (100-150nm thick) and then viewed with JEOL 1200EX transmission electron microscope, accelerating voltage 80Kv.

X-ray powder diffraction (XRD) of bio-Pd (0)

For XRD analysis, bioPd (0) was washed three times in distilled water and once in acetone, then resuspended in a small volume of acetone. This was then air dried and ground into a fine black powder in an agate mortar with pestle. The X-ray powder diffraction patterns were acquired from a Bruker AXS D8 Autosampler (Transmission) Diffractometer using a monochromatic high-intensity $CuK_{\alpha 1}$ radiation (λ = 1.5406 Å) equipped with a solid-state LynxEye position sensitive detector (PSD) with a 3^o electronic window. The XRD patterns of the bio-Pd samples were then compared to a reference standard in the International Committee for Diffraction Data (ICDD)

database. The particle size of the bioPd (0) was determined using Scherrer's equation using just the major peaks (Jaboyedoff et al., 1999).

Atomic force Microscopy (AFM)

Aliquots of palladized and Pd-free live cells of *D. desulfuricans* NCIMB 8307 and NCIMB 8326 were washed (16,000 x g, 4min) and distributed uniformly in sterile distilled water (for the metallised cells) and MOPS-NaOH buffer, pH 7.0 (live cells). The samples were then diluted appropriately, mounted on a silicon wafer and dried in air at room temperature (20-26^{o}C). Topographies were acquired using a NanoWizard II atomic force microscope (JPK Instruments, UK) operating in intermittent contact mode at a tip velocity of 20 μm/s, employing pyramidal tipped Si cantilevers (PPP-NCL, Windsor Scientific, UK) while the data analysis was processed using the " PK data processing software."

Catalytic hydrogenation of soybean oil

Catalytic test was carried out by partial hydrogenation of soybean oil. This was performed in a 0.5 litre capacity batch reactor (Baskerville reactors and autoclaves Ltd Manchester, England) at 100^{o}C and 5 bar hydrogen pressure (5 h) by using a 150 mg of 5% bio-Pd (0) catalyst produced on cells of *D. desulfuricans* NCIMB 8307 and NCIMB 8326 respectively (agitation speed of 800 rpm). 150 ml of soybean oil was introduced into the reactor followed by catalyst addition and the reactor and its contents were purged with nitrogen. The first sample was withdrawn as the reaction temperature reached100^{o}C prior to hydrogenation. Nitrogen was then released before hydrogen was introduced immediately for hydrogenation to proceed. Small amounts of samples were then taken at various suitable time intervals for 5 hours and stored in the dark until GC analysis. Prior to sample analysis, the fatty acid content of the soybean oil was converted to fatty acid methyl esters (FAMEs) by derivatisation according to the method of Christy et al. (2009) with slight modification. In the derivatization of hydrogenated soybean oil, 2ml of 0.5M NaOH/methanol was added to 0.2ml of hydrogenated soybean oil sample followed by heating in a water bath at 60^{0}C (15 min). After cooling, boron triflouride in methanol (BF3/methanol v/v) was added (2 ml) and heated for an additional 10 min. Then, 2ml of a saturated solution of NaCl and 1ml of hexane was added and shaken for a few minutes. The content was allowed to settle for a

few minutes and the top hexane (organic) layer was extracted into a clean vial and stored in the dark prior to GC analysis. GC analysis of samples was done in a gas chromatograph (Varian CP-3380) equipped with a flame ionization detector (FID) with a 75 m SP^{TM}-2560 capillary column (Sigma-Aldrich, UK) by injecting 0.5 µl of sample in an analysis time of 30 min.

Pd (II) sorption and X-ray photoelectron spectroscopy analysis (XPS)

These tests were done with fresh cells of *D. desulfuricans* in 20 mM MOPS-NaOH buffer (pH 7) challenged with 2mM Pd (II) solution initially adjusted to pH 2.0 with 0.01M HNO_3. After the addition of cells, the final pH was 2.3 (*D. desulfuricans* NCIMB 8307) and pH 2.4 (*D. desulfuricans* NCIMB 8326) which was followed by sorption for 30 minutes at 30 ^{o}C. For the XPS studies, aliquots of biosorbed samples of Pd (II) solution on cells were washed with distilled water, dropped and dried on a boron-doped silicon wafer (7x7mm) in diameter. The X-ray photoelectron spectroscopy (XPS) data were collected at the Science City Photoemission Facility, University of Warwick. The samples were mounted on Omicron sample plates using electrically conductive carbon tape and loaded in to the fast-entry chamber. Once a pressure of less than 1 x 10^{-7} mbar was achieved (approx. 1 hour), the samples were transferred to a 12-stage storage carousel, located between the preparation and main analysis chambers, for storage at pressures of less than 2 x 10^{-10}mbar. XPS measurements were made in the main analysis chamber (base pressure 2 x 10^{-11} mbar), with the sample being illuminated using an XM1000 monochromatic Al k_{α} x-ray source (Omicron Nanotechnology). The measurements were done at room temperature and at a take-off angle of 90°, allowing a maximum probe depth of approximately 5-10nm. The photoelectrons were detected using a Sphera electron analyser (Omicron Nanotechnology), with the core levels recorded using a pass energy of 10 eV (resolution approx. 0.47eV). Due to the insulating nature of the samples, a CN10 charge neutralizer (Omicron Nanotechnology) had to be used in order to prevent surface charging, whereby a low energy (typically 1.5 eV) beam of electrons was directed on to the sample during XPS data acquisition. The data were converted into VAMAS format and analysed using the CasaXPS package, using Shirley backgrounds, mixed Gaussian-Lorentzian (Voigt) lineshapes and asymmetry parameters where appropriate. All

binding energies were calibrated to the C 1s peaks originating from adventitious carbon at 284.6 eV. Control samples include metal-free biomass, heat-killed cells and Pd (II) metal solution.

Results and Discussion

Comparison of catalytic activity of Bio-Pd_{Dd8307} and Bio-Pd_{Dd8326} in the hydrogenation of soybean oil

The 5% bio-Pd (0) produced by both strains of *D. desulfuricans* NCIMB 8307 (Bio-Pd_{Dd8307}) and NCIMB 8326 (Bio-Pd_{Dd8326}) were compared in the partial catalytic hydrogenation of soy bean oil. This test showed using one-way anova that bio-Pd_{Dd8307} was more active ($P < 0.05$) than bio-Pd_{Dd8326} (17% and 6% conversion of linoleic acid (C18:2) respectively) (Fig 1a) with no significant difference for the first 2h of reaction. This conclusion was supported by the higher hydrogen consumption by Bio-Pd_{Dd8307} than Bio-Pd_{Dd8326} ($P < 0.05$; Fig 1b). Small differences was also seen in the pattern of selectivity to *cis* (Fig 1c) and *trans* (Fig 1d) monounsaturated (C18:1) fatty acid methyl esters but with little differences between the overall selectivity of ~ 45-60% towards the *cis* product. A full mass balance was not attempted. This better activity of Bio-Pd_{Dd8307} may be partly due to surface roughness of the bacterial cell support (see below) as differences in surface morphology of supports are critical in defining catalytic behaviour. For example, the surfaces of SBA-15, a mesoporus silicate support for vanadium oxide catalyst, influenced catalytic activity, a smooth surface catalyst conferring less selectivity (~20% lower) to formaldehyde conversion from methanol than rough surface (Smith et al., 2014) due to the varying distribution of surface hydroxyl groups on the silica support. Higher textural (roughness) cell surface and oxygen-containing surface ligands results in increased dispersion of the Pd-NPs surface (Du et al., 2012; Zienkiewickz-Strzalka and Pikus, 2012). It has been proven that metal dispersion on the surface of Pd on activated carbon increases with increasing amount of oxygen-containing surface groups (Dong et al., 1993).

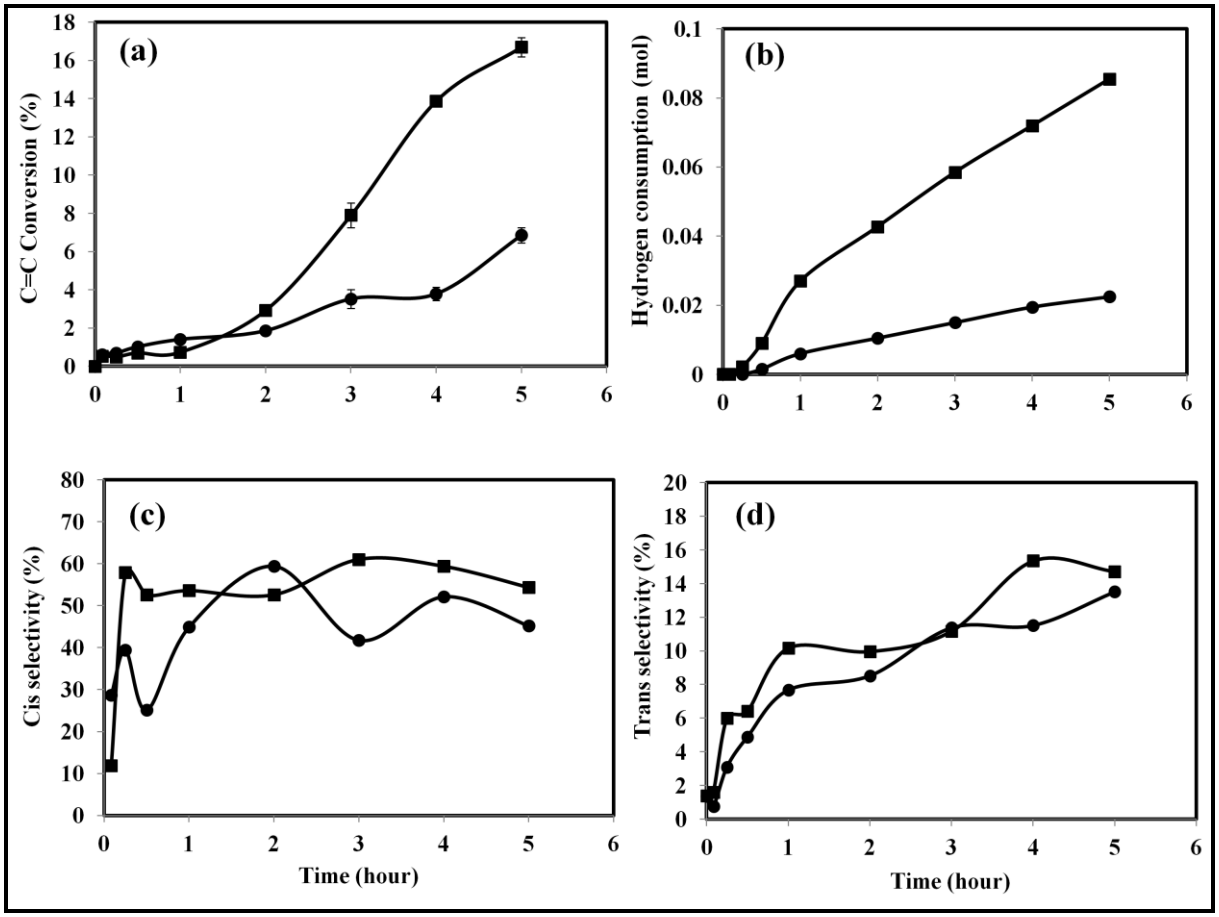

Figure 1 (a) Conversion of linolate (C18:2) by bio-$Pd_{D.d8307}$ (■) and bio-$Pd_{D.d8326}$ (●) (b) Hydrogen consumption (mole) by each bio-Pd (0) in the course of hydrogenation of soybean oil. (c) Selectivity to monounsaturated (C18:1) *cis* fatty acid methyl ester and (d) Selectivity to monounsaturated (C18:1) *trans* fatty acid methyl ester. Results are replicates of three independent experiments with Mean ± SEM. Where not shown error bars were within the dimension of the symbol.

Comparison of cell surface roughness using Atomic Force Microscopy (AFM)

In order to compare the roughness of the two bacterial supports, AFM was used to further characterize the cellular morphology of the two strains of *D. desulfuricans* with and without Pd (0). Images of Pd-free live and palladized cells of *D. desulfuricans* per se are shown in Figure 2 but little detail is discernable visually between non-palladized (Fig 2 a-d) and palladized (Fig 2 e-g) cells. The rate and extent of removal of Pd (II) onto both types of cells was identical (Fig 3). However differences were revealed

in topography and surface roughness when calculated using the in-built functions of a JPK imaging software. The surface roughness of both cells increased as a result of metallization with palladium (Table 1). There was a significant difference in the arithmetic average roughness (Ra, $P < 0.05$) and root mean square roughness (RMS, $P < 0.05$) after palladium sorption on both strains of bacteria, with *D. desulfuricans* NCIMB 8307 (Figure 2e, f) having a higher Ra and RMS (Table 1) when compared to *D. desulfuricans* NCIMB 8326 (Figure 21g, h). An increase in the surface roughness of *Pseudomonas* cells was reported following the sorption of uranium and thorium (Kazy et al., 2009).Wang et al., (2007) also showed an increase in the size of *E.coli* cells after nickel metallisation while an increase in cell size due to dye sorption was reported by Du et al., (2012). Therefore, we conclude that surface roughness increases as a result of metallization, by ~3-fold. However, the observation that unpalladized cells of *D. desulfuricans* NCIMB 8326 are 3-fold less rough (smoother) than cells of *D. desulfuricans* NCIMB 8307 suggest that it is a feature of roughness rather than Pd (0) nanoparticles per se which is key; this is discussed in detail later.

Table 1 AFM topography of live and palladized cells of *D. desulfuricans*

	Surface roughness (nm)			
Surface parameters	NCIMB 8307		NICMB 8326	
	Live cells	Palladized cells	Live cells	Palladized cells
R_a	1.80 ± 0.36	5.36 ± 0.34	0.60 ± 0.33	1.78 ± 0.23
RMS	2.24 ± 0.40	6.88 ± 0.29	0.76 ± 0.38	2.19 ± 0.31

R_a = Arithmetic average roughness; RMS = Root mean square roughness; n = 3; Results are Mean ± SEM.

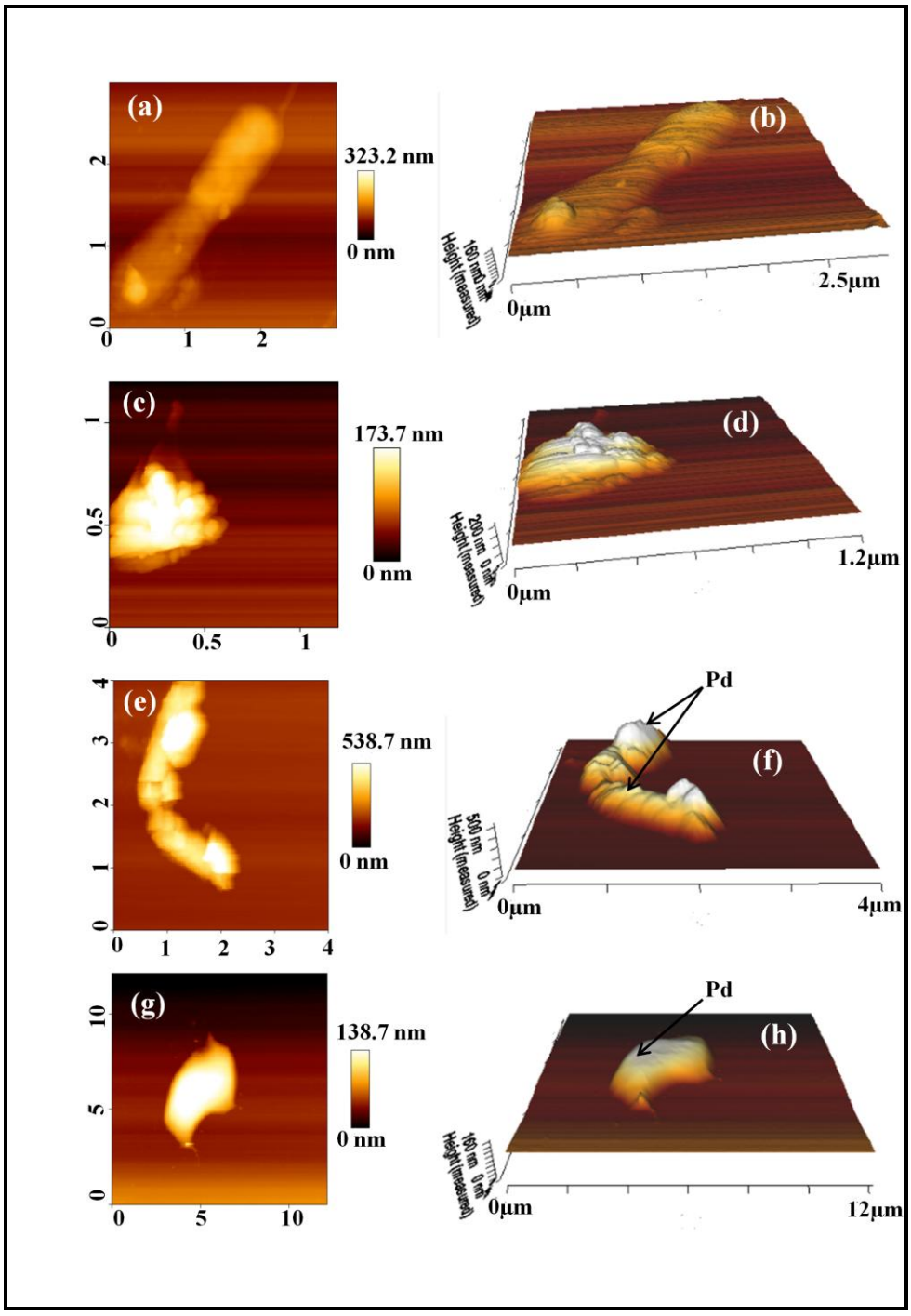

Figure 2 AFM images of live cells of (a) *D. desulfuricans* NCIMB 8307 and (b) 3D image representation on the right with corresponding images of *D. desulfuricans* NCIMB 8326 (c) and (d). Images of palladized cells of (e) *D. desulfuricans* NCIMB 8307 and (f) 3D image representation on the right with corresponding images of *D. desulfuricans* NCIMB 8326 (g) and (h). Image analysis was done using an AFM JPK data and imaging processing software. However, Pd on cells is not clearly visible from images f and h (metallized cells).

Examination of bio-Pd by Electron Microscopy

The complete reduction of palladium on the surfaces of resting cells of *D. desulfuricans* NCIMB 8307 and *D. desulfuricans* NCIMB 8326 occurred identically within a few minutes (Figure 3). TEM images (Figure 4a, b) of thin sections showed that Pd was predominantly deposited in the periplasmic space of both with some intracellular localization in both strains (Fig 4a, b, insets). Scanning electron microscopy (SEM) showed the presence of extracellular materials in *D. desulfuricans* NCIMB 8326 (Figure 2d) which tends to hold the cells together but this was not visible in *D. desulfuricans* NCIMB 8307 (Figure 4c). However, the TEM and SEM were carried out in a vacuum, under which conditions heavily hydrated extracellular polymeric materials collapse to become visible as a stranded mesh (Fig 4d, arrowed). Energy dispersive X-ray spectroscopy (EDX) further confirmed the presence of palladium within the electron-dense regions of the cells with characteristic Pd peaks (Figures 4e, f) in NCIMB 8307 and NCIMB 8326 respectively.

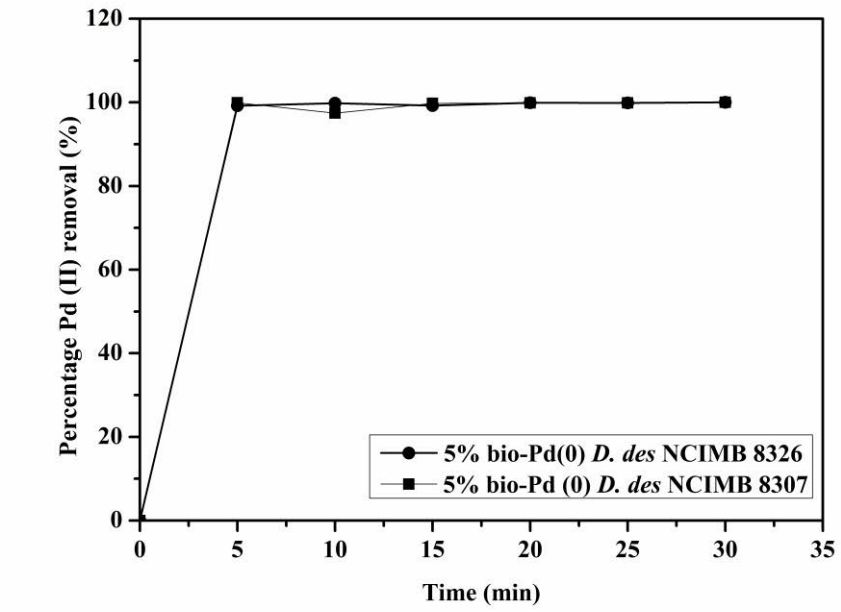

Figure 3 Pd (II) removal by *D. desulfuricans* in the presence of hydrogen as electron donor. Results are replica of three independent determinations (Mean ± SEM). Error bars are within the limits of the symbol. Note that Pd (II) reduction was not measured directly.

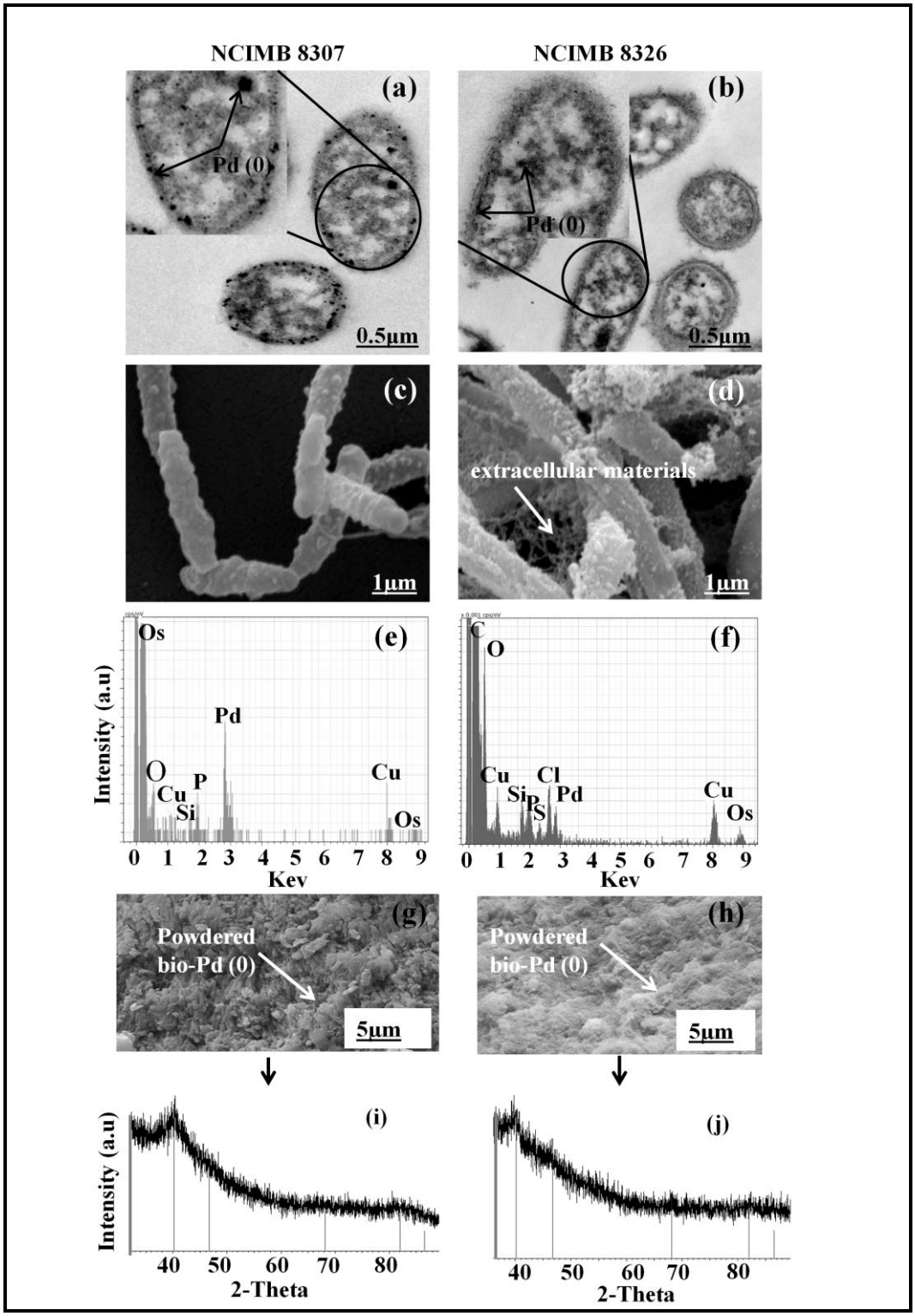

Figure 4 Results shows TEM (a, b) and SEM (c. d) images, elemental composition using EDX (e, f) powdered bio-Pd (g, h) and XRD patterns of 5wt% bio-Pd made using *D. desulfuricans* NCIMB 8307 (left) and *D. desulfuricans* NCIMB 8326 (right) respectively. Vertical lines are Pd peak positions. Insets show magnified images.

XRD analysis of Bio-Pd

XRD powder patterns enabled the determination of crystallite sizes of powdered (Figures 1g, h) materials as shown in Figs 4i, j. The presence of broad peaks observed in the XRD patterns (Figs 4i, j) which was more prominent in *D. desulfuricans* NCIMB 8307 (figure 1i) is a typical characteristic of amorphous nanoparticle preparations with small sizes resulting in poor crystal formation. The main peak observed in both bio-Pd at $2\Theta = \sim 40^{o}$ (111 plane) matched the Pd peaks found in the ICDD (International Committee for Diffraction Data) database. Average crystallite sizes were calculated using Scherrer's equation (Jaboyedoff et al., 1999). The calculated average crystallite sizes of the Pd-NPs were broadly comparable at 3.34 ± 0.09 nm for *D. desulfuricans* NCIMB 8307 and 3.81 ± 0.05 nm for *D. desulfuricans* NCIMB 8326 but it was not possible to measure these accurately due to the lack of peak definition (Figure 4i, j). The XRD results (particle sizes) obtained in this study are similar to the particle sizes determined from previous studies. Redwood et al., (2008) reported that biopalladium NPs from *Desulfovibrio desulfuricans* were approximately 3-10 nm. This was also shown previously by Creamer et al., (2007) when they determined Pd-NPs made by *Desulfovibrio desulfuricans* with size range of 1 – 6 nm, while Omajali et al., (2015) described the crystal structure and sizes of the intracellular Pd-NPs in both strains of *D. desulfuricans*. However, the ill-defined peaks shown in Fig 2 confirm that XRD is unreliable as it is very difficult to delineate the peaks precisely in this study. For this reason, direct measurement using high resolution electron microscopy may be preferable (Omajali et al., 2015).

Over all, little differences was apparent in the bio-Pd (0) produced by the two strains of *D. desulfuricans*. However, the mechanism of palladium (II) reduction by both strains of *D. desulfuricans* may vary due to differences in cell surfaces (see SEM images). Hydrogenases are known (Lloyd et al., 1998) to be involved in the periplasmic reduction of Pd (II) to Pd (0) in *D. desulfuricans* and may be involved in performing a similar function in both strains. Studies on mutant strains of *Desulfovibrio fructosovorans* lacking periplasmic hydrogenases (Mikheenko et al., 2008) confirmed this finding as Pd (0) deposition was observed to be transferred to the cytoplasmic hydrogenases (or some other oxidoreductases).

Analysis of cell surface functional groups before palladization using XPS

The thickness of the periplasmic space is ~10-50 nm (Stock et al., 1977) and that of the outer membrane is ~3-8 nm (Ahimou et al., 2007; Rouxhet et al., 1994; Hoffman et al., 2008) and hence XPS (probes depth ~5-10; Gilbert et al., 2013) reports on events at the outer membrane and its interface with the periplasm. Assuming that Pd (0) deposition occurs at or near the site of hydrogenases (Mikheenkho et al., 2008; Deplanche et al., 2010) a recognition site and translocation mechanism within and across the outer membrane are envisaged, possibly *via* Pd (II) having affinity for mechanisms that 'traffic' Ni (II) since this metal is a structural component of hydrogenases and both elements share some similar chemical behaviours (see Omajali et al., 2015).

XPS was used to probe the initial events in Pd (II) coordination to the cells during Pd (II) sorption prior to bio-Pd-NP synthesis. XPS has shown that both strains of bacteria behaved differently when contacted with a metal solution of Pd (II) at pH 2.0 and hence a new mechanism is proposed. One of the objectives of the study was to determine the involvement of fatty acid amides in Pd (II) bonding to cells prior to reduction and biocatalyst manufacture and whether the hypothesis of amide coordination is valid and hence the reason for the better catalytic properties observed above with the catalyst produced by NCIMB 8307. Table 2 shows the variation in atomic concentrations of elements (C, O, N, P, S and Ca) found on the surface of Pd-free live cells of each bacterium. Most notably is the concentration of phosphorus, sulphur and calcium on each strain. There is a significantly higher concentration of both phosphorus (3.4%) and calcium (3.45%) in the Pd-free live cells of *D. desulfuricans* NCIMB 8326 than was found in *D. desulfuricans* NCIMB 8307 (0.99% and 0.26%) respectively. See Figure 5 for the XPS spectral details of the elemental composition of Pd-free live cells.

Table 2 XPS atomic concentration of Pd-free cell surfaces of *D. desulfuricans*

	Atomic concentrations (%)	
Elemental composition	NCIMB8307	NCIMB8326
C1s	68.86 ± 2.86	61.45 ± 2.96
O1s	27.61 ± 2.99	25.58 ± 1.33
N1s	9.24 ± 2.20	9.03 ± 2.32
S2p	1.34 ± 0.40	0.93 ± 0.71
P2p	0.99 ± 0.32	3.40 ± 0.63
Ca2p	0.26 ± 0.51	3.45 ± 0.21

Results are replicates of two independent batches of experiments. Mean ± SEM

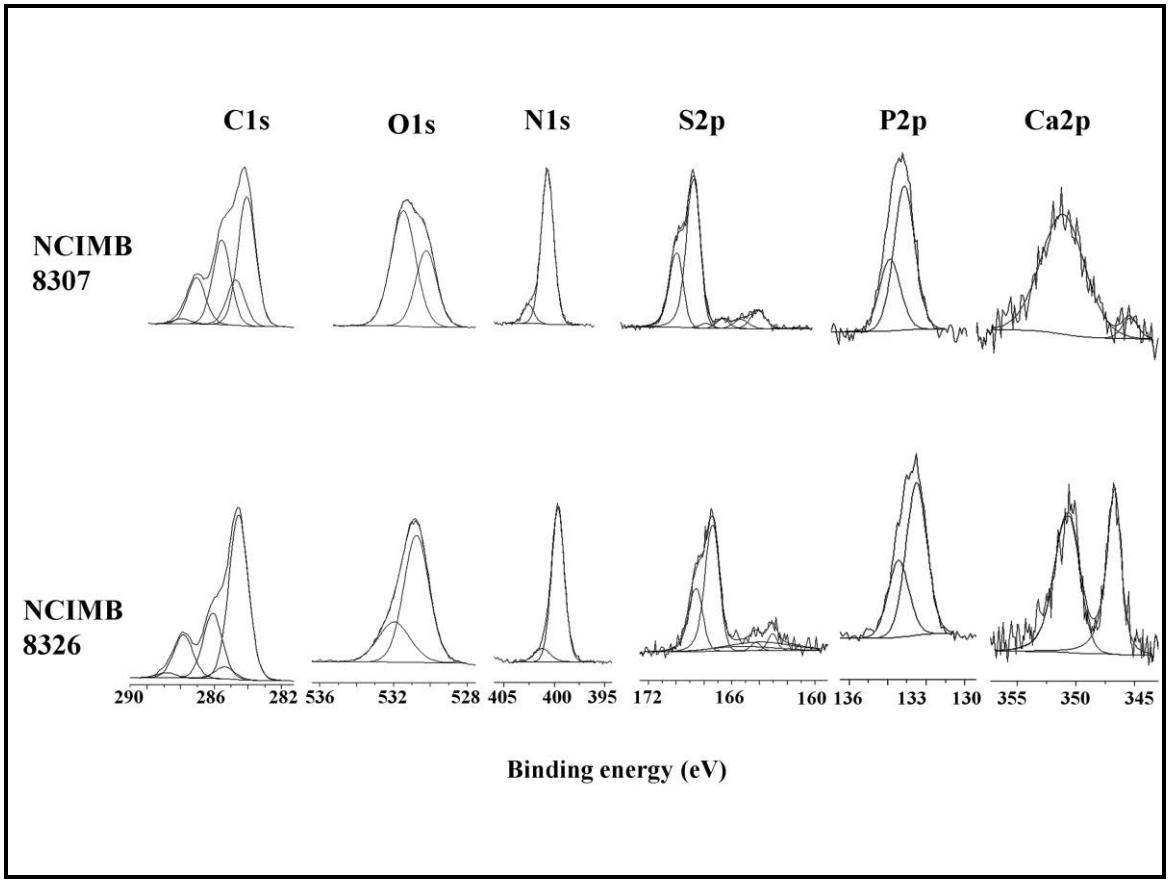

Figure 5 XPS spectra of elemental components on Pd-free cells of *D. desulfuricans* NCIMB 8307 and *D. desulfuricans* NCIMB 8326. Corresponding spectra following Pd (II) sorption is shown in Fig 7.

Group 1: C, N and S

Carbon (C1s) peaks associated with each bacterial cell surface were delineated into five components, each with an associated binding energy (Figure 5). Carbon bound to only hydrogen and carbon (C-(C, H) is attributed to a binding energy at 284.6 eV and this was the standard reference for both Pd-free live cells, Pd-sorbed and autoclaved (heat-killed) cells (Table 3 and 4, Figure 7). From the Pd-free live cells of *D. desulfuricans* NCIMB 8307, the binding energy at 285.51 eV was assigned to carbon singly bound to nitrogen (C-NH_2) and is attributed to amine. Bonding to ether, alcohol, amine or amide through single bond with oxygen or nitrogen C-(O, N) is also attributed to a higher binding energy at 286.42 eV and carbon interaction through one double bond or single bond with oxygen (O-C-O, O=C) can be assigned to the binding energy at 287.75 eV of hemiacetal, acetal, amide and carboxylate while carbon bonded through one double bond and one single bond with oxygen (O=C-OH, O=C-OR) at a binding energy of 288.73 eV is associated with ester and carboxyl groups (Table 3 and 4). In a similar way, the C1s binding energies of Pd-free cells of *D. des* NCIMB 8326 occurred at: 284.6 eV, 285.47 eV, 286.20 eV, 287.81 eV and 288. 87 eV (Table 3) respectively. Considering the nitrogen (N1s) peaks, two binding energies appeared at 399.58 eV which is associated with unprotonated (-NH-) amine or amide functions of peptide and at 401.36 eV known for protonated (-NH^+) amine or ammonium (Ahimou et al., 2007) were found on the surface of Pd-free live cells of strain NCIMB 8307, while in strain NCIMB 8326, they occurred at 399.60 eV and 401.29 eV. In addition, the presence of sulphur (S2p) peaks on the cell surfaces may be due to organic sulphur in proteins (Dufrene et al., 1996), which was slightly at a higher binding energy of 165.39 eV and 165.14 eV in both NCIMB 8307 and NCIMB 8326 respectively with corresponding peaks at higher binding energies of 167.37 eV and 167.33 eV.

Group 2: O, P and Ca

Two oxygen (O1s) peaks were associated with Pd-free live cells of *D. desulfuricans* NCIMB 8307 (Figure 5). The oxygen peak at the binding energy of 530.93 eV is due to oxygen doubly bonded with carbon (O=C) from amide and carboxyl functions and to oxygen of carboxylate while the binding energy at 531.94 eV is associated with a singly bonded oxygen to hydrogen or carbon (C-O-H of alcohol and

carboxyl, C-O-C of acetal and hemiacetal) while in *D. desulfuricans* NCIMB 8326 this bonding interaction appears at 530.96 eV and 532.69 eV respectively. Furthermore, two peaks of phosphorus (P2p) appeared at 132.93 eV and 133.68 eV in Pd-free live cells of strain NCIMB 8307 and at 132.49 eV and 133.42 eV in strain NCIMB 8326 and the binding energy at ~ 133 eV is associated with phosphate groups. Calcium, a likely exchangeable ion, was found on the cell surfaces of each Pd-free live cell of both bacteria and it appeared as a doublet at 347.65eV and 351.64 eV in *D. des* NCIMB 8307 and at 346 eV and 350.60 eV in *D. des* NCIMB 8326. Identification of the above functional groups using XPS has been reported previously in Gram-positive (Ahimou et al., 2007) and Gram-negative bacteria (Dufrene et al., 1996) but reports on interaction with Pd are very limited as explained below, while specific composition of the bacterial outer surface is likely to vary between individual species and indeed strains.

Proposed mechanism of Pd (II) coordination to cell surface ligands informed using XPS analysis

Further to the above, oxygen-containing groups have been shown to be the most important surface functional groups with respect to Pd binding in activated carbon and oxidic supports like alumina, silica and other metallic oxides (Toebes et al. 2001) which is analogous with the numerous presence of oxygen-containing groups on *D. desulfuricans* (Table 3 and 4, Figure 7). The surfaces of these support materials contain oxygen groups that are acidic, basic or neutral with both positive and negative charged surface sites present in aqueous solution and these surfaces have been shown to influence the rearrangement of metal NPs in chemical catalyst (Divins et al., 2014) (in a pH dependent way). Negatively charged surfaces (*e.g*. deprotonated acidic groups) will attract cations while positively charged (protonated basic groups) surfaces will bind to anions present in solution (Rodríguez-reinoso, 1998). In an analogous way, the oxygen-containing groups of biomass such as carboxyl, quinones and lactones are acidic in nature and have been shown to attract positively charged metal ions in solution due to their negative charges and ability to decrease the hydrophobicity of carbonated surfaces (Prado-Burguete et al. 1989; Rodríguez-reinoso, 1998). The dispersion of Pd on activated carbon was shown to be increased as a result of increased number of surface oxygen functional groups (Dong et al., 1993) analogous to the high atomic

concentration of oxygen on the surfaces of the two strains of *D. desulfuricans* (Table 2). Weakly acidic to neutral oxygen groups of phenol, carbonyls (aldehydes, amide, ketones, esters, and carboxylic acids) and ether have been shown to increase the interaction of metal precursors or metal particles with the support (Prado-Burguete et al. 1989). In terms of basic sites *e.g.* nitrogen and sulfide, their quantities are lower than acidic surface sites (Table 2) but may be found around the same location. An increase in the number of basic sites increases electrostatic attraction with metal anions and reduces repulsion (Barton et al., 1997).

Consequent upon the above surface ligands found in the Pd-free live cells of both bacteria, differences were subsequently observed during Pd (II) sorption as changes or shifts in binding energies due to Pd (II) interaction with various cell surface functional groups using XPS (Table 3 and 4). The binding energy of sulphur to Pd surface in strain NCIMB 8307 was negatively shifted (1.44 eV) to a lower binding energy of 163.97 eV which suggests the formation of a Pd-S bond (Gotterbarm et al 2012) and another to a higher energy level of 167.56 eV with a positive shift in binding energy of 0.17 eV which may be due to the formation of Pd-sulphate bond (Table 3). This could be due to stabilization of the sulphate (SO_4^{2-}) by neighbouring oxygen atoms as observed on the surface of chemically synthesized Pd (Gotterbarm et al 2012) which suggests chemical interactions with cell surface groups, *e.g.* protein-thiols. A similar trend was also observed with strain NCIMB 8326 (Table 3) and the heat-killed cells (Table 4). Azcarate et al. (2014) in their work and a previous review by Sperling and Parak (2010) showed that thiol groups (R-SH- or C-SH-containing groups) lead to strong sulphur head-metal covalent bonding and intermolecular interactions which affects the properties and reactivity of metal NPs. In this work , the atomic concentration of the metal-free surface of strain NCIMB 8307 is about 1.34% sulphur as compared to 0.93% found in strain NCIMB 8326 (Table 2) and this might affect the catalytic properties of the resulting bio-NPs. Also, Dunleavy (2006) reported that the addition of very low concentrations (<10 ppb) of H_2S and S species can prolong the life of PGM catalysts.

A previous study by de Vargas et al., (2005) only demonstrated the presence of Pd (II) binding to amine nitrogen but binding to sulfur was not examined. The presence of sulphur at the surface may be due to the presence of a sulfur-containing amino acid

located on the cell surface (Fauque et al 1988) with the ability to interact with incoming metals, since precious metals have great affinity for sulphur (Dunleavy, 2006). Pd (II) coordination to disulphides, sulphinic acids, thioethers and sulphur-containing amino acids has been shown previously (Luo et al., 1999).

The presence of phosphate groups (PO_4^{3-}) in *D. desulfuricans* was not reported or sought in previous XPS studies on Pd binding in this bacterium. In both strains of bacteria, a positive shift in binding energies of phosphate in both live and heat-killed cells (Tables 3 and 4) were observed. There was a higher positive shift (0.49 eV) in binding energy observed after contact with Pd (II) in live cells of *D. des* NCIMB 8326 (Table 3) than that of strain NCIMB 8307 (0.26 eV) which suggest a more pronounced interaction with strain NCIMB 8326 to form Pd-phosphate bond at 133.19 eV and 132.98 eV respectively. Binding of Pd to phosphate in *B. subtilis* containing immobilized Au^{3+} (Southam and Beveridge, 1996) have been reported. In the Gram-negative enterobacterium *Serratia* sp a ^{31}P NMR study specifically identified the phosphate groups of the lipid A component of the lipopolysaccharide as being the site of initial coordination of Cu (II) to the Gram-negative bacterial surface (Bonthrone et al., 2000; Macaskie et al., 2000) which is in accordance with the possibility of the presence of this feature in strain NCIMB 8326 in relation to the different surface topographies reported by AFM (Table 1). In this present study Pd-O bonding was confirmed due to the positive shifts in the binding energy of the O1s regions (Table 3 and 4). As the cells come in contact with Pd (II), the O1s in the Pd-free cells of *D.des* NCIMB 8307 peak at 530.93 eV increased to 531.09 eV as a result of a positive shift (0.16eV) which has been shown to be due to Pd-O interaction *via* –OH groups on the cells (Chen et al., 2011; Divins et al., 2014) while a positive shift (0.53 eV) in the second peak of O1s was due to oxidized carbon on the cell surface or the silicon substrate used. A higher shift in binding energy was observed in both live and heat-killed cells of *D. des* NCIMB 8326 (Table 3 and 4). de Vargas et al., (2005) also reported bonding to oxygen in *D. desulfuricans*. This interaction of the Pd-O bonding could also be due to phosphorus at the cell surface, as phosphoryl groups *via* oxygen on bacterial surfaces are known to be involved in bonding to divalent cations (Warthmann et al., 2000) in addition to the involvement of lipid A as noted above. The above

discussions points to interaction of incoming Pd (II) *via* coordination to cell surface components of polymers, proteins and phospholipids.

The involvement of Pd bonding to amine nitrogen was very prominent when the C1s region was considered. There was a significant positive shift (0.22 eV) in binding energy of the C1s amine region (~285 eV) of strain NCIMB 8307 than in strain NCIMB 8326 which is negative (0.01eV) with a corresponding positive shift in the nonprotonated amine nitrogen (0.13 eV and 0.01eV) and protonated amine nitrogen (0.17 eV and 0.12 eV) respectively. It has long been shown that when the amide is neutral (as in bacterial cell) protonation and metallization occurs at the amide oxygen (Sigel and Martin, 1982) and when anionic amide nitrogen becomes protonated, metallization occurs at the amide nitrogen *via* hydrogen substitution (as in this case of bio-Pd, where Pd (II) is presented at pH 2.3) due to the protonation of the bacterial cell. The interaction of the Pd-N bond appears more prominent in strain NCIMB 8307 than in strain NCIMB 8326 with an increased area ratio of 0.25 to 0.18 in the latter with corresponding lower values of 0.12 and 0.06 in heat-killed cells when the N1s peak areas were considered. The lack of clear difference in the C1s amide regions (~287 eV), with resultant negative shifts in binding energies (Table 3 and 4) supports a lack of evidence to the hypothesis of Pd (II) binding to fatty acid amide in *D. desulfuricans*. The above positive chemical shifts may be explained as a consequence of electron density transfer from Pd (II) to the surface ligands on the bacterial cells which has been shown in chemical systems to lead to strong metal-support interaction (Kim and Winograd, 1975) while negative shifts in Pt-supported on Al_2O_3 was attributed to the inability of the system formed by the support and metal to conductively couple the Fermi edge of two components (Venezia et al., 1992). Notably, the molar ratios of the elements to total carbon (Figure 6) on the cell surface groups of Pd-free cells appears to differ considerably between heat-killed (Figure 7b) and Pd-treated live cells probably (Figure 7a) as a result of cell surface modification due to Pd (II) interaction and heat-treatment of cells. Modification of the cell wall by chemicals was suggested to have altered the architecture and restricted the exposure of available groups (Beveridge and Murray, 1980) in *B. subtilis.* In the present case this would account for the difference between live and heat-killed cells as evidenced in Figure 6 and 7 but not the difference between the two strains. The most striking feature of figure 6 was the high

concentration of surface phosphorus and calcium, attributed as described above to the presence of lipid A and the presence of Ca coordinating to this in live cells of strain NCIMB 8326 but not strain NCIMB 8307.

The binding mechanisms of the two strains may be *via* an ion-exchange mechanism of Pd (II) with calcium bound to Pd-free live cells (Table 2) prior to Pd (II) uptake which was not detected after Pd (II) sorption (Figure 6) akin to the binding mechanism of in-coming Cd (II) to *Serratia* sp (see previously). The atomic concentration of the calcium varies, with 3.45% on the Pd-free cells of strain NCIMB 8326 compared to 0.26% in strain NCIMB 8307 (Table 2, Figure 6) and also phosphate in parallel. The presence of extracellular matrix in strain NCIMB 8326 as suggested by SEM (Figure 4d) above may be the reason for the higher amount of calcium ion which may also influence the binding mechanism of Pd (II) to oxygen-containing groups. Polysaccharides are the major components of most EPS, commonly in combination with polypeptides, nucleic acids, phospholipids, and other polymeric compounds (Decho, 2010). Calcium ions adsorbed onto the bacterial surface can induce the precipitation of fine grained calcium carbonate by the complexation of counter ions (Schultze-Lam et al., 1996) – a possible route by which bio-cement is produced by some bacteria. Further studies have reported (Gao et al., 1995) that the oxygen site of carboxylic acids may donate a lone pair of electron to a transition metal ion (Lewis acid) and such ion exchange mechanism between a transition metal and the O-binding site with Ca ion may occur, leaving calcium behind in solution, a possible reason for its absence after Pd sorption in both bacteria (Figure 6) which was not tested. A similar result was reported by Southam and Beveridge (1996) whereby a metal-free cell of *B. subtilis* was found to contain Ca in the range of 7-8% atomic concentration which was later not detected in Au^{3+}-immobilzed cells. This supports a possible ion-exchange mechanism of Pd (II) with oxygen-containing carboxylic acid groups on the bacterial cell surfaces during Pd (II) uptake. It has been experimentally proven that the carboxyl groups are more on bacterial cell surface and are mostly involved in palladium binding than the amino groups (Remoudaki et al 1999). Beveridge and Murray (1980) have further shown that in *B. subtilis*, the carboxyl group of glutamic acid are the main site of Au (III) binding while the amino group does not make a significant contribution. This is because of the ability of soluble metals to bind easily to the more reactive COO^- group once they

penetrate the extensive peptidoglycans of *B. subtilis*. This study also suggests that exchange mechanisms between protons of the identified sulfur-containing ligands and nitrogen containing ligands (protonated amine) with Pd (II) ions in the solution during sorption which is stronger in strain NCIMB 8307, may occur.

This study identifies the ligand binding sites on the surface of *D. desulfuricans* but is not able to provide specific information about the biochemical mechanism of translocation and patterning of Pd at the surface. Given the greater extent of putative lipid A in strain NCIMB 8326 it seems likely that this 'diverts' in-coming Pd (II) away from specific translocation mechanism to the point of 'correct' patterning for maximum catalytic activity (Omajali et al., 2015). Future studies would aim to support this hypothesis by the use of ^{31}P NMR but the strong magnetic property of Pd-bionanoparticles (Creamer et al., 2011; A.R. Williams, PhD thesis in preparation) would complicate interpretation of NMR data which is the reason underpinning early work to use " NMR-silent" Cd (II) (Bonthrone et al.,2000; Macaskie et al., 2000). A molecular method to delete lipid A would be a simpler approach to obtain proof but in conclusion this study provides no evidence for a role of fatty acid amides in Pd (II) binding but evidence for a 'nuisance' effect of lipid A. The possibility of lipid A "masking" access to Pd (II) to the sites responsible for giving materials of the highest catalytic activity should be noted as a potential adverse effect and hence a future molecular strain modification would be required for improved catalytic synthesis.

Table 3 Binding of Pd (II) on cell surface of live cells of *D. desulfuricans* probed using XPS analysis

Elements	Chemical functions	Binding Energies (eV) of peak positions					
		NCIMB 8307			NCIMB 8326		
		before sorption	after sorption	shift in BE	before sorption	after sorption	shift in BE
C1s	C-(C,H) C-NH2 C-(O,N) C=O,O-C-O O=C-OH, O=C-OR	284.60 285.51 286.24 287.75 288.73	284.60 285.73 286.31 287.71 288.69	0.00 (+) 0.22 (+) 0.07 (-) 0.04 (-) 0.04	284.60 285.47 286.20 287.81 288.66	284.60 285.46 286.21 287.73 288.87	0.00 (-) 0.01 (+) 0.01 (-) 0.08 (+) 0.21
O1s	O=C,P=O, P-O$^-$ HO-C,C-O-C P-O-C	530.93 531.94	531.09 532.47	(+) 0.16 (+) 0.53	530.96 531.69	531.26 532.37	(+)0.30 (+)0.68
N1s	-NH- -NH$^+$	399.58 401.36	399.71 401.53	(+)0.13 (+)0.17	399.60 401.29	399.61 401.41	(+)0.01 (+)0.12
P2p	PO_4^{3-}	132.93 133.68	133.19 134.12	(+)0.26 (+)0.44	132.49 133.42	132.98 133.61	(+)0.49 (+)0.19
S2p	S^{2-} SO_4^{2-}	165.39 167.39	163.97 167.56	(-)1.44 (+)0.17	165.14 167.33	163.65 167.43	(-)1.49 (+)0.1
Ca2p	Ca^{2+}	347.65 351.64	n.d	-	346.68 350.60	n.d	-

Peak positions are signals of photoelectrons from various energy levels from two independent batches of experiments. Shift in binding energies (BE) is due to the difference between the binding energies of metal-free cells (before Pd (II) sorption) and after interaction of live cells with Pd (II) solution (after sorption) in *D. desulfuricans* NCIMB 8307 and *D. desulfuricans* NCIMB 8326 as adsorbents. n.d = Not detected.

Table 4 Binding of Pd (II) on cell surface of autoclaved (heat-killed) cells of *D. desulfuricans* probed using XPS analysis

Elements	Chemical functions	Binding Energies (eV) of peak positions					
		NCIMB 8307			NCIMB 8326		
		before sorption	after sorption	shift in BE	before sorption	after sorption	shift in BE
C1s	C-(C,H)	284.60	286.60	0.00	284.60	284.60	0.00
	C-NH2	285.51	285.53	(+)0.02	285.47	285.51	(+)0.04
	C-(O,N)	286.24	286.35	(+)0.11	286.20	286.29	(+)0.09
	C=O,O-C-O	287.75	287.69	(-)0.06	287.81	287.70	(-)0.11
	O=C-OH,	288.73	288.76	(+)0.03	288.66	288.71	(+)0.05
	O=C-OR						
O1s	O=C,P=O,	530.93	530.93	0.00	530.96	531.52	(+)0.56
	P-O^-						
	HO-C,C-O-C	531.93	532.27	(+)0.34	531.69	532.31	(+)0.62
	P-O-C						
N1s	-NH-	399.58	399.66	(+)0.08	399.60	399.66	(+)0.06
	$-NH^+$	401.36	401.41	(+)0.05	401.29	401.50	(+)0.21
P2p	PO_4^{3-}	132.93	133.02	(+)0.09	132.49	132.96	(+)0.47
		133.68	134.04	(+)0.36	133.42	133.98	(+)0.56
S2p	S^{2-}	165.39	163.81	(-)1.58	165.14	163.75	(-)1.39
	SO_4^{2-}	167.39	167.24	(-)0.15	167.33	167.49	(+)0.16
Ca2p	Ca^{2+}	347.65	n.d	-	346.68	n.d	-
		351.64			350.60		

Peak positions are signals of photoelectrons from various energy levels from two independent batches of experiments. Shift in binding energies (BE) is due to the difference between the binding energies of metal-free cells (before Pd (II) sorption) and after interaction of heat-killed cells with Pd (II) solution in *D. desulfuricans* NCIMB 8307 and *D. desulfuricans* NCIMB 8326 as adsorbents. n.d = Not detected.

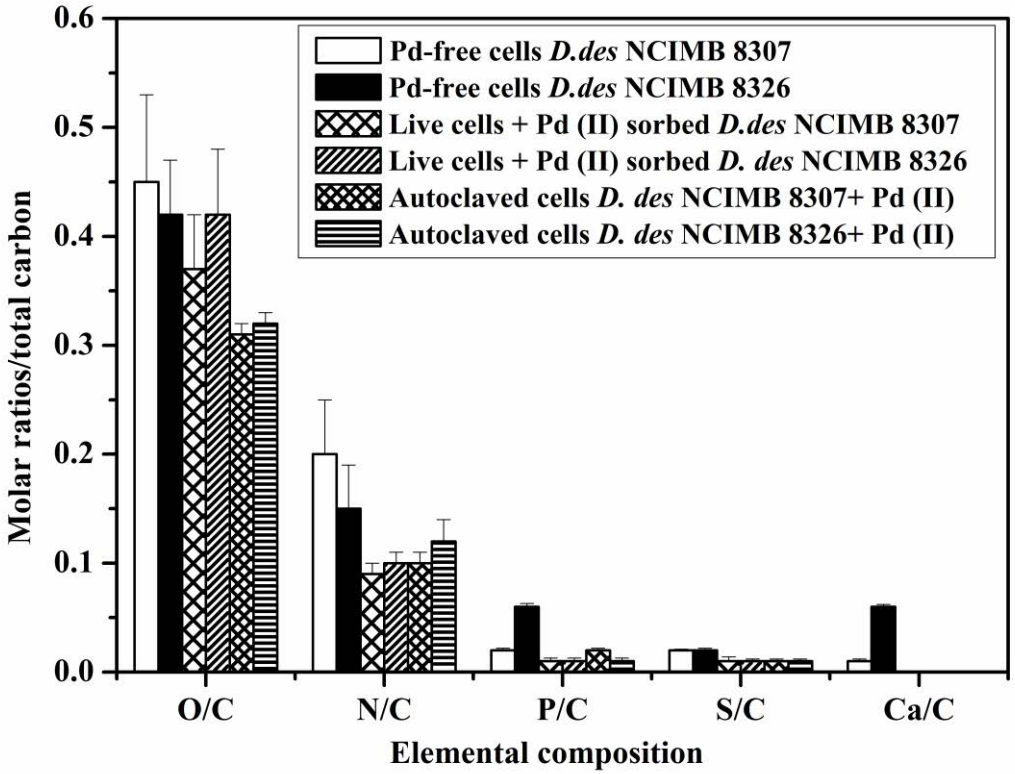

Figure 6 Elemental compositions (molar ratios *vs* total carbon) on Pd-free, Pd (II) –sorbed and heat-killed cells of *D. desulfuricans* from two independent batches of experiments.

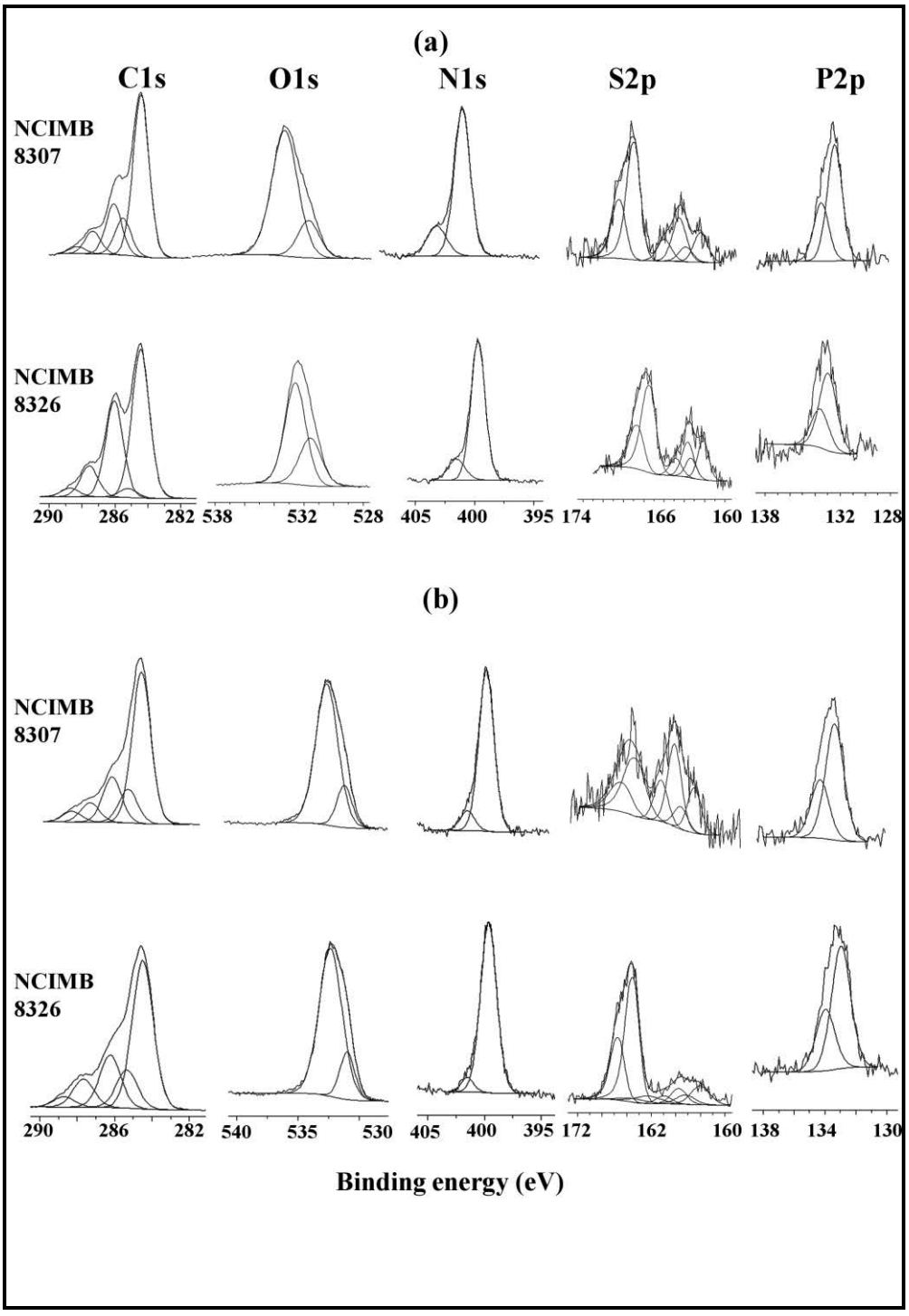

Figure 7 XPS spectra of elemental components of live cells of *D. desulfuricans,* NCIMB 8307 and NCIMB 8326 (a) and corresponding spectra for heat-killed cells (b) following Pd (II) sorption.

Conclusion

This study does not show a direct interaction of Pd (II) to fatty acid amide in *D. desulfuricans* NCIMB 8307 as hypothesized but to protein amides. However, it has been found that *D. desulfuricans* binds to more ligands than previously reported *via* XPS analysis and a new mechanism of ion-exchange and proton-exchange is therefore proposed. It was confirmed in this study, however, that differences exist in terms of morphology, catalytic ability and binding mechanism to Pd (II) between the two strains of *D. desulfuricans*. The catalytic properties of 5% bio-Pd made by strain NCIMB8307 in the hydrogenation of soybean oil towards monosaturated fatty acid methyl esters was better than that made by *D. des* NCIMB 8326 which may be the result of several factors such as higher textural (roughness) cell surface (outer membrane) and also due to increased number of oxygen-containing surface ligands. Furthermore, stronger interaction to the amine nitrogen group by the cell surface of strain NCIMB 8307 compared to strain NCIMB 8326 considering positive shifts in binding energies is also a potentially important factor towards improved catalytic property as amine-functionalized abiotic surfaces for Pd-synthesized catalyst showed improved catalytic properties (De corte et al ., 2013). However, further analysis [X-ray absorption spectroscopy (XAS) coupled with extended X-ray absorption fine structure (EXAFS) and X-ray absorption near edge structures (XANES)] may be required to show that these factors are directly linked.

The extracellular layer of strain NCIMB 8326 potentially masks the passage of Pd (II) to where it ought to get in order to make a good catalyst contrary to better interaction observed in strain NCIMB 8307.

Acknowledgements

The authors are thankful to the Commonwealth scholarships for funding JBO. The atomic force microscope used in this research was obtained, through Birmingham Science City: Innovative Uses for Advanced Materials in the Modern World (West Midlands Centre for Advanced Materials Project 2), with support from Advantage West

Midlands (AWM) and part funded by the European Regional Development Fund (ERDF).

References

Ahimou, F.; Boonaert, C. J. P.; Adriaensen, Y.; Jacques, P.; Thonart, P.; Paquot, M.; Rouxhet, P. G., XPS analysis of chemical functions at the surface of *Bacillus subtilis*. *Journal of Colloid and Interface Science* **2007,** *309*, 49-55.

Azcarate, J. C.; Floridia Addato, M. A.; Rubert, A.; Corthey, G.; Kuerten Moreno, G. S.; Benitez, G.; Zelaya, E.; Salvarezza, R. C.; Fonticelli, M. H., Surface Chemistry of thiomalic acid adsorption on planar gold and gold nanoparticles. *Langmuir* **2014,** *30*, 1820-1826.

Barton, S. S.; Evans, M. J. B.; Halliop, E.; MacDonald, J. A. F., Acidic and basic sites on the surface of porous carbon. *Carbon* **1997,** *35*, 1361-1366.

Baxter-Plant, V. S.; Mikheenko, I. P.; Macaskie, L. E., Sulphate reducing bacteria, palladium and the reductive dehalogenation of chlorinated compounds. *Biodegradation* **2003,** *14*, 83-90.

Beauregard, D. A.; Yong, P.; Macaskie, L. E.; Johns, M. L., Using non-invasive magnetic resonance imaging (MRI) to assess the reduction of Cr(VI) using a biofilm–palladium catalyst. *Biotechnology and Bioengineering* **2010,** *107*, 11-20.

Bennett, J. A.; Mikheenko, I. P.; Deplanche, K.; Shannon, I. J.; Wood, J.; Macaskie, L. E., Nanoparticles of palladium supported on bacterial biomass: New re-usable heterogeneous catalyst with comparable activity to homogeneous colloidal Pd in the Heck reaction. *Applied Catalysis B: Environmental* **2013,** *140–141*, 700-707.

Beveridge, T. J.; Murray, R. G., Sites of metal deposition in the cell wall of Bacillus subtilis. *Journal of Bacteriology* **1980,** *141*, 876-87.

Bonthrone, K. M.; Quarmby, J.; Hewitt, C. J.; Allan, V. J. M.; Paterson-Beedle, M.; Kennedy, J. F.; Macaskie, L. E., The effect of the growth medium on the composition and metal binding behaviour of the extracellular polymeric material of a metal-accumulating *Citrobacter* sp. *Environmental Technology* **2000,** *21*, 123-134.

Bouriazos, A., S. Sotiriou, C. Vangelis, and G. Papadogianakis. Catalytic conversions in green aqueous media: Part 4. Selective hydrogenation of polyunsaturated methyl esters of vegetable oils for upgrading biodiesel. *Journal of Organometallic Chemistry*. **2010**, *695*, 327-337.

Casalot, L.; Hatchikian, C. E.; Forget, N.; de Philip, P.; Dermoun, Z.; Belaich, J. P.; Rousset, M., Molecular study and partial characterization of iron-only hydrogenase in *Desulfovibrio fructosovorans*. *Anaerobe* **1998,** *4*, 45-55.

Chen, L.; Yelon, A.; Sacher, E., X-ray photoelectron spectroscopic studies of Pd nanoparticles deposited onto highly oriented pyrolytic graphite: interfacial interaction, spectral asymmetry, and size determination. *Journal of Physical Chemistry C* **2011,** *115*, 7896-7905.

Christy, A. A.; Xu, Z.; Harrington, P. d. B., Thermal degradation and isomerisation kinetics of triolein studied by infrared spectrometry and GC-MS combined with chemometrics. *Chemistry and Physics of Lipids* **2009,** *158*, 22-31.

Creamer, N. J.; Mikheenko, I. P.; Yong, P.; Deplanche, K.; Sanyahumbi, D.; Wood, J.; Pollmann, K.; Merroun, M.; Selenska-Pobell, S.; Macaskie, L. E., Novel supported Pd hydrogenation bionanocatalyst for hybrid homogeneous/heterogeneous catalysis. *Catalysis Today* **2007,** *128*, 80-87.

Creamer, N. J.; Mikheenko, I. P.; Johnson, C.; Cottrell, S. P.; Macaskie, L. E., Local magnetism in palladium bionanomaterials probed by muon spectroscopy. *Biotechnology Letters* **2011,** *33*, 969-976.

Das, N., Recovery of precious metals through biosorption — A review. *Hydrometallurgy* **2010,** *103*, 180-189

Decho, A. W., Overview of biopolymer-induced mineralization: What goes on in biofilms? *Ecological Engineering* **2010,** *36*, 137-144.

De Corte, S.; Bechstein, S.; Lokanathan, A. R.; Kjems, J.; Boon, N.; Meyer, R. L., Comparison of bacterial cells and amine-functionalized abiotic surfaces as support for Pd nanoparticle synthesis. *Colloids and Surfaces B: Biointerfaces* **2013,** *102*, 898-904.

Deplanche, K. New nanocatalysts made by bacteria from metal solutions and recycling of metal wastes. PhD Thesis, University of Birmingham, UK, 2008

Deplanche, K.; Caldelari, I.; Mikheenko, I. P.; Sargent, F.; Macaskie, L. E., Involvement of hydrogenases in the formation of highly catalytic Pd(0) nanoparticles by bioreduction of Pd(II) using *Escherichia coli* mutant strains. *Microbiology* **2010,** *156*, 2630-2640.

Deplanche, K.; Murray, A.; Taylor, S.; Macaskie, L.E. Biorecycling of precious metals and rare earth elements. In *Nanomaterials*, Rahman, M.M. Ed. In Tech publishing, Rijeka, Croatia: **2011**, pp 279-314. ISBN: 978-953-307-913-4.

Deplanche, K.; Merroun, M. L.; Casadesus, M.; Tran, D. T.; Mikheenko, I. P.; Bennett, J. A.; Zhu, J.; Jones, I. P.; Attard, G. A.; Wood, J.; Selenska-Pobell, S.; Macaskie, L. E., Microbial synthesis of core/shell gold/palladium nanoparticles for applications in green chemistry. *Journal of the Royal Society Interface* **2012,** *9*, 1705-1712.

Deplanche, K.; Bennett, J. A.; Mikheenko, I. P.; Omajali, J.; Wells, A. S.; Meadows, R. E.; Wood, J.; Macaskie, L. E., Catalytic activity of biomass-supported Pd nanoparticles: Influence of the biological component in catalytic efficacy and potential application in 'green' synthesis of fine chemicals and pharmaceuticals. *Applied Catalysis B: Environmental* **2014,** *147*, 651-665.

de Vargas, I.; Macaskie, L. E.; Guibal, E., Biosorption of palladium and platinum by sulfate-reducing bacteria. *Journal of Chemical Technology and Biotechnology* **2004,** *79*, 49-56.

de Vargas, I.; Sanyahumbi, D.; Ashworth, M. A.; Hardy, C. M.; Macaskie, L. E. In *Use of X-ray photoelectron spectroscopy to elucidate the mechanism of palladium and platinum biosorption by Desulfovibrio desulfuricans biomass*, 25th - 29th September; 16th int. Biohydrometallurgy Symp., Cape Town, Harrison, S. T. L., Rawlings, D.E., Petersen, J., Ed. Cape Town, **2005**; pp 605-616.

De Windt, W.; Aelterman, P.; Verstraete, W., Bioreductive deposition of palladium (0) nanoparticles on *Shewanella oneidensis* with catalytic activity towards reductive dechlorination of polychlorinated biphenyls. *Environmental Microbiology* **2005,** *7*, 314-325.

Divins, N. J.; Angurell, I.; Escudero, C.; Perez-Dieste, V.; Llorca, J., Influence of the support on surface rearrangements of bimetallic nanoparticles in real catalysts. *Science* **2014,** *346*, 620-623.

Dong Jin, S.; Tae-Jin, P.; Son-Ki, I., Effect of surface oxygen groups of carbon supports on the characteristics of Pd/C catalysts. *Carbon* **1993,** *31*, 427-435.

Du, L.-N.; Wang, B.; Li, G.; Wang, S.; Crowley, D. E.; Zhao, Y.-H., Biosorption of the metal-complex dye Acid Black 172 by live and heat-treated biomass of *Pseudomonas* sp. strain DY1: Kinetics and sorption mechanisms. *Journal of Hazardous Materials* **2012,** *205–206*, 47-54.

Dufrêne, Y. F.; Rouxhet, P. G., X-ray photoelectron spectroscopy analysis of the surface composition of *Azospirillum brasilense* in relation to growth conditions. *Colloids and Surfaces B: Biointerfaces* **1996,** *7*, 271-279.

Dufrêne, Y. F.; Boonaert, C. J. P.; Rouxhet, P. G., Adhesion of *Azospirillum brasilense*: role of proteins at the cell-support interface. *Colloids and Surfaces B: Biointerfaces* **1996,** *7*, 113-128.

Dunleavy, J. K., Sulfur as a catalyst poison. *Platinum Metals Review* **2006,** *50*, 110.

Fauque, G.; Peck, H. D., Jr.; Moura, J. J.; Huynh, B. H.; Berlier, Y.; DerVartanian, D. V.; Teixeira, M.; Przybyla, A. E.; Lespinat, P. A.; Moura, I.; et al., The three classes of hydrogenases from sulfate-reducing bacteria of the genus *Desulfovibrio*. *FEMS Microbiology Review* **1988,** *4*, 299-344.

Fernández, M. B.; Sánchez M, J. F.; Tonetto, G. M.; Damiani, D. E., Hydrogenation of sunflower oil over different palladium supported catalysts: Activity and selectivity. *Chemical Engineering Journal* **2009,** *155*, 941-949.
Gadd, G. M., Metals, minerals and microbes: geomicrobiology and bioremediation. *Microbiology* **2010,** *156*, 609-643.

Gao, Y.-M.; Sengupta, A. K.; Simpson, D., A new hybrid inorganic sorbent for heavy metals removal. *Water Research* **1995,** *29*, 2195-2205.

Gilbert, J. B.; Rubner, M. F.; Cohen, R. E., Depth-profiling X-ray photoelectron spectroscopy (XPS) analysis of interlayer diffusion in polyelectrolyte multilayers. *Proceedings of the National Academy of Sciences of the United States of America* **2013,** *110*, 6651-6656.

Goldsworthy, M. J. H. Hydrocarbon biosynthesis in *Mycobacterium* sp. NCIMB 10403 and *Desulfovibrio desulphuricans*. PhD Thesis, Unversity of Exeter, Exeter, UK **2011**.

Gotterbarm, K.; Luckas, N.; Hoefert, O.; Lorenz, M. P. A.; Streber, R.; Papp, C.; Vines, F.; Steinrueck, H.-P.; Goerling, A., Kinetics of the sulfur oxidation on palladium: A combined in situ x-ray photoelectron spectroscopy and density-functional study. *Journal of Chemical Physics* **2012,** *136*.

Harrad, S.; Robson, M.; Hazrati, S.; Baxter-Plant, V. S.; Deplanche, K.; Redwood, M. D.; Macaskie, L. E., Dehalogenation of polychlorinated biphenyls and polybrominated dipheny ethers using a hybrid bioinorganic catalyst. *Journal of Environmental Monitoring* **2007,** *9*, 314-318.

Hoffmann, C.; Leis, A.; Niederweis, M.; Plitzko, J. M.; Engelhardt, H., Disclosure of the mycobacterial outer membrane: Cryo-electron tomography and vitreous sections reveal the lipid bilayer structure. *Proceedings of the National Academy of Sciences of the United States of America* **2008,** *105*, 3963-3967.

Jaboyedoff, M.; Kubler, B.; Thelin, P. H., An empirical Scherrer equation for weakly swelling mixed-layer minerals, especially illite-smectite. *Clay Minerals* **1999,** *34*, 601-617.

Kazy, S. K.; D'Souza, S. F.; Sar, P., Uranium and thorium sequestration by a *Pseudomonas* sp.: mechanism and chemical characterization. *Journal of Hazardous Materials* **2009,** *163*, 65-72.

Kim, K. S.; Winograd, N., X-ray photoelectron spectroscopic binding energy shifts due to matrix in alloys and small supported metal particles. *Chemical Physics Letters* **1975,** *30*, 91-95.

Lloyd, J. R.; Yong, P.; Macaskie, L. E., Enzymatic recovery of elemental palladium by using sulfate-reducing bacteria. *Applied and Environmental Microbiology* **1998,** *64*, 4607-4609.

Luo, X. M.; Huang, W.; Mei, Y. H.; Zhou, S. Z.; Zhu, L. G., Interaction of palladium (II) complexes with sulfur-containing peptides studied by electrospray mass spectrometry. *Inorganic Chemistry* **1999,** *38*, 1474-1480.
Macaskie, L. E.; Bonthrone, K. M.; Yong, P.; Goddard, D. T., Enzymically mediated bioprecipitation of uranium by a *Citrobacter* sp: a concerted role for exocellular lipopolysaccharide and associated phosphatase in biomineral formation. *Microbiology* **2000,** *146*, 1855-67.

Macaskie, L. E.; Creamer, N. J.; Essa, A. M. M.; Brown, N. L., A new approach for the recovery of precious metals from solution and from leachates derived from electronic scrap. *Biotechnology and Bioengineering* **2007,** *96*, 631-639.

Maillard, F.; Schreier, S.; Hanzlik, M.; Savinova, E. R.; Weinkauf, S.; Stimming, U., Influence of particle agglomeration on the catalytic activity of carbon-supported Pt nanoparticles in CO monolayer oxidation. *Physical Chemistry Chemical Physics* **2005,** *7*, 385-393.

Mikheenko, I. P.; Rousset, M.; Dementin, S.; Macaskie, L. E., Bioaccumulation of palladium by *Desulfovibrio fructosovorans* wild-type and hydrogenase-deficient strains. *Applied and Environmental Microbiology* **2008,** *74*, 6144-6146.

Mozaffarian, D., Trans fatty acids - Effects on systemic inflammation and endothelial function. *Atherosclerosis Supplements* **2006,** *7*, 29-32.

Murray, A. J.; Singh, S.; Vavlekas, D.; Tolley, M. R.; Macaskie, L. E., Continuous biocatalytic recovery of neodymium and europium. *RSC Advances* **2015,** *5*, 8496-8506.

Murray, A. J.; Taylor, S.; Zhu, J.; Wood, J.; Macaskie, L. E., A novel biorefinery: Biorecovery of precious metals from spent automotive catalyst leachates into new catalysts effective in metal reduction and in the hydrogenation of 2-pentyne. Min Eng. In Press. **2015**.

Okura, I., Hydrogenase and its application for photoinduced hydrogen evolution. *Coordination Chemistry Reviews* **1985,** *68*, 53-99.

Omajali, J.B; Mikheenkho, I.P; Merroun, L.M; Wood, J; Macaskie L.E.,
Characterization of intracellular palladium nanoparticles synthesized by *Desulfovibrio desulfuricans* and *Bacillus benzeovorans*. *Journal of Nanoparticle Research* **2015,** *17*, 1-17.

Prado-Burguete, C.; Linares-Solano, A.; Rodríguez-Reinoso, F.; de Lecea, C. S.-M., The effect of oxygen surface groups of the support on platinum dispersion in Pt/carbon catalysts. *Journal of Catalysis* **1989,** *115*, 98-106.

Redwood, M. D.; Deplanche, K.; Baxter-Plant, V. S.; Macaskie, L. E., Biomass-supported palladium catalysts on *Desulfovibrio desulfuricans* and *Rhodobacter sphaeroides*. *Biotechnology and Bioengineering* **2008,** *99*, 1045-1054.

Remoudaki E; Tsezos M; Hatzikioseyian A; Y, K., Mechanism of palladium biosorption by microbial biomass. The effects of metal ionic speciation and solution co-ions. *Process Metallurgy* **1999,** *9B*, 449-462.
Rodríguez-Reinoso, F., The role of carbon materials in heterogeneous catalysis. *Carbon* **1998,** *36*, 159-175.

Rouxhet, P. G.; Mozes, N.; Dengis, P. B.; Dufrêne, Y. F.; Gerin, P. A.; Genet, M. J., Application of X-ray photoelectron spectroscopy to microorganisms. *Colloids and Surfaces B: Biointerfaces* **1994,** *2*, 347-369.

Schlüter, M.; Hentzel, T.; Suarez, C.; Koch, M.; Lorenz, W. G.; Böhm, L.; Düring, R.-A.; Koinig, K. A.; Bunge, M., Synthesis of novel palladium(0) nanocatalysts by microorganisms from heavy-metal-influenced high-alpine sites for dehalogenation of polychlorinated dioxins. *Chemosphere* **2014,** *117*, 462-470.

Schultze-Lam, S.; Fortin, D.; Davis, B. S.; Beveridge, T. J., Mineralization of bacterial surfaces. *Chemical Geology* **1996,** *132*, 171-181.

Sigel, H.; Martin, R. B., Coordinating properties of the amide bond-stability and structure of metal-ion complexes of peptides and related ligands. *Chemical Reviews* **1982,** *82*, 385-426.

Southam, G.; Beveridge, T. J., The occurrence of sulfur and phosphorus within bacterially derived crystalline and pseudocrystalline octahedral gold formed in vitro. *Geochimica et Cosmochimica Acta* **1996,** *60*, 4369-4376

Smith, M. A.; Zoelle, A.; Yang, Y.; Rioux, R. M.; Hamilton, N. G.; Arnakawa, K.; Nielsen, P. K.; Trunschke, A., Surface roughness effects in the catalytic behavior of vanadia supported on SBA-15. *Journal of Catalysis* **2014,** *312*, 170-178.

Sperling, R. A.; Parak, W. J., Surface modification, functionalization and bioconjugation of colloidal inorganic nanoparticles. *Philosophical Transactions of the Royal Society a-Mathematical Physical and Engineering Sciences* **2010,** *368*, 1333-1383.

Stock, J. B.; Rauch, B.; Roseman, S., Periplasmic space in *Salmonella typhimurium* and *Escherichia coli*. *J Biol Chem* **1977,** *252* (21), 7850-61.

Toebes, M. L.; Dillen, J. A. v.; Jong, K. P. d., Synthesis of supported palladium catalysts. *Journal of Molecular Catalysis A-chemical* **2001,** *173*, 75-98.

van der Mei, H. C.; de Vries, J.; Busscher, H. J., X-ray photoelectron spectroscopy for the study of microbial cell surfaces. *Surface Science Reports* **2000,** *39*, 1-24.

Venezia, A. M.; Duca, D.; Floriano, M. A.; Deganello, G.; Rossi, A., XPS study of pumice-supported palladium and platinum catalysts. *Surface and Interface Analysis* **1992,** *19*, 543-547.

Vijayaraghavan, K.; Mao, J.; Yun, Y.-S., Biosorption of methylene blue from aqueous solution using free and polysulfone-immobilized *Corynebacterium glutamicum*: batch and column studies. *Bioresource Technology* **2008,** *99*, 2864-2871.
Volesky, B., Detoxification of metal-bearing effluents: biosorption for the next century. *Hydrometallurgy* **2001,** *59*, 203-216.

Warthmann, R.; van Lith, Y.; Vasconcelos, C.; McKenzie, J. A.; Karpoff, A. M., Bacterially induced dolomite precipitation in anoxic culture experiments. *Geology* **2000,** *28*, 1091-1094.

Wang, J.; He, S. Y.; Xu, L. N.; Gu, N., Transmission electron microscopy and atomic force microscopy characterization of nickel deposition on bacterial cells. *Chinese Science Bulletin* **2007,** *52*, 2919-2924.

Won, S. W.; Kotte, P.; Wei, W.; Lim, A.; Yun, Y. S., Biosorbents for recovery of precious metals. *Bioresource Technology* **2014,** *160*, 203-212.

Wood, J.; Bodenes, L.; Bennett, J.; Deplanche, K.; Macaskie, L. E., Hydrogenation of 2-butyne-1,4-diol using novel bio-palladium catalysts. *Industrial & Engineering Chemistry Research* **2010,** *49*, 980-988.

Yong, P.; Rowson, N. A.; Farr, J. P. G.; Harris, I. R.; Macaskie, L. E., Bioaccumulation of palladium by *Desulfovibrio desulfuricans*. *Journal of Chemical Technology and Biotechnology* **2002,** *77*, 593-601.

Yong, P.; Liu, W.; Zhang, Z.; Beauregard, D.; Johns, M. L.; Macaskie, L. E., One step bioconversion of waste precious metals into Serratia biofilm-immobilized catalyst for Cr(VI) reduction. *Biotechnology Letters* **2015**, 1-11.

Zienkiewicz-Strzalka, M.; Pikus, S., The study of palladium ions incorporation into the mesoporous ordered silicates. *Applied Surface Science* **2012,** *261*, 616-622.

Zhu, J. Synthesis of Precious Metal Nanoparticles Supported on Bacterial Biomass for Catalytic Applications in Chemical Transformations. PhD Thesis, University of Birmingham, **2014.**

3.1.2 Uptake of Pd (II) by *Desulfovibrio desulfuricans*: coordination to cell surface functional groups and endogenous reduction at the cell surface shown by X-ray photoelectron spectroscopy

J. B. Omajali[1], I. de Vargas[2], D. Sanyahumbi[3], A. M. Ashworth[4], C.M. Hardy[5], M.Walker[6], L.E. Macaskie[1]*

[1]*Unit of Functional Bionanomaterials, Institute of Microbiology and Infection, School of Biosciences, The University of Birmingham, Edgbaston, Birmingham B15 2TT, United Kingdom* [4]*Interdisciplinary Research Centre in Materials Processing, University of Birmingham, Edgbaston, Birmingham B15 2TT, United Kingdom.*
[6] *Department of Physics University of Warwick,* Coventry*, CV4 7AL, United Kingdom*

*Corresponding author. Tel.: fax:

Email address:

Journal: Biotechnology and Bioengineering, in submission

This paper was written by J.B. Omajali. Data on Pd (II) sorption and uptake in chloride and sulphate solutions were obtained previously by de Vargas. I performed the experiments on endogenous reduction and hydrogen reduction and also carried out the analysis. Technical help with XPS was provided by Dr Marc Walker, Warwick University.

ABSTRACT

The uptake of palladium (II) ions onto cells of *Desulfovibrio desulfuricans*, *D. vulgaris* and *D. fructosovorans* was investigated. *D. desulfuricans* accumulated > 50% Pd (II) more than the other *Desulfovibrio* spp. The interaction between Pd (II) ions and the latter cell surface was investigated using X-ray photoelectron spectroscopy in chloride and sulfate matrices at pH 2. A mechanism of palladium coordination involving protonated amine groups was demonstrated but endogenous reduction of Pd (II) was equivocal. Subsequent tests used Pd (II) in a nitrate matrix with two strains of *D. desulfuricans* (pH 2.3) to confirm endogenous metabolic reduction of Pd (II) in the absence of added electron donor. The data are discussed with respect to the binding behaviour of Pd (II) to known polymer functional groups and with respect to the potential for building nanostructured metallic catalysts.

KEYWORDS: Catalyst; *D. desulfuricans*; *D. fructosovorans*; *D. vulgaris*; Pd reduction; Palladium; X-ray Photoelectron Spectroscopy.

INTRODUCTION

Recent studies have shown the potential for using biomanufacturing processes to produce stable metallic nanoparticles on bacterial cells. By using precious metals novel nanocatalysts can be produced which have potential applications in green chemistry, energy and environment (see Bennett et al., 2013; De Corte et al., 2012; Deplanche et al., 2011; 2014; Foulkes et al., 2011).

Metallic nanoparticles (NPs) are difficult to make commercially due to problems of agglomeration requiring the use of capping agents to retain NP stability. In contrast the use of bacteria as scaffolding matrices confers particle stability and, following an initial nucleation step, nanoparticle growth occurs under enzymatic control under hydrogen or with formate via hydrogenase activity (Deplanche et al., 2010; Mikheenko et al., 2008). Biogenic metallic nanoparticles are stable against attrition and agglomeration during repeated use in chemical catalysis (Bennett et al., 2013) and, being recoverable, represent a step change in combining the most advantageous aspects of homogeneous and heterogeneous catalysis (Bennett et al., 2013; Creamer et al., 2007).

Most studies to date have focused on metallic NPs deposited at the surfaces of bacterial cells but, following initial observations of Pd-NPs beneath cell surface layers (Deplanche et al., 2014; Foulkes et al., 2011), clear evidence was provided by high resolution sccanning transmission electron microscopy to confirm an ordered array of cytoplasmic Pd-NPs of size 1-6 nm within the cytoplasm of *Desulfovibrio desulfuricans* and *Bacillus benzeovorans* (Omajali et al., 2015). The mechanisms by which the Pd uptake and NP deposition processes occur is unknown and bioprocessing of Pd (II) is unreported. However, in order to develop applications of synthetic biology for controlled catalyst manufacture for specific applications the mechanism of cells uptake and processing of Pd (II) require elucidation following hypothesis that Pd (II) may act as a 'surrogate' for Ni (II), a metal essential for the functioning of hydrogenase and ureases for example (Omajali et al., 2015).

The initial nucleation step prior to Pd (II) uptake involves its coordination onto cell surface functional groups, (Yong et al., 2002). The initially-deposited metal is below the limit of visualization using electron microscopy but metallic clusters become apparent later when they are enlarged *via* additional enzymatically-reduced metal onto initial nucleation foci

(Bennett et al., 2013; Humphries et al., 2006). It is not known whether the initially bound Pd (II) ions or small Pd clusters are translocated into the cells or are processed further at the cell surface into nanoparticles following e.g. cellular uptake of Pd (II) followed by efflux of mobile Pd species from the cells as a possible detoxification mechanism.

This study focuses on the initial stages in uptake of the soluble metallic species of Pd (II) ions since this entails the first step in the generation of biomass-supported catalysts and underpins the bio-patterning which was shown to be key to the development of active catalysts (Macaskie et al., 2012). Understanding of the mechanism(s) involved in the Pd (II) uptake process (and further metabolic processes) would underpin potential improvement of catalyst biomanufacture; if the coordination groups are identified and can be linked to further translocation processes, this will open the possibility to 'steer' the patterning of the catalyst and potentially also the catalytic activity, as was exemplified by a fuel cell bionano-catalyst using a pleiotropic mutation (Orozco et al., 2010).

Metal uptake processes are often quantified in overall terms of initial sorption kinetics and metal-binding capacity. Relatively fewer studies focus on elucidating the mechanism of binding, which depends on the composition of the microbial cell surface ligands. Coordination of metal ions onto cell surface chemical groups has been comprehensively reviewed (Kratochvil and Volesky, 1998). Early work (Doyle et al. 1980) showed that when amino groups were replaced by neutral or negatively charged groups in Gram-positive *Bacillus subtilis*, the number of sites for cation complexing increased, revealing a contribution of sites available for metal ion interaction in teichoic acid and peptidoglycan moieties. A mechanism for Pd(0) deposition in *B. licheniformis* was postulated (Lin et al., 2002) to involve a mechanism whereby Pd(0) locates within the wall layers beneath the S-layer with hydrolysates of polysaccharides or peptidoglycan (i.e. reducing sugars) serving as endogeneous electron donors for its reduction from Pd (II) in an essentially abiotic (non-metabolic) process.

The Gram-negative bacterial cell surface is more complex than that of the cells comprising a cell surface 'compartment' (the periplasm) bounded by inner and outer membranes (Beveridge, 1990). The periplasm comprises a hydrated gel containing peptidoglycan polymers (*N*-acetyl glucosamine and *N*-acetyl muramic acid) in addition to enzymes and redox carriers (Babic et al., 2008) that have been exported from the cytoplasm.

The possibility of 'endogeneous' reduction of Pd (II) was masked in previous work by the addition of formate or hydrogen as exogenous electron donors. A coordination/reduction mechanism for processing Au (III) was described in organism that involved thiol groups (Briñas et al., 2008). However, sulfide is a powerful 'poison' of Pd (0) (Pinna et al., 2001) which is inconsistent with the high catalytic activity of cell-bound Pd (0) (see above).

Metal speciation, related to the chemistry of the metal, is an important factor in investigating metal-cell interactions. In early work, Tsezos and Volesky (1982a, b) showed differences in the uptake of uranium and thorium and Holan and Volesky (1994) between lead and nickel. Evidence for the mechanism of initial coordination of precious metals such as gold, palladium or platinum on bacterial cells is more sparse due to the complex metal chemistries. The platinum group metals and gold almost always predominate in solution as neutral or negatively charged chloride complexes although some free Pd^{2+} can exist in solution at low chloride concentrations and under acidic conditions (Colombo et al., 2008).

Desulfovibrio desulfuricans has a high capacity for Pd (II) uptake at pH 2-3 (de Vargas et al., 2004) when compared to other Gram-negative bacteria (Deplanche et al., 2014). However, the latter study, comparing five Gram-negative organisms (*D. desulfuricans, Escherichia coli, Serratia sp., Shewanella oneidensis* and *Cupriavidis metallidurans*) found no correlation between the extent of initial exogenous electron donor- independent uptake of Pd (II) and the catalytic activity of the finished Pd-catalyst (5% of the bacterial dry weight) with respect to reduction of Cr (VI) or the Heck coupling of phenyl iodide and styrene (Deplanche et al., 2014). On the other hand, within the genus *Desulfovibrio*, palladized cells (5% of the dry weight) of *D. desulfuricans* were more than twice as active in the reduction of 7 mM CrO_4^{2-} than similar cells of *D. fructosovorans* (Skibar et al., 2005), and they were 1.8-fold as active in hydrogenolytic dehalogenation (Pd (0) at 50% of the bacterial dry weight) than *D. vulgaris* (Baxter-Plant et al., 2003). The initial uptake of Pd (II) in these species of *Desulfovibrio* has not been compared previously and this formed the first objective of this study.

The second objective was to provide insight into the behaviour of Pd (II) on the cell surface through a direct approach using X-ray photoelectron spectroscopy (XPS). Since *Desulfovibrio* spp. are well known to cycle hydrogen metabolically (Odom and Peck, 1984), it is possible that a hydrogenase-mediated or other metal reduction mechanism may occur at the expense of endogenously-generated electron donor (H_2 or an organic compound). Therefore,

the possibility of endogenous Pd (II) reduction was evaluated in a background matrix of NO_3^- to preclude both excessive formation of Pd-chloride complexes and also the possibility of H_2S production from SO_4^{2-} *via* dissimilatory sulfate reduction

MATERIALS AND METHODS

Organisms, growth conditions and harvesting

Desulfovibrio desulfuricans (NCIMB 8307 and NCIMB 8326), *D. vulgaris* NCIMB 8303 and *D. fructosovorans* DSM 3604 were grown anaerobically under oxygen-free nitrogen (OFN) in Postgate medium C (Postgate, 1979) at 30 °C (48 h; inoculated from a 24 hour pre-culture, 10% v/v) in sealed bottles to OD_{600} (0.5-0.7). Cells were harvested (Beckman J2-21M/E) by centrifugation in the bottle (9094 x g, 15 min, 4^{o}C), washed three times in air with MOPS-NaOH buffer (20mM, pH 7.0) (Yong et al., 2002), resuspended in the MOPS buffer and stored in air at 4°C before use (usually within 24h). In some cases cells were lyophilized. Heat-killed cells (121^{o}C, 30 minutes) of *D. desulfuricans* (NCIMB 8307 and NCIMB 8326) were also prepared in parallel for examination. Deviations from this procedure are noted where appropriate.

Study of Pd (II) uptake

Palladium solution was prepared by dissolving the chloride salt $Na_2PdCl_4.6H_2O$ (Sigma, UK) in de-ionised, distilled water. The solution pH was adjusted to pH 2 (found previously to be optimal for subsequent catalytic activity of Pd (0); Yong et al., 2002) using HCl, HNO_3 or H_2SO_4. For tests, a constant amount of cell concentrate in the MOPS buffer (as above) (150 mg dry cell weight/L i.e. 1.5 mg biomass/ 10 mL final volume of metal solution) was contacted with a set volume (V) of metal solutions (usually to 10 mL) at initial metal concentrations (C_o) of 5 - 50 mg/L in sterile and sealed serum bottles (30 ^{o}C, agitation 150 rpm, under N_2; pH 2 ± 0.1). After incubation (up to 96 h), samples of the supernatant from centrifuged samples were analysed for the final equilibrium residual metal concentration (C_{eq}) spectrophotometrically using $SnCl_2$/HCL (Balcerzak et al., 2001). The method was cross-validated previously using polarography (Yong et al., 2002) and by using samples analysed commercially (H_2b Analytical Services Ltd., Capenhurst UK). All experiments were done twice using separate batches of cells. The standard error of mean between experiments was

always less than 2%. The uptake capacity (q; mg metal per g cells; m = mass of cells in mg) (assuming no further bioprocessing of Pd (II)) was calculated using the following equation: $q = [V (C_o - C_{eq}]/m$.

X-ray photoelectron spectroscopy

Tests using a background matrix of chloride or sulfate at pH 2 using lyophilized cells

Initial metal uptake tests used known volumes of 2 mM metal solution of $Na_2PdCl_4 \cdot 6H_2O$ salt with known mass (dry weight) of *Desulfovibrio* spp as described (1 h; 30 ^oC; pH adjusted to 2.0 with HCl or H_2SO_4). XPS analysis was done on lyophilized (overnight) cells before and after Pd (II) exposure and XPS spectra were acquired using metal solutions without cells for comparison.

XPS analysis was carried out in a VG Escalab II instrument using VGX 900 data acquisition software. Analyses were typically performed under a base pressure of 10^{-9} mbar using a non-focused monochromatic Al kα (1486.6 eV) radiation with the X-ray source operated at 15 kV and 20mA emission current. High resolution scans were recorded in constant pass energy mode at 20 eV and expressed as intensity on y-axis versus binding energy (BE) on the x-axis, measured in eV. A non-linear curve fitting program with a Gaussian-Lorentzian mix function and Shirley background subtraction was used to de-convolute the XPS peaks. The carbon 1s electron binding energy corresponding to adventitious carbon was referenced at 284.6 eV. Silver and gold peaks at 368.27 eV and 84.00 eV respectively were also referenced for instrumental calibration. The de-convolution of the peaks was performed maintaining a similar full width half maximum (FWHM) per each individual element.

Tests using a background matrix of nitrate at pH 2 using fresh cells

These tests were carried out with fresh (non-lyophilized) cells of *D. desulfuricans* (NCIMB 8307 and NCIMB 8326) suspended in 20mM MOPS-NaOH buffer (pH 7) and challenged with 2mM Pd (II) solution initially adjusted to pH 2.0 with 0.01M HNO_3.

The mass ratio of metal to biomass was 1:19. After addition of cells, the pH increased to 2.3 (NCIMB 8307) and pH 2.4 (NCIMB 8326) respectively, which was followed by uptake of Pd (II) ions (30 minutes at 30 ^{o}C). Other studies using flow cytometry confirmed cellular integrity and metabolism during this period (see section 3.3.2). Cells were washed twice with distilled water and aliquots of sorbed samples of Pd (II) solution on the cells were dropped (approximately 0.01ml at a time) and dried on a boron-doped silicon wafer. X-ray photoelectron spectroscopy (XPS) data were collected at the Science City Photoemission Facility, University of Warwick, UK. The samples investigated in this part of the study were mounted on Omicron sample plates using electrically conductive carbon tape and loaded into the fast-entry chamber. Once a pressure of less than 1 x 10^{-7} mbar had been achieved (approx. 1 hour), the samples were transferred to a 12-stage storage carousel, located between the preparation and main analysis chambers, for storage at pressures of less than 2 x 10^{-10} mbar. XPS measurements were conducted in the main analysis chamber (base pressure 2 x 10^{-11} mbar), with the sample being illuminated using an XM1000 monochromatic Al k_{α} x-ray source (Omicron Nanotechnology). The measurements were conducted at room temperature and at a take-off angle of 90°, allowing a maximum probe depth of approximately 10nm, i.e. reporting on the cell surface and within the periplasm, but not cytoplasmic layers of the cell. The photoelectrons were detected using a Sphera electron analyser (Omicron Nanotechnology), with the core levels recorded using a pass energy of 10 eV (resolution approx. 0.47eV). Due to the insulating nature of the samples, a CN10 charge neutralizer (Omicron Nanotechnology) was used in order to prevent surface charging, whereby a low energy (typically 1.5 eV) beam of electrons was directed on to the sample during XPS data acquisition. The data generated were converted into VAMAS format and analysed using the CasaXPS package (Fairley, 2013), using Shirley backgrounds, mixed Gaussian-Lorentzian (Voigt) line shapes and asymmetry parameters where appropriate. All binding energies were calibrated to the C 1s peak originating from adventitious carbon at 284.6 eV. Controls include Pd (II) solution, heat-killed (autoclaved) cells and Pd reduced under hydrogen (exogenous reduction).

RESULTS & DISCUSSION

Comparison of Pd (II) uptake by *Desulfovibrio* spp in nitrate, chloride and sulfate matrices

Initial studies to identify the best species for detailed study compared Pd (II) uptake by three *Desulfovibrio* spp. in three background ionic matrices. The Pd (II) uptake at equilibrium for *D. desulfuricans* was 1.7-fold greater in a nitrate background than with the other two *Desulfovibrio* species (Fig. 1). In each case, the equilibrium uptake of Pd (II) with the pH set using HCl was approximately halved (to respectively 70, 56 and 45 mg Pd/g dry cell mass (not shown; c.f. Fig. 1) as compared to that taken up from HNO_3 matrix. Substitution of sulfate for chloride increased the Pd (II) uptake by *D. desulfuricans* to 120 mg/g but this was still less than the uptake seen in NO_3^- (Fig. 1). Formation of H_2S and the nature of the Pd-deposit were not investigated.

Pd (II) exists in solution at acidic pH as a mixture of some free cationic Pd^{2+}, but mainly as chloride species in solution ($PdCl^+$, $PdCl_2$, $PdCl_3^-$); the Pd(II) chloride salt Na_2PdCl_4, has four chloride ions. Hence, it is likely that cationic Pd^{2+} and anionic chloride species would co-exist and would be attracted to anionic and cationic groups respectively on the cell surface. The biphasicity of the *D. desulfuricans* (and to a lesser extent *D. vulgaris)* uptake isotherm for Pd (II) (Fig 1) may well reflect the binding affinity of two types of site (the steeper the gradient, the higher the affinity: (Reis and Rosa, 2005)) but this was not investigated further.

The three *Desulfovibrio* spp. gave different patterns of Pd (II) uptake. *D. desulfuricans* and *D. vulgaris* had similar high affinity sites (a steep isotherm) at low values for C_{eq}. *D. fructosovorans* had lower affinity sites but showed a similar metal uptake at equilibrium to *D. vulgaris*. A second set of lower affinity sites was clearly apparent in *D.desulfuricans* which would have accounted for the nearly 2-fold higher uptake seen over and above the uptake observed with the other two *Desulfovibrio* species (Fig. 1). It is not known to what extent the 'additional' sites may have contributed to the higher catalytic activity observed using palladized cells of *D.desulfuricans* as compared to the other two strains (i.e more sites for catalyst development would lead to smaller

nanoparticles for a given amount of Pd (II)) but Fig 1 would suggest three types of discrete binding for Pd (II) within different species within the same genus. Since *D. desulfuricans* appeared to offer two distinct sites, one of high and one of lower affinity, as well as forming the most catalytically active Pd-NPs (as above), this species formed the focus of subsequent studies. The use of pH 2 for metal uptake studies may be seen as counterintuitive to the need for continued cellular metabolism during subsequent Pd-NP deposition *via* reduction to Pd (0). An early study (Yong et al., 2002) identified empirically that such "sorption" of metal prior to reduction "predisposes" the cells towards making a more active catalyst subsequently with the pronounced effects at pH 2. Continued cell integrity and metabolism was confirmed using flow cytometry (see section 3.3.2 and 3.4.2) and will be reported in full in a subsequent publication, but the degree of cell injury was not assessed.

"Acid shock" is a well-known promoter of a suite of bacterial stress responses (Johnson et al., 2014) any of which may relate to the production of a more effective Pd-catalyst by acid-shocked cells: indeed metal toxicity would be expected to itself involve a stress response but further investigation was beyond the remit of this study. Also, it should be noted that while the Pd (II) bulk solution was held at pH 2, the presence of extensive carboxylate groups on periplasmic polymers could tend to have a buffering function as they become protonated.

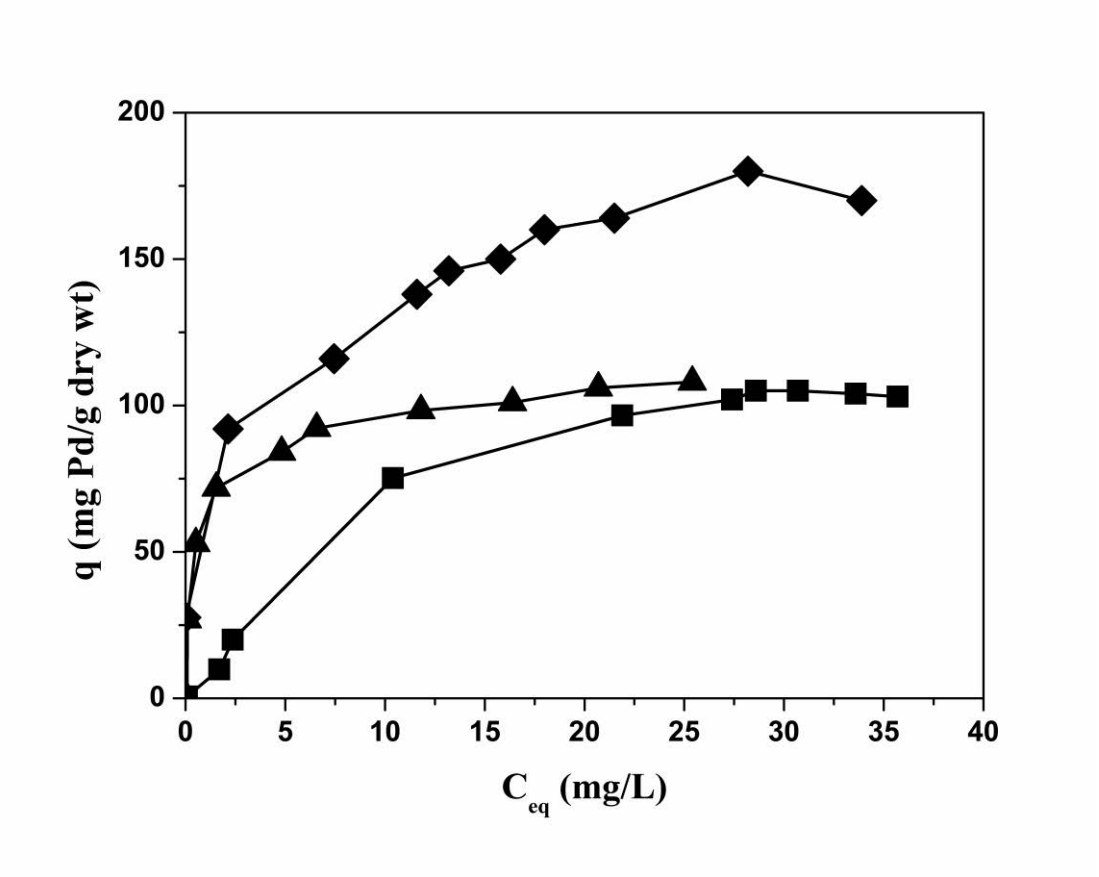

Figure 1 Uptake isotherms for Pd (II) in HNO_3 solution at pH 2 by: ♦, *D. desulfuricans* NCIMB 8307; ▲, *D. vulgaris* and ■, *D. fructosovorans***.**

Studies on background Pd (II) solution and cells using X-ray photoelectron spectroscopy

Background XPS spectra were obtained for the palladium solutions and for *D. desulfuricans* cells suspended from lyophilisate without Pd (Figure 4 and 5). Initial tests examined C, N and O X – ray photoelectron peaks of cells of *D. desulfuricans* before Pd (II) sorption (Fig. 4) and Table 1 shows the main assignments of these peaks. The atomic concentration of N was 10.3% and two peaks, identified at 399.7 eV and 398.6 eV respectively (Fig. 2a), suggest a surface that is not extensively protonated in the absence of the acidic metal solution (as NH_4^+ groups would be expected at around 401.7eV). O peak positions were 536.4 eV and 532.0 eV (Table 1). The C atomic concentration was 64.3% and two C peaks were found at 287.0 eV and 284.6 eV (Table 1), which were attributed to aliphatic carbon or carboxylic acid groups on the cell surface (Table 1).

The binding energies and the peak assignments associated with the main spectral bands observed for Pd (II) solution (pH adjusted with HCl, H_2SO_4 and HNO_3) without cells (Fig 3) are shown in Table 2. This shows the solution chemistry to be least complex in the HNO_3 matrix and some free Pd^{2+} was seen in all three cases but this was not quantified.

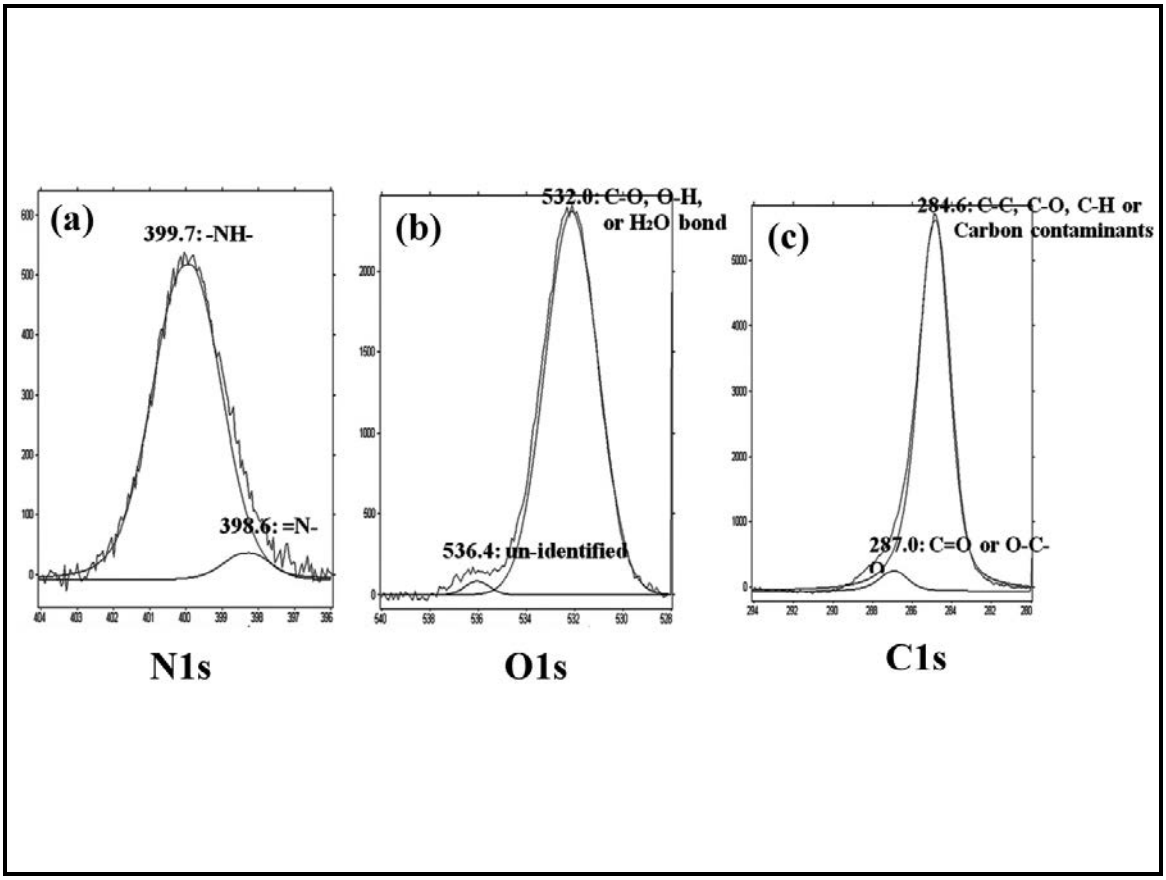

Figure 2 XPS spectra with peak assignments for a: nitrogen (N), b: oxygen (O) and c: carbon (C) groups for *D. desulfuricans* cells prior to Pd (II) uptake. The x-axis = binding energy (eV) and intensity shown on the y-axis. Total atomic concentration for each group are shown in Table 1.

Table 1 Assignment of the main spectral bands based on their binding energies (BE) and atomic fractions (AF) on the surface of *D. desulfuricans* NCIMB 8307 before metal exposure. (See Fig 2).

Element	BE (eV)	AF (%)	Assignments
N 1s	399.7	17.7	-NH-
N 1s	398.6	2.2	=N-
Total N 1s		10.3	
O 1s	536.4	1.6	Na auger
O 1s	532.0	81.4	C-O, O-H or Pd-O
Total O 1s		16.8	
C 1s	287.0	8.4	C=O or O-C-O groups
C 1s	284.6	91.5	C-C, C-O, C-H or contaminant carbon
Total C 1s		64.3	

Together the N, O and C components of the cell accounts for 91.4% of the atomic fraction (Table 1). However, those data do not take into accounts loosely bound water or cellular S (thiols or S-containing amino acids) or P (membrane phospholipids)-(see section 3.1.1). Total values represent the total atomic concentration of each element idenfied in the bacterial cell before metal exposure obtained from CasaXPS software after line fitting

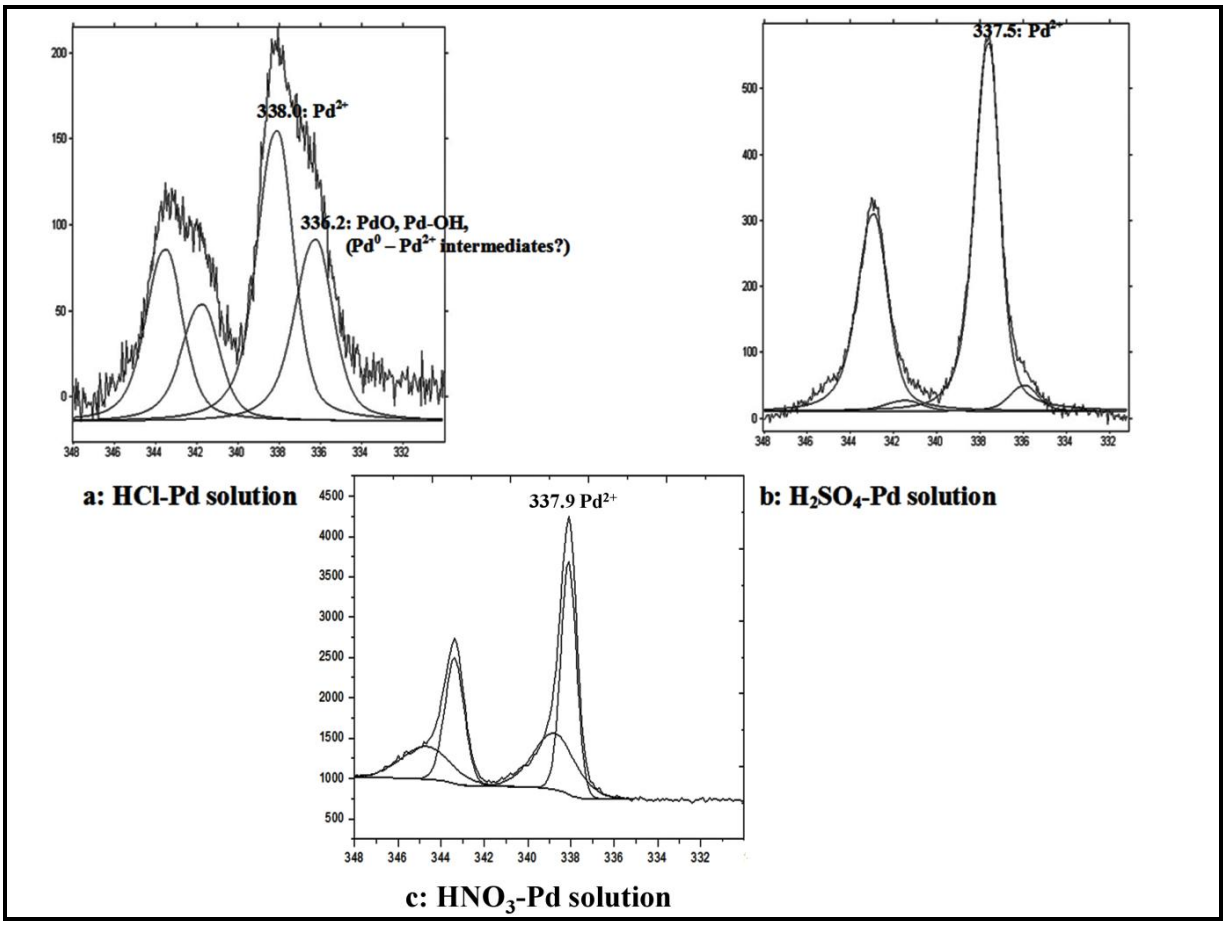

Figure 3 XPS spectra showing Pd 3d peaks in solution of palladium in the absence of cells where the pH 2 was set with a: HCl, b: H_2SO_4, c: HNO_3. The x-axis = binding energy (eV), the y-axis = intensity. Peaks assigned are shown in Table 2a, 2b and 2c.

Table 2 Assignment of main spectral bands based on their binding energies (BE) for the Pd (II) solutions at pH 2 in HCl, H_2SO_4 or HNO_3 in the absence of bacterial cell (Figure 3).

(a) HCl matrix

Element	BE (eV)	Assignments
O 1s	533.3	Atmospheric oxygen
O 1s	536.9	Na auger
Cl 2p $_{3/2}$	199.3	Pd-Cl or covalently bonded chloride
Pd 3d $_{5/2}$	336.2	PdO, Pd-OH and unknown groups; possible intermediate state between Pd^0, Pd^{2+}
Pd 3d $_{5/2}$	338.0	Pd^{2+}

(b) H_2SO_4 matrix

Element	BE (eV)	Assignments
O 1s	533.4	Atmospheric oxygen
O 1s	531.7	Pd-O or Pd-OH
O 1s	535.6	Na auger
Cl 2p $_{3/2}$	199.7	Pd-Cl or covalently bonded chloride
Pd 3d$_{5/2}$	337.5	Pd^{2+}

(c) HNO_3 matrix

Element	BE (eV)	Assignments
O 1s	535.1	Na auger
O 1s	532.3	C=O or C-O-C
Pd 3/5	377.9	Pd^{2+}

Palladium uptake in aqueous solution with HCl

XPS spectra for the bacterial cells after Pd (II) uptake (Fig. 2) from chloride solution was compared to the spectra of the original palladium-chloride solution (Fig 3). The latter alone was evidence of Pd-Cl bonds or covalently bonded chlorine (199.3 eV, Table 2) (Drelinkiewicz et al., 1998; Hasik et al., 2002). However, this chlorine peak shifted to 197.4 eV when the Pd-challenged cells were examined (Table 3, Figure 5), corresponding to the energy of N^+-Cl, which suggests involvement of an anion-

exchange mechanism (Drelinkiewicz et al., 1998). The high concentration of chloride anions would result in the formation of $PdCl_4^-$ anionic species which are able to attach to protonated amine groups on the bacterial cell surface by an anion exchange mechanism with Cl^- as counter anion and a proposed sorbed species of N-Cl-Pd. The high tendency of Pd (II) to coordinate with nitrogen groups is well known (Hicks et al., 2009) and formation of Pd-N is likely.

Nitrogen groups on the bacterial cell surface were assigned to two peaks, one corresponding to - NH – group (399.7 eV) and the other, with a smaller contribution (lower intensity), corresponding to the = N – group (398.6 eV: Table 1, Fig 3). In the cells following Pd (II) sorption only the – NH – peak could be identified, slightly shifted to 399.9 eV (Table 3, Fig. 4). The disappearance of the = N – peak in Fig. 4 may be due to electron transfer.

Oxygen peaks present at 536.4 eV and 536.9 eV for the cell surface alone and the palladium – HCl solution matrix respectively (Table 1, Table 2a) were not identified but may be an auger sodium (Na) peak from the sodium palladate salt used (Dambies et al., 2001). A difference was observed for other identified O peaks, between the bacterial surface before and after palladium uptake. A peak at ~532.0 eV (Table 1, Fig 2) for the cells before Pd (II) uptake slightly shifted to 532.6 eV (Table 3, Fig. 4) subsequently (Dambies et al., 2001) as O 1s in C – O , O – H or PdO. A peak appeared at 531.3 eV (Table 3, Fig. 4) after palladium was added and was identified as O 1s in C = O or C-O-C bonds, a PdO-like state or stochiometric hydroxide (Dambies et al., 2001).

Four palladium peaks were identified by XPS analysis for the metal solution before contacting with cells (Fig 2), the first pair corresponding to Pd 3d 5/2 and 3/2 peaks at 338.0 eV and 343.4 eV for Pd^{2+} and the second pair at 336.2 eV and 341.7 ev; according to the literature (Huang et al., 1998); these could not be unambiguously characterized but may represent an intermediate palladium state between Pd^0 and Pd^{2+} or possibly also Pd bonds to oxygen or hydroxide. These peaks were retained following palladium uptake (Fig. 4) but the dominant Pd contribution was from Pd bonding environment.

In Pd solutions where the pH was adjusted using HCl, the dominant Pd species in solution would be anionic $PdCl_4^{2-}$ but, in general, all the species in solutions are hydrated.

Therefore it is possible that the Pd peak observed at 336.2 eV could also correspond to the hydration of the anionic species which, after contact with the biomass, becomes the predominant species due to a proposed competitive effect with chloride anions for the binding sites (de Vargas et al., 2004). This competitive effect may also account for the shift in the chloride peak (199.3 eV, Table 2 to 197.4 eV, Table 3), which was identified as N^{+}-Cl bonds. The peak position at approximately 338 eV has also been assigned to a Pd-N bond (Hasik et al, 2002).

Notably, no peaks could be conclusively assigned to the presence of the reduced species Pd (I) and Pd (0), although an uncharacterized peak was found at approximately 336 eV. Therefore, no clear conclusion could be made under these conditions with respect to the contribution of any endogenous reductive process towards palladium uptake.

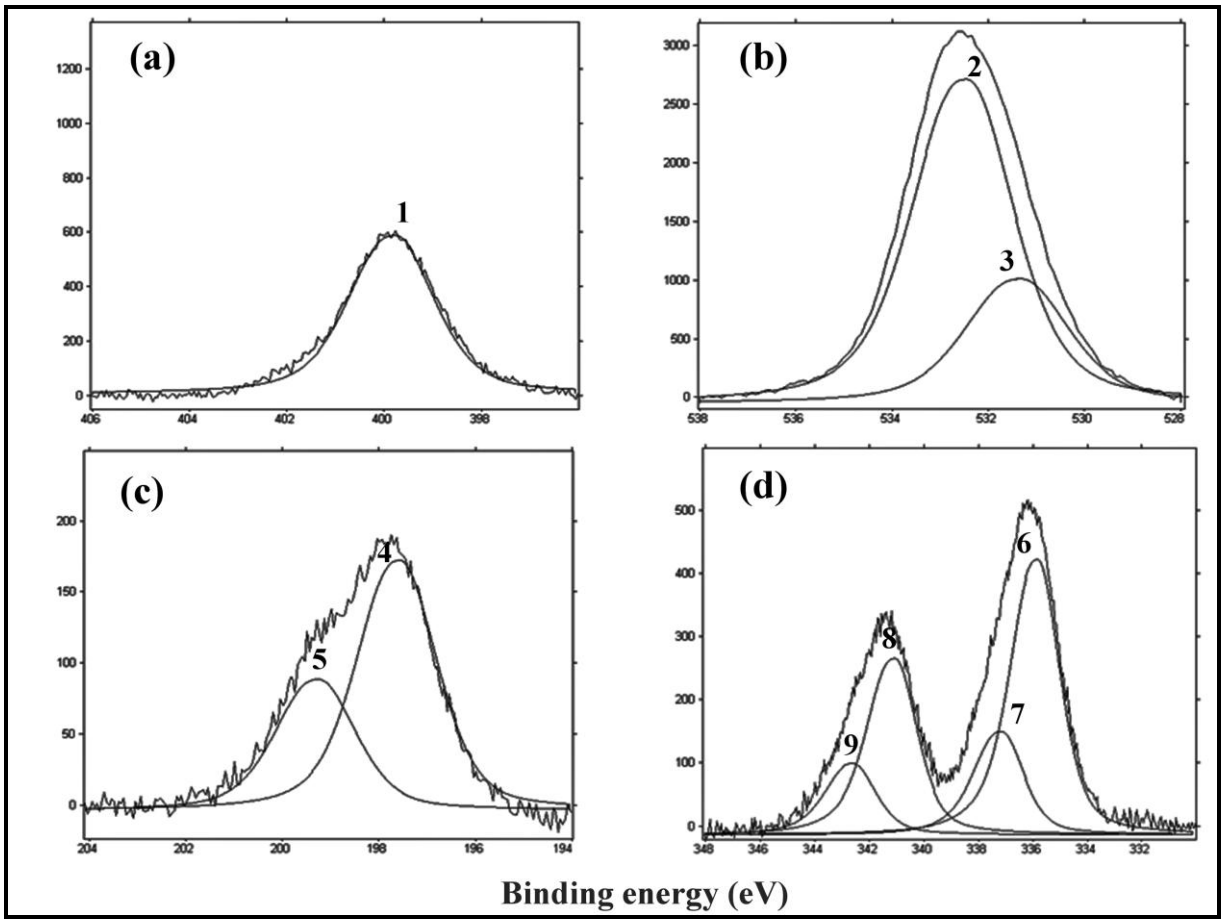

Figure 4 XPS spectra showing a:N, b:O, c:Cl and d:Pd peaks for *D. desulfuricans* NCIMB 8307 cell surface after Pd (II) uptake from HCl solution. The main peak assignments for these spectra are summarised in Table 3a and are shown as numbers in the above figure: 1= N 1s; 2 = O1 s higher BE; 3 = O 1s lower BE; 4 = Cl $2p_{3/2}$; 5 Cl 2p1/2, 6 = Pd $3d_{5/2}$ lower BE; 7 = Pd $3d_{5/2}$ higher BE with corresponding doublets (8, 9). BE = Binding energy is on x-axis and y – axis = intensity.

Palladium uptake in aqueous solutions with H_2SO_4

The main spectral bands assigned for *D. desulfuricans* cells after palladium uptake in solution at pH 2.0 adjusted with H_2SO_4 are shown in Table 3. The corresponding XPS spectra are shown in Fig. 5.Where the pH was adjusted with HCl (above) the dominant palladium species were anionic, but where other anions predominate, (here SO_4^{2-}), Pd (II) was less extensively complexed to chloride ion and hence neutral or cationic species would occur in higher proportions.

XPS spectra of palladium solution at pH 2.0 in H_2SO_4 (Table 2, Fig 3) and corresponding to cells after Pd uptake are shown in Table 3 and Fig. 5. Of the two nitrogen peaks (339.7 eV, -NH- and 398.6 eV, =N-) identified on the cells prior to metal uptake (Table 1), the peak at 399.7 eV was shifted to 400.15 eV (Table 3, Fig. 5) and the 398.6 eV peak disappeared. This was possibly related to protonation of sites on the cell surface and may indicate the presence of neutral and cationic Pd species, where less interaction with protonated nitrogen groups has taken place *via* 'bridging' chloride ions (c.f. the chloride solution matrix).

The chloride peak identified at 199.7 eV (Table 2) for the Pd – H_2SO_4 background matrix, and a similar peak assigned to Pd-Cl (Table 3) following Pd (II) uptake, suggested no significant contribution by the chloride groups in this case.

Table 3 Assignment of main spectral bands based on their binding energies (BE) of the surface species on cells of *D. desulfuricans* after Pd sorption at pH 2 in HCl or H_2SO_4 (see figures 4 and 5 respectively).

(a) HCl matrix

Element	BE (eV)	Assignment
O 1s	532.6	C-C, O-H or PdO
O 1s	531.3	C=O or C-O-C
N 1s	399.9	-NH-
Cl $2p_{3/2}$	197.4	Pd-Cl
Pd $3d_{5/2}$	336.2	PdO, Pd-OH and unknown groups; possible intermediate state between Pd^0, Pd^{2+}
Pd $3d_{5/2}$	338.0	Pd^{2+} and Pd-N

(b) H_2SO_4 matrix

Element	BE (eV)	Assignment
O 1s	5532.5	C-O, O-H or PdO
N 1s	400.1	$–NH^+$-
Cl $2p_{3/2}$	199.1	Pd-Cl
Pd $3d_{5/2}$	337.1	Pd^{2+}

Palladium peaks corresponding to Pd^{2+} were present at 337.5 eV (Table 2, Fig 3) in the background solution and at 337.1 eV (Table 3, Fig. 5) following Pd (II) uptake. The presence of this peak indicates the presence of neutral and cationic palladium species. No Pd (0) peak was identified, suggesting that there was no endogenous reductive process; note that the previously identified but un-characterised peak at approximately 336 eV (c.f. above) was not present in this case. As with the Pd-HCl solution matrix system, the oxygen peak detected at 532.5 eV (Table 3, Fig. 4) was assigned to O 1s C-O or O-H or bonded H_2O on the cell surface, according to the known occurrence of heavily hydrated polymers in the periplasm (*N*-acaetyl glucosamine and *N*-acetyl muramic acid) and within extracellular polymeric substances (Beveridge, 1990).

In conclusion, no unequivocal evidence was seen for endogenous reduction of Pd (II) in chlorine or sulfate matrices. The fate of SO_4^{2-} via possible reduction to H_2S (and formation of possible PdS) was not investigated but no evidence was seen for the formation of Pd-sulfide species.

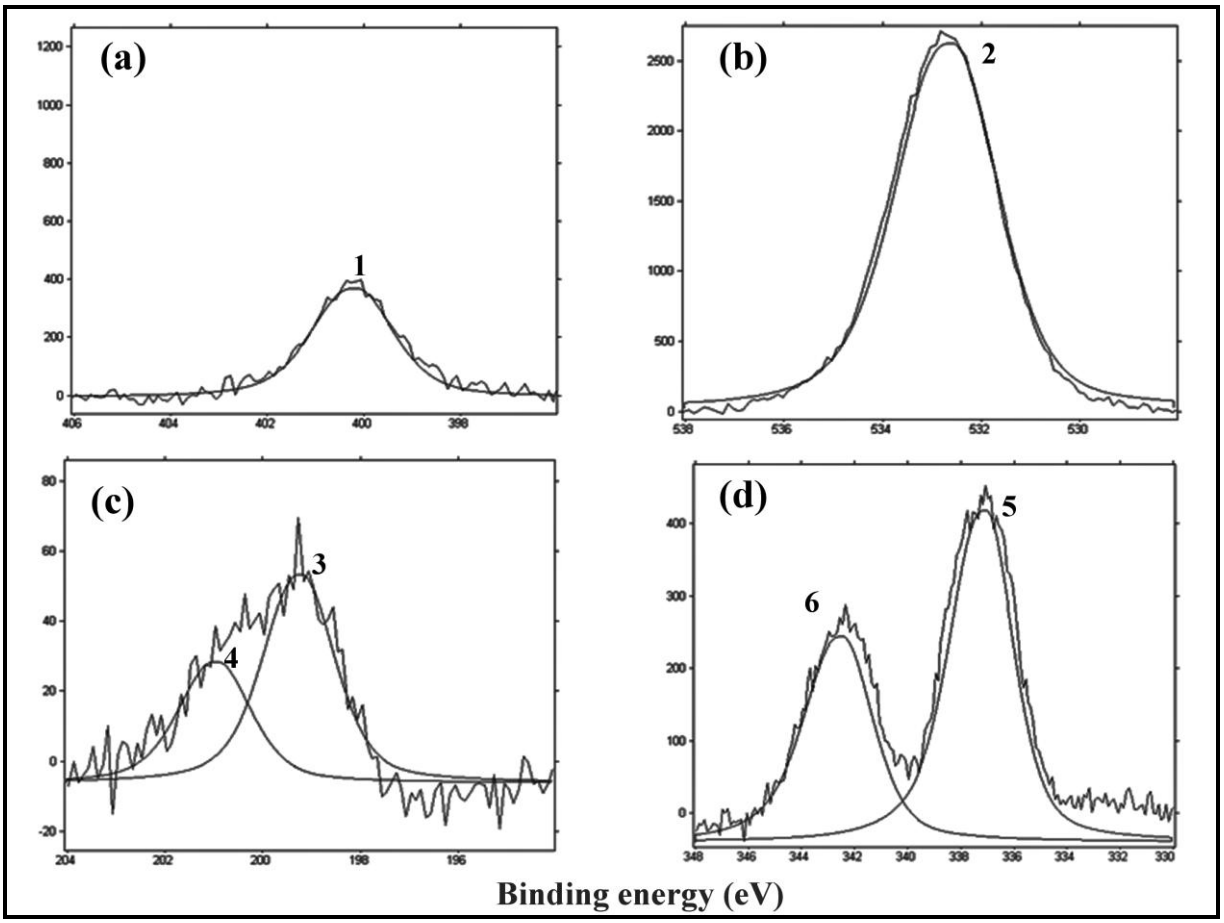

Figure 5 XPS spectra showing a: N, b: O, c: Cl and d: Pd peaks for *D. desulfuricans* NCIMB 8307 cell surface after Pd (II) uptake from H_2SO_4 solutions. The main peak assignments for these spectra are summarised in Table 3b and are shown as numbers in the above figure: 1= N 1s; 2 = O1 s; 3 = Cl $2p_{3/2}$; 4 = Cl $2p_{1/2}$, 5 = Pd $3d_{5/2}$ 6 Pd $3d_{3/2}$ and y – axis = intensity.

Uptake of Pd (II) from nitrate solution by cells of *D. desulfuricans* NCIMB 8307 and NCIMB 8326

As a result of the higher Pd (II) sorption capacity of *D. desulfuricans* NCIMB 8307 observed earlier when compared with other *Desulfovibrios*, it is important to compare the former with a close relative, *D. desulfuricans* NCIMB 8326 in order to exploit any strain-dependent differences where possible. The above studies initially assumed little or no active contribution by the cells since the pH of the suspensions was 2.0. The possibility of Pd (II) reduction, if confirmed, was unexpected and was investigated further. Studies using

flow cytometry have shown that metabolism is retained during the 30-45 minutes "pH shock" (see section 3.3.2 and 3.4.2) while I. Mikheenkho and M. Rousset (personal communication) confirmed the persistence of hydrogenase activity for this duration. Hence, the persistence of a small amount of hydrogen trafficking and, indeed, of residual sulfate reduction in the absence of added electron donor, cannot be excluded. Since the initial evidence for endogenous reduction of Pd (II) was equivocal (above), a small series of experiments was designed using a nitrate solution matrix (i.e. no additional chloride was present for complexation of Pd (II) nor substrate for H_2S generation) and, here, using non-lyophilized fresh cells kept in 20 mM MOPS-NaOH buffer, pH 7. Upon addition of the Pd (II) solution (pH 2.0 in HNO_3) the pH increased to 2.3 and 2.4 respectively using *D. desulfuricans*, NCIMB 8307 and NCIMB 8326 and, in parallel, using heat-killed cell of each. A positive control was hydrogen-reduced Pd (II) on cells to make 'bio-Pd' *via* a previously established method (Deplanche et al., 2014).

Generally, the binding energies of Pd appear as doublets in XPS analysis. In this study, reduction of Pd (II) was observed using live but not heat-killed cells of both strains, confirming that this process may be metabolically driven (Figure 6). There was a 1.51 eV shift in binding energy (BE) of Pd $3d_{5/2}$ peaks as a result of the endogenous reduction of the total Pd (II) sorbed by *D. desulfuricans* NCIMB 8307 with a shift to a lower energy (from 337.87 eV of the Pd (II) solution in the absence of biomass to 336.36 eV and a 1.50 eV shift in BE in *D. desulfuricans* NCIMB 8326 while for the heat-killed cells the shift in BE of Pd (II) was reduced in either case (Table 4, Figure 6). However, the binding energy of Pd during endogenous reduction by live cells of *D. desulfuricans* NCIMB 8307 (336.36 eV) and *D. desulfuricans* NCIMB 8326 (336.37 eV) was similar to that of palladium on carbon catalyst (Pd/C) with a binding energy of 336.4 eV (Bertolini et al., 1990) and this may explain a Pd interaction with the carbonaceous bacterial cell surface as Pd (II) was endogenously reduced by the live cells "donating" electrons *via* a mechanism absent from killed counterparts. However, in the hydrogen reduced live cell controls, Pd (II) was reduced directly to Pd (0) in *D. desulfuricans* NCIMB 8307 with binding energies of the doublet at 335.50 eV and 340.76 eV (Figure 6e) and a corresponding doublet at 335.78 eV and 341.54 eV in *D. desulfuricans* NCIMB 8326 (Figure 6f). The Pd (0) reduced in the presence of exogenous electron donor (hydrogen) can be assigned to a Pd-Pd bonding for metallic palladium or zero-valent state (Park et al., 2010; Zienkiewickz-Strzalka and Pikus,

2012) and the binding energies shifted with about 2.37 eV in *D. desulfuricans* NCIMB 8307 and 2.09 eV in *D. desulfuricans* NCIMB 8326 when referenced to Pd $3d_{5/2}$ of palladium (II) unreduced solution (Table 4, Figure 6). Although the Pd reduction in the absence of exogenous electron donor was not very prominent in both strains of *D. desulfuricans*, it is concluded that an electron transfer mechanism is present in the surface layers of live but not heat-killed cells. Studies by Gericke and Pinches (2006) examined a purely biogenic method to reduce and synthesize Au-NPs in some bacteria without exogenous electron donors and suggested that protein and enzymes present in either cell wall or cytoplasm may play a role in the reductive process. This suggests the participation of metabolic electron transport process in Pd (II) reduction that is confirmed here by direct analysis of the Pd-speciation on the periplasm of the cells during the initial period of Pd (II) uptake. With respect to Gram-positive bacteria, dry cells of *Bacillus licheniformis* R08 capable of reducing Pd (II) to Pd (0) in the absence of exogenous electron donors (Lin et al., 2002) was reported. Here, the reduction of Pd (II) to Pd (0) may have occurred *via* the peptidoglycan (N-acetyglucosamine and N-acetyl muramic acid) of the bacterium with partial hydrolysate (i.e. sugar reducing groups) on the cells serving as an electron donor *in-situ* (essentially an abiotic mechanism; Lin et al., 2002) but the possibility of biochemical electron transport was not precluded. The current observation that Pd (II) reduction is largely abolished in heat-killed cells suggests the participation of metabolic and not chemical or abiotic processes.

Table 4 Endogenous reduction of Pd (II) by *D. desulfuricans*

Adsorbents	Binding energy (eV) of Pd				
	Pd (II) solution Pd $3d_{5/2}$	Endogenous reduction	Shift in BE	Hydrogen reduction	Shift in BE
D. desulfuricans NCIMB 8307 (live cells)	337.87	336.36	1.51	335.50	2.37
D. desulfuricans NCIMB 8307 (heat-killed)	337.87	337.70	0.17	-	-
D. desulfuricans NCIMB 8326 (live cells)	337.87	336.37	1.50	335.78	2.09
D. desulfuricans NCIMB 8326 (heat-killed)	337.87	337.80	0.07	-	-

XPS data showing endogenous reduction of Pd (II) in a solution of Na_2PdCl_4 salt adjusted to pH 2 with 0.01M HNO_3. Reduction is accompanied by significant shifts in binding energies of Pd 3d on live cells, hydrogen reduced controls but not heat-killed cells. BE: Binding energy. Note that Pd $3d_{5/2}$ peak was considered in each case with shift in binding energy during reduction deduced from binding energy of Pd (II) unreduced reference solution.

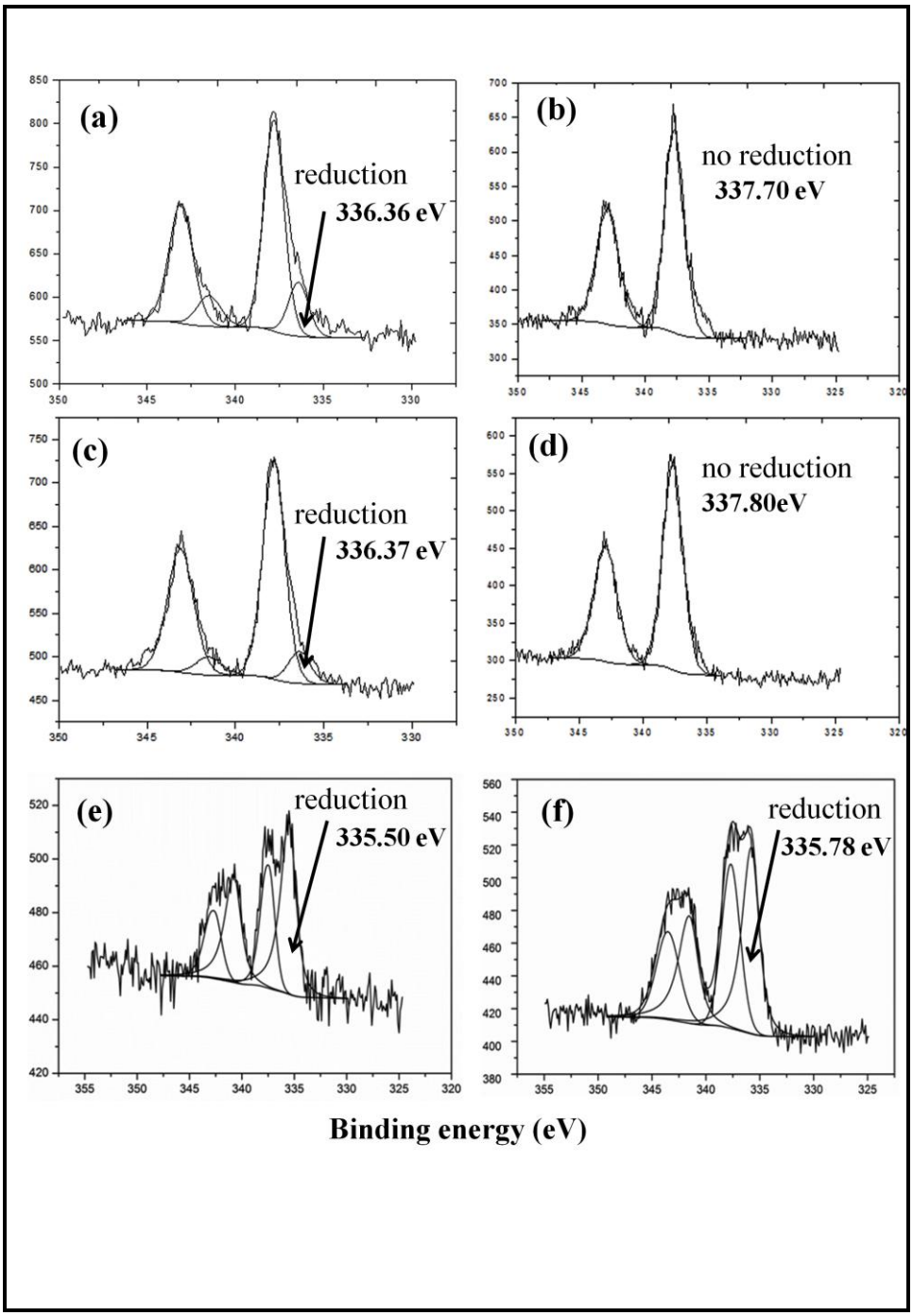

Figure 6 XPS spectra of cells of *D. desulfuricans* NCIMB 8307 (a) and NCIMB 8326 (c) and corresponding heat-killed cells (b and d) following uptake of Pd (II) with control reduced *via* hydrogen as exogenous electron donor in *D. desulfuricans* NCIMB 8307 (e) and NCIMB 8326 (f).Arrows indicate peaks evident in live cells and H_2-reduced cells but not heat-killed cells. The putative endogenous reduction in both cases is accompanied by a shift in binding energy (eV) of Pd $3d_{5/2}$ after Pd (II) uptake by cells in Pd (II) solution adjusted to pH 2 with 0.01M HNO_3. The y-axis = intensity. Details of shift in binding energy (eV) due to reduction are given in Table 4.

Nickel shares similar chemistry with palladium which exists in 0, +1, +2, +3 and +4 redox states (Powers and Ritter, 2011) and Ni is able to cycle through three redox states (+1, +2 and +3) (Ragsdale, 2009). This introduces the possibility of Pd (II) trafficking (Omajali et al., 2015) *via* Ni (II)-transporter. Based on electron paramagnetic resonance (EPR) studies of the membrane-bound NiFe hydrogenase of *D. fructosovorans*, the catalytic phase of hydrogen oxidation for hydrogenase activation leads to the formation of an active Ni (I) species (Lil and Siegbahn, 2009). It is possible that during the endogenous reduction process, the cell reduces Pd (II) to Pd (I) and then Pd (0) instead of Ni (II) which has a lower redox potential (Hayes, 1993), hence, the detection of reduced Pd on bacterial cell surfaces (outer most membrane) *via* XPS.

XPS is a surface technique that probes to a depth of ~5-10 nm. The bacterial periplasm is about 10-50 nm thick (Graham et al., 1991; Sochacki et al., 2011), and hence the endogenous reduction reported here would occur in the periplasm or outer membrane. This could be attributed to a hydrogenase (Mikheenkho et al., 2008) but, since no hydrogen was added, Pd (II) would have been reduced *via* H_2 produced endogenously by the SRB (Odom and Peck, 1984). Alternatively, our observations may be attributed to another, as yet unidentified "Pd-reductase." If Pd (0) is made in the periplasm, then, the question arises as to how metallic Pd (0) nanoparticles are translocated into the cytoplasm (Omajali et al., 2015). It is possible that there are two routes for 'handling' Pd (II); one route yielding Pd (0) in the cell surface layers while another 'traffics' Pd (II) by an as yet unknown mechanism (e.g. Ni (II) uptake system (see Deplanche et al. 2014; Omajali et al., 2015 for discussion).

CONCLUSIONS

Following metal uptake at pH 2 in chloride or sulfate matrices, coordinations to amine and carboxyl groups were confirmed. It was not possible to assign conclusively any of the palladium peaks to Pd^0, although an identified but un-characterised peak appearing at 336 eV may possibly be partly contributed by Pd^0. Clear evidence was found for the presence of PdO. In a nitrate background evidence was seen for metabolically-mediated reduction of Pd (II) to Pd (0) in the absence of added electron donor. However, having used XPS which is a high vacuum system, there is the possibility of damage to sample integrity but since the binding

between Pd (II) and functional groups on bacterial surface had occurred prior to placing samples under high vacuum, the main goal was to determine the chemical environment of the covalently bound Pd (II) to functional groups on bacterial cell. It should be noted that at such high vauum, loosely bound materials would be lost due to poor interaction. The potential application of X-ray absorption spectroscopy (XAS) may be useful in determining a Pd intermediate between Pd (II) and Pd (0).

ACKNOWLEDGEMENTS

The authors wish to acknowledge the financial support of the European Commission, Project number GRD1-2000-25156 and also the kind collaboration of IRC centre, University of Birmingham. The Science City Photoemission Facility used in this research was funded by the Science Cities Advanced Material's Project 1: Creating and Characterizing the Next Generation of Advanced Materials with support from AWM and ERDF JBO acknowledges with thanks funding *via* a Commonwealth scholarship and support for collaboration was also provided by EPSRC *via* a block grant to University of Birmingham.

REFERENCES

Babic A, Gobec S, Gravier-Pelletier C, Le Merrer Y, Pecar S. 2008. Synthesis of 1-C-linked diphosphate analogues of UDP-N-Ac-glucosamine and UDP-N-Ac-muramic acid. Tetrahedron 64: 9093-9100.

Balcerzak M, Bystronska D, Swiecicka E. 2001. Derivative spectrophotometric methods for the determination of rhodium, palladium and platinum in mixtures. Chem Anal 46: 547-560.

Bertolini JC, Delichere P, Khanra BC, Massardier J, Noupa C, Tardy B. 1990. Electronic-properties of supported Pd aggregates in relation with their reactivity for 1, 3-butadiene hydrogenation Catalysis Letters 6: 215-223.

Baxter-Plant VS, Mikheenko IP, Macaskie LE. 2003. Sulphate-reducing bacteria, palladium and the reductive dehalogenation of chlorinated aromatic compounds. Biodegradation 14: 83-93.

Bennett JA, Mikheenko IP, Deplanche K, Shannon IJ, Wood J, Macaskie LE. 2013. Nanoparticles of palladium supported on bacterial biomass: new re-usable heterogeneous catalyst with comparable activity to homogeneous colloidal Pd in the Heck reaction. Appl Catal B 144-141: 700-707.

Beveridge TJ. 1990. Mechanism of Gram variability in select bacteria. J Bacteriol 172: 1609-1620.

Briñas RP, Hu M, Qian L, Lymar ES, Hainfeld JF. 2008. Gold nanoparticle size controlled by polymeric Au (I) thiolate precursor size. J Am Chem Soc 130: 975-982.

Colombo C, Oates CJ, Monhemius AJ, Plant, JA. 2008. Complexation of platinum, palladium and rhodium with inorganic ligands in the environment. Geochem Explor Env A 8: 91-101.

Creamer NJ, Mikheenko I P, Yong P, Deplanche K, Sanyahumbi D, Wood J, Pollmann K, Merroun M, Selenska-Pobell S, Macaskie LE. 2007. Novel supported Pd hydrogenation bionanocatalyst for hybrid homogeneous/heterogeneous catalysis. Catal Today 128: 80-87.

Dambies L, Guimon C, Yiacoumi S, Guibal E. 2001.Characterization of metal interactions with chitosan by X-ray photoelectron spectroscopy. Colloids Surf A. 177: 203-214.

De Corte S, Hennebel T, de Gusseme B, Verstraete W, Boon N. 2012. Bio-palladium: from metal recovery to catalytic applications. Microb Biotechnol 5: 5-17.

Deplanche K, Murray AJ, Mennan C, Taylor S, Macaskie LE. 2011. Biorecycling of precious metals and rare earth elements. In: *Nanomaterials*. Chapter12. Rahman MM, editor. InTech Publications. ISBN 978-953-307-913-4: pp 279-283.

Deplanche K, Bennett JA, Mikheenko IP, Omajali J, Wells AS, Meadows RE, Wood J, Macaskie LE. 2014. Catalytic activity of biomass-supported Pd nanoparticles: Influence of the biological component in catalytic efficacy and potential application in 'green' synthesis of fine chemicals and pharmaceuticals. Appl Catal B 147: 651-665.

Deplanche K, Caldelari I, Mikheenko IP, Sargent F, Macaskie LE. 2010. Involvement of hydrogenases in the formation of highly catalytic Pd (0) nanoparticles by bioreduction of Pd (II) using *Escherichia coli* mutant strains. Microbiol 156: 2630–2640.

de Vargas I, Macaskie L, Guibal E. 2004. Biosorption of palladium and platinum by sulphate-reducing bacteria. J Chem Technol Biotechnol 79: 49-56.

Doyle R, Matthews T, Streips U. 1980. Chemical basis for selectivity of metal ions by the *Bacillus subtilis* cell wall. J Bacteriol 143:471-80.

Drelinkiewicz A, Hasik M, Choczyński M. 1998. Preparation and propreties of polyaniline containing palladium. Mater Res Bull 33: 739-762.

Fairley N. 2013. CasaXPS. Casa Software Ltd. www.casaxps.com.

Foulkes JM, Malone KJ, Coker VS, Turner NJ, Lloyd JR. 2011. Engineering a biometallic whole cell catalyst for enantioselective deracemization reactions. ACS Catal 11: 1589-94.

Gericke M, Pinches A. 2006. Biological synthesis of metal nanoparticles. Hydrometallurgy 83, 132-140.

Graham LL, Harris R, Villiger W, Beveridge TJ. 1991. Freeze-substitution of eubacteria - general cell morphology and envelope profile. J Bacteriol. 173: 1623-1633.

Hasik M, Bernasik A, Drelinkiewicz A, Kowalski K, Wenda E, Camra J. 2002. XPS studies of nitrogen-containing conjugated polymers-palladium system. Surf Sci 507:916-921.

Hayes PC. 1993. Standard reduction potentials. In: Process principles in minerals and materials production. 2nd edition. Brisbane: Hayes publishing co. pp 660-665.

Hicks JD, Hyde AM, Cuezva AM, Buchwald SL. 2009. Pd-Catalyzed N-Arylation of Secondary Acyclic Amides: Catalyst Development, Scope, and Computational Study. J Am Chem Soc 131:16720-16734.

Holan ZR, Volesky B.1994. Biosorption of lead and nickel by biomass of marine algae. Biotechnol Bioeng 43: 1001-1009.

Huang SW, Neoh KG, Shih CW, Lim DS, Kang ET, Han HS, Tan KL. 1998. Synthesis, characterization and catalytic properties of palladium-containing electroactive polymers. Synth Met 96: 117-122.

Humphries AC, Mikheenko IP, Macaskie LE. 2006. Chromate reduction by immobilized palladized sulfate-reducing bacteria. Biotechnol Bioeng 94: 81-90.

Johnson MD, Bell J, Clarke K, Chandler R, Pathak P, Xia Y, Marshall RL, Weinstock GM, Loman NJ, Winn PJ, Lund PA. 2014. Characterization of mutations in the PAS domain of the EvgS sensor kinase selected by laboratory evolution for acid resistance in Escherichia coli. Mol Microbiol 93: 911-927.

Kratochvil D, Volesky B. 1998. Advances in the biosorption of heavy metals. Trends Biotechnol 16: 291-300.

Lin Z, Zhou C, Wu J, Cheng H, Liu B, Ni Z, Zhou J, Fu J. 2002. Adsorption and reduction of palladium (Pd^{2+}) by *Bacillus licheniformis* R08. Chin Sci Bull 47: 1262-1266.

Lill SO, Siegbahn PE. 2009. An autocatalytic mechanism for NiFe-hydrogenase: reduction to Ni (I) followed by oxidative addition. Biochemistry 48:1056-66.

Macaskie LE, Humphries AC, Mikheenko IP, Baxter-Plant VS, Deplanche K, Redwood MD, Bennett JA, Wood J. 2012. Use of *Desulfovibrio* and *Escherichia coli* Pd-nanocatalysts in reduction of Cr (VI) and hydrogenolytic dehalogenation of polychlorinated biphenyls and used transformer oil. J Chem Technol Biotechnol 87: 1430-1435.

Mikheenko I, Rousset M, Dementin S, Macaskie LE. 2008. Bioaccumulation of palladium by *Desulfovibrio fructosovorans* and hydrogenase deficient mutants. Appl Environ Microbiol 74: 6144-46.

Odom JM, Peck HD. 1984. Hydrogenase, electron-transfer proteins, and energy coupling in the sulfate-reducing bacteria *Desulfovibrio*. Annu Rev Microbiol 38: 551-592.

Omajali JB, Mikheenkho IP, Merroun LM, Wood J, Macaskie LE. 2015. Characterization of intracellular palladium nanoparticles synthesized by *Desulfovibrio desulfuricans* and *Bacillus benzeovorans*. J Nanopart Res 17: 1-17.

Orozco RL, Redwood MD, Yong P, Caldelari I, Sargent F, Macaskie LE. 2010. Towards an integrated system for bio-energy: H_2 production by *Escherichia coli* and use of palladium-coated waste cells for electricity generation in fuel cell. Biotechnol Letts 32: 1837-1845.

Park J, Won SW, Mao J, Kwak IS, Yun Y-S. 2010. Recovery of Pd(II) from hydrochloric solution using polyallylamine hydrochloride-modified Escherichia coli biomass. J Hazard Mater 181: 794-800.

Pinna F, Menegazzo F, Signoretto M, Canton P, Fagherazzi G, Pernicone N. 2001. Consecutive hydrogenation of benzaldehyde over Pd catalysts - Influence of supports and sulfur poisoning. Appl Catal A 219: 195-200.

Postgate JR. 1979. The sulphate-reducing bacteria. Cambridge University Press, Cambridge U.K. 26 p.

Powers DC, Ritter T. 2011. Palladium (III) in Synthesis and Catalysis. Top organomet chem 503: 129-156.

Ragsdale SW. 2009. Nickel-based Enzyme Systems. J Biol Chem 284:18571-18575.

Redwood MD, Deplanche K, Baxter-Plant VS, Macaskie LE. 2008. Biomass-supported palladium catalysts on *Desulfovibrio desulfuricans* and *Rhodobacter sphaeroides*. Biotechnol Bioeng. 99: 1045-1054.

Reis AH, Rosa R. 2005. Role of sorption isotherms in the analysis of coupled heat and mass fluxes in porous media. J Porous Med 8: 259-269.

Skibar W, Macaskie LE, Selenska-Pobell S, Pompe W, Jager I, Rousset M, Hofinger J, Cances C. 2005. Novel precious metal-based bionanocatalysts from scrap Final Report EU contract G5 RD-CT-2002-00750.

Sochacki KA, Shkel IA, Record MT, Weisshaar JC. 2011**.** Protein diffusion in the periplasm of E-*coli* under osmotic stress. Biophys J. 100: 22-31.

Tsezos M, Volesky B. 1982a.The mechanism of uranium biosorption by *Rhizopus arrhizus*. Biotechnol Bioeng 24: 385-401.

Tsezos M, Volesky B. 1982b. The mechanism of thorium biosorption by *Rhizopus arrhizus*. Biotechnol Bioeng 24: 955-969.

Volesky B. 1994. Advances in biosorption of metals: selection of biomass types. FEMS Microbiol Rev 14: 291-302.

Yong P, Rowson NA, Farr JPG, Harris IR, Macaskie LE. 2002. Bioaccumulation of palladium by *Desulfovibrio desulfuricans*. J Chem Technol Biotechnol 77: 593-601.

Zienkiewicz-Strzalka M, Pikus S. 2012. The study of palladium ions incorporation into the mesoporous ordered silicates. Appl Surf Sci 261: 616-622.

3.2 Catalytic Activities of Bionanocatalysts Made by *Bacillus benzeovorans* and *Desulfovibrio desulfuricans*

This section contains the following studies:

3.2.1 Biomanufacture of Heterogeneous Palladium Catalyst: Effects of Biomass Type in the Reductive Dechlorination of Chorobenzene

Journal: Applied Microbiology and Biotechnology, awaiting submission.

3.2.2 *In-situ* Catalytic Upgrading of Heavy Oil Using Dispersed Bionanoparticles Supported on Gram-Positive and Gram-Negative Bacteria

Journal: Applied Catalysis B: Environmental, in submission

3.2.1 Bio-manufacture of Heterogeneous Palladium catalysts: Effects of Biomass Type in the Reductive Dechlorination of Chlorobenzene

Jacob B. Omajali [1], Iryna P. Mikheenko [1], Mohamed L. Merroun [2], Lynne E. Macaskie [1, *]

[1] Unit of Functional Bionanomaterials, Institute of Microbiology and Infection, School of Biosciences, University of Birmingham, Edgbaston, Birmingham, B15 2TT, United Kingdom

[2] Department of Microbiology, Faculty of Sciences, University of Granada, Campus Fuentenueva, 18071, Granada, Spain

*Corresponding author. Tel.: fax:

Email address:

Journal: Appled Microbilogy and Biotechnology, awaiting submission

This paper was written by J.B. Omajali. All experiments and analysis were performed by the author.

Abstract

Chlorinated aromatic contaminants like chlorobenzene are known for their toxicity and persistence in the environment mainly due to the presence of the halogen substituent. Palladized bacteria are reported to effect reductive dehalogenation. This study reports reductive dechlorination of chlorobenzene with 'bio-Pd' (20% by mass) synthesized *via* hydrogen and formate as electron donors using Gram-positive (*Bacillus benzeovorans* NCIMB 12555) and Gram-negative (*Desulfovibrio desulfuricans*, NCIMB 8307 and NCIMB 8326) bacteria as catalyst supports. The catalyst made under hydrogen showed smaller Pd crystallites using TEM and XRD than equivalent bio-catalyst made *via* formate. Bio-Pd$_{D.desulfuricans\ 8307}$ produced the most active catalyst with a chloride removal efficiency of 40-52% at removal rates of 0.058-0.100 mmol/min/mg Pd (~1.5-2) fold faster than those made by the other Gram-negative (Bio-Pd$_{D.\ desulfuricans\ 8326}$) and Gram-positive (Bio-Pd$_{B.benzeovorans\ 12555}$) bacteria after 24h of reaction. Generally, bio-Pd was more active at 20% loading than commercial Pd/C in dehalogenation reactions with rates ~20-61 times faster, depending on the biomass type.

Keywords: *Bacillus benzeovorans*; Chlorobenzene; *Desulfovibrio desulfuricans*; Palladized bacteria; Reductive dehalogenation

Introduction

Chlorinated aliphatic and aromatic compounds are produced by agricultural and chemical industries (Field and Sierra-Avarez, 2008; Liang et al., 2013) *e.g.* in the manufacture of agricultural and industrial chemicals such as biocides, degreasing agents, solvents, flame retardants, heat transfer liquids and pharmaceuticals (Adrian and Gorisch, 2002; Field and Sierra-Avarez, 2008; Zanaroli et al. 2015). Despite that major production of these chemicals is in decline they have continued to persist, bioaccumulate and biomagnify mainly from hazardous waste disposal sites leading to extensive environmental contamination and toxicity (Field and Sierra-Avarez, 2008). Compounds such as polychlorinated biphenyls (PCBs), polychlorinated dibenzo *p*-dioxins (PCDDs), polybrominated diphenyl ether (PBDE), polychlorinated dibenzofurans (PCDFs) and low-chlorinated benzenes (monochlorinated benzenes (*e.g.* chlorobenzen) and dichlorinated benzenes) have become major pollutants in soil, ground water and aquatic sediments (Wong et al., 2007). While chlorinated aromatic compounds like PCBs, PCDDs and PCDFs are carcinogenic, mutagenic, and stable (Henry and DeVito, 2015), the toxicity of chlorobenzene can lead to adverse effects on the liver, kidney, thyroid and lungs (den Besten et al., 1991).

Chlorobezene is a priority pollutant according to the US Environmental protection agency. When the Safe Water Act was passed by the US congress in 1974, becoming effective in 1989, the maximum contaminant level of chlorobenzene in drinking water was set at 100µg/L (100ppb) and can lead to health related complications when present above drinking water standard limits (EPA, 2015).

Various methods have been developed to either reduce the toxicity of chlorinated compounds or completely degrade them. Biological processes such as oxidative and reductive microbial degradations have been used in the destruction of harmful chlorinated aromatic contaminants. Aerobically, bacteria utilize oxidative mechanism *via* enzymes *e.g.* dioxygenase which uses oxygen directly as a reactant to convert chlorinated aromatic compound first into an intermediate called chlorocatechol which is further metabolized *via* ortho or meta – ring cleavage pathways (Field and Sierra-Alvarez, 2008) to CO_2. However, the chlorinated organic compounds readily form dense non-aqueous phase liquids (DNAPLs) which move into the anaerobic deep

zones of sediments and ground water which requires the activity of anaerobic or halorespiring bacteria (Nelson et al., 2014).

Under anoxic conditions, bacteria such as sulfate-reducing bacteria (SRB) and other halorespiring bacteria have developed a mechanism called reductive dechlorination (Lesage et al., 1998; Fung et al., 2009) which replaces the halogen substituent with hydrogen or hydroxyl group. Reductive dechlorination reduces the difficulty in degradation and potential toxicity of intermediates during the degradative steps (Janssen et al., 2001). The activities of some species of bacteria such as *Desulfovibrio*, *Desulfomonile* and *Desulfoluna* spp. was recently reviewed (Zanaroli et al., 2015). These organisms couple the oxidation of organic electron donors to the dehalogenation of less hydroxylated or carboxylated monoaroamtic organohalides. According to Miller et al (2005), *Dehalobium chlorocoercia* couples the oxidation of hydrogen or formate to reductive dechlorination of tetrachloroethene to trichloroethene while hexa-chlorobenzene was reductively dechlorinated to pentachlorobenzene (Wu et al., 2002).

However, biological processes are quite limited due to inefficiency and slow rate in the treatment of particularly ground water contaminated with chlorinated aromatic compounds (Adrian and Gorisch, 2002). For instance, aerobic oxidation of PCBs only results in slight attack on chlorinated congeners while anaerobic processes involve reductive dechlorination which may lead to a reduction in toxicity, but accumulation of intermediates in aquifers (Heidrich et al., 2004) are examples of low-chlorinated benzenes.

Alternatively the use of catalytic reductive dechlorination is considered more advantageous because it is safe, simple and effective (Alonso et al., 2002). There is a renewed interest in the use of nanostructured materials in catalysis as a result of their potential as effective catalyst in water or biphasic water-organic solvents for reactions such as oxidation (Cornils et al., 2005) and reductive dehalogenation (hydrogenolysis) (Baxter-Plant et al., 2003) only if recovered or immobilized. An initial study using palladized zero-valent iron (Kort et al., 1997) was reported but was found to foul up quickly with the product leading to limited extent of breakdown. Commercially supported catalysts of Pd/C and Pd/$AlPO_4$-SiO_2 have been previously utilized under

different experimental conditions to treat chlorobenzenes (Aramendia et al., 1999; Konuma et al., 2002). However, the use of commercial catalyst has major disadvantages as they are very expensive at large scale and also involves the use of toxic chemicals and without passivation, nano catalysts agglomerate, therefore blocking active surfaces (Choudhary and Goodman, 2002). Hence, the use of palladized bacteria (bio-Pd) becomes a suitable alternative in the reductive dehalogenation of chlorobenzene as bio-Pd are more sustainable, cheaper and the precious metals *e.g.* Pd, Pt and Au can be sourced or recovered from waste streams (Murray et al., 2007; Yong et al. 2010).

Previous studies using palladized bacteria have demonstrated its effectiveness in the reductive dehalogenation of various chlorinated aromatic contaminants. De Windt et al (2005) used a facultative anaerobe, *Shewanella oneidensis* in the presence of both hydrogen and formate as electron donors to synthesized 'bio-Pd' which facilitated the reductive dehalogenation of PCB while De Corte et al (2012) used a similar bacterium (*Shewanella oneidensis*) metallized with both Pd and Au for the dehalogenation of diclofenac within 24 h. Under a fermentative condition, Hennebel et al. (2011a) produced bio-Pd using *Citrobacter braakii* to dehalogenate 22 mg of diatrizoate from a 20 mg/L source. In the same year, the authors coupled hydrogen in the cathode of a microbial electrolytic cell (MEC) to dehalogenate ground water contaminant of trichloroethylene and diatrizoate with the concomitant release of both Cl^- and ethane (Hennebel et al., 2011b). Other studies have shown that *Desulfovibrio desulfuricans* and *Rhodobacter sphaeroides* grown anaerobically can also serve as platforms for the synthesis of bio-Pd and utilized subsequently in the reductive dehalogenation of PCBs and chlorinated phenols (Baxter-Plant et al 2003; Redwood et al. 2008). The dehalogenation of PCBs and PBDE has also been shown using palladized *Desulfovibrio desulfuricans* (Harrad et al., 2007; Deplanche et al., 2009) while Baldi et al., (2011) used Fe and Pd binding to extracellular polymeric substances (EPS) from *Klebsiella oxytoca* BAS-10 grown under an anaerobic condition in the reductive dehalogenation of chlorobenzene. In this study, we considered the use of chlorobenzene (low-chlorinated benzene) because the degradation of highly chlorinated aromatic compounds leads to the formation and accumulation of low-chlorinated benzenes commonly found in ground water which have been known to be toxic above a certain concentration in drinking water (EPA, 2015).

The first objective of this study was to evaluate the influence of cell type *i.e.* of Gram-positive *Bacillus benzeovorans* (facultatively anaerobic) and Gram-negative *Desulfovibrio desulfuricans* (obligately anaerobic) as catalyst (bio-Pd) support in the reductive dechlorination of chlorobenzene. Previous studies (De Windt et al., 2005) on catalytic reductive dehalogenation of polychlorinated biphenyls (PCBs) considered only the use of bio-Pd made *via* reduction with hydrogen and formate on a Gram-negative facultative anaerobe, *Shewanella oneidensis*. Hence, this study compares the catalytic reductive dechlorination of chlorobezene *via* bio-Pd synthesized by aerobic (Gram-positive) and anaerobic (Gram-negative) bacteria. Since observed effects could not only be attributed to simple differences in nanoparticle size, the second aim was to compare the structural differences in the two types of bio-Pd to provide further insight into the nature of catalytic efficacy.

Materials and Methods

Microorganisms, growth conditions and synthesis of biomass-supported Pd-catalysts

Desulfovibrio desulfuricans (NCIMB 8307 and NCIMB 8326) were grown anaerobically (Deplanche et al., 2014) while *B. benzeovorans* NCIMB 12555 was grown aerobically (Omajali et al 2015). Cells were harvested, washed and concentrated in a small amount of the same buffer. Then degassed and stored under oxygen-free nitrogen (OFN) at 4^{o}C until use. Concentrated resting cell suspension of each bacterium was transferred into an appropriate volume of degassed (30 minutes) 2mM Pd (II) salt solution (Na_2PdCl_4, pH 2 ± 0.1 adjusted with 0.01 M HNO_3) to make a 20% loading (1:5) on biomass. Complete removal of Pd onto cells was determined by a method described previously (Deplanche et al., 2010). Biosorption of Pd (II) onto cell surfaces was done by allowing the palladium mixture to stand in water for 30 min, at 30^{o}C with occasional shaking. The reduction of Pd (II) to Pd (0) was achieved *via* hydrogen and formate as exogenous electron donors based on the method of Omajali et al., (2015). The resulting bio-Pd (0) was washed with water and acetone and then dried to constant weight, finely ground in an agate mortar with pestle and sieved.

Electron Microscopy and Energy dispersive X-ray Spectrometry (EDX) analysis

The method of Deplanche et al. (2010) was adopted for electron microscopy and EDX analysis. Electron opaque deposits were examined by EDX (Yong et al., 2002) with peaks sought corresponding to X-ray emission energies of Pd. The HAADF-STEM analysis was done according to a previous method (Omajali et al., 2015).

X-Ray Powder Diffraction (XRD) Analysis

Washed samples of bio-Pd were air dried and ground into a fine black powder in an agate mortar with pestle according to previous methods (Deplanche et al., 2014). The X-ray powder diffraction patterns were acquired from a Bruker AXS D8 autosampler (transmission) diffractometer using a monochromatic high-intensity $CuK_{\alpha 1}$ radiation (λ = 1.5406 Å) and the XRD patterns were then compared to a reference standard in the International Committee for Diffraction Data (ICDD) database.

Reductive dehalogenation of chlorobenzene using bio-Pd catalyst

Catalytic activity of bio-Pd was determined by the release of chloride from chlorobenzene. Bio-Pd (0) (2mg) was suspended in 9ml of sterile and degassed MOPS-NaOH buffer (20mM, pH 7.0) in a 12ml serum bottle. The metal loading on biomass was 20wt% bio-Pd (0) (0.4 mg Pd) or 0.4mg Pd of palladium on carbon catalyst (Pd/C) (Sigma-Aldrich, UK). This was followed by the addition of 1ml of chlorobenzene in hexane (1:1 v/v) and chlorobenzene concentration was 5mM. The hexane partitioned the catalyst and chloride product (aq) (Redwood et al., 2008). After shaking (5 mins) and separation, sample (1 ml aq) was taken to determine the chloride concentration (time = 0) and the catalyst separated by centrifugation. The reductive dehalogenation was initiated by the addition of sodium formate (1M, pH 7.0) to a final concentration of 10 mM (Baxter-Plant et al., 2003). Samples were then taken from the aqueous phase at suitable time intervals, centrifuged (16,000 x g, 4min), and the supernatant was transferred into cuvettes. Reductive dehalogenation was monitored by the release of Cl^- (Deplanche, 2008) monitored at 460 nm. Controls included catalyst free mixture and unpalladized biomass (metal-free control). All experiments were conducted in triplicate.

Results

Examination of bio-Pd of the three strains made under hydrogen and formate

Examination of the Pd-NPs shows that these are indistinct by electron microscopy with some larger nanoparticles but use of EDX shows Pd to be present in all the samples (Fig 1).

X-ray powder diffraction (XRD) (Fig 2) confirms the presence of Pd-crystallites. The average crystallite sizes were calculated using Scherrer equation (Jaboyedoff et al, 1999). The average crystallite size of Pd made *via* formate were confirmed as generally larger, with Dd8326 producing the largest size (25.8±1.9 nm) with no significant difference (P = 0.547) between the sizes of Dd8307 (14.7±1.1 nm) and Bb (14.9±3.7 nm) respectively (Table 1). Made under hydrogen, the average crystallize size follows a similar trend with Dd8326 producing the largest size (18.8±1.6 nm) followed by Dd8307 (13.2±1.5nm) but with Bb producing the smallest size (7.5±0.7 nm) (Table 1).

Table 1 XRD analysis of crystallite size of bio-Pd made by bacteria using hydrogen and formate as electron donors

	Average crystallite size (nm) Electron donors	
Catalyst type	Hydrogen	Formate
Bio-Pd*B. Benzeovorans* 12555	7.5 ± 0.7	14.9 ± 3.7
Bio-Pd*D. desulfuricans* 8307	13.2 ± 1.5	14.7 ± 1.1
Bio-Pd*D. desulfuricans*8326	18.8 ± 1.6	25.8 ± 1.9
Commercial (Pd/C) catalyst	3.8 ± 0.9	

Crystallite size (Mean ± SEM) was estimated *via* the scherrer equation (Jaboyedoff et al, 1999) from the X-ray powder diffraction patterns shown in Fig 2.

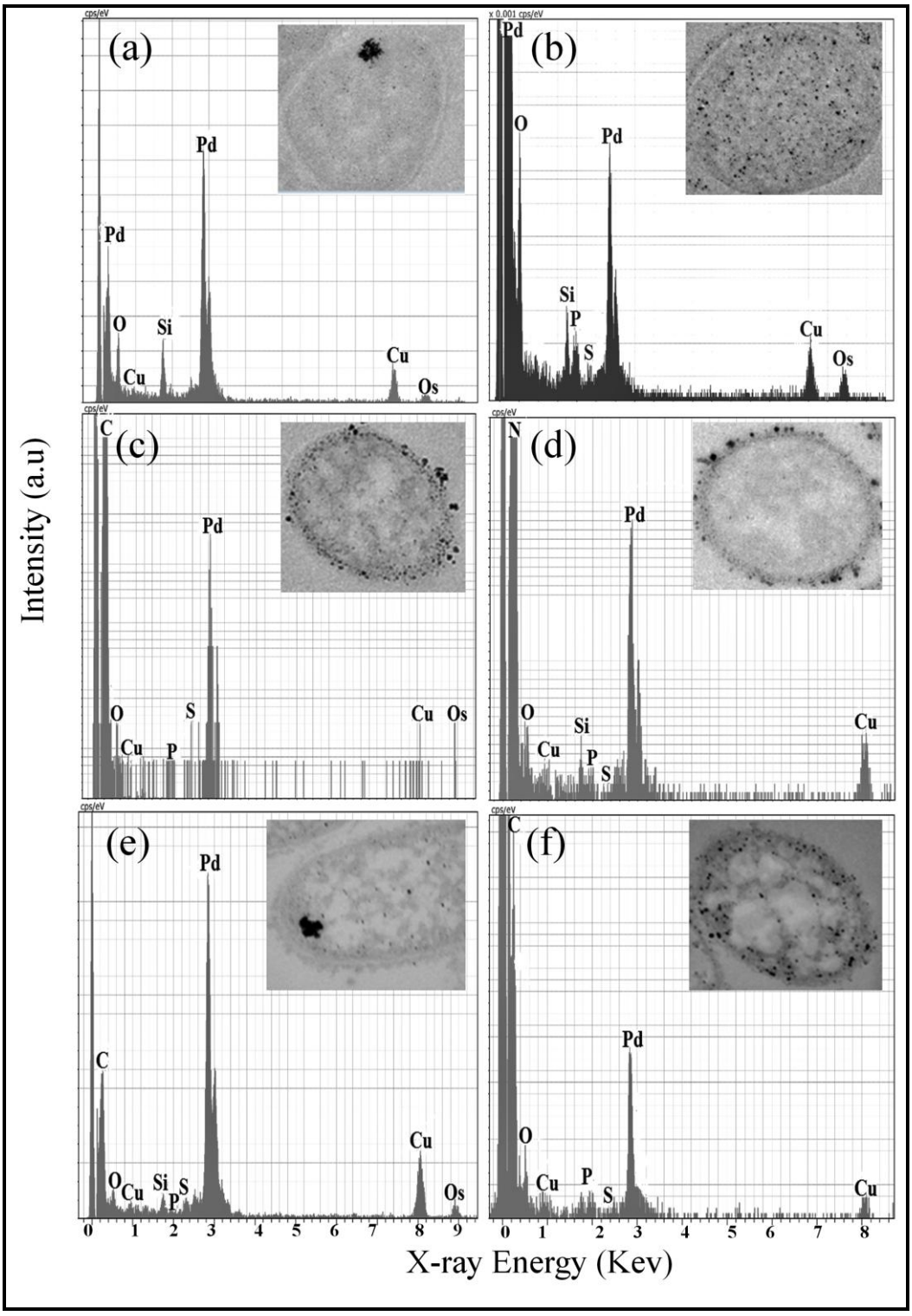

Figure 1 EDX results showing the presence of Pd in 20wt% bio-Pd made using hydrogen (right) and formate (left) as electron donors by *B. benzeovorans* (top, a, b), *D. desulfuricans* NCIMB 8307 (middle, c, d) and *D. desulfuricans* NCIMB 8326 (bottom, e, f). Insets are corresponding TEM images of bio-Pd.

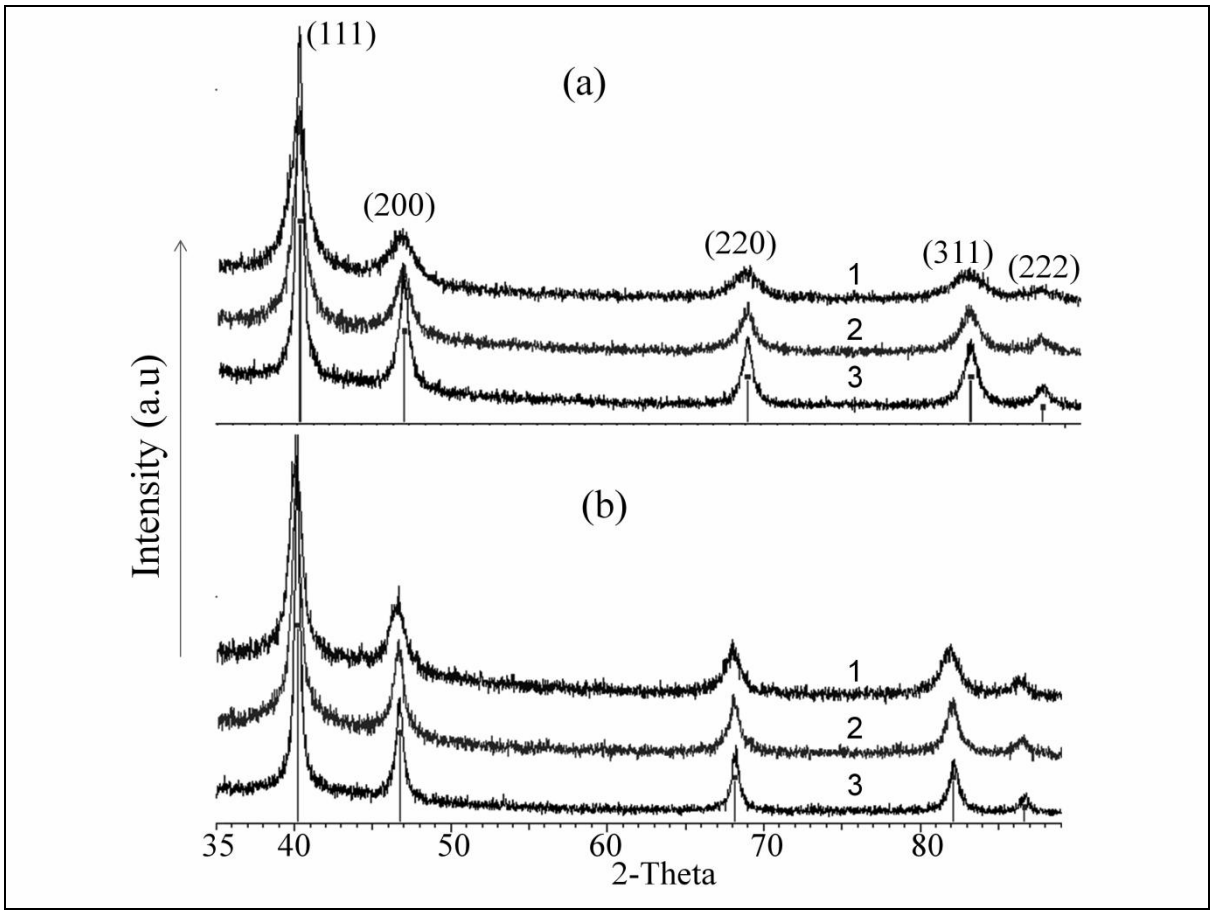

Figure 2 XRD patterns of 20wt% bio-Pd synthesized using hydrogen (a) and formate (b) as electron donors by 1. Bb; 2. Dd8307 and 3. Dd8326 respectively. Vertical lines correspond to peak intensity of Pd planes: (111), (200), (220), (311) and (222) as obtained from ICCD database while horizontal axis represents angle of diffraction.

Evaluation of reductive dechlorination of chlorobenzene

Reductive dechlorination was done as a catalytic test to determine the influence of bacterial biomass and electron donors on catalytic properties of bio-Pd (0). Bio-Pd synthesized using hydrogen as electron donor gave, after 24h, efficiency of chloride removal from chlorobenzene of 52.0%, 42.4% and 40.1% (Fig 3a, Table 2) for bio-Pd$_{D\ desulfuricans8307}$, bio-Pd$_{B.\ benzeovorans}$, and bio-Pd$_{D.\ desulfuricans\ 8326}$ respectively i.e. bio-Pd$_{D\ desulfuricans8307}$) was ~18-23% more effective catalytically. There was a significant difference (P = 0.0034) at 95% confidence level in the final amount of chloride released by bio-Pd$_{B.\ benzeovorans\ 12555}$ and bio-Pd$_{D.\ desulfuricans\ 8326}$. The initial rate determined for the first 30 mins of reaction, indicated that bio-Pd$_{D\ desulfuricans8307}$ was ~1.5-2 fold faster than

both bio-Pd$_{B.\ benzeovorans\ 12555}$ and bio-Pd$_{D.\ desulfuricans\ 8326}$ (Table 2). The difference between the two *Desulfovibrio* strains was highly significant ($P < 0.01$).

Bio-Pd synthesized using formate was less active than that made *via* hydrogen. After 24 h of reaction, bio-Pd$_{D\ desulfuricans8307}$ was more active (2.01 mmol of chloride released) than that of bio-Pd$_{D.\ desulfuricans\ 8326}$ and bio-Pd$_{B.\ benzeovorans\ 12555}$ (1.49 and 1.42 mmol) respectively. This corresponds to a removal efficiency of 40.1%, 29.8% and 28.4% of bound chloride in chlorobenzene respectively (Fig 3b). The control reaction using commercial palladium catalyst on carbon (Pd/C) gave chloride removal of 4.7% (rate of 0.00164 mmol/min/mg Pd) (Table 2). It was observed that during the dehalogenation reaction, the Pd/C catalyst agglomerates and formed larger particles as compared to the bio-Pd made by bacteria which remained dispersed in the reaction media throughout the reaction time. The release of chloride from catalyst-free control and metal-free biomass (Table 2) reaction was insignificant.

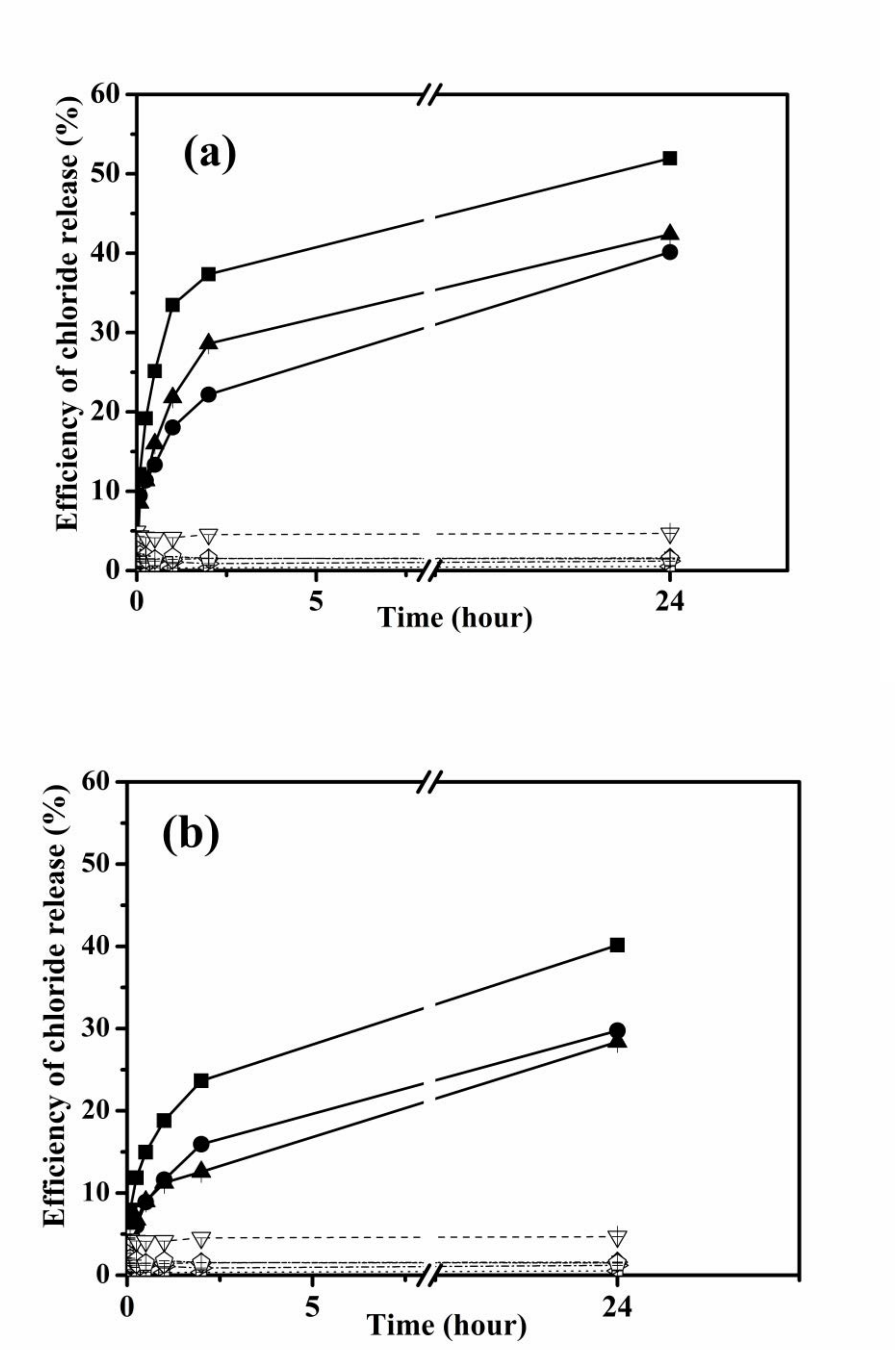

Figure 3 Efficiency of chloride release after 24 hours from chlorobenzene using 20% bio-Pd reduced using (a) hydrogen and (b) formate as electron donors. Closed symbols represent 0.4 mg Pd catalyst loading for bio-Pd$_{D\ desulfuricans}$8307 (■), bio-Pd$_{B.\ benzeovorans}$ 12555 (▲), bio-Pd$_{D.\ desulfuricans}$ 8326 (●) while open symbols represent controls; 0.4 mg palladium on carbon (Pd/C) commercial catalyst (▽), catalyst free control (◅), non-metalized biomass of Bb (▻), Dd8307 (◇) and Dd8326 (⬠). Results are Mean ± SEM of three independent experiments. Error bars are within the dimension of the symbols. Bb: *Bacillus benzeovorans*; Dd: *Desulfovibrio desulfuricans.*

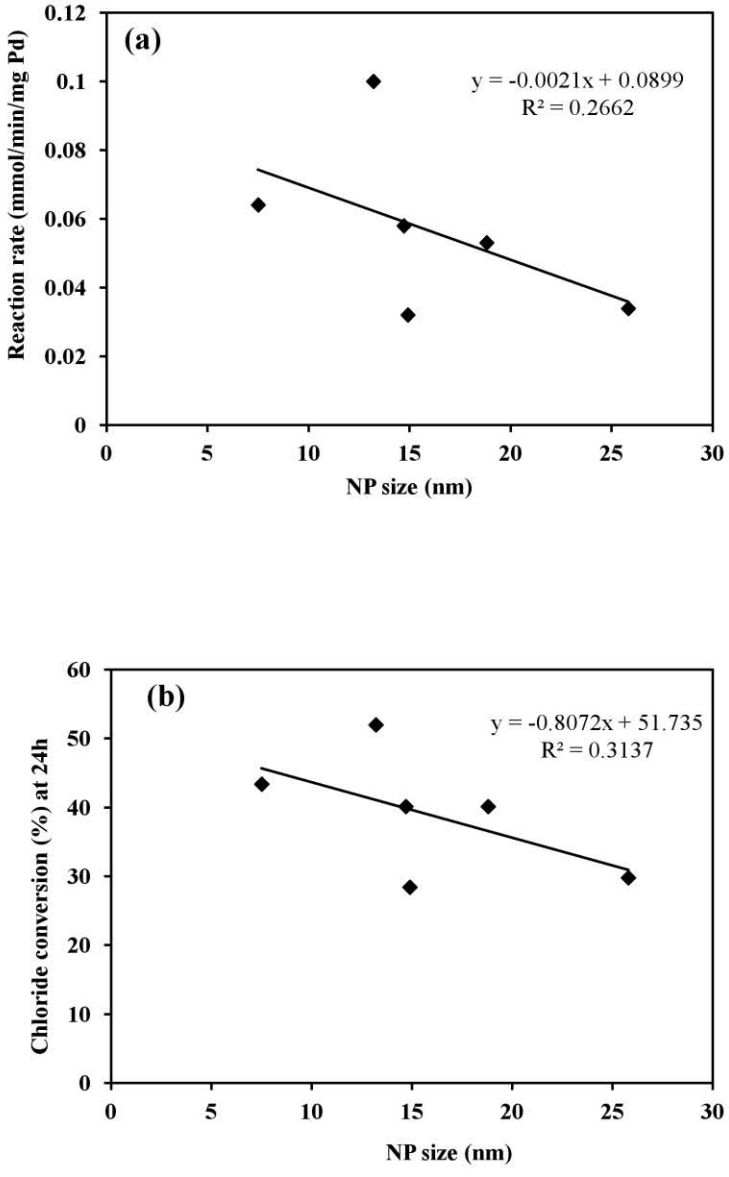

Figure 4 Relationship between reaction rate *vs* NP size (a) and chloride conversion *vs* NP size (b) at 24 h of reaction. Test of correlation coefficients shows that there was no significant correlation ($p = 0.31$) in (a) and $p = 0.34$ in (b) respectively.

Table 2 Dehalogenation of chlorobenzene using bio-Pd made with hydrogen and formate as electron donors

Catalyst	Electron donor	Final amount (mmol) and Efficiency (%) of chloride release			Initial rate of reaction (mmol/min/mg Pd)		
		Bb	Dd8307	Dd8326	Bb	Dd8307	Dd8326
20% bio-Pd	Hydrogen	2.11±0.002 (42.4%)	2.60±0.036 (52.0%)	2.01±0.036 (40.1%)	0.064	0.100	0.053
	Formate	1.42±0.109 (28.4%)	2.01±0.313 (40.1%)	1.49±0.069 (29.8%)	0.032	0.058	0.034
Non-metallized biomass	None	<1	<1	<1	-	-	-
5% Pd/C	Commercially Supplied	0.23±0.005 (4.7%)			0.00164		
Catalyst-free control	None	<1			-		

Initial rate was obtained for the first 30 minutes of reaction per mass of catalyst used (normalized). 5mM chlorobenzene in hexane was used as substrate. Figures in brackets represent efficiency of chloride released after 24 hours of dechlorination. Formate (10 mM) was used as the electron donor for reductive dehalogenation reaction. 0.4 mg Pd catalyst loading was used in each sample for the reaction. Bb: *Bacillus benzeovorans*; Dd: *Desulfovibrio desulfuricans*. Results are Mean ± SEM. Catalyst-free control contains neither catalyst nor biomass. Bio-Pd (0) cleaves formate into highly reactive hydrogen by weakening the C-H bond and inducing reductive dehalogenation reaction to proceed (see Mabbet et al., 2006).

Discussion

In this study, when hydrogen was used as an electron donor, the two strains of *Desulfovibrio* behaved differently in terms of the mechanism of Pd-NP deposition on their surfaces or within the cell matrices. Dd8307 produced Pd-NPs mainly within the periplasmic space while Dd8326 produced mainly intracellular Pd-NPs with little or no extracellular Pd deposition. Hydrogenases are known to cycle hydrogen (Odom and Peck, 1981) and were implicated in the formation of Pd-NPs in Gram-negative bacteria *via* hydrogen oxidation anaerobically (Mikheenko et al., 2008; Deplanche et al., 2010). The formation of Pd-NPs within the periplasmic space of Dd8307 (Fig 1c) could have

been facilitated by hydrogenases and/or cytochromes. The involvement of hydrogenase was proposed by Mikheenko et al (2008) by using a mutant of *D. fructosovorans* devoid of periplasmic hydrogenases and was later confirmed in *E. coli* by Deplanche et al., (2010). The absence of bound Pd-NPs within the periplasmic space of Dd8326 when hydrogen was used as electron donor (Fig 1e) suggests a new mechanism or the absence of periplasmic hydrogenases. The mechanism of Pd nanoparticle deposition *via* formate by Dd8307 and Dd8326 differs from that made under hydrogen as the Pd-NPs were more on the outer membrane and cell wall (Fig 1d, f). It is plausible that the biochemical oxidation of formate *via* formate hydrogen lyase (Axley et al. 1990) might be in part responsible for this observation.

Furthermore, in the presence of hydrogen as electron donor the formation of Pd-NPs in Bb (Fig 1a) is mostly intracellular suggesting the possible roles of an alternative mechanism for Pd synthesis. Bunge et al (2010) reported that hydrogenases are not involved in the formation of Pd nanopartciles in *Cupriavidus necator* H16, but suggested the possible role of fortuitous enzyme activities or cellular interfaces and that directed processes were not involved. In the presence of formate as electron donor, the Pd-NPs produced by Bb (Fig 1b) were larger than that synthesized using hydrogen which may be due to the possible influence of chemical or biochemical oxidation through formate dehydrogenase. This is because of the possible role of the enzyme in biochemically splitting formate (Costa et al., 1997; Ding et al., 2011) to generate hydrogen which splits in the presence of Pd (Livingstone 1973; Rhodin and Ertl, 1979) to give more reactive hydrogen radical. In *Shewanella oneidensis* (De Windt et al., 2005), smaller particles associated with cell surface and inside periplasm were seen when hydrogen was used as an electron donor to synthesize Pd (0) nanoparticles while in formate reduced Pd, fewer and larger particles were observed.

The use of bio-Pd (0) in *in-situ* environmental remediation could be more attractive when augmented with purely microbial processes. In this study, when hydrogen was used as an electron donor to synthesize Pd-NPs, bio-Pd$_{D\ desulfuricans8307}$ demonstrated the best activity in the dechlorination of chlorobenzene when compared with bio-Pd$_{D.\ desulfuricans\ 8326}$ and bio-Pd$_{B.\ benzeovorans\ 12555}$. Considering the activities of the *Desulfovibrios*, bio-Pd$_{D\ desulfuricans8307}$ had a chloride removal efficiency of 52% better

than 40.1% for bio-Pd$_{D.\ desulfuricans\ 8326}$ and the rates of reaction was about 1.89 fold faster. This can be explained by looking at the nature of Pd-NP patterning on each bacterium from TEM images (Omajali et al 2015). It is possible that the accessibility of substrates to bio-Pd$_{D\ desulfuricans8307}$ was better due to the nature of the Pd-NPs on the periplasmic surface and inside the cell providing more contact at the hexane-water interface than bio-Pd$_{D.\ desulfuricans\ 8326}$ where there were little or no surface localized Pd-NPs, except for the presence of fewer intracellular Pd-NPs. This can also explain the slower reaction in Bb where there was no surface bound NPs, meaning that there was less synergy between surface bound and intracellular NPs. This explanation is also valid for the formate reduced Pd-NPs. However, even though Pd-NPs by bio-Pd$_{D\ desulfuricans8307}$ was more active than the other two, the activity of bio-Pd$_{D.\ desulfuricans\ 8326}$ was comparable to bio-Pd$_{B.\ benzeovorans\ 12555}$ where both catalysts displayed more intracellular NPs than bio-Pd$_{D\ desulfuricans8307}$. Such intracellular NPs might be difficult for the aromatic substrate to contact at the hexane-water interface during dechlorination, leading to reduced activity and slower rates of reaction as observed (Table 2).

The Pd crystallite size also matters with regards to catalyst activity (Chaturvedi et al., 2012). From the XRD analysis (Fig 2, Table 1), the reduction of Pd (II) in the presence of hydrogen produced Pd with smaller crystallite sizes than when formate was used. The smaller Pd crystals made *via* hydrogen were catalytically more active overall (Fig 3a) than the larger Pd crystals made *via* formate (Fig 3b) with bio-Pd$_{D.\ desulfuricans\ 8326}$ having the largest crystallite size but having comparable activity with bio-Pd$_{B.\ benzeovorans\ 12555}$ but less active than bio-Pd$_{D\ desulfuricans8307}$. This shows that electron donors have the ability to tune the size and possibly shapes of Pd-NPs (Shi et al., 2013; Omajali et al., 2015) leading to new materials with different catalytic properties. De Windt et al (2005) showed that when hydrogen was used to synthesize bio-Pd in *S. oneidensis*, higher extent of dechlorination was observed after 48h when compared to bio-Pd synthesized *via* formate which also produced larger Pd-NPs. Smaller non-aggregated NPs are known to have a larger surface area to volume ratio which exposes the active Pd surface to substrates and hence faster rates of reactions and activity (Chaturvedi et al., 2012). However, the catalyst synthesized by Bb *via* hydrogen with the smallest size was not the most active which explains that size alone does not control the entire mechanism of catalyst activity (Zhang et al. 2013). A similar result for the formate reduced bio-Pd

showed that despite bio-Pd$_{D\ desulfuricans8307}$ and bio-Pd$_{B.\ benzeovorans\ 12555}$ Pd-NPs having comparable crystallite size, bio-Pd$_{D\ desulfuricans8307}$ was more active (about 1.57 fold faster) in reaction rate. The reason for this kind of difference may be attributed to the various biochemical mechanisms and surface groups (Schluter et al 2014) by which Pd-NPs are stabilized and patterned on each bacterium as observed from the differences in Pd NP arrangement on cells shown *via* TEM images (Fig 1). Therefore, this study confirms that the catalyst activity in terms of rate ($r^2 = 0.2662$) and chloride conversion ($r^2 = 0.3137$) at 24h does not correlate with crystallite size when both catalyst made *via* formate and hydrogen were considered together or separately (Fig 4). However, XPS analysis has shown some differences in the concentration of surface groups in both *D. desulfuricans* and *B. benzeovorans* (Omajali et al unpublished). Previous studies have shown that bio-Pd produced by *D. desulfuricans* (bio-Pd$_{D\ desulfuricans8307}$) was a better catalyst in reductive dehalogenation when compared to other species of *Desulfovibrios* (Baxter-Plant et al., 2003) and *Rhodobacter sphaeroides* (Redwood et al., 2008).

By using a cell suspension of anaerobic bacteria (*e.g*. *Desulfomonile tiedjei* DBC-1), the rate of reductive dehalogenation of chlorinated aromatic compounds was found to be below 3.9×10^{-3}nmol/min/mg biomass (Tiedjel et al., 1993; Haggblom and Young, 1995). Bio-Pd has shown to be faster and within the range of ~32 – 100 nmol/min/mg Pd (this study). This suggests that bacterial processes could be augmented with bio-Pd to treat aquifers, underground water and sediments contaminated with low-chlorinated benzenes instead of using bacteria alone. The synergy can result in faster treatment of contaminants. The rate of dehalogenation tends to slow down eventually after 24 hours which may be due to steric hinderance or flocculation by the chlorinated aromatic compound. Mikheenko et al, (unpublished) has demonstrated this mechanism of flocculation using scanning probe microscopy (SPM). Such flocculation is a challenge to the life span and performance of a catalyst.

In general bio-Pd was a better catalyst ($P < 0.05$) in the dehalogenation of chlorobenzene than commercial catalyst of palladium on carbon (Pd/C). The rate of reductive dechlorination of chlorobenzene using bio-Pd was ~ 25 and 44 fold faster than Pd/C when formate and hydrogen were used respectively to synthesize bio-Pd. Baxter-Plant et al (2003) showed that bio-Pd made using *D. desulfuricans* (bio-Pd$_{D\ desulfuricans8307}$) was ~30 times more active (9nmol/min/mg Pd) than chemical Pd (0) in the

dechlorination of 2, 3, 4, 5-tetrachlorobiphenyl. In this study, it was observed that the bio-Pd (0) catalysts were well dispersed during the reaction while the commercial Pd/C catalyst agglomerates soon after the reaction was initiated and may explain the reason for slow activity and poor performance in the dehalogenation of chlorobenzene. The agglomeration must have led to particle growth and blockage of active surfaces preventing access to the aromatic substrate (chlorobenzene) at the hexane-water interface and eventually leading to a slow rate of reaction and deactivation of the catalyst. Biosynthesized Pd might be more active, resistant to deactivation as they are more dispersed and stable due to binding of the Pd-NPs to functional groups on the cell surface leading to specific cell-molecule interaction with the organic substrate (Schluter et al 2014) which justifies the differences observed between bio-Pd and commercial Pd/C. A similar result was also shown by De Windt et al., (2005) whereby commercial Pd (0) catalyst showed a slower rate in the dechlorination of PCBs than bio-Pd made by *S. oneidensis*. Schluter et al (2014) have also shown that chemically synthesized Pd did not actively catalyse dioxin dechlorination when compared with bio-Pd synthesized using *Pseudomonas* spp. Other studies have further supported this finding (Baxter-Plant et al., 2003; Redwood et al., 2008; Hennebel et al., 2011a). However, Deplanche et al (2009) observed that chemically synthesized and commercial Pd catalyst were more active than bio-Pd in the debromination of PBDE #47 within 24 h than bio-Pd and it was suggested that the lower metal loading (1:19) to biomass ratio could be the possible reason. In a separate experiment by the authors, bio-Pd catalyst was about five times more active than commercial Pd (0) catalyst in the dechlorination of ground water containing tris chloroisopropyl phosphate (TCPP). Redwood et al., (2008) further supported that higher metal loading tend to be more active in dehalogenation. Catalyst-free control (hexane alone without chlorbenzene) and metal-free biomass have shown neglible chloride release. This is in line with the findings of Baxter-Plant et al., (2003), De Windt et al., (2005) and De Corte et al., (2012) where negligible to no chloride release was witnessed. This confirms the absence of chloride release due to induction by these controls.

Conclusion

This study has revealed the influence of biomass type and electron donors on catalytic synthesis and the subsequent effects of each catalyst in reductive dechlorination of chlorbenzene. The patterning of Pd-NPs on the various bacteria differs and this was seen to be one of the key reasons for the catalytic performance of the catalyst. We have also shown that catalytic reductive dechlorination of chlorobenzene is independent of crystallite size. Therefore, biochemical arrangement of Pd-NPs and the influence of cell surface groups may potentially determine the nature of Pd-NPs. Gram-negative *D. desulfuricans* (bio-$Pd_{D\ desulfuricans8307}$) was a better catalyst overall due to size and the nature of surface bound and intracellular localization of the Pd-NPs. However, *D. desulfuricans* (bio-$Pd_{D.\ desulfuricans\ 8326}$) and Gram-positive *B. benzeovorans* (bio-$Pd_{B.\ benzeovorans\ 12555}$) produced more intracellular Pd-NPs. Generally, the bio-Pd catalysts are more active in the dehalogenation of chlorobenzene than the commercial Pd/C catalyst and could augment microbial biotransformation of chlorinated aromatic contaminants because of their dispersion and stability in reaction media.

Acknowledgement

The authors acknowledge with thanks a Commonwealth scholarship to JBO.

References

Adrian, L.; Gorisch, H., Microbial transformation of chlorinated benzenes under anaerobic conditions. *Research in Microbiology* **2002,** *153* (3), 131-137.

Alonso, F.; Beletskaya, I. P.; Yus, M., Metal-mediated reductive hydrodehalogenation of organic halides. *Chemical Reviews* **2002,** *102* (11), 4009-4091

Aramend a, M. A.; Bor u, V.; Garc a, I. M.; Jiménez, C.; Lafont, F.; Marinas, A.; Marinas, J. M.; Urbano, F. J., Influence of the Reaction Conditions and Catalytic Properties on the Liquid-Phase Hydrodechlorination of Chlorobenzene over Palladium-Supported Catalysts: Activity and Deactivation. *Journal of Catalysis* **1999,** *187* (2), 392-399.

Axley, M.J; Grahame, D.A; Stadtman, T.C. *Escherichia coli* formate-hydrogen lyase purification and properties of the selenium-dependent formate dehydrogenase component. J Biol Chem. **1990**, *265*, 18213-8.

Baldi, F.; Marchetto, D.; Paganelli, S.; Piccolo, O., Bio-generated metal binding polysaccharides as catalysts for synthetic applications and organic pollutant transformations. *New Biotechnology* **2011,** *29* (1), 74-78.

Baxter-Plant, V. S.; Mikheenko, I. P.; Macaskie, L. E., Sulphate reducing bacteria, palladium and the reductive dehalogenation of chlorinated compounds. *Biodegradation* **2003,** *14* (2), 83-90.

Bennett, J. A.; Mikheenko, I. P.; Deplanche, K.; Shannon, I. J.; Wood, J.; Macaskie, L. E., Nanoparticles of palladium supported on bacterial biomass: New re-usable heterogeneous catalyst with comparable activity to homogeneous colloidal Pd in the Heck reaction. *Applied Catalysis B: Environmental* **2013,** *140–141* (0), 700-707.

Bunge, M.; Sobjerg, L. S.; Rotaru, A. E.; Gauthier, D.; Lindhardt, A. T.; Hause, G.; Finster, K.; Kingshott, P.; Skrydstrup, T.; Meyer, R. L., Formation of Palladium(0) Nanoparticles at Microbial Surfaces. *Biotechnology and Bioengineering* **2010,** *107* (2), 206-215.

Chaturvedi, S.; Dave, P. N.; Shah, N. K., Applications of nano-catalyst in new era. *Journal of Saudi Chemical Society* **2012,** *16* (3), 307-325.

Choudhary, T. V.; Goodman, D. W., Oxidation Catalysis by Supported Gold Nano-Clusters. *Top Catal* **2002,** *21* (1-3), 25-34.

Cornils, B; Herrmann, W.A; Horvath, I.T; Leitner, W; Mecking, S; Olivier-Bourbigou, H; Vogt, D (Eds). Multiphase heterogeneous catalysis. **2005**, Vol 1. Wiley-VCH

Costa, C; Teixeira, M; LeGall, J; Moura, J.J.G; Moura I., Formate dehydrogenase from *Desulfovibrio desulfuricans* ATCC 27774: Isolation and spectroscopic characterization of the active sites (heme, iron-sulfur centers and molybdenum). *J. Biol Inorg Chem*. **1997**, *2*, 198-208.

Creamer, N. J.; Mikheenko, I. P.; Yong, P.; Deplanche, K.; Sanyahumbi, D.; Wood, J.; Pollmann, K.; Merroun, M.; Selenska-Pobell, S.; Macaskie, L. E., Novel supported Pd hydrogenation bionanocatalyst for hybrid homogeneous/heterogeneous catalysis. *Catalysis Today* **2007,** *128* (1–2), 80-87.

De Corte, S.; Sabbe, T.; Hennebel, T.; Vanhaecke, L.; De Gusseme, B.; Verstraete, W.; Boon, N., Doping of biogenic Pd catalysts with Au enables dechlorination of diclofenac at environmental conditions. *Water Research* **2012,** *46* (8), 2718-2726.

den Besten, C.; Vet, J. J.; Besselink, H. T.; Kiel, G. S.; van Berkel, B. J.; Beems, R.; van Bladeren, P. J., The liver, kidney, and thyroid toxicity of chlorinated benzenes. *Toxicol Appl Pharmacol* **1991,** *111* (1), 69-81.

Deplanche, K. New nanocatalysts made by bacteria from metal solutions and recycling of metal wastes. PhD Thesis. PhD Thesis, University of Birmingham, UK. **2008.**

Deplanche, K.; Snape, T. J.; Hazrati, S.; Harrad, S.; Macaskie, L. E., Versatility of a new bioinorganic catalyst: Palladized cells of *Desulfovibrio desulfuricans* and application to dehalogenation of flame retardant materials. *Environmental Technology* **2009,** *30* (7), 681-692.

Deplanche, K.; Caldelari, I.; Mikheenko, I. P.; Sargent, F.; Macaskie, L. E., Involvement of hydrogenases in the formation of highly catalytic Pd(0) nanoparticles by bioreduction of Pd(II) using *Escherichia coli* mutant strains. *Microbiology-Sgm* **2010,** *156*, 2630-2640.

Deplanche, K.; Merroun, M. L.; Casadesus, M.; Tran, D. T.; Mikheenko, I. P.; Bennett, J. A.; Zhu, J.; Jones, I. P.; Attard, G. A.; Wood, J.; Selenska-Pobell, S.; Macaskie, L. E., Microbial synthesis of core/shell gold/palladium nanoparticles for applications in green chemistry. *Journal of the Royal Society Interface* **2012,** *9* (72), 1705-1712.

Deplanche, K.; Bennett, J. A.; Mikheenko, I. P.; Omajali, J.; Wells, A. S.; Meadows, R. E.; Wood, J.; Macaskie, L. E., Catalytic activity of biomass-supported Pd nanoparticles: Influence of the biological component in catalytic efficacy and potential application in 'green' synthesis of fine chemicals and pharmaceuticals. *Applied Catalysis B: Environmental* **2014,** *147* (0), 651-665.

De Windt, W.; Aelterman, P.; Verstraete, W., Bioreductive deposition of palladium (0) nanoparticles on *Shewanella oneidensis* with catalytic activity towards reductive dechlorination of polychlorinated biphenyls. *Environmental Microbiology* **2005,** *7* (3), 314-325.

de Vargas, I.; Sanyahumbi, D.; Ashworth, M. A.; Hardy, C. M.; Macaskie, L. E. In *Use of X-ray photoelectron spectroscopy to elucidate the mechanism of palladium and platinum biosorption by Desulfovibrio desulfuricans biomass*, 25th - 29th September; 16th int. Biohydrometallurgy Symp., Cape Town, Harrison, S. T. L., Rawlings, D.E., Petersen, J., Ed. Cape Town, 2005; pp 605-616.

Ding, H.T; Liu, D.F; Li, Z.L; Du, Y.Q; Xu, X.H; Zhao, Y.H., Characterization of a thermally stable and organic solvent-adaptative NAD^+-dependent formate dehydrogenase from *Bacillus* sp. F1. *J Appl Microbiol*. **2011**, *111*, 1075-1085.

EPA. Water: Basic information about chlorobenzene in drinking water http://water.epa.gov/drink/contaminants/basicinformation/chlorobenzene.cfm. (Accessed, 27/04/2015)

Field, J.; Sierra-Alvarez, R., Microbial degradation of chlorinated benzenes. *Biodegradation* **2008,** *19* (4), 463-480

Fung, J. M.; Weisenstein, B. P.; Mack, E. E.; Vidumsky, J. E.; Ei, T. A.; Zinder, S. H., Reductive Dehalogenation of Dichlorobenzenes and Monochlorobenzene to Benzene in Microcosms. *Environmental Science & Technology* **2009,** *43* (7), 2302-2307.

Haggblom, M. M.; Young, L. Y., Anaerobic degradation of halogenated phenols by sulfate-reducing consortia. *Applied and Environmental Microbiology* **1995,** *61* (4), 1546-1550.

Harrad, S.; Robson, M.; Hazrati, S.; Baxter-Plant, V. S.; Deplanche, K.; Redwood, M. D.; Macaskie, L. E., Dehalogenation of polyclorinated biphenyls and polybrominated dipheny ethers using a hybrid bioinorganic catalyst. *J.Environ Monito* **2007,** *9* (4), 314-318.

Hennebel, T.; Van Nevel, S.; Verschuere, S.; De Corte, S.; De Gusseme, B.; Cuvelier, C.; Fitts, J. P.; Van der Lelie, D.; Boon, N.; Verstraete, W., Palladium nanoparticles produced by fermentatively cultivated bacteria as catalyst for diatrizoate removal with biogenic hydrogen. *Applied Microbiology and Biotechnology* **2011a,** *91* (5), 1435-1445.

Hennebel, T.; Benner, J.; Clauwaert, P.; Vanhaecke, L.; Aelterman, P.; Callebaut, R.; Boon, N.; Verstraete, W., Dehalogenation of environmental pollutants in microbial electrolysis cells with biogenic palladium nanoparticles. *Biotechnology Letters* **2011b,** *33* (1), 89-95.

Henry, T.R; DeVito, M.J. Non-dioxin like PCBs: Effects and consideration in ecological risk assessment. http://www.epa.gov/oswer/riskassessment/pdf/1340-erasc-003.pdf. (Accessed, 01/05/2015)

Heidrich, S.; Weiss, H.; Kaschl, A., Attenuation reactions in a multiple contaminated aquifer in Bitterfeld (Germany). *Environ Pollut* **2004,** *129* (2), 277-88.

Jaboyedoff, M.; Kubler, B.; Thelin, P. H., An empirical Scherrer equation for weakly swelling mixed-layer minerals, especially illite-smectite. *Clay Minerals* **1999,** *34* (4), 601-617.

Janssen, D. B.; Oppentocht, J. E.; Poelarends, G. J., Microbial dehalogenation. *Current Opinion in Biotechnology* **2001,** *12* (3), 254-258.

Konuma, K.; Kameda, N., Effect of substituents on the hydrodechlorination reactivity of para-substituted chlorobenzenes. *Journal of Molecular Catalysis A: Chemical* **2002,** *178* (1–2), 239-251.

Kominami, H; Nishi, J; Foku, K; Hashimoto, K. Photocatalytic reductive dechlorination of chlorobenzene in alkali-free aqueous alcoholic suspensions of palladium-loaded titanium (IV) oxide particles in the absence or presence of oxygen. *RSC Adv.*, **2013**, ***3***, 6058-6064

Korte, N; Lang, L; Muftikan, R; Grittini, C; Fernando, Q Palladised iron utilised for ground water purification. *Platin. Metals Rev*. **1997**, 41: 2–7

Lee, S. H.; Carberry, J. B., Biodegradation of PCP enhanced by chemical oxidation pretreatment. *Water Environment Research* **1992,** *64* (5), 682-690.

Liang, X. M.; Devine, C. E.; Nelson, J.; Lollar, B. S.; Zinder, S.; Edwards, E. A., Anaerobic Conversion of Chlorobenzene and Benzene to CH4 and CO2 in Bioaugmented Microcosms. *Environmental Science & Technology* **2013,** *47* (5), 2378-2385.

Livingstone SE (1973) Palladium: The Element. In: Bailer JC, Nyholm R, Trotman-Dickenson AF (eds). Comprehensive Inorganic Chemistry. Vol. 3. Pergamon Press: Oxford, UK. pp 1274-1276.

Lesage, S.; Brown, S.; Millar, K., A different mechanism for the reductive dechlorination of chlorinated ethenes: Kinetic and spectroscopic evidence. *Environmental Science & Technology* **1998,** *32* (15), 2264-2272

Mabbett, A. N.; Sanyahumbi, D.; Yong, P.; Macaskie, L. E., Biorecovered precious metals from industrial wastes. Single step conversion of a mixed metal liquid waste to a bioinorganic catalyst with environmental applications. *Environmental Science and Technology* **2006,** *40*, 1015-1021.

Mikheenko, I. P.; Rousset, M.; Dementin, S.; Macaskie, L. E., Bioaccumulation of palladium by *Desulfovibrio fructosovorans* wild-type and hydrogenase-deficient strains. *Applied and Environmental Microbiology* **2008,** *74* (19), 6144-6146.

Miller, G. S.; Milliken, C. E.; Sowers, K. R.; May, H. D., Reductive dechlorination of tetrachloroethene to trans-dichloroethene and cis-dichloroethene by PCB-dechlorinating bacterium DF-1. *Environmental Science & Technology* **2005,** *39* (8), 2631-2635.

Murray, A. J.; Mikheenko, I. P.; Goralska, E.; Rowson, N. A.; Macaskie, L. E., Biorecovery of platinum group metals from secondary sources. In *Biohydrometallury: From the Single Cell to the Environment*, Schippers, A.; Sand, W.; Glombitza, F.; Willscher, S., Eds. 2007; Vol. 20-21, pp 651-654.

Nelson, J. L.; Jiang, J.; Zinder, S. H., Dehalogenation of chlorobenzenes, dichlorotoluenes, and tetrachloroethene by three Dehalobacter spp. *Environ Sci Technol* **2014,** *48* (7), 3776-82

Odom, J. M.; Peck Jr, H. D., Hydrogen cycling as a general mechanism for energy coupling in the sulphate-redcuing bacteria, *Desulfovibrio* sp. *FEMS Microbiol. Lett* **1981,** *12*, 47-50.

Omajali, J.B; Mikheenkho, I.P; Merroun, L.M; Wood, J; Macaskie L.E., Characterization of intracellular palladium nanoparticles synthesized by *Desulfovibrio desulfuricans* and *Bacillus benzeovorans*. *J Nanopart Res* **2015,** *17* (6), 1-17.

Redwood, M. D.; Deplanche, K.; Baxter-Plant, V. S.; Macaskie, L. E., Biomass-supported palladium catalysts on Desulfovibrio desulfuricans and Rhodobacter sphaeroides. *Biotechnology and Bioengineering* **2008,** *99* (5), 1045-1054.

Rhodin TN, Ertl G (1979) The Nature of the Surface Chemical Bond. Oxford, UK: North-Holland. pp 104-108.

Schluter, M.; Hentzel, T.; Suarez, C.; Koch, M.; Lorenz, W. G.; Bohm, L.; During, R. A.; Koinig, K. A.; Bunge, M., Synthesis of novel palladium(0) nanocatalysts by microorganisms from heavy-metal-influenced high-alpine sites for dehalogenation of polychlorinated dioxins. *Chemosphere* **2014,** *117*, 462-70.

Shi, S.-Y.; Teng, H.-H.; Chang, L.-M.; Wang, Y.; Xiao, L.-N.; Cui, X.-B.; Xu, J.-Q., New compounds constructed from bi-antimony capped Keggin polyoxoanions and different coordination fragments. *Inorganica Chimica Acta* **2013,** *399* (0), 172-176.

Tiedje, J. M.; Quensen, J. F., 3rd; Chee-Sanford, J.; Schimel, J. P.; Boyd, S. A., Microbial reductive dechlorination of PCBs. *Biodegradation* **1993,** *4* (4), 231-40.

Wiegel, J.; Wu, Q., Microbial reductive dehalogenation of polychlorinated biphenyls. *FEMS Microbiology Ecology* **2000,** *32* (1), 1-15.

Wong, M. H.; Wu, S. C.; Deng, W. J.; Yu, X. Z.; Luo, Q.; Leung, A. O. W.; Wong, C. S. C.; Luksemburg, W. J.; Wong, A. S., Export of toxic chemicals – A review of the case of uncontrolled electronic-waste recycling. *Environmental Pollution* **2007,** *149* (2), 131-140.

Wu, Q. Z.; Watts, J. E. M.; Sowers, K. R.; May, H. D., Identification of a bacterium that specifically catalyzes the reductive dechlorination of polychlorinated biphenyls with doubly flanked chlorines. *Applied and Environmental Microbiology* **2002,** *68* (2), 807-812.

Yong, P.; Farr, J. P. G.; Harris, I. R.; Macaskie, L. E., Palladium recovery by immobilized cells of *Desulfovibrio desulfuricans* using hydrogen as the electron donor in a novel electrobioreactor. *Biotechnology Letters* **2002,** *24* (3), 205-212.

Yong, P.; Mikheenko, I. P.; Deplanche, K.; Redwood, M. D.; Macaskie, L. E., Biorefining of precious metals from wastes: an answer to manufacturing of cheap nanocatalysts for fuel cells and power generation via an integrated biorefinery? *Biotechnology Letters* **2010,** *32* (12), 1821-1828.

Zanaroli, G.; Negroni, A.; Häggblom, M. M.; Fava, F., Microbial dehalogenation of organohalides in marine and estuarine environments. *Current Opinion in Biotechnology* **2015,** *33* (0), 287-295.

Zhang, H.; Jin, M. S.; Xiong, Y. J.; Lim, B.; Xia, Y. N., Shape-Controlled Synthesis of Pd Nanocrystals and Their Catalytic Applications. *Accounts of Chemical Research* **2013,** *46* (8), 1783-1794.

3.2.2 *In-Situ* Catalytic Upgrading of Heavy Oil Using Dispersed Bionanoparticles Supported on Gram-Positive and Gram-Negative Bacteria

Jacob B. Omajali [1], Abarasi Hart [2], Joseph Wood [2], Marc Walker [3] and Lynne E. Macaskie [1, *]

[1] Unit of Functional Bionanomaterials, Institute of Microbiology and Infection, School of Biosciences, University of Birmingham, Edgbaston, Birmingham, B15 2TT, United Kingdom

[2]School of Chemical Engineering, University of Birmingham, Edgbaston, Birmingham, B15 2TT, United Kingdom

[3]Department of Physics, University of Warwick, Coventry, CV4 7AL, United Kingdom

*Corresponding author. Tel.: fax:

Email address:

Journal: Applied Catalysis B: Environmental, in submission.

This paper was written by J.B.Omajali. Catalytic test and analysis was done by Dr Hart Abarasi, University of Birmingham while technical assistance on XPS was provided by Dr Marc Walker, University of Warwick. The author also carried out the synthesis and characterization of the bionanoparticles.

ABSTRACT

With the continuous depletion of global oil reserves, unconventional alternative oil resources like heavy oil and bitumen have become increasingly attractive. However, heavy oils and bitumen have undesirable properties such as high viscosity, low API (American Petroleum Institute) gravity, high molecular weight compounds and high contents of heavy metals and hetero-atoms. The use of commercial cracking catalysts in heavy oil upgrading is expensive and the catalyst may become prematurely deactivated due to coking. Bimetallic bio-nanoparticles (bio-NPs), a potential alternative, were made by sequential reduction of precious metal (Pd and Pt) ions with hydrogen as the electron donor at 5% and 20% metal loading using bacteria (*Desulfovibrio desulfuricans* and *Bacillus benzeovorans*). The bio-NPs were characterized using transmission electron microscopy (TEM), X-ray powder diffraction (XRD) and X-ray photoelectron spectroscopy (XPS). Heavy oil was upgraded with the bio-NPs in a stirred batch reactor which simulates the dispersed CAPRI (catalytic upgrading process *in-situ*) add-on of the THAI (Toe-to-heel air injection) process. The bimetallic bio-NPs produced an increment of ~2^{o} in API gravity (~9.1^{o}) better than monometallic bio-NPs (~7.6^{o}) on average while the API gravity using thermal upgrading was lower (6.3^{o}). The API gravity of a commercial Ni-Mo/Al_2O_3 catalyst was 11.1^{o}. However, more coking was produced using this than with the bio-NPs. The extent of viscosity reduction was: 98.7% (thermal), 99.2% (bio-NPs) and 99.6% (Ni-Mo/Al_2O_3) of the baseline 1031 mPa.s for the feed heavy oil reference. The potential advantage of using bio-NPs is that the precious metals can be sourced cheaply from waste streams, which could serve as a potential platform for the green synthesis of catalytically active materials using bacteria for *in-situ* catalytic upgrading of heavy oils.

Keywords: Bio-nanoparticles; Coking; Heavy oil; Upgrading; Viscosity.

Highlights

- Heavy oil are characterized by high viscosity, high heavy ends and heavy metals with low API gravity, hence the need for upgrading into lighter components.
- Use of commercial catalyst is quite expensive and results in coking which may lead to eventual deactivation of the catalyst.

- Bacterial cells provide a green approach with reduced coking, increased oil yield and comparable catalytic activity with commercial catalyst. The precious metals (Pd and Pt) can also be sourced cheaply from waste streams.

Introduction

The world's energy consumption continues to grow and has been projected by the US Energy and Information Administration (EIA) to reach 56%, a value of approximately 8.6 x 10^6 joules per annum by 2040 [1]. Oil is considered the world's leading fuel source, supporting 32% of global energy consumption, which increased by 2.3% in 2013 [2]. It has been reported that most of the future energy demand will be dominated (95%) by the non-OECD (non-Organization for Economic Cooperation and Development) countries where demand is driven by strong economic growth [2]. As consumption of world energy continues to rise, fossil fuels are expected to remain the predominant sources of supply, satisfying about 80% of global needs [3] despite continuing concerns about environmental consequences.

A consequence of the increase in demand and consumption of light crude oil is a global decline in reserves and supply. Therefore, there is a need to supplement short-and-long term needs through less conventional oil resources, like heavy oil and bitumen, whose current production stands at 2-3% (2 Million barrels/day, Mb/d) of global supply, with output predicted to reach 7 Mb/d in 2030 [4]. Large deposits of heavy oil and bitumen occur in locations such as Canada (the Alberta Basin) and Venezuela (the Orinoco Belt), which together comprise about 80% of world's remaining oil reserves [5] However, the exploitation of these forms a major challenge due to their inherent properties *i.e.* high viscosity, low hydrogen content, presence of high molecular weight compounds (resins and asphaltenes) and richness in hetero-elements (nitrogen, sulfur and oxygen), as well as high metal contents, especially nickel and vanadium. These properties of heavy oil are thought to be the consequence of subsurface water flows and also microbial activities within a shallow depth of low temperature environments as the oil accumulates over time [6]. Microbial processes introduce changes, especially in the light end of the oil, specifically the hydrocarbon molecules (oxidation of C_{6+} components), leading to fluids characterized by high contents of heavy molecules rich in sulfur, nitrogen, oxygen and metals but with decreased API gravity

and increased viscosity and acidity [6, 7]. Other challenges include environmental concerns such as water management, specifically production water for steam generation, and the control of greenhouse gases and other pollutants during the extra refining required for heavy oils [7]. While strict regulations are being implemented for the latter, current developments in carbon storage (CSC: Capture and Sequestration of CO_2) and the possibility of using nuclear reactors to generate steam, together with cold production technologies in Venezuela [8] would lead to reduction in CO_2 emission. However, the viscous rheology of heavy oil affects production, upgrading and transport throughout surface pipelines which indirectly impacts upon the economics [9].

Consequently heavy oil, unlike conventional oil, must be upgraded into synthetic light crude components in order to increase their market values (increase in API gravity, reduced viscosity and lower contents of heavy ends [asphaltenes, resins and metals]) which should expedite transport *via* pipelines and also provide light crude oil better able to meet the specific needs of refineries [10]. The relevance of some upgrading technologies such as cold production, steam injection, steam assisted gravity drainage, *in-situ* combustion and partial upgrading processes (De-asphalting, visbraking or coking) have been extensively highlighted [11, 12]. Visbraking for instance, thermally cracks heavy oil non-catalytically under mild temperature conditions, increasing distillate yield which in turn reduces the viscosity of heavy oil, by modifying the structure of oil compounds [13, 14]. Subsequently, this leads to increase in the light saturate fractions of maltenes. However, the challenge is to prevent asphaltene precipitation and maximize viscosity reduction while limiting the formation of gas and coke.

In-situ upgrading technologies such as catalytic thermal conversions in the presence of hydrogen, hydrogen donor solvents and the use of microbial communities generating methane (biodegradation of C_2-C_5 hydrocarbons) are currently in use but not yet at industrial scale [15] coupled with other emerging technologies [12] which all have environmental advantages because of their ability to trap most of the pollutants generated from heavy oil in the reservoir well. They also reduce the need for surface upgrading, which results in the cleaner production of lower viscosity oil, which is more easily transported without the use of diluents. The THAI-CAPRI (Toe-to-Heel Air

Injection coupled with Catalytic Upgrading Process *In-situ*) technology combines thermally enhanced oil recovery with down-hole *in-situ* catalytic upgrading of heavy oil into light fractions [16, 17]. This technology, shown for the *in-situ* catalytic upgrading of heavy oil in the presence of steam, hydrogen and methane has demonstrated significant improvements over non-catalytic thermal processes [17].

However commercial cracking catalysts such as noble metals on chemical supports are prohibitively expensive for a large scale once-through technology; an alternative source of cheaper catalyst is therefore essential. One of the options is to utilize regenerated catalysts from treated oils as reported previously [17] which could reduce catalyst cost but the disadvantage is in their low activity. The emergent use of bacteria as new systems for catalytic synthesis [18] provides alternative sources of cheaper support for the patterning of metallic nanoparticles (NPs) called bio-nanoparticles (bio-NPs) which are held supported on the cells as micron-sized carriers. Advantages of using bacteria include scalability of NP synthesis, as non-toxic reducing agents/support when compared to strong toxic chemical reductants used in commercial systems and as remediation platforms for precious metal-containing wastes [19]. In addition, the various functional groups (amine, carboxyl, hydroxyl and phosphoryl) found on bacterial cell surfaces, tend to control and stabilize particle growth [20] *via* 'bio-patterning' as compared to the use of surfactants and capping agents which introduce artefacts into commercial catalysts. In some cases the metallic bio-NPs made from wastes can have higher activity than monometallic bio-NPs [21]. When biomanufactured from a source such as road dust the concept of a 'once-through' loss into the environment becomes conceptually and economically acceptable and this forms the goal of this investigation.

The use of *Desulfovibrio desulfuricans* (Gram-negative) and *Bacillus sp* (Gram-positive) bacteria has been widely examined in the context of bio-NPs catalyst production [22-24]. However, the production of hydrogen sulfide (normally a strong catalyst poison) by the former, coupled with the problem of production at scale, would make *Bacillus* preferable but on the other sulfidation of metals by sulfur leads to activation of catalyst [25]. *Bacillus* spp. are produced in large quantities *via e.g.* the commercial manufacturing of enzymes and hence waste biomass could provide a

sustainable source for the synthesis of new catalytic materials. Various precious metals (*e.g*. Pd, Pt and Au) have been reductively precipitated into bio-NPs by various strains of Gram-negative and Gram-positive bacteria and utilized in a range of catalytic reactions of industrial importance, with activities comparable to commercial catalysts [26, 27]. However, there are no reports on the use of bio-NPs for *in-situ* catalytic upgrading of heavy oil prior to this study. It was reported that bimetallic bio-NPs are more catalytically active in various reactions than their monometallic counterparts [28], attributed to the synergistic effects of the two metals, which has also been shown in chemical synthesis [29]. For example, a bio-Pd/Au core-shell bimetallic catalyst synthesized using *E-coli* was shown to be comparable to a commercial catalyst in the oxidation of benzyl alcohol [30] while De Corte et al. [28] synthesized Pd/Au bimetallic using *S. oneidensis* MR-1 to make a better dechlorination catalyst of dichlofenac than monometallic bio-Pd.

This study evaluates the potential for use of bio-NPs for the upgrading of heavy oil and compares the efficacy of the bio-NPs synthesized on *Desulfovibrio desulfuricans* (bio-Pd_{Dd}) with counterparts synthesized on *Bacillus benzeovorans* (bio-Pd_{Bb}). Other catalytic tests have shown some strain-dependent differences using monometallic NPs following differences shown between Gram-negative and Gram-positive supports [24]. Hence, the second aim, prerequisite to the biomanufacturing of active bimetallic Pd/Pt NPs from wastes [31] is to compare bimetallic bio-NPs of two different bacteria with those made using Pd alone.

Experimental

Materials. The heavy oil feedstock used in this study was recovered from oil sands at Kerrobert, Saskatchewan by THAI and was provided by Touchstone Exploration Inc, Canada. Since the feedstock was produced by the THAI process, it was partially upgraded by pyrolysis and its properties are shown in Table 1. A commercial catalyst (Ni-Mo/Al_2O_3) was supplied by Akzo Nobel (Amsterdam, Netherlands).

Table 1 Properties and composition of heavy oil used in this study

Parameter	Value
API gravity (^{o})	13.8
Viscosity at 20 ^{o}C (mPa.s)	1031
Nickel (ppm)	41
Vanadium (ppm)	108
Ni + V (ppm)	149
Asphaltene (wt. %)	10.3
Elemental analysis	
C	88.82 wt.%
H	10.17 wt.%
N	0.57 wt.%
H/C	0.114
S	3.52(wt. %)

Data provided by Touchstone Exploration Inc.

Bacterial strains and growth conditions

Bacillus benzeovorans NCIMB 12555 (Bb) (aerobic) and *Desulfovibrio desulfuricans* NCIMB 8307 (Dd) (anaerobic) were grown as follows: *B. benzeovorans* was grown aerobically [32] in a rotary shaker (180 rpm at 30^{o}C) in nutrient medium (pH 7.3 ± 0.2) comprising (per litre) 1.0g beef extract (Sigma-Aldrich), 2.0g yeast extract (Sigma-Aldrich), 5.0g peptone (Sigma-Aldrich) and 15.0g NaCl. *D. desulfuricans* was grown anaerobically under oxygen-free nitrogen (OFN) in Postgate's medium C [24] (pH 7.5 ± 0.2) at 30^{0}C (inoculated from a 24 hour pre-culture, 10%v/v) in sealed anaerobic bottles without shaking. Bacterial cells were harvested by centrifugation (9,000 x g, 15 minutes, 4^{o}C) at mid exponential growth phase (OD_{600} 0.7-1.0 and OD_{600} 0.5-0.7 respectively) washed three times in air with 20 mM MOPS (morpholinepropanesulfonic acid)-NaOH buffer, pH 7.0 and then concentrated in a small amount of the same buffer [33] and stored at 4^{o}C under OFN (oxygen-free nitrogen) until use, within 24 hours. Bacterial density (mg/ml) was calculated from the OD_{600} *via* a previously determined calibration.

Preparation of bionanoparticles (bio-NPs)

The resting cell suspensions (as above) were transferred into a degassed solution of 2mM Na_2PdCl_4 (Sodium tetrapalladate (II)) salt adjusted to pH 2 with 0.01M HNO_3 and left for biosorption (30 min, 30^oC) to make a monometallic (5wt%Pd and 20wt%Pd) bio-NPs. This was achieved by bubbling hydrogen through a Pd (II)-supplemented cell suspension for 15 min and then saturating the mixture (in a closed bottle) for an additional 15 min for reduction to reach completion. The bimetallic Pd/Pt catalysts were prepared by sequential reduction of 2mM Pd (II) solution. This was washed twice with distilled water and then resuspended in water based on the method of Deplanche et al. [30] for Pd/Au synthesis with slight modifications, followed by the addition of 1mM K_2PtCl_6 (potassium hexachloroplatinate (IV)) salt solution to a final metal loading of 5wt% (2.5wt%Pd/2.5wt% Pt) and 20wt% (10wt%Pd/10wt%Pt) on bacterial cells. The content was purged with hydrogen for 15 min and left for 1 h (180 rpm, 30^oC) for reduction. The removal of residual Pd (II) and Pt (IV) from solution was confirmed according to a method previously described [33]. The final bio-catalysts (Bio-Pd and BioPd/Pt) were then washed three times (9,000 x g, 4^oC, 15 minutes) with distilled water and once in acetone, dried and then ground by hand for characterization and catalysis.

Characterization of Bio-NPs

Transmission Electron Microscopy

Bio-NPs-loaded cells (bio-Pd/Pt) of *B. benzeovorans* and *D. desulfuricans* were washed twice with distilled water, fixed with 2.5% (w/v aq) glutaraldehyde in 0.1M cacodylate buffer (pH 7.0) at 4^oC and stained with 1% osmium tetraoxide. The cells were dehydrated using an ethanol series, washed twice in propylene oxide [33], embedded in epoxy resin, cut into sections (100-150nm thick) and viewed with a JEOL 1200EX transmission electron microscope, accelerating voltage of 80kV.

X-Ray Powder Diffraction

X-ray powder diffraction (XRD) patterns of samples (bio-NPs) were acquired from a Bruker AXS D8 Autosampler (Transmission) Diffractometer using a monochromatic

high-intensity $CuK_{\alpha 1}$ radiation (λ = 1.5406 Å) equipped with a solid-state LynxEye position sensitive detector (PSD) with a 3^{o} electronic window. The XRD patterns were then compared to a reference standard from the International Committee for Diffraction Data (ICDD) database and the crystallite size of the bio-NPs was determined using Scherrer's equation [34].

X-ray Photoelectron Spectroscopy

Surface chemical composition and oxidation state analysis of bio-Pd/Pt were analysed using X-ray photoelectron spectroscopy (XPS). Data were collected using a Sphera electron analyser (Omicron Nanotechnology), with the core levels recorded using a pass energy of 10 eV (resolution approx. 0.47eV). Due to the insulating nature of the samples, a CN10 charge neutralizer (Omicron Nanotechnology) was used in order to prevent surface charging. A low energy (typically 1.5 eV) beam of electrons was directed on to the sample during XPS data acquisition. Measurements were made at room temperature and at a take-off angle of 90°, allowing a maximum probing depth of approximately 5-10 nm to evaluate bio-NPs bound to the outermost cell surfaces. The data generated were converted into VAMAS format and analysed using the CasaXPS package [35] employing Shirley backgrounds, mixed Gaussian-Lorentzian (Voigt) lineshapes and asymmetry parameters where appropriate. All binding energies were calibrated to the C 1s peak originating from C-H or C-C groups at 284.6 eV.

Catalytic upgrading of heavy oil. The catalytic activity of the bio-NPs and commercial catalyst was tested in a stirred batch reactor (100 mL capacity, Baskerville, United Kingdom) using 15 g of heavy oil as feedstock. The optimum reaction temperature was used based on previous investigations using a fixed-bed of pelleted commercial catalysts [36, 37] with an optimum reaction condition of; 30 min at 450^{o}C, stirring speed of 500 rpm and nanoparticles-to-oil ratio of 1 mg/g as reported by Hart et al. [38] with an initial heat-up-time (~2h 15 min). The gas atmosphere was nitrogen with initial pressure of 20 bar which increases with the ramp temperature rise and the added gas from the cracking reactions to 74-80 bar (during cooling the pressure decreases to 24-26 bars). Detailed experimental procedure can be found in Hart et al. [38]. In order to evaluate the effect of the bioNP catalyst, experiments were conducted in parallel

without bioNPs (thermal cracking only) and also with bacterial biomass (without metals) as controls.

Product analysis. The products of the upgrading reaction consist of light oil (*i.e.*, liquid), non-condensable gas and coke. The produced coke was determined as a percentage of the deposit after reaction using a thermogravimetric analyser (TGA) (NETZSCH-Geratebau GmbH, TG 209 F1 Iris®). The TGA was carried out with a ramp temperature increase from 25 to 900 ^{o}C under air flow of 50 mL/min. The composition of the produced gas was determined using an Agilent 7890A gas chromatograph. The liquid product (i.e. upgraded oil samples) was collected; measurements of viscosity were made as previously described [17, 39] (Advanced Rheometer AR1000, TA Instruments), API gravity (portable density meter DMA 35, Anton Paar, UK) and the true boiling point (TBP) (by simulated distillation using an Agilent 6850N Network gas chromatograph in accordance with the ASTM-2887D method; the Agilent 6850N was calibrated using a mix containing C_5 to C_{40}). The asphaltene content before and after the reactions was determined through precipitation using n-C_7H_{16}. A detailed description of these analytical procedures was reported elsewhere [17, 39]. Fig 1 summarises the experimental and analytical methods used in this study.

Product distribution

The mass balances of the three products i.e., liquid, gas, and coke were calculated as percentage of the mass of feed oil into the reactor using equations 1 and 2:

$$\text{Yield (wt. \%)} = W_i/W_F \times 100 \quad (1)$$

$$\text{Yield of gas (wt \%)} = (W_F - W_A) / W_F \times 100 \quad (2)$$

Where W_i is the weight of component i and W_F is the weight of the feed oil (heavy oil fed into the reactor) and W_A is weight of autoclaved content after reaction.

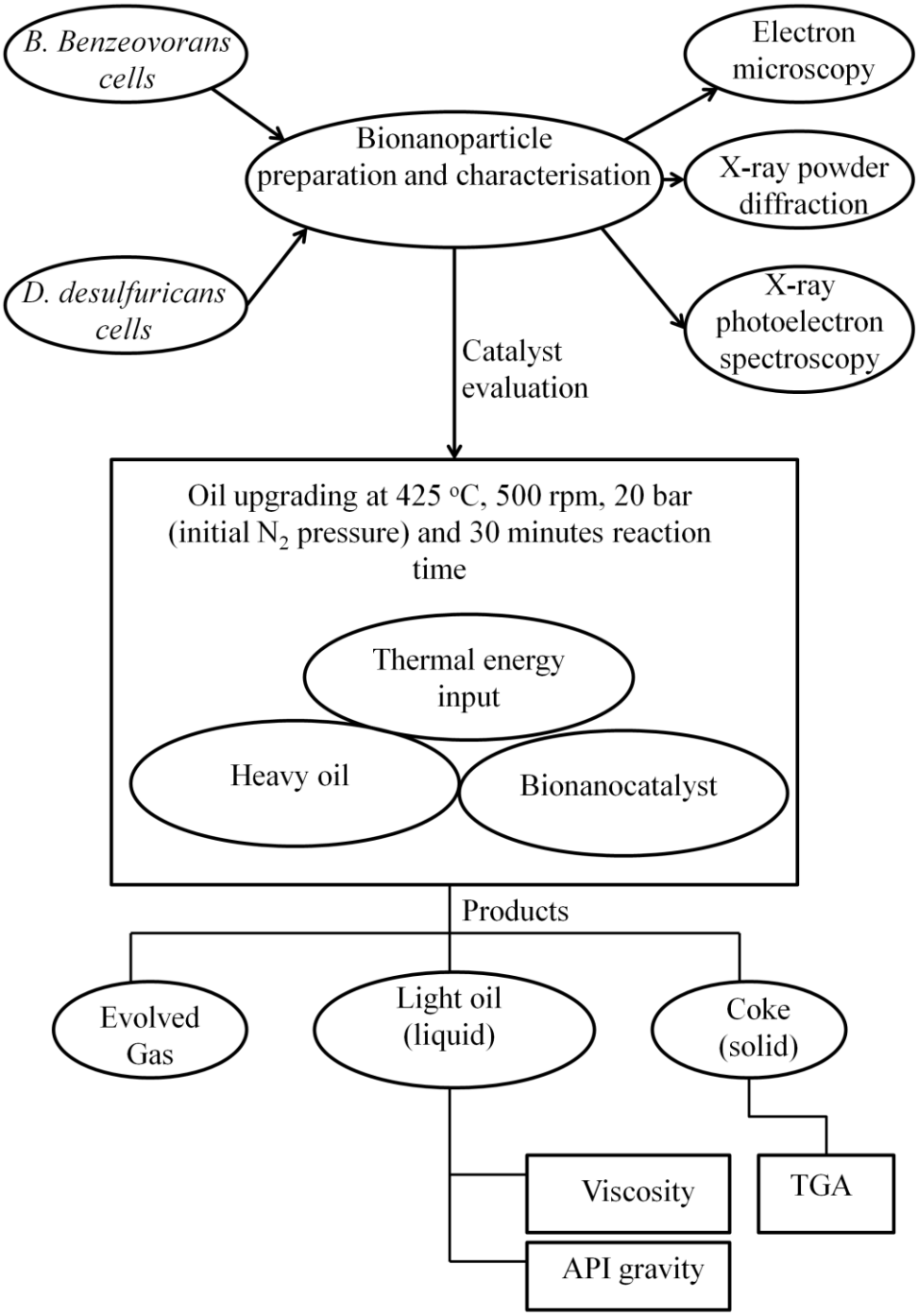

Figure 1 An overview of experimental methods.

TGA: Thermogravimetric analysis
API gravity: American petroleum institute gravity (a standard reference for measuring the quality of oil and transportability)

Results and Discussion

Examination by Transmission electron microscopy (TEM)

Analysis by TEM of selected samples [5wt% (2.5%Pd/2.5%Pt) and 20wt% (10%Pd/10%Pt) bimetallic bio-Pd/Pt] produced by *B. benzeovorans* (Bb) and *D. desulfuricans* (Dd) is shown in Fig 2. With 5wt% bio-Pd/Pt produced by the two bacteria, TEM showed more nanoparticles (NPs) distributed within the intracellular matrix in *B. benzeovorans* (Fig 2a) than in *D. desulfuricans* where no discrete intracellular NPs were visible (Fig 2b); however most of the NPs formed an electron opaque 'shell' around both types of cell. This is more apparent with the higher metal loadings (20wt% bioPd/Pt) (Fig 2c and 2d) but with agglomerates of bio-NPs in *D. desulfuricans* (Fig 2d) which were found mostly on the surface or periplasmic space of the bacteria.

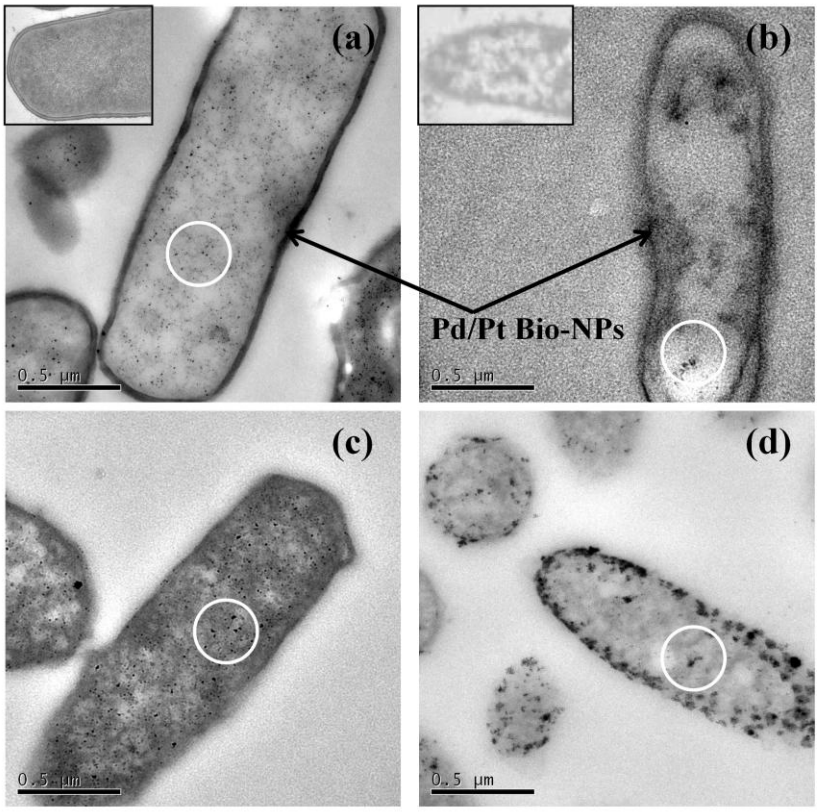

Figure 2 TEM images of 5wt% bimetallic bio-NPs made by a) *B. benzeovorans* and b) *D. desulfuricans* with corresponding 20wt% bimetallic bio-NPs c) and d) respectively. Scale bar is 0.5µm. Insets are cells with no metals. Intracellular NPs are circled.

Examination by X-ray powder diffraction (XRD)

XRD analysis (Fig 3, Table 2) was used to determine the average Pd and Pd/Pt crystallite size of synthesized mono-and bi-metallic bio-NPs (as dry powders) produced by *B. benzeovorans* and *D. desulfuricans* using Scherrer's equation [34]. The XRD powder patterns of 5wt% monometallic Pd in both organsims showed only amorphous materials (Fig 3a) while at 20wt% Pd the characteristic emission peaks of Pd at 2θ approx. = 40.1^o, 46.7^o, 68.2^o, 82.1^o, 86.6 (Fig 3b) were clearly visible with broader peaks in B. Pd_{Bb}. At 5wt% (Fig 3c) of the bimetallic (i.e 2.5%Pd/2.5%Pt) crystalline Pd/Pt was apparent in Bb only while Dd showed only amorphous Pd/Pt. However, at a higher loading of 20wt% (10%Pd/10%Pt) both cell types gave clearly defined patterns which were crystalline (Fig 3d). The Pd peaks at 2θ approx. = 40.1^o, 46.7^o, 68.2^o, 82.1^o, 86.6^o in both mono and bimetallic bio-NPs corresponds to the lattice planes; (111), (200), (220), (311) and (222) which is consistent with a previous report [40] and a face cubic centre (fcc) crystal structure [41] and the Pt peaks in the bimetallic appeared at 2θ approx. = 39. 93^o, 46.3^o, 67.7^o, 81.46^o and 85.9^o with the same lattice planes as those in Pd except for 5wt% bio-Pd/Pt NPs by *D. desulfuricans* and 5% bio-Pd made by both bacteria where only one prominent peak at 2θ = 39.8^o or 40.1^o (attributed to the (111) plane) was present, in accordance with the ICDD database.

Overall, the monometallic Pd (111) and bimetallic Pd-Pt (111) lattice planes at 40.1^o and 39.93^o, respectively displayed the strongest diffraction peaks (Fig 3) indicating high crystallinity [42] with the exceptions of 5wt% bimetallic Pd/Pt made by *D. dulfuricans* (Fig 3c) and the 5wt% monometallic Pd made by both bacteria (Fig 3a). The Average crystallite size was calculated from the Scherrer equation:

$$D = 0.9\lambda/\beta\cos\theta\,, \qquad (3)$$

Where D is the crystallite size in Å, λ is the X-ray wavelength, $CuK_{\alpha 1}$ radiation (λ = 1.5406 Å), θ is the Braggs angle, and β is the full width at half maximum (fwhm, in radians) of the peaks considered.

The average crystallite sizes calculated using Eq.3 for the bimetallic Pd/Pt (5wt% and 20wt%) made by *B. benzeovorans* were generally larger than those produced by *D. desulfuricans* (Table 2) with the exception that the average crystallite

size of the 20wt% monometallic Pd-NPs produced by *B. benzeovorans* was smaller (7.45 ± 0.71nm) than *D. desulfuricans* (13.15 ± 1.15nm) but were larger than the corresponding 5% monometallic Pd-NPs respectively (Table 3). Using combined imaging and surface probing teachniques, Deplanche et al. [30] reported a size of 16 nm for 5wt% Pd/Au bimetallic NPs synthesized using *E.coli*. In previous studies [30, 43] on the formation of Pd/Au core-shell bionanoparticles (Au core/Pd shell) the initial Pd-deposit (crystalline) became amorphous when the bimetallic was formed, consistent with migration of Pd atoms to form a shell around the Au core [30]. In this case reduction of Au (III) was mediated by Pd (0) under H_2. It is not known in the present case whether reduction of Pt (IV) was mediated chemically (*via* Pd (0) 'seed') or enzymatically but the XRD patterns (Fig 3c and d) clearly demonstrates the existence of Pt NPs. Note that XRD is a 'bulk' characterisation technique and hence the values reported in Table 2 represent both surface-localized and intracellular NPs, and no attempt was made to distinquish between them.

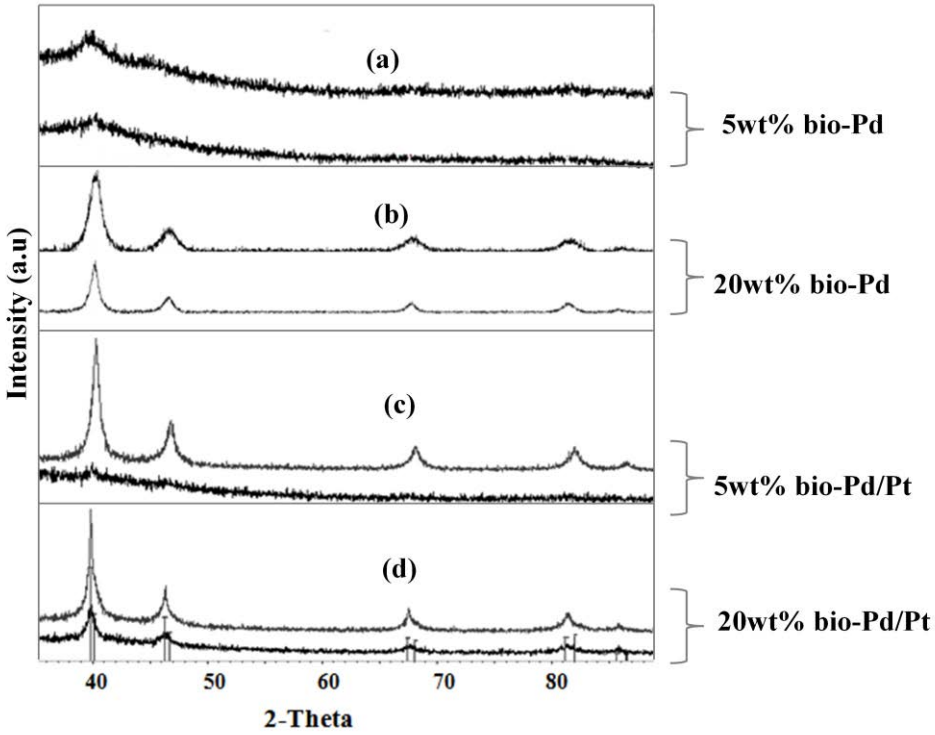

Figure 3 XRD patterns shows a sequence of bio-NPs made by *B. benzeovorans* (top spectrum) and *D. desulfuricans* (bottom spectrum). In the bimetallic bio-NPs only, the vertical line (right) represents Pt peak position while the vertical line (left) is Pd.

Table 2 Average Pd crystallite size of bio-NPs analysed using XRD

	Crystallite size (nm)	
Catalyst type	Bb	Dd
5wt% bio-Pd	5.10 ± 1.10	3.34 ± 0.10
20wt% bio-Pd	7.45 ± 0.71	13.15 ± 1.51
5wt% bio-Pd/Pt	21.16 ± 8.84	13.97 ± 0.17
20wt% bio-Pd/Pt	28. 87 ± 4.78	16.25 ± 3.10

Bb: *Bacillus benzeovorans*; Dd: *Desulfovibrio desulfuricans*. Results are Mean ± SEM, n=3.

Examination of surface NPs by X-ray photoelectron spectroscopy

In order to determine the surface chemical composition of bio-NPs and the oxidation states of the resulting Pd/Pt, X-ray photoelectron spectroscopy (XPS) was used to analyze the bimetallic bio-NPs (5wt% and 20wt% bio-Pd/Pt). Fig 4 and Table 3a show the XPS spectra of Pd 3d and Pt 4f for Pd and Pt respectively present on the surface of the bio-NPs. There are two oxidation states for both Pd and Pt in the bio-NPs as shown by two binding energy doublets. For 5wt% and 20wt% bio-Pd/Pt bimetallics, two different oxidation states of Pd (0) and Pd (II) were observed. The peaks in 5wt% bio-Pd/Pt produced by *B. benzeovorans* appeared at 335.23eV and 337.69eV and at binding energies of 335.55eV and 337.42eV (Fig 4a) in *D. desulfuricans* (Fig 4c) respectively. The Pd peaks around 335.23 eV, 335.55 eV, can be assigned to zero-valent Pd [44, 45] while the chemical state Pd (II) can be attributed to the peaks at 337.69eV and 337.42 eV respectively [46] (Table 3a) and may be due to incomplete reduction or oxidation of metallic Pd during sample preparation consistent with the finding of Deplanche et al., [30] for Pd/Au bimetallic synthesis. The 20wt% bio-Pd/Pt also shows zero-valent Pd peaks at 335.72eV and 335.17eV and peaks for Pd (II) at 337.62eV and 337.26eV for both Bb (Fig 4e) and Dd (Fig 4g) respectively (Table 3a). The shifts observed in the binding energies of the Pd (0) between the 5wt% and 20wt% bio-Pd/Pd of Bb than in Dd may be due to differences in the surface properties of both bacteria (Table 5) as the cells interact to stabilize Pd NPs.

Considering the binding energies of Pt 4f in both cells, the binding energies of the 5% bio-Pd/Pt were below detection which appears to have been covered by Pd (Table 3a, Figure 4b, d) whereas for the 20wt% bio-Pd/Pt, the binding energies from 71-72eV can be assigned to Pt (0) [47] in the bio-NPs made by both cells (Table 3a). The appearance of these binding energies of Pt in the 20wt% bio-Pd/Pt NPs (Fig 4f, h) may be due to the higher metal loading which favours an increase in electron density [45] around Pd as the addition of Pt withdraws electrons from the Pd to be reduced to Pt (0) during the sequential reduction of the bio-NPs as suggested by the observation of Pd (II) (above). The peaks representative of higher binding energies (74-76 eV) may be as a result of the formation of Pt (II), PtO_2 or $Pt(OH)_4$ from Pt (IV) species [48]. It can be concluded that Pt exists primarily in the bio-NPs as Pt (0). This interaction suggests the

existence of Pd/Pt bimetallic on the surface of the bio-NPs. The presence of Pt (0) in the bimetallic may have generated some residual Pd (II) at the end of the reduction process, characteristic of the binding energies seen above or this may have been 'biosorbed' Pd (II) that was not reduced to Pd (0) 'seeds'.

Table 3b and supplementary Tables 4, 5 and Fig 4 shows that the bacterial cell surfaces also contain C, N, O and P which can be attributed to carboxyl, amine, hydroxyl and phosphoryl groups found as organic components [49] around the bio-NPs with varying binding energies. These components are responsible stabilizing [50] the bio-NPs against agglomeration. Table 5 also shows the various molar ratios of the bio-NPs to total carbon. It was observed that the bio-NPs produced by *Bacillus* contain a higher molar ratio of each elemental component (N, P and O) to total carbon than *D. desulfuricans*. Probably, the elemental ratios in supplementary Table 5 reflect that the probe is detecting the thick layer of peptidoglycan/teichoic acids in *Bacillus* and the outer membrane/periplasm in *Desulfovibrio*. A detailed study on the mechanism of binding of precious metal ions to the two bacterial cell surfaces will be reported elsewhere. Notably, the O1s of the bimetallic bio-NPs (5wt % and 20wt %) produced by the two bacteria have a similar binding energy around 532eV [44]. However, looking at the 5wt % bimetallic NPs, they have a binding energy of approximately 531eV which could be attributed to the interaction of the bacterial surfaces with the NPs due to oxygen from phosphate groups and amide functions [51]. The shift of the O1s peaks to a lower binding energy of around 530eV observed in bio-NPs with 20wt % metal loading could be attributed to the formation of metal oxides of Pd and Pt [52, 53] on both bacteria. In conclusion, the various surfaces of the bimetallic NPs are mainly covered with Pd and Pt metallic states and could be Pd/Pt core-shell structures, but this requires further verification. Using a similar approach of sequential synthesis, Flynn and Gewirth [54] chemically synthesized Au/Pt core-shell nanoparticles.

Table 3a XPS binding energies of bio-Pd/Pt bimetallic bio-NPs

Bimetallic	Pd $3d_{5/2}$ BE (eV)		Pt $4f_{7/2}$ BE (eV)		Pt $4f_{5/2}$ BE (eV)	
bio-NPs	Bb	Dd	Bb	Dd	Bb	Db
5wt%	335.23	335.55	-	-	-	-
bio-Pd/Pt	337.69	337.42				
20wt%	335.72	335.17	72.04	71.28	75.37	74.61
bio-Pd/Pt	337.62	337.26	72.90	72.14	76.23	75.47

XPS binding energies of palladium and platinum bimetallic bio-NPs made by *B. benzeovorans* (Bb) and *D. desulfuricans* (Dd) indicating the presence of Pd $3d_{5/2}$ and Pt 4f doublets. BE = Binding energy of electrons.

Table 3b XPS elemental fractions of bio-Pd/Pt

Bimetallic	N1s BE (eV)		P2p BE (eV)		O1s BE (eV)	
bio-NPs	Bb	Dd	Bb	Dd	Bb	Dd
5wt%	399.72[a]	399.68[a]	133.22	133.99	531.20	531.02
bio-NPs	401.50[b]	401.59[b]	134.08	134.85	532.34	532.49
20wt%	399.68[a]	399.54[a]	133.72	133.96	530.98	530.81
bio-NPs	401.61[b]	401.64[b]	134.62	134.82	532.43	532.39

XPS binding energies of elemental fractions; N1s, P 2p and O1s of bimetallic bio-NPs. Details of the C1s component is presented in Table S2 and Fig S3. [a]Non-protonated nitrogen group; [b]Protonated nitrogen group; Bb = *Bacillus benzeovorans;* Dd = *Desulfovibrio desulfuricans;* BE = Binding energy of electrons.

Table 4 Functional groups and XPS binding energies of C1s peaks

	Binding energy (eV)							
Bimetallic bio-	C- (C-H)		C- (O, N)		C = O, O-C-O		O =C-OH,O=C-OR	
NPs	Bb	Dd	Bb	Dd	Bb	Dd	Bb	Dd
5% bio-Pd/Pt	284.6	284.6	286.09	286.23	287.79	287.95	288	-
20% bio-Pd/Pt	284.6	284.6	286.13	286.33	287.94	287.93	-	-

Results show binding energies of the various functional groups on C1s peak (see Figure 5) on the bio-NPs as analysed using XPS and how carbon interacts with various groups at certain binding energies. Bb = *Bacillus benzeovorans*; Dd = *Desulfovibrio desulfuricans*

Table 5 Elemental composition (molar ratios *vs* total carbon) on bio-NPs analysed by XPS

Bimetallic bio-	O/C		N/C		P/C	
NPs	Bb	Dd	Bb	Dd	Bb	Dd
5% bio-Pd/Pt	0.403	0.276	0.144	0.065	0.020	0.012
20% bio-Pd/Pt	0.619	0.384	0.128	0.094	0.034	0.015

O =oxygen, C = carbon, N = nitrogen, P = phosphorous, Bb = *Bacillus benzeovorans*; Dd = *Desulfovibrio desulfuricans*

.

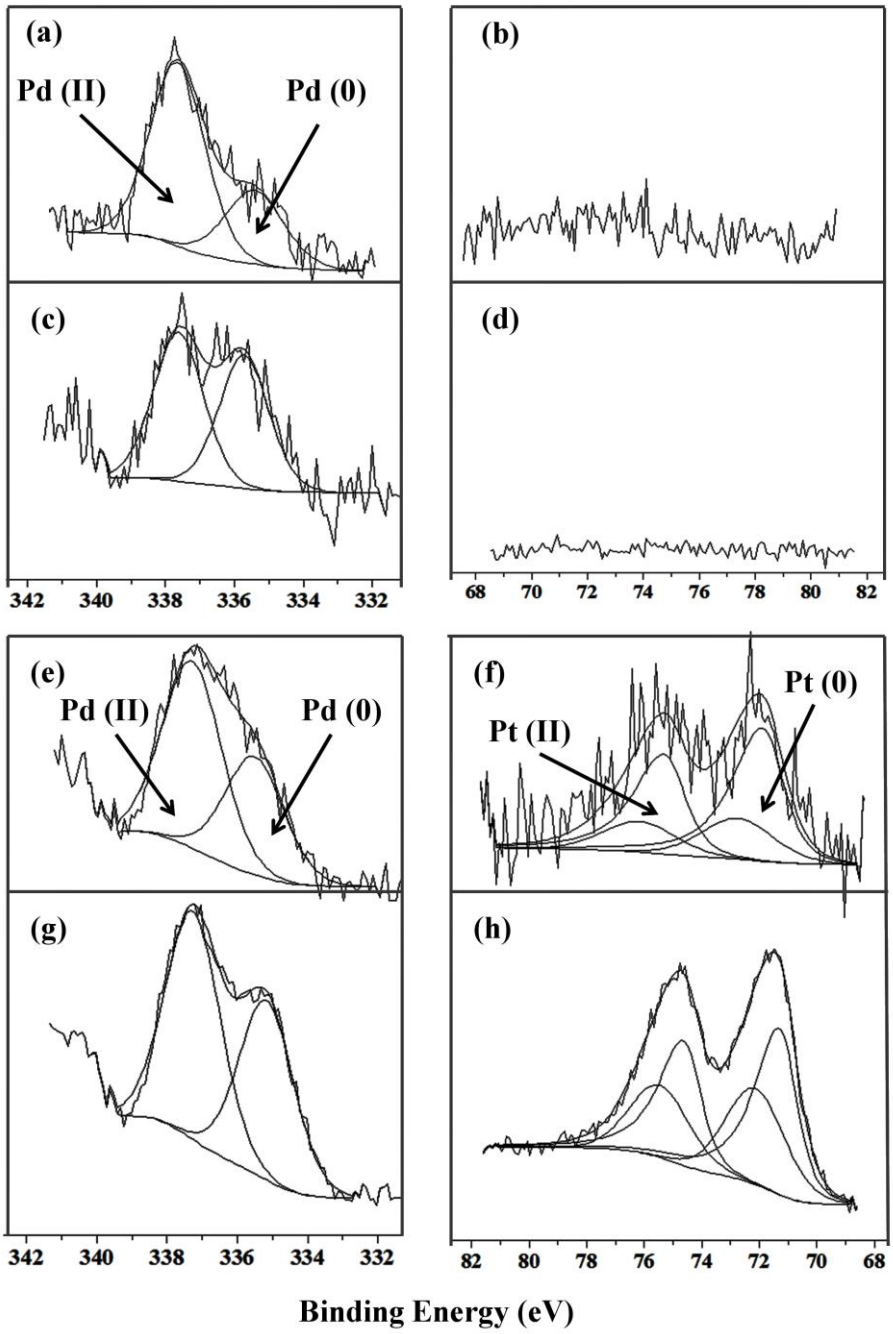

Figure 4 XPS spectra of Pd $3d_{5/2}$ and Pt 4f peaks in 5% bimetallic Pd/Pt bio-NPs made by *B. benzeovorans* (a) and (b); *D. desulfuricans* (c) and (d) and 20% bimetallic Pd/Pt bio-NPs made by *B. benzeovorans* (e) and (f); *D. desulfuricans* (g) and (h) respectively. Fitting was done using Shirley backgrounds, mixed Gaussian-Lorentzian (Voigt) lineshapes.

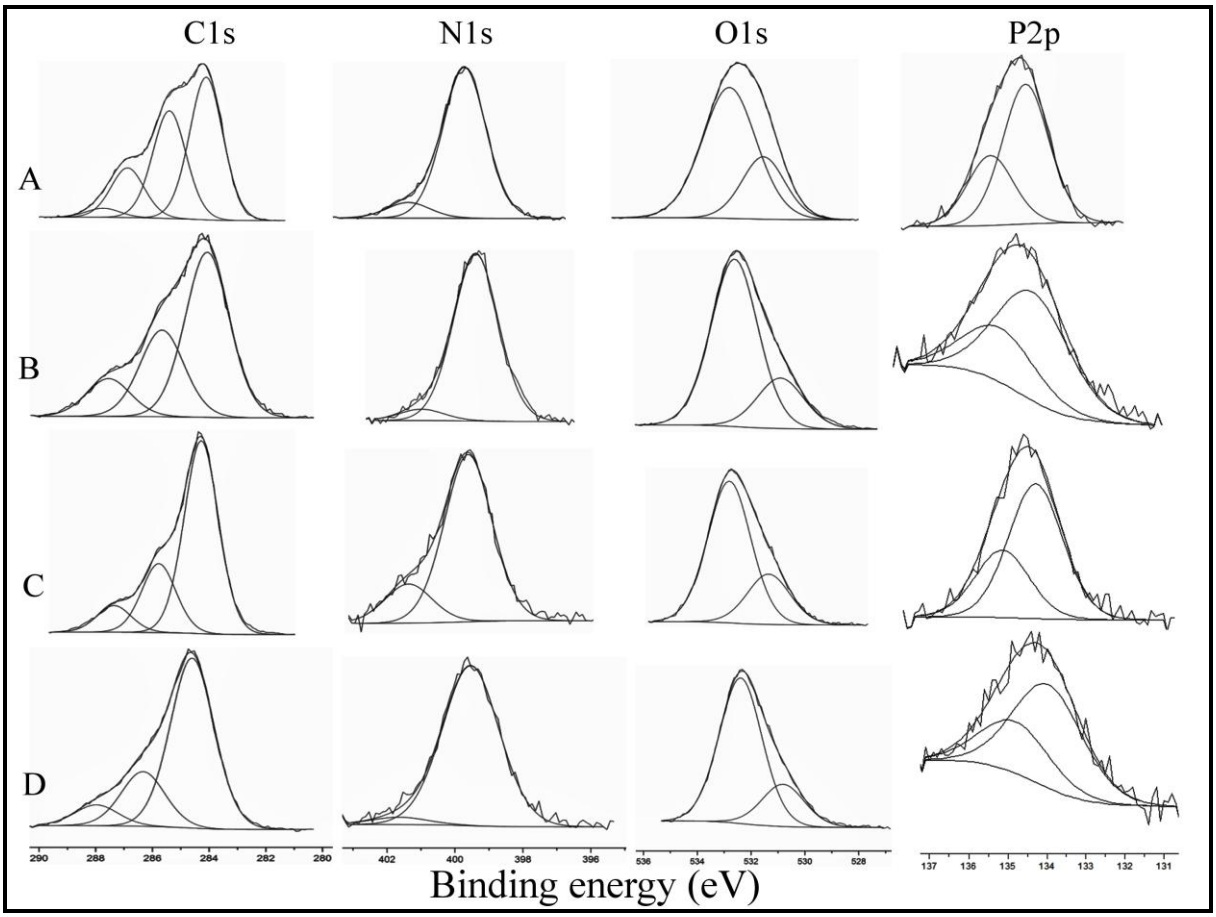

Figure 5 Results are XPS spectra of C1s, N1s, O1s and P2p on 5wt% bimetallic bio-NPs made by a) *B. benzeovorans* b) *D. desulfuricans* and the corresponding 20wt% bimetallic bio-NPs (c) and (d) respectively.

The cracking of heavy oil involves breaking of C-C, C-H, and C-heteroatom bonds as it is exposed to elevated temperatures. This reaction produces upgraded oil, together with non-condensable gases (e.g., nC_1-C_5, iC_4-C_5, olefin C_2-C_4, H_2, H_2S, CO and CO_2) and coke.

Coke determination

It has been reported that a major cause of catalyst deactivation is the formation of fouling deposits of "coke" i.e. solid or carbonaceous materials that arise due to side reactions that occur on the catalyst surface [55]. An estimate of coke can be made by thermogravimetric analysis (i.e. progressive weight loss) of materials before and after

reaction. Residual asphaltene, catalysts and other deposits were separated from the reaction as described in materials and methods. The percentage of the deposit after reactions that comprises coke was determined using the thermogravimetric analyser (TGA), as the material burnt-off beyond that of n-heptane separated asphaltene. Fig 6 shows the thermograms or weight loss curves as a function of ramp temperature for n-heptane-separated asphaltene, fresh Ni-Mo/Al_2O_3 and deposit after reaction with Ni-Mo/Al_2O_3 (Fig 6a) and also the metal-unsupplemented bacterial cells, fresh bio-NPs and the deposits after reaction with *D. desulfuricans* (Fig 6b) and *B. benzeovorans* (Fig 6c).

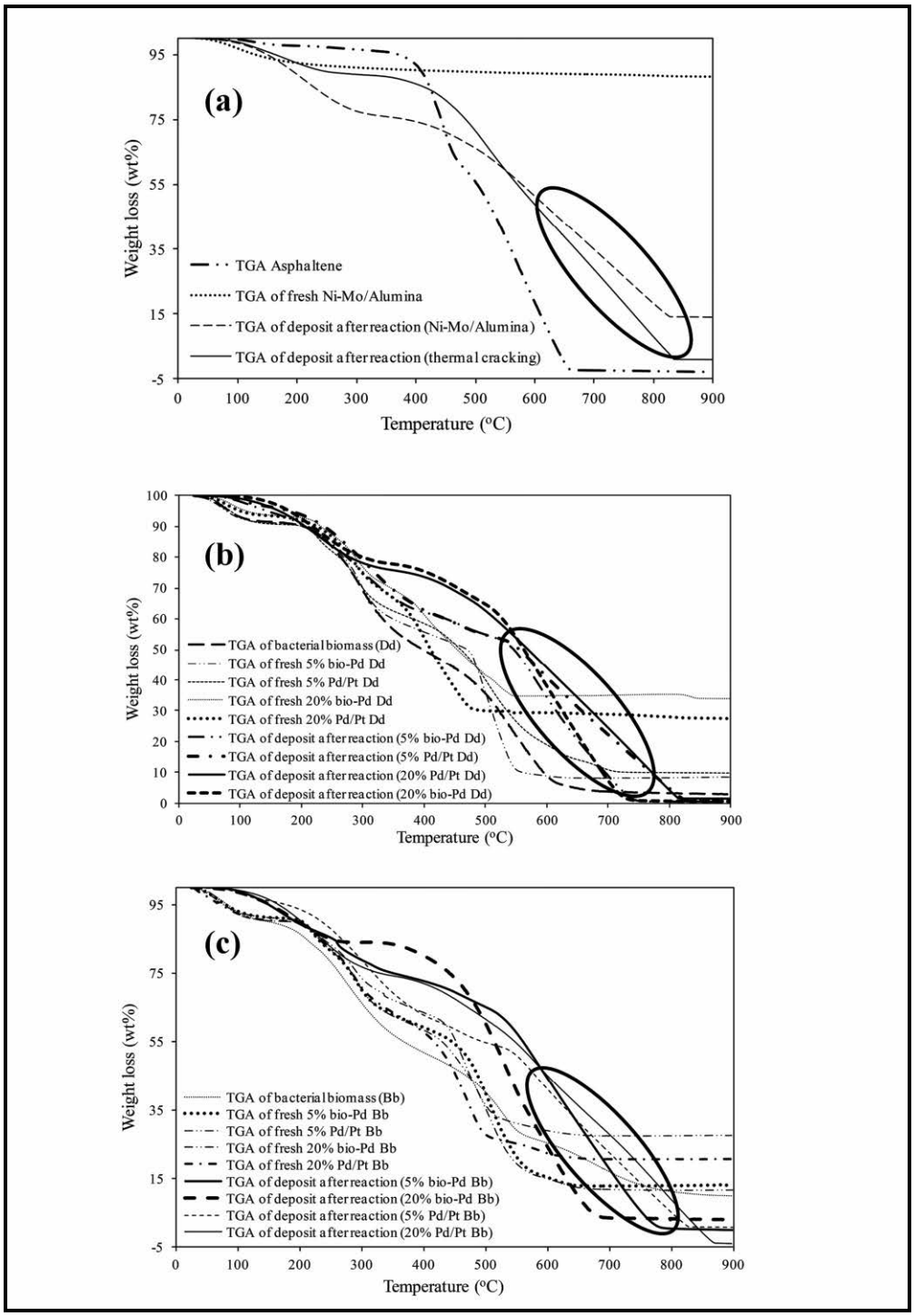

Figure 6 TGA curves of fresh bio-Pd and Pd/Pt, n-heptane separated asphaltene, and deposits after reactions at 425 ^{o}C, 500 rpm, and 30 minutes reaction time. Circled regions: responses attributed to coke and residual catalyst.

The fresh 5 or 20wt % bio-catalysts (Pd or Pd/Pt) lost 65 wt. % of their masses during the temperature rise to 550 ^{o}C in air. This is as a result of moisture removal (from 25 to 80 ^{o}C), charring of the biomass (80 – 300 ^{o}C) and subsequent burn-off of the formed carbon (from 300 – 550 ^{o}C). The thermogram curves of the air-dried bacterial cells decorated with Pd or Pd/Pt NPs (i.e., fresh bionanoparticles) show that the residual mass ranged from 8.7-13wt% (5wt% Pd and 5wt%Pd/Pt) and 20.6-27.7wt % (20% Pd and 20%Pd/Pt). Most of the residual masses are metals (i.e., Pd or Pd/Pt) with little biomass char formed, which accounts for about 4 wt% from the TGA of the bacterial cells without metals (Figs 6b, c). There was a complete burn-off of the separated asphaltenes using n-heptane as the temperature increased from 430 to 600 ^{o}C. Therefore, the burn-off above 600 ^{o}C (Fig 6a) for the deposit after reaction is attributed to rejected coke after upgrading [56]. Hence, from the weight loss curves of deposits after reaction the residues after burn-off from 600 to 820 ^{o}C was coke. (Figs 6a, b, c). The weight loss from 25-100 ^{o}C for the fresh Ni-Mo/Al_2O_3 represent the removal of moisture, beyond this temperature (100^{o}C) the catalyst is thermally stable. However, 41.3% of the deposit after reaction with Ni-Mo/Al_2O_3 particles was coke (Fig 6a). The coke content of the deposits after reaction with 5wt% (Pd or Pd/Pt) on bacterial cells ranged from 25 to 29.2 wt. % while that of 20wt% ranged from 20.2 to 38.1 wt% (Figs 6b, c). The coke content of the deposit after reaction ranges from 20 to 43 wt. % of amount of deposit. The deposit after reaction with particles of Ni-Mo/Al_2O_3 showed a higher coke content and burn-off temperature (about 820 ^{o}C) compared to those of bioNPs (750-800 ^{o}C). This high burn-off temperature can be attributed to the hardness of the produced coke resulting from the acidity of the alumina support [56]. The coke deposits for the samples are shown in Table 6, from which it can be concluded that thermal cracking and metal-free biomass, followed by commercial catalyst, produced more coke than the bio-NPs.

The yields of light oil (*i.e*. liquid), gas and coke after upgrading with thermal cracking, biomass alone, commercial catalyst and bionanoparticles are shown in Table 6.

Table 6 Mass balance of liquid (*i.e.,* light oil), gas and coke yields after reaction

	Liquid (wt %)		Gas (wt %)		Coke (wt %)	
Experiments	Bb	Dd	Bb	Dd	Bb	Dd
Thermal	79.83 ± 1.6		10.02 ± 1.2		10.15 ± 2.0	
Biomass alone	84.86±1.1	82.64±0.0	8.51±0.8	9.72±0.0	6.63±1.3	7.64±0.0
5wt% bio-Pd	89.32±0.4	89.09±0.2	7.48±0.2	7.62±0.2	3.20±0.4	3.30±0.1
20wt% bio-Pd	89.45±0.7	89.80±0.4	7.61±0.1	7.04±0.4	2.94±0.1	3.16±0.5
5wt%bio-Pd/Pt	89.20±0.3	89.40±0.5	7.07±0.2	6.73±1.1	3.73±0.2	3.87±0.2
20wt%bio-Pd/Pt	89.02±0.5	89.13±0.3	6.78±0.1	6.80±0.2	4.20±0.2	4.07±0.6
Commercial catalyst	87.25 ± 0.5		7.73 ± 0.7		5.02 ± 0.8	

Note: Bb = *B. benzeovorans;* Dd = *D. desulfuricans*; Commercial catalyst = Ni-Mo/Al_2O_3

Table 6 shows that the coke yield was decreased significantly after reaction with 5wt.% and 20 wt.% bionanoparticles of Pd and Pd/Pt promoted catalysts; Although there is no significant difference ($P > 0.05$) between the NPs made by the two bacteria at 0.05 significance level (except for 20wt.% bio-Pd: $P = 0.004$) the bionanoparticles displayed significant pronounced effects in suppressing coke formation compared to thermal cracking (10.15 wt.% of coke) and commercial catalyst (5.02 wt.%) while biomass alone yielded 6.63 wt.% for Bb and 7.64 wt.% for Dd of coke respectively.

Analysis of the produced gas during heavy oil upgrading has shown that hydrogen is produced [39], e.g. 20 mol% hydrogen was found in the produced gas from an *in situ* combustion pilot at Marguerite Lake, Alberta, Canada [57] and subsequently Hart et al. [38] found 1.5 to 2.5 vol. % hydrogen in the produced gas after the use of

dispersed ultrafine Co-Mo/Al_2O_3 catalyst upgrading of heavy oil in a batch reactor. It is well known that metals perform a hydroconversion function; hence this observation can be explained by the fact that the produced hydrogen gas molecules, which are readily adsorbed onto the surfaces of nanoparticles, could be dissociated to produce reactive hydrogen species which subsequently reacts with the cracked intermediates to produce stable lower molecular weight products. Correspondingly, the increased yield of coke resulted in a decrease yield of the desired liquid product [57, 58]. On the other hand, thermal cracking without catalyst has shown a greater tendency to form coke due to free radical addition polymerisation reaction [38].

Table 6 shows that the nanoparticles of Ni-Mo/Al_2O_3 hydrodesulfurisation (HDS) catalyst yielded higher coke than bioNPs. This is attributable to a cracking function provided by the alumina acidic support which increases the cracking reaction leading to more coke formation [59] unlike the bio-NPs that are well dispersed and stabilized by various functional groups on the neutral bacterial support [50] (see above).

For all bionanoparticles of Pd or Pd/Pt catalysts, the amount of gaseous hydrocarbon produced was lower than that of the thermal cracking and the biomass-promoted reaction with no metal NPs (Table 6). A typical composition of the produced gas has been reported elsewhere [17, 39]. The presence of nanoparticles suppresses gas formation probably as a result of the transfer of active hydrogen, methyl and ethyl radical additions *via* the NPs to stabilise hydrocarbon radicals formed by thermal cracking into the liquid phase [61]. A similar observation of a lower yield of gas was reported by Hossain et al. [29] for a synergistic effect of Pd/Rh promoted Co/HPS [cobalt decorated with high porous saponite (clay)] catalyst for upgrading of vacuum gas oil at 400 ^{o}C in a batch autoclave reactor. These results are expected because of the availability of reactive hydrogen due to hydrogen spillover i.e. the dissociation and chemisorption/physisorption of hydrogen atom/molecule on metals such as Pd, Pt, Ni, Mo, etc., followed by incorporation of the active hydrogen onto the nearest receptor [61] which, in this case, could be attack on biomass components, introduced by the nanoparticles that helps to suppress the formation of lighter gases and coke [29]. Hence, the over cracking of produced hydrocarbon intermediates leading to undesirable light gaseous products is inhibited. This conclusion can be reinforced by the high yield of gas in thermal cracking and upgrading with biomass only. Hence, the bimetallic bioNPs

may have enhanced hydrogen, methyl and ethyl transfer because of the synergistic effect of Pd/Pt and their 'biochemical' environment to stabilise cracked fragments of heavy oil molecules. In this manner, the formation of large molecular weight hydrocarbons as a result of free radical addition reactions would be significantly suppressed. All metallised samples gave a higher proportion of liquid post-reaction than either thermal cracking or biomass alone (Table 6).

API gravity and viscosity

API (American Petroleum Institute) gravity is a standard parameter that determines the transportability of crude oil *via* pipelines [62]. For heavy oil to be transported, the viscosity must be reduced and lower than 250 mPa.s at 100^{o}F [63]. The viscosity and API gravity of heavy oil depends to a large extent on its macromolecular weight constituents such as resins and asphaltenes. It is well known that hydrocarbons with larger weight and high boiling point exhibit high density and viscosity. Table 6 shows the API gravity increments and viscosities of produced oil samples after reaction with thermal cracking, biomass alone, bio-supported NPs of Pd or Pd/Pt, and NPs of Ni-Mo/Al_2O_3. The oil produced by thermal cracking had a lower API gravity increment and higher viscosity compared to the produced oil samples after reaction with bio-NPs of Pd or Pd/Pt. Moreover, the produced oils after upgrading with bimetallic NPs (Pd/Pt) had approximately 2^{o} further increase in API gravity compared to those upgraded with monometallic Pd (~7.6 ^{o}API on average). The extent of viscosity reduction after upgrading therefore can be summarised as follows: 98.7 % (thermal), 99.2 % (bioNPs) and 99.6 % (nanoparticles of Ni-Mo/Al_2O_3) below 1031 mPa.s for the received heavy oil reference. This level of viscosity reduction would improve production and pipeline transport than the feed oil. A similar level of viscosity reduction of 98.9 % for Liaohe extra-heavy oil using nano-nickel catalyst in batch reactor has been reported [64]. While, for small quantities, the small improvement gave by catalytic augmentation is questionable, the beneficial effects at scale and overall process economics, awaits evaluation.

Table 7 Produced oil API gravity increment and viscosity after reaction (feed oil: 13.8 ^{o}API and 1031 mPa.s)

	API gravity increments (^{o})		Viscosity (mPa.s)	
Experiments	Bb	Dd	Bb	Dd
Thermal	6.3 ± 0.3		13.8 ± 0.4	
Biomass alone	6.1 ± 0.5	6.2 ± 0.0	16.0 ± 2.2	14.8 ± 0.0
5wt% bio-Pd	7.8 ± 0.3	7.8 ± 0.2	9.7 ± 0.6	8.1 ± 0.4
20wt% bio-Pd	7.4 ± 0.4	7.5 ± 0.2	8.8 ± 0.7	10.7 ± 2.5
5wt% bio-Pd/Pt	9.1 ± 0.4	9.6 ± 0.8	7.0 ± 0.3	5.8 ± 0.6
20wt%bio-Pd/Pt	9.2 ± 0.9	8.4 ± 0.6	7.4 ± 1.2	6.2 ± 0.7
Commercial catalyst	11.1 ± 0.3		3.7 ± 0.6	

Note: Bb = *B. benzeovorans;* Dd = *D. desulfuricans;* Commercial catalyst = Ni-Mo/Al_2O_3

Thermal reaction involves cracking of C-C and C-heteroatom bonds, cracking of side chains from aromatics and asphaltenes, aromatization of aliphatic structures, and condensation of aromatic radicals to form coke. Hence, generated fragments commonly undergo addition reaction to larger molecular weight species which adversely impacts on the produced oil API gravity and viscosity after upgrading by thermal cracking. In a catalytic environment, the presence of metals such as Pd and Pt are thought to activate hydrogen-transfer reactions from C-H bond cleavage to cap some of the produced radicals [38, 39, 58], thereby narrowing the molecular weight of the product compared to thermal cracking alone (see later).

An industrial hydrodesulfurisation (HDS) Ni-Mo/γAl_2O_3 catalyst was also evaluated under the same reaction conditions and the activity of this catalyst was also included for comparison purposes. This produced better upgrading than the bio-catalysts (Table 7) but correspondingly more coke (Table 6) instead of the dual benefit obtained by using the biomaterials. Comparing the extent of upgrading by Pd/Pt/bio-NPs and Ni-

Mo/Al_2O_3, the produced oil API gravity for the bio-derived and commercial catalysts was 9.6^o (Pd/Pt 5wt. %) and 11.1^o ($Ni\text{-}Mo/Al_2O_3$). The ~1.5 ^{o}API increment obtained with the commercial HDS Ni-Mo catalyst can be attributed to the additional cracking role of acid sites of the alumina support whereas bio-nanoparticles of Pd/Pt lacks such sites (although immobilization of catalyst on alumina support is entirely feasible as a self-adhering film [65, 66]. However, the alumina support would lack the potential sites for amelioration of the coking problem (see above); the bio-Pd/Pt is superior to the commercial catalyst in this regard.

Furthermore, the macromolecules such as resins and asphaltenes are known coke precursors because of their high aromaticity, molecular weight, and heteroatom content. These components confer the characteristic low API gravity, high viscosity and low yield of light distillates with lower boiling points upon distillation. The higher API gravity observed after upgrading therefore indicates that the produced oil composition has shifted towards lighter components with lower molecular weight (but still accompanied with polymerisation and condensation of some of the macromolecules to form coke). Heavy oil is known to be hydrogen-deficient, thus coke formation can be suppressed remarkably if hydrogen/hydrogen-donor is available to stabilise generated free radicals during reaction [40, 59]. In this respect the well known property of Pd (0) to hold H_2 within its lattice may help transfer hydrogen into the reaction [67]. The authors showed that Pd nanocrystals covered with a metal-organic framework has twice the hydrogen storage capacity as compared to bare Pd nanocrystals [67].

True boiling point (TBP) distribution

The crude oil boiling point distribution curve is an important yardstick of quality evaluation and refinery process design. It has been reported that aliphatic-rich oil generally has a higher API gravity and high yield of fuel distillates than aromatic-rich oils [68]. Additionally, a high content of sulfur, metals and nitrogen-containing compounds of the heavy oil adds to their low API gravity and low fuel distillate yields [56]. The true boiling point (TBP) distribution curves for the feed and produced oils after reaction with the different bioNPs and thermal cracking are shown in Fig 7. The shift of the TBP distribution curves of the produced oils after reaction to the left of TBP

curve of the feed oil is an indication of the extent of upgrading achieved, representing the extent of conversion of heavy molecular weight compounds into low-boiling fractions.

The performance of the bioNPs was evaluated in comparison to the control experiments such as the feed heavy oil, upgraded oil by thermal cracking, and upgraded oil with biomass only (without metals), with the upgraded oils with bioNPs of Pd and Pd/Pt all subjected to the same operating conditions.

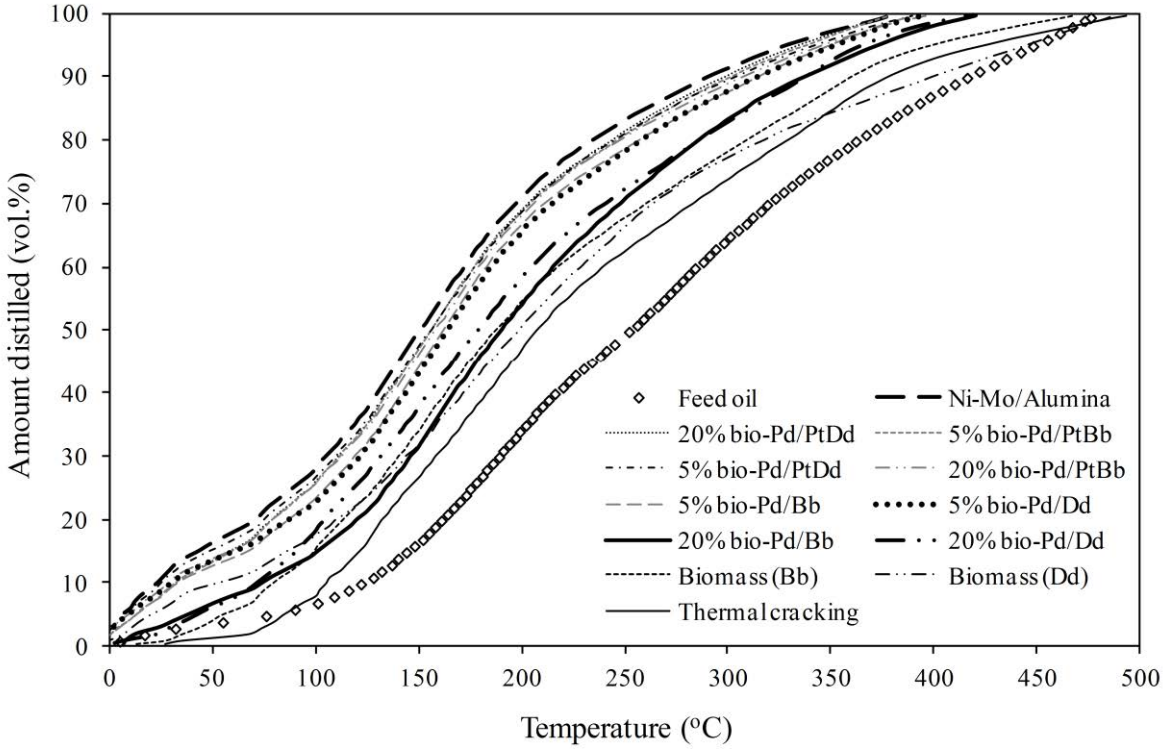

Figure 7 Simulated distillation curves of feed and produced oils after reaction with the different nanoparticles at temperature 425 °C, agitation 500 rpm, metal NP-to-oil ratio 1 (mg/g), initial pressure 20 bar and 30 minutes reaction time.

Fig 7 shows that oil upgrading with the addition of bionanoparticles of Pd and Pd/Pt favours a significant shift towards lighter distillate fractions in comparison to thermal cracking, upgrading with biomass only (no metal nanoparticles) and the feed oil reference. A 53 and 65 °C shift to the left in the boiling point axis at 50 vol. % yield can be observed for thermal cracking and with biomass only in comparison to the feed oil TBP curve. This rose to 90 °C (5 wt.% Pd_{Bb}), 94 °C (20 wt.% Pd/Pt_{Bb}) and 96 °C (20 &

5 wt.% Pd/Pt_{Dd} and 5 wt.% Pd/Pt_{Bb}) but only 73 ^{o}C (20 wt.% Pd_{Bb} and 20 wt Pd_{Dd}) at 50 vol.% yield after the reactions using Pd and Pd/Pt/bio-NPs. This shift in temperature to the left of the TBP curve of the feed oil can be attributed to the increased amount of low-boiling fractions in the upgraded oil samples after reaction with metallic bionanoparticles. An important observation is made with the use of commercial Ni-Mo/Alumina catalyst and 5 w% bio-Pd/Pt of both bacteria, as the shift towards lower distillable temperatures is comparable.

Conclusions

This study shows the use of bio-NPs made by cells of Gram-positive (*B. benzeovorans*) and Gram-negative (*D. desulfuricans*) bacteria in heavy oil upgrading. The bio-NPs of Pd and Pd/Pt were better catalysts as they suppressed coke formation when compared to using non-metallized biomass, a thermal non-catalytic process and NPs of commercial catalyst of Ni-Mo/Al_2O_3, and also produced more volumes of liquid fractions on average. The API gravity produced by commercial catalyst, Ni-Mo/Al_2O_3 was higher but hindered by coking when compared with the bio-NPs. There was generally no significant difference in terms of the catalytic behaviour of the bio-NPs made by the two bacteria, *B. benzeovorans* would be considered a better platform of choice in catalytic synthesis, as it is easier to produce at scale than by using the slow growing *D. desulfuricans*. The differences in the bioentities (particle size *via* XRD and TEM and elemental surface composition *via* XPS analysis) make little difference to the outcome of heavy oil upgrading.

For process economics, bio-NPs can be bio-fabricated from waste sources and this is a potentially useful future approach; the impact of such ‘green’ fabrication on the catalytic efficacy will be reported elsewhere.

Notes

The authors declare no competing financial interests.

Acknowledgements

The authors acknowledge, with thanks, financial supports from a Commonwealth scholarship of the United Kingdom to JBO. The project was also supported by EPSRC (grant number EP/J008303/1) to JW and LEM. The Science City Photoemission Facility used in this research was funded through the Science Cities Advanced Materials Project 1: Creating and Characterising Next Generation of Advanced Materials with support from AWM and ERDF funds.

References

[1] Anon. US Energy Information Administration (EIA): International Energy Outlook. Report number: Doe/EIS-0484. Sep. 9th, 2014.

[2] Anon. BP Statistical review of world energy. June, 2014

[3] Anon. World Energy Outlook. International Energy Agency (IEA),. ISBN: 978 9264 12413 4. November, 2014.

[4] Anon. Total Oil and Gas. Reserves for the future. http://www.total.com/en/energies-expertise/oil-gas/exploration-production/strategic-sectors/heavy-oil/challenges/reserves-future. (Accessed online 05/05/2015).

[5] M. F. M. de Sena, L. P. Rosa, A. Szklo, Energy Policy. 61 (2013) 51-9.

[6] I. M. Head, D. M. Jones, S. R. Larter, Nature 426 (2003) 344-352.

[7] A. Y. Huc, Geological origin of heavy oil: In heavy crude oil: From geology to upgrading. An overview: Alain-Yves Huc, Ed. Editions Technip, Paris ISBN 978-2-7108-0890-9. 2011, pp 25-31.

[8] B. Tremblay, Chapter 22 - Cold Production of Heavy Oil. In *Enhanced Oil Recovery Field Case Studies*, J. J. Sheng, Ed. Gulf Professional Publishing: Boston, 2013, pp 615-666.

[9] K. J. Chew, Philos. Trans. A Math. Phys. Eng. Sci. 372 (2014) 201203.

[10] C. E. Galarraga, P. Pereira-Almao, Energy Fuels 24 (2010) 2383-2389.

[11] L. C. Castaneda, J. A. D. Munoz, J. Ancheyta, Fuel 100 (2012) 110-127.

[12] L. C. Castaneda, J. A. D. Munoz, J. Ancheyta, Catal. Today 220 (2014) 248-273.

[13] Z. Shen, Z. Cao, X. Zhu, X. Li, Petrol Sci Technol 26 (2008) 1676-1683.

[14] L. Wang, A. Zachariah, S. F. Yang, V. Prasad, A. de Klerk, Energy Fuels 28 (2014) 5014-5022.

[15] J.P. Heraud, A. Kamp, J.F. Argiller, *In-situ* upgrading of heavy oil and Bitumen: In Heavy Crude Oil: From Geology to Upgrading. An Overview: Alain-Yves Huc, Ed. Editions Technip, Paris ISBN978-2-7108-0890-9. 2011, pp 388-402.

[16] M. Greaves, A. El-Saghr, T. X. Xia, Prepr. ACS, Div. Pet. Chem. 47 (2000) 595−598.

[17] A. Hart, G. Leeke, M. Greaves, J. Wood, Energy Fuels 28 (2014) 1811-1819.

[18] K. Deplanche, A. Murray, S. Taylor, L. E. Macaskie, Biorecycling of precious metals and rare earth elements. In *Nanomaterials*, M. M. Rahman, Ed. In Tech publishing, Rijeka, Croatia: 2011, pp 279-314. ISBN: 978-953-307-913-4.

[19] A. N. Mabbett, D. Sanyahumbi, P. Yong, L. E. Macaskie, Environ. Sci. Technol. 40 (2006) 1015-1021.

[20] Narayanan, K. B.; Sakthivel, N., Biological synthesis of metal nanoparticles by microbes. Adv. Colloid Interface Sci. 156 (2010)1-13.

[21] P. Yong, I. P. Mikheenko, K. Deplanche, M. D. Redwood, L. E. Macaskie, Biotechnol. Lett. 32 (2010) 1821-1828.

[22] S. Selenska-Pobell, P. Panak, V. Miteva, I. Boudakov, G. Bernhard, H. Nitsche, FEMS Microbiol. Ecol. 29 (1999) 59-67.

[23] J. M. Foulkes, K. J. Malone, V. S. Coker, N. J. Turner, J. R. Lloyd, ACS Catal. 11 (2011) 1589-1594.

[24] K. Deplanche, J. A. Bennett, I. P. Mikheenko, J. Omajali, A. S. Wells, R. E. Meadows, J. Wood, L. E. Macaskie, Appl. Catal. B 147 (2014) 651-665.

[25] H. Ortiz-Moreno, J. Ramírez, F. Sanchez-Minero, R. Cuevas, J. Ancheyta, Fuel 130 (2014) 263-272.

[26] Creamer, N. J.; Mikheenko, I. P.; Yong, P.; Deplanche, K.; Sanyahumbi, D.; Wood, J.; Pollmann, K.; Merroun, M.; Selenska-Pobell, S.; Macaskie, L. E., Novel supported Pd hydrogenation bionanocatalyst for hybrid homogeneous/heterogeneous catalysis. Catal. Today 128 (2007) 80-87.

[27] J. A. Bennett, I. P. Mikheenko, K. Deplanche, I. J. Shannon, J. Wood, L. E. Macaskie, Appl. Catal. B 140-141 (2013) 700-707.

[28] S. De Corte, T. Sabbe, T. Hennebel, L. Vanhaecke, B. De Gusseme, W. Verstraete, N. Boon, Water Res. 46 (2012) 2718-2726.

[29] M. M. Hossain, M. A. Al-Saleh Shalabi, T. Kimura, T. Inui, Appl. Catal. A 278 (2004) 65–71.

[30] K. Deplanche, M. L. Merroun, M. Casadesus, D. T. Tran, I. P. Mikheenko, J. A Bennett, J. Zhu, I. P. Jones, G. A. Attard, J. Wood, S. Selenska-Pobell, L. E. Macaskie, J. R. Soc. Interface 9 (2012) 1705-1712.

[31] A. J. Murray, S. Taylor, J. Zhu, J. Wood, L. E. Macaskie, Min. Eng. In Press. (2015)

[32] J. B. Omajali, I. P. Mikheenko, M. L. Merroun, J. Wood, L. E. Macaskie, J. Nanopart. Res. 17 (2015) 1-17.

[33] K. Deplanche, I. Caldelari, I. P. Mikheenko, F. Sargent, L. E. Macaskie, Microbiology 156 (2010) 2630-2640.

[34] M. Jaboyedoff, B. Kubler, P. H. Thelin, Clay Miner. 34 (1999) 601-617.

[35] N. Fairley, CasaXPS. Casa Software Ltd. www.casaxps.com. 2013.

[36] A. Hart, A. Shah, G. Leeke, M. Greaves, J. Wood, Ind. Eng. Chem. Res. 52 (2013) 15394-15406.

[37] A. Shah, R. P. Fishwick, A. G. Leeke, J. Wood, S. P. Rigby, M. Greaves, J. Can. Petrol. Technol. 50 (2011) 33-47.

[38] A. Hart, M. Greaves, J. Wood, Chem. Eng. J. (2015). http://dx.doi.org/10.1016/ j.cej.2015.01.101.

[39] A. Hart, G. Leeke, M. Greaves, J. Wood, Fuel 119 (2014) 226-235.

[40] C.-M. Lin, T.-L. Hung, Y.-H. Huang, K.-T. Wu, M.-T. Tang, C.-H. Lee, C. T. Chen, Y. Y. Chen, Phys Rev B 75 (2007) 125426-1-125426-2.

[41] G. T. Fu, X. Jiang, L. F. Ding, L. Tao, Y. Chen, Y. W. Tang, Y. M. Zhou, S. H. Wei, J. Lin, T. H. Lu, Appl. Catal. B 138 (2013) 167-174.

[42] Y. Chen, B. He, T. Huang, H. Liu, Colloids Surf A Physicochem. Eng. Asp. 348 (2009) 145-150.

[43] J. Zhu, *Synthesis of precious metal nanoparticles supported on bacterial biomass for catalytic applications in chemical transformations*. PhD Thesis, University of Birmingham, 2014

[44] J. Park, S. W. Won, J. Mao, I. S. Kwak, Y.-S. Yun, J. Hazard. Mater. 181 (2010) 794-800.

[45] L. Wu, S. Shafii, M. R. Nordin, K. Y. Liew, J. Li, Mater. Chem. Phys. 137 (2012) 493-498.

[46] M. Hasik, A. Bernasik, A. Drelinkiewicz, K. Kowalski, E. Wenda, J. Camra, Surf. Sci. 507-510 (2002) 916-921.

[47] F. Sen, G. Gokagac, J. Phys. Chem. C 111 (2007) 5715-5720.

[48] Z. Q. Tian, S. P. Jiang, Y. M. Liang, P. K. Shen, J. Phys. Chem. B 110 (2006) 5343-5350.

[49] Y. F. Dufrêne, P. G. Rouxhet, Colloids Surf. B 7 (1996) 271-279.

[50] C. Rodriguez-Navarro, C. Jimenez-Lopez, A. Rodriguez-Navarro, M. T. Gonzalez-Muñoz, M. Geochim. Cosmochim. Acta 71 (2007) 1197-1213.

[51] F. Ahimou, C. J. P. Boonaert, Y. Adriaensen, P. Jacques, P. Thonart, M. Paquot, P. G. Rouxhet, J. Colloid Interf. Sci. 309 (2007) 49-55.

[52] J. S. Corneille, J.-W. He, D. W. Goodman, Surf. Sci. 338 (1995) 211-224.

[53] M. C. Biesinger, B. P. Payne, L. W. M. Lau, A. Gerson, R. S. C. Smart, Surf. Interface Anal. 41 (2009) 324-332.

[54] N. T. Flynn, A. A. Gewirth, J. Raman. Spectrosc. 33 (2002) 243-251.

[55] P. Forzatti, L. Lietti, Catal. Today 52 (1999) 165-181.

[56] A. Hart, *Advanced studies of catalytic upgrading of heavy oils*, PhD thesis, University of Birmingham, UK. 2014.

[57] R. J. Hallam, L. E. Hajdo, J. K. Donnelly, R. P. Baron, SPE Reserv. Eng. 4 (1989) 178-186.

[58] A. Zachariah, L. Wang, S. F. Yang, V. Prasad, A. de Klerk, Energy Fuels 27 (2013) 3061-3070.

[59] S. Alkhaldi, M. M. Husein, Energy Fuels 28 (2014) 643-649.

[60] H. Purón, J. L. Pinilla, I. Suelves, M. Millan, Catal. Today 249 (2015) 79-85.

[61] J. H. Guo, H. Zhang, Y. J. Tang, X. L. Cheng, Phys. Chem. Chem. Phys. 15 (2013) 2873-2881.

[62] F. Sánchez-Minero, G. Sánchez-Reyna, J. Ancheyta, G. Marroquin, Fuel 138 (2014) 193-199.

[63] A. P. Szilas (Ed). *Production and transport of oil and gas*. Elsevier city; 1975. pp. 1–496

[64] L. Wei, Z. Jian-hua, Q. Jian-hua, J. Fuel Chem. Technol. 35 (2007) 176-180.

[65] D. A. Beauregard, P. Yong, L. E. Macaskie, M. L. Johns, Biotechnol. Bioeng. 107 (2010) 11-20.

[66] P. Yong, W. Liu, Z. Zhang, D. Beauregard, M. L. Johns, L. E. Macaskie, Biotechnol. Lett. (2015) 1-11.

[67] G. Q. Li, H. Kobayashi, J. M. Taylor, R. Ikeda, Y. Kubota, K. Kato, M. Takata, T. Yamamoto, S. Toh, S. Matsumura, H. Kitagawa, Nature Mater 13 (2014) 802-806.

[68] X. Y. Chen, J. J. Gao, Y. Z. Lu, H. Meng, C. X. Li, Fuel Process. Technol. 130 (2015) 7-11.

3.3 Interaction of Palladium with Bacterial Cells

This section contains the following studies:

3.3.1 Characterization of Intracellular Palladium Nanoparticles Synthesized by *Desulfovibrio desulfuricans* and *Bacillus benzeovorans*

Journal: Journal of Nanoparticle Research, Published.

3.3.2 Probing the Viability of Palladium-Challenged Cells Using Flow Cytometry

Journal: FEMS Microbioloy Letters, in submission

3.3.1 Characterization of intracellular palladium nanoparticles synthesized by *Desulfovibrio desulfuricans* and *Bacillus benzeovorans*

Jacob B. Omajali [*, 1], Iryna P. Mikheenko [1], Mohamed L. Merroun [2], Joseph Wood [3], Lynne E. Macaskie [1]

[1] Unit of Functional Bionanomaterials, Institute of Microbiology and Infection, School of Biosciences, University of Birmingham, Edgbaston, Birmingham, B15 2TT, United Kingdom

[2] Departments of Microbiology, Faculty of Sciences, University of Granada, Campus Fuentenueva, 18071, Granada, Spain

[3]School of Chemical Engineering, University of Birmingham, Edgbaston, Birmingham, B15 2TT, United Kingdom

*Corresponding author. Tel.: [redacted] fax: [redacted]

Email address: [redacted]; [redacted]

This paper has been published in Journal of Nanoparticle Research. 17 (6), 2015:1-17

This paper was written by J.B. Omajali. All experiments and analysis were performed by the author. Technical assistance on HAADF-STEM was provided by Maria del Mar Abad Ortega (Centro de Instrumentación Científica, University of Granada, Spain).

Abstract

Early studies have focused on the synthesis of palladium nanoparticles within the periplasmic layer or on the outer membrane of *Desulfovibrio desulfuricans* and on the S-layer protein of *Bacillus sphaericus*. However, it has remained unclear whether the synthesis of palladium nanoparticles also takes place in the bacterial cell cytoplasm. This study reports the use of high resolution STEM (Scanning-Transmission Electron Microscopy) with a HAADF (High-Angle Annular Dark Field) detector and EDX (Energy Dispersive X-ray Spectrometry) attachment to investigate the intracellular synthesis of palladium nanoparticles (Pd-NPs). We show the intracellular synthesis of Pd-NPs within cells of two anaerobic strains of *D. desulfuricans* and an aerobic strain of *B. benzeovorans* using hydrogen and formate as electron donors. The Pd nanoparticles were small and largely monodispersed, between 0.2 and 8nm, occasionally from 9 to 12nm with occasional larger nanoparticles. With *D. desulfuricans* NCIMB 8307 (but not *D. desulfuricans* NCIMB 8326) and with *B. benzeovorans* NCIMB 12555 the NPs were larger when made at the expense of formate, co-localizing with phosphate in the latter, and were crystalline, but were amorphous when made with H_2, with no phosphorus association. The intracellular Pd nanoparticles were mainly icosahedrons with surfaces comprising {111} facets and about 5% distortion when compared with that of bulk palladium. The particles were more concentrated in the cell cytoplasm than the cell wall, outer membrane or periplasm. We provide new evidence for synthesis of palladium nanoparticles within the cytoplasm of bacteria, which were confirmed to maintain cellular integrity during this synthesis.

Keywords: *Bacillus benzeovorans*. *Desulfovibrio desulfuricans*. Icosahedron. Intracellular. Palladium nanoparticles.

Introduction

There is an increasing demand for precious metals in the areas of electronics and catalysis. Since the introduction of catalytic converters in the USA in 1975 and in Europe in 1986 (Wiseman and Zereini, 2009), platinum group metals have been widely used to control emission of harmful pollutants like carbon monoxide, nitrogen oxides and unburnt hydrocarbons from automobiles. The ability of palladium to catalyse a wide range of reactions in chemical synthesis makes it the most sought after precious metal in a range of industrial applications (Holt et al. 1999). As a consequence, the high demand for palladium has led to a parallel increase in price (Cowley, 2013) resulting in increasing focus on the clean and sustainable recovery of palladium from waste sources (Cui and Zhang, 2008; Macaskie et al. 2011; Lee and Pandey, 2012) with the potential for bioconversion of wastes into new catalytic materials (Mabbet et al. 2006; Murray et al. 2015).

Microbial recovery of palladium is considered more promising than the conventional methods of bulk recovery (Narayanan and Sakthivel, 2010; Thakkar et al. 2010). Recovery traditionally involves the dissolution of metals from spent catalysts using acids at high temperatures and then application of strong chemical reductants, which are toxic (De corte et al. 2013) and generate undesirable waste products. Bacterial cells act as reducing agents using enzymes, avoiding the use of toxic reagents, and also controlling particle growth *via* 'bio-patterning' (Mikheenko et al. 2008) while minimizing artefacts from surfactants and capping agents (Narayanan and Sakthivel, 2010).

Several studies have focused on the reductive precipitation of soluble precious metal ions to insoluble metals using various pure cultures of dissimilatory sulphate-reducers (de Vargas et al. 2005; Wood et al. 2010; Bennett et al. 2013), *E. coli* (Deplanche et al. 2010; 2012; Foulkes et al. 2011), other facultative anaerobes (Deplanche et al. 2014) and also aerobic bacteria such as *Bacillus sphaericus* (Selenska-Pobell et al. 1999; Fahmy et al. 2006; Creamer et al. 2007). Studies on the use of bacteria in the synthesis of metallic nanoparticles have centred mainly on metal reducing bacteria such as *Geobacter*, *Shewanella* (De Windt et al. 2005; Law et al.

2008; Heugebaert et al. 2012; Yates et al. 2013) and also sulphate-reducers of the genus *Desulfovibrio* (Riddin et al. 2009; Bennett et al. 2010).

The precipitation of palladium by the anaerobic sulphate-reducing bacterium *D. desulfuricans* has been well demonstrated *via* several studies; *e.g.* a primary route for nanoparticle synthesis is *via* hydrogenases (Mikheenko et al. 2008) but other components of the 'nanofactory' are not known. Indeed, *E. coli* stripped genetically of its hydrogenases (Deplanche et al. 2010), or *E. coli* (Foulkes et al. 2011) and *Serratia* spp. (Deplanche et al. 2014) grown aerobically (where hydrogenases are not expressed) reduced Pd (II) to Pd (0), while the aerobic *Bacillus sphaericus* also reduced Pd (II) to Pd (0) nanoparticles very similar to those of *D. desulfuricans,* with similar catalytic activity in hydrogenation of itaconic acid (Creamer et al. 2007) *Bacillus* spp. have long been known to accumulate heavy metals selectively (Selenska-Pobell et al. 1999). Their ability to reduce metals has been studied by various authors (Boone et al. 1995; Cheng and Li, 2009) but the only known route towards the synthesis of nanosized Pd deposits was *via* metal deposition on an S-layer protein (Pollman et al. 2005; Fahmy et al. 2006) which, of several strains examined, was only associated with *B. sphaericus* (Selenska-Pobell et al. 1999). Cells of this strain bind to cationic metals strongly *via* carboxylic groups (*e.g.* glutamic acid) and also to phosphate groups as a result of the extensive phosphorylation of its S-layer protein (Pollman et al. 2005; Merroun et al. 2007). However, Pd nanoparticles were also observed to be localized below the S-layer, and Pd deposition was attributed to other factors (Deplanche et al. 2014). Fahmy et al. (2006) showed that carboxylates of aspartate and glutamate residues are coordination sites for Pd (II) in *Bacillus* spp. S-layer protein. However, the nature and localization of the additional putative "Pd reductase" beneath the S-layer are not known.

The reduction of palladium at the cell surface by various bacterial species has been well documented. However, the formation of intracellular palladium nanoparticles (Pd NPs) in terms of characterization has not been previously examined and this forms the focus of this study. Examination of EDX data (Foulkes et al. 2011) showed intracellular Pd located on the inner surface of the plasma membrane of *E.coli* but details on the nature of the intracellular particles were not discussed further. It has been shown, however, that intracellular metallic nanoparticles could be synthesized by

various micro-organisms. Beveridge and Murray (1980) reported precipitation of gold nanoparticles within bacterial cells from Au^{3+} which was confirmed in later work (Southman and Beveridge, 1996). Using cells of lactic acid bacteria, Nair and Pradeep (2002) synthesized intracellular nanoparticles of gold, silver and also alloys. Other examples include intracellular gold nanoparticles made *via* a novel alkalotolerant actinomycete, *Rhodococcus* species (Ahmad et al. 2003) and *Shewanella alga* (Konishi et al. 2006). More recent studies continue to report the synthesis of intracellular non-precious metal nanoparticles (Peng et al. 2010; Navarrete et al. 2011; Polti et al. 2011; Ravindranath et al 2011; Sousa et al. 2013) but the characterization of intracellular Pd-NPs has never been performed. Confirmation of the formation of intracellular Pd NPs not associated with the cell membrane will prompt further fundamental questions into the underlying mechanisms of intracellular 'trafficking' of non-essential precious metals to key locations within bacteria; identification of the underlying biochemical mechanisms, would, in turn, provide tools for the application of synthetic biology towards enhancing nanoparticle production.

This current study examines intracellular Pd (0) deposition by two strains of *D. desulfuricans* and a strain of *B. benzeovorans* using hydrogen and formate as electron donors. *D. desulfuricans* NCIMB 8307 was noted to have a higher biosorption capacity (de Vargas et al. 2005) than other strains of the same genus which is key to making catalytically very active bio-Pd. However, *D. desulfuricans* NCIMB 8307 has never been compared with a closer relative within the same species. *D. desulfuricans* NCIMB 8326 was chosen since this strain (unlike NCIMB 8307) lacks fatty acid ethanolamide (Goldsworthy, 2011), a candidate species for the initial amide-coordination (de Vargas et al., 2005) of incoming Pd (II). A better understanding of the mechanism of patterning of Pd NPs in *D. desulfuricans*, and exploiting subtle strain-dependent differences, could provide useful tools in potential molecular design to improve bio-Pd catalyst. This would provide insight as to what improvements could be expected or aimed for, and on how to potentially improve catalyst selectivity in a range of reactions and products. The literature in this area of research continues to expand but there is relatively little focus on the mechanisms of Pd (0) deposition and patterning.

This study compares two methods for the synthesis of intracellular bio-Pd nanoparticles in *Desulfovibrio and Bacillus*. The first method involves the reduction of

Pd (II) in the presence of hydrogen as the electron donor at room temperature while in the second method the temperature was set at 30^{o}C in order to increase the reaction rate using formate (Shi et al. 2013). A marked difference in the patterning or formation of the bio-Pd nanoparticles was sought as the first indication of the potential for nanoparticle "steerage" according to the condition of biomanufacture.

Materials and methods

Bacterial strains, culture conditions and harvest

The following bacteria were used in this study: two strains of anaerobic *Desulfovibrio desulfuricans* (NCIMB 8307 and NCIMB 8326) and one strain of aerobic *Bacillus benzeovorans* NCIMB 12555. The *D. desulfuricans* were grown anaerobically under oxygen-free nitrogen in Postgate's medium C (pH 7.5 ± 0.2) at 30^{o}C (inoculated from a 24 hour pre-culture, 10%v/v) in sealed anaerobic bottles (Deplanche et al. 2010) while *B. benzeovorans* was grown aerobically (rotary shaker; 180 rpm, 30^{o}C) in nutrient medium (pH 7.3 ± 0.2) of the following composition: 1.0g beef extract (Sigma-Aldrich, UK), 2.0g yeast extract (Sigma-Aldrich, UK), 5.0g peptone (Sigma-Aldrich, UK) and 15.0g NaCl per litre of distilled water. Cells were harvested (Beckman Coulter Avati J-25 Centrifuge, U.S.A) by centrifugation (9,000 x g, 15minutes at 4^{o}C) at mid-exponential phase (OD_{600} 0.5-0.7 for *D. desulfuricans*; OD_{600} 0.7-1.0 for *B. benzeovorans*), washed three times in air with 20mM MOPS (4-morpholinepropanesulfonic acid)-NaOH buffer, pH 7.0 and then concentrated in a small amount of the same buffer to usually 20-30mg/ml as determined by reference to a pre-determined OD_{600} to dry weight conversion as previously described (Deplanche et al. 2010). The concentrated cells of known OD_{600} were degassed and stored under oxygen-free nitrogen (OFN) at 4^{o}C until use, usually within 24h.

Preparation of palladium-challenged cells

A known volume of a concentrated resting cell suspension was transferred into an appropriate volume of degassed (30 minutes) 2mM Pd (II) salt solution (Na_2PdCl_4, pH 2 ± 0.1 adjusted with 0.01 M HNO_3) to make a 20% loading (1:5) on biomass of *D.*

desulfuricans and *B. benzeovorans.* Complete removal of Pd onto cells was determined by assay (below). The cells and palladium mixture were allowed to stand in a water bath (30 min, 30^{o}C) for biosorption of the Pd (II) onto the cell surfaces of each strain with occasional shaking. Hydrogen and formate were used separately as exogenously-applied electron donors for Pd (II) reduction to Pd (0). The first method involves reduction under hydrogen at room temperature by bubbling hydrogen through the suspension (15 minutes) and then leaving in the head-space for reduction to reach completion (15 minutes). In the second method, sodium formate was added to a final concentration of 20mM from a 1M stock with shaking at 30^{0}C (overnight). The products were harvested by centrifugation (9,000 x g, 4^{o}C, 15 minutes) prior to examination by electron microscopy.

Pd (II) assay using tin (II) chloride

Prior to harvesting the palladized cells, the complete removal of Pd (II) from the solution was confirmed by the tin (II) chloride assay method as described previously (Deplanche et al. 2010) spectrophotometrically (Ultraspec III, Pharmacia Biotech, Little Chalfront, Buckinghamshire, UK). Stock tin (II) chloride was prepared by dissolving 29.9 g $SnCl_2$ powder into 500 ml HCl and diluted fresh (aq) with the samples for use as required.

High resolution scanning-transmission electron microscopy (STEM) with HAADF (high-angle annular dark field) detector and EDX analysis

Pd-loaded cells of *D. desulfuricans* and *B. benzeovorans* prepared using both hydrogen and formate as electron donors were harvested as above, washed twice with distilled water and fixed with 2.5% (w/v) glutaraldehyde fixative in 0.1M cacodylate buffer (pH 7.0) at 4^{o}C and stained with 1% aq osmium tetraoxide. For STEM (Scanning and Transmission Electron Microscopy) and EDX (Energy Dispersive X-ray spectroscopy), the Pd-loaded cells were dehydrated using an ethanol series and washed twice in propylene oxide (Deplanche et al. 2010). The cells were embedded in epoxy resin and cut into sections (100-150nm thick) and mounted on carbon-coated copper TEM grids.

Electron opaque deposits were examined by EDX with peaks sought corresponding to X-ray emission energies of Pd (Yong et al. 2002). STEM and EDX were done using a FEI image Cs-corrector configuration Titan^{TM} G2 60-300 STEM microscope equipped with HAADF detector, accelerating voltage of 300kV.

Image processing, lattice spacing and particle size analysis

The images obtained with HAADF-STEM were imported into image processing software, "Image " and analysed (Abramoff et al. 2004; Schneider et al. 2012). The bandpass filter function was applied in order to distinguish the Pd nanoparticles on cells of the three bacteria from background signals and artefacts by adjustment. This was followed by image thresholding and the total number of the Pd nanoparticles on bacterial cells was counted and the particles size diameter was calculated. The particle size distribution was then estimated ("Origin C"). From these values, the dispersity of Pd nanoparticles was calculated using a Gaussian function. The lattice spacings were also determined using "Image " through profiling of high resolution HAADF-STEM images and compared against lattice spacing of bulk palladium from the database generated using "Powder cell 2.4" software.

Results

Examination of Pd-nanoparticles by electron microscopy and EDX

High-resolution HAADF-STEM (High-Angle Annular Dark Field-Scanning Transmission Electron Microscopy) with EDX (Energy Dispersive X-ray Spectrometry) was used to confirm the identity of cellular nanoparticles as Pd within cells of *B. benzeovorans* and *D. desulfuricans* (Figs. 1A-L). Sections of samples produced with hydrogen as electron donor (Figs. 1A, B, E, F, I, and J) show bacteria with intracellular nanosized particles identified as Pd (below) and occasional larger inclusions. Cells unchallenged with Pd (II) showed no accumulated nanoparticles at their surfaces or intracellularly (S1). Few Pd nanoparticles were visible at the surface of *B. benzeovorans* NCIMB 12555 (Figs. 1A, B) while *D. desulfuricans* NCIMB 8307 (Figs. 1E, F)

supported surface-bound Pd (0) but none was apparent on *D. desulfuricans* NCIMB 8326 (Figs. 1I, J). In *B. benzeovorans* NCIMB 12555 reduced with formate (Fig 1D), there were more numerous Pd nanoparticles located within the intracellular matrices than in the outer layers. At high magnification, HAADF-STEM images revealed many intracellular Pd nanoparticles in *B. benzeovorans* NCIMB 12555 (Fig. 1B) and *D. desulfuricans* NCIMB 8307 (Fig. 1F) but fewer in *D. desulfuricans* NCIMB 8326 (Fig. 1J). However, it would be very useful to compare these difference based on variation in bacterial cell volume to the amount of intracellular Pd NPs.

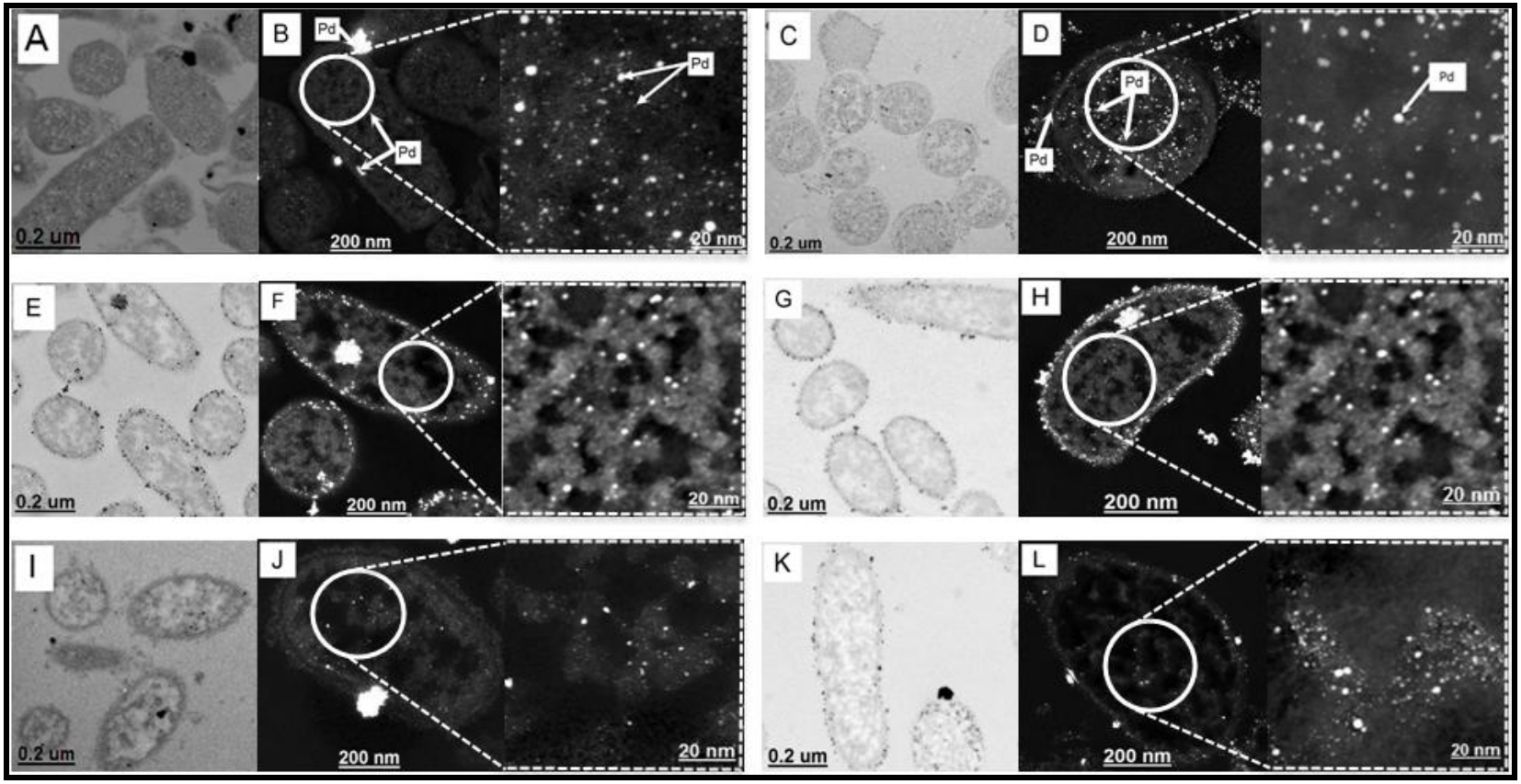

Fig 1 HAADF-STEM micrographs of intracellular Pd nanoparticles synthesized using 20% by mass Pd loading (1:5) on bacterial cells from 2mM Na_2PdCl_4 solution, in 0.01M HNO_3 using hydrogen (left) and formate (right) as electron donors: Ordinary TEM images of Pd nanoparticle deposits on bacteria (A, C, E, G, I, K); HAADF-STEM of Pd nanoparticles in cells coupled with high resolution HAADF-STEM of a section of intracellular Pd nanoparticles (B, D, F, H, J, L) in *B. benzeovorans* NCIMB 12555 (top), *D. desulfuricans* NCIMB 8307 (middle) and *D. desulfuricans* NCIMB 8326 (bottom)

A similar trend was observed when formate was used as the electron donor, (Figs. 1C, D, G, H, K, and L) with some extracellular Pd-nanoparticles present in each case. However, under hydrogen or formate as electron donors, only *D. desulfuricans* NCIMB 8307 had a major deposition of surface-bound nanoparticles (Figs. 1E, F, G, and H). While mostly invisible in TEM micrographs (Figs. 1A, E, I, C, G, K), intracellular nanoparticles were visible in all three strains at high resolution using electron backscattering (Figs. 1 B, F, J, D, H, L).

It was confirmed that irrespective of the electron donors used, Pd NPs were present in the cytoplasm of cells by using STEM –EDX mapping of palladized bacteria. This allowed the identification of Pd clusters with phosphorus (P) and sulphur (S), as the major inorganic elements (Figs. 2 A-F). Elemental mapping (Fig. 2 and S2) shows that only cells that had significant detectable Pd also showed S and P detected above the background. The co-localization of Pd and S in larger deposits within *D. desulfuricans* (Fig. 3A) was assumed to be PdS as a result of biogenic H_2S production but was not investigated further. No clear co-localization of S otherwise, nor of P, was seen in *D. desulfuricans* (Fig. 3A) but *B. benzovorans* evidenced co-localization (Fig 3C) of Pd and P (Fig. 3B, circled). The presence of S is seen as a normal constituent of bacterial proteins and P within deoxyribonucleic acids, ribonucleic acids, phospholipids, techoic acids and other compounds (Southman and Beveridge, 1996) but it is not clear why these elements are more evident in cells that showed internal Pd desposition. Southman and Beveridge (1996) showed the co-appearance of intracellular gold crystals with S and P in *B. subtilis*, in which it was suggested that the signals from S and P could have been contributed due to organic film from the bacteria and coatings on the Au crystals used. It is possible that complexation of macromolecules with Pd depletes available cellular reserves, stimulating overproduction to compensate. It could also mean a detoxification mechanism which reduces the mobility, and in turn, the toxicity of Pd nanoparticles by neutralizing the negative charges of Pd nanoparticles by P and S containing molecules in the cell. The incorporation of palladium nanoparticles within organic materials may help to stabilize them and control their size *e.g.* proteins within the network of calcium carbonates in *Myxococcus xanthus* have been shown to stabilize the structure of these biogenic Ca carbonates (Rodriguez-Navarro et al. 2007). We conclude that, while surface-bound Pd-NPs have been reported extensively using

many microorganisms (Creamer et al. 2007; Foulkes et al. 2011; Bennett et al. 2013; De Corte et al. 2013; Deplanche et al. 2014) we now show evidence for intracellular localization of palladium and hence an inference of the ability of Pd (II) to be translocated *via* cellular transport and deposition mechanisms which await further study. Other studies, to be reported in a subsequent publication, used flow cytometry to confirm continued cell integrity and metabolism during the process of Pd deposition.

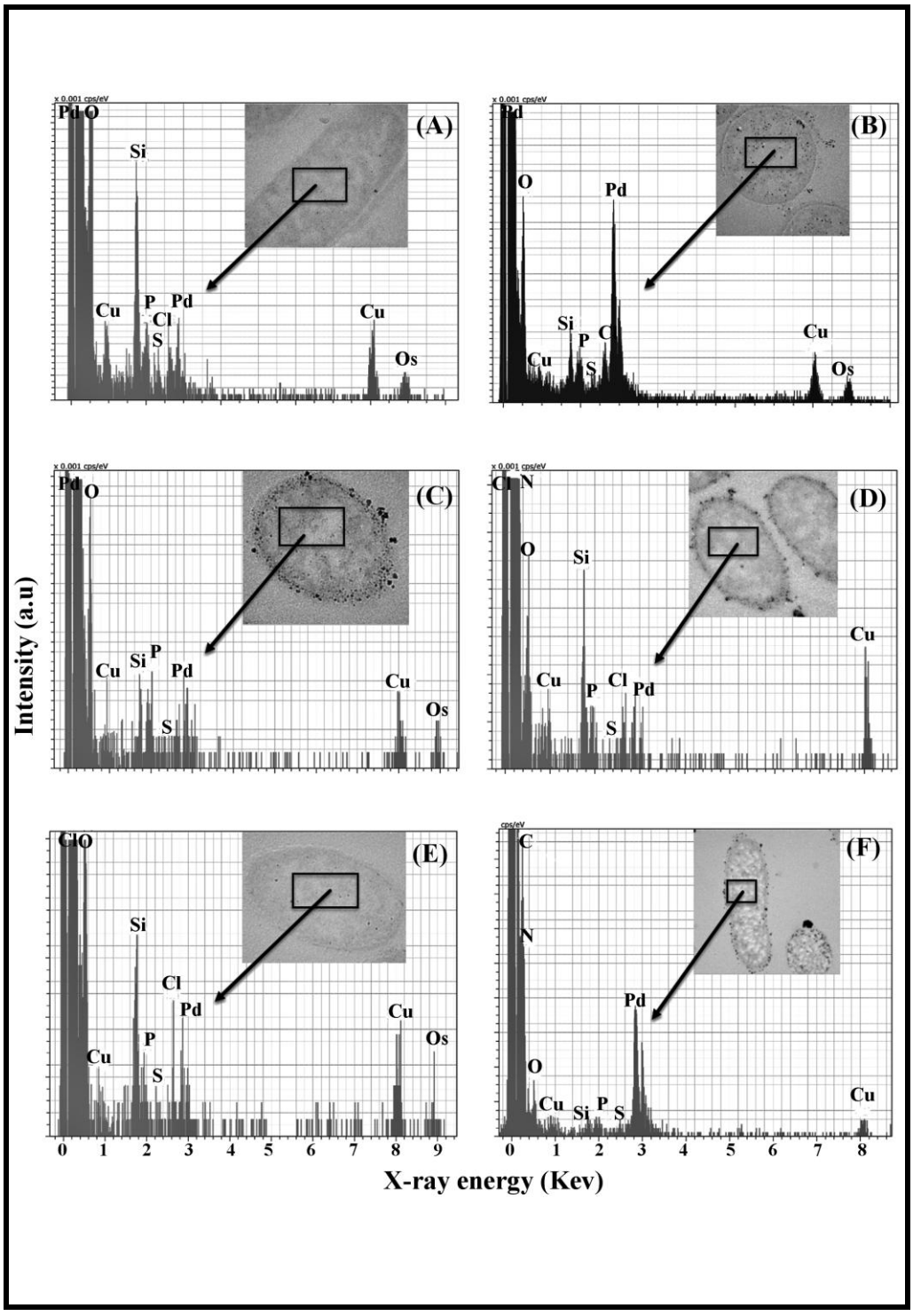

Fig 2 HAADF-STEM-EDX analysis of intracellular Pd nanoparticles (selected areas shown) with phosphorus (P) and sulfur (S) in *B. benzeovorans* NCIMB 12555 (A, B-top), *D. desulfuricans* NCIMB 8307 (C, D-middle) and *D. desulfuricans* NCIMB 8326. The Cu is from the TEM grid while the silicon results from the oil in the diffusion pump of the column of the TEM system

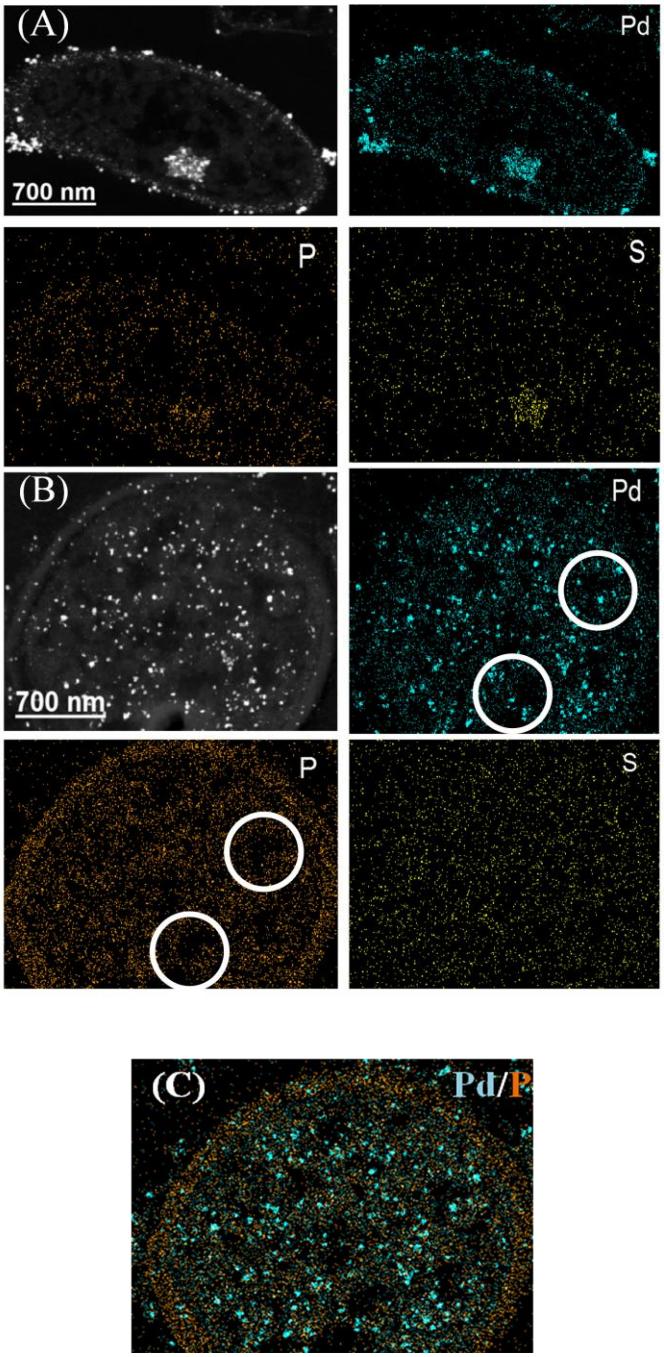

Fig 3 EDX Elemental mapping showing Pd, P and S in *D. desulfuricans* NCIMB 8307 (3A) and *B. benzeovorans* (3B) while 3C shows an overlay of Pd and P from 3B . Only *B. benzeovorans* shows co-localization of Pd with P (white circle) but not S within the cell cytoplasm. From imagej, Costes test for colocalization shows a correlation (R = 0.96) and Mander's overlap coefficient (R = 0.998) indicative of high colocalization between Pd and P.

Dispersity and distribution of intracellular Pd nanoparticles.

High resolution images allowed the calculation of particle size distribution using "Image " software (Abramoff et al. 2004; Schneider et al. 2012). The mean particle sizes of the intracellular Pd nanoparticles were calculated as shown in Figs. 4A-F and Table 1. When hydrogen was used as the electron donor, the ranking of the mean particle size followed the order *D. desulfuricans* NCIMB 8307 > *B.benzeovorans* NCIMB 12555 > *D. desulfuricans* NCIMB 8326 (Figs. 4C, A, E). A similar ranking of the mean particle diameter of the Pd-NPs produced was observed using formate (Figs. 4D, B, F and Table 1). The particle size distributions were similar in the case of *B. benzeovorans* and *D. desulfuricans* NCIMB 8307 (Figs. 4A, B, C, D), especially cells in Figs. 1B, D from formate but skewed towards small NPs when Pd (II) was reduced under H_2 (cells in Figs. 1A, C). Very little difference was apparent using the two electron donors with *D. desulfuricans* NCIMB 8326 (Figs. 4E, F) skewed in each case, although larger NPs were produced at the expense of formate by the other two strains (Table 1).

Table 1 Particle size distribution of intracellular Pd nanoparticles

Cell type	Mean Particle size (nm)		Dispersity			
			Polydispersity index		Monodispersity (%)	
	Reducing agents					
	Hydrogen	Formate	Hydrogen	Formate	Hydrogen	Formate
B. benzeovorans NCIMB 12555	1.70 ± 0.41	5.80 ± 2.24	0.24	0.39	76	61
D. desulfuricans NCIMB 8307	3.57 ± 0.77	6.97 ± 2.46	0.22	0.35	78	65
D. desulfuricans NCIMB 8326	1.10 ± 0.95	1.20 ± 0.69	0.86	0.58	14	42

Mean particle size distribution of intracellular Pd nanoparticles produced by three strains of bacteria using hydrogen and formate as electron donors. The polydispersity index was calculated from the particle size distribution using a Gaussian function and the monodispersity values were converted into percentage values. In all, >100 particles were counted in each case using "Image " software. 20% by mass Pd loading (1:5) on cells of each bacterium was used from 2mM Na_2PdCl_4 solution, in 0.01M HNO_3. Data are Means ± Standard deviation of the means. The polydispersity index was derived from the standard deviation of a Gaussian function fitted to the data. From this, the monodispersity was calculated as a percentage. Polydispersity is the degree of heterogeneity (non-uniformity) of sizes of molecules or particles while mondispersity is the degree of homogeneity (uniformity) of sizes of molecules or particles.

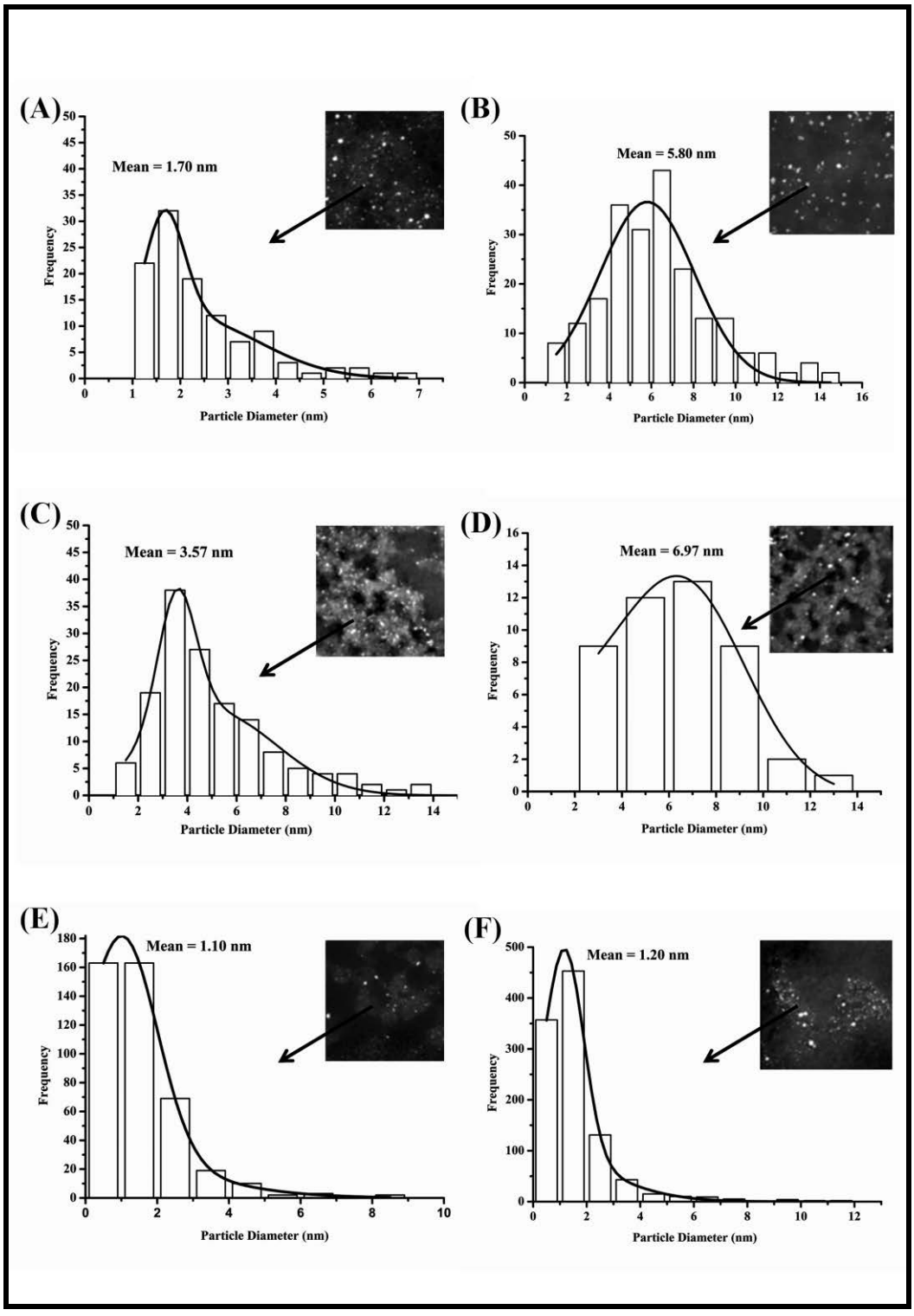

Fig 4 Particle size distribution of intracellular Pd nanoparticles made using hydrogen (left) and formate (right) as electron donors with *B. benzeovorans* NCIMB 12555 (A, B -top), *D. desulfuricans* NCIMB 8307 (C, D-middle) and *D. desulfuricans* NCIMB 8326 (E, F -bottom) respectively and > 100 particles were counted in each case.

In order to determine the degree of dispersity of the Pd nanoparticles, the polydispersity indices were calculated from the size distribution of the nanoparticles, while the monodispersity was presented in percentages (Table 1). *D. desulfuricans* NCIMB 8326 produced the most heterogeneous Pd nanoparticles with a polydispersity index of 0.86, resulting in 14% monodispersity (Table 1) under hydrogen as electron donor. In contrast, the Pd-NPs of *D. desulfuricans* NCIMB 8307 and *B. benzeovorans* NCIMB 12555 were less polydispered with similar polydispersity indices of 0.22 and 0.24 respectively, meaning that 78% and 76% (Table 1) of the Pd nanoparticles were monodispersed. Overall, the degree of homogeneity of intracellular Pd nanoparticles produced by the three strains of bacteria followed the order *D. desulfuricans* NCIMB 8307 > *B. benzeovorans* NCIMB 12555 > *D. desulfuricans* NCIMB 8326.

The polydispersity indices of the intracellular Pd nanoparticles reduced with formate were higher than the indices of Pd NPs reduced by using hydrogen except for *D. desulfuricans* NCIMB 8326 (Table 1). Under formate-mediated reduction, the polydispersity indices calculated for *B. benzeovorans* NCIMB 12555, *D. desulfuricans* NCIMB 8307 and *D. desulfuricans* NCIMB 8326 Pd NPs were 0.39, 0.35 and 0.58 respectively, corresponding to a degree of homogeneity (monodispersity) of the Pd nanoparticles of 61%, 65% and 42% respectively (Table 1), revealing that *D. desulfuricans* NCIMB 8326 had the least homogeneously distributed intracellular Pd nanoparticles. According to Nidhin et al. (2008) a polydispersity index of > 0.7 is associated with samples with very broad size distribution and only the NPs of *D. desulfuricans* NCIMB 8326 exceeded this value under hydrogen. Using formate as an electron donor, Shi et al. (2013) chemically synthesized Au-Pd alloy nanocrystals and obtained very large (~20nm) and irregularly shaped nanoparticles when compared with stronger reducing agents like $NaBH_4$ and ascorbic acid. This was attributed to the differences in reaction kinetics (Shi et al. 2013). Formate is a weaker reducing agent than hydrogen taking more time for bio-reduction to reach completion using bacterially-mediated reduction (I.P Mikheenko and L.E. Macaskie, unpublished). Hence, the reduction of Pd (II) by formate was done at 30^0C with constant agitation to increase the reaction rate while hydrogen reduction was accomplished at room temperature by bubbling it through the cell suspension. The rates of uptake and reduction of Pd (II) in each case were not measured.

Crystallinity and lattice spacing of intracellular Pd nanoparticles

High resolution TEM images revealed that, while the Pd nanoparticles produced by *B. benzeovorans* (Fig. 5A) were amorphous under hydrogen as electron donor, those produced by this strain from formate and in both cases by *D. desulfuricans* NCIMB 8307 (Fig. 5C) and *D. desulfuricans* NCIMB 8326 (Fig. 5E) were crystalline. The lattice spacings of representative crystalline particles were 0.250nm, 0.243nm and 0.258nm for *D. desulfuricans* NCIMB 8307 (Fig. 5C), which is consistent with the {111} facet of Pd, exposing mainly the {111} facets to the surface (Fig. 5C) with some particles appearing to be icosahedral in shape (Bennett et al., 2013) comprising mainly single crystal structures for *B.benzeovorans* NCIMB 12555 (Fig. 5B) and multiply twinned structures for *D. desulfuricans* NCIMB 8307 (Figs. 5C, D) and *D. desulfuricans* NCIMB 8326 (Figs. 5E, F) which may have formed as a result of particle growth *via* coalescence (Lim et al. 2008). The values of the Pd planes showed a distortion of about 5% when compared with the values generated for bulk palladium from the database using "Powder cell 2.4" software. About 10% distortion of the {111} facet for extracellular Pd nanoparticles from *D. desulfuricans* NCIMB 8307 (Bennett et al. 2013) and a 12.5% expansion of the {200} facet of Pd nanoparticles synthesized chemically on amorphous carbon (José-Yacamán et al. 2001) were reported. Shapes are characterized according to the type of facets exposed to the surface; octahedrons and icosahedrons have their surfaces covered mainly by {111} facets (Zhang et al. 2013). Only *D. desulfuricans* NCIMB 8326 reduced under hydrogen showed a mix-facet arrangement of Pd nanoparticles with lattice spacings of 0.208nm and 0.248nm (Fig. 5E), corresponding to the {200} and {111} facets respectively (Fig. 5E). This Pd nanostructure is similar to a cubo-octahedron or its truncation (José-Yacamán et al. 2001). The reason for the production of amorphous Pd nanoparticles by *B. benzeovorans* under hydrogen (Fig. 5A) remains unclear and is the focus of an ongoing study which also aims to compare the catalytic activities of the different Pd-types. Reduction *via* formate, however, showed that the resulting intracellular Pd-NPs were crystalline and very similar (Figs. 5B, D, F) for all three strains. The lattice spacing for these nanocrystals was analysed for *B. benzeovorans* NCIMB 2555 (0.250nm), *D. desulfuricans* NCIMB 8307 (0.250nm) and *D.desulfuricans* NCIMB 8326 (0.241nm and 0.250nm) corresponding to the {111} facets exposed to the surface as shown by

representative TEM images (Figs. 5B, D, F) with similar distortions as the Pd reduced by hydrogen (Figs. 5A, C, E).

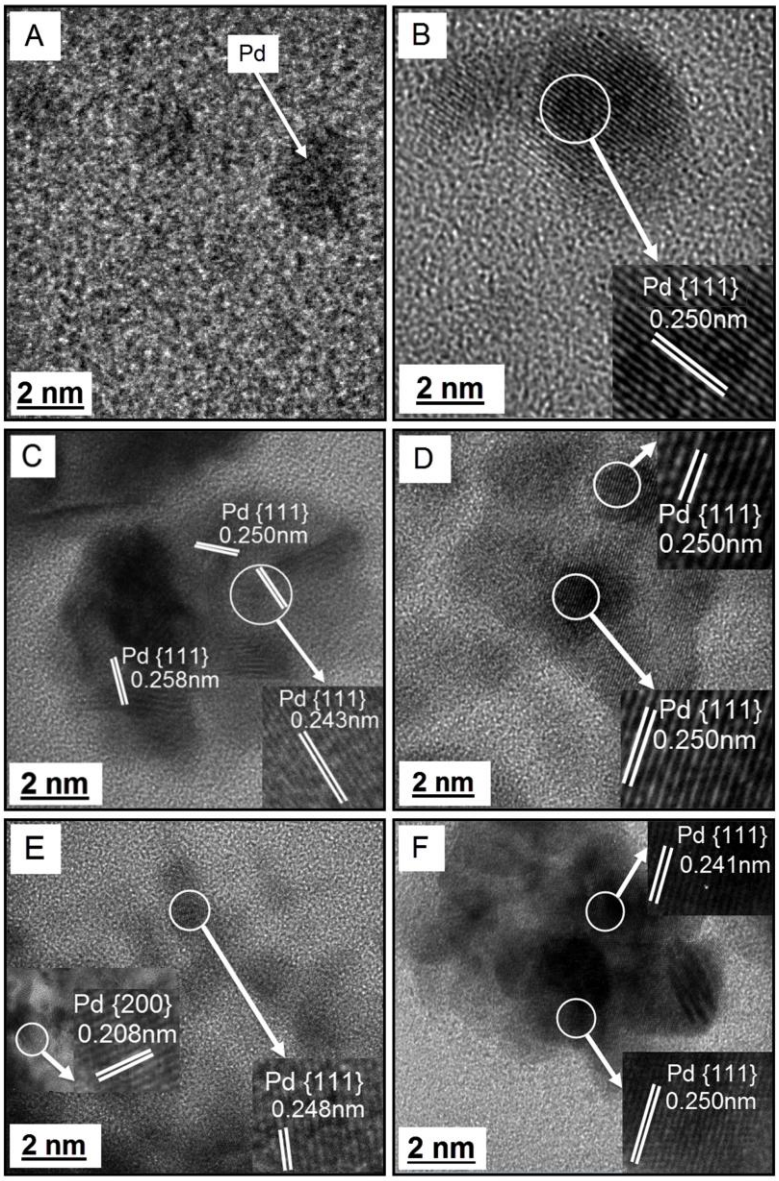

Fig 5 High resolution TEM images of intracellular Pd crystals with insets revealing lattice spacing in crystals made using hydrogen (left) and formate (right) as reducing agents; *B. benzeovorans* NCIMB 12555 (top), *D. desulfuricans* NCIMB 8307 (middle) and *D. desulfuricans* NCIMB 8326 (bottom) respectively.

Discussion

This study focuses on the synthesis and characterization of intracellular palladium nanoparticles in aerobic and anaerobic bacteria made *via* hydrogen and formate as electron donors, whereas most previous studies have been focused on surface Pd-NPs. Hydrogen and formate are metabolized differently with the possibility of affecting the synthesis and patterning of Pd nanoparticles in bacterial cells. Chemical reduction of palladium (II) under hydrogen or formate using killed bacterial cells was significantly slower (Mikheenko et al. 2008). A substantial number of surface-bound Pd nanoparticles was shown on the surface of *D. desulfuricans* NCIMB 8307 but not apparent in the cells of NCIMB 8326 using H_2 as electron donor which is supported by previous reports of Pd binding on cell surfaces and within the periplasmic layer (Bennett et al. 2010). For use as catalysts the palladized bacteria are routinely washed in acetone which destabilizes and removes lipid membrane structures, to allow access to intracellular as well as surface-localized NPs, but during NP synthesis continued membrane integrity (and hence the permeability barrier) was confirmed using flow cytometry (see section 3.3.2). Hydrogenases are located predominantly periplasmically in *D. desulfuricans* (Hatchikian et al. 1990; Casalot et al. 1998) and have been implicated to play important roles in Pd (II) reduction (Mikheenko et al. 2008). In the case where hydrogen was used as electron donor, it is possible that hydrogenases play a dominant role (alongside other enzymes and electron-generating biomolecules) in determining the nature of the final Pd NPs in the two strains of *D. desulfuricans* (Figs. 5C, E) but the absence of surface-bound Pd in *D. desulfuricans* NCIMB 8326 suggests that alternative mechanism(s) predominate in this strain. In *B. benzeovorans* (grown aerobically where hydrogenases are not present) only amorphous Pd nanoparticles were visible (Fig. 5A) suggesting a possible involvement of other mechanisms. In previous studies, Mikheenkho et al. (2008) observed that *Desulfovibrio fructosovorans* deficient in its periplasmic hydrogenases relocated the bio-Pd (0) deposits to the cytoplasmic membrane, which was the site of the remaining hydrogenases. This was further supported by similar work involving hydrogenase deficient *E. coli* mutants (Deplanche et al. 2010), where alternative supplementary mechanisms were implied.

While there were differences in terms of the shapes of the intracellular Pd NPs under hydrogen, the shapes of the Pd NPs using formate as an electron donor appeared to be mainly crystalline icosahedrons. However, this major, thermodynamically stable, nanostructure (formed due to its lowest surface energies and slower growth rate: Xiong et al. 2007; Zhang et al. 2013), differs between the bacterial types. Most of the final Pd nanocrystals made within Gram-positive *B. benzeovorans* were single nanocrystals while those within the two Gram-negative strains of *D. desulfuricans* could be seen as multiply twinned nanoparticles (Ascencion et al. 1998). It is possible that an association with cellular phosphate structures (Fig. 3B) reduced the mobility of the NPs within the cells of the former and stabilized them against agglomeration whereas no apparent associations were seen in the Gram-negative cells. Chemically synthesized nanoparticles of Pd on carbon have been shown with four basic shapes: FCC (face-centred cubic), cubo-octahedral, icosahedral and twinned shapes (José-Yacamán et al. 2001). Shapes, together with the atoms at corners and edges, define the facets and surface structure of nanoparticles *e.g.* icosahedrons are formed only by {111} planes (Xiong et al. 2007). Several factors like the metal salt precursors, capping agents, stabilizers and reducing agents can influence the final shapes of nanoparticles. For example, the chemical reduction of palladium (II) acetylacetonate (Pd $(acac)_2$) in the presence of tetraethylene glycol (TTEG) resulted in the formation of tetrahedral Pd NPs while octahedrons with {111} facets (Wang et al. 2013) were formed with Na_2PdCl_4 and a Pd cubo-octahedron was synthesized in the presence of ethylene glycol (EG) and polyvinylpyrrolidone (PVP) (Zhang et al. 2013). Icosahedral Pd nanoparticles were formed chemically by reducing H_2PdCl_4 in the presence of TTEG (Chen et al. 2009) which was suggested to be due to the higher viscosity and milder reducing property of TTEG than EG. That could indicate a reason for the formation of mainly icosahederal crystalline intracellular Pd nanostructures by the three bacteria in the presence of formate, a milder reducing agent than hydrogen, within heavily hydrated gel-type cellular matrices. However, it is equally possible that, intracellularly, formate is oxidized enzymatically with another biomolecule effecting the final electron transfer onto Pd (II).

Palladium nanoparticles made *via* using formate as electron donor were shown to be similar (crystalline) for each bacterial strain. Formate, like hydrogen, must be

broken down to release the electrons needed for the reduction of Pd (II). The first deposited Pd (0) can split formate chemically by weakening the C-H bond due to interaction of a delocalized electron pair with the surface of Pd (0) (Rhodin and Ertl, 1979). This mechanism releases CO_2 and H_2. H_2 is then split on the surface of Pd (0) to yield single electrons for the subsequent reduction of Pd (II) to Pd (0) (Livingstone, 1973); hence, enzymatic involvement is not obligatory.

Biochemically, in anaerobic bacteria, formate bio-oxidation provides electrons for pathways that utilize final electron acceptor molecules other than dioxygen (Mota et al. 2011) while NAD^+ is an intermediate electron/proton acceptor in aerobes using oxygen as the terminal electron acceptor. However, it was shown that an anaerobic growth condition lowers the production of NAD^+ in *Bacillus cereus* (de Sarrau et al. 2012) at low temperature suggesting a possible use of other alternative electron carriers under these conditions. Enzymatic formate oxidation is made possible by formate dehydrogenases (FDH) (Costa et al. 1997; Ding et al. 2011). An early study (Weimer, 1984) reported that formate, a product of glucose fermentation in *Bacillus macerans,* was gradually depleted with a resultant detection of CO_2 and H_2; the addition of exogenous formate led to the formation of CO_2 and H_2. Pyruvate formate lyase and formate dehydrogenase (FDH) activities were then detected in cell extracts which confirmed the enzymatic oxidation of formate in this strain. In anaerobes, formate hydrogen-lyase (FHL) (Axley et al. 1990) is responsible for splitting formate to make hydrogen. The metal-containing FDH *e.g.* the molybdenum-containing FDH in *E.coli* (Jormakka et al. 2002) and tungsten-containing FDH in *D. gigas* (Raaijmakers et al. 2002) are typical of anaerobic bacteria, while the NAD^+-dependent FDH found in *e.g. Bacillus* spp. F1 (Ding et al. 2011) and *Rhodobacter capsulatus* (Hartmann and Leimkuhler, 2013) are located in the cytoplasm and differ in composition and in the mechanism of formate metabolism (Hartmann and Leimkuhler, 2013). Regardless of the specific enzymatic mechanism, the process of formate oxidation provides the source of electrons needed for the reduction of Pd (II) into nanoparticles by the bacteria.

Intracellular Pd nanoparticles were visible in each strain using both electron donors. The intracellular nanoparticles, generally too small to be readily visible in TEM micrographs, were shown to be present *via* electron backscattering and confirmed as Pd

via EDX analysis. The behavior of *B. benzeovorans* and *D. desulfuricans* NCIMB 8307 was similar in terms of the dispersity of their intracellular Pd-NPs when compared with *D. desulfuricans* NCIMB 8326. Deplanche et al. (2014) highlighted a possible 'Pd (II)-trafficking' across the cytoplasmic membrane developed from a report (Foulkes et al. 2011) whereby Pd (II) reduction by anaerobic *E. coli* was attributed in part to the Pd (II) travelling across the cytoplasmic membrane by an unknown translocation mechanism. However, this was not characterized, nor the mechanism by which further transport into and across the cytoplasm was facilitated. Ni (II) is a key component of metalloenzymes like hydrogenases and ureases (Mulrooney and Hausinger, 2003; Liermann et al. 2007) and both enzymes are commonly found in the bacterial cytoplasm. Since Pd (II) shares some similar chemistry with Ni (II), it was suggested that Pd (II) could be transported through Ni (II) 'trafficking' systems (Deplanche et al. 2014) as a possible route to its unproductive delivery into intracellular enzymes, with deposition as cytoplasmic inclusions as a possible method for 'packaging' physiologically redundant but potentially cytotoxic metals. Like Pt, Pd is well known to bind to DNA (Shoukry and Mohamed, 2012). In this context, although the occasional larger Pd-inclusions visible in *D. desulfuricans* (Fig. 3A) resemble cell nuclei, this is unlikely to be the explanation as the DNA of bacteria is distributed around the cell and not within nuclear bodies and, furthermore, DNA binding would account for the co-occurrence of Pd with P in *B. benzeovorans* but not S. Molecular "destinations" for Pd (II) in lieu of Ni (II) would provide a possible rationale for the presence of intracellular Pd nanoparticles as many metalloproteins can select the wrong metals when presented with a mixture of other metals because protein metal-coordination sites can be quite receptive to inorganic or non-essential partners (Waldron and Robinson, 2009). For example, Cd (II) can replace Zn (II) in carbonic anhydrase in *Thalassiosira weissflogii* (a diatom), a possible evolution of enzyme capable of working with Cd in prokaryotes in Cd-polluted environments (Xu et al., 2008). Also, the high affinity of Hg and Cd to thiols makes them liable to outcompete Zn for protein-binding sites that contain cysteine which can result in the inactivation of Zn-requiring proteins (Frausto da Silva and Williams, 2001) just as Ag and Au (non-essential metals) can inactivate Cu in proteins (Gupta et al., 1999). However, as far as we are aware, Pd (II) cannot substitute biochemically for Ni (II) and hence in this study the cell would be left with a burden of Pd (II). Since Pd (II)

(redox potential of +0.99V) (Hayes, 1993) is reduced more easily than Ni (II) (-0.27V), it is possible that in order to maintain the homeostasis of the intracellular environment, the cell attempts to expel Pd (II) as a consequence of a stress response *via* Ni exporters such as the ABC transporter or P-type ATPases (Silver and Phung, 1996; Hendricks and Mobley, 1997) but instead fortuitously reduces Pd (II) and deposits Pd (0) within the intracellular matrix as a by product of a failed attempt to incorporate Pd (II) instead of Ni (II) into enzymes or proteins. It is still unknown how Pd (II) is trafficked within the cell. The literature on Ni-trafficking is extensive and the reader is referred to other published works (see Maroney, 1999; Eitinger and Mandrand-Berthelot, 2000; Waldron and Robinson, 2009) as the mechanistic aspects of Pd-metabolism are beyond the scope of this paper.

Conclusions

This study has demonstrated the synthesis of intracellular Pd nanoparticles by *B. benzeovorans* NCIMB 12555 (Gram-positive, aerobic bacterium), *D. desulfuricans* NCIMB 8307 and *D. desulfuricans* NCIMB 8326 (Gram-negative, anaerobic bacteria). The structure of the Pd-NPs was analyzed to establish the influence of factors such as the nature of the electron donor and bacterial cell type. The fundamentally different *D. desulfuricans* NCIMB 8307 and *B. benzeovorans* produced similar homogeneously distributed (monodispersed) intracellular Pd-NPs, with those produced *via* formate oxidation being larger (5-7 nm) than those produced *via* oxidation of hydrogen (1-4 nm). The intracellular Pd nanoparticles produced by the three bacteria in the presence of formate were mainly crystalline icosahedrons enclosed by {111} facets. In *B. benzeovorans* amorphous intracellular Pd NPs were observed under hydrogen. The mechanism of Pd (II) trafficking in the cell is unknown, but this study indicates a possible 'trafficking' of palladium ions into the cytoplasm of both aerobic and anaerobic bacteria which may serve as a platform for 'fine-tuning' and bio-manufacture of novel targeted catalysts. In this respect, the intracellular nanoparticles produced by ethanolamide-deficient *D. desulfuricans* NCIMB 8326 were smaller than in NCIMB 8307 and the polydispersity index was higher; the comparative catalytic activities of the two types of 'bio-Pd' will be reported in subsequent publications.

Acknowledgements The authors acknowledge with thanks a Commonwealth scholarship to JBO and to Maria del Mar Abad Ortega (Centro de Instrumentación Científica, University of Granada, Spain) with technical assistance on the STEM/HAADF measurement. They also acknowledge the financial support of EPSRC (grant number EP/J008303/1).

Conflict of interest: The authors report no conflict of interest.

References

Abramoff MD, Magalhaes PJ, Ram SJ (2004) "Image Processing with ImageJ". Biophotonics Int. 11**:** 36-42.

Ahmad A, Senapati S, Khan MI, Kumar R, Ramani R. Srinivas V, Sastry M (2003) Intracellular synthesis of gold nanoparticles by a novel alkalotolerant actinomycete, *Rhodococcus* species. Nanotechnology. 14: 824-828. doi: 10.1088/0957-4484/14/7/323

Ascencio JA, Gutierrez-Wing C, Espinosa ME, Marin M, Tehuacanero S, Zorrilla C, Jose-Yacaman M (1998) Structure determination of small particles by HREM imaging: Theory and experiment. Surf Sci. 396: 349-368. doi: 10.1016/s0039-6028(97)00689-4

Axley MJ, Grahame DA, Stadtman TC (1990) *Escherichia coli* formate-hydrogen lyase purification and properties of the selenium-dependent formate dehydrogenase component. J Biol Chem. 265: 18213-8.

Bennett JA, Creamer NJ, Deplanche K, Macaskie LE, Shannon IJ, Wood J (2010) Palladium supported on bacterial biomass as a novel heterogeneous catalyst: A comparison of Pd/Al_2O_3 and bio-Pd in the hydrogenation of 2-pentyne. Chem Eng Sci. 65: 282-90. doi: 10.1016/j.ces.2009.06.069

Bennett JA, Mikheenko IP, Deplanche K, Shannon IJ, Wood J, Macaskie LE (2013) Nanoparticles of palladium supported on bacterial biomass: New re-usable heterogeneous catalyst with comparable activity to homogeneous colloidal Pd in the heck reaction. Appl Catal B. 140–141: 700-707. doi: 10.1016/j.ces.2009.06.069

Beveridge TJ, Murray RG (1980) Sites of metal deposition in the cell wall of *Bacillus subtilis*. J Bacteriol. 141: 876-887.

Boone DR, Liu YT, Zhao ZJ, Balkwill DL, Drake GR, Stevens TO, Aldrich HC (1995) *Bacillus-infernus* sp-nov, an Fe(III)-reducing and Mn(IV)-reducing anaerobe

from the deep terrestrial subsurface. Int J Syst Bacteriol. 45: 441-448. doi: 10.1099/00207713-45-3-441

Casalot L, Hatchikian EC, Forget N, de Philip P, Dermoun Z, Bélaich J.-P, Rousset M (1998) Molecular study and partial characterization of iron-only hydrogenase in *Desulfovibrio fructosovorans*. Anaerobe. 4: 45-55.doi:doi:10.1006/anae.1997.0137

Chen Y, He B, Huang T, Liu H (2009) Controlled synthesis of palladium icosahedra nanocrystals by reducing H_2PdCl_4 with tetraethylene glycol. Colloids Surf A. 348: 145-150. doi: 10.1016/j.colsurfa.2009.07.007

Cheng GJ, Li XH (2009) Bioreduction of chromium (VI) by *Bacillus* sp. isolated from soils of iron mineral area. Eur J Soil Biol. 45: 483-487. doi: 10.1016/j.ejsobi.2009.06.009

Costa C, Teixeira M, LeGall J, Moura JJG, Moura I (1997) Formate dehydrogenase from *Desulfovibrio desulfuricans* ATCC 27774: Isolation and spectroscopic characterization of the active sites (heme, iron-sulfur centers and molybdenum). J. Biol Inorg Chem. 2: 198-208. doi: 10.1007/s007750050125

Cowley A (2013) "Platinum 2013 interim review." Johnson Matthey PLC: Hertfordshire, England, pp. 2-35.

Creamer NJ, Mikheenko IP, Yong P, Deplanche K, Sanyahumbi D, Wood J, Pollmann K, Merroun M, Selenska-Pobell S, Macaskie LE. 2007. Novel supported Pd hydrogenation bionanocatalyst for hybrid homogeneous/heterogeneous catalysis. Catal Today. 128: 80-87. doi: 10.1016/j.cattod.2007.04.014

Cui J, Zhang L (2008) Metallurgical recovery of metals from electronic waste: A review. J Hazard Mater. 158: 228-56 doi:10.1016/j.jhazmat.2008.02.001

De Corte S, Bechstein S, Lokanathan AR, Kjems J, Boon N, Meyer RL (2013) Comparison of bacterial cells and amine-functionalized abiotic surfaces as support for Pd nanoparticle synthesis. Colloids Surf B. 102: 898-904. doi: 0.1016/j.colsurfb.2012.08.045

Deplanche, K, Caldelari I, Mikheenko IP, Sargent F, Macaskie LE (2010) Involvement of hydrogenases in the formation of highly catalytic Pd(0) nanoparticles by bioreduction of Pd(II) using *Escherichia coli* mutant strains. Microbiol-SGM. 156: 2630-2640. doi: 10.1099/mic.0.036681-0

Deplanche K, Merroun ML, Casadesus M, Tran DT, Mikheenko IP, Bennett JA, Zhu J, Jones IP, Attard GA, Wood J, Selenska-Pobell S & Macaskie LE (2012) Microbial synthesis of core/shell gold/palladium nanoparticles for applications

in green chemistry. J R Soc Interface. 9:1705-1712. doi: 10.1098/rsif.2012.0003

Deplanche K, Bennett JA, Mikheenko IP, Omajali J, Wells AS, Meadows RE, Wood J, Macaskie LE (2014) Catalytic activity of biomass-supported Pd nanoparticles: Influence of the biological component in catalytic efficacy and potential application in 'green' synthesis of fine chemicals and pharmaceuticals. Appl Catal B. 147: 651-65. doi:10.1016/j.apcatb.2013.09.045

De Corte S, Bechstein S, Lokanathan AR, Kjems J, Boon N, Meyer RL (2013) Comparison of bacterial cells and amine-functionalized abiotic surfaces as support for Pd nanoparticle synthesis. Colloids Surf B 102: 898-904. doi.org/10.1016/j.colsurfb.2012.08.045

de Sarrau B, Clavel T, Clerte C, Carlin F, Ginies C, Nguyen-The C (2012) Influence of anaerobiosis and low temperature on *Bacillus cereus* growth, metabolism, and membrane properties. Appl Environ Microbiol. 78: 1715-23. doi:10.1128/AEM.06410-11

de Vargas I, Sanyahumbi D, Ashworth MA, Hardy CM, Macaskie LE (2005) Use of X-ray Photoelectron Spectroscopy to elucidate the mechanism of palladium and platinum biosorption by *Desulfovibrio desulfuricans* biomass. 16th Int. Biohydrometallurgy Symp. Harrison STL, Rawlings DE, Petersen J. (eds). University of Cape Town. pp 605-616.

De Windt W, Aelterman P , Verstraete W (2005) Bioreductive deposition of palladium (0) nanoparticles on *Shewanella oneidensis* with catalytic activity towards reductive dechlorination of polychlorinated biphenyls. Environ. Microbiol. 7: 314-25. doi: 10.1111/j.1462-2920.2004.00696.x

Ding HT, Liu DF, Li ZL, Du YQ, Xu XH, Zhao YH (2011) Characterization of a thermally stable and organic solvent-adaptative NAD^+-dependent formate dehydrogenase from *Bacillus* sp. F1. J Appl Microbiol. 111: 1075-1085. doi: 10.1111/j.1365-2672.2011.05124.x

Eitinger T, Mandrand-Berthelot MA (2000) Nickel transport systems in microorganisms. Arch Microbiol 173: 1-9.

Fahmy K, Merroun M, Pollmann K, Raff J, Savchuk O, Hennig C, Selenska-Pobell S (2006) Secondary structure and Pd-(II) coordination in S-layer proteins from *Bacillus sphaericus* studied by infrared and X-ray absorption spectroscopy. Biophys J. 91: 996-1007. doi: 10.1529/biophysj.105.079137

Foulkes JM, Malone KJ, Coker VS, Turner NJ, Lloyd JR (2011) Engineering a biometallic whole cell catalyst for enantioselective deracemization reactions. ACS Catal. 11: 1589-94. doi: 10.1021/cs200400t

Frausto da Silva JJR, Williams RJP (2001) Biological chemistry of the elements: the inorganinc chemistry of life. (Oxford University Press)

Goldsworthy MJH (2011) Hydrocarbon biosynthesis in *Mycobacterium* spp NCIMB 10403 and *Desulfovibrio desulfuricans*. PhD Thesis. University of Exeter, United Kingdom.

Gupta A, Matsui K, Lo JF, Silver S (1999) Molecular basis for resistance to silver cations in *Salmonella*. Nature Medicine 5: 183-188. doi: 10.1038/5545

Hartmann T, Leimkuhler S (2013) The oxygen-tolerant and NAD (+)-dependent formate dehydrogenase from *Rhodobacter capsulatus* is able to catalyze the reduction of CO_2 to formate. FEBS J. 280: 6083-96. doi: 10.1111/febs.12528

Hatchikian EC, Traore A, Fernandez VM, Cammack R (1990) Characterization of the nickel-iron periplasmic hydrogenase from *Desulfovibrio fructosovorans*. Eur J Biochem. 187: 635-643. doi: 10.1111/j.1432-1033.1990.tb15347.x

Hayes PC (1993) Standard reduction potentials. In: Process principles in minerals and materials production. 2nd edition. Brisbane: Hayes publishing co. pp 660-665.

Hendricks JK, Mobley HLT (1997) Helicobacter pylori ABC transporter: Effect of allelic exchange mutagenesis on urease activity. J Bacteriol 179: 5892-5902.

Heugebaert TSA, De Corte S, Sabbe T, Hennebel T, Verstraete W, Boon N, Stevens CV (2012) Biodeposited Pd/Au bimetallic nanoparticles as novel Suzuki catalysts. Tetrahedron Lett. 53**:** 1410-2. doi: 10.1016/j.tetlet.2012.01.030

Holt EM, Kelly GJ, King F (1999) Catalyst design and manufacture. In: Winterbotton JM, King MB (eds) Reactor Design for Chemical Engineers. Stanley Thornes Ltd: Cheltenham, UK. pp 276-300.

Jormakka M, Tornroth S, Byrne B, Iwata S (2002) Molecular basis of proton motive force generation: Structure of formate dehydrogenase-N. Science. 295: 1863-8. doi: 10.1126/science.1068186

José-Yacamán M, Mar n-Almazo M, Ascencio JA (2001) High resolution TEM studies on palladium nanoparticles. J Mol Catal A: Chem. 173: 61-74. doi: 10.1016/S1381-1169(01)00145-5

Konishi Y, Tsukiyama T, Ohno K, Saitoh N, Nomura T, Nagamine S (2006) Intracellular recovery of gold by microbial reduction of $AuCl_4^-$ ions using the anaerobic bacterium *Shewanella alga*. Hydrometallurgy. 81: 24-29. doi: 10.1016/j.hydromet.2005.09.006

Law N, Ansari S, Livens FR, Renshaw JC, Lloyd JR (2008) Formation of nanoscale elemental silver particles *via* enzymatic reduction by *Geobacter sulfurreducens*. Appl Environ Microbiol. 74: 7090-7093. doi: 10.1128/aem.01069-08

Lee J-C, Pandey BD (2012) Bio-processing of solid wastes and secondary resources for metal extraction – A review. Waste Manage. 32: 3-18. doi:10.1016/j.wasman.2011.08.010

Liermann LJ, Hausrath EM, Anbar AD, Brantley SL (2007) Assimilatory and dissimilatory processes of microorganisms affecting metals in the environment. J Anal At Spectrom. 22: 867-877. doi: 10.1039/b705383e

Lim B, Kobayashi H, Camargo PC, Allard L, Liu J, Xia Y (2010) New insights into the growth mechanism and surface structure of palladium nanocrystals. Nano Res. 3: 180-188. doi: 10.1007/s12274-010-1021-5

Livingstone SE (1973) Palladium: The Element. In: Bailer JC, Nyholm R, Trotman-Dickenson AF (eds). Comprehensive Inorganic Chemistry. Vol. 3. Pergamon Press: Oxford, UK. pp 1274-1276.

Mabbett AN, Sanyahumbi D, Yong P, Macaskie LE (2006) Biorecovered precious metals from industrial wastes: single step conversion of a mixed metal liquid waste to a bioinorganic catalyst with environmental applications. Environ Sci Technol. 40: 1015-1021. doi: 10.1021/es0509836

Macaskie LE, Mikheenko IP, Yong P, Deplanche K, Murray AJ, Paterson-Beedle, M, Coker VS, Pearce CI, Cutting R, Pattrick RAD et al. (2011) Today's wastes, tomorrow's materials for environmental protection. In: Moo-Young B. et al. (eds) *Comprehensive Biotechnology.* Vol. 6: *Environmental Biotechnology and Safety.* Pergamon, New York. pp 719-725.

Maroney MJ (1999) Structure/function relationships in nickel metallobiochemistry. Curr Opin Chem Biol 3: 188-199. 10.1016/s1367-5931(99)80032-5

Merroun M, Rossberg A, Hennig C, Scheinost AC, Selenska-Pobell S (2007) Spectroscopic characterization of gold nanoparticles formed by cells and S-layer protein of *Bacillus sphaericus* JG-A12. Mater Sci Eng C. 27: 188-92. doi: 10.1016/j.msec.2006.05.001

Mikheenko IP & Rousset M, Dementin S, Macaskie LE (2008) Bioaccumulation of palladium by *Desulfovibrio fructosovorans* wild-type and hydrogenase-deficient strains. Appl Environ Microbiol. 74: 6144-6146. doi: 10.1128/aem.02538-07

Mota CS, Rivas MG, Brondino CD, Moura I, Moura JJG, Gonzalez PJ, Cerqueira N. (2011) The mechanism of formate oxidation by metal-dependent formate dehydrogenases. J Biol Inorg Chem. 16: 1255-1268. doi: 10.1007/s00775-011-0813-8

Mulrooney SB, Hausinger RP (2003) Nickel uptake and utilization by microorganisms. FEMS Microbiol Rev. 27: 239-261. doi: 10.1016/S0168-6445(03)00042-1

Murray AJ, Taylor S, Zhu J, Wood J, Macaskie LE (2015) A novel biorefinery: Biorecovery of precious metals from spent automotive catalyst leachates into new catalysts effective in metal reduction and in the hydrogenation of 2-pentyne. Min Eng. In Press.

Nair B, Pradeep T (2002) Coalescence of nanoclusters and formation of submicron crystallites assisted by *Lactobacillus* strains. Cryst Growth Des. 2: 293-298. doi: 10.1021/cg0255164

Narayanan KB, Sakthivel N (2010) Biological synthesis of metal nanoparticles by microbes. Adv Colloid Interface Sci. 156: 1-13. doi: 10.1016/j.cis.2010.02.001

Navarrete JU, Borrok DM, Viveros M, Ellzey JT (2011) Copper isotope fractionation during surface adsorption and intracellular incorporation by bacteria. Geochim Cosmochim Acta. 75: 784-799. doi: 10.1016/j.gca.2010.11.011

Nidhin M, Indumathy R, Sreeram KJ, Nair BU (2008) Synthesis of iron oxide nanoparticles of narrow size distribution on polysaccharide templates. Bull Mater Sci. 31: 93-96. doi: 10.1007/s12034-008-0016-2

Peng X, Zhou H, Li J, Li J, Chen S, Yao H, Wu Z (2010) Intracellular and extracellular mineralization of a microbial community in the Edmond Deep-Sea Vent field environment. Sediment Geol. 229: 193-206. doi: 10.1016/j.sedgeo.2010.06.003

Pollmann K, Raff J, Schnorpfeil M, Radeva G, Selenska-Pobell S (2005) Novel surface layer protein genes in *Bacillus sphaericus* associated with unusual insertion elements. Microbiol-SGM. 151: 2961-2973. doi: 10.1099/mic.0.28201-0

Polti MA, Amoroso MJ, Abate CM (2011) Intracellular chromium accumulation by *Streptomyces* sp. MC1. Water Air Soil Poll. 214: 49-57. doi: 10.1007/s11270-010-0401-5

Raaijmakers H, Macieira S, Dias JM, Teixeira S, Bursakov S, Huber R, Moura JJG, Moura I, Romao MJ (2002) Gene sequence and the 1.8 Å crystal structure of the tungsten-containing formate dehydrogenase from *Desulfovibrio gigas*. Structure. 10: 1261-72. doi: 10.1016/S0969-2126(02)00826-2

Ravindranath SP, Henne KL, Thompson DK, Irudayaraj J (2011) Surface-enhanced Raman imaging of intracellular bioreduction of chromate in *Shewanella oneidensis*. PLOS ONE. 6. doi: 10.1371/journal.pone.0016634

Riddin TL, Govender Y, Gericke M, Whiteley CG (2009) Two different hydrogenase enzymes from sulphate-reducing bacteria are responsible for the bioreductive mechanism of platinum into nanoparticles. Enzyme Microb Tech. 45: 267-73. doi: 10.1016/j.enzmictec.2009.06.006

Rhodin TN, Ertl G (1979) The Nature of the Surface Chemical Bond. Oxford, UK: North-Holland. pp 104-108.

Rodriguez-Navarro C, Jimenez-Lopez C, Rodriguez-Navarro A, Gonzalez-Muñoz MT, Rodriguez-Gallego M (2007) Bacterially mediated mineralization of vaterite. Geochim Cosmochim Acta. 71: 1197-1213. (doi: 10.1016/j.gca.2006.11.031)

Schneider CA, Rasband WS, Eliceiri KW (2012) NIH image to imageJ: 25 years of image analysis. Nat Methods 9: 671-5. doi: 10.1038/nmeth.2089

Selenska-Pobell S, Panak P, Miteva V, Boudakov I, Bernhard G, Nitsche H (1999) Selective accumulation of heavy metals by three indigenous *Bacillus* strains, *B-cereus*, *B-megaterium* and *B-sphaericus*, from drain waters of a uranium waste pile. FEMS Microbiol Ecol. 29: 59-67. doi: 10.1111/j.1574-6941.1999.tb00598.x

Silver S, Phung LT (1996) Bacterial heavy metal resistance: New surprises. Annu Rev Microbiol 50: 753-789. 10.1146/annurev.micro.50.1.753

Shi LH, Wang AQ, Zhang T, Zhang BS, Su DS, Li HQ, Song YJ (2013) One-step synthesis of Au-Pd alloy nanodendrites and their catalytic activity. J Phys Chem C. 117: 12526-36. doi: 10.1021/jp4013202

Shoukry AA, Mohamed MS (2012) DNA binding, spectroscopic and antimicrobial studies of palladium(II) complexes containing 2,2'-bipyridine and 1-phenylpiperazine. Spectrochim Acta A Mol Biol Spectrosc. 96: 586-593. doi: 10.1016/j.saa.2012.07.012

Sousa T, Chung AP, Pereira A, Piedade AP, Morais PV (2013) Aerobic uranium immobilization by *Rhodanobacter* A2-61 through formation of intracellular uranium-phosphate complexes. Metallomics. 5: 390-397. doi: 10.1039/c3mt00052d

Southam G, Beveridge TJ (1996) The occurrence of sulfur and phosphorus within bacterially derived crystalline and pseudocrystalline octahedral gold formed in vitro. Geochim Cosmochim Acta. 60: 4369-4376. doi: 10.1016/S0016-7037(96)00235-9

Thakkar KN, Mhatre SS, Parikh RY (2010) Biological synthesis of metallic nanoparticles. Nanomedicine: Nanotech. Biol. Med. 6: 257-62. doi: 10.1016/j.nano.2009.07.002

Waldron KJ, Robinson NJ (2009) How do bacterial cells ensure that metalloproteins get the correct metal? Nat Rev Microbiol. 7: 25-35. doi:10.1038/nrmicro2057

Wang Y, Xie SF, Liu JY, Park J, Huang CZ & Xia YN. 2013. Shape-controlled synthesis of palladium nanocrystals: A mechanistic understanding of the evolution from octahedrons to tetrahedrons. Nano Lett. 13: 2276-2281. doi: 10.1021/nl400893p

Wiseman CLS, Zereini F (2009) Airborne particulate matter, platinum group elements and human health: A review of recent evidence. Sci Total Environ. 407: 2493-2500 doi: 10.1016/j.scitotenv.2008.12.057

Weimer PJ (1984) Control of product formation during glucose fermentation by *Bacillus macerans*. Microbiology. 130: 103-111. doi: 10.1099/00221287-130-1-103

Wood J, Bodenes L, Bennett J, Deplanche K, Macaskie LE (2010) Hydrogenation of 2-butyne-1,4-diol using novel bio-palladium catalysts. Ind Eng Chem.Res. 49: 980-988. doi: 10.1021/ie900663k

Xiong Y, McLellan JM, Yin Y, Xia Y (2007) Synthesis of palladium icosahedra with twinned structure by blocking oxidative etching with citric acid or citrate ions. Angew Chem. 119: 804-808. doi: 10.1002/ange.200604032

Xu Y, Feng L, Jeffrey PD, Shi YG, Morel FMM (2008) Structure and metal exchange in the cadmium carbonic anhydrase of marine diatoms. Nature 452: 56-U3. 10.1038/nature06636

Yates MD, Cusick RD, Logan BE (2013) Extracellular palladium nanoparticle production using *Geobacter sulfurreducens*. ACS Sustain Chem Eng. 1:1165-1171. doi: 10.1021/sc4000785

Yong P, Rowson NA, Farr JPG, Harris IR, Macaskie LE. (2002) Bioaccumulation of palladium by *Desulfovibrio desulfuricans*. J Chem Technol Biotechnol. 77: 593-601. doi: 10.1002/jctb.606

Zhang H, Jin MS, Xiong YJ, Lim B, Xia YN (2013) Shape-controlled synthesis of Pd nanocrystals and their catalytic applications. Acc Chem Res 46: 1783-1794. doi: 10.1021/ar300209w

3.3.2 Probing the Viability of Palladium-Challenged Bacterial Cells Using Flow Cytometry

Jacob B. Omajali [*, 1], Iryna P. Mikheenko [1], Mohamed L. Merroun [2], Lynne E. Macaskie [1]

[1] Unit of Functional Bionanomaterials, Institute of Microbiology and Infection, School of Biosciences, University of Birmingham, Edgbaston, Birmingham, B15 2TT, United Kingdom

[2] Departments of Microbiology, Faculty of Sciences, University of Granada, Campus Fuentenueva, 18071, Granada, Spain

*Corresponding author. Tel.: fax:

Email address:

Journal: FEMS Microbiology Letters, in submission

This paper was written by J.B. Omajali. All experiments and analysis were carried out by the author. Technical assistance on flow cytometry was provided by Prof. M.L. Merroun and Dr. Jaime Lazuen-Alcon from the Flow Cytometry Unit, Centro de Instrumentación Cientifica, University of Granada, Spain.

Abstract

This study investigates the use of flow cytometry coupled with fluorescent probes to determine membrane integrity and membrane potential of cells of *Desulfovibrio desulfuricans* and *Bacillus benzeovorans* challenged with 1 mM of sodium tetrachloropalladate (II) (Na_2PdCl_4) solution at pH 2 followed by reduction of palladium (II) (Pd (II)) with formate to give 1% loading of Pd on cells. The bacterial cells retained membrane integrity and membrane potential when challenged with Pd (II) solutions. Since cells containing Pd (0) can still retain metabolic activity this provides the potential for combining chemical catalysis with biochemical activity in reactions that require metabolic synergy.

Key words: Catalysis; Cell viability; Flow cytometry; Membrane integrity; Membrane potential; Palladium.

Introduction

Flow cytometry has widespread applications in biotechnology, industrial and medical research (Fouchet et al., 1993; Brown, 2000; Diaz et al., 2010). It provides qualitative and quantitative analytical measurement of individual cells using fluorescence emission of labelled cells when they pass individually through a light source (*e.g.* laser) (Fulwyler, 1980; Davey and Kell, 1996; Davies, 2007).

Cell viability determination plays a strategic role particularly in, for example food microbiology and microbial pharmacology (Fouchet et al., 1993). The flow cytometry method depends on the uptake by dead or non-viable cells of dyes that are normally excluded by viable cells or those with intact membranes. Propidium iodide (PI) for instance is a membrane impermeable molecule (~ 668Da) with the ability to bind to nucleic acid due to loss of cellular integrity in dying, dead or necrotic cells, producing red fluorescence, but PI cannot cross an intact cytoplasmic membrane (Chan et al., 2015). Fluorescein diacetate (FDA) is a non-fluorescent dye but when taken up by active cells it is hydrolysed by a non-specific intracellular esterase to produce fluorescence that is retained by cells with intact cell membranes (Ziglio et al., 2012). A charged and slightly lipophilic dye like 3, 3'-dihexyloxacarbocyanine (DiO_6 (3) has been used to determine the membrane potential of *E. coli* as a measure of cell viability, resulting in green fluorescence (Monfort and Baleux, 1996) in intact cells (polarised membranes), while anionic dyes will interact with depolarized membranes (Hyka et al., 2013). There are other dyes known for their relevance in the determination of cell viability (Kaprelyants and Kell, 1992; Pedreira et al., 2013) and these can be used in combination with others or conjugated with antibodies in most cases. Appropriate dyes can be used to quantify the effects of stress or toxic chemicals on the cytoplasmic membrane integrity and physiology of a bacterial population (Boswell et al., 1998; Lopez-Fernandez et al., 2014).

Using flow cytometry, cell viability measurement has been applied in the rapid enumeration of probiotic bacteria (Muller et al., 2010), pathogenic bacteria (Qin et al., 2008), root-associated bacteria (Valdameri et al., 2015) and *Lactobacillus rhamnosus* in chocolate (Raymond and Champagne, 2015). Other parameters such as light scattering, DNA, RNA, protein contents, identification of antibody-antigen interaction, altered cell

states such as apoptosis and cell death (Fouchet et al., 1993; Davies, 2007) can also be measured.

Studies on cells 'decorated' with metallic nanoparticles (NPs) such as Pd (0) have been widely reported using various bacterial strains (Hennebel et al., 2012; Deplanche et al., 2014). However catalytically active materials synthesized using these bacteria have mostly been produced in dry powdered form following drying of the metallised cells. A recent study has shown that, contrary to reports that Pd-NP localization is restricted to the surface layers (Creamer et al., 2008; Mikheenko et al., 2008; Deplanche et al., 2014), cells of *Bacillus benzeovorans*, *Desulfovibrio desulfuricans* (Omajali et al., 2015) and *Escherichia coli* (Priestley, 2015) show extensive deposition of small intracellular Pd-NPs which implies a mechanism of cellular 'trafficking' of the Pd (II) initially applied. 'Next generation' biocatalysis would involve 'tandems' whereby both Pd-NPs and biochemical processes contribute to single cell 'nanofactories' as illustrated by Foulkes et al., (2011) in a deracemization reaction whereby application of palladized cell suspension of engineered *E. coli* was used for the sequential oxidation and reduction coupled with biotransformation of 1-methyltetrahydroisoquinoline (MTQ). De Windt et al (2006) reported the determination of cell viability of Pd-challenged cells of *Shewanella oneidensis* using flow cytometry. However, to our knowledge, there are no in-depth studies on the determination of both cell viability and integrity of palladium-challenged cells and this forms the major focus of this study. This study reports the viability and integrity of "palladized" cells of Gram-positive *Bacillus benzeovorans* NCIMB 12555 and two strains of Gram-negative *Desulfuricans desulfuricans* (NCIMB8307 and NCIMB8326) which have shown different patterns of Pd-deposition (Omajali et al., 2015). Therefore, the main objective of the study was to determine the viability of Pd-challenged cell suspension through the measurement of membrane integrity and membrane potential as indices of cell viability using flow cytometry. This will underpin a new direction in the synthesis of potentially novel catalysts which combine biochemical and chemical catalysis in single cells.

Materials and methods

Bacterial growth and cell preparation

Gram-negative *Desulfovibrio desulfuricans* (NCIMB 8307 and NCIMB 8326) were grown anaerobically based on the method of Deplanche et al (2014) in Postgate's C medium while Gram-positive *Bacillus benzeovorans* (NCIMB 12555) was grown aerobically (Omajali et al. 2015) in a nutrient medium. Cells were harvested by centrifugation during exponential growth, concentrated in a small amount of MOPS (4-morpholinepropanesulfonic acid)-NaOH buffer, pH 7 and stored under oxygen-free nitrogen (OFN) at 4^{o}C until use, usually within 24 h.

Pd (II) –challenge of cells and reduction of Pd (II) with formate

Harvested cell suspensions (20 mg/ml) were estimated based on predetermined OD_{600} and dry weight conversion for *D. desulfuricans* (Deplanche, 2008) and *B. benzeovorans* (J. B. Omajali unpublished) and challenged with 1 mM Pd (II) solution of Na_2PdCl_4 (pH 2) to make a 1wt% Pd loading on cells. Samples were divided into two; a Pd-cell suspension was supplemented with 1 M sodium formate (final concentration of 20 mM) for 1 h with shaking and the control was without formate. Both samples were then stored (4^{o}C) overnight (16-20 h) prior to flow cytometry measurement. Control comprised cells not supplemented with Pd (II) and cells killed by heat treatment (70^{o}C; 1 h).

Measurement of membrane integrity and membrane potential *via* flow cytometry

Cell samples (5 ml) each were divided into four: Pd (II)-challenged cells (without formate), Pd-challenged cells with Pd (II) reduced using formate, Pd-free live cells and heat-killed cells as controls. After incubation as above and prior to flow cytometry measurement, the cells were washed by centrifugation (12, 175 x g, 15 min, 4^{o}C) to remove unbound metal ion and MOPS-NaOH buffer and then suspended in ice cold (10 ml) phosphate buffered saline (PBS) (10 mM PBS, containing NaCl (8g), KCl (0.2g), Na_2HPO_4 (1.44g), KH_2PO_4 (0.2g) per L), pH 7.4, washed twice (12, 175 x g, 15 min, 4^{o}C) and 0.1 ml of each type of cell was resuspended to approx 10^6 cells/ml in PBS (1.9 ml) to a final volume of 2 ml (Lopez-Fernandez et al., 2014). For measurement of

membrane integrity, solutions of fluorochromes, fluorescein diacetate (FDA) (40µl, 0.1 mg/ml aq) and of propidium iodide (IP) (4µl, 1 mg/ml aq) were added simultaneously to the 2 ml cell mixture. Meanwhile, for the measurement of membrane potential, 3, 3'-Dihexyloxacarbocyanine iodide [$DiOC_6$ (3)] (20µl, 1 µM) was added to a separate sample. Mixtures were stored in the dark for 15 minutes. Flow cytometry measurements were taken immediately in triplicates (viable cells stain green while non-viable or dead cells stain red) using a FACS Cantoll flow cytometer, Becton Dickson (San Jose Palo Alto, California) equipped with three lasers: 488 nm blue, 620 nm red and 405 nm UV. Samples were measured in a green fluorescence detector or filter, FL1 (fluorescein isothiocyanate, FITC) and a red fluorescence detector or filter, FL2 (phycoerythrin-propidium iodide, PE-IP) mode in logarithmic scale channels at medium speed. The band pass filters used were 530 nm and 580 nm and results were analysed using BD Diva 6.1 software.

Results

Evaluation of membrane integrity of Pd-challenged cells

Initial measurements were made to differentiate between viable, non-viable (dead) and damaged cells (i.e. neither viable nor dead) based on double staining with the dyes flourescein diacetate (FDA) and propidium iodide (PI). Four test samples of Dd8307, Dd8326 and Bb (Fig 1, Table 1) were examined: Pd-free live cell controls, Pd (II)-sorbed cells (non-formate), reduced Pd (II) (with formate) and heat-killed cell controls. In the case of Pd (II)-treatment, a 1mM Na_2PdCl_4 of 1% Pd (II) loading on cells was used with 20 mM final formate concentration as an electron donor to reduce Pd (II) in cells that had been allowed to take up Pd (II) for 45 min before formate addition. The work was done at pH 2 because an acidic optimum was previously established (Yong et al., 2002) for the catalytic synthesis of biogenic Pd (0).

The results of cell viability are interpreted based on the state of the cell population given in percentage, i.e. viable cells or cells with enzymatic activity (lower-right quadrants) are indicated with green fluorescence, dead or non-viable cells (upper-left quadrants) with red fluorescence, damaged cells (upper-right quadrant) with dark-

blue fluorescence while fluorescence due to noise or background (lower-left quadrant) was given as light blue (cyan) fluorescence in dot or two-parameter plots (Fig 1). With the Pd-free live cell controls, the activities of the intact cell membranes are shown by green fluorescence (Figure 1a, b, c) when in contact with FDA. The population of viable cells in Pd-free live cells was 95- 100% (Table 1) with no dead cells detected. The proportion of damaged cells in Dd8307 and Bb was significantly lower than Dd8326 when cells were challenged with Pd (II) (Table 1). When Pd (II) was reduced on the cells using formate as electron donor, the cell viability was not significantly reduced when compared to Pd-free live cells except for Dd8326 (Fig 1i) with a population of 35.30% viable cells and 52.55% damaged cells (Table 1). In contrast, no non-viable cells were detected in Bb and Dd8307 although 12.13 % were found in Dd8326. In the heat-killed cell controls > 99% of the cell population of Bb, Dd8307 and Dd8326 were dead or non-viable (Table 2) indicated by red fluorescence (Figs 1j, k, l) with <1% sub-population of damaged cells.

Table 1 Determination of membrane integrity using flow cytometry

Test samples	State of cells	Cell viability (%) Bb	Dd8307	Dd8326
Pd-free live cells	viable	100 ± 0.00	99.90 ± 0.10	95.33 ± 0.50
	non-viable	0.00 ± 0.00	0.00 ± 0.00	0.00 ± 0.00
	damaged	0.00 ± 0.00	0.16 ± 0.16	4.71 ± 0.51
Pd (II)-sorbed cells	viable	89.29± 2.06	99.30 ± 0.33	9.51 ± 1.32
	non-viable	0.55 ± 0.11	0.00 ± 0.00	3.85 ± 0.22
	damaged	10.12 ± 1.92	0.36 ± 0.19	86.64 ± 1.17
Reduced (bio-Pd (0) on cells)	viable	99.89 ± 0.04	99.93 ± 0.07	35.30 ± 1.15
	non-viable	0.00 ± 0.00	0.00 ± 0.00	12.13 ± 1.31
	damaged	0.15 ± 0.04	0.00 ± 0.00	52.55 ± 1.52
Heat-killed cells	viable	0.00 ± 0.00	0.00 ± 0.00	0.00 ± 0.00
	non-viable	99.54 ± 0.19	99.83 ± 0.00	99.91 ± 0.09
	damaged	0.42 ± 0.20	0.17 ± 0.17	0.04 ± 0.04

Results are replicates of three separate determinations, Mean ± SE.

1% loading of 1mM Pd (II) solution (Na_2PdCl_4) was used on cells. Reduction of Pd (II) solution was *via* 20 mM sodium formate as electron donor. Bb: *Bacillus benzeovorans*, Dd8307: *Desulfovibrio desulfuricans* NCIMB8307, Dd8326: *Desulfovibrio desulfuricans* NCIMB 8326. Samples were stained with flourochromes, flourescein diacetate (FDA) and propidium iodide (PI) resulting in green and red fluorescence for viable and dead cells respectively; and blue fluorescence for damaged cells (see text).

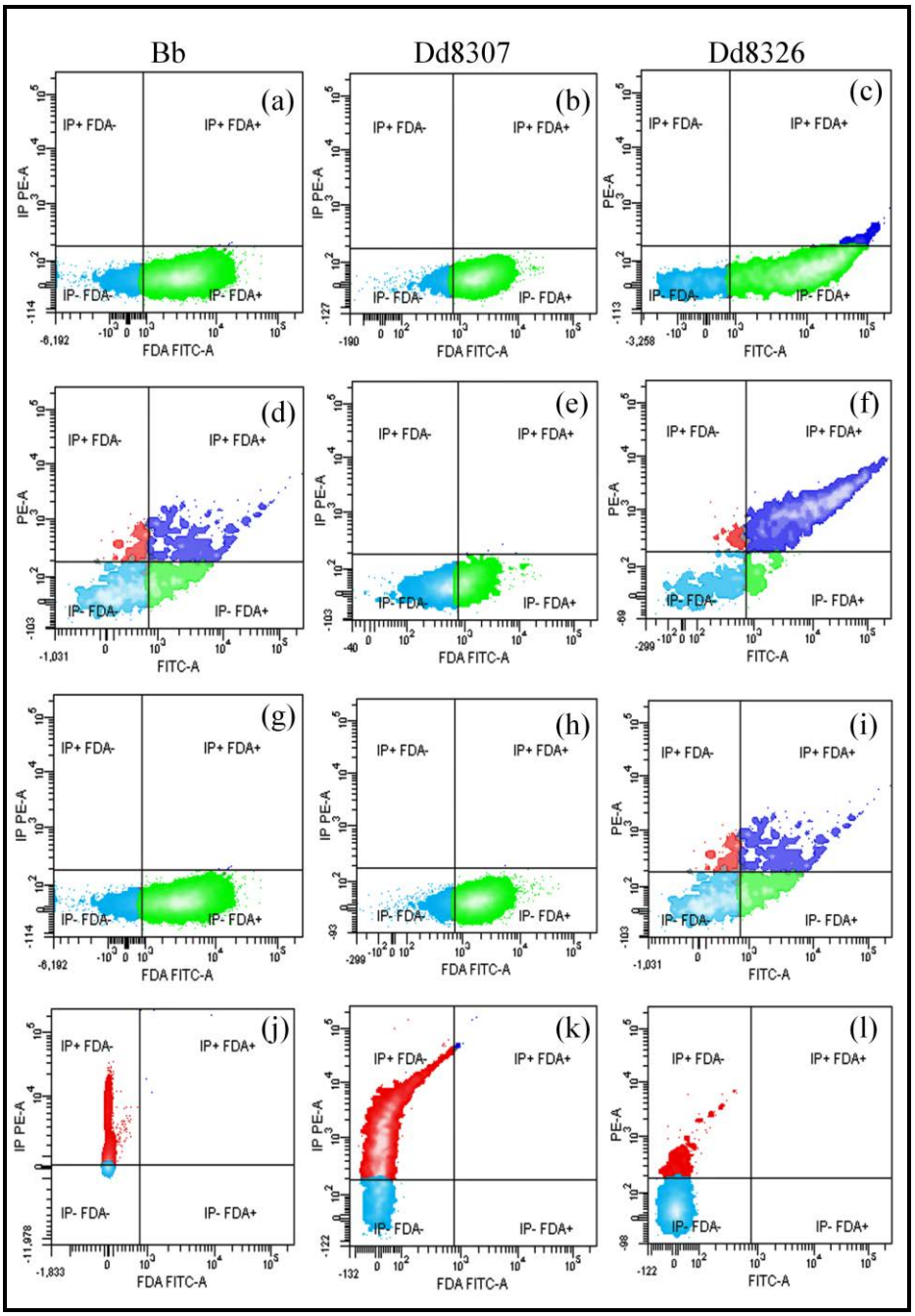

Figure 1 Dot or two-parameter plots of cell viability showing IP PE-A/FDA FITC-A with four regions (viable cells in green, non-viable cells in red, damaged cells in dark blue and noise or background signals as light blue fluorescence) in Pd-challenged cells of *B. benzeovorans* (Bb), *D. desulfuricans* (Dd8307 and Dd8326). Pd-free live cells (a, b, c); Pd (II)-sorbed cells (d, e, f); Reduced Pd (II)[bio-Pd(0)] on cells (g, h, i) and heat-killed cells (j, k, l). X-axis is increase in the fluorescence of FDA FITC-A (fluorescein diacetate or fluorescein isothiocyanate). Y-axis is increase in the fluorescence of IP PE-A (propidium iodide or phycoerythrin).

Assessment of metabolic or membrane potential of Pd-challenged cells

Metabolic or membrane potential is an alternative way to assess damage to Pd-challenged cells using cationic 3, 3'-dihexyloxacarbocyanine iodide [DiO_6 (3)] dye which interacts with intact cells (polarised membranes) but not permeabilized, dead or resting cells (depolarised membranes) (Hyka et al., 2013). Apart from metal-free live cell controls, cell samples were first treated with Pd (II) then with dye. There was no heat-killed control as dead cells do not have membrane potential (the cationic dye does not interact with depolarised cell membranes: Hyka et al., 2013). The results of cell viability (membrane potential) are described in terms of active and inactive state of the cell membrane due to interaction of the dye with lipophilic sites within the membrane (Table 2) while the fluorescence histograms (Fig 2) show the metabolic state of the cell membrane as active (P2) or inactive (P3). P2 and P3 are event markers, designating positive and negative events respectively (Fig 2).

The Pd-free live cells (positive control) of Bb, Dd8307 and Dd8326 showed that about 100%, 99.7% and 98.9% of the cell population were metabolically active with less than 2% of cells being inactive (Fig 2a, b, c and Table 2). When challenged with Pd (II), the membrane activity of Bb reduced to 35.1% and over 60% of the cell population were inactive (Fig 2d, Table 2). With Dd8307 and Dd8326, the number of cells with intact membranes reduced to 88.8% and 94.0% respectively (Figs 2e, f and Table 2) with a correspondingly increased number of inactive cells. However, when Pd (II) on the challenged cells was reduced with formate to Pd (0) in all three strains, the membrane potential of the cells was sustained and there was no significant difference when compared with Pd-free live cells (Figs 2g, h, i) while the number of inactive cells was also low (Table 2).

Table 2 Determination of membrane (metabolic) potential of cells using flow cytometry

Test samples	Metabolic state	Membrane potential of cells (%) Bb	Dd8307	Dd8326
Pd-free live cells	active cells	100 ± 0.00	99.73 ± 0.00	98.87 ± 0.41
	inactive cells	0.27 ± 0.03	0.27 ± 0.03	1.13 ± 0.41
Pd (II)-sorbed cells	active cells	32.05± 1.15	88.83 ± 2.37	94.03 ± 0.42
	inactive cells	67.95± 1.15	11.17 ± 2.37	5.97 ± 0.42
Reduced (bio-Pd (0) on cells)	active cells	99.97 ± 0.03	98.70 ± 0.40	94.87 ± 1.47
	inactive cells	0.03 ± 0.03	1.30 ± 0.40	5.90 ± 0.90

Results are replicates of three separate determinations, Mean ± SE.

1% loading of 1mM Pd (II) solution (Na_2PdCl_4) was used on cells. Reduction of Pd (II) solution was *via* 20 mM sodium formate as electron donor. Bb: *Bacillus benzeovorans*, Dd8307: *Desulfovibrio desulfuricans* NCIMB8307, Dd8326: *Desulfovibrio desulfuricans* NCIMB 8326. Interaction of an intact cell membrane with the dye, 3, 3'-dihexyloxacarbocyanine iodide [DiO_6 (3)] verifies metabolic or membrane potential of the cells.

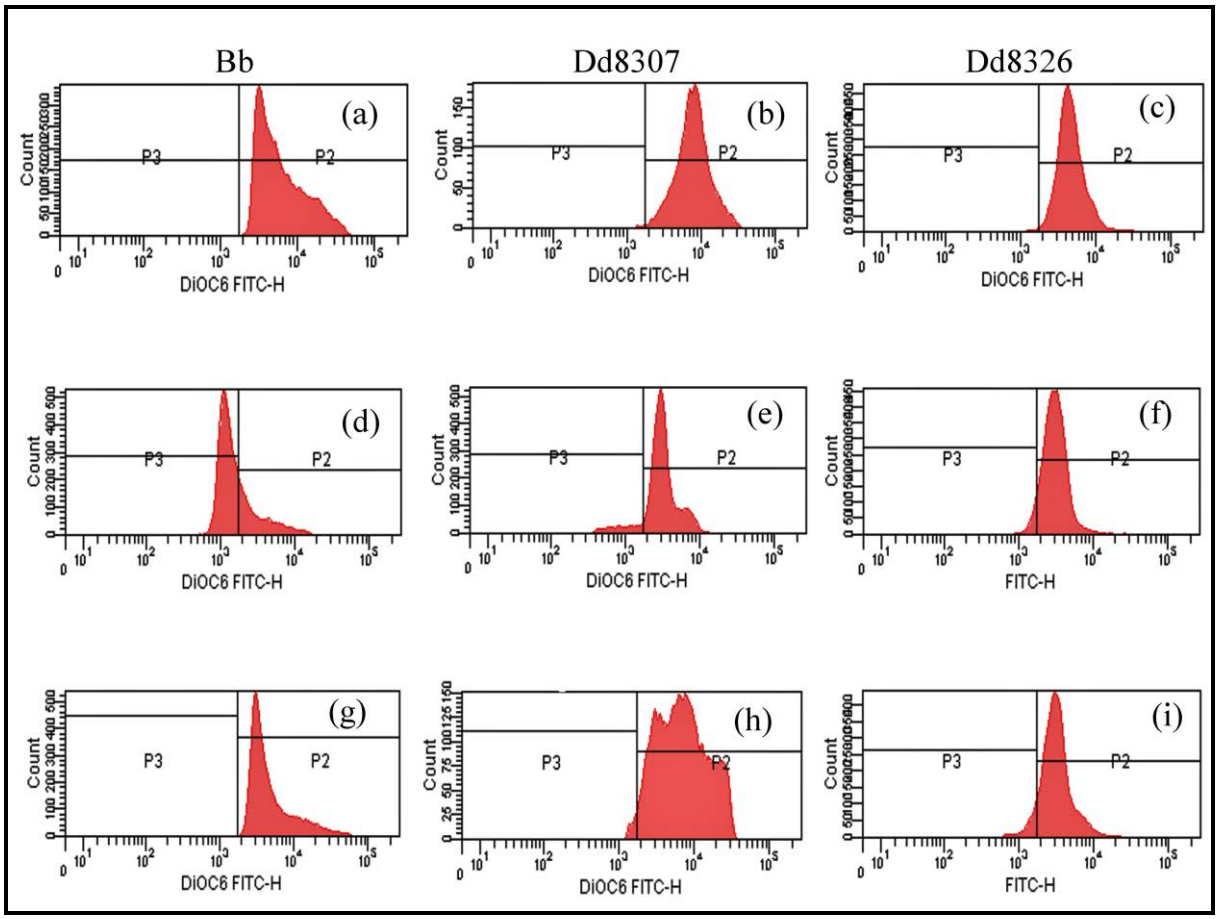

Figure 2 Fluorescence histogram showing membrane potential of Pd-challenged cells of *B. benzeovorans* (Bb), *D. desulfuricans* (Dd8307 and Dd8326) with two markers: P2 designating active membrane; P3 for inactive membrane. Cell samples were divided into Pd-free live cells (a, b, c); Pd (II)-sorbed cells (d, e, f) and reduced Pd (II) (with formate) on cells (g, h, i). X-axis is increase in the fluorescence of DiOC6 (3) or FITC-H (3', 3-dihexyloxacarbocyanine or fluorescein isothiocyanate). Y-axis is increase in cell count or population. P2 and P3 were determined directly from the flow cytometer.

Discussion

This study investigated the viability of Pd-challenged cells of two strains of Gram-negative *Desulfovibrio desulfuricans* (Dd8307 and Dd8326) and a Gram-positive *Bacillus benzeovorans* (Bb) by measuring membrane integrity and membrane potential. The double staining of cells with fluorescein diacetate (FDA) and propidium iodide (PI) was used to determine membrane integrity and differentiated between viable and non-viable cells (Chan et al., 2015). A slight decrease in the population of viable cells when

challenged with palladium (II) (Table 1) due to its toxicity was more pronounced in *D. desulfuricans* (Dd8326) where only 9.51% of the cell population remain viable. Notably, over 80% of the cells were damaged, i.e. these cells were neither viable nor dead (Ziglio et al., 2002). In contrast the other two strains appeared more resistant to Pd toxicity. An alternative explanation for this significant effect on Dd8326 could be that, while *Desulfovibrio* spp. are strict anaerobes some of them are more tolerant to O_2 than others (Cypionka, 2000; Mogensen et al., 2005) and during flow cytometry analysis, the cells were unavoidably exposed and analysed in air which could have resulted in additional stress or injury (Caron and Bradley, 1995). However, since there was an overall improvement in the viability of the cells (Figs 1g, h, i) when the Pd (II) was reduced in the presence of formate as an electron donor (especially in Dd8326; Fig 1i, Table 1). This suggests that the stress suffered by this organism was Pd (II)-related. It is well known that metallic ions have the ability to bind to DNA, enzymes or proteins, exhibiting cytotoxic or genotoxic effects (Qiao and Ma, 2013). This was exemplified by Boswell et al (1998) who used flow cytometry to study the effects of some heavy metals on *Acinetobacter johnsonii*, which resulted in permeabilized cytoplasmic membranes as confirmed by transmission electron microscopy. The mechanism of metal toxicity is beyond the scope of this work while comparison with other work is complicated since the cells were placed under pH stress in this study. However, in this study, once reduced to Pd (0) this additional stress had no effect on the viability of Bb and Dd8307 and the small effect observed in Dd8326 may be associated with a greater toxicity of Pd (II). Note also, however, that the Pd (II) challenge was done at pH 2 and metal toxicity may have been differentially augmented by acid-stress although, again this does not account for the recovery of the cells once Pd (II) was reduced to Pd (0). According to De Windt et al (2006), Pd (II) treated cells (without electron donors) of *Shewanella oneidensis* resulted in a 60% reduction of cell viability while the addition of hydrogen or formate to Pd (II) challenged cells reduced the toxicity of Pd (II) on the cells without significantly reducing cell viability. However, the addition of formate proved to be less effective in reducing Pd (II) toxicity than hydrogen. Since the pK_a of formic acid is 3.75 and undissociated formic acid can enter cells, dissociating within the cell to H^+ and COO^- (Pronk et al., 1991, Johnson, 1998), intracellular acidification leads to cell death (Thomas et al., 2014). Fermentative bacteria have effective formate hydrogen lyase

activity to effect formate breakdown; this enzyme has been reported in *D. desulfuricans* but its differential expression in the two *Desulfovibrio* strains would not account for the recovery seen following reduction of Pd (II) to Pd (0) which suggests that the effects observed are attributable to the free Pd (II) species, either as free Pd^{2+} or the $PdCl_4^{2-}$ that predominates in a chloride solution (Hubicki and Wolowicz, 2009). The cell membrane contains organic compounds, mainly phospholipids, and also proteins and attached polysaccharide chains (Dolezalova and Lukes, 2015) and attack on various functional groups of the membrane by oxidation may be a key mechanism leading to heat-induced cell death (Davidson et al., 1996) and lipids are the most vulnerable. In support of this, studies using XPS (a surface technique, which probes the outer membrane ~5-10 nm) have shown an effect of Pd on cells of *E. coli* (Priestley et al., 2015) while some reduction of Pd (II) in the absence of added electron donor was observed using *D. desulfuricans* (NCIMB 8307 and NCIMB 8326) suggesting a function of Pd (II) as an oxidant (Omajali et al., unpublished).

The metabolic or membrane potential of the cell is very important to cell viability. There was no significant difference in the membrane potential of the Pd-free live cells of the three bacteria when compared to cells containing reduced Pd (0) (Table 2). Intracellular palladium nanoparticles were synthesized *via* formate and hydrogen reduction in all three strains could not prove membranes were intact (Omajali et al., 2015). However, the present study shows that, even though ~90% of the Pd (II)-sorbed cells of Bb were viable, the metabolic activity of these cells was low with ~68% of the population in an inactive state. In contrast, even though the population of viable cells of Dd8326 (Table 2) was low, over 90% of the cell population were still metabolically active. This suggests that the distinction between life and non-life is not absolute as many cells may exist in a dormant (Stevenson, 1977) state but may give a viable direct count (Gottschal, 1990). Hence, most of the cells that appeared non-viable in Dd8326 could still carry out metabolic functions while the sub-population of Pd (II)-challenged cells of Bb that appeared viable was not active metabolically. A similar response, over all, was given by both strains of *D. desulfuricans* since these Gram-negative cells contained both outer membrane and periplasmic capabilities which are absent in Gram-positive cells, speculations as to the root of the observed differences is unwarranted.

The ability of these bacteria to exhibit intact cell membrane and maintain metabolic activity when challenged with 1mM Pd (II) solution may be relevant in catalysis. The use of palladized bacteria in catalysis used dried, powdered preparations (e.g. De Corte et al., 2012; Deplanche et al., 2014) but Foulkes et al (2011) demonstrated the synthesis of bio-Pd by using a 1mM Na_2PdCl_4 solution to a final Pd loading of 1wt% on an engineered *E.coli* cell expressing monoamine oxidase activity, making an aqueous catalyst suspension with application in both oxidation and reduction reaction as well as biotransformation. However, even though the cells had monoamine oxidase activity, the potential for 'long term' tandem catalysis was not considered. The present results using *D. desulfuricans* and *B. benzeovorans* confirm cellular resilience under challenge with 1 mM Pd (II) which resulted in a loading of 1wt% of the dry mass without apparent adverse effects.

Acknowledgements

The authors acknowledge with thanks a Commonwealth scholarship to BO's PhD and Dr. Jaime Lazuen-Alcon from the Flow Cytometry Unit, Centro de Instrumentación Cientifica, University of Granada, Spain with technical help on flow cytometry analysis.

References

Boswell, C. D.; Hewitt, C. J.; Macaskie, L. E., An application of bacterial flow cytometry: Evaluation of the toxic effects of four heavy metals on *Acinetobacter* sp. with potential for bioremediation of contaminated wastewaters. *Biotechnology Letters* **1998,** *20*, 857-863.

Brown, M.; Wittwer, C., Flow cytometry: Principles and clinical applications in hematology. *Clinical Chemistry* **2000,** *46*, 1221-1229.

Caron, G. N. V.; Badley, R. A., Viability assessment of bacteria in mixed populations using flow-cytometry. *Journal of Microscopy* **1995,** *179*, 55-66.

Chan, L. L. Y.; Kuksin, D.; Laverty, D. J.; Saldi, S.; Qiu, J., Morphological observation and analysis using automated image cytometry for the comparison of trypan blue and fluorescence-based viability detection method. *Cytotechnology* **2015,** *67*, 461-473.

Creamer, N. J.; Deplanche, K.; Snape, T. J.; Mikheenko, I. P.; Yong, P.; Sanyahumbi, D.; Wood, J.; Pollmann, K.; Selenska-Pobell, S.; Macaskie, L. E., A biogenic catalyst for hydrogenation, reduction and selective dehalogenation in non-aqueous solvents. *Hydrometallurgy* **2008,** *94*, 138-143.

Cypionka, H., Oxygen respiration by *Desulfovibrio* species. *Annual Review of Microbiology* **2000,** *54*, 827-848.

Davey, H. M.; Kell, D. B., Flow cytometry and cell sorting of heterogeneous microbial populations: the importance of single-cell analyses. *Microbiol Rev* **1996,** *60*, 641-96.

Davidson, J. F.; Whyte, B.; Bissinger, P. H.; Schiestl, R. H., Oxidative stress is involved in heat-induced cell death in *Saccharomyces cerevisiae*. *Proceedings of the National Academy of Sciences of the United States of America* **1996,** *93*, 5116-5121.

Davies, D., Cell sorting by flow cytometry. In *flow cytometry: Principles and applications.* Macey, M. G., Ed. Humana Press Inc: Totowa, New Jersey, 2007; pp. 257-276.

De Corte, S.; Hennebel, T.; De Gusseme, B.; Verstraete, W.; Boon, N., Bio-palladium: from metal recovery to catalytic applications. *Microbial Biotechnology* **2012,** *5*, 5-17.

Deplanche, K. New nanocatalysts made by bacteria from metal solutions and recycling of metal wastes. PhD Thesis, University of Birmingham, UK, **2008**.

Deplanche, K.; Bennett, J. A.; Mikheenko, I. P.; Omajali, J.; Wells, A. S.; Meadows, R. E.; Wood, J.; Macaskie, L. E., Catalytic activity of biomass-supported Pd nanoparticles: Influence of the biological component in catalytic efficacy and potential application in 'green' synthesis of fine chemicals and pharmaceuticals. *Applied Catalysis B: Environmental* **2014,** *147*, 651-665.

De Windt, W.; Boon, N.; Van den Bulcke, J.; Rubberecht, L.; Prata, F.; Mast, J.; Hennebel, T.; Verstraete, W., Biological control of the size and reactivity of catalytic Pd(0) produced by *Shewanella* oneidensis. *Antonie Van Leeuwenhoek* **2006,** *90*, 377-89.

Fouchet, P.; Jayat, C.; Héchard, Y.; Ratinaud, M.-H.; Frelat, G., Recent advances of flow cytometry in fundamental and applied microbiology. *Biology of the Cell* **1993,** *78*, 95-109

Díaz, M.; Herrero, M.; García, L. A.; Quirós, C., Application of flow cytometry to industrial microbial bioprocesses. *Biochemical Engineering Journal* **2010,** *48*, 385-407.

Dolezalova, E.; Lukes, P., Membrane damage and active but nonculturable state in liquid cultures of *Escherichia coli* treated with an atmospheric pressure plasma jet. *Bioelectrochemistry* **2015,** *103*, 7-14.

Foulkes, J. M.; Malone, K. J.; Coker, V. S.; Turner, N. J.; Lloyd, J. R., Engineering a biometallic whole cell catalyst for enantioselective deracemization reactions. *ACS Catalysis* **2011,** *1*, 1589-1594.

Fulwyler, M. J., Flow cytometry and cell sorting. *Blood Cells* **1980,** *6*, 173-84.

Gottschal, G. J., Phenotypic responses to environmental changes. *FEMS Microbiology Ecology* **1990,** *74*, 93-102.

Hennebel, T.; De Corte, S.; Verstraete, W.; Boon, N., Microbial production and environmental applications of Pd nanoparticles for treatment of halogenated compounds. *Current Opinion in Biotechnology* **2012,** *23* (4), 555-561.

Hutter, K. J.; Eipel, H. E., Microbial determinations by flow cytometry. *J Gen Microbiol* **1979,** *113*, 369-75.

Hubicki, Z.; Wolowicz, A., Adsorption of palladium(II) from chloride solutions on Amberlyst A 29 and Amberlyst A 21 resins. *Hydrometallurgy* **2009,** *96*, 159-165.

Hyka, P.; Lickova, S.; Přibyl, P.; Melzoch, K.; Kovar, K., Flow cytometry for the development of biotechnological processes with microalgae. *Biotechnology Advances* **2013,** *31*, 2-16.

Johnson, D. B., Biodiversity and ecology of acidophilic microorganisms. *FEMS Microbiology Ecology* **1998,** *27*, 307-317.

Kaprelyants, A. S.; Kell, D. B., Rapid assessment of bacterial viability and vitality by rhodamine 123 and flow-cytometry. *Journal of Applied Bacteriology* **1992,** *72*, 410-422.

Lopez-Fernandez, M.; Fernandez-Sanfrancisco, O.; Moreno-Garcia, A.; Martin-Sanchez, I.; Sanchez-Castro, I.; Merroun, M. L., Microbial communities in bentonite formations and their interactions with uranium. *Applied Geochemistry* **2014,** *49*, 77-86.

Mikheenko, I. P.; Rousset, M.; Dementin, S.; Macaskie, L. E., Bioaccumulation of palladium by *Desulfovibrio fructosivorans* wild-type and hydrogenase-deficient strains. *Applied and Environmental Microbiology* **2008,** *74*, 6144-6146.

Monfort, P.; Baleux, B., Cell cycle characteristics and changes in membrane potential during growth of *Escherichia coli* as determined by a cyanine fluorescent dye and flow cytometry. *Journal of Microbiological Methods* **1996,** *25*, 79-86.

Mogensen, G. L.; Kjeldsen, K. U.; Ingvorsen, K., *Desulfovibrio aerotolerans* sp. nov., an oxygen tolerant sulphate-reducing bacterium isolated from activated sludge. *Anaerobe* **2005,** *11*, 339-349.

Muller, J. A.; Stanton, C.; Sybesma, W.; Fitzgerald, G. F.; Ross, R. P., Reconstitution conditions for dried probiotic powders represent a critical step in determining cell viability. *Journal of Applied Microbiology* **2010,** *108*, 1369-1379.

Omajali, J.B; Mikheenkho, I.P; Merroun, L.M; Wood, J; Macaskie L.E., Characterization of intracellular palladium nanoparticles synthesized by *Desulfovibrio desulfuricans* and *Bacillus benzeovorans*. *J Nanopart Res* **2015,** *17*, 1-17.

Pedreira, C. E.; Costa, E. S.; Lecrevisse, Q.; van Dongen, J. J. M.; Orfao, A., Overview of clinical flow cytometry data analysis: recent advances and future challenges. *Trends in Biotechnology* **2013,** *31*, 415-425.

Priestley, R. E.; Macaskie, L. E.; Mansfield, A.; Bye, J.; Deplanche, K.; Jorge, A. B.; Bret, D.; Sharma, S. 2015. Pd nanoparticles supported on reduced grapheme-*E. coli* hybrid with enhanced crystallinity in bacterial biomass. *RSC Advances* (In submission).

Pronk, J. T.; Meijer, W. M.; Hazeu, W.; Vandijken, J. P.; Bos, P.; Kuenen, J. G., Growth of *Thiobacillus-ferrooxidans* on formic acid. *Applied and Environmental Microbiology* **1991,** *57*, 2057-2062.

Qiao, Y.; Ma, L., Quantification of metal ion induced DNA damage with single cell array based assay. *Analyst* **2013,** *138*, 5713-8.

Raymond, Y.; Champagne, C. P., The use of flow cytometry to accurately ascertain total and viable counts of *Lactobacillus rhamnosus* in chocolate. *Food Microbiology* **2015,** *46*, 176-183.

Qin, D.; He, X.; Wang, K.; Tan, W., Using fluorescent nanoparticles and SYBR Green I based two-color flow cytometry to determine *Mycobacterium tuberculosis* avoiding false positives. *Biosensors and Bioelectronics* **2008,** *24*, 626-631

Stevenson, L. H., A case for bacterial dormancy in aquatic systems. *Microbial Ecology* **1977,** *4*, 127-133.

Thomas, V. C.; Sadykov, M. R.; Chaudhari, S. S.; Jones, J.; Endres, J. L.; Widhelm, T. J.; Ahn, J. S.; Jawa, R. S.; Zimmerman, M. C.; Bayles, K. W., A central role for carbon-overflow pathways in the modulation of bacterial cell death. *PLOS Pathogens* **2014,** *10*.

Valdameri, G.; Kokot, T. B.; Pedrosa, F. D.; de Souza, E. M., Rapid quantification of rice root-associated bacteria by flow cytometry. *Letters in Applied Microbiology* **2015,** *60*, 237-241.

Yong, P.; Rowson, N. A.; Farr, J. P. G.; Harris, I. R.; Macaskie, L. E., Bioaccumulation of palladium by *Desulfovibrio desulfuricans*. *Journal of Chemical Technology and Biotechnology* **2002,** *77*, 593-601.

Ziglio, G.; Andreottola, G.; Barbesti, S.; Boschetti, G.; Bruni, L.; Foladori, P.; Villa, R., Assessment of activated sludge viability with flow cytometry. *Water Research* **2002,** *36*, 460-468.

3.4 Towards Tandem Catalysis

This section contains the followings studies:

3.4.1 Synthesis of Biogenic Palladium Catalyst by *Bacillus benzeovorans* pregrown by two methods

Journal: Biotechnology Letters, in submission

3.4.2 Potential of Palladized Cells of *Bacillus Benzeovorans* in Tandem Catalytic Remediation of Chlorobenzene

Journal: Awaiting submission.

3.4.1 Synthesis of Biogenic Palladium Catalyst by *Bacillus benzeovorans* Pregrown by Two Methods

Jacob B. Omajali [1] and Lynne E. Macaskie [*, 1]

[1] Unit of Functional Bionanomaterials, Institute of Microbiology and Infection, School of Biosciences, University of Birmingham, Edgbaston, Birmingham, B15 2TT, United Kingdom

*Corresponding author. Tel.: fax:

Email address

Journal: Biotechnology Letters, in submission

This paper was written by J.B.Omajali. All experiments were perfomed by the author. Technical assistance on XPS was provided by Dr Marc Walker, Warwick University.

Abstract

In this study, two catalysts (bio-Pd) made by pre-growing *Bacillus benzeovorans* NCIMB 12555 in a nutrient-rich aerobic medium and a fermentative medium were compared in the reductive dehalogenation of chlorobenzene. The catalysts were characterized using transmission electron microscopy (TEM), X-ray powder diffraction (XRD) and X-ray photoelectron spectroscopy (XPS). The average crystallite size of palladium nanoparticles (Pd-NPs) made *via* anaerobically pregrown cells was larger than those made using aerobically pregrown cells. There was no difference in terms of the morphological or Pd speciation when examined using TEM and XPS. The bio-Pd made using aerobic cells had ~26% higher conversion than that made *via* anaerobic cells after 24 h of reductive dechlorination of chlorobenzene.

Keywords: Aerobic; Anaerobic; *Bacillus benzeovorans*; Chlorobenzene; Dechlorination

Introduction

Nanoparticles of palladium have found widespread applications in a number of important catalytic reactions as a result of their effective chemical and physical properties (Nishihata et al., 2002; Boutinguiza et al., 2014). However, in the absence of catalyst support nanoparticle (NP) instability eventually leads to particle growth by coalescence or ripening (Choudhary and Goodman, 2002). Chemical catalyst supports (Toebes et al., 2001; Petrucci et al., 2015) have the ability to reduce particle growth and they also alter the functionalities and properties of catalyst due to various functional groups on support surface. However, the challenges of manufacturing chemical catalysts include high metal cost and toxic effects of the chemicals used (Cole-Hamilton, 2003).

A number of 'green chemistry' approaches *e.g.* the use of biological supports for the synthesis of metal NPs (e.g. bacteria, fungi, yeast, algae, plants and viruses) have received substantial attention (Gericke and Pinches, 2006; Narayanan and Sakthivel, 2010; Faramarzi et al., 2013). Among these, the use of bacterial support is now well developed (e.g. Bunge et al., 2010; Deplanche et al., 2014; Omajali et al., 2015). Various bacteria have been used to synthesize palladium nanoparticles, usually yielding comparable catalytic properties to commercial catalysts. For example, biogenic catalyst of palladium (bio-Pd) made on cells of *Desulfovibrio desulfuricans* was more active than colloidal palladium catalyst in the Heck reaction of styrene and iodobenzene (Bennett et al., 2013) while Sobjerg et al., (2009) looked at the relevance of biogenic palladium catalyst in commercially important Suzuki-Miyaura and Mizoroki-Heck reactions. The use of biogenic Pd-nanoparticle catalysts in reductive dehalogenation of many chlorinated compounds including pesticides like lindane (Mertens et al., 2007) is well established (Baxter-Plant et al., 2003; Hennebel et al., 2012) with potential environmental applications.

Although bacterial dehalogenation and metabolism of chlorinated compounds is well-reported (Zanaroli et al., 2015) these metabolic processes are slow, attributed to interference by the chlorine substituent (Fung et al., 2009). The oxidative route (*via* dioxygenase enzyme) is well known and selectively rapid (Schmidt et al., 2013) whereas the anaerobic route (*via* reductive dechlorination or halorespiration (Nelson et al., 2014)) is much slower and less established. A landmark study combined catalytic

activity of Pd NPs on engineered cells of *E. coli* coupled with a biotransformation to form a 'tandem' catalyst (Foulkes et al., 2011) and the possibility exist to apply this concept to the Pd-catalysed dehalogenation and degradation of chlorinated aromatic contaminants. The use of bacteria as supports for catalytic Pd-nanoparticles that degrade aromatic compounds has not been investigated. This formed the first objective of this study using *Bacillus benzeovorans*. Relatively little attention has been paid to the use of *Bacillus* spp. in the manufacture of Pd-NPs except for *B. subtilis* (Gericke and Pinches, 2006) and *B. sphaericus* (Creamer et al., 2008) to synthesize "bio-Pd" with comparable activity to that made by *Desulfovibrio desulfuricans* in the hydrogenation of itaconic acid and 3-nitrostyrene (Creamer et al., 2008).

Bacillus spp. *e.g. B. subtilis* was generally considered to be aerobic but *Bacillus* spp. are now well known to grow by either respiration or fermentation (Cruzramos et al., 1995; Nakano et al., 1997). Anaerobic growth of *B. subtilis* was known to occur *via* anaerobic respiration using nitrate as the electron acceptor and also *via* fermentation, although some *Bacillus* spp. have shown the ability to use arsenic [As(V)] and selenium [Se(VI)] as electron acceptors (Switzer Blum et al., 1998). Using nuclear magnetic resonance (NMR), it was shown that *B. subtilis* can grow by mixed acid fermentation in the absence of any external electron acceptor with no formate produced (Nakano et al., 1997). This finding has led to the identification of various genes responsible for anaerobiosis in *B. subtilis* (Geng et al., 2007) including formate hydrogenlyase, a complex enzyme which degrades formate and the hydrogenase-3 component of which is responsible in part for the reduction of Pd (II) to Pd (0) (Deplanche et al., 2010). The use of aerobic cells of *B. benzeovorans*, a soil bacterium (Tzeneva et al., 2004) which degrades aromatic compounds (Walker and Weatherley, 2000) to synthesize palladium nanoparticles (Omajali et al., 2015) has raised the possibility of producing bio-Pd from anaerobic cells for reductive dechlorination of chlorobenzene under hydrogen in a 'one pot' reaction; followed by metabolism of the residual aromatic compound. There are no current reports on the use of anaerobic cells of *Bacillus* in this form of application, although the use of 'palladized' cells of *Eschericia coli* to perform a 'tandem' chemical catalysis and biotransformation was reported (Foulkes et al., 2011).

The objective of this study was to develop a biogenic palladium catalyst from anaerobically grown cells of *B. benzeovorans*. This may introduce novel physical characteristics into the catalyst, capable of influencing the catalytic behaviour. For example, assuming *B. benzeovorans* expresses hydrogenase-3 akin to the palladium synthesis mechanism in *E. coli* (Deplanche et al., 2010) and with previous work with *Desulfovibrio desulfuricans* showing that Pd (0) nanoparticles (NPs) locate to the site of the hydrogenase enzyme involved in their synthesis (Mikheenko et al., 2008), a comparison of their catalytic property with those made on aerobically grown cells in reductive dechlorination of chlorobenzene was the final objective of this study. Previous work has used a rich growth medium based on meat (beef) extract and peptone which is now the subject of restrictive legislation (Anon, 2008). Hence the opportunity was taken to develop the growth of *B. benzeovorans* in a defined minimal medium which also reduces implications of process waste disposal.

Materials and methods

Aerobic and anaerobic growth of *B. benzeovorans*

Bacillus benzeovorans was grown aerobically in rich beef extract/peptone medium (N) containing 100 ml in 250 ml shake flasks with constant agitation (180 rpm, 30^{o}C) on a rotary shaker (Omajali et al., 2015). Eight different minimal media (Table 1) were formulated (A-H) for anaerobic growth with medium F (see Table 1) selected for the subsequent anaerobic growth studies. For anaerobic growth, a 10% overnight inoculum of an aerobic culture was transferred into an anaerobic medium F in an anaerobic bottle with a butyl rubber stopper and aluminium cap. This was left to stand (30^{o}C) in an incubator without shaking. Cells were harvested during exponential growth (OD_{600} = 0.7-1.5) for the aerobic culture and OD_{600} = 0.5-0.6 for the anaerobic culture, washed three times in MOPS (4-morpholinepropanesulfonic acid)-NaOH buffer (pH 7) and stored at 4^{o}C prior to use.

Synthesis of biogenic palladium catalyst

Cell suspensions of both aerobic and anaerobic *B. benzeovorans* made *via* medium N and F respectively were used to synthesize 20wt% bio-Pd [80% dry mass of cell and 20% mass of Pd (0)] based on the method of Omajali et al., (2015). “Palladized” cells

(bio-Pd) were washed three times in distilled water and once in acetone, dried at room temperature and ground.

Characterization of biogenic Pd

The physical characteristics of palladized cells were examined *via* transmission electron microscopy (TEM) and X-ray powder diffraction (XRD) using previously described methods (Deplanche et al., 2014; Omajali et al. 2015). X-ray photoelectron spectroscopy (XPS).

Reductive dechlorination of chlorobenzene

Reductive dechlorination of chlorobenzene (5 mM) was used to compare catalytic properties of the bio-Pd made from aerobic and anaerobic cells identical to the methods of Baxter-Plant et al., (2003) and Redwood et al., (2008) except that the substrate was chlorobenzene (in hexane)- (see chapter 2 and section 3.3.1 for details of methods used).

Results

Medium selection for anaerobic growth

Preliminary tests established medium F as the most useful for anaerobic growth of *Bacillus benzeovorans* (Fig 1a, Table 1). Growth in medium F was compared with that in nutrient-rich medium N aerobically (Fig 1b). For Pd production, the cells were harvested during exponential growth at OD_{600} 0.7-1.5 for aerobically grown cells and 0.5-0.6 for anaerobically grown cells (see point of harvest in Fig 1b) and the cells were then resuspended to equivalent metal proportions to make bio-Pd.

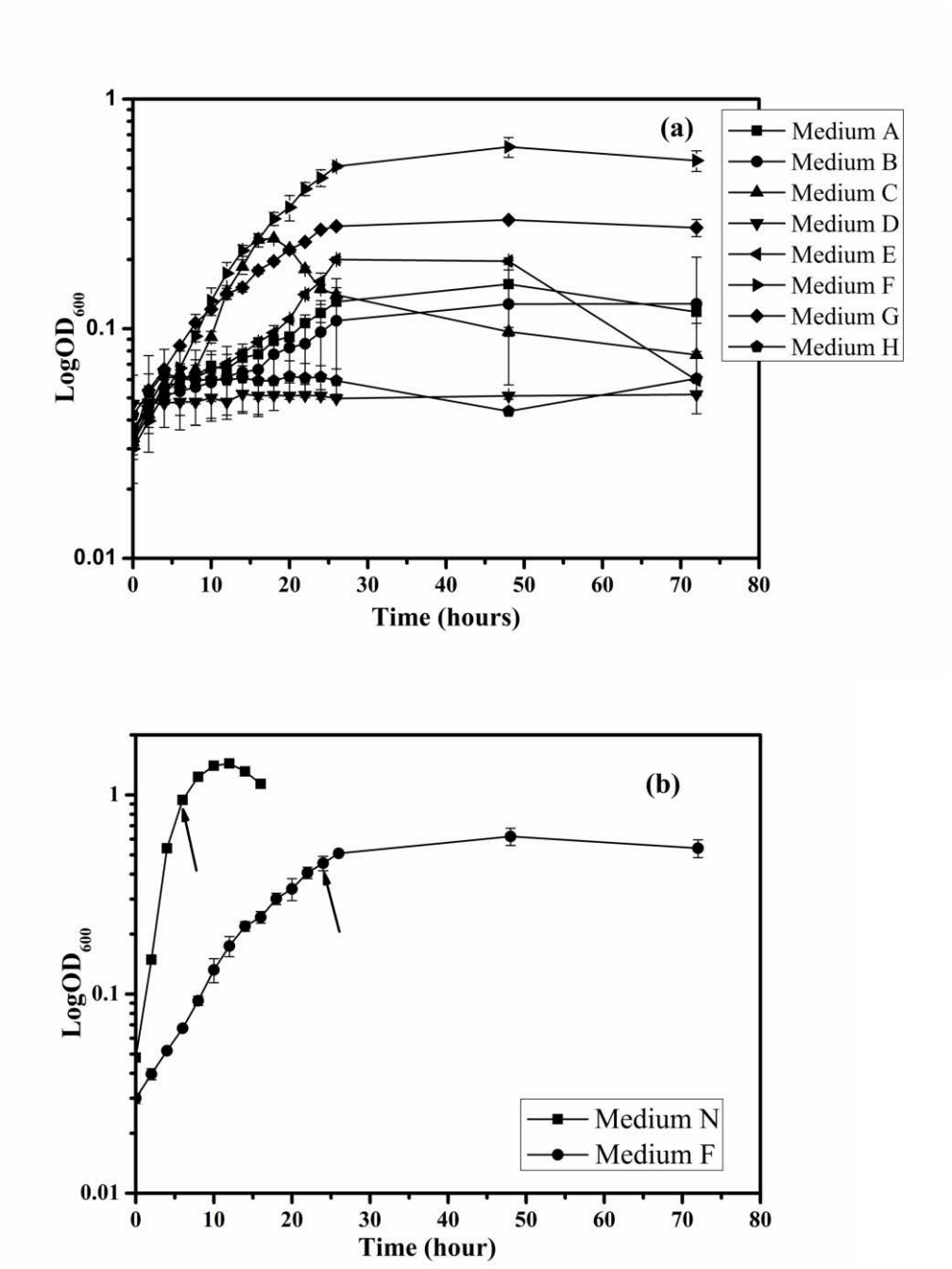

Figure 1 Anaerobic growth of *B. benzeovorans* in (a) eight modified media (A-H, Table 1) within 72 hours and comparison of the best anaerobic medium F with an aerobic medium N (b). Anaerobic media were modified using various electron acceptors and carbon sources (Table 1). Aerobic nutrient medium N was according to Omajali et al., (2015). Arrows: point of harvest of cultures for bio-Pd production.

Table 1 Modified media for anaerobic respiration and fermentative growth of *B. benzeovorans*

Media components		Medium composition							
		A	**B**	**C**	**D**	**E**	**F**	**G**	**H**
KCl	0.62g	+	+	+	+	+	+	+	+
Tris buffer	12g	+	+	+	+	+	+	+	+
$(NH_4)_2HPO_4$	0.96g	+	+	+	+	+	+	+	+
$MgSO_4.7H_2O$	0.063	+	+	+	+	+	+	+	+
$NaNO_2$	0.20%	-	-	-	+	-	-	-	-
$NaNO_3$	0.20%	-	-	+	-	+	-	-	-
$Na_2C_4H_2O_4$	0.40%	+	+	-	-	-	-	-	-
Glucose	20 mM	+	+	+	+	-	+	-	+
Glycerol	0.50%	-	+	-	-	+	-	-	-
$FeSO_4.7H_2O$	0.00033g	+	+	+	+	+	+	+	+
Pyruvate	1%	-	-	-	-	-	+	+	-
Distilled Water	1000ml	+	+	+	+	+	+	+	+

Glucose was prepared separately, degassed, autoclaved and added aseptically to already autoclaved and cooled media to a final concentration of 20mM. pH of media was adjusted to 7.3 with 2M HCl. A-E represent media for anaerobic respiration while F-H is for fermentative growth. Abbreviated symbols: Ammonium phosphate dibasic $(NH_4)_2HPO_4$, Magnesium sulphate heptahydrate ($MgSO_4.7H_2O$), Sodium nitrite ($NaNO_2$), Sodium nitrate ($NaNO_3$), Sodium fumarate dibasic ($Na_2C_4H_2O_4$), Iron (II) sulphate heptahydrate ($FeSO_4.7H_2O$). Components of nutrient medium N; 1.0g beef extract (Sigma-Aldrich), 2.0g yeast extract (Sigma-Aldrich), 5.0g peptone (Sigma-Aldrich) and 15.0g NaCl per litre of distilled water (Omajali et al., 2015). +, positive and -, negative is presence or absence of a media component.

Characterization of bio-Pd made by two methods

20wt% bio-Pd catalyst was synthesized from 2mM Na_2PdCl_4 solution (pH 2) using hydrogen as electron donor and cells of *B. benzeovorans* as catalyst support. The bio-Pd synthesized by aerobically and anaerobically-grown cells was characterized using transmission electron microscopy (TEM) which showed surface and intracellular localization of bio-Pd in both cell types (Fig 2a, b). In both preparations, most of the Pd-NPs were localized as small NPs within the intracellular compartments (circles in Fig 2 a, b) with occasional larger deposits. X-ray photoelectron spectroscopy (XPS) (Fig 2 c, d) shows the presence of two valence states (Pd (0) and Pd (II)) of palladium with two doublets each in both types of cells. In the aerobic cells, the two doublets of Pd (0)

appeared at binding energy levels of 334.94eV and 340.21eV with corresponding Pd (II) doublets at 337.75eV and 343.21eV (Fig 1c). With anaerobic cells, the doublets at 335.64eV and 341.10eV were similarly assigned to zero-valent Pd (0) and the peaks at 337.34 eV and 342.73eV to Pd (II) valence state (Fig 2d). There was a difference of about 0.7 eV in the binding energies of the zero-valent Pd between both cell types. XPS is a surface technique informing on the outermost (3-5 nm) of the cell (Ahimou et al., 2007) with a detection limit of ~5-10 nm (Fairley, 2013) below the cell surface; here XPS showed no major difference between the surface-Pd of both types of cells but confirmed its Pd its presence and reduction to Pd (0). In contrast, XRD is a 'bulk technique' to provide information about the Pd-NPs located on the surface and also within the cells. Fig 2e shows that both cells produced crystalline Pd with differences in the average crystallite size of the Pd. The anaerobically grown cells produced larger (18.0 ± 6.4 nm) NPs than those obtained in aerobically grown cells (7.5 ± 1.4 nm) which is consistent with the smaller intracellular NPs of the latter as shown in Fig 2a. Average crystallite size was calculated using Scherrer equation (Jaboyedoff et al., 1999).

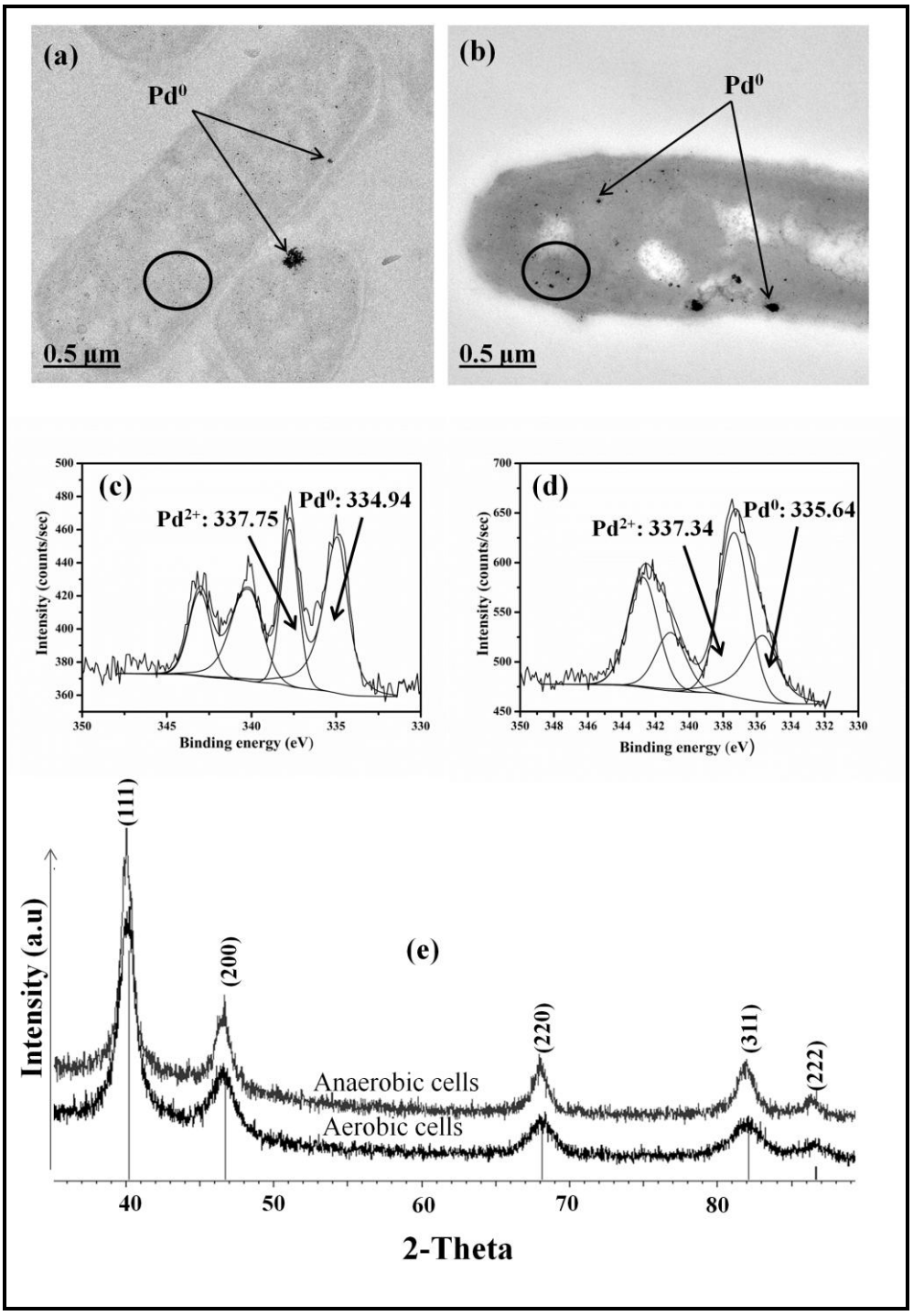

Figure 2 Characterization of bio-Pd catalyst made using aerobic cells (left) and anaerobic cells (right) *via* TEM (a, b), XPS (c, d) and XRD (e). XPS shows the various binding energies of the oxidation states of Pd while XRD powder diffraction patterns show the various planes (vertical lines) and peak intensities of Pd. Bb: *Bacillus benzeovorans*. Scale bar of the TEM images is 0.5 µm. Note that the binding energies of the Pd 3d peaks appear as doublets in each case.

Catalytic property of biogenic Pd (0)

Reductive dechlorination of chlorobenzene was used to compare the catalytic property of the bio-Pd made by aerobic and anaerobic cells that had been washed in acetone to dissolve membrane materials and acetone has been reported to permeabilize cells (Jamur and Oliver, 2010). In this study, the first 20 min showed no difference in the catalyst activities but after 30 min the catalyst made *via* aerobic cells was more active. There was a significant difference ($p < 5\%$) in the total chloride released after 24 h (Fig 3a) with 75.2 mg/L and 63.6 mg/L by aerobic and anaerobic cells respectively. Both reactions were rapid initially (15-20 min) with the rate then decreasing exponentially (Fig 3b). The reaction rate decreased from, initially, 0.199 mmol/min/mg Pd to 0.004 mmol/min/mg Pd after 24 h using catalyst from aerobic cells while that made using anaerobic cells decreased identically from 0.191to 0.003 mmol/min/mg Pd (Fig 3b). Hence, the bio-Pd catalyst made from aerobic cells was more than twice as effective and the final chloride released as well as at the point where reaction slowed (2 h) showed ~26% difference between them. Since *B. benzeovorans* is known to metabolize benzene (Walker and Weatherley, 2000) and other studies have shown that 'palladized' cells retain metabolic activity (J.B. Omajali, unpublished) analysis for the benzene co-product was not carried out as its consumption within the reaction was not known.

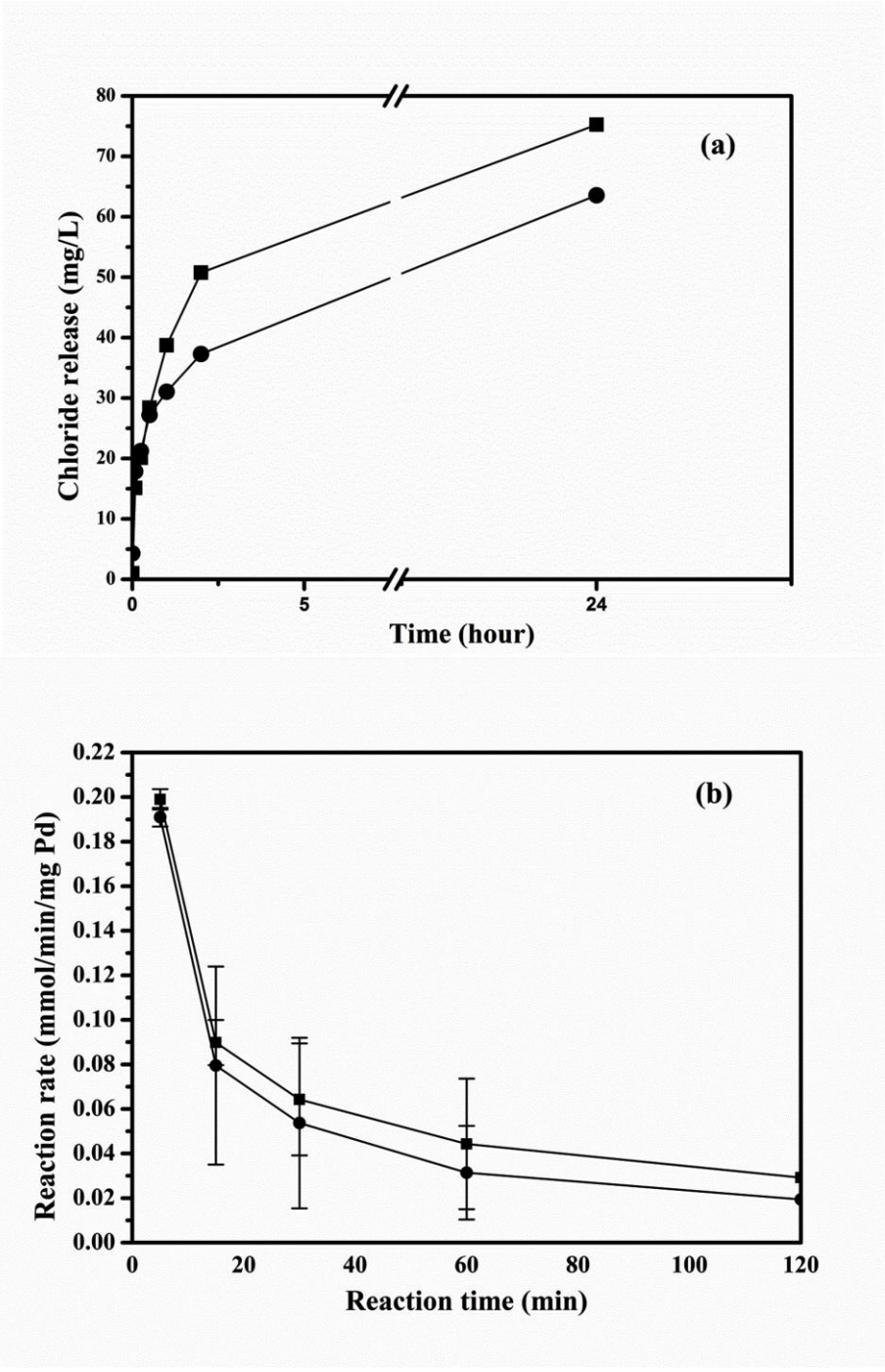

Figure 3 Amount of chloride released from chlorobenzene (5mM starting concentration) in 24 h (a) using catalyst synthesized from aerobic (■) and anaerobic cells (●) of *B. benzeovorans.* Rate of reaction for a chosen period of 2h (120 min) is shown in (b). Results are Mean ± SEM (three preparations) and error bars are within the dimension of the symbols where none is apparent.

Discussion

The synthesis of bio-Pd from anaerobically grown cells of *B. benzeovorans* and subsequent application in catalytic reductive dechlorination of chlorobenzene was demonstrated in this study. *Bacillus* species e.g. *B. subtilis* have been generally considered to be aerobic. However, studies have now shown that several *Bacillus* spp. can grow anaerobically in the presence of external electron acceptors (Geng et al., 2007) or by fermentation (Clements et al., 2002). In this study, *B. benzeovorans* grew anaerobically by both respiration and fermentation, but fermentative growth was better (Fig 1a). Under anaerobic respiration *via* nitrate, nitrite and fumarate, medium with nitrate (medium C) produced the best growth. It is well known that when *B. subtilis* is grown with nitrate and glucose, its dissimilatory nitrate reduction (Nakano and Hulet, 1997) produces nitrite which is toxic and is expelled into the medium (Schirawski and Unden, 1995). Dissimilatory nitrite reduction leads to build up of ammonium ion, known to be toxic (Kadam and Boone, 1996), which may explain the poor growth observed in medium D. The poor growth observed with fumarate (medium A) is not surprising since fumarate is known to be a less efficient electron acceptor than nitrate in *B. subtilis* but not in *B. licheniformis* (Clements et al., 2002).

Fermentative medium F, containing both glucose and pyruvate gave the best growth (Fig 1a). Nakano et al (1997) showed that *B. subtilis* grows better when glucose utilization is stimulated in the presence of pyruvate but not in the presence of either glucose or pyruvate alone (as already known in *E. coli*: Nakano et al., 1997). The mechanism of such stimulation is yet to be elucidated but *B. benzeovorans* fermented pyruvate alone (medium G) better than glucose alone (medium H). Glucose fermentation *per se* in *B. subtilis* was reported to be very poor (Shariati et al., 1995).While the use of glucose alone could not induce the expression of genes required for pyruvate catabolism (substrate induction) (Nakano et al., 1997); the metabolism of pyruvate by pyruvate dehydrogenase (PDH) generates endogeneous electron acceptors like acetyl CoA therefore generating energy (ATP) *via* substrate-level phosphorylation. Genes necessary for anaerobic and fermentative growth in *Bacillus* spp. have now been well reported (Geng et al., 2007) especially the fumarate and nitrate reductase gene (*fnr*) requiring a ResD-ResE two component signal transduction system. When the aerobic

nutrient-rich medium N was compared with the anaerobic medium F, the growth rate and cell yield were better in the former (Fig 1b) as previously reported by Ohara and Yahata, (1996).

Cells of *B. benzeovorans* pre-grown anaerobically were used to synthesize bio-Pd and compared with bio-Pd made from aerobic cells in the dehalogenation of chlorobenzene. The rate of reaction between the two types of catalysts was indistinguishable and rapid initially but decreases finally possibly attributable to fouling of active sites of the Pd-NPs by the chlorinated aromatic substrate as was shown directly using scanning probe microscopy (SPM) and polychlorinated biphenyls (I. P. Mikheenko, unpublished) and it could also be as a result of the fact that the reaction reaches thermodynamic equilibrium. The physical characterisation of the Pd-NPs *via* TEM and XRD (Fig 2) showed that from anaerobically grown cells, the Pd-NPs were overall approximately twice as large as their counterparts made from aerobically grown cells i.e. less total catalyst surface area per unit mass of Pd (0) and hence an earlier saturation of catalyst by fouling deposits.

How various growth conditions influence subsequent particle growth and stability is yet to be determined. In addition to the size of nanoparticles (i.e. surface area), shape and facets are important in catalysis (Zhang et al., 2013). The smaller size of Pd made *via* aerobic cells is sufficient to explain the differences in catalytic property of the two types of bio-Pd in the reductive dechlorination of chlorobenzene but future further examination may be warranted.

Previous studies showed cleavage of benzene by *B. benzeovorans* to be *via* the action of dioxygenases and hence the process is dependent on molecular oxygen. Hence, an integrated 'tandem' catalyst to perform catalytic dechlorination of chlorobenzene followed by metabolism of benzene would require Pd (0) to operate in air as an electron donor other than H_2. Pd-catalysis has been employed to reduce Cr (IV) using formate as the electron donor in air (Beauregard et al., 2010; Yong et al., 2015) and the ability of bio-Pd to reductively dehalogenate chlorobenzene under a similar condition requires confirmation. As an alternative, an anaerobic route (dehalogenation *via* bio-Pd under H_2 and then anaerobic metabolism if shown to exist in *B. benzeovorans*) would be possible. However, since the activity of cells grown aerobically in rich medium was shown in this

study future work will focus on developing bio-Pd in air for this application. In addition, since experiments were not done in aerobic medium F or anaerobic medium N, the observed effect may be completely independent of aerobic/anaerobic conditions and this would also form part of future investigation. However, further studies are needed in order to check the physiological state of the cultures by measuring redox potential and dissolved oxygen of the aerobic cultures.

Conclusion

This study has shown that palladium nanoparticles (bio-Pd) can be synthesized using anaerobic cells of *B. benzeovora*ns as biogenic support. However, the mean nanoparticle size was larger, and the catalytic activity with respect to dehalogenation of chlorobenzene was lower than by using bio-Pd made using cells grown aerobically in rich medium. However, it is unclear whether the rates are significantly different.

Acknowledgements

A Commonwealth Scholarships to JBO is acknowledged, with thanks to Marc Walker of Warwick University for help with XPS measurements.

References

Ahimou, F.; Boonaert, C. J. P.; Adriaensen, Y.; Jacques, P.; Thonart, P.; Paquot, M.; Rouxhet, P. G., XPS analysis of chemical functions at the surface of *Bacillus subtilis*. *Journal of Colloid and Interface Science* **2007,** *309*, 49-55.

Anon. Deadline for EU flavour legislation. http://www.flavourhorizons.com/wp-content/uploads/2011/12/fhissue6.pdf. [1334/2008, Article 3 (2) (e) (ii)]. Issue 6, summer, 2013. Accessed online (27/06/2015).

Baxter-Plant, V. S.; Mikheenko, I. P.; Macaskie, L. E., Sulphate reducing bacteria, palladium and the reductive dehalogenation of chlorinated compounds. *Biodegradation* **2003,** *14*, 83-90.

Beauregard, D. A.; Yong, P.; Macaskie, L. E.; Johns, M. L., Using non-invasive magnetic resonance imaging (MRI) to assess the reduction of Cr(VI) using a biofilm–palladium catalyst. *Biotechnology and Bioengineering* **2010,** *107*, 11-20.

Bennett, J. A.; Mikheenko, I. P.; Deplanche, K.; Shannon, I. J.; Wood, J.; Macaskie, L. E., Nanoparticles of palladium supported on bacterial biomass: New re-usable heterogeneous catalyst with comparable activity to homogeneous colloidal Pd in the Heck reaction. *Applied Catalysis B: Environmental* **2013,** *140–141*, 700-707.

Boutinguiza, M.; Comesaña, R.; Lusquiños, F.; Riveiro, A.; del Val, J.; Pou, J., Palladium nanoparticles produced by CW and pulsed laser ablation in water. *Applied Surface Science* **2014,** *302*, 19-23.

Bunge, M.; Sobjerg, L. S.; Rotaru, A. E.; Gauthier, D.; Lindhardt, A. T.; Hause, G.; Finster, K.; Kingshott, P.; Skrydstrup, T.; Meyer, R. L., Formation of palladium(0) nanoparticles at microbial surfaces. *Biotechnology and Bioengineering* **2010,** *107*, 206-215.

Clements, L. D.; Miller, B. S.; Streips, U. N., Comparative growth analysis of the facultative anaerobes *Bacillus subtilis*, *Bacillus licheniformis*, and *Escherichia coli*. *Systematic and Applied Microbiology* **2002,** *25*, 284-286.

Cole-Hamilton, D. J., Homogeneous catalysis: new approaches to catalyst separation, recovery, and recycling. *Science* **2003,** *299*, 1702-1706.

Creamer, N. J.; Deplanche, K.; Snape, T. J.; Mikheenko, I. P.; Yong, P.; Sanyahumbi, D.; Wood, J.; Pollmann, K.; Selenska-Pobell, S.; Macaskie, L. E., A biogenic catalyst for hydrogenation, reduction and selective dehalogenation in non-aqueous solvents. *Hydrometallurgy* **2008,** *94*, 138-143.

Cruzramos, H.; Boursier, L.; Moszer, I.; Kunst, F.; Danchin, A.; Glaser, P., Anaerobic transcription activation in *Bacillus-subtilis* identification of distinct of distinct FNR-dependent and FNR-independent regulatory mechanisms. *EMBO Journal* **1995,** *14*, 5984-5994.

Choudhary, T. V.; Goodman, D. W., Oxidation catalysis by supported gold nano-clusters. *Top Catalysis* **2002,** *21*, 25-34.

De Corte, S.; Bechstein, S.; Lokanathan, A. R.; Kjems, J.; Boon, N.; Meyer, R. L., Comparison of bacterial cells and amine-functionalized abiotic surfaces as support for Pd nanoparticle synthesis. *Colloids and Surfaces B: Biointerfaces* **2013,** *102*, 898-904.

Deplanche, K.; Caldelari, I.; Mikheenko, I. P.; Sargent, F.; Macaskie, L. E., Involvement of hydrogenases in the formation of highly catalytic Pd(0) nanoparticles by bioreduction of Pd(II) using *Escherichia coli* mutant strains. *Microbiology* **2010,** *156*, 2630-2640.

Deplanche, K.; Bennett, J. A.; Mikheenko, I. P.; Omajali, J.; Wells, A. S.; Meadows, R. E.; Wood, J.; Macaskie, L. E., Catalytic activity of biomass-supported Pd nanoparticles: Influence of the biological component in catalytic efficacy and potential application in

'green' synthesis of fine chemicals and pharmaceuticals. *Applied Catalysis B: Environmental* **2014,** *147*, 651-665.

de Vargas, I.; Sanyahumbi, D.; Ashworth, M. A.; Hardy, C. M.; Macaskie, L. E. In Use of X-ray photoelectron spectroscopy to elucidate the mechanism of palladium and platinum biosorption by *Desulfovibrio desulfuricans* biomass, 25th - 29th September; 16th int. Biohydrometallurgy Symp., Cape Town, Harrison, S. T. L., Rawlings, D.E., Petersen, J., Ed. Cape Town, 2005; pp 605-616.

Faramarzi, M. A.; Sadighi, A., Insights into biogenic and chemical production of inorganic nanomaterials and nanostructures. *Advances in Colloid and Interface Science* **2013,** *189–190*, 1-20.

Fairley N. 2013. CasaXPS. Casa Software Ltd. www.casaxps.com.

Fung, J. M.; Weisenstein, B. P.; Mack, E. E.; Vidumsky, J. E.; Ei, T. A.; Zinder, S. H., Reductive dehalogenation of dichlorobenzenes and monochlorobenzene to benzene in Microcosms. *Environmental Science & Technology* **2009,** *43*, 2302-2307.

Jaboyedoff, M.; Kubler, B.; Thelin, P. H., An empirical Scherrer equation for weakly swelling mixed-layer minerals, especially illite-smectite. *Clay Minerals* **1999,** *34*, 601-617.

Jamur, M. C.; Oliver, C., Permeabilization of cell membranes. *Methods in Molecular Biology* **2010,** *588*, 63-6.

Geng, H.; Zhu, Y.; Mullen, K.; Zuber, C. S.; Nakano, M. M., Characterization of ResDE-dependent *fnr* transcription in *Bacillus subtilis*. *Journal of Bacteriology* **2007,** *189*, 1745-1755.

Gericke, M.; Pinches, A., Biological synthesis of metal nanoparticles. *Hydrometallurgy* **2006,** *83*, 132-140.

Hennebel, T.; De Corte, S.; Verstraete, W.; Boon, N., Microbial production and environmental applications of Pd nanoparticles for treatment of halogenated compounds. *Current Opinion in Biotechnology* **2012,** *23*, 555-561.

Kadam, P. C.; Boone, D. R., Influence of pH ammonia accumulation and toxicity in halophilic, methylotrophic methanogens. *Applied and Environmental Microbiology* **1996,** *62*, 4486-4492.

Klaus-Joerger, T.; Joerger, R.; Olsson, E.; Granqvist, C.-G., Bacteria as workers in the living factory: metal-accumulating bacteria and their potential for materials science. *Trends in Biotechnology* **2001,** *19*, 15-20.

Mertens, B.; Blothe, C.; Windey, K.; De Windt, W.; Verstraete, W., Biocatalytic dechlorination of lindane by nano-scale particles of Pd (0) deposited on Shewanella oneidensis. *Chemosphere* **2007,** *66*, 99-105.

Mikheenko, I. P.; Rousset, M.; Dementin, S.; Macaskie, L. E., Bioaccumulation of palladium by *Desulfovibrio fructosovorans* wild-type and hydrogenase-deficient strains. *Applied and Environmental Microbiology* **2008,** *74*, 6144-6146.

Nakano, M. M.; Hulett, F. M., Adaptation of *Bacillus subtilis* to oxygen limitation. *FEMS Microbiology Letters* **1997,** *157*, 1-7.

Nakano, M. M.; Dailly, Y. P.; Zuber, P.; Clark, D. P., Characterization of anaerobic fermentative growth of *Bacillus subtilis*: Identification of fermentation end products and genes required for growth. *Journal of Bacteriology* **1997,** *179*, 6749-6755.

Narayanan, K. B.; Sakthivel, N., Biological synthesis of metal nanoparticles by microbes. *Advances in Colloid and Interface Science* **2010,** *156*, 1-13.

Nelson, J. L.; Jiang, J.; Zinder, S. H., Dehalogenation of chlorobenzenes, dichlorotoluenes, and tetrachloroethene by three Dehalobacter spp. *Environ Sci Technol* **2014,** *48*, 3776-82.

Nishihata, Y.; Mizuki, J.; Akao, T.; Tanaka, H.; Uenishi, M.; Kimura, M.; Okamoto, T.; Hamada, N., Self-regeneration of a Pd-perovskite catalyst for automotive emissions control. *Nature* **2002,** *418*, 164-167.

Ohara, H.; Yahata, M., L-Lactic acid production by *Bacillus* sp. in anaerobic and aerobic culture. *Journal of Fermentation and Bioengineering* **1996,** *81*, 272-274.

Omajali, J.B; Mikheenkho, I.P; Merroun, L.M; Wood, J; Macaskie L.E., Characterization of intracellular palladium nanoparticles synthesized by *Desulfovibrio desulfuricans* and *Bacillus benzeovorans*. *Journal of Nanoparticle Research* **2015,** *17*, 1-17.

Petrucci, C.; Cappelletti, M.; Piermatti, O.; Nocchetti, M.; Pica, M.; Pizzo, F.; Vaccaro, L., Immobilized palladium nanoparticles on potassium zirconium phosphate as an efficient recoverable heterogeneous catalyst for a clean Heck reaction in flow. *Journal of Molecular Catalysis A: Chemical* **2015,** *401*, 27-34.

Redwood, M. D.; Deplanche, K.; Baxter-Plant, V. S.; Macaskie, L. E., Biomass-supported palladium catalysts on *Desulfovibrio desulfuricans* and *Rhodobacter sphaeroides*. *Biotechnology and Bioengineering* **2008,** *99*, 1045-1054.

Schirawski, J.; Unden, G., Anaerobic respiration of *Bacillus-macerans* with fumarate, tmao, nitrate and nitrite and regulation of the pathway by oxygen and nitrate. *Archives of Microbiology* **1995,** *163*, 148-154.

Schmidt, E.; Mandt, C.; Janssen, D. B.; Pieper, D. H.; Reineke, W., Degradation of chloroaromatics: structure and catalytic activities of wild-type chlorocatechol 2,3-dioxygenases and modified ones. *Environmental Microbiology* **2013,** *15*, 183-190.

Shariati, P.; Mitchell, W. J.; Boyd, A.; Priest, F. G., Anaerobic metabolism in *Bacillus-licheniformis* NCIB-6346. *Microbiology* **1995,** *141*, 1117-1124.

Sobjerg, L. S.; Gauthier, D.; Lindhardt, A. T.; Bunge, M.; Finster, K.; Meyer, R. L.; Skrydstrup, T., Bio-supported palladium nanoparticles as a catalyst for Suzuki-Miyaura and Mizoroki-Heck reactions. *Green Chemstry* **2009,** *11*, 2041-2046.

Switzer-Blum, J.; Burns-Bindi, A.; Buzzelli, J.; Stolz, J. F.; Oremland, R. S., *Bacillus arsenicoselenatis*, sp. nov., and *Bacillus selenitireducens*, sp. nov.: two haloalkaliphiles from Mono Lake, California that respire oxyanions of selenium and arsenic. *Archieves of Microbiology* **1998,** *171*, 19-30

Toebes, M. L.; Dillen, J. A. V.; Jong, K. P. D., Synthesis of supported palladium catalysts. *Journal of Molecular Catalysis A-Chemical* **2001,** *173*, 75-98.

Tzeneva, V. A.; Li, Y. G.; Felske, A. D. M.; de Vos, W. M.; Akkermans, A. D. L.; Vaughan, E. E.; Smidt, H., Development and application of a selective PCR-denaturing gradient gel electrophoresis approach to detect a recently cultivated *Bacillus* group predominant in soil. *Applied and Environmental Microbiology* **2004,** *70*, 5801-5809.

Walker, G. M.; Weatherley, L. R., Biodegradation and biosorption of acid anthraquinone dye. *Environmental Pollution* **2000,** *108*, 219-223.

Yong, P.; Liu, W.; Zhang, Z.; Beauregard, D.; Johns, M. L.; Macaskie, L. E., One step bioconversion of waste precious metals into Serratia biofilm-immobilized catalyst for Cr(VI) reduction. *Biotechnology Letters* **2015**, 1-11.

Zanaroli, G.; Negroni, A.; Häggblom, M. M.; Fava, F., Microbial dehalogenation of organohalides in marine and estuarine environments. *Current Opinion in Biotechnology* **2015,** *33*, 287-295.

Zhang, X.; Wang, H.; Xu, B. Q., Remarkable nanosize effect of zirconia in Au/ZrO_2 catalyst for CO oxidation. *Journal of Physical Chemistry B* **2005,** *109*, 9678-9683.

Zhang, H.; Jin, M.S.; Xiong, Y.J.; Lim, B.; Xia, Y.N. Shape-controlled synthesis of Pd nanocrystals and their catalytic applications. *Accounts of Chemical Research*. **2013**, *46*, 1783-1794.

3.4.2 Potential of Palladized Cells of *Bacillus Benzeovorans* in Tandem Catalytic Remediation of Chlorobenzene

This aspect was written by the J.B. Omajali. All experiments and analysis were also perfomed by the author.

Abstract

The ability to synthesize and use bio-supported Pd catalyst in a multi-step catalytic process would provide a new direction in bio-catalysis and bio-nanotechnology**.** Ensuring the viability and membrane potentials of bacterial cells used in the synthesis of bio-Pd while using sub-lethal concentrations of the metal ions could open up a new direction in the fields of bioremediation, chemical synthesis and other technologies of the future. As a preliminary step, this study demonstrates that 'palladized' cells of *B. benzeovorans* which were confirmed to be viable using growth studies and flow cytometry showed catechol-1, 2- dioxygenase activity. The enzyme activity decreases with increased metal loading with 1wt% bio-Pd having the highest enzyme activity of (130.3 U/ml). There was a significant decrease in enzyme activity when unmetallised cells were grown with various concentrations of chlorobenzene. However, the ability of the cells of *B. benzeovorans* to remain viable after metallisation while still expressing enzyme activity is potentially relevant to the design of a tandem bio-inorganic catalyst with multifunctional properties in the remediation of chlorinated aromatic pollutants.

Introduction

Anthropogenic processes and the widespread use of industrial solvents, pesticides, chemical raw materials, organic synthetic intermediates and deodorants are some of the major sources of chlorinated organic pollutants (e.g. chlorobenzene) in the environment, mainly *via* solids, liquid wastes and atmospheric discharges (Chakraborty and Coates, 2004; Zanaroli et al., 2015). Chlorobenzene is particularly persistent in soil and ground water with the ability to accumulate in fatty tissues thereby resulting in toxic effects in both animals and humans (den Besten et al., 1991). Various strategies have been developed to remediate chlorobenzene (*e.g.* Adrian and Gorisch, 2002; Konuma and Kameda, 2002; Kominami et al., 2013). However, microbial treatment is considered more sustainable *via* either aerobic or anaerobic processes.

In general, microbial treatment requires a supply of electron acceptors such as oxygen, ferric iron, nitrate, and sulphate and electron donors like ferrous iron, hydrogen, methane and sulphide (Liang et al., 2013) which support their growth and biodegradation has also been reported under fermentative conditions (Ramos et al., 2013). Under aerobic condition, oxygen is considered to be the preferred electron acceptor and as a result aerobic bacteria have evolved enzymes capable of degrading chlorobenzene in the presence of oxygen as a reactant, which in polluted water, occurs at the oxic phase of the oxic/anoxic interface (Witt et al., 2002). These enzymes are called dioxygenases and are subdivided into catechol 1, 2-dioxygenase (intradiol dioxygenase) and catechol 2, 3-dioxygenase (extradiol dioxygenase) and are also called ring-cleaving dioxygenases (Schmidt et al., 2013). The enzymes which has an absolute requirement for molecular oxygen, consist of a non-haem iron as the cofactor, ferric iron (Fe^{3+}) in the intradiol cleaving enzyme and ferrous ion (Fe^{2+}) in the extradiol cleaving enzyme (Vetting and Ohlendorf, 2000); the latter does not require a reducing equivalent when inserting hydroxyl groups derived from molecular oxygen into the aromatic ring (Caglio et al., 2009). Many bacteria have been identified to possess both enzymes with the ability of using various chlorobenzenes (Field and Sierra-Alvarez, 2008) as substrates. However, the activity of the enzyme can be reduced under limited oxygen availability, which can also lead to the accumulation of chlorocatechol, a key intermediate in the aerobic breakdown of chlorobenzene (Fritz et al., 1991). The activity

of anaerobic dehalogenating bacteria (Nelson et al., 2014) is an alternative approach where molecular oxygen is limiting but the rate of metabolism is very slow. While chlorinated aromatics can be biodegraded, the rate is much slower than the non-chlorinated equivalents (Adrian and Gorisch, 2002) and it would be advantageous to design a tandem catalytic system using a bacterium known to degrade aromatic compounds with the possibility to accelerate a rate-limiting dehalogenation step prior to entry of the compound into the cell. Apart from the use of inorganic catalysts (Alonso et al., 2002; Yoneda et al., 2007), bio-Pd has been shown in previous studies to reductively dehalogenate chlorinated aromatic compounds (Baxter-Plant et al., 2003; Hennebel et al., 2012) but this can lead to the accumulation of the more toxic benzene (Liang et al., 2013) unless it is metabolised concurrently. Therefore, a system capable of removing both the chlorine substituent and benzene in a one-pot reaction would be more sustainable and this forms the overall goal of this investigation.

Tandem catalysis (Mata et al., 2014) is a coupled catalytic process where sequential transformation of substrates occurs *via* two or more mechanistically distinct processes (Fogg and Santos, 2004). This is further divided into orthogonal, assisted and auto-tandem catalysis. While the orthogonal tandem catalysis requires the use of two or more functionally distinct and non-interfering catalysts, assisted tandem catalysis involves addition of a reagent to trigger the activity of the catalyst and in auto-tandem catalysis the activity of a single catalyst is involved in multifunctional catalysis (Fogg and Santos, 2004; Ostrowski et al., 2015). Until recently, studies on tandem catalysis have been focused on the use of inorganic catalysts in various reactions (Rezayee et al., 2015), e.g. the use of Ir, Rh, Pd and Ru metal complexes in hydrogen autotransfer, also called "borrowing hydrogen" in the formation of C-C and C-N bonds (Choo et al., 2015) and nickel-exchange zincosilicate catalyst in the upgrading of light hydrocarbon *via* a tandem alkane/alkene coupling (Labinger et al., 2015).

The coupling of inorganic; bio-Pd mediated catalysis with a metabolic biotransformation pathway (Foulkes et al., 2011) represented a step change towards integration of chemical and metabolic processes. More recently, Wallace and Balskus (2014) overviewed the potential applications of transition metal catalyst with enzymes due to their high selectivity and synthetic efficiency while Denard et al., (2015)

combined organo-metallic Ru catalyst and an enzymatic system in the tandem conversion of a mixture of alkenes to a single epoxide product with high enantioselectivity and moderate yield (alkene metathesis). The use of whole cell metabolic pathways of bacteria in tandem catalytic process was exemplified by Foulkes et al (2011) using an engineered *E. coli* with the ability to overexpress monoamine oxidase in a deracemization reaction coupled with biotransformation. The aim of this study was to utilize cells of *Bacillus benzeovorans,* a bacterium capable of degrading benzene, as a platform for the synthesis of a bio-inorganic catalyst using a sub-lethal concentration of palladium and to establish that key enzymes of benzene degradation remain active in 'palladized' cells of *B. benzeovorans*. This forms an essential prerequisite in the use of tandem system for accelerated oxidative biodegradation of chlorinated aromatic compounds. While "bio-Pd" has been shown to function in catalysis in the presence of oxygen (I.P.Mikheenko, unpublished) if provided with formate as the electron donor (Yong et al., 2015), the high sensitivity of oxygenase enzymes (*e.g.* methane monoxygenase) to heavy metals (Grosse et al., 1999) means that the ability of the enzyme to be compromised by metal addition must be established, particularly since it is now established that incoming palladium metal can overcome cellular permeability barriers by a mechanism that is still unknown (Omajali et al., 2015). Hence, the objective was to assay the metallised cells for dioxygenase activity, an important aromatic ring-cleavage enzyme under aerobic condition.

Materials and methods

Growth of *B. benzeovorans* with Chlorobenzene

B. benzeovorans strain NCIMB 12555 was grown in nutrient medium as described previously (Omajali et al., 2015). 1% inoculum of overnight grown cells of *Bacillus benzeovorans* was transferred into 100 ml nutrient medium in triplicate in 250 ml shake flasks. A range of initial concentrations of chlorobenzene (0.5, 1.0, 1.5, 3.5 and 5 mM) was added to each flask and controls were without chlorobenzene. Initial OD_{600} was determined and each flask transferred onto a shaker at 180 rpm, 30^{o}C for aerobic

growth. OD_{600} of the culture was determined at the time of harvest and the cell was harvested as described below.

Harvest and preparation of cell extracts

Cells were harvested by centrifugation (9,000 x g, 10 min at 4^{o}C) and washed twice in ice cold 100 mM potassium phosphate buffer (50 mM KH_2PO_4: 50 mM K_2HPO_4 mixture) at pH 7.2. The cells were suspended in ice cold phosphate buffer (10 ml) in triplicate and disrupted with a homogenizer (Aminco, Md; 140 Pa, 0^{o}C) for 2-cycles of 2 minutes with cooling on ice (30 sec) between each cycle. The cell pellets were centrifuged (74,000 x g, 1 h at 4^{o}C) and the clear supernatant solution was used as a source of crude cell extract (Reinke and Knackmuss, 1984; Zaki, 2006) for enzyme assay. Metabolites in the culture fluid ((without cells) were determined by gas chromatography (GC). The entire culture fluid 100 ml) was extracted with hexane (10 ml) and the top layer collected and then concentrated using anhydrous magnesium sulphate (Schenck et al., 2002). The organic layer was collected in glass vials for GC analysis. The GC sample (0.5µl) was injected into a gas chromatograph (Varian CP-3380) equipped with a flame ionization detector (FID) and a RTX-1701 (30 x 0.25 mm x 0.25µm) column (Restek, USA) using helium as a carrier gas (flow rate, 30 ml/min). The following parameters were set: injector temperature (200^{o}C), column temp (70^{o}C), oven temperature (200-250^{o}C), and detector temperature (250^{o}C) at a stabilization time of 50 min and total sample analysis time of 17 min.

Enzyme assay

The enzymes, catechol 1, 2-dioxygenase and catechol 2, 3-dioxygenase were measured separately based on two combined methods (Reinke and Knackmuss, 1984; Hupert-Kocurek et al., 2012). The activity of catechol 1, 2- dioxygenase was determine spectrophotometrically at 260 nm by measuring the formation of the product, *cis, cis*-muconic acid (CCMA) with a molar extinction coefficient (ε_{CCMA} = 16800 M^{-1} cm^{-1}) (Hupert-Kocurek et al., 2012) at 40^{o}C for 10 min. The reaction mixture contained a total volume of 1 ml: 20 µl of crude cell extract was incubated with 30% H_2O_2 (30 µl) for 5 min in order to inactivate catechol 2, 3-dioxygenase activity (Hupert-Kocurek et al., 2012) followed by addition of 67 µl (20 mM) of Na_2EDTA, 863 µl (50 mM) of

phosphate buffer and finally 20 µl (50 Mm) of catechol. The determination of catechol-2, 3- dioxygenase was done based on the formation of the product 2-hydroxymuconic semialdehyde (2-HMS) at 375 nm ($^{\varepsilon}_{2\text{-HMS}}$ = 36, 000 M^{-1} cm^{-1}) under the same experimental conditions as above in a total reaction volume of 1 ml. Reaction mixture contained 20 µl crude cell extract, 960 µl (50 mM) of phosphate buffer and 20 µl (50 Mm) of catechol. All samples were kept on ice during analysis. One unit (U) of enzyme activity was defined as the enzyme amount generating 1µmol of product per min at 40^{o}C.

Preparation of bio-Pd

In a separate preparation, cells of *Bacillus benzeovorans* were grown aerobically without chlorobenzene as described previously (Omajali et al., 2015). Cells were harvested (9,000 x g, 15 m, and 4^{o}C), washed three times with 20mM MOPS-NaOH buffer (pH 7) and resuspended in a small amount of MOPS to a predetermined OD_{600} and dry weight conversion (see appendix). The cells were challenged (30 min, 30^{o}C) with degassed solution (sterile syringe-filtered) of 1 mM Na_2PdCl_4 (pH 2, in 0.01M HNO_3 final pH 2.3) to make 1wt%, 5wt% and 20wt% bio-Pd on cells. Metalized cells were then reduced under H_2 for 15 min and the samples were then transferred onto a shaker at 180 rpm overnight. Residual Pd (II) was assayed by tin (II) chloride method (Omajali et al., 2015). The 'bio-Pd' samples were divided into two: Those for enzyme assay were washed twice (9,000 x g, 15 min, 4^{o}C) and resuspended in phosphate buffer (pH 7.2) as above. The second sets of samples were washed twice in MOPS-NaOH buffer (pH 7.0) and resuspended in a small amount of MOPs (30 ml) and stored at 4^{o}C for the subsequent determination of subsequent growth in nutrient medium and examination by flow cytometry.

Growth study of 'palladized' cells and cell sorting *via* flow cytometry

Palladized cells (1wt%, 5wt% and 20wt% bio-Pd) of *B. benzeovorans* stored at 4^{o}C for one week were each then transferred (1 ml) into a 250 ml shake flask containing 100 ml of freshly prepared nutrient medium in triplicate. Each flask was then incubated (30^{o}C, 180 rpm) and the growth of the palladized cells was monitored. Controls include metal-free cells (untreated) and metal-free cells challenged with 0.01 M HNO_3. Samples were

harvested after 48 h and their dry weight was determined based on a dry weight and OD_{600} conversion (appendix A). Samples (1wt%, 5wt% and 20wt% bio-Pd) of *B. benzeovorans* stored in MOPS buffer for 6 days (4^oC) were also selected for cell sorting using flow cytometry: 2 ml of each palladized cells were washed (12,000 x g, 15 min, 4^oC) to remove MOPS and then washed twice with ice cold phosphate buffered saline-PBS (pH 7.4). 0.1 ml of each sample was added to 1.9 ml of PBS to make up a final volume of 2 ml. The cell mixture was then incubated with 40 µl flourescein diacetate (FDA) and 4 µl of propidium iodide (PI) fluorochrome mixture in the dark. Samples were then analysed using flow cytometry (see details in materials and methods, chapter two).

TEM analysis of metallised cells

Palladized cells before and after onward growth were washed twice with distilled water and fixed with 2.5% glutaraldehyde in 0.1 M cacodylate buffer (Omajali et al., 2015), dehydrated, stain, sectioned and viewed using JEOL 1200EX transmission electron microscope (TEM) with an accelerating voltage of 80kV (Deplanche et al., 2014).

Results

Effects of chlorobenzene on growth and enzyme activity

Bacillus benzeovorans was challenged with four different initial concentrations of chlorobenzene (0.5, 1.5, 3.0 and 5.0 mM) as a first step towards establishing the potential of this bacterium in tandem catalysis. The effect of chlorobenzene on growth and activity of dioxygenases (catechol 1, 2- dioxygenase and catechol 2, 3-dioxygenase) was determined. This was to evaluate the effect of chlorobenzene on growth to be able to select a suitable concentration for subsequent work in the absence of added metal. Controls include cells not treated with chlorobenzene. The final OD_{600} was checked after growth of cells within 20-48 h depending on the concentration of the compound used. It was observed that the growth of cells occured within 20 h for the cells treated with 0.5 mM OD_{600} of 1.68 as compared to the untreated cells (OD_{600} = 1.90). Higher concentrations of chlorobenzene produced a longer lag phase (about 32 h for cells treated with 1.5 and 3.0 mM) to reach a final OD_{600} of 1.54 and 1.31 respectively. Even after 24 h, there was no growth in the cells treated with 5.0 mM

chlorobenzene and hence the flasks were left for another 24 h (i.e 48 h) before growth was observed; here the cells reached an OD_{600} of 1.67 **(Figure 1a)**. However, measurement of growth curves would have been a better way to study the changes due to chlorobenzene concentration. Since chlorobenzene is volatile, it would be more useful to add a control without cells to determine the loss of chlorobenzene.

To be able to determine the effects of chlorobenzene on the activity of the dioxygenase, crude cell extracts of each cell treatment were examined. Catechol 2, 3-dioxygenase activity was almost absent in extracts from treated and untreated cells (**Figure 1b**). Hence, only catechol 1, 2- dioxygenase was monitored in subsequent experiments. The activity of catechol 1, 2-dioxygenase decreased with increase in the concentration of chlorobenzene during growth, from 53.7 – 17 U/ml using 0.5 and 5.0 mM chlorobenzene respectively (**Table 1**). The untreated cell control had an activity of 246.5 U/ml. However, the activity of catechol 2, 3-dioxygenase remained between 0.37 U/ml for untreated cells and 0.28 U/ml when treated with 5.0 mM of chlorobenzene. **Figure 1** shows that 0.5 mM chlorobenzene gave an activity of catechol 1, 2-dioxygenase of ~50% of the activity of untreated cells and this concentration was chosen for subsequent work. Gas chromatography (GC) analysis of organic extract of depleted growth medium did not show the presence of either chlorobenzene or benzene, meaning that chlorobenzene must have been metabolized into other products which could not be determined using the GC method.

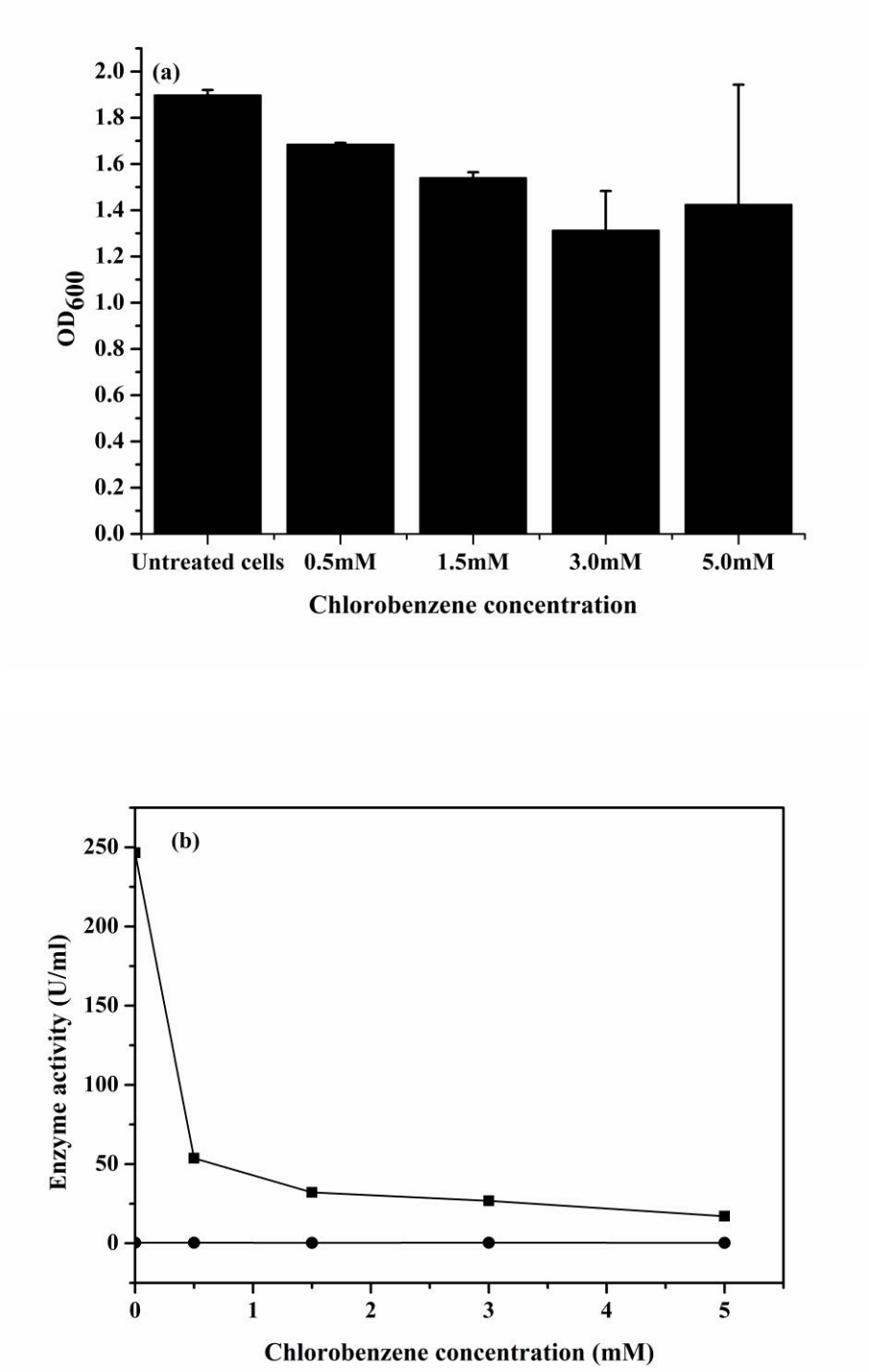

Figure 1 Growth of *B. benzeovorans* on chlorobenzene (a) between 20 and 48 h and activity of catechol 1, 2- dioxygenase (■) and catechol 2,3-dioxygenase (●) in crude cell extract of *B. benzeovorans* grown in the presence of various concentrations of chlorobenzene. Incubation time for the cells ranges between 20-48h (20h, 32h, 32h, 48h) depending on the concentration (0.5, 1.5, 3.0, 5.0 mM) of chlorobenzene used respectively.

Growth and determination of enzyme activity of metallised cells of *B. benzeovorans*

Once the growth and enzyme activity of the cells and cell extract of *B. benzeovorans* was established in the presence of chlorobenzene, the next step was to determine the onward growth of 'palladized' cells of *B. benzeovorans* in nutrient-rich medium and subsequently analyse the cell extracts for catechol 1, 2-dioxygenase activity. Various metal loadings on cells from a 1 mM Pd (II) solution were used (1wt% bio-Pd, 5wt% bio-Pd and 20wt% bio-Pd) and controls included cells treated with 0.01M HNO_3 and cells not treated with Pd. The growth was monitored for 48 h before cells were harvested and extracted for the determination of catechol 1, 2-dioxygenase activity. During growth, the untreated cells were the best in terms of growth which was within 20-24h (OD_{600} = 1.4). The cells treated with 0.01M HNO_3 showed the worst growth but there lag phase was within 3h which was better when compared to the lag phase of 8-10 h of metallised cells. However, after 48 h, the final OD_{600} of the metallised cells were 0.6, 0.4, 0.4 (for 20wt%, 5wt% and 1wt% bio-Pd) whereas the acid-treated cells had the least OD_{600} of 0.3 (**Figure 2a**). A similar result can also be seen with the determined dry weight after 48 h of growth, resulting in the following order: untreated cells > 20wt% bio-Pd > 5wt% bio-Pd = 1wt% bio-Pd > cells treated with 0.01M HNO_3 (47.7, 24.8, 18.6, 18.5 and 14.8 mg) respectively **(Figure 2b)**. In order to determine the relative number of viable cells in the 1wt% and 5wt% bio-Pd populations (since dry weight was the same) flow cytometry was used (**Figure 2c**) with 1wt % bio-Pd (~200,000 cells) compared to ~100,000 cells of 5wt% bio-Pd. The controls without Pd and HNO_3 could not be done due to equipment breakdown and should be considered in a subsequent study.

After 48 h of growth of metallised in nutrient medium the cell extracts of metallised cells were used for catechol 1, 2-dioxygenase activity determination and the activity was compared with those challenged with chlorobenzene (**Table 1**). That the cell extracts of the metallised cells during the onward growth still retained some catechol 1, 2-dioxygenase activities with cells metallised at 1wt% having the highest activity (130.3 U/ml) and 20wt% loaded cells with least (20.1 U/ml) (**Table 1**). Electron microscopy images (**Figure 3**) revealed that prior to onward growth of the metallised cells in nutrient medium; cells had deposits of metals both on the surface and inside the

cells (**Figure** 3c, d and e). When representative cells of 20wt% bio-Pd which was harvested after growth in nutrient medium was viewed using electron microscopy, it showed that cells still retained some Pd both within and on the cell surface (**Figure 3f**). However, cells treated with 0.01M HNO_3 showed apparent membrane stress (**Figure 3b**).

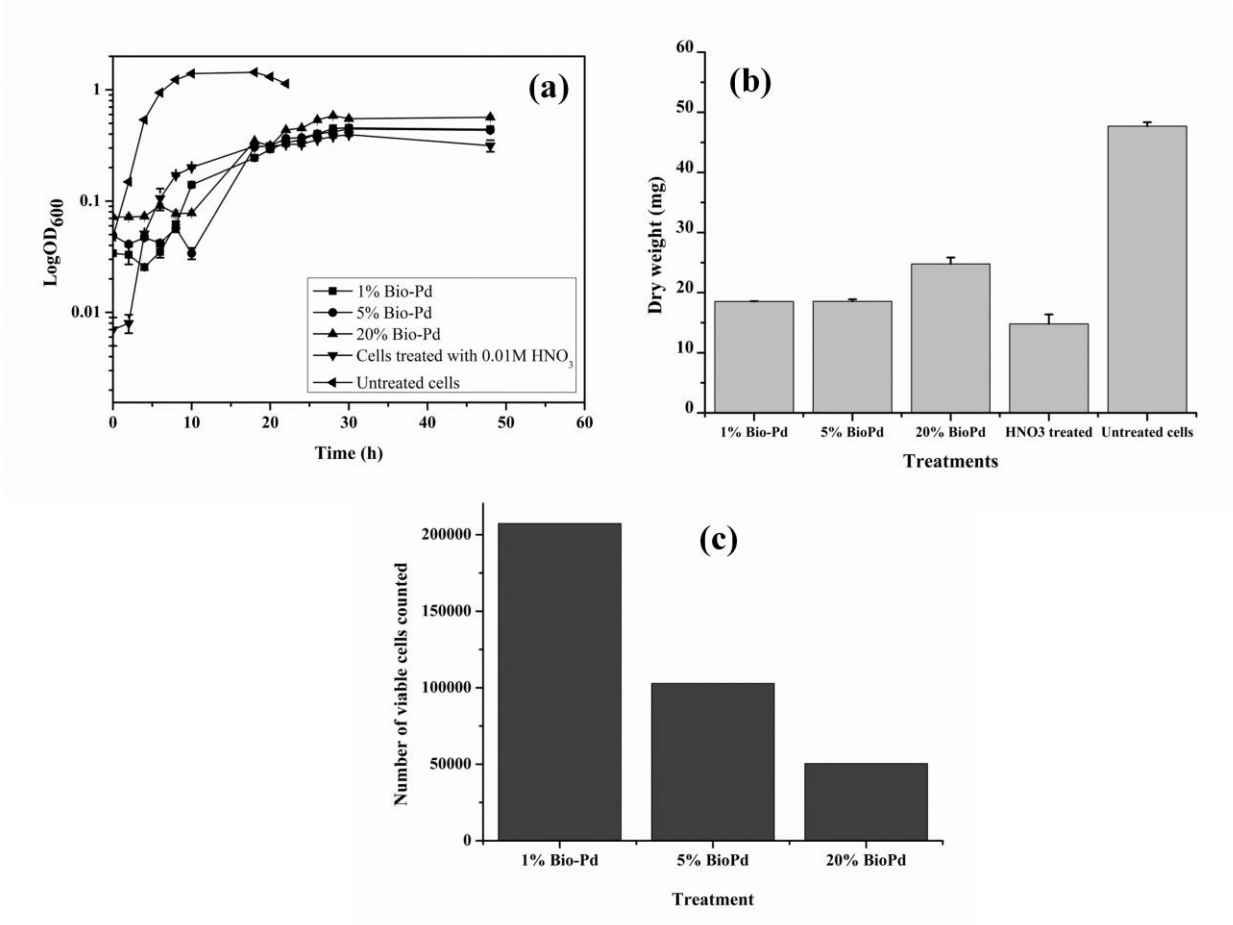

Figure 2 Growth of untreated cells, metallised cells and HNO_3-treated cells of *B. benzeovorans* in nutrient-rich medium (a) and dry weight (b) within 48 hours. Flow cytometry of viable cells of *B. benzeovorans* metallised at 1wt%, 5wt% and 20wt% bio-Pd (c) with the following number of viable cells counted respectively: 207,366, 102,810 and 50,460 after 1 hour of analysis.

Table 1 Summary of the activity of catechol 1, 2- dioxygenase

Treatments	Enzyme activity (U/ml)	Relative enzyme activity (%)
Untreated cells	246.5 ± 0.06	100
0.5 mM chlorobenzene	53.7 ± 0.04	21.8
1.5 mM	32.1 ± 0.02	13.0
3.0 mM	26.8 ± 0.02	10.9
5.0 mM	17.1 ± 0.01	6.9
1wt% bio-Pd	130.3 ± 0.06	52.9
5wt% bio-Pd	61.0 ± 0.01	24.8
20wt% bio-Pd	20.1 ± 0.02	8.2

1 unit of enzyme, U = 1 μmol/min. A relative enzyme activity was calculated as a percentage relative to the untreated cell control (without exposure to either chlorobenzene or palladium solution). Enzyme activities are shown in cells exposed to chlorobenzene, cells not exposed to Pd and cells that had been palladized at 1-20wt% bio-Pd (but not exposed to chlorobenzene).

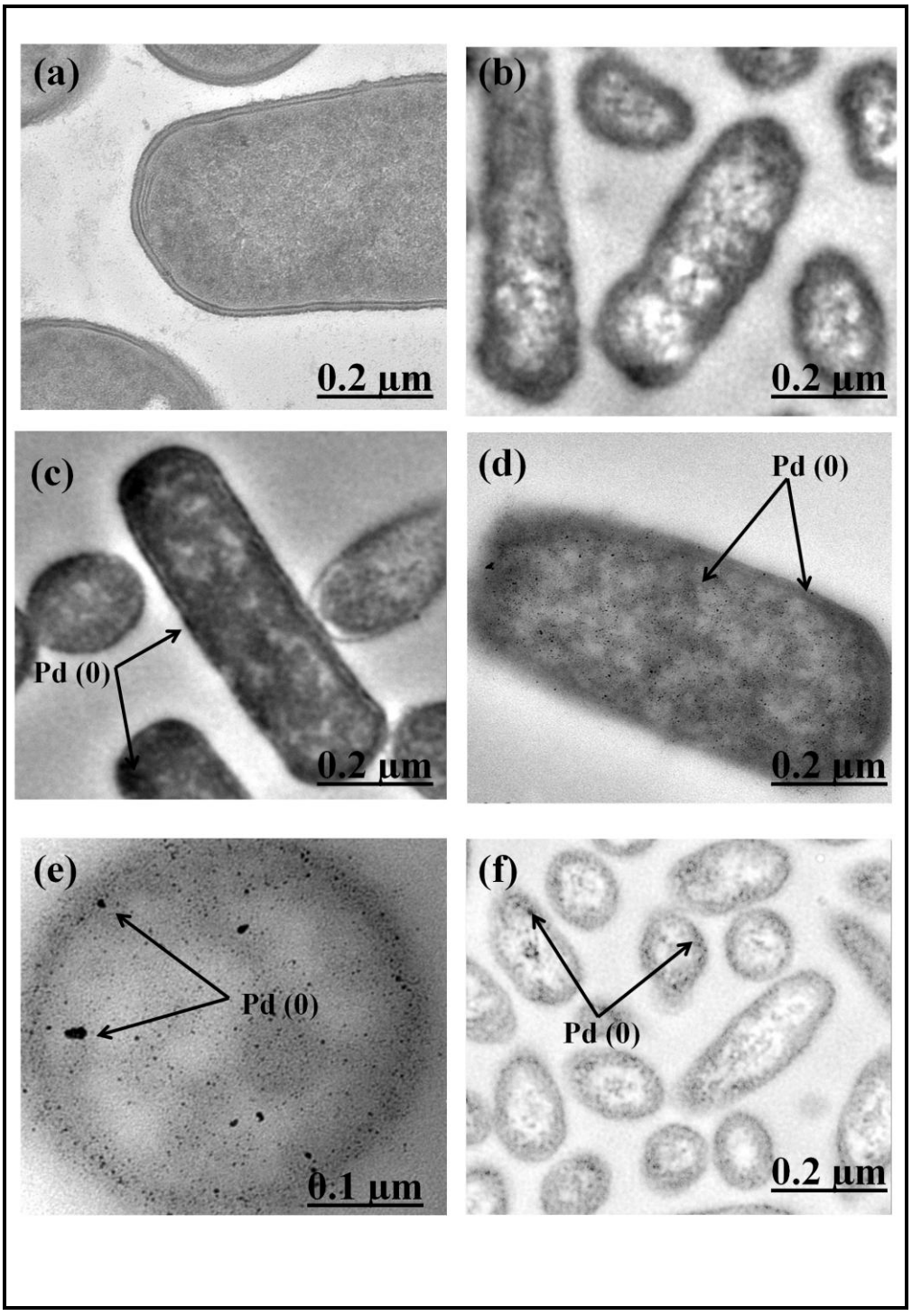

Figure 3 TEM images of metal-free cells (a), HNO_3-treated cells (b) and metal-loaded (1wt%, 5wt% and 20wt% bio-Pd) cells prior to onward growth in nutrient medium (c, d, e) and 20wt% bio-Pd after subsequent growth in nutrient medium (f).

Discussion

Bacteria have evolved degradative or ring cleavage enzymes (Schmidt et al., 2013) in the remediation of environmental pollutants like chlorobenzene but are hindered by the chloro-substituent resulting in slow rate of activity or an outright inhibition (Janssen et al., 2001). Previous work has shown the ability of Pd (0) nanoparticles immobilized on cells of *B. benzeovorans* to reductively dehalogenate chlorobenzene (see section 3.2.1). This preliminary investigation as the first step towards chemical removal of the halogen substituent to release the aromatic compound for metabolic degradation, establishes potential methodologies and platforms towards tandem or multifunctional catalytic remediation of simple chlorinated compounds like chlorobenzene using metallised cells of *Bacillus benzeovorans* which in this study was found to possess catechol 1, 2-dioxygenase activity in the presence Pd (0) nanoparticle in/on the cells.

Initial studies determined the growth of *B. benzeovorans* on various concentrations of chlorobenzene prior to designing a tandem metallo-biological catalyst with a potential for reductive dehalogenation of chlorobenzene and oxic metabolism of the resulting benzene. The lag phase noticed during the growth of *B. benzeovorans* in higher concentration of chlorobenzene did not affect maximal yield. A similar result was shown in a *Planococcus* strain S5 which was able to show maximal yield in phenol despite prolonged lag phase at higher phenol concentration (Hupert-Kocurek et al., 2012). However, at higher chlorobenzene concentration, the activity of catechol 1, 2-dioxygenase decreases compared to lower concentrations of chlorobenzene and that of untreated cells of *B. benzeovorans*. Notably, a concentration of chlorobenzene higher than 3.5 mM was found to be toxic to cells of *Pseudomonas* sp. strain RHO1 (Fritz et al., 1991) due to the accumulation of toxic compounds (2-chlorophenol and 3-chlorocatechol) which were isolated from cell extracts. Generally, chlorobenzoates degraded by aerobic bacteria are de-aromatized from chlorocatechols and then into chloro-cyclohexadiene-1, 2-diol-1-carboxylic acid (DHB) (Suzuki et al., 2002).The accumulation of this DHB as a dead end metabolite could chelate the Fe^{3+} ion of the active site of the *ortho*-cleaving enzyme leading to decreased activity or turnover rate (Broderick and O'Halloran, 1991) and hence prompting consideration of a catalytic dehalogenation step to forestall DHB production by the cells. In this study, despite the

inhibitory effect of chlorobenzene on the *ortho*-cleaving enzyme (catechol 1, 2-dioxygenase), it appears to be the key enzyme in *B. benzeovorans* as the activity of the *meta*-cleaving catechol 2, 3-dioxygenase in both treated and untreated cells of *B. benzeovorans* was negligible.

When cells of *B. benzeovorans* without chlorobenzene were metallised with Pd (0) at various metal loading, the cells still retained catechol 1, 2-dioxygenase activity despite the reduced activity due to metallisation, which was more pronounced in 20 wt% Pd loaded cells than those loaded at 5wt% and 1wt%. The reduced activity of enzyme in metallised cells and extent of growth in acid-treated cells could be as a result of stress induction by acid (intracellular acidification) (Johnson et al., 2014) and free metal ion during uptake by the cells prior to reduction as Pd (0), potentiating the repression of key degradative genes such as *Cat* genes for catechol degradation. The repression of *Cat* gene in *Burkholderia* sp. strain TH2 led to non-transformation of chlorobenzoate (Suzuki et al., 2002). Methane monoxygenase was highly inhibited by heavy metal ions *e.g.* Hg^{+}, Cu^{2+} and Zn^{2+} in *Methylocystis* sp. strain WI 14 (Grosse et al., 1999). However, Guzik et al (2013) reported that while protocatechuate 3, 4-dioxygenase from *Stenotrophomonas maltophilia* was inhibited to a higher extent by heavy metal ions, catechol 1, 2-dioxygenase retained a higher relative activity in the presence of metal ions (e.g. Co^{2+}, Zn^{2+}, Cd^{2+}, Cu^{2+}) with a lesser inhibition. This observation is due to the fact that many metal ions are known inhibitors of sulf-hydryl groups which is capable of changing the conformation of a protein structure (Ha et al., 2000).

This study has demonstrated that metallised cells of *B. benzeovorans* remain viable and retained catechol 1, 2-dioxygenase activity when challenged with a sub-lethal concentration of palladium confirming earlier flow cytometry. For a tandem catalytic process, higher concentrations of chlorobenzene could increase the inhibitory effect of the chloro-substituent and hence concentrations less than 0.5 mM should be considered in a laboratory scale design of a viable bio-inorganic catalyst using *B. benzeovorans*. The fact that benzene or chlorobenzene was not detected in the liquid growth medium *via* GC analysis suggests the transformation of chlorobenzene into the corresponding non-aromatic chlorinated intermediate (e.g. chlorocatechol) or other metabolites that

was not determined using GC analysis. Subsequent studies will utilized the Pd-loaded viable cells in tandem catalysis, whereby the viable cells will act under aerobic condition to de-aromatize chlorobenzene and the Pd (0) to perform a reductive dehalogenation. The application of this technology *in-situ* would require an aerobic/anaerobic cycle to break aromatic ring and reductively dehalogenate the chlorinated compound which may involve the use of alginate beads to immobilize the bio-Pd suspension towards the point of contact with chlorinated compound. However, this awaits future consideration.

References

Adrian, L.; Gorisch, H., Microbial transformation of chlorinated benzenes under anaerobic conditions. *Research in Microbiology* **2002,** *153*, 131-137.

Alonso, F.; Beletskaya, I. P.; Yus, M., Metal-mediated reductive hydrodehalogenation of organic halides. *Chemical Reviews* **2002,** *102*, 4009-4091.

Baxter-Plant, V. S.; Mikheenko, I. P.; Macaskie, L. E., Sulphate reducing bacteria, palladium and the reductive dehalogenation of chlorinated compounds. *Biodegradation* **2003,** *14*, 83-90.

Bartels, I.; Knackmuss, H. J.; Reineke, W., Suicide inactivation of catechol 2, 3-dioxygenase from *Pseudomonas-putida* MT-2 by 3-halocatechols. *Applied and Environmental Microbiology* **1984,** *47*, 500-505.

Braeckevelt, M.; Rokadia, H.; Imfeld, G.; Stelzer, N.; Paschke, H.; Kuschk, P.; Kastner, M.; Richnow, H. H.; Weber, S., Assessment of in situ biodegradation of monochlorobenzene in contaminated groundwater treated in a constructed wetland. *Environmental Pollution* **2007,** *148*, 428-437.

Broderick, J. B.; O'Halloran, T. V., Overproduction, purification, and characterization of chlorocatechol dioxygenase, a non-heme iron dioxygenase with broad substrate tolerance. *Biochemistry* **1991,** *30*, 7349-7358.

Caglio, R.; Valetti, F.; Caposio, P.; Gribaudo, G.; Pessione, E.; Giunta, C., Fine-Tuning of Catalytic Properties of Catechol 1,2-Dioxygenase by Active Site Tailoring. *Chembiochem* **2009,** *10*, 1015-1024.

Choo, G. C. Y.; Miyamura, H.; Kobayashi, S., Synergistic cascade catalysis by metal nanoparticles and Lewis acids in hydrogen autotransfer. *Chemical Science* **2015,** *6*, 1719-1727.

Chakraborty, R.; Coates, J. D., Anaerobic degradation of monoaromatic hydrocarbons. *Appl Microbiol Biotechnol* **2004,** *64*, 437-46.

den Besten, C.; Vet, J. J.; Besselink, H. T.; Kiel, G. S.; van Berkel, B. J.; Beems, R.; van Bladeren, P. J., The liver, kidney, and thyroid toxicity of chlorinated benzenes. *Toxicol Appl Pharmacol* **1991,** *111*, 69-81.

Denard, C. A.; Bartlett, M. J.; Wang, Y. J.; Lu, L.; Hartwig, J. F.; Zhao, H. M., Development of a One-pot tandem reaction combining ruthenium-catalyzed alkene metathesis and enantioselective enzymatic oxidation to produce aryl epoxides. *ACS Catalysis* **2015,** *5*, 3817-3822.

Deplanche, K.; Bennett, J. A.; Mikheenko, I. P.; Omajali, J.; Wells, A. S.; Meadows, R. E.; Wood, J.; Macaskie, L. E., Catalytic activity of biomass-supported Pd nanoparticles: Influence of the biological component in catalytic efficacy and potential application in 'green' synthesis of fine chemicals and pharmaceuticals. *Applied Catalysis B: Environmental* **2014,** *147*, 651-665.

Field, J. A.; Sierra-Alvarez, R., Microbial transformation and degradation of polychlorinated biphenyls. *Environmental Pollution* **2008,** *155*, 1-12.

Fogg, D. E.; dos Santos, E. N., Tandem catalysis: a taxonomy and illustrative review. *Coordination Chemistry Reviews* **2004,** *248*, 2365-2379.

Foulkes, J. M.; Malone, K. J.; Coker, V. S.; Turner, N. J.; Lloyd, J. R., Engineering a biometallic whole cell catalyst for enantioselective deracemization reactions. *ACS Catalysis* **2011,** *1*, 1589-1594.

Fritz, H.; Reineke, W.; Schmidt, E., Toxicity of chlorobenzene on *Pseudomonas* sp. strain RHO1, a chlorobenzene-degrading strain. *Biodegradation* **1991,** *2*, 165-70.

Grosse, S.; Laramee, L.; Wendlandt, K.-D.; McDonald, I. R.; Miguez, C. B.; Kleber, H.-P., Purification and Characterization of the Soluble Methane Monooxygenase of the Type II Methanotrophic Bacterium *Methylocystis* sp. Strain WI 14. *Applied and Environmental Microbiology* **1999,** *65*, 3929-3935.

Guzik, U.; Hupert-Kocurek, K.; Sałek, K.; Wojcieszyńska, D., Influence of metal ions on bioremediation activity of protocatechuate 3,4-dioxygenase from *Stenotrophomonas maltophilia* KB2. *World J Microbiol Biotechnol* **2013,** *29*, 267-273.

Ha, Y. M.; Jung, Y. H.; Kwon, D. Y.; Kim, Y.; Kim, C. K.; Min, K. H., Reaction characteristics of 4-methylcatechol 2,3-dioxygenase from *Pseudomonas* putida SU10. *Journal of Microbiology and Biotechnology* **2000,** *10*, 35-42.

Hennebel, T.; De Corte, S.; Verstraete, W.; Boon, N., Microbial production and environmental applications of Pd nanoparticles for treatment of halogenated compounds. *Current Opinion in Biotechnology* **2012,** *23*, 555-561.

Hupert-Kocurek, K.; Guzik, U.; Wojcieszynska, D., Characterization of catechol 2, 3-dioxygenase from *Planococcus* sp strain S5 induced by high phenol concentration. *Acta Biochimica Polonica* **2012,** *59*, 345-351.
Janssen, D. B.; Oppentocht, J. E.; Poelarends, G. J., Microbial dehalogenation. *Current Opinion in Biotechnology* **2001,** *12*, 254-258.

Johnson, M. D.; Bell, J.; Clarke, K.; Chandler, R.; Pathak, P.; Xia, Y.; Marshall, R. L.; Weinstock, G. M.; Loman, N. J.; Winn, P. J.; Lund, P. A., Characterization of mutations in the PAS domain of the EvgS sensor kinase selected by laboratory evolution for acid resistance in *Escherichia coli*. *Molecular Microbiology* **2014,** *93*, 911-927.

Kominami, H.; Nishi, T.; Fuku, K.; Hashimoto, K., Photocatalytic reductive dechlorination of chlorobenzene in alkali-free aqueous alcoholic suspensions of palladium-loaded titanium (iv) oxide particles in the absence or presence of oxygen. *RSC Advances* **2013,** *3*, 6058-6064.

Konuma, K.; Kameda, N., Effect of substituents on the hydrodechlorination reactivity of para-substituted chlorobenzenes. *Journal of Molecular Catalysis A: Chemical* **2002,** *178*, 239-251.

Labinger, J. A.; Leitch, D. C.; Bercaw, J. E.; Deimund, M. A.; Davis, M. E., Upgrading light hydrocarbons: a tandem catalytic system for alkane/alkene coupling. *Top Catal* **2015,** *58*, 494-501.

Liang, X. M.; Devine, C. E.; Nelson, J.; Lollar, B. S.; Zinder, S.; Edwards, E. A., Anaerobic Conversion of Chlorobenzene and Benzene to CH4 and CO2 in Bioaugmented Microcosms. *Environmental Science & Technology* **2013,** *47*, 2378-2385.

Mars, A. E.; Kasberg, T.; Kaschabek, S. R.; vanAgteren, M. H.; Janssen, D. B.; Reineke, W., Microbial degradation of chloroaromatics: Use of the meta-cleavage pathway for mineralization of chlorobenzene. *Journal of Bacteriology* **1997,** *179*, 4530-4537.

Mata, J. A.; Hahn, F. E.; Peris, E., Heterometallic complexes, tandem catalysis and catalytic cooperativity. *Chemical Science* **2014,** *5*, 1723-1732.

Nelson, J. L.; Jiang, J.; Zinder, S. H., Dehalogenation of chlorobenzenes, dichlorotoluenes, and tetrachloroethene by three Dehalobacter spp. *Environ Sci Technol* **2014,** *48*, 3776-82.

Omajali, J. B; Mikheenko, I. P; Merroun, M. L; Wood, J.; Macaskie, L. E, Characterization of intracellular palladium nanoparticles synthesized by *Desulfovibrio desulfuricans* and *Bacillus benzeovorans*. *Journal of Nanoparticle Research* **2015,** *17*, 1-17.

Ostrowski, K. A.; Fassbach, T. A.; Vorholt, A. J., Tandem hydroformylation/acyloin reaction - the synergy of metal catalysis and organocatalysis yielding acyloins directly from olefins. *Advanced Synthesis & Catalysis* **2015,** *357*, 1374-1380.

Ramos, D. T.; da Silva, M. L.; Chiaranda, H. S.; Alvarez, P. J.; Corseuil, H. X., Biostimulation of anaerobic BTEX biodegradation under fermentative methanogenic conditions at source-zone groundwater contaminated with a biodiesel blend (B20). *Biodegradation* **2013,** *24*, 333-41.

Reineke, W.; Knackmuss, H. J., Microbial metabolism of haloaromatics: isolation and properties of a chlorobenzene-degrading bacterium. *Applied and Environmental Microbiology* **1984,** *47*, 395-402.

Riegert, U., Burger, S., Stolz, A. Altering catalytic properties of 3-chlorocatechol-oxidizing extradiol dioxygenase from *Sphingomonas xenophaga* BN6 by random mutagenesis. *Journal of Bacteriology* **2001,** *183*, 2322-2330.

Rezayee, N. M.; Huff, C. A.; Sanford, M. S., Tandem amine and ruthenium-catalyzed hydrogenation of CO_2 to methanol. *Journal of the American Chemical Society* **2015,** *137*, 1028-1031.

Schenck, F. J.; Callery, P.; Gannett, P. M.; Daft, J. R.; Lehotay, S. J., Comparison of magnesium sulfate and sodium sulfate for removal of water from pesticide extracts of foods. *Journal of Aoac International* **2002,** *85*, 1177-1180.

Schmidt, E.; Mandt, C.; Janssen, D. B.; Pieper, D. H.; Reineke, W., Degradation of chloroaromatics: structure and catalytic activities of wild-type chlorocatechol 2,3-dioxygenases and modified ones. *Environmental Microbiology* **2013,** *15*, 183-190.

Suzuki, K.; Ichimura, A.; Ogawa, N.; Hasebe, A.; Miyashita, K., Differential expression of two catechol 1,2-dioxygenases in Burkholderia sp strain TH2. *Journal of Bacteriology* **2002,** *184*, 5714-5722.

Vetting, M. W.; Ohlendorf, D. H., The 1.8 angstrom crystal structure of catechol 1, 2-dioxygenase reveals a novel hydrophobic helical zipper as a subunit linker. *Structure with Folding & Design* **2000,** *8*, 429-440.

Wallace, S.; Balskus, E. P., Opportunities for merging chemical and biological synthesis. *Current Opinion in Biotechnology* **2014,** *30*, 1-8.

Witt, M. E.; Klecka, G. M.; Lutz, E. J.; Ei, T. A.; Grosso, N. R.; Chapelle, F. H., Natural attenuation of chlorinated solvents at Area 6, Dover Air Force Base: groundwater biogeochemistry. *Journal of Contaminant Hydrology* **2002,** *57*, 61-80.

Yoneda, T.; Takido, T.; Konuma, K., Hydrodechlorination reactivity of para-substituted chlorobenzenes over platinum/carbon catalyst. *Journal of Molecular Catalysis A: Chemical* **2007,** *265*, 80-89.

Yong, P.; Liu, W.; Zhang, Z.; Beauregard, D.; Johns, M. L.; Macaskie, L. E., One step bioconversion of waste precious metals into *Serratia* biofilm-immobilized catalyst for Cr(VI) reduction. *Biotechnology Letters* **2015**, 1-11.

Zaki, S., Detection of *meta*- and *orthor*-cleavage dioxygenase in bacterial phenol-degraders. *Journal of Applied Science and Environmental Management* **2006,** *10*, 75-81.

Zanaroli, G.; Negroni, A.; Häggblom, M. M.; Fava, F., Microbial dehalogenation of organohalides in marine and estuarine environments. *Current Opinion in Biotechnology* **2015,** *33*, 287-295.

CHAPTER 4 Discussion, conclusion and future work

This project has achieved all of its major objectives and hence this chapter summarizes the key findings *via* a final discussion, conclusions and future projects arising from this work. This research has demonstrated the effects of bacterial support surfaces in catalysis by elucidating the key functional groups involved in coordination during Pd (II) uptake and by also confirming endogenous reduction of Pd (II) in *Desulfovibrio desulfuricans*. Catalytic applications of catalysts made by both *Bacillus benzeovorans* and *Desulfovibrio desulfuricans* were demonstrated in reductive dehalogenation of chlorobenzene, hydrogenation of soy bean oil and heavy oil upgrading. This study also revealed intracellular synthesis of palladium nanoparticles which was previously thought to be mainly a cell surface phenomenon. This was followed by the finding that Pd-carrying cells were both viable and metabolically active *via* flow cytometry analysis. Finally, towards the design of a tandem catalyst, *B. benzeovorans* was chosen as a candidate of choice due to its ability to degrade benzene, grow under anaerobic condition and as a platform for nanoscale palladium synthesis while still maintaining cell viability and retaining dioxygenase enzyme activity, paving the way to synthesis of Pd (0) anaerobically followed by a tandem oxic process for chlorobenzene degradation.

4.1 Concluding discussion

This study has demonstrated the ability of *Bacillus benzeovorans* and two strains of *Desulfovibrio desulfuricans* (NCIMB 8307 and NCIMB 8326) to precipitate palladium nanoparticles of defined sizes and morphologies on both cell surfaces and intracellular matrices. The motivation behind the hypothesis on the two strains of *D. desulfuricans* lay in understanding why NCIMB 8307 makes better catalysts than other *Desulfovibrio* species studied previously, by comparing this with a close relative, strain NCIMB 8326.This followed a study by Goldsworthy (2011) whereby the two strains were compared based on their ability to biosynthesize hydrocarbons. That study found the presence of fatty acid ethanolamide in NCIMB 8307 which was suggested by Goldsworthy (2011) to be due to the under-expression of a membrane enzyme aspartyl/glutamyl t-RNA amidotransferase (with an amidase signature) which was found to be over expressed in NCIMB 8326 thereby eliminating the persistence of fatty

acid ethanolamide in this strain. Binding of Pd (II) to amide groups had been reported by G.A. Attard (personal communication, 2011). The initial working hypothesis of this study was that the fatty acid ethanolamide could serve as a binding platform for in-coming Pd (II) during catalyst preparation which was suggested to be responsible for the synthesis and patterning of a more active catalyst in NCIMB 8307. However, physical characterisation and cell surface studies using XPS (see previous chapter) revealed that fatty acid ethanolamide was not involved. The key factors responsible for the differences in catalytic properties when the two strains of *Desulfovibrio desulfuricans* were compared in hydrogenation reaction (see previous chapter) include strain-dependent surface structures such as the presence of extracellular materials, cell surface roughness and the influence of surface functional groups identified from XPS studies.

It was found in this study that *D. desulfuricans* NCIMB 8326 which over expresses the enzyme aspartyl/glutamyl t-RNA amidotransferase (Goldsworthy, 2011) also contains extracellular materials which were absent in *D. desulfuricans* NCIM 8307 (the strain with better Pd (0) catalytic properties). It is possible that the presence of the EPS prevents direct interaction of in-coming Pd with the bacterial cell surface and may explain the observation of smooth cell surface in *D. desulfuricans* NCIMB 8326 *via* AFM studies (see earlier section). In addition, the presence of high concentration of phosphorus (a lipid A component of lipopolysaccharide) and calcium (well known to cross-link EPS' polysaccharide) would have been contributed by the EPS which are known to comprise proteins, carbohydrates, lipids and nucleic acids (Pal and Paul, 2008; Jain et al., 2015) leading to interaction and high dispersion of in-coming Pd (II) thereby reducing interaction of Pd (II) with the cell surface. This is a plausible explanation for the limited deposition of Pd (0) observed on both the surface and intracellular matrices of NCIMB 8326 as compared to outer membrane, periplasmic and intracellular deposition in *D. desulfuricans* NCIMB 8307 (see previous sections). However, the under-expression of this enzyme in *D. desulfuricans* NCIMB 8307 and the corresponding persistence of fatty acid ethanolamides may contribute to increased surface roughness that was observed in this strain, possibly subsequently leading to rearrangement of Pd-NPs (Zienkiewickz-Strzalka and Pikus, 2012) on the cell surface and increased catalytic properties. This observation of how smooth or rough the

bacterial surface looks may be due to the type of lipopolysaccharides (**Figure 4**) which extends outward to about 10 nm from the surface of the bacterial outer membrane (Anwar and Choi, 2014). The lipid A component is found mainly in Gram-negative bacteria including some *D. desulfuricans,* as characterized using GC/MS (Wolny et al., 2011) and MALDI mass spectrometry (Zhang-Sun et al., 2015) and was shown to also contain hydroxyl fatty acid-bound amides and esters. The hydroxyl or phosphate linked components of lipid A may be substituted for ethanolamine-phosphate as reported based on the identification of a phosphoethanolamine substituted penta-acyl lipid A in a strain of *D. desulfuricans* (Zhang-Sun et al., 2015). This may explain the surface roughness and formation of fatty acid ethanolamide in NCIMB 8307 and a corresponding smooth surface of NCIMB 8326. In addition to these observations, the binding mechanisms and changes in binding energies of the various functional groups especially the positive shifts observed in the nitrogen groups in NCIMB 8307 may have been partially contributed by nitrogen groups from the fatty acid ethanolamide produced by this strain (NCIMB 8307) but this claim would need further investigation. Amide nitrogen is known to bind to transition metals under acidic condition (Sigel and Martin, 1982), as was used during Pd (II) sorption prior to bio-Pd synthesis. Abiotic amine-functionalized surfaces have been shown to produce more active Pd catalyst (De Corte et al., 2013); however, this is yet to be reported in biological support systems. Notably, apart from binding of metal ion to protein amide nitrogen (Uvdal et al., 1992), binding of metals to fatty acid amide has not yet been observed using XPS.

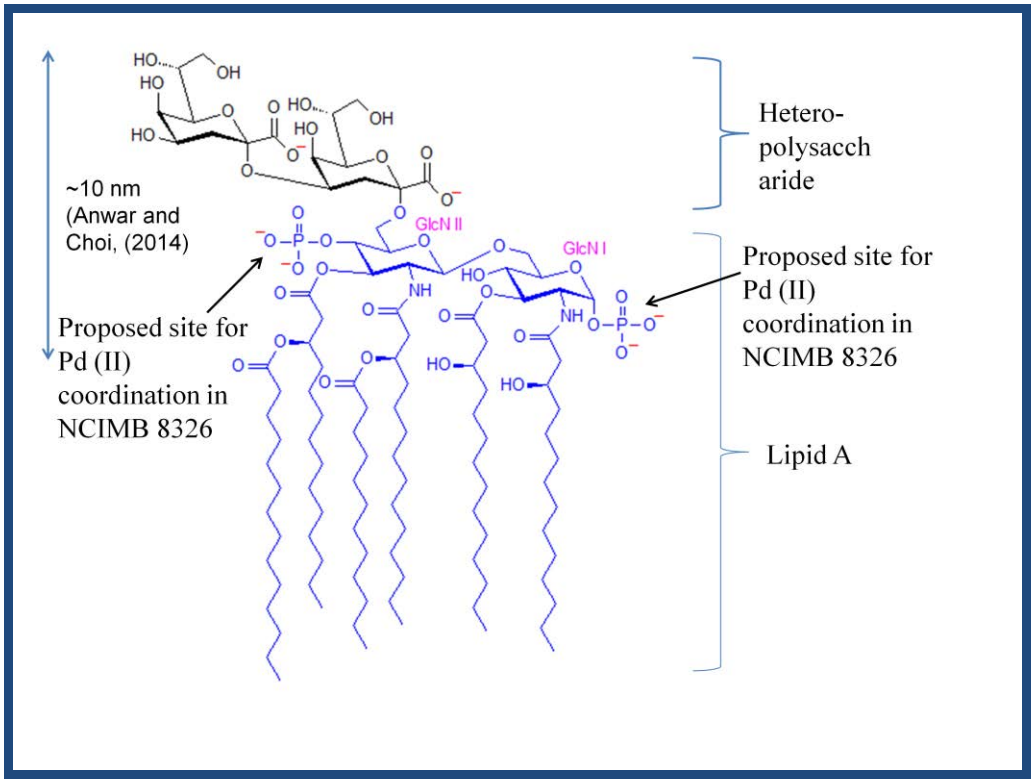

Figure 4 Schematic structure of a basic lipopolysaccharide divided into two major components: covalently bonded lipid A (blue) and hydrophilic hetero-polysaccharide (black). GlcN: glucosamine. Adapted from Anwar and Choi (2014). Note the phosphate groups which are responsible for binding incoming divalent metal ions and thereby crosslinking and densifying the structure (Macaskie et al., 2000; Bonthrone et al., 2000)

Previous investigations have shown the ability of catalyst made using cells of *D. desulfuricans* in a number of catalytic reactions (Bennett et al., 2013; Deplanche et al., 2014). However, in order to move towards large scale synthesis of catalyst under a limited time frame, a *Bacillus* was selected (see previous section for details) since *Bacillus* spp are grown industrially at scale for production of (e.g. commercial enzymes resulting in waste biomass). This would also overcome the challenges of hydrogen sulphide production, a known catalyst poison (Dunleavy, 2006) and also slow (obligately anaerobic) growth of *D. desulfuricans*. Therefore, an initial investigation was made to compare the catalytic properties of *B. benzeovorans* with the two strains of *D. desulfuricans* (NCIMB 8326 and NCIMB 8307) in reductive dehalogenation of chlorobenzene which was extensively discussed in a previous section. This study

however has shown that *D. desulfuricans* NCIMB 8307 produces a better catalyst in the dehalogenation reaction than *D. desulfuricans* NCIMB 8326 and *B. benzeovorans*. XPS has revealed a higher concentration of sulfur in *D. desulfuricans* NCIMB 8307, which might have increased the life span (Dunleavy, 2006) of the catalyst leading to better improvement seen later in the dehalogenation reaction when compared to the other strains. As a result of the poor performance of the catalyst made by *D. desulfuricans* NCIMB 8326, it was not selected in a subsequent reaction involving upgrading of heavy oil.

Bacillus benzeovorans and *Desulfovibrio desulfuricans* NCIMB 8307, which were more active in the reductive dehalogenation test, were selected for the synthesis of mono-metallic and bimetallic catalysts for heavy oil upgrading. Studies on bimetallic synthesis have shown in previous investigations that the synergistic properties of both metals contributed to better catalytic performance than their monometallic counterparts in various applications (Hossain et al., 2004; De Corte et al., 2012). However, this observation is not absolute as other studies have shown situations where monometallic catalyst (bio-Pd) was better (Heugebaert et al., 2012) than bio-Pd/Au in e.g. Suzuki-coupling of arylboronic acid. In this current study, the activities of the 5w t% bimetallic catalyst (Pd/Pt) appeared better than the higher metal loadings (20wt %). There was no difference in the activities of the catalysts made by both cells but when comparing factors like ease of cell growth and potential for large scale production, *B. benzeovorans* was considered a better support for the synthesis of catalyst for heavy oil upgrading than *D. desulfuricans* NCIMB 8307, considering the several challenges involved in using the latter as explained above. In terms of life cycle analysis, bio-Pd will be cheaper to make when compared to commercial catalyst as the bacterial biomass can be sourced cheaply as waste from pharmaceutical industries while the precious metals (Pd and Pt) can also be obtained from wastes (e.g. road dusts and electronic scraps).

Contrary to earlier studies that palladium is mainly deposited on the cell surface and outer compartments of bacteria (outer membrane, periplasm and S-layer protein), the discovery of intracellular synthesis of Pd in both *D. desulfuricans* and *B. benzovorans* in this study and also Pt and Pd in *E. coli* (Priestley et al., 2015; Williams, A. unpublished) has opened up an entirely new direction not only in catalytic synthesis

but also in understanding the mechanism of intracellular trafficking of non-essential metal ions which may further explain the mechanism of cytotoxic non-essential metal ions (e.g. Pd and Pt) in cancer therapy (Cutillas et al., 2013) or as antimicrobial agents (Prasad et al., 2013). The mechanism of bacterial Pd (II) trafficking is yet to be fully understood but a possible trafficking mechanism *via* the Ni (II) trafficking system was recently discussed (Deplanche et al., 2014; Omajali et al., 2015). Unlike mammalian systems, many bacteria have Ni-containing key hydrogenases requiring 'fine control' of metabolism of Ni (Mulrooney and Hausinger, 2003) while ureases are also Ni-enzymes (Eitinger and Mandrand-Berthelot, 2000). A detailed overview is outside the scope of this study and the reader is referred to an extensive review by (Waldron and Robinson, 2009). The formation of the intracellular NPs may also be linked to endogenous reduction at the cell surface that was confirmed in *D. desulfuricans* using XPS (see section 3.1.2). Since XPS only probes bacterial surfaces to the depth of ~5-10 nm, it would not have been possible to probe the intracellular reduction of Pd (II) as indicated by the intracellular localization of metallic crystalline Pd NPs within the cells of bacteria examined. However, another plausible explanation for intracellular NP synthesis is that due to the positive standard redox potential of Pd (II), it could serve as an electron acceptor during bio-Pd synthesis possibly intercepting fortuitously electron acceptors in order to overcome the challenge of moving electrons generated by intracellular metabolism, since flow cytometry has confirmed cell viability and metabolic activity (see later). During respiration, electrons are released from NADH and $FADH_2$ and eventually transferred to oxygen (aerobic respiration) and to other species like nitrate and sulphate in anaerobic respiration. These electrons are generated by the metabolism (glycolysis, β-oxidation and tricyclic acid cycle) inside the bacterial cell (Gottschalk, 2004).

Electron carrier proteins (NADH dehydrogenase, Succinate dehydrogenase and cytochromes) and hydrogen carriers (flavoproteins, Coenzyme Q and menaquinone) of the electron transport chain (ETC) in bacterial cytoplasmic membrane may be utilized based on their standard reduction potentials (Table 4) to transfer electrons for the intracellular reduction of Pd (II) ions. The NADH dehydrogenase (complex I) contains flavin mononucleotide (FMN) and iron-sulfur proteins and has been known to transfer hydride ion from NADH to Coenzyme Q, while succinate dehydrogenase (complex II)

which has a flavin adenine dinucleotide (FAD)-containing protein also transfers hydrogen into the respiratory chain at the Conenzyme Q level. In eukaryotic organisms, this electron transfer process proceeds through the reduction of cytochrome *c* by coenzyme Q *via* complex III and finally complex IV catalysis the transfer of reducing power to oxygen (Equation 12, Table 4) and water is produced (Nicholls and Ferguson, 2013).

However, in some bacteria this mechanism appears to be complex but simpler in *E.coli*. In *E. coli* cytochrome *c* is not involved and in aerobic growing cells, the reducing powers flows from coenzyme Q, cytochrome b_{556} and cytochrome *o* to oxygen; in anaerobic conditions, conenzyme Q or menaquinone and cytochrome b_{558}, *a* and *d* are utilized as carriers (Gottschalk, 2004). It might be assumed that during the synthesis of bio-Pd in both *D. desulfuricans* and *B. benzeovorans*, an available terminal electron acceptor (other than metabolic intermediates) was the soluble Pd (II) ions in the cytoplasm since the standard reduction potential of Pd (II) is higher than that of the other electron carriers (Equation 14, Table 4), particularly Ni (II) (Equation 13, Table 4) which shares similar chemical properties with Pd (II) and is a component of cytoplasmic metallo-enzymes (Maroney, 1999). Electron transfer from cytochrome *c* to an inorganic chemical hexacyanoferrate (VI) has been shown which is often used experimentally as a nonphysiological electron acceptor (see Nicholls and Ferguson, 2013).

Flow cytometry has subsequently confirmed that the metallized cells of *D. desulfuricans* and *B. benzeovorans* maintained cellular integrity and membrane potential which was more prominent when the Pd (II) was reduced with hydrogen or formate as electron donors than left in the corresponding ionic forms. The ionic state of Pd (II) and also the acidic condition (pH ~2) during Pd (II) sorption would be responsible for the reduced cell viability in the bacteria. Acid stress is a well known phenomenon that has been extensively described in Gram-positive (Senouci-Rezkallah et al., 2015) and Gram-negative (Stincone et al., 2011) bacteria whereas free metal ions have been shown to be more toxic above certain threshold concentrations than their metallic counterparts (Gadd, 2010) with lower redox state and reduced mobility. This explains the reduced viability and membrane potentials observed in cells kept in acidic solution of Pd (II) without external reducing agents (see section 3.3.2). However, the

ability of the cells to remain viable when palladized was used to potentially underpin the selection of *B. benzeovorans* as catalyst support for the synthesis of a possible tandem catalyst in the remediation of chlorobenzene. Although this strain can grow fermentatively (see section 3.4.1) an oxic route was chosen for development of the tandem; bio-Pd, once made under H_2 or formate, functions as a chemical catalyst in oxic conditions even in the presence of highly oxidising species such as Cr (VI) (Humphries et al., 2006; Mabbett et al., 2004), reducing them, while reductive dehalogenation was shown in well-agitated suspensions of chlorinated aromatic compounds (Baxter-Plant et al 2003). However, going forward in the application of this work in-situ might require the use an aerobic/anaerobic system for the dual treatmenat of chlorinated compounds and the resulting aromatic ring.

Table 4 Standard oxidation-reduction potentials of respiratory chain components at pH 7.0 and 30^0C in comparison to Ni^{2+} and Pd^{2+}

Components	E'_0 (V)
1. $NAD^+ + 2H^+ + 2e^- \rightleftharpoons NADH + H^+$	-0.320
2. $FAD + 2H^+ + 2e^- \rightleftharpoons FADH_2$	-0.220
3. $FMN + 2H^+ + 2e^- \rightleftharpoons FMNH_2$	-0.190
4. Fumarate + $2H^+$ + 2e- $\rightleftharpoons$ Succinate	+0.033
5. Flavoprotein + $2H^+ + 2e^- \rightleftharpoons$ red. flavoprotein	-0.450-0.0[a]
6. FeS-protein + $2e^- \rightleftharpoons$ red. FeS-protein	-0.400-0.200[a]
7. Menaquinone + $2H^+ + 2e^- \rightleftharpoons$ red. menaquinone	-0.074
8. Ubiquinone + $2H^+ + 2e^- \rightleftharpoons$ red. ubiquinone	+0.113
9. 2 cyt b_{ox} + 2e- $\rightleftharpoons$ 2 cyt b_{red}	+0.070
10. 2 cyt c_{ox} + 2e- $\rightleftharpoons$ 2 cty c_{red}	+0.254
11. 2 cty a_{ox} + $2e^- \rightleftharpoons$ 2 cty a_{red}	+0.384
12. $1/2O_2 + 2H^+ + 2e^- \rightleftharpoons H_2O$	+0.818
13. $Ni^{2+} + 2e^- \rightleftharpoons Ni^0$	-0.27

14. $Pd^{2+} + 2e^- \rightleftharpoons Pd^0$ +0.990

Abbreviations: [a]The redox potential (*E'*$_0$) value of certain flavoproteins or FeS-proteins could be within this range as a result of interaction of the prosthetic groups with the protein. Adapted from Hayes (1993) and Gottschalk (2004).

NAD^+: Nicotinamide Adenine Dinucleotide
NADH: Nicotinamide Adenine Dinucleotide hydride
FAD: Flavin Adenine Dinucleotide
$FADH_2$: Flavin Adenine Dinucleotide Dihydride
FMN: Flavin Mononucleotide
$FMNH_2$: Flavin Mononucleotide Dihydride
Fe-S-Protein: Iron Sulfur Protein
Cyt: Cytochrome
red: Reduced
oxy: Oxidized
H^-: Hydride ion
Pd^{2+}: Palladium ion
Ni^{2+}: Nickel ion

Another major finding from this study was the discovery of the ability of *B. benzeovorans* to retain catechol 1, 2-dioxygenase activity in metallised cells (bio-Pd) which can therefore serve as a potential catalyst in the tandem catalytic remediation of chlorobenzene as a model compound for more complex halogenated aromatics. Chlorinated benzenes, as described earlier, are persistent in the environment and can cause various health problems; hence a one-pot system for remediation could be advantageous since this is mostly very slow under purely biological conditions. Although metallised cells of *B. benzeovorans* were able to retain catechol 1, 2-dioxygenase activity, the challenge remains in its application which would form the basis for future studies.

In conclusion, this study has resulted in the following findings:

i. Fatty acid ethanolamide was not directly responsible for the better catalytic property of bio-Pd (0) observed in *D. desulfuricans* NCIMB 8307 when compared with *D. desulfuricans* NCIMB 8326.

ii. Crystallite size of palladium nanoparticles alone does not influence catalytic property but in combination with factors like bacterial cell surface roughness and variations in cell surface functional groups.

iii. Endogenous reduction was confirmed in *D. desulfuricans* but the main mechanism is yet to be understood.

iv. Lower loading of metals (Pd and Pt) in the synthesis of bimetallic catalyst appeared to be more active than both higher loadings and monometallic catalyst in heavy oil upgrading.

v. Intracellular synthesis of palladium nanoparticles were confirmed in both *Desulfovibrio desulfuricans* and *Bacillus benzeovorans* using either formate or hydrogen as exogenous electron donors.

vi. Metallised cells (1wt% bio-Pd) of *B. benzeovorans* and *D. desulfuricans* maintained both membrane integrity and membrane potential as confirmed *via* flow cytometry.

vii. Bio-Pd can be synthesised using *B. benzeovorans* grown anaerobically with activity in reductive dehalogenation of chlorobenzene.

viii. Metallised cells (1-20wt% bio-Pd) of *B. benzeovorans* retained catechol 1, 2-dioxygenase activity and hence a potential platform for the synthesis of a bio-inorganic catalyst in a tandem (one-pot) catalytic remediation of chlorinated benzenes.

4.2 Future work arising from this research

Due to time constraints, some areas identified during the course of this research could not be investigated and have now formed potential future projects as detailed in the sections below:

4.2.1 *Desulfovibrio desulfuricans*

This study revealed that *D. desulfuricans* NCIMB 8307 which contains fatty acid ethanolamide (Goldsworthy, 2011) produced a better catalyst than *D. desulfuricans* NCIMB 8326 without fatty acid ethanolamide in all the reactions investigated. However, the discovery of extracellular polymeric substances (EPS) in *D. desulfuricans* NCIMB 8326 has raised a new question of whether the presence of such material has

the potential to prevent the cells from making catalytically active catalysts by masking key coordination sites responsible for bio-patterning of Pd (0) NPs. It is hypothesised that the bacterial surface structure could play a major role in determining catalytic activity. Hence, the following future studies are suggested:

i. Extraction of the extracellular polymeric substances (EPS) from *D. desulfuricans* NCIMB 8326 followed by characterization and metallization with processes followed by e.g. carbon and phosphorus NMR. The EPS observed in NCIMB 8326 is supported by the presence of higher concentrations of phosphorus and calcium found *via* XPS, in addition to the fact that palladized extracellular materials have been shown to be active in the dehalogenation of chlorobenzene (Baldi et al., 2011).

ii. Comparison of the palladized EPS with EPS-free cells in a number of catalytic tests.

iii. Comparison of palladized EPS-free cells of NCIMB 8326 with NCIMB 8307 and other strains where EPS has not been found in a series of catalytic reactions.

iv. Extraction and characterization (GC/MS and MALDI-MS) of the lipid A components of NCIMB 8307 and NCIMB 8326 to determine the type of lipid A (smooth or rough) found in each strain in order provide more insights into the property of the cell surfaces (outer-membrane) of Gram-negative bacteria.

v. For many of these studies *E. coli* should be considered as a model organism as it makes catalytically active bio-Pd and is the standard 'workhorse' for molecular engineering and strain development.

4.2.2 *Bacillus benzeovorans*

Bacillus benzeovorans has demonstrated the ability to grow both aerobically and anaerobically and also the activity of the enzyme catechol 1, 2-dioxygenase was confirmed to be retained in metallised cells (bio-Pd). The viability of the cells was also confirmed *via* flow cytometry, suggesting the possibility of producing a bio-inorganic tandem catalyst with potential environmental applications. These initial findings are platforms for the following future project:

i. Design of a tandem catalyst (bio-Pd) for the remediation of a simple chlorinated aromatic compound such as chlorobenzene. Since cells of *B. benzeovorans* can degrade

benzene and palladized cells have shown activity in reductive dehalogenation of chlorobenzene, catechol 1, 2- dioxygenase activity of palladized cells could be used as a bio-inorganic tandem catalyst for reductive dehalogenation of chlorobenzene accompanied by enzymatic degradation of the aromatic ring. Other tests for the determination of cell viability and physiology of bacteria could potentially be used in order to compare results with that of flow cytometry. Such tests could include the determination of lipid peroxidation and use of other molecular techniques to determine changes in proteins (e.g acid-shock proteins). Also, the ability to differentiate metal-containing cells and non-metalised cells should be considered in future work.

ii. Use of gas chromatography or GC-MS to determine the formation of intermediates or identification of metabolites from degradation of the aromatic ring *via* HPLC analysis.

iii. Application to more complex halogenated aromatic compounds

4.2.3 *Bacillus benzeovorans* and *Desulfovibrio desulfuricans*

The discovery of intracellular synthesis of palladium nanoparticles made by cells of *Bacillus benzeovorans* and *Desulfovibrio desulfuricans* is key to understanding the mechanism of intracellular trafficking of non-essential precious metals; hence, the following future project recommendations are suggested:

i. Incorporation of *E. coli* as a model organism since intracellular Pd (0) NPs have been shown in this organism (Williams, A unpublished, Priestley et al., 2015). These NPS were also visible in earlier preparations of *E. coli* (Deplanche et al., 2010) but were not explored further.

ii. Design of a suitable procedure to access the intracellular nanoparticles (NPs) which are small, highly monodispersed and stabilized by the internal biological materials and hence may possess important catalytic properties. Different approaches to cell lysis or cell membrane digestion such as the use of enzyme digestion of cell membrane to release the intracellular particles should be sought and the resulting palladium NPs used in a range of catalytic test. ‘Markers’ for periplasmic and membrane components would need to be incorporated to confirm removal of these components.

iii. To understand the mechanism of trafficking, two major approaches could be adopted; since Pd (II) shares similar chemical properties with Ni (II), the first approach would involve starving the cells of nickel then feed Pd (II). The resulting metallised cell can then be examined using a high resolution STEM followed by EDX for the identification of intracellular Pd and/or Ni.

iv. The second approach could involve the design of mutants devoid of Ni (II) transporter genes and the cells should be treated with Pd (II) and/or Ni (II) while using appropriate controls in order to understand whether intracellular trafficking of these metal ions can still take place in mutants.

Finally, since the cells of *B. benzeovorans* can be used in the synthesis of bimetallic catalyst (Pd/Pt) coupled with the advantage of ease of scale up than *D. desulfuircans*, it should be considered in the synthesis of bimetallic catalyst from wastes sources such as road dust which contains precious metals (Pd and Pt) in addition to other metals. The use of road dust would provide a sustainable and cheaper source of these metals in the production of catalysts in a number of reactions such as heavy oil upgrading, oxidation, reductive dehalogenation, hydrogenation, biomass conversion and other important synthetic reactions.

4.3 References

Anwar, M. A.; Choi, S., marine bacteria: structural features of lipopolysaccharides and their relevance for economically important diseases. *Marine Drugs* **2014,** *12*, 2485-2514.

Baldi, F.; Marchetto, D.; Paganelli, S.; Piccolo, O., Bio-generated metal binding polysaccharides as catalysts for synthetic applications and organic pollutant transformations. *New Biotechnology* **2011,** *29*, 74-78.

Baxter-Plant, V. S.; Mikheenko, I. P.; Macaskie, L. E., Sulphate reducing bacteria, palladium and the reductive dehalogenation of chlorinated compounds. *Biodegradation* **2003,** *14*, 83-90.

Bennett, J. A.; Mikheenko, I. P.; Deplanche, K.; Shannon, I. J.; Wood, J.; Macaskie, L. E., Nanoparticles of palladium supported on bacterial biomass: New re-usable

heterogeneous catalyst with comparable activity to homogeneous colloidal Pd in the Heck reaction. *Applied Catalysis B: Environmental* **2013,** *140–141*, 700-707.

Bonthrone, K. M.; Quarmby, J.; Hewitt, C. J.; Allan, V. J. M.; Paterson-Beedle, M.; Kennedy, J. F.; Macaskie, L. E., The effect of the growth medium on the composition and metal binding behaviour of the extracellular polymeric material of a metal-accumulating Citrobacter sp. *Environmental Technology* **2000,** *21*, 123-134.

Cutillas, N.; Yellol, G. S.; de Haro, C.; Vicente, C.; Rodriguez, V.; Ruiz, J., Anticancer cyclometalated complexes of platinum group metals and gold. *Coordination Chemistry Reviews* **2013,** *257*, 2784-2797.

De Corte, S.; Bechstein, S.; Lokanathan, A. R.; Kjems, J.; Boon, N.; Meyer, R. L., Comparison of bacterial cells and amine-functionalized abiotic surfaces as support for Pd nanoparticle synthesis. *Colloids and Surfaces B: Biointerfaces* **2013,** *102*, 898-904.

Deplanche, K.; Caldelari, I.; Mikheenko, I. P.; Sargent, F.; Macaskie, L. E., Involvement of hydrogenases in the formation of highly catalytic Pd(0) nanoparticles by bioreduction of Pd(II) using *Escherichia coli* mutant strains. *Microbiology* **2010,** *156*, 2630-2640.

Deplanche, K.; Bennett, J. A.; Mikheenko, I. P.; Omajali, J.; Wells, A. S.; Meadows, R. E.; Wood, J.; Macaskie, L. E., Catalytic activity of biomass-supported Pd nanoparticles: Influence of the biological component in catalytic efficacy and potential application in 'green' synthesis of fine chemicals and pharmaceuticals. *Applied Catalysis B: Environmental* **2014,** *147*, 651-665.

Dunleavy, J. K., Sulfur as a catalyst poison. *Platinum Metals Review* **2006,** *50*, 110.

Eitinger, T.; Mandrand-Berthelot, M. A., Nickel transport systems in microorganisms. *Arch Microbiology* **2000,** *173*, 1-9.

Gadd, G. M., Metals, minerals and microbes: geomicrobiology and bioremediation. *Microbiology* **2010,** *156*, 609-643.

Goldsworthy MJH (2011) Hydrocarbon biosynthesis in *Mycobacterium* spp NCIMB 10403 and *Desulfovibrio desulfuricans*. PhD Thesis. University of Exeter, United Kingdom.

Gottschalk , G., *Bacterial Metabolism. 2nd Edition*. 2nd Edition ed.; Springer Verlag: New York Inc.: **2004**; p pp 22-36.

Hayes P. C., Standard reduction potentials. In: Process Principles in Minerals and Materials Production. 2nd edition. Brisbane: Hayes publishing co.**1993**, pp 660-665.

Hossain, M.M.; Al-Saleh M. A.; Shalabi, M. A.; Kimura, T.; Inui, T., Pd–Rh promoted Co/HPS catalysts for heavy oil upgrading, *Applied Catalysis A* **2004**, *278*, 65–71.

Heugebaert, T. S. A.; De Corte, S.; Sabbe, T.; Hennebel, T.; Verstraete, W.; Boon, N.; Stevens, C. V., Biodeposited Pd/Au bimetallic nanoparticles as novel Suzuki catalysts. *Tetrahedron Letters* **2012,** *53*, 1410-1412.

Humphries, A. C.; Mikheenko, I. P.; Macaskie, L. E., Chromate reduction by immobilized palladized sulfate-reducing bacteria. *Biotechnology and Bioengineering* **2006,** *94*, 81-90.

Jain, R.; Jordan, N.; Weiss, S.; Foerstendorf, H.; Heim, K.; Kacker, R.; Hubner, R.; Kramer, H.; van Hullebusch, E. D.; Farges, F.; Lens, P. N. L., Extracellular Polymeric Substances Govern the Surface Charge of Biogenic Elemental Selenium Nanoparticles. *Environmental Science & Technology* **2015,** *49*, 1713-1720.

Mabbett, A. N.; Yong, P.; Farr, J. P. G.; Macaskie, L. E., Reduction of Cr(VI) by "Palladized" - Biomass of *Desulfovibrio desulfuricans* ATCC 29577. *Biotechnology and Bioengineering* **2004,** *87*, 104-109.

Macaskie, L. E.; Bonthrone, K. M.; Yong, P.; Goddard, D. T., Enzymically mediated bioprecipitation of uranium by a *Citrobacter* sp.: a concerted role for exocellular lipopolysaccharide and associated phosphatase in biomineral formation. *Microbiology* **2000,** *146*, 1855-67.

Maroney, M. J. Structure/function relationships in nickel metallobiochemistry. *Current Opinion Chemical Biology* **1999**, *3,* 188-199.

Mulrooney, S. B.; Hausinger, R. P., Nickel uptake and utilization by microorganisms. *FEMS Microbiology Reviews* **2003,** *27*, 239-261.

Nicholls, D. G.; Ferguson, S. J., 5 - Respiratory Chains. In *Bioenergetics (Fourth Edition)*, Nicholls, D. G.; Ferguson, S. J., Eds. Academic Press: Boston, 2013; pp 91-157.

Omajali, J. B; Mikheenkho, I. P; Merroun, L. M; Wood, J; Macaskie, L. E., Characterization of intracellular palladium nanoparticles synthesized by *Desulfovibrio desulfuricans* and *Bacillus benzeovorans*. *Journal of Nanoparticle Research* **2015**, *17*, 1-17.

Pal, A.; Paul, A. K., Microbial extracellular polymeric substances: central elements in heavy metal bioremediation. *Indian Journal of Microbiology* **2008,** *48*, 49-64.

Prasad, K. S.; Kumar, L. S.; Chandan, S.; Naveen Kumar, R. M.; Revanasiddappa, H. D., Palladium(II) complexes as biologically potent metallo-drugs: Synthesis, spectral characterization, DNA interaction studies and antibacterial activity. *Spectrochimica Acta Part A: Molecular and Biomolecular Spectroscopy* **2013,** *107*, 108-116.

Priestley, R. E.; Macaskie, L. E.; Mansfield, A.; Bye, J.; Deplanche, K.; Jorge, A. B.; Bret, D.; Sharma, S., Pd nanoparticles supported on reduced grapheme-*E. coli* hybrid with enhanced crystallinity in bacterial biomass. *RSC Advances* (accepted subject) **2015**

Senouci-Rezkallah, K.; Jobin, M. P.; Schmitt, P., Adaptive responses of *Bacillus cereus* ATCC14579 cells upon exposure to acid conditions involve ATPase activity to maintain their internal pH. *Microbiology open* **2015,** *4*, 313-322.

Sigel, H.; Martin, R. B., Coordinating properties of the amide bond-stability and structure of metal-ion complexes of peptides and related ligands. *Chemical Reviews* **1982,** *82*, 385-426.

Stincone, A.; Daudi, N.; Rahman, A. S.; Antczak, P.; Henderson, I.; Cole, J.; Johnson, M. D.; Lund, P.; Falciani, F., A systems biology approach sheds new light on *Escherichia coli* acid resistance. *Nucleic Acids Research* **2011,** *39*, 7512-7528.

Uvdal, K.; Bodö, P.; Liedberg, B., l-cysteine adsorbed on gold and copper: An X-ray photoelectron spectroscopy study. *Journal of Colloid and Interface Science* **1992,** *149*, 162-173.

Waldron, K. J.; Robinson, N. J., How do bacterial cells ensure that metalloproteins get the correct metal? *Nature Reviews Microbiology* **2009,** *7*, 25-35.

Wolny, D.; Lodowska, J.; Jaworska-Kik, M.; Kurkiewicz, S.; Weglarz, L.; Dzierzewicz, Z., Chemical composition of *Desulfovibrio desulfuricans* lipid A. *Archives of Microbiology* **2011,** *193*, 15-21.

Williams, A. PhD thesis-In preparation. University of Birmingham, UK

Zienkiewicz-Strzalka, M.; Pikus, S., The study of palladium ions incorporation into the mesoporous ordered silicates. *Applied Surface Science* **2012,** *261*, 616-622.

Zhang-Sun, W.; Augusto, L. A.; Zhao, L.; Caroff, M., *Desulfovibrio desulfuricans* isolates from the gut of a single individual: structural and biological lipid A characterization. *FEBS Lett* **2015,** *589*, 165-71.

CHAPTER 5 Appendices

This section contains additional information not covered elsewhere in the thesis. This includes some preliminary investigations and work not yet ready for publication and also quantitative methods involved in the preparation of standards and reagents.

5.1 Appendix A

5.1.1 Determination of OD_{600} to dry weight (OD_{600}/DW) conversion factor

The determination of the OD_{600}/dry weight conversion factors for the strains used in this study was important in order to calculate accurate loading of metals on cells. In previous studies, this factor was determined for *Desulfovibrio desulfuricans* (see summary table 5.1.1) (Deplanche, 2008). To determine the OD_{600} to dry weight conversion factor, cells of *B. benzeovorans* (4 L) were grown for 24 h and then harvested (9,000 x g, 15 min, 4^{o}C) and washed in 20 mM MOPS-NaOH buffer (pH 7.0). Triplicate serial dilutions of the stock cells (total volume of 30 ml) were made in a pre-weighed 50 ml tubes and the OD_{600} were then recorded before pelleting the cells (4000 rpm, 15 min, 4^{o}C). The cell pellets were dried to constant weight in an oven overnight at 104^{o}C and then transferred into a desiccator (4 h). The final weight of dried cell pellets was then correlated to OD_{600} and the OD_{600}/DW conversion factor was calculated as determined from the regression line for an OD_{600} of 1. See Figure below for the calibration curve of OD_{600}/DW conversion for *B. benzeovorans*.

Table 5.1.1 Summary for OD_{600}/DW conversion factors of strain used in this study

Bacterial Strain	OD_{600}/DW conversion factor (mg/ml)
B. benzeovorans	0.42
D. desulfuricans	0.72

Calibration curve for OD_{600}/DW conversion

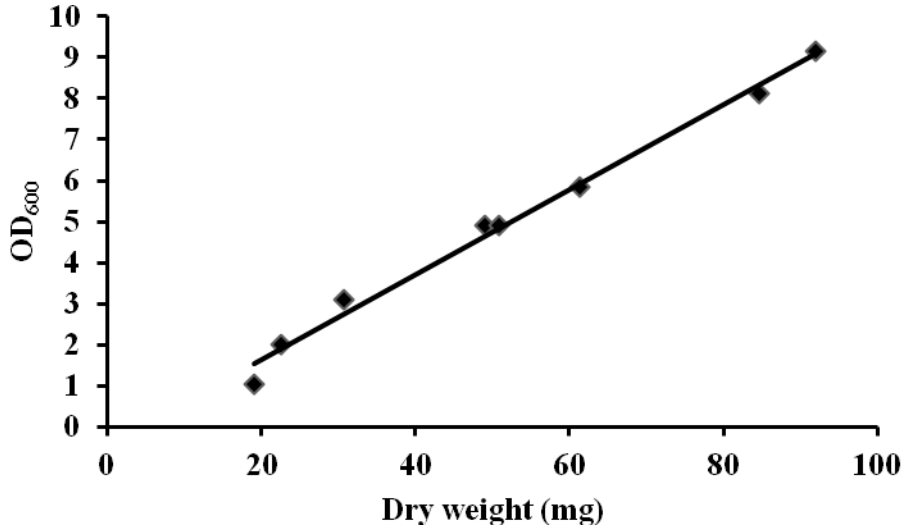

Equation of linear regression:

$Y = 0.1012X - 0.2669$; $R^2 = 0.9918$

A- Absorbance at 600 nm

X- Dry weight in mg

Unknown dryweight at $A_{600} = 1$, $X = (A_{600} + 0.2669)/0.1012$

Considering the total volume of diluent (MOPS) used (30 ml), dry weight conversion factor per ml at $A_{600} = 1$

= X/30 ml = mg/ml.

Errors are negligible on the scale of this graph

5.2 Appendix B: Quantification of standards

5.2.1 Protein assay (Bicinchonic acid (BCA) method)

This method was adapted from Sigma protein kit

Solution A- Bicinchonic acid (from manufacturer's kit)

Solution B- Copper (II) sulphate solution (from manufacturer's kit)

Solution C- Add 1 part of solution B to 50 parts of solution A and mix the contents very well to achieve a homogeneous solution.

Assay method

1. Set the incubator to 30^{o}C

2. Add 0.4 ml of sample to 1 ml of solution C in a 1.5 ml plastic cuvette

3. Mix very well to homogeneity and then incubate for 30 min at 30^{o}C

4. Record the absorbance at 562 nm; Note that blank is distilled water in lieu of sample.

Standard: bovine serum protein solution (1 mg/ml) from Sigma-Aldrich, UK was diluted in the range of the following concentration:

µg protein/ml test solution	µl of standard protein solution	µl of H_2O
0	0	1000
10	10	990
20	20	980
30	30	970
40	40	960
50	50	950
100	100	900
150	150	850
200	200	800

Calibration curve for protein concentration

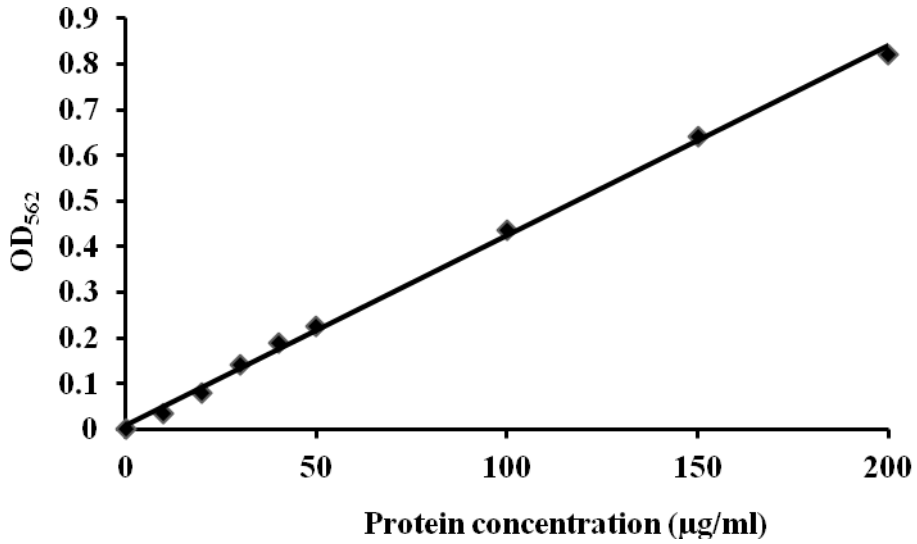

Equation of linear regression

$Y = 0.0042X + 0.0086$; $R^2 = 0.9979$

Y- Absorbance at 562 nm

X- Protein concentration (µg/ml)

Unknown protein concentration, $X = (A_{562}-0.0086)/0.0042$

Error bars are negligible on the scale of this graph.

5.2.2 Pd (II) assay (Tin (II) chloride method)

Reagents

Solution A – $SnCl_2$ solution: dissolve 29.9g of $SnCl_2$ in 500 ml of concentrated HCl

Assay method:

1. Set incubator at 30^{o}C

2. Add 0.2 ml of sample (200µl) to 0.8 ml (800µl) of solution A in a 1.5 ml plastic cuvette.

3. Mix the contents very well, and then incubate for 30 min at 30^{o}C to allow for the development of the coloured complex.

4. Record the absorbance at 463 nm. Blank is distilled water in lieu of sample.

For the calibration curve, 2 mM Pd (II) solution from sodium tetrachloropalladate (II) (Na_2PdCl_4) set to pH 2 with 0.01M HNO_3 was used and diluted in the following range of concentrations:

[Na_2PdCl_4], mM
0
0.2
0.4
0.6
0.8
1
1.2
1.4
1.6
1.8
2

Calibration curve for Pd (II) assay

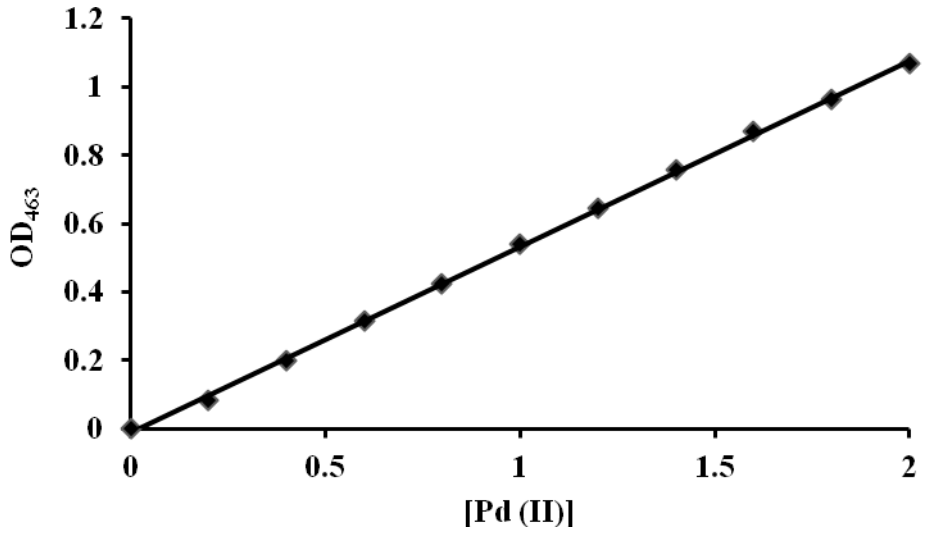

Equation of linear regression

$Y = 0.544X - 0.0106$; $R^2 = 0.9994$

Y – Absorbance at 463 nm

X- Concentration of palladium (II) solution (mM)

Unknown concentration, $X = (A_{463} + 0.0106)/0.544$

Error bars are negligible on the scale of this graph

5.2.3 Ru (III) assay (Tin (II) chloride method)

Reagents

Solution A – $SnCl_2$ solution: dissolve 29.9g of $SnCl_2$ in 500 ml of concentrated HCl

Determination of optimum absorption spectrum of 2 mM aqueous solution ($RuCl_3.H_2O$) of Ru (III) was done using wavelength 400-600 nm. 400 nm was selected as the optimum absorption wavelength (see table below)

Table 5.3 Optimum absorption wavelength of Ru (III)

Wavelength (nm)	Maximum absorbance
400	0.311666667
410	0.237666667
420	0.187
450	0.146
463	0.116333333
500	0.095333333
600	0.161333333

Assay method for Ru (III):

1. Set incubator at 30^{o}C

2. Add 0.2 ml of ruthenium sample (200µl) to 0.8 ml (800µl) of solution A in a 1.5 ml plastic cuvette.

3. Mix the content very well, and then incubate for 30 min at 30^{o}C to allow for the development of the coloured complex.

4. Record the absorbance at 400 nm. Blank is distilled water in lieu of sample.

For the calibration curve, 2 mM Ru (III) solution from ruthenium (III) chloride hydrate ($RuCl_3.H_2O$) set to pH 2.3 with 0.01M HNO_3 was used and diluted in the following range of concentrations:

[$RuCl_3.H_2O$], mM
0
0.2
0.4
0.6
0.8
1
1.2
1.4
1.6
1.8
2

Calibration curve for Ru (III) assay

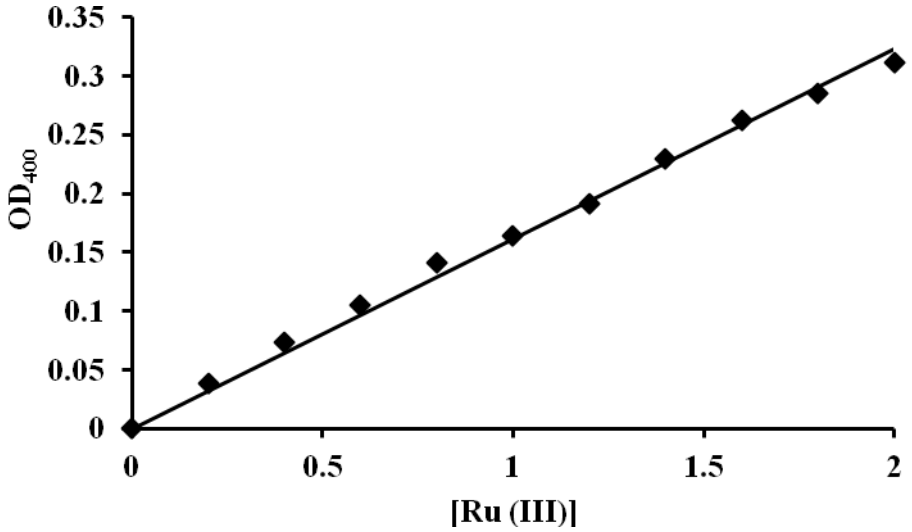

Equation of linear regression

$Y = 0.1614X$; $R^2 = 0.995$

Y – Absorbance at 400 nm

X- Concentration of ruthenium (III) solution (mM)

Unknown concentration, $X = (A_{400})/0.1614$

Error bars are negligible on the scale of this graph

5.2.4 Chloride (Cl^-) assay (mercury (II) thiocyanate method)

Reagents

Solution A- dissolve 5g of mercury (II) thiocyanate ($Hg(SCN)_2$) in 1 L of type (II) water (18.2 MΩ) or in ethanol, a concentration of 0.01578 M. Then decant and filter (whatman paper, 0.3µm) a portion of the saturated supernatant liquid and store at room temperature.

Solution B- dissolve 60 g of ammonium iron (III) sulfate solution ($FeNH_4(SO_4)_2.12H_2O$ in 500 ml of type (II) water (18.2 MΩ). Then add 355 ml of concentrated HNO_3 and dilute to 1 L with type (II) water. Finally, filter (whatman paper, 0.3µm) and store at room temperature.

Assay method

1. To 1 ml of sample add 0.1 ml of solution A and 0.1 ml of solution B

2. Mix very well and leave to stabilize for 10 minutes

3. Record the absorbance at 460 nm. Blank is distilled water or 20 mM MOPS-NaOH buffer (pH 7.0) depending on which solvent was used for the preparation of NaCl standard stock solution.

For the calibration curve - dissolve 0.8241 g of sodium chloride in type (II) water or 20 mM MOPS and dilute to 1 L in a volumetric flask to final stock concentration of 0.0141 M. Prepare a series of standard below by diluting suitable volumes (concentrations) of stock solutions. Then plot a calibration curve of absorbance against concentration.

$[Cl^-]$, mM
0
0.282
0.564
0.846
1.128
1.41

Calibration curve for Cl^- assay

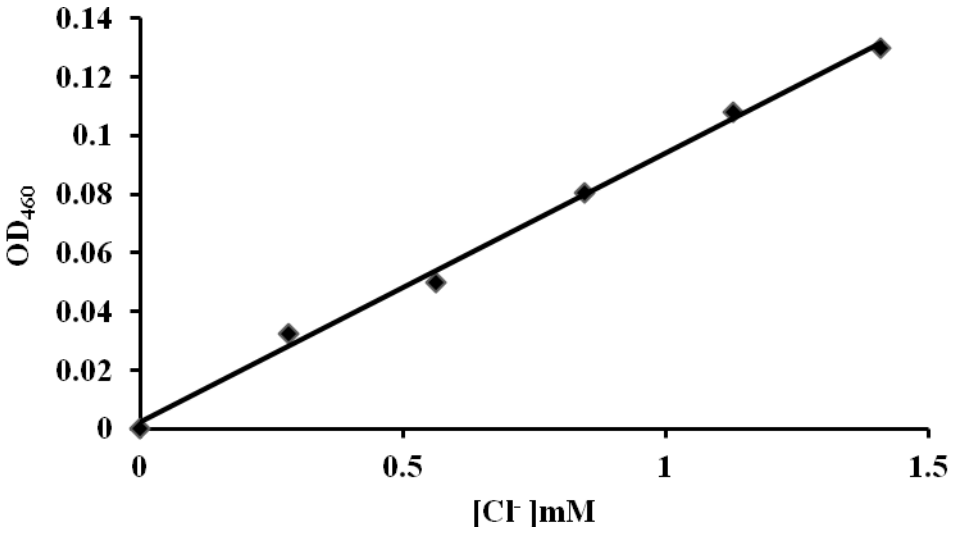

Equation of linear regression:

$Y = 0.0917X + 0.0022$; $R^2 = 0.9957$

Y- Absorbance at 460 nm

X- Chloride concentration (mM)

$[Cl^-] = (A_{460}-0.0022)/0.0917$

Error bars are neglible on the scale of this graph

5.2.5 Gas chromatographic determination of chlorobenzene and benzene standards

To establish the series of concentration for chlorobenzene and benzene, the following equation was adopted:

Mol = Volume x density/molar mass

1. Benzene: Density: 0.8765 g/cm3 (876.50 kg/m^3), molar mass: 78.11 g/mol.

2. Chlorobenzene: Density: 1.11g/cm3 (1110 kg/m^3), molar mass: 112.56 g/mol

The following ranges of initial concentrations were used, using hexane as diluents to the required concentrations below. Samples (0.5 µl) were each injected into a GC with a flame ionization detector (FID) with a RTX-1701 (30 x 0.25 mm x 0.25µm) column (Restek, USA). Injector temperature, 200^oC, detector temperature, 250^oC and a column temperature of 70^oC increasing at the rate of 20^oC/min, split ratio (200:1), and hold time of 8 min and total sample analysis time of 15 min. Carrier gas was helium at a flow rate of 30 ml/min and sample injection volume of 0.5µl.

Concentration (mM)	
Benzene	Chlorobenzene
0	0
0.2	0.1
0.4	1.5
0.6	2.5
0.8	3.5
1	5

A. Calibration curve for benzene standard

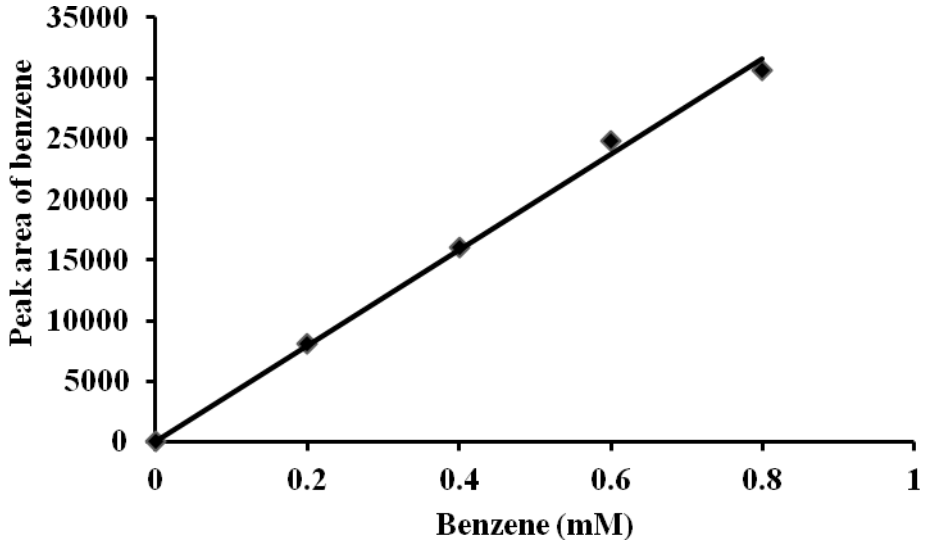

Equation of linear regression:

$Y = 39533X$; $R^2 = 0.9965$

Y – Peak area as determined from GC; X – benzene concentration (mM)

Unknown benzene concentration [X] = Peak area/39533

Note: peak area of undiluted benzene determined = 93797.2

Retention time of benzene during GC analysis = 2.5-2.65 min

Retention time for hexane solvent = 2.1-2.4 min

Error bars are negligible on the scale of this graph

B. Calibration curve for chlorobenzene standard

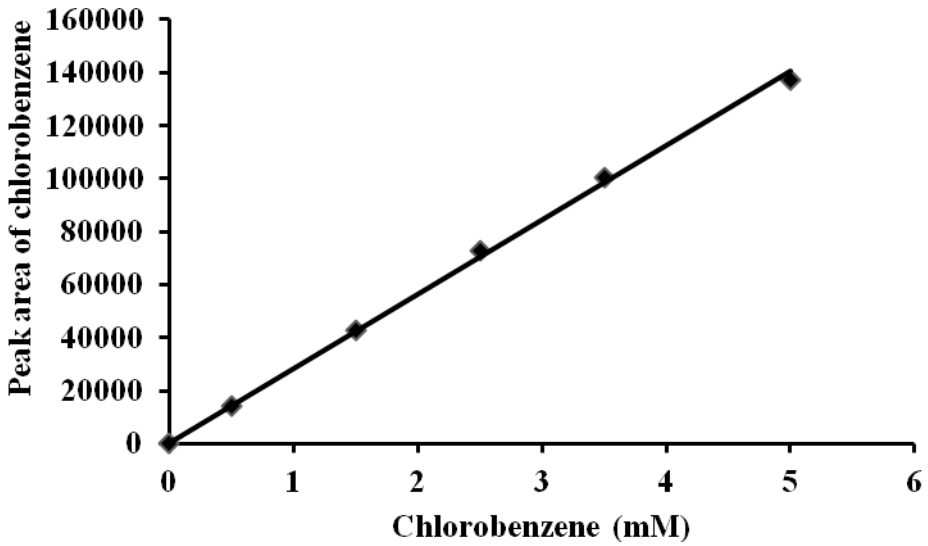

Equation of linear regression:

$Y = 28080X$; $R^2 = 0.9985$

Y – Peak area determined from GC; X – chlorobenzene concentration (mM)

Unknown chlorobenzene concentration [X] = Peak area/28080

Note: that peak area of undiluted chlorobenzene determined = 188491.8

Retention time of chlorobenzene during GC analysis = 4.1- 4.4 min

Error bars are negligible on the scale of this graph

5.3 Appendix C

This section includes some preliminary results of new synthetic methods of biomass-supported catalyst which are not yet ready for publication.

5.3.1 A Facile and Cost Effective Synthesis of Biomass-supported Palladium Nanoparticles Using Sodium Hypophosphite for Catalytic Dechlorination of Chlorobenzene

5.3.1.1 Introduction

Hydrogen is a source of environmentally clean and sustainable energy of the future. It has great potential in power generation e.g. in polymer electrolyte membrane (PEM) fuel cell technology (Bose et al., 2011). However, molecular hydrogen has been described as a gas of low molecular weight, high diffusibility with ease of ignition resulting in hazards, especially in large scale production (Johnstone et al., 1985). Despite extensive efforts there is still no hydrogen storage method with a sufficiently high H_2/weight ratio. Hence, hydrogen donor compounds are becoming increasingly viable alternatives for both storage and generation of hydrogen gas, requiring no hydrogen vessels for storage and major challenges of containment and transport are avoided. Examples of such alternative hydrogen donor compounds include $NaBH_4$, formic acid, formate and NaH_2PO_2 which are safer, environmentally greener alternatives and can be more easily handled than molecular hydrogen.

The objective of this study was to investigate the use of sodium hypophosphite (Na_2HPO_2) as a simple and cost-effective alternative source of hydrogen for the catalytic synthesis of Pd nano-catalysts supported on bacteria and the subsequent application in reductive dechlorination of chlorobenzene.

5.3.1.2 Materials and methods

Bacillus benzeovorans NCIMB 12555 and *Desulfovibrio desulfuricans* NCIMB 8307 were grown according to the method of Omajali et al., (2015). Cells were harvested by centrifugation followed by sorption of Pd (II) (30^oC, 30 min) in a given volume of Na_2PdCl_4 (pH 2 adjusted with 0.01M HNO_3) to make a final 20wt % bio-Pd on cells. Reduction to Pd (0) was done with a 20 mM solution of sodium hypophosphite ($NaPO_2H_2$) from a 500 mM stock without shaking the content. The reduction occurred

immediately. Samples were washed with distilled water and prepared for various characterization techniques (TEM, XRD and XPS) (see chapter two: materials and methods for details of these techniques). The catalyst made by both *B. benzeovorans* and *D. desulfuricans* were compared in reductive dehalogenation of chlorobenzene (see chapter two for details of analysis).

5.3.1.3 Results and discussion

The reduction of palladium by both bacteria using sodium hypophosphite ($NaPO_2H_2$) occurred almost immediately with black deposits of Pd on and within cells. The black deposits were examined using TEM (Figures 5.3 a, b) on *D. desulfuricans* and *B. benzeovorans* respectively. More Pd was found localized on the periplasm and outer membrane of *D. desulfuricans* than inside the cells while intracellular deposition was more apparent in *B. benzeovorans*. Similar palladium nanoparticle (Pd-NP) formation was reported by Omajali et al., (2015) using both formate and hydrogen as electron donors. Some larger Pd-particles were visible on the outside of the cells (Figures 5.3 a, b) which were not seen in the previous work (Omajali et al., 2015). In this study the Pd NPs were confirmed as palladium *via* XRD (X-ray powder diffraction) (Figure 5.3 e). However, the average Pd crystallite size made by *B. benzeovorans* was larger (10.7 ± 069 nm) than that made by *D. desulfuricans* (8.7 ± 0.94 nm). This difference is very clear when the XRD patterns from both cells were compared; with bio-Pd (0) of *D. desulfuricans* producing mostly broader Pd peaks (Figure 5.3d) than that of *B. benzeovorans* (Figure 5.3 e). The peak broadening in both bio-Pd may be due to interaction of phosphorus (P) from the reductant (NaH_2PO_2) with Pd, forming a PdP alloy on cells; using XRD a similar result was reported (Cheng et al., 2008) in the synthesis of PdP/ on carbon by NaH_2PO_2 reduction, leading to peak broadening.

X-ray photoelectron spectroscopy (XPS) provided information on the oxidation states and elemental composition of the surface of each catalyst made by both cells. Both catalysts were reduced mostly to metallic palladium with corresponding binding energies at 335.6 eV and 335.2 eV for *D. desulfuricans* and *B. benzeovorans* respectively, with some residual palladium (II) occurring at binding energies of 337.6 eV and 337.1eV (Figures 5.3 c, d). However, differences were apparent in O1s (Figure 5.3.1c, d) and P2p (Figures 5.3.1g, h) surface elements. There were shifts to higher

binding energies (531.9 eV and 533.2 eV) of the O1s in the catalyst made by bio-Pd of *D. desulfuricans* compared to lower binding energies (530.5 eV and 532.1 eV) seen in *B. benzeovorans* . A similar difference seen with P2p shows two key binding energies of 134.33 eV and 133.1 eV while three different peaks and binding energies at 132.5 eV, 133.81 eV and 135.1 eV were associated with *B. benzeovorans*. This difference in binding energy may be as a result of Pd interaction with phosphorus during Pd reduction with NaH_2PO_2. The differences in the surface elements are more prominent when the atomic concentrations were determined (Table 5.3).

Reductive dechlorination of chlorobenzene resulted in the removal of 82 mg/L of chloride (46.2%) and 77.6 mg/L (43.7%) by bio-Pd made by *D. desulfuricans* and *B. benzeovorans* after 24 h (Figure 5.3.2). The rate of removal after the first 30 min of reaction was faster (0.072 mmol/min/mg Pd) for the catalyst made by *D. desulfuricans* than that made by *B. benzeovorans* (0.04 mmol/min/mg Pd).

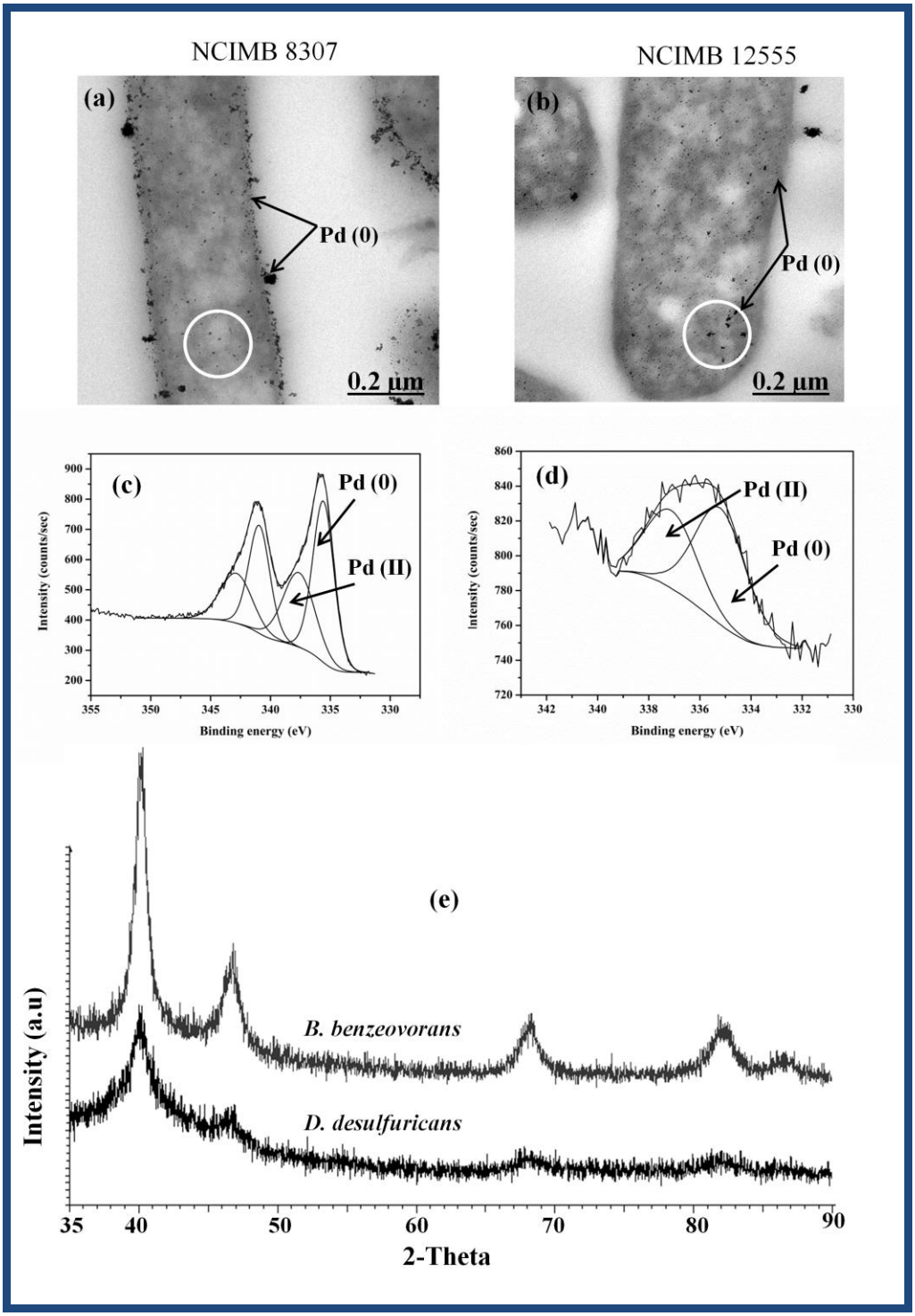

Figure 5.3 TEM images (a, b), XPS spectra of Pd 3d (c, d) and XRD (e) patterns of catalyst made *via* sodium hypophosphite mediated Pd (II) reduction on cells of *D. desulfuricans* (left) and *B. benzeovorans* (right). White circles highlight intracellular palladium nanoparticles.

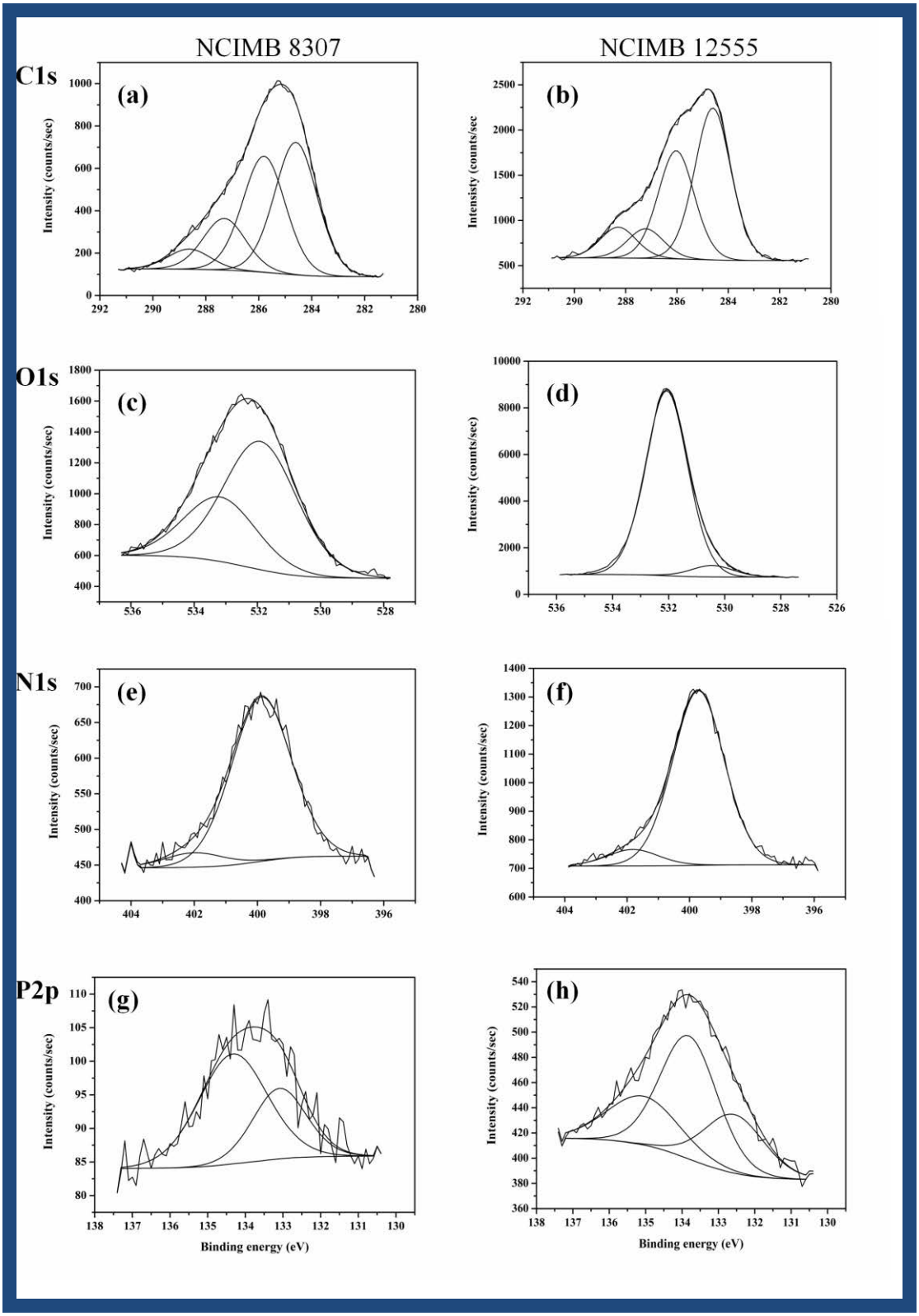

Figure 5.3.1 XPS spectra of surface composition of elements found on catalyst reduced *via* sodium hypophosphite by *D. desulfuricans* NCIMB 8307 (left) and *B. benzeovorans* NCIMB 12555 (right).

Table 5.3 Atomic concentration of elements on catalyst surface made by bacteria after Pd addition

Element	Atomic concentration (%)	
	NCIMB 8307	NCIMB 12555
C1s	62.1	48.0
N1s	6.7	6.1
O1s	25.9	43.3
P2p	0.95	2.43

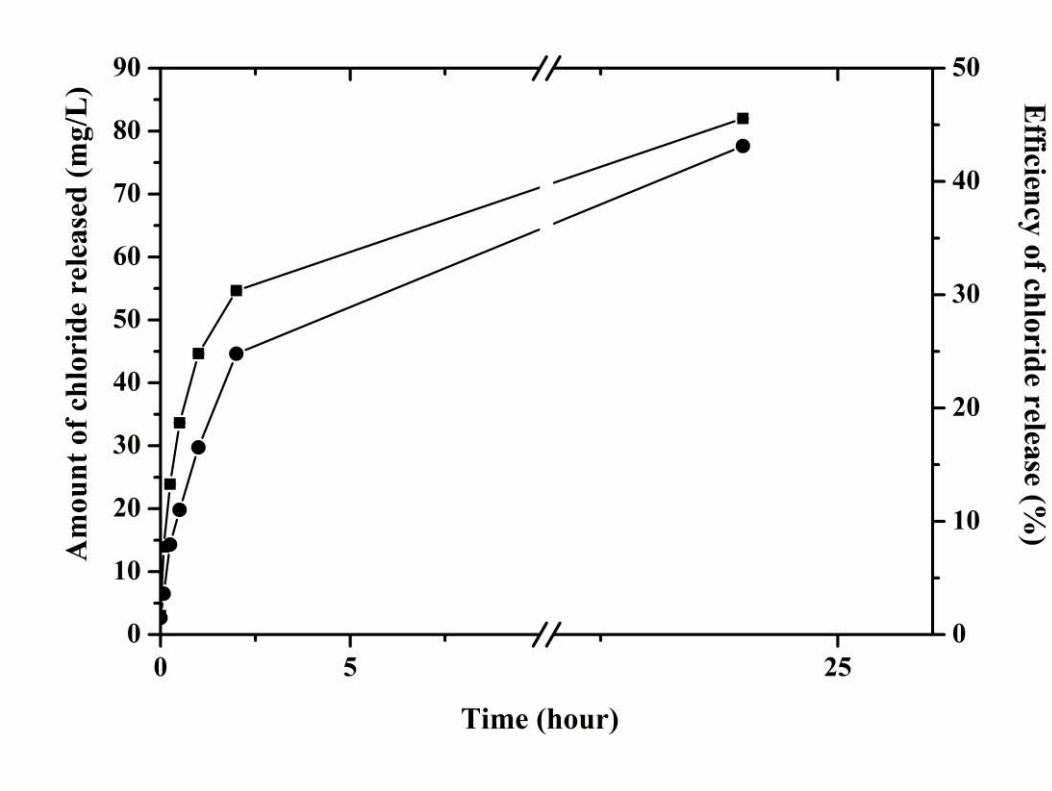

Figure 5.3.2 Efficiency and amount of chloride released by bio-Pd catalyst made by sodium hypophosphite reduction on cells of *D. desulfuricans* (■) and *B. benzeovorans* (●) after 24 h of reductive dechlorination of chlorobenzene.

5.3.1.4 References

Bose, S.; Kuila, T.; Thi, X. L. N.; Kim, N. H.; Lau, K. T.; Lee, J. H., Polymer membranes for high temperature proton exchange membrane fuel cell: Recent advances and challenges. *Progress in Polymer Science* **2011,** *36*, 813-843.

Cheng, L.; Zhang, Z.; Niu, W.; Xu, G.; Zhu, L., Carbon-supported Pd nanocatalyst modified by non-metal phosphorus for the oxygen reduction reaction. *Journal of Power Sources* **2008,** *182*, 91-94.

Johnstone, R. A. W.; Wilby, A. H.; Entwistle, I. D., Heterogeneous catalytic transfer hydrogenation and its relation to other methods for reduction of organic compounds. *Chemical Reviews* **1985,** *85*, 129-170.

Omajali, J. B; Mikheenko, I. P; Merroun, M. L; Wood, J.; Macaskie, L. E, Characterization of intracellular palladium nanoparticles synthesized by Desulfovibrio desulfuricans and Bacillus benzeovorans. *Journal of Nanoparticle Research* **2015,** *17*, 1-17.

5.4 Appendix D

5.4.1 Time-dependent reduction of bio-Pd: Crystallite size analysis *via* XRD

5.4.2 Summary

This study was done to investigate the influence of time-dependent reduction of Pd (II) on the crystallite size when analysed using X-ray powder diffraction. Any difference would provide an idea on the influence of reduction time on crystallite size and subsequent catalytic effects.

5.4.3 Materials and methods

Cells of *Desulfovibrio desulfuricans* NCIMB 8307 were grown and harvested according to the method of Omajali et al., (2015). 20wt % bio-Pd was prepared by using an appropriated volume of Na_2PdCl_4 (pH 2 adjusted with 0.01 M HNO_3) after sorption of Pd (II) (30 min, 30^oC). Reduction was done by bubbling hydrogen for 1 h. Hydrogen bubbling was stopped after 1, 5, 10, 15, 30 and 60 min. At the end of each reduction time, the content was depressurized immediately by removing the rubber stopper on each bottle. Samples were then washed twice with distilled water and once with acetone and the crystallite size was determined by X-ray powder diffraction (XRD) using Scherrer equation (see chapter two materials and methods).

5.4.4 Results and discussion

Time-dependent reduction of palladium by cells of *D. desulfuricans via* hydrogen as a source of electron donor had no effect on crystallite size for the first 30 min (Table 5.4 and Figures 5.4, 5.4.1). There was no observable difference in crystallite size between 1 and 30 mins but a difference was apparent between 30 and 60 mins.

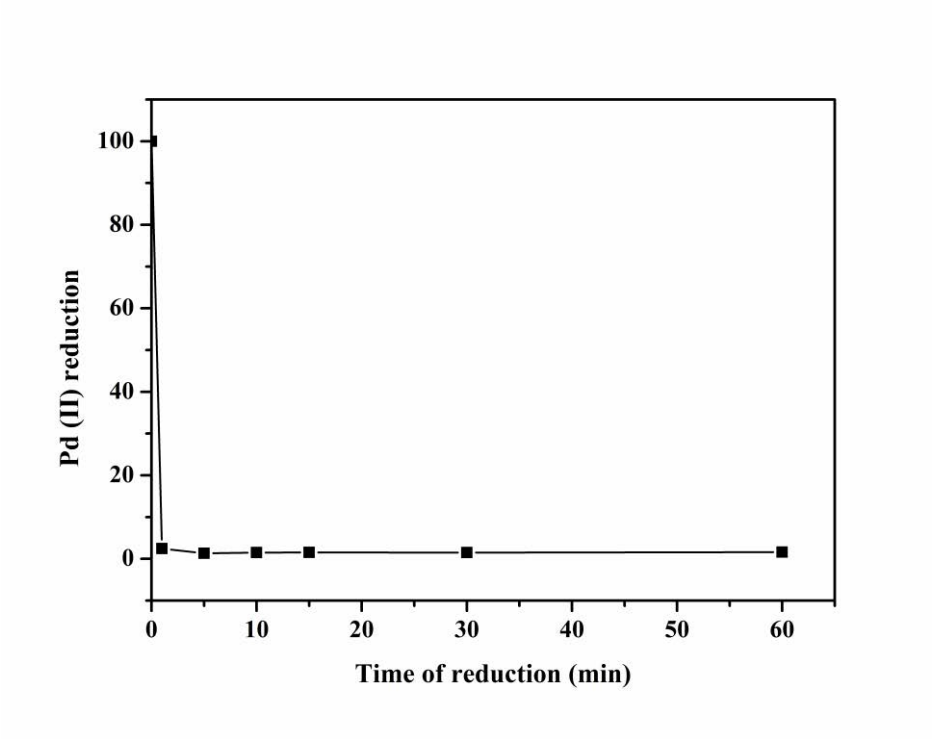

Figure 5.4 Amount of Pd (II) left after a time-dependent Pd (II) reduction at 1, 5, 10, 15, 30 and 60 min intervals. 2 mM Pd (II) solution of Na_2PdCl_4 (pH 2) was used on cells of *Desulfovibrio desulfuricans* to make a 20wt % bio-Pd. Pd (II) removal was determined using tin (II) chloride assay.

Table 5.4 Pd crystallite size after time-dependent reduction

Bio-Pd reduction time (min)	Pd Crystallite size (nm)
1	13.80 ± 0.76
5	13.75 ± 1.35
10	13.54 ± 1.12
15	13.49 ± 0.83
30	12.25 ± 0.93
60	15.51 ± 2.11

Crystallite size of palladium nanoparticles made by reducing Pd (II) to make 20wt % bio-Pd on cells of *D. desulfuricans via* bubbling hydrogen at various time intervals as determine by XRD.

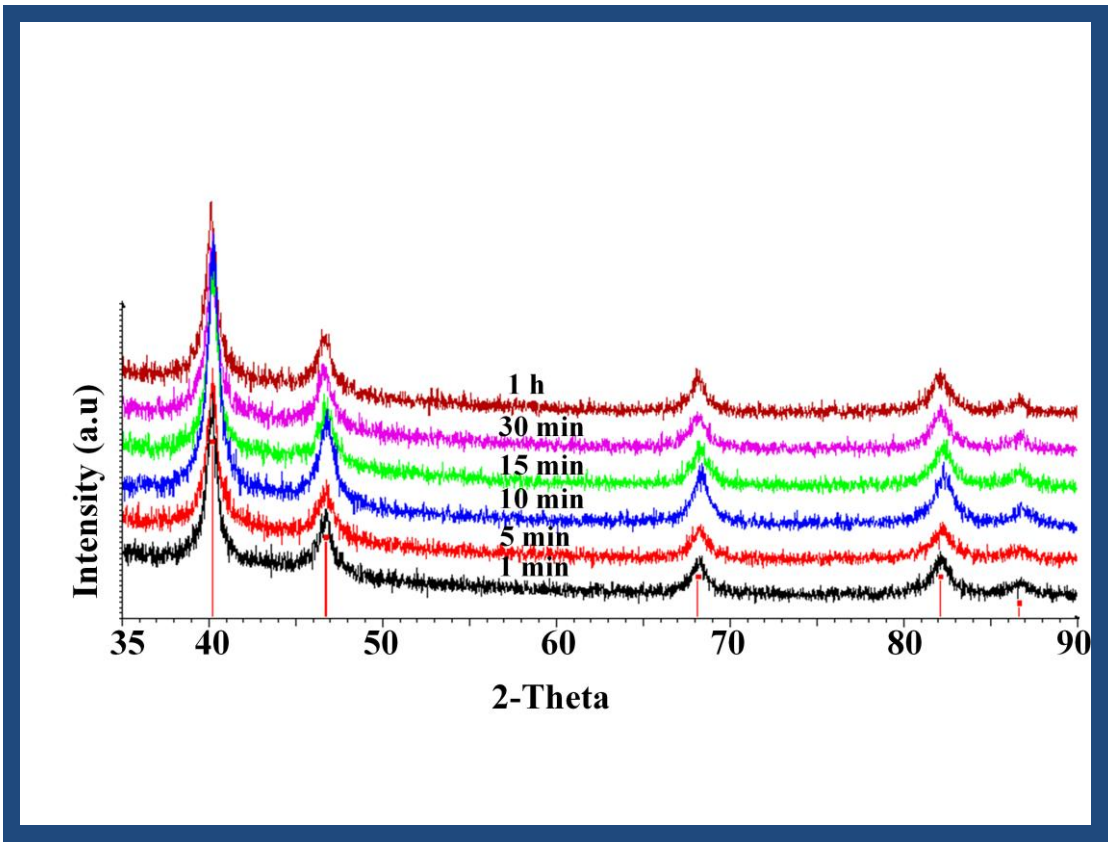

Figure 5.4.1 XRD patterns of time-dependent reduction of 20wt % bio-Pd made by *D. desulfuricans* NCIMB 8307.

5.4.5 References

Omajali, J. B; Mikheenko, I. P; Merroun, M. L; Wood, J.; Macaskie, L. E, Characterization of intracellular palladium nanoparticles synthesized by Desulfovibrio desulfuricans and Bacillus benzeovorans. *J Nanopart Res* **2015,** *17*, 1-17.

5.5 Appendix E

5.5.1 *In-situ* reduction of bio-Pd made by *Desulfovibrio desulfuricans* using XPS

5.5.2 Summary

In-situ reduction was done in this study as a fast way of analysing Pd (II)-doped cells without the need to reduce Pd (II) on cells with an external hydrogen donor prior to XPS analysis. Therefore by using the in-built hydrogen source of the XPS spectrometer, real-time reduction and analysis of metal ions on cells can be done followed by analysis of surface composition of materials. This will save time and the need to reduce metals on cells prior to XPS analysis. This study was intended to pioneer an *in-situ* reduction of palladium (II) on cells of two strains of Gram-negative bacteria (*Desulfovibrio desulfuricans*, NCIMB 8307 and NCIMB 8326).

5.5.3 Materials and methods

Cells of two strains of *Desulfovibrio desulfuricans* (NCIMB 8307 and NCIMB 8326) were grown and harvested (see chapter two: materials and methods). Palladium (Na_2PdCl_4) (II) solution was biosorbed (30^oC, 30 min) on each strain to make 5wt% Pd loading without using external reducing agents. Degree of biosorption was not determined. Samples were washed with distilled water and then prepared for XPS (see chapter two: materials and methods) and *in-situ* reduction was done using X-ray photoelectron spectrometer by dosing samples with atomic hydrogen at a pressure of 1.0 x 10^{-6} mbar (1800L) for 30 min and the data were acquired and analysed as in chapter two.

5.5.4 Results and discussion

For the first time a new method was developed *in-situ* for the reduction of Pd (II) on cells of *D. desulfuricans* using atomic hydrogen within the cell of an XPS spectrometer, which made it easier to monitor the reduction with the simultaneous scanning of the sample to obtain chemical information, avoiding the reduction of samples with exogenous hydrogen sources prior to XPS measurement. A Similar approach was used by Lim et al., (2010) in the reduction of Pd (II) on tobacco mosaic virus (TMV) as a template for the production of palladium nanowires without the addition of external reducing agent. The reduction of Pd (II) was done by an *in-situ* hydrogenation in an

environmental cell transmission electron microscopy (E-TEM) by flowing hydrogen gas while an *ex-situ* hydrogenation was done in a reaction cell of an XPS spectrometer. Using this approach could serve as a new way for synthesizing nanomaterials using *D. desulfuricans* as a template. The results in **Figure 5.5** shows that *in-situ* reduction of Pd (II) on cells of both *D. desulfuricans* was confirmed due to changes in binding energy of unreduced Pd (II) solution from 377.87 eV to 335.80 eV and 335.42 eV in *D. desulfuricans* NCIMB 8307 and NCIMB 8326 respectively after reduction. This binding energy of ~335 eV is due to metal-metal interaction in Pd (0) whereas the binding energy at ~336.9-388 eV is due to Pd in +2 valence state (Hasik et al., 2002). The differences in elemental compositions (Table 5.5, Figure 5.5.1) on both cells of bacteria may be due to differences in surface structure of both *Desulfovibrios* as observed in a previous section.

Table 5.5 Atomic concentration of elements on metallised cells of *D. desulfulricans*

Element	**Atomic concentration (%)**	
	NCIMB 8307	**NCIMB 8326**
C1s	77.6	69.7
N1s	4.3	6.6
O1s	17.4	22.6
P2p	0.65	0.39
S2P	0.26	0.44

Table shows the various elemental compositions determined on each metallised cells during *in-situ* reduction with XPS spectrometer.

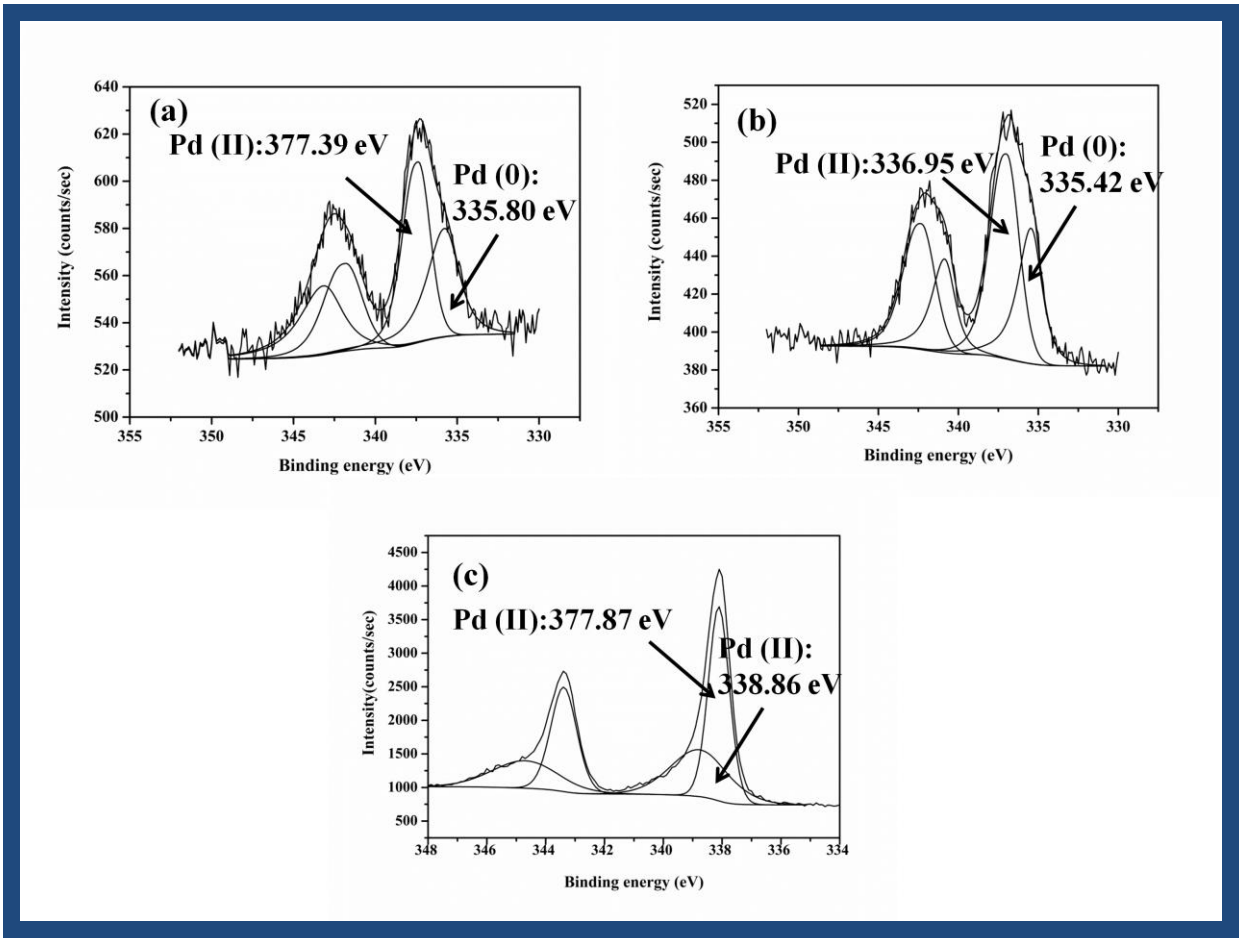

Figure 5.5 XPS spectra of Pd 3d after *in-situ* reduction on metallise cells of *D. desulfuricans* NCIMB 8326 (a) and NCIMB 8326 (b) with Pd 3d spectra of palladium (II) solution serving as unreduced palladium control. Note that Pd 3d peaks appeared as doublets.

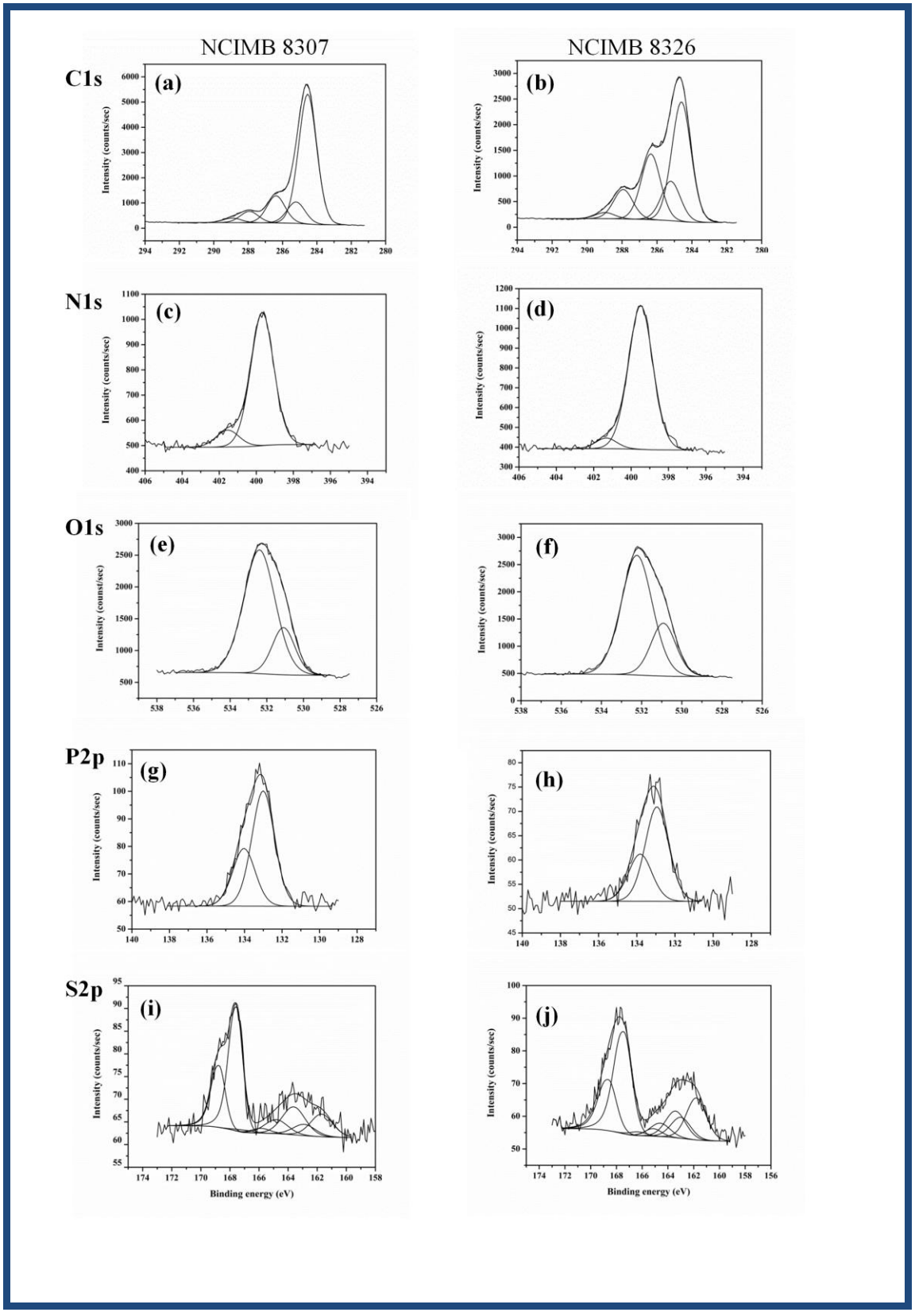

Figure 5.5.1 XPS spectra of various elemental surface components found on metallised cells reduced in-situ using XPS spectrometer.

5.5.5 References

Lim, J.-S.; Kim, S.-M.; Lee, S.-Y.; Stach, E. A.; Culver, J. N.; Harris, M. T., Biotemplated Aqueous-Phase Palladium Crystallization in the Absence of External Reducing Agents. *Nano Letters* **2010,** *10*, 3863-3867.

Hasik, M.; Bernasik, A.; Drelinkiewicz, A.; Kowalski, K.; Wenda, E.; Camra, J., XPS studies of nitrogen-containing conjugated polymers–palladium systems. *Surface Science* **2002,** *507–510*, 916-921.

5.6 Appendix F

5.6.1 Application of a novel Pd/Ru catalysts synthesized by *Bacillus benzeovorans* in transfer hydrogenation of 5-Hydroxymethylfurfural (5-HMF) to 2, 5-Dimethylfuran (DMF)

5.6.2 Introduction

The increasing global energy demand and concerns on global warming has put pressure on the search for alternative sources of energy of which biomass conversion is receiving massive attention in recent times as one of the environmentally viable areas of energy development. Carbohydrates form about 75% of the annual renewable biomass (Schmidt and Dauenhauer, 2007) and as a result of the abundance of the six-carbon fuel derivatives, 5-hydroxymethyl furfural (5-HMF), a derivative of fructose or glucose (van Putten et al., 2013) has become a key precursor in the production of platform chemicals like 2, 5-dimethylfuran (DMF).

The synthesis of 2, 5-DMF from 5-HMF was first reported by Román-Leshkov et al., (2007) through hydrogenoloysis. They started by first converting fructose (by removing three atoms of oxygen) to HMF in a biphasic reactor *via* acid-catalysed dehydration and then removing two oxygen atom by hydrogenolysis of a C-O bond over a bimetallic CuRu/C catalyst to produce 2, 5 DMF (71% in yield). 2, 5-DMF has more advantageous fuel qualities than ethanol because of its higher gravimetric energy density (about 40%), higher boiling point (by 20K) and insolubility in water, however, 5-HMF is not suitable as fuel due to a very high normal boiling point (Román-Leshkov et al., 2007). These properties of 2, 5-DMF has made it a potential gasoline-alternative biofuel (Luque, 2008).

Various catalytic applications have been developed over the years to ensure better yield and selectivity to 2, 5-DMF. However, most developments have focused on commercial heterogeneous mono and bimetallic catalysts based on *e.g.* Ru, Pd, Pt, Au, Cu (Hansen et al., 2012; Zu et al., 2014; Nishimura et al., 2014; Luo et al., 2015) which are very expensive, particularly those from precious metals. The use of a bacterial platform for this application, which has not yet been sought, will provide a cheaper and sustainable source of supported catalyst coupled with the fact that precious metals can be obtained from waste sources.

The first objective of this study was to develop the synthesis of ruthenium based catalyst using cells of *Bacillus benzeovorans* as support in the transfer hydrogenation of 5-HMF to 2, 5-DMF. The second objective was to compare the catalytic transfer hydrogenation of the 5-HMF using alternative hydrogen donor solvents with respect to molecular hydrogen.

5.6.3 Materials and methods

5.6.3.1 Materials. 5-HMF (≥ 99%) FG, DMF (99%), Triethylamine (Et_3N) (≥ 99%), Pd/C (5 wt% Pd on activated carbon dry mass basis) were purchased from Sigma Aldrich, UK. Formic acid (HCOOH) (99%) Acros Organics was supplied by Fisher Scientific, UK. Ru/C (5 wt % Ru on activated carbon paste type 619) and Pd/C (10 wt% Pd on activated carbon type 487 dry) were purchased from Johnson Matthey, UK. All chemicals were used without further purification.

5.6.3.2 Bacteria and growth conditions

Bacillus benzeovorans NCIMB 12555 was selected for the preparation of bio-NPs as a result of ease for potential scale up. *B. benzeovorans* was grown under an aerobic condition (180 rpm at 30^{o}C) in a nutrient medium with the following composition: 1.0g beef extract (Sigma-Aldrich), 2.0g yeast extract (Sigma-Aldrich), 5.0g peptone (Sigma-Aldrich) and 15.0g NaCl per litre of distilled water and adjusted to pH 7.3 (Omajali et al., 2015). The bacterial cells were then harvested (Beckman Coulter Avati J-25 Centrifuge, U.S.A) by centrifugation (9,000 x g, 15minutes at 4^{o}C) during exponential phase, OD_{600} 0.7-1.0, washed three times in air with 20mM MOPS (morpholinepropanesulfonic acid)-NaOH buffer, pH 7.0 and then concentrated in a small amount of the same buffer. These were stored at 4^{o}C and subsequently used for bio-NPs preparation, usually within 24 h.

5.6.3.3 Preparation of monometallic and bimetallic bionanoparticles (bio-NPs)

The bio-NP catalyst preparation was done in two ways: The syntheses of monometallic and bimetallic biocatalysts were made differently. For all monometallic bio-NPs preparation, cell suspensions were transferred into 2 mM Pd (II) solution of Na_2PdCl_4 or 2 mM Ru (III) of $RuCl_3.2H_2O$ solution (adjusted to pH 2) and left for biosorption (30 minutes at 30^{o}C). During the preparation of monometallic bio-Ru using a 2 mM

solution of $RuCl_3.H_2O$, H_2 was bubbled for about 1hr and then saturated and then transferred onto a shaker (180 rpm and 30^oC) for 96h. For the synthesis of the bimetallic Pd/Ru, a 2mM Pd (II) and 1 mM Ru (III) was used in line with the method of Deplanche et al (2012) for Pd/Au synthesis with modifications. Here, the 2 mM Pd (II) solution was first reduced under hydrogen for 30 min. The resulting bio-Pd was then washed twice with distilled water and then some quantity of water (2:1) was added in respect to the initial Pd solution used. The reduced bio-Pd was then used to sequentially reduce 1 mM Ru (III). The content was then saturated with hydrogen for 15 min and then transferred onto a shaker (180 rpm, 30^oC) for 96h for further reduction of Ru (III) by the bio-Pd seed. The reduced bimetallic bio-NPs were then washed three times with distilled water and once with acetone (9,000 x g, 15minutes at 4^oC) and then dried. The dried samples were ground in a mortar with pestle for catalytic reactions.

5.6.3.4 Transmission electron microscopy

Selected samples of the bio-NPs-deposited on bacterial cells were washed twice with distilled water and then fixed with 2.5% (w/v) glutaraldehyde fixative in 0.1M cocadylate buffer (pH 7.0) at 4^oC and stained with 1% osmium tetraoxide. The cells were then dehydrated in an ethanol series. This was followed by embedding cells in epoxy resins and then cutting into sections about 100-150 nm thick. Finally, the samples were viewed under a transmission electron microscope (JEOL 1200 EX) with an accelerating voltage of 80 kV (Omajali et al., 2015). For easy image visualization using JEOL 1200 EX electron microscope, higher metal loadings (20%) of the bio-NPs were considered.

5.6.4 Catalytic testing

Catalytic testing and product analysis was performed and written by Bayonle Kayode, School of Chemical Engineering, University of Birmingham.

5.6.4.1 Procedure for the catalytic transfer hydrogenation of 5-HMF to 2, 5-DMF in formic acid/triethylamine ($HCOOH/Et_3N$) solvent. The catalytic transfer hydrogenation reactions were carried out in a 100 mL stainless steel Parr reactor with an external temperature and stirring controllers. For a typical reaction, 0.3 M 5-HMF, 100

mg catalyst and 25 mL of HCOOH/Et_3N were added to the reactor, sealed and purged three times with N_2 at 10 bar pressure, heated to 210^oC, and stirred at a speed of 300 rpm for 4 hours. After completion of the reaction, the reactor was cooled to room temperature in an ice-water bath; and the reaction mixture was filtered through 8µm Whatman quantitative filter paper.

5.6.4.2 Procedure for catalytic transfer hydrogenation of 5-HMF to 2, 5-DMF in 2-propanol solvent. The catalytic transfer hydrogenation reactions were carried out in a 100 mL stainless steel Parr reactor autoclave with an external temperature and stirring controllers. For a typical reaction, 0.05M 5-HMF, 100 mg catalyst and 25 ml of 2-propanol were added to the reactor, sealed, purged of air with 5 bar N_2 and charged with 20 bar N_2. The reactor was heated to 260^oC reaction temperature and stirred at a speed of 300 rpm for 2 hours. After completion of the reaction, the reactor was quenched to room temperature in ice-water bath; and the reaction mixture was filtered through 8µm Whatman quantitative filter paper.

5.6.4.3 Product Analysis. 5-HMF, 2,5-DMF, and intermediates formed were analysed by GC (Shimadzu 2010) equipped with a FID detector and a ZB-SemiVolatile column (30 m × 0.25 mm × 0.50 µm) and Waters GCT Premier time-of-flight mass spectrometer (Micromass, Manchester, UK) with a ZB-SemiVolatile-MS column. For GC-FID analysis, the injection volume was 1 µL, the injector temperature was 300^oC, the detector temperature was 300^oC, inlet pressure was 100 KPa, split ratio of 100:1, and the carrier gas was He with a flow rate of 1 mL/min. The initial column temperature of 50^oC was held for 5 min, and then, the temperature was ramped 16.6^oC/min until 133.3^oC was reached and held for 1.5 min; after that, the temperature was ramped until 300^oC was reached and held for 3.5 min. For GC-MS analysis, Waters MassLynx software (version 4.1) was used to operate the GC-TOFMS system. The source temperature was 200^oC and electron energy was 70 eV. It should be noted here that 5-HMF conversion and DMF yield were based on external standard method and calculated using the equations below:

$$\text{HMF Conversion (\%)} = \frac{(\text{Initial moles of HMF} - \text{Final moles of HMF})}{\text{Initial moles of HMF}} \times 100 \quad (1)$$

$$\text{DMF Yield (\%)} = \frac{\text{Moles of DMF in products}}{\text{Initial moles of HMF}} \times 100 \quad (2)$$

$$\text{Selectivity (\%)} = \frac{\text{Moles of DMF in products}}{(\text{Initial moles of HMF} - \text{Final moles of HMF})} \times 100 \quad (3)$$

5.6.5 Results and discussion

5.6.5.1 Surface characteristics of bio-NPs

TEM images in figure 5.6 present some morphological characteristics of the bio-ruthenium catalysts. The reduction was quite slow (for about 96 h) and incomplete, which was confirmed by tin (II) chloride assay. However, allowing reduction to occur at higher temperature in future preparation may improve and speed up the reduction process. The synthesis of monometallic bio-Ru by *B. benzeovorans* was mostly on the extracellular cell surface (Fig 5.6a) with no intracellular deposition of ruthenium nanoparticles (NPs) which was different from the synthesized bimetallic bio-Pd/Ru (Fig 5.6b) with intracellular deposition of NPs. There was both extracellular and intracellular deposition of bio-Pd/Ru in *B. benzeovorans* (Fig 5.6b). The absence of intracellular NPs observed in bio-Ru produced cells is quite intriguing because Omajali et al., (2015) confirmed the intracellular synthesis of Pd (0) in both Gram-negative and Gram-positive bacteria and suggested that Pd could have been "trafficked" *via* which may explain the presence of intracellular NPs in cells with bio-Pd/Ru. However, this needs further investigation as it seems possible that Ru (III) may not be trafficked and hence the absence of intracellular NPs in Figure 5.6a.

The catalytic transfer hydrogenation of 5-HMF to 2, 5-DMF using biomass-supported ruthenium catalyst (mono and bimetallic) was demonstrated using hydrogen donor solvents; formic acid/triethylamine mixture and 2-propanol in comparison with molecular hydrogen. When formic acid/triethylamine mixture was used as a source of

hydrogen, the commercial 5wt% Ru/C catalyst produced the highest yield (92.1%) and selectivity (98.6%) to 2, 5-DMF followed by bio-ruthenium catalysts which produced comparable selectivities (51-58.5%) but with the 20wt% bimetallic Pd/Ru producing the best yield (56.7%) to 2, 5-DMF. Pd/C catalysts were the poorest in terms of activity (Table 5.6). A similar trend was seen when 2-propanol was used (Table 5.6.1). However, in this case, the 5wt% Pd/Ru was more selective (42.6%) to 2, 5-DMF with better yield (45.1%) than both 20wt% Pd/Ru and 20wt% Ru catalysts. The bio-ruthenium catalyst also showed superiority over commercial Pd/C catalyst. Finally, using molecular hydrogen as the source of hydrogen produced a better activity than using the hydrogen donor solvents, with Ru/C producing the best result (Table 5.6.2). A similar trend was seen with the bio-ruthenium catalysts in the following order: 20wt% Pd/Ru > 5wt% Pd/Ru > 20wt% Ru. Generally, the final conversion of 5-HMF to 2, 5-DMF using the hydrogen donor sources did not differ significantly (93-97%) using the various hydrogen donor sources.

This study has shown that formic acid/triethylamine mixture and 2-propanol can serve as alternative sources of hydrogen to molecular hydrogen in the synthesis of 2, 5-DMF. However, the transfer hydrogenation was less effective than using molecular hydrogen but would be a cheaper and less hazardous approach. Despite the less effective activities of the bio-ruthenium catalysts when compared with Ru/C, they were more effective than Pd/C catalysts used and are also a more sustainable source of catalyst supply. However, improvements are needed in order to compete with commercial counterparts.

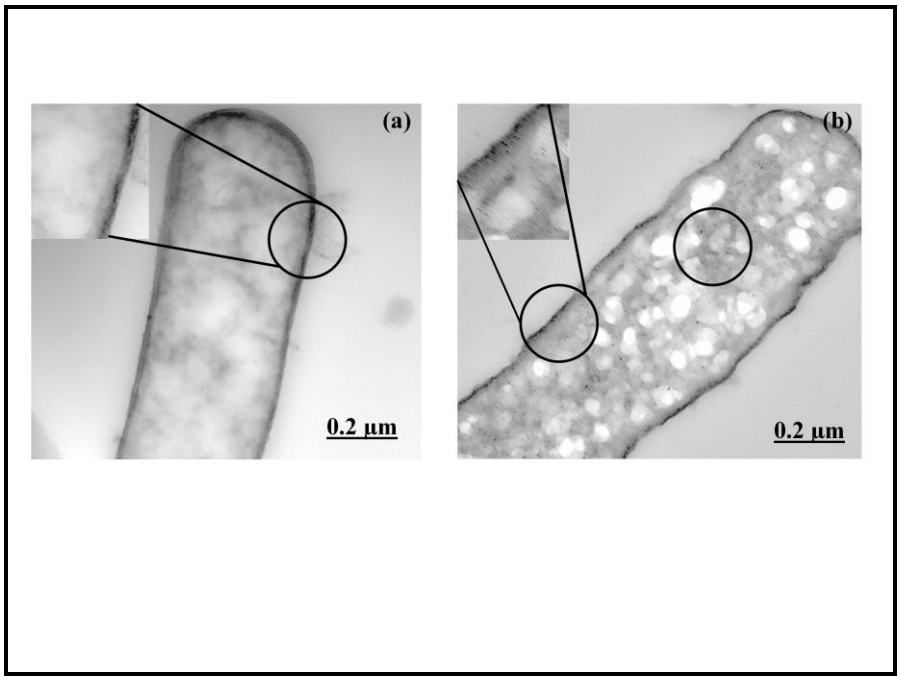

Figure 5.6 TEM images of 20wt% bio-Ru (a) and 20wt% bio-Pd/Ru (b) made by *Bacillus benzeovorans*. Insets are enlarged images (50 nm) of the metallised surfaces (black circle). Intracellular NPs (black circle) can be seen only in cells that produced bio-Ru/Pd. Scale bars are 0.2µm.

Table 5.6 Comparison of catalyst in 5-HMF transfer hydrogenation with formic acid/triethylamine ($HCOOH/Et_3N$) mixture

Test	5wt% bio-Pd/Ru	20wt% bio-Pd/Ru	20wt% bio-Ru	5wt% Ru/C	5wt% Pd/C	10wt% Pd/C
DMF Yield (%)	49.8 ± 0.6	56.7 ± 0.2	52.7 ± 1.2	92.1 ± 0.4	26.5±2	24.4±1.6
5-HMF Conversion (%)	96.8	96.9	96.8	93.4	97.5	97.3
Selectivity (%)	51.5	58.5	54.5	98.6	27.2	25.0

Result of hydrogenation of 5-HMF using $HCOOH/Et_3N$ (formic acid/triethylamine) mixture as hydrogen donor. Yield of DMF, conversion of 5-HMF and selectivity to DMF are represented in percentage.

Table 5.6.1 Comparison of catalyst in 5-HMF transfer hydrogenation with 2-propanol

Test	5wt% bio-Pd/Ru	20wt% bio-Pd/Ru	20wt% bio-Ru	5wt% Ru/C	5wt% Pd/C	10wt% Pd/C
DMF Yield (%)	42.6±1.2	38.6±1.6	37.2±0.7	70.2±2.4	32.6±1.8	32.8±1.2
5-HMF Conversion (%)	94.5	94.3	94.5	94.3	94.5	94.3
Selectivity (%)	45.1	40.9	39.3	74.4	34.5	34.8

Result of hydrogenation of 5-HMF using 2-propanol as hydrogen donor. Yield of DMF, conversion of 5-HMF and selectivity to DMF are represented in percentage.

Table 5.6.2 Comparison of catalyst in 5-HMF transfer hydrogenation with hydrogen

Test	5wt% bio-Pd/Ru	20wt% bio-Pd/Ru	20wt% bio-Ru	5wt% Ru/C
DMF Yield (%)	55.5 ± 2	60.3 ± 3	47.9 ± 2	95.1±0.5
[5-HMF Conversion (%)	94.7	95.3	95.1	96.4
Selectivity (%)	58.5	63.3	50.4	98.7

Result of hydrogenation of 5-HMF using hydrogen as hydrogen donor. Yield of DMF, conversion of 5-HMF and selectivity to DMF are represented in percentage.

5.6.5 References

Deplanche K.; Merroun M.L.; Casadesus M.; Tran D.T.; Mikheenko I.P.; Bennett J.A.; Zhu J.; Jones I.P.; Attard G.A.; Wood J.; Selenska-Pobell, S.; Macaskie, L.E. Microbial synthesis of core/shell gold/palladium nanoparticles for applications in green chemistry. *Journal of the Royal Society Interface* **2012**, *9*, 1705-1712.

Hansen, T. S.; Barta, K.; Anastas, P.T. One-pot reduction of 5-hydroxymethylfurfural via hydrogen transfer from supercritical methanol. *Green Chemistry,* **2012**, *14*, 2457-2461

Luque, R.; Herrero-Davila, L.; Campelo, J.M.; Clark, J.H.; Hidalgo, J.M.; Luna, D.; Marinasa, J.M.; Romeroa, A.A. "Biofuels: a technological perspective." *Energy & Environmental Science* **2008**, *1*, 542-564.

Luo, J.; Arroyo-Ramirez, L.; Gorte, R. J.; Tzoulaki, D.; Vlachos, D. G., Hydrodeoxygenation of HMF Over Pt/C in a Continuous Flow Reactor. *AICHE Journal* **2015,** *61*, 590-597.

Nishimura, S.; Ikeda, N.; Ebitani, K. Selective hydrogenation of biomass-derived 5-hydroxymethylfurfural (HMF) to 2, 5-dimethylfuran (DMF) under atmospheric hydrogen pressure over carbon supported PdAu bimetallic catalyst. *Catalysis Today*. **2014**, *232*, 89-98.

Omajali, J.B; Mikheenkho, I.P; Merroun, L.M; Wood, J; Macaskie L.E., Characterization of intracellular palladium nanoparticles synthesized by *Desulfovibrio desulfuricans* and *Bacillus benzeovorans*. *Journal of Nanoparticle Research* **2015,** *17*, 1-17.

Román-Leshkov, Y.; Barrett, C. J., Liu, Z. Y.; Dumesic, J. A. Production of dimethylfuran for liquid fuels from biomass-derived carbohydrates. *Nature* **2007**, *447*, 982–985.

Schmidt, L. D.; Dauenhauer, P. J. Hybrid routes to biofuels. *Nature* **2007**, *447*, 914.

van Putten, R. J.; van der Waal, J. C.; de Jong, E.; Rasrendra, C. B.; Heeres, H. J.; de Vries, J. G., Hydroxymethylfurfural, A Versatile Platform Chemical Made from Renewable Resources. *Chemical Reviews* **2013,** *113*, 1499-1597.

Zu, Y.H.; Yang, P.P.; Wang, J.J.; Liu, X.H.; Ren, J.W.; Lu, G.Z.; Wang, Y.Q. Efficient production of the liquid fuel 2, 5-dimethylfuran from 5-hydroxymethylfurfural over Ru/Co_3O_4 catalyst. *Applied Catal*ysis, B, **2014**, *146*, 244-248.

5.7 Appendix G

This section covers journal publications, conference proceedings, posters, seminars and abstracts not covered elsewhere.

5.7.1 Journal Publications

i. **Omajali, J.B**; Mikheenkho, I.P; Merroun, L.M; Wood, J; Macaskie L.E., Characterization of intracellular palladium nanoparticles synthesized by *Desulfovibrio desulfuricans* and *Bacillus benzeovorans*. *J Nanopart Res* **2015,** *17* (6), 1-17

This paper was written by me, including all experiments and analyses. Technical assistance on STEM-HAADF was given by Maria del Mar Abad Ortega (Centro de Instrumentación Científica, University of Granada, Spain).

ii. Deplanche, K.; Bennett, J. A.; Mikheenko, I. P.; **Omajali, J**.; Wells, A. S.; Meadows, R. E.; Wood, J.; Macaskie, L. E., Catalytic activity of biomass-supported Pd nanoparticles: Influence of the biological component in catalytic efficacy and potential application in 'green' synthesis of fine chemicals and pharmaceuticals. *Applied Catalysis B: Environmental* **2014,** *147* (0), 651-665

My contribution in this paper was in terms of X-ray powder (XRD) analysis of bio-Pd of *D. desulfuricans*

iii. Hart, Abarasi.; **Omajali, J.B**.; Macaskie, L. E.; Greaves, M.; Wood, J. Nanoparticles of Pd supported on bacterial biomass have comparable activity to carbon and alumina for in-situ upgrading of heavy oil during toe-to-heel air injection (THAI) process. Submitted to Fuel

My contribution in this paper was in terms of synthesis and characterization of the bio-Pd catalyst on *D. desulfuricans*

5.7.2 Conference proceedings

i. A.J Murray; **J.B. Omajali**; Y. Del Mastio; A. Hart; J. Wood; L. E. Macaskie. Conversion of waste platinum group metals in road dust into biocatalysts for cracking heavy oil. Accepted for presentation at the International Biohydrometallurgy Symposium, Bali, Indonesia, October 2015

My contribution in this paper was in terms of synthesis and characterization of the bio-Pd catalyst on *D. desulfuricans, E. coli* and *B. benzeovorans.* I also wrote a section of the materials and methods.

ii. Hart A.; **Omajali, J.B**.; Macaskie, L. E.; Greaves, M.; Wood, J. In-situ catalytic upgrading of heavy oil using nanoparticulate catalysts during toe-to-heel air injection (THAI). World heavy oil congress, Edmonton, Alberta, Canada, 2015

My contribution in this paper was in terms of synthesis and characterization of the bio-Pd catalyst on *D. desulfuricans*

5.7.3 Conference abstracts, posters, seminars and symposia

i. Bayonle Kayode, **Jacob B. Omajali**, Mohamed Farah, Joseph Wood, Lynne Macaskie and Bushra Al-Duri. Novel Nanoparticles of Ru and Pd supported on Bacterial Biomass for Catalytic Hydrogenation of 5-HMF to Produce 2, 5-DMF. Green chemistry conference, September 2015, Orlando, Florida, USA

ii. **Omajali, J. B.**; Mikheenko, I. P.; Merroun, L. M.; Wood, J.; Macaskie, L. E. Intracellular synthesis of palladium nanoparticles by Gram-negative and Gram-positive bacteria and their characterization via high resolution STEM-HAADF. Redeal meeting, Colloid and Surface Chemistry group, Society of Chemical Industry, London 2015

iii. **Omajali, J. B**.; Wood, J.; Macaskie, L. E. Biomanufactured nanoscale palladium catalyst: Effects of biomass type on catalyst activity in the reductive dechlorination of chlorobenzene. 3rd International conference on Nanotek and Expo, Las Vegas, USA, 2013

iv. **Omajali, J. B**.; Macaskie, L. E. Understanding the catalytic properties of bio-palladium nanocatalyst produced by *Desulfovibrio desulfuricans*. Postgraduate research conference, University of Birmingham, 2013

v. **Omajali, J. B.** Synthesis of bio-palladium nanocatalyst by reduction of bacterial surfaces. Image of research conference, University of Birmingham, 2013

vi. **Omajali, J. B.**; Walker, M.; Wood, J.; Macaskie, L. E. Biomanufactured nanoscale palladium catalyst from *Desulfovibrio desulfuricans* in hydrogenation and hydrogenolysis. Surface science summer seminar, University of Warwick, 2013